Brunel University

NOVEL RETROFIT TECHNOLOGIES INCORPORATING SILICA AEROGEL FOR LOWER ENERGY BUILDINGS

Mark Dowson

A thesis submitted in partial fulfilment for the degree of Engineering Doctorate in Environmental Technology

School of Engineering and Design, September 2012

Declaration of Authorship

I, Mark Dowson, declare that this thesis entitled '*Novel retrofit technologies incorporating silica aerogel for lower energy buildings"* and the work presented in it are my own. I confirm that:

- This work was done wholly or mainly while in candidature for a research degree at this University.
- Where any part of this thesis has previously been submitted for a degree or any other qualification at this University or any other institution, this has been clearly stated.
- Where I have consulted the published work of others, this is always clearly attributed.
- Where I have quoted from the work of others, the source is always given.
- With the exception of such quotations, this thesis is entirely my own work.
- I have acknowledged all main sources of help.
- Where the thesis is based on work done by myself jointly with others, I have made clear exactly what was done by others and what I have contributed myself.

Signed: 

Date: *1st September 2012*

Brunel University

ABSTRACT

NOVEL RETROFIT TECHNOLOGIES INCORPORATING SILICA AEROGEL FOR LOWER ENERGY BUILDINGS

by Mark Dowson

The aim of this Engineering Doctorate is to design, build and test novel environmental retrofit technologies to reduce energy consumption in existing buildings. Three contributions to knowledge are documented. The first contribution is the technical verification of a novel proof-of-principle prototype incorporating translucent silica aerogel granules to improve the thermal performance of existing windows without blocking out all of the useful natural light. The study demonstrates that a 10 mm thick prototype panel can reduce heat loss by 80 %, without detrimental reductions in light transmission. Payback periods of 3.5-9.5 years are predicted if applied as openable shutters or removable secondary glazing. The second contribution is a streamlined life cycle assessment of silica aerogel following the ISO 14000 standards. The study assesses the raw materials and electricity use associated with two of the three known methods of aerogel production. Despite being produced in a laboratory that had not been refined for mass manufacture, the production energy and CO_2 burden from aerogel production can be recovered within 0-2 years when applied in a glazing application. The third contribution is the development and verification of a novel solar air heater incorporating granular aerogel, retrofitted to an external south facing wall, preheating the air in a mechanical ventilation system with heat recovery on a hard-to-treat domestic property. During the 7-day in-situ test, peak outlet temperatures up to 45 °C were observed and validated to within 5 % of predictions, preheating the dwelling's fresh air supply up to 30 °C, facilitating internal temperatures of 21-22 °C without auxiliary heating. The predicted financial and CO_2 payback for a range of cover thicknesses is 7-13 years and 0-1 years, respectively. Efficiency up to 60 % and a financial payback of 4.5 years is predicted with an optimised design incorporating a 10 mm thick granular aerogel cover.

Acknowledgements

This doctorate would not have been possible without the support and time of numerous people. Firstly, I would like to thank Professor David Harrison for being a reliable, positive and supportive academic supervisor throughout the whole process. Dr Andrew Cripps for giving me the position at Buro Happold and Dr Nicola Combe for starting her EngD with me, making the whole process less daunting. Dr Salmaan Craig deserves credit for his critical and motivational approach to industrial supervision. Thanks to Dr Ian Pegg for picking up this role during the second half and to Dr Gideon Susman for his willingness and guidance as industrial supervisor at the final hurdle.

Dr Zack Gill was very helpful, teaching me how to set up the monitoring equipment for the pilot study at early stages of this project. Thanks to Dr Paul Baker for calibration support. A phone call to Dr Michael Grogan at the University of Bath, led to a great collaboration involving the manufacture of aerogel samples, allowing the task of a life cycle assessment to be feasible. Thanks to his supervisor, Professor Tim Birks for supporting this collaboration. Thanks to Professor Yanmeng Xu at Brunel University, for his support with the high resolution photography of the aerogel samples. Dan Knott was also helpful, taking the time to share his parametric modelling understanding.

'Retrofit for the Future' was a key driving force allowing the Aerogel Solar Collector to be installed and tested on a real house. Thanks go to all of the team working on this refurbishment project, including Martin Montgomery of Gallions Housing Association, Angus Brown and Viviana Vivanco of FBM architects, Jim Martin and Stephen Mitchell of Martin-Arnold Associates and the team at Axis Europe. Thanks go to Richard Lowe of Xtralite Ltd, Colin Biggs of Nuaire Ltd and Dr Jeremy Richings of Permarock Products Ltd for their design support. Thanks to Alan Gilbert of BSRIA Ltd and the team at MD electrical for monitoring and control installation support. Thanks to Sam Proctor for his interest to install the Spacetherm™ Door at the property. Thanks to Dr Zahir Dehouche for his time spent reviewing the thermal modelling calculations.

This research would not have been possible without funding from the Engineering and Physical Sciences Research Council (EPSRC) and Buro Happold Ltd. I also want to thank all of my family and friends for their support. Lastly, a big thanks to Anna Menezes (soon to submit and pass her own EngD) for being by my side the whole time, through the trials, tribulations and all of the proof reading!

Contents

Glossary

APD	Ambient pressure drying
BRE	Building Research Establishment
BSRIA	Building Services Research and Information Association
CERT	Carbon Emissions Reduction Target
CESP	Community Energy Savings Programme
CIBSE	Chartered Institution of Building Services Engineers
DEC	Display Energy Certificate
DER	Dwelling Emission Rate
EPC	Energy Performance Certificate
EPS	Expanded polystyrene
FIT	Feed in Tariff
GRP	Glass reinforced plastic
HTSCD	High temperature supercritical drying
LCA	Life cycle assessment
LTSCD	Low temperature supercritical drying
MVHR	Mechanical ventilation system with heat recovery
PHPP	Passive House Planning Package
PIR	Passive infrared sensor / polyurethane insulation
PV	Photovoltaic
RHI	Renewable Heat Incentive
SAP	Standard Assessment Procedure
SBEM	Simplified Building Energy Model
SEM	Scanning electron microscopy
TER	Target Emission Rate
TIM	Translucent insulation material
TSB	Technology Strategy Board
TST	Total solar transmission
VIP	Vacuum insulation panel
WER	Window Energy Rating
XPS	Expanded polystyrene

Executive summary

Background

The thermal performance of our existing building stock must improve significantly for the UK to meet its target of an 80 % reduction in CO_2 emissions by 2050, against the 1990 baseline. According to recent forecasts, the nation's 26 million dwellings account for 27 % of all UK CO_2 emissions and more than 80 % of the houses we will be living in by 2050 have already been built. Similarly, the non domestic building stock is accountable for a further 20 % of all UK CO_2 emissions.

Heat loss through the fabric of existing buildings is responsible for a large portion of these emissions. Across England, approximately 8.4 million homes still contain single glazed windows and up to 12 million homes contain first generation double glazing installed over 20 years ago. Many of these units do not meet modern standards and are not cost effective to improve through conventional double glazing. By comparison, 6.6 million homes contain 'hard-to-treat' solid brick walls, which are expensive and disruptive to insulate, often limited by available space and planning restrictions. Up to half of these properties might never be upgraded without stronger incentive schemes, active promotion and technological innovation.

There is an opportunity to design better retrofit solutions using translucent insulation materials, the most promising of which is 'silica aerogel'. This unique, nano-porous material has the best insulation properties of any solid, retaining up to four times as much heat as conventional insulation, whilst being highly translucent to light and solar radiation. Solid monolithic tiles of transparent silica aerogel, produced in laboratories, have been cited as the 'holy grail' of future glazing technology due to their unrivalled low thermal conductance and high solar and light transmission. Alternatively, low cost translucent aerogel granules, produced commercially, achieve similar properties and can be encapsulated and retrofitted to buildings in a variety of applications.

This research project focuses on designing, building and testing concepts for novel retrofit products incorporating granular aerogel that have potential to reduce energy consumption in existing buildings. Working in collaboration with Brunel University, the project is sponsored by Buro Happold, an international engineering consultancy. The research was conducted within the Sustainability and Building Physics team in the London branch of Buro Happold.

Research aims & objective

At the outset of this project, the brief set by the sponsor company was to design a new 'green' building fabric technology to reduce demand for heating and/or artificial lighting in existing buildings. To justify the project as 'Environmental Technology', the solution(s) would need to demonstrate a measurable benefit across the life cycle, i.e. the energy and CO_2 saved in use must not be outweighed by the respective energy and CO_2 used during manufacture. The core objectives were to:

(i) Conduct a literature review of the UK retrofit market identifying a suitable technology to develop and the research gaps to address

(ii) Build a basic prototype and verify its technical performance through in-situ testing, steady state thermal modelling and payback calculations

(iii) Undertake a streamlined life cycle assessment (LCA) to estimate the energy and CO_2 used to manufacture the technology, which can be compared to the estimated energy and CO_2 saved by the basic prototype

(iv) Design and install a fully functional prototype and validate its performance through in-situ testing, steady state thermal modelling, payback calculations and a streamlined life cycle assessment

Methodology

The diagram overleaf illustrates the overarching methodology in this project and where each contribution to knowledge (CTK) arises. The first step was to define the research questions to drive the literature review and technology selection process. These were:

(i) Where is current research into the UK retrofit challenge focused?

(ii) Which technologies have potential to achieve deep reductions in energy consumption in existing buildings from heating and/or artificial lighting?

(iii) Which technology is the most promising to research further? How has this technology been applied in building research and what is its environmental performance? Where are the research gaps?

Addressing the first research question highlighted the low level of thermal insulation in millions of existing buildings as well as the barriers to retrofitting, particularly due to

the long payback periods associated with measures such as solid wall insulation and new double glazing. This then led to a review of emerging technologies suitable for retrofitting to the walls and windows of existing buildings. In a review of translucent insulation, silica aerogel was identified as a promising technology to research further due to its notable thermal and optical properties, low weight and recent emergence in the construction sector. There is scope to develop a host of novel retrofit technologies with this unique material, and also scope to verify its environmental impact.

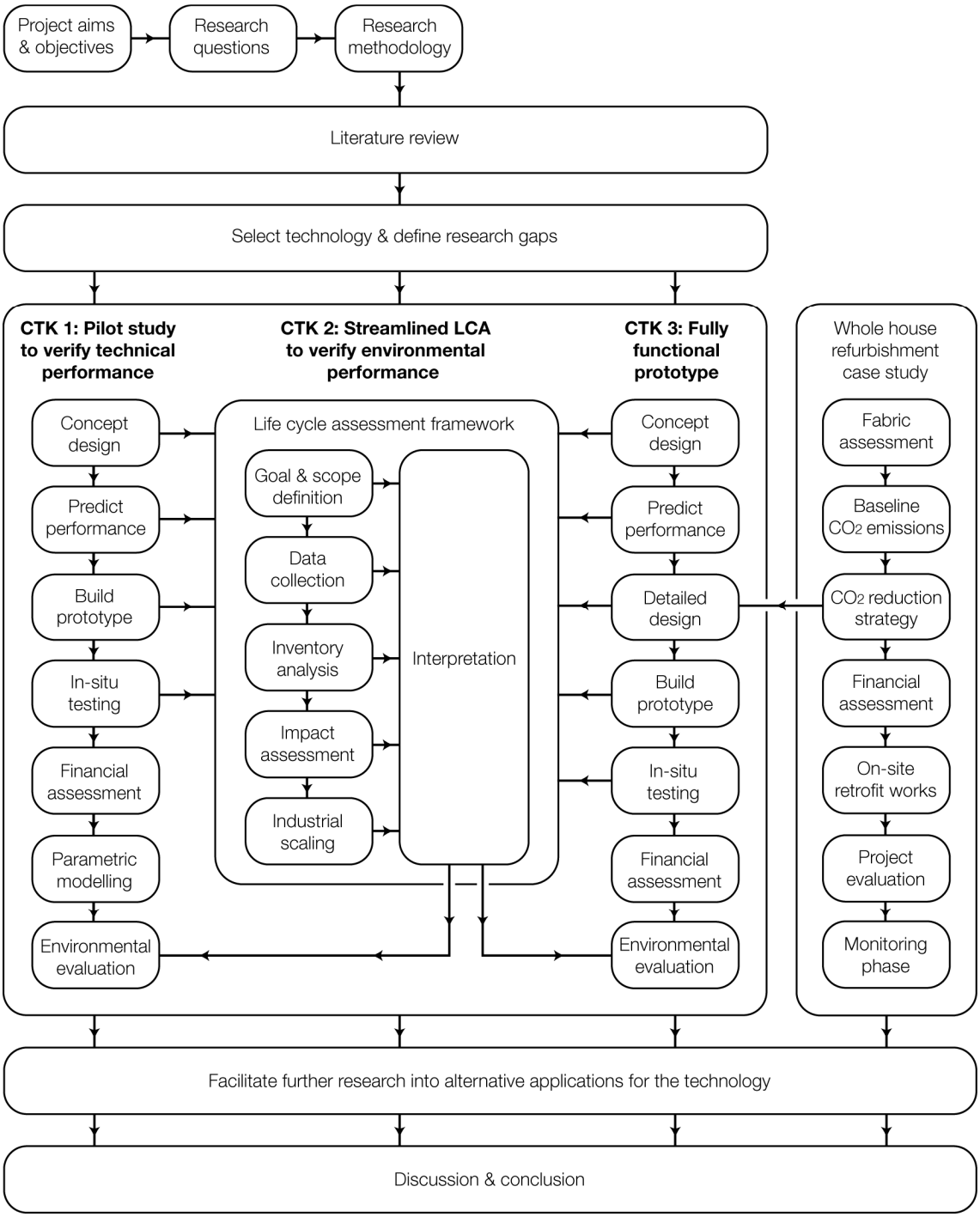

Figure i *Overarching methodology of this thesis.*

Three research gaps associated with the use and environmental impact of silica aerogel were identified during the literature review. These are:

(i) There is a lack of studies assessing the predicted and in-situ performance or payback period of a translucent retrofit solution, incorporating granular aerogel to improve the thermal performance of existing single glazed windows without blocking out all of the useful natural light.

(ii) There is a lack of publically available life cycle assessments of the silica aerogel following the ISO 14000 standards, despite many solvents being used in its production, often accompanied by intensive drying processes, which may consume large amounts of energy and CO_2.

(iii) There is a lack of studies assessing the predicted and in-situ performance or payback period of an active solar air collector incorporating translucent granular aerogel into the cover, retrofitted to the external south facing wall of a domestic property to provide insulation and solar heated warm air.

The three contributions to knowledge are achieved in this thesis by addressing each of these research gaps individually. The first gap was addressed via a pilot study to verify the technical performance of aerogel granules in a window renovation application. A basic prototype was designed, its performance was predicted and a prototype was built to verify the in-situ performance. The second research gap was then addressed through a streamlined life cycle assessment (LCA) to verify environmental performance of silica aerogel. An LCA compliant with the ISO 14000 standards was sought, meaning the study needed to have a defined goal, scope and functional unit, followed by an open data collection and interpretation process, with all results subjected to a third party review (achieved by publishing the study in a peer reviewed journal). The third research gap was addressed through designing a fully functional prototype permanently installed on a 6-bedroom house. Key differences between this study and the first prototype were the added complexity in design and the product's impact on the occupied space. A supporting case study on the whole house refurbishment where this prototype was incorporated is presented as a stand-alone chapter in this thesis. This refurbishment also incorporates two further applications of aerogel: in the floor and an external door. The final study in the thesis is a preliminary modelling investigation of granular aerogel applied in a passive solar 'Trombe' wall application. These additional investigations into aerogel are studies to facilitate further research into alternative applications of the technology. Collectively, all studies feed into the final conclusion.

Summary of studies and results

This thesis contains 8 chapters. Chapter 1 is the introduction. Chapter 2 is the literature review. Chapters 3, 4 and 6 contain the studies forming the three contributions to knowledge. Chapter 5 contains the whole house retrofitting case study supporting the work contained in Chapter 6. Chapter 7 contains a further modelling study. Chapter 8 contains the main conclusions of the thesis, including proposals for further work.

The literature review is split into three sub chapters investigating (i) the UK retrofit challenge, (ii) emerging retrofit technologies and (iii) the thermal and environmental performance of silica aerogel insulation. The reader is taken through the journey that resulted in the selection of silica aerogel as a suitable material for further research and product development. The 'UK retrofit challenge' sub chapter was accepted and published as a stand-alone review article to the *Energy Policy* journal. Content on translucent insulation materials in the second sub chapter and silica aerogel in the final sub chapter was used to provide context for three further journal papers containing the studies forming each of the contributions to knowledge. The literature review conclusion highlights the main research gaps to be addressed.

Chapter 3 contains the pilot study verifying the technical performance of granular aerogel in a glazing retrofit application. Findings were published in the *International Journal of Sustainable Engineering*. The study investigates the thermal performance and light transmission of a single glazed window retrofitted with a translucent polycarbonate panel filled with granular aerogel insulation. Two basic prototype panels (one 6 mm thick, the other 10 mm thick) were built, installed, and then compared against an unmodified single glazed window acting as a control. The core contribution to knowledge arising from this study was demonstrating that a 10 mm thick aerogel panel can reduce the rate of heat loss through a single glazed window by 80 % without detrimental reductions in light transmission. When installed, the measured centre pane U-value for this prototype was 1.17 $W/m^2 K$, meeting the Building Regulations requirements for glazing renovations. Steady state thermal modelling was used to validate figures and conduct payback calculations accounting for inevitable thermal bridging from openable retrofit solutions such as pop-in secondary glazing or aerogel shutters. Payback periods of 3.5-9.5 years were calculated if products are consistently used over the heating season, which is significantly less than new double glazing, which often exceeds its 20 year product lifespan. A further study in this chapter is a parametric assessment of heating, cooling and day lighting in offices with different glazing types. Findings indicate that a translucent aerogel shutter, capable of operating

automatically, retrofitted to single glazed or first generation double glazed office can meet or exceed the performance of new triple glazing across all facade orientations.

Chapter 4 contains the streamlined life cycle assessment of silica aerogel following the ISO 14000 standards to verify the material's environmental performance. Findings were published in the *Applied Energy* Journal. The goal of this study was to identify whether the production impacts of silica aerogel can be recovered by its operational savings within a realistic product lifespan. The study is streamlined since the scope is a 'cradle-to-factory gate' assessment focused only on the material's energy and CO_2 burden. Primary data, such as the mass of raw materials and electricity usage was collected for two of the three known methods of silica aerogel production, providing a unique comparison between these techniques. The functional unit was the energy use (kWh) and CO_2 burden ($kgCO_2$), required to produce 1 m^3 of aerogel. Findings were compared against the predicted annual savings arising from retrofitting a translucent aerogel panel to single glazing. Results are treated as a conservative estimate as the aerogel was produced in a laboratory which had not been developed for mass manufacture or refined to reduce its environmental impact. Furthermore, the samples are small and assumptions to upscale the manufacturing volume occur without major changes to production steps or equipment used. Despite these factors, the core contribution to knowledge was demonstrating that parity between the CO_2 burden and CO_2 savings is achieved in less than 2 years, indicating that silica aerogel can provide a measurable environmental benefit. Additional scaling to represent economies of scale in mass production demonstrates that these figures can be reduced even further.

Chapter 5 contains a case study of a whole house refurbishment which took place over the duration of this EngD. This work was included in this thesis, since it deals with a number of issues related to the core themes of this research, such as upgrading hard-to-treat homes, and the challenges associated with meeting stringent standards for insulation and air tightness. It is also the location of the solar air collector prototype described in Chapter 6. The project was initiated by successfully acquiring funding through "Retrofit for the Future", a competition launched by the Technology Strategy Board, challenging teams to develop innovative refurbishment strategies with potential to reduce 80 % of CO_2 emissions in low rise social housing. In total, 86 teams across the country were successfully awarded funding to implement their proposals. Buro Happold, led internally by the research engineer, were involved in one project aiming to upgrade a 1960s pre-cast concrete end terrace house in the Thamesmead estate, South-East London, working with Gallions Housing Association, Fraser Brown MacKenna architects, Martin-Arnold Associates surveyors and Axis Europe contractors. Through

retrofit works the property has been transformed from a four bedroom hard-to-treat property into a six bedroom super insulated home. Aerogel was applied to an area of the ground floor and in an external plant room door. It was also applied in an innovative solar air collector integrated into the external insulation on the south façade, preheating air in a newly installed mechanical ventilation system. The design team aspired to obtain the German "Passivhaus standard", but this was not achieved due to difficulties achieving the required air tightness targets on-site. Nonetheless, the air tightness is 3 times better than UK new build standard and a number of valuable experiential lessons were learnt. Ongoing research (after this EngD) will include a two year whole house energy monitoring programme with residents in-situ.

Chapter 6 contains a detailed study investigating the predicted and in-situ performance of the 'Aerogel Solar Collector', preheating the air in a mechanical ventilation system with heat recovery (MVHR) installed at the retrofit property. Findings were published in the *Energy and Buildings* Journal. This prototype was sized to provide supply air temperatures of 30 °C during cold sunny days, whilst achieving a U-value below the Passivhaus target for glazed openings of 0.8 W/m² K. The collector area is 6 meters wide by 0.9 meters high and it incorporates a 40 mm thick translucent polycarbonate cover filled with granular aerogel insulation. Efficiency calculations for a range of cover thicknesses were carried out, with results compared to single and double glazed covers, as well as a monolithic silica aerogel cover. The core contribution to knowledge is the technical verification of the installed prototype through in-situ testing which took place during cool sunny conditions in October 2011, validated by steady state thermal modelling. During the 7-day test, peak outlet temperatures up to 45 °C were observed and validated to within 5 % of predictions, preheating the dwelling's fresh air supply up to 30 °C, facilitating internal temperatures of 21-22 °C without auxiliary heating. Peak efficiencies of 22-36 % were calculated based on the proposed design across a range of cover types. Estimated energy outputs ranged from 118-166 kWh/m²/year for collectors with different thickness granular aerogel covers, compared to 110 kWh/m²/year for a single glazed collector, 140 kWh/m²/year for a double glazed collector and 202 kWh/m²/year for a collector incorporating high performance monolithic aerogel. Financial payback periods of 9-16 years and CO_2 payback periods of 0-1 years were calculated across all cover types. An efficiency of up to 60 % and a financial payback period as low as 4.5 years was predicted for an optimised collector incorporating a 10 mm thick granular aerogel cover. Preliminary findings from long term monitoring as part of Retrofit for the Future funding from November 2011 to August 2012 can be found in the Appendices.

Chapter 7 contains two thermal modelling studies to facilitate future research into 'Trombe' walls incorporating granular aerogel. Trombe walls are passive solar heated collector storage walls that do not rely on mechanical ventilation, thus may be more widely applicable to retrofit to existing housing, compared to active solar-air collectors. The concept of a granular 'Aerogel Trombe wall' has been proposed in the literature and there are built examples. However, there is a lack of publically available information on their predicted or in-situ performance, limiting their widespread implementation. In 2010, Buro Happold provided design guidance for new detached pilot house being built in the Whitehill Bordon Eco-town, East Hampshire. It was proposed that an 8 m^2 Trombe wall incorporating a 10 mm thick cover be built. With permission from the client, the predicted performance of this system, compared to a conventional single glazed Trombe wall has been modelled for this EngD. Results demonstrate that the 'Aerogel Trombe wall' is capable of reducing the building's annual heat load by 26 % with a minimum payback period of 7.5 years, compared to an energy saving of 18 % and a 9 year payback for the single glazed system. Applying the methodology to a further modelling study, a parametric assessment of different Aerogel Trombe wall areas retrofitted to different house types and construction standards was conducted. Calculated energy savings ranged from 183 kWh/m^2/year for an 8 m^2 Trombe wall retrofitted to a solid walled detached house, to 62 kWh/m^2/year for a 32 m^2 Trombe wall retrofitted to a super insulated flat. A series of look-up tables for preliminary design guidance were created based on these results. Future research should validate these figures through dynamic thermal modelling and experimentation.

Conclusions

The main aim of this thesis was to design, build and test novel environmentally responsible retrofit technologies with potential to reduce demand for heating and/or artificial lighting in existing buildings. This has been achieved through the development of two prototypes incorporating translucent granular aerogel insulation in novel applications and a streamlined life cycle assessment verifying the material's production impact. Each study addresses an important research gap associated with the use and environmental assessment of silica aerogel. Three contributions to knowledge in the resulting studies are achieved, all of which have been published in peer reviewed scientific journal papers.

The proof-of-principle prototype built to improve the thermal performance of existing glazing without blocking out all of the useful natural light demonstrates that it is possible to meet Building Regulations requirements for glazing renovation U-values in

a cost effective manner, without replacement windows. This is important as a large portion of the existing UK building stock has single glazed or first generation double glazed windows, where improvements are limited by the long payback periods of new glazing, low incentives for private landlords or planning restrictions in listed buildings and conservation areas. There is scope to develop the prototype further into a range of translucent products, such as pop-in secondary glazing, sliding shutters or roller blinds capable of fitting to a wide range of window types and sizes. If operated effectively by users or automated controls, these products could achieve significant reductions in energy consumption for heating and cooling, without detrimental impact on the artificial lighting loads.

Applied to external south facing walls, granular aerogel can be used to insulate and harness free solar energy for heating, making better use of the nation's stock of un-insulated solid walled properties. These products can be applied as stand-alone systems retrofitted directly to the walls (or roofs) of existing properties, or as integrated systems combined with external insulation and mechanical ventilation systems to enhance their performance. The prototype built for this research demonstrates that a small area of an integrated solar collector can provide a significant source of free warm air heating, enabling the property to retain comfortable living conditions without the need for auxiliary heating throughout most of the year. Despite not achieving Passivhaus certification in the whole house retrofit, the Aerogel Solar Collector was capable of achieving a Passivhaus U-value whilst also boosting the performance of the heat recovery system. As such, this system may be well suited as a Passivhaus component, most applicable for properties aiming to achieve deep reductions in CO_2 emissions beyond the limits of conventional measures.

Streamlined life cycle assessment has proved to be an invaluable tool to verify the environmental performance of the prototypes following a systematic approach, which considers both operational savings and embodied impacts; a critical balance that is typically ignored. Findings have demonstrated that the energy use and CO_2 burden in aerogel manufacture can be quickly recovered by the operational savings obtained from both retrofit technologies, despite conservative scaling to represent mass production. Studies like this will become increasingly important as Building Regulations become more stringent, resulting in lower operational energy use, increasing the significance of embodied energy and CO_2 over the life cycle of buildings. Silica aerogel is a unique material, with potential for many applications in new insulation products. Innovative materials such as this should not be overlooked in the effort to reduce the life cycle CO_2 emissions across our existing building stock.

Chapter 1

INTRODUCTION

This Engineering Doctorate (EngD) was undertaken from September 2008-2012 with Brunel University. The research was sponsored by Buro Happold Ltd and funded by the Engineering and Physical Sciences Research Council (EPSRC). At the outset of this project, the preliminary working title was “Product design for lower energy buildings". The brief set by the sponsor company was to design a new green building fabric technology to reduce demand for heating and/or artificial lighting in existing buildings.

Throughout the four year process, the title of this thesis has been refined to: “Novel retrofit technologies incorporating silica aerogel for lower energy buildings”. The literature review takes readers through the journey that resulted in the selection of silica aerogel insulation as a suitable area for further research and product development. Three research gaps associated with the use and environmental assessment of silica aerogel are identified. In the resulting studies, two prototypes incorporating granular silica aerogel have been built and tested on real buildings to verify their performance in a working environment. Using streamlined life cycle assessment, their predicted energy and CO_2 savings have been verified against the energy and CO_2 burden associated with their production.

1.1 Contributions to knowledge

Addressing each research gap individually forms the three contributions to knowledge in this thesis. These studies can be found in Chapters 3, 4 and 6 respectively. Edited versions of these studies have also been published in separate peer reviewed scientific journals. Each contribution to knowledge falls under the category of “*empirical work which has not been done before covering scientific measurement and/or engineering development”* (Francis, 1976; Phillips and Pugh, 1992). These contributions are:

(i) **Study investigating the steady state & in-situ performance of translucent granular aerogel retrofitted to an existing single glazed window.** During in-situ testing a 10 mm thick prototype reduced the rate of heat loss through single glazing by 80 % without detrimental reductions in light transmission. Payback periods of 3.5-9.5 years are predicted depending on use.

(ii) **Streamlined life cycle assessment (LCA) of transparent silica aerogel made by supercritical drying following the ISO 14000 standards.** Silica aerogel was made using two of the three known aerogel production methods in a laboratory which had not been refined for mass manufacture. Despite this, the production energy and CO_2 burden from silica aerogel manufacture can be recovered within 0-2 years when retrofitted to buildings in a glazing application.

(i) **Study investigating the steady state & in-situ performance of a solar air collector incorporating granular aerogel in the cover, preheating air in a mechanical ventilation system with heat recovery in a domestic property.** During in-situ testing, peak outlet temperatures up to 45 °C were observed and validated to within 5 % of predictions, preheating the dwelling's fresh air supply up to 30 °C, facilitating internal temperatures of 21-22 °C without auxiliary heating. The predicted financial and CO_2 payback for a range of cover thicknesses is 7-13 years and 0-1 years, respectively. An efficiency up to 60 % and a financial payback of 4.5 years is predicted with an optimised design incorporating a 10 mm thick granular aerogel cover.

1.2 Supporting studies

Whilst undertaking this EngD, the research engineer was also involved in a whole house refurbishment project working with the sponsor company. Chapter 5 contains a full case study of this whole house retrofit from conceptualisation to handover. The scheme aimed to achieve deep reductions in operational CO_2 emissions through a combination of innovative materials, products and Passivhaus design. It was this property, where the innovative solar air heater incorporating aerogel was incorporated. Two further applications of aerogel were also implemented in a hard-to-treat area of the ground floor and in an external plant room door.

Chapter 7 investigates the potential for aerogel to be applied in a passive solar Trombe wall application, not reliant on mechanical ventilation. Two preliminary thermal modelling studies have been conducted to facilitate further research in this area. The first thermal modelling study predicts the theoretical performance of Trombe wall incorporating granular aerogel built on a new house, comparing its performance to a conventional single glazed Trombe wall. The second is a parametric modelling study investigating the performance of Aerogel Trombe walls applied to different house types and construction standards across the existing UK building stock.

1.3 Statement of thesis

The following statement summarises the key argument in this thesis, based on the evidence in the three contributions to knowledge and two supporting studies.

> *When applied appropriately in translucent insulation applications, granular aerogel can be a cost effective and environmentally sustainable material suitable for retrofitting into existing buildings to achieve deep reductions in energy consumption for heating, without detrimental impact in natural lighting or solar transmission.*

1.4 Motivation

The thermal performance of our existing building stock must improve significantly for the UK to meet its target to reduce CO_2 emissions by 80 % by 2050, against the 1990 baseline (Climate Change Act, 2008). This is a major issue, since millions of these properties contain poorly performing elements such as solid walls, single glazing and un-insulated roofs/floors responsible for a significant amount of wasted heat. Technological innovation and life-cycle thinking focused on the development of new retrofit products is one of many areas of research capable of alleviating this burden.

1.5 Journal publications

Three original research studies and one review article have been published in peer reviewed journals. These papers are in the Appendices. Details are as follows:

(i) **Domestic UK Retrofit Challenge: Drivers, Barriers and Incentives leading into the Green Deal**, *Energy Policy, 2012, Volume 50, pp 294-305.*

(ii) **Improving the thermal performance of single-glazed windows using translucent granular aerogel**, *International Journal of Sustainable Engineering, 2011, Volume 4 (3), pp 266-280.*

(iii) **Streamlined life cycle assessment of transparent silica aerogel made by supercritical drying**, *Applied Energy, 2011, Volume 97, pp 396-404.*

(iv) **Predicted and in-situ performance of a solar air collector incorporating a translucent granular aerogel cover**, *Energy and Buildings, 2012, Volume 49, pp 173-187.*

1.6 Industrial publications

Three articles have been published in trade magazines. Most notably, a feature article, found in the Appendices, was written in the CIBSE journal. Details are given below:

(i) **Box of tricks:** CIBSE Journal, Chartered Institute of Building Services Engineers, Feature article on Retrofit for the Future, June issue, 2012.

(ii) **Sustainability needs new thinking as well as technology:** Patterns Magazine, Buro Happold in association with Architects Journal, Feature article on novel aerogel applications, Issue 16, 2012, p30-31.

(iii) **Retrofit does not mean retro**, ABC+D magazine, Fraser Brown MacKenna Architects in collaboration with Buro Happold, March 2011, p71.

1.7 Research conferences

Seven conference presentations have been given including the International Conference on Applied Energy, Greenbuild Expo and the CIBSE Building Simulation Conference:

(i) **Innovative use of aerogel in passive and active solar storage walls**: Energy Storage in Buildings: Simulation and modelling, CIBSE building simulation group, University College London, UK, June 2nd 2011.

(ii) **Innovative use of PCM and aerogel in low energy buildings:** Greenbuild International Conference & Expo, San Francisco, November 14th-16th 2012.

(iii) **Streamlined life cycle assessment of transparent silica aerogel made by supercritical drying:** Third International Conference on Applied Energy (ICAE 2011), Perugia, Italy, May 16th-18th, 2011.

(iv) **The Aerogel Solar Collector: background and preliminary modelling:** Full length paper produced for the Annual EngD conference, Surrey University, 20-21st June 2011.

(v-vii) **Product design and life cycle assessment of novel retrofit technologies incorporating silica aerogel:** AMEE / Design research seminar, Brunel University, 3rd June 2009. Annual EngD conference, Brunel University, 7th January 2010. ResCon conference, Brunel University, 18st-20nd June 2012.

Chapter 2

LITERATURE REVIEW

Abstract

This chapter reviews (i) the UK retrofit challenge, (ii) emerging retrofit technologies, and (iii) the thermal and environmental performance of silica aerogel insulation. The UK faces a major challenge to improve the thermal performance of its existing building stock. Millions of buildings possess hard-to-treat walls and have single glazed windows which are difficult to improve cost effectively. A number of conventional retrofit solutions are available to improve these buildings. However, there are limits to the actual energy savings that can be achieved and several barriers to their successful implementation. There is scope to improve existing buildings using translucent insulation materials. These materials can reduce energy use arising from heating and artificial lighting, since they can retain heat effectively, whilst diffusing natural light and transmitting useful solar energy. Cutting edge research focuses on utilising *silica aerogel,* a unique nano-porous translucent insulation material with the lowest thermal conductivity of any solid. Solid monolithic tiles of transparent silica aerogel have been cited as the 'holy grail' of future glazing technology due to their unrivalled low thermal conductance and high solar and light transmission. However they are fragile and expensive to produce on a commercial scale. By comparison there is an opportunity to apply lower cost, commercially available translucent aerogel granules to the walls and glazing of existing buildings in a variety of novel applications. Moreover, there is an opportunity verify the environmental performance of aerogel through a streamlined life cycle assessment verifying that the energy and CO_2 burden in manufacture does not outweigh the respective savings in use.

2.1 UK Retrofit Challenge

2.1.1 Introduction

The thermal performance of our existing building stock must improve significantly for the UK to meet its target to reduce CO_2 emissions by 80 % by 2050, against the 1990 baseline (Climate Change Act, 2008). In 2008, the country's 26 million dwellings were estimated to be responsible for 27 % of all UK CO_2 emissions (Utley and Shorrock, 2008). Non domestic buildings were accountable for a further 20 % (RCEP, 2007). According to recent forecasts, 75 – 85 % of the current UK building stock will still be in use by 2050 (Ravetz, 2008; Power, 2008). This is a major issue, since millions of these properties contain poorly performing elements such as solid walls, single glazing and un-insulated roofs/floors responsible for a significant amount of wasted heat. These features can be expensive and disruptive to improve and associated improvements can be limited by available space and planning restrictions (Beaumont, 2007; EEPH, 2008). There is scope to retrofit these buildings to make deep cuts in CO_2 emissions, but effective implementation is no trivial task. Solutions must account for variety in age, size, quality, composition, function and social value of existing building stock, as well as the different needs, expectations and budgets of homes owners and occupiers.

2.1.2 Survey of English housing stock

The English Housing Survey is a national survey commissioned by the Department for Communities and Local Government (CLG) to monitor the age, type, tenure and condition of the English housing stock. Approximately 6,200 houses undergo physical inspections annually by qualified surveyors, with findings extrapolated to represent the 20.4 million dwellings in the English housing stock (CLG, 2004a). Figure 2.1 shows a profile based on the available data segmenting the housing stock by age and type, across each major construction period (CLG, 2001).

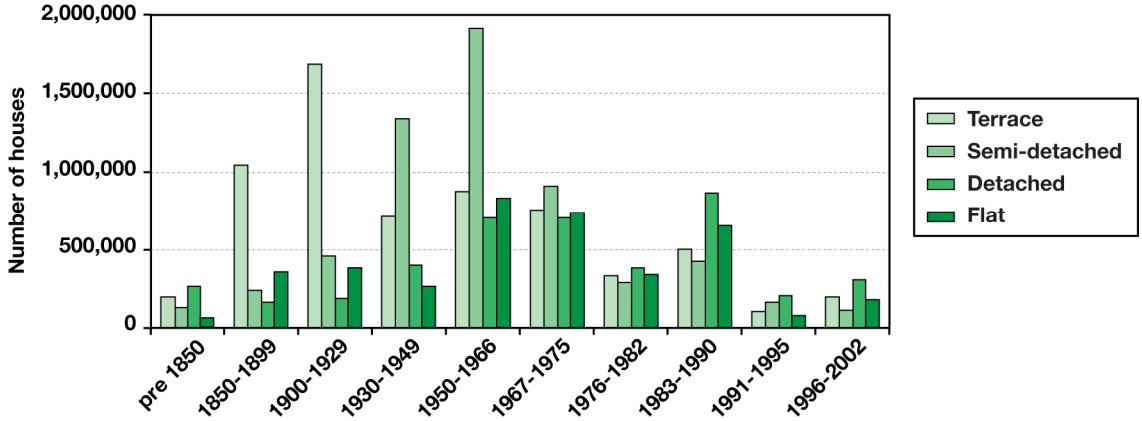

Figure 2.1 *English housing stock by age and type (Generated using data from CLG 2001).*

As shown, England contains millions of Victorian and Edwardian terraced houses, post-war semi-detached houses and flats built during the 1960s. Building Regulations setting minimum standards for insulation were only enforced after 1976. As a result solid walls, un-filled cavity walls, single glazing, un-insulated roofs and un-insulated floors were common construction features before this time.

Increasing housing demand, as well as the availability of construction materials and machinery over the past century, has led to distinctive types of dwellings across the English housing stock (Beaumont, 2007). Figure 2.2 displays a stock profile segmented by type and region (CLG, 2003). As shown, London has a particularly high proportion of flats and terraced houses, whereas Northern regions tend to have higher concentrations of terraced houses and semi-detached houses.

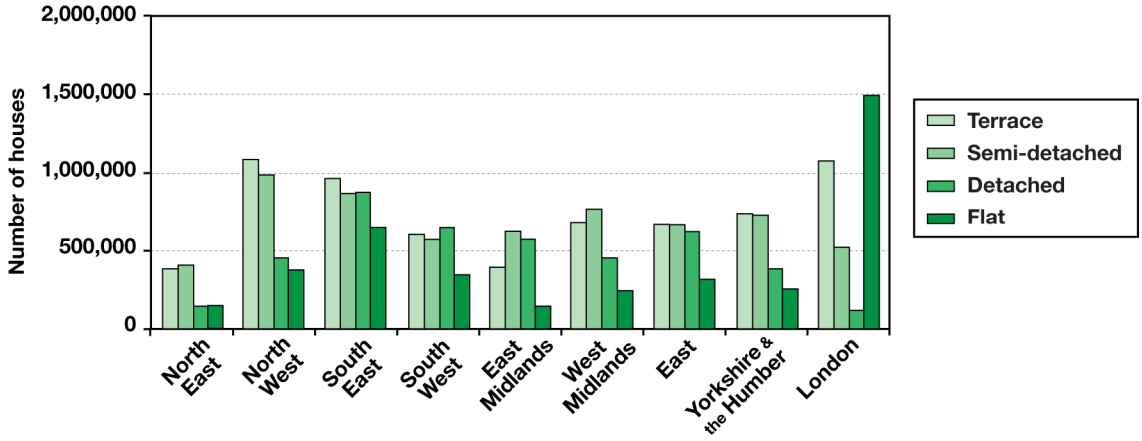

Figure 2.2 *English housing stock by region (Generated using data from CLG 2003).*

During the Industrial Revolution the mass migration of workers into towns and cities lead to millions of terrace houses being built in the late 18th and early 19th centuries. Typically these homes were single glazed and were of brick or stone solid wall construction (Muthesius, 1984). By the 1930s, a rise in the number of building developers combined with a decline in material, labour and land costs resulted in a boom of owner occupied semi-detached houses across suburban England. These homes tended to contain un-filled cavity walls, consisting of two separate skins of brick as a method to prevent damp penetration (Roberts, 2008a). Following the Second World War, housing shortages lead to a resurgence of terrace and semi-detached houses across the country, constructed with un-filled cavity walls containing a brick or concrete inner leaf. By the 1950s, demand for social housing in dense urban areas lead to the growth of high-rise flats up to 10 storeys high, constructed using load bearing masonry walls and concrete floors. Throughout the 1960s and early 1970s, flats up to 30 storeys high were constructed mainly using pre-fabricated steel reinforced concrete

panels built in factories then erected on-site to overcome the skills and labour shortages. Originally intended to be temporary constructions, millions of these flats are still in use today, with many suffering from poor thermal insulation and structural problems due the corrosion of the steel reinforcements in the concrete panels (Beaumont, 2007).

2.1.3 History of Building Regulations in the UK

The thermal efficiency of the UK building stock is governed through the Building Regulations. The UK's first mandatory Building Regulations were enforced in Scotland in 1964. England and Wales soon followed with separate regulations in 1966, as did Northern Ireland in 1967 (Killip, 2005). Each set of regulations was produced largely in response to public health issues rather than a need to improve the energy efficiency of dwellings. The standards were revised in 1976 to provide maximum U-value standards to limit the heat losses through the walls, roof and floors in new dwellings, following the 1973 energy crisis (Killip, 2005). Table 2.1 tabulates the historic maximum U-values for compliance with Building Regulations for England and Wales from 1976-2006. As shown, continual revisions to Building Regulations have caused U-value targets for all new buildings to become increasingly stringent. It should be noted that U-value requirements for exposed walls only imply the presence of full cavity wall insulation in new buildings registered after 1995. Furthermore, maximum U-values for windows were only raised beyond single glazing standards by 1990. Additional measures such as eliminating continuous thermal bridges and limiting air permeability to reduce heat losses by infiltration occurred as part of the 1990 Building Regulations.

Table 2.1 *Historic U-values and air permeability targets in the England and Wales Building Regulations (Generated using data from Killip 2005).*

Building Regulations	Exposed walls (W/m^2K)	Roof (W/m^2K)	Floor (W/m^2K)	Windows (W/m^2K)	Air permeability ($m^3/m^2\,h$ @50Pa)
1976	1.0	0.6	Not specified	Not specified	Not specified
1982	0.6	0.35	Not specified	Not specified	Not specified
1990	0.45	0.25	0.45	3.3	10
1995	0.45	0.25	0.35	3.3	10
2000	0.35	0.25	0.25	2.2	10
2006	0.35	0.16-0.25	0.25	2.0-2.2	10

From 2006, Part L1A of the Building Regulations for England and Wales required all new dwellings to demonstrate design compliance using the Standard Assessment Procedure (SAP). SAP is a government approved calculation methodology, which estimates a dwelling's CO_2 emissions, in $kgCO_2/m^2/year$, based upon the design U-values, air tightness level, efficiency of space heating, lighting and hot water systems, as

well as pumps/fans and any savings from renewable technologies. For Part L1A compliance, the calculated Dwellings Emissions Rate (DER) must demonstrate a 25 % improvement over a Target Emission Rate (TER) calculated from a notional building constructed to 2002 standards. In 2010, compliance levels were raised to a 25 % reduction over a notional building constructed to 2006 standards. In 2013, the Building Regulations (still under consultation) are expected to raise compliance levels further to a 44 % reduction over 2006 standards. Future revisions of the Building Regulations, are anticipated to set 'zero carbon' then 'net carbon' targets for all developers, resulting in an increasing need for well insulated building fabrics and efficient systems, with reliance on renewable technologies. Currently, Building Regulations only deal with 'regulated' loads, excluding energy use and CO_2 emissions associated with small power plug loads. Moreover SAP currently does not allow variations in factors such as household size, heating patterns or geographic location.

2.1.4 Thermal efficiency of English housing stock

The SAP methodology results in a 'SAP rating' from 1-100, which provides an indication of the overall efficiency of a dwelling. Higher scores represent higher efficiencies and lower running costs. For existing buildings, the SAP rating can be calculated from a reduced SAP method (RdSAP) based upon an on-site survey, which considers the dwelling's size, construction characteristics, thermal insulation levels, annual running costs as well as the installed heating and hot water systems and lighting types (DECC, 2010a). Figure 2.3 displays SAP ratings across the existing housing stock, based upon data from the English Housing Survey. Each bar represents an age band of dwellings and each colour shows how the SAP ratings are divided between the stocks.

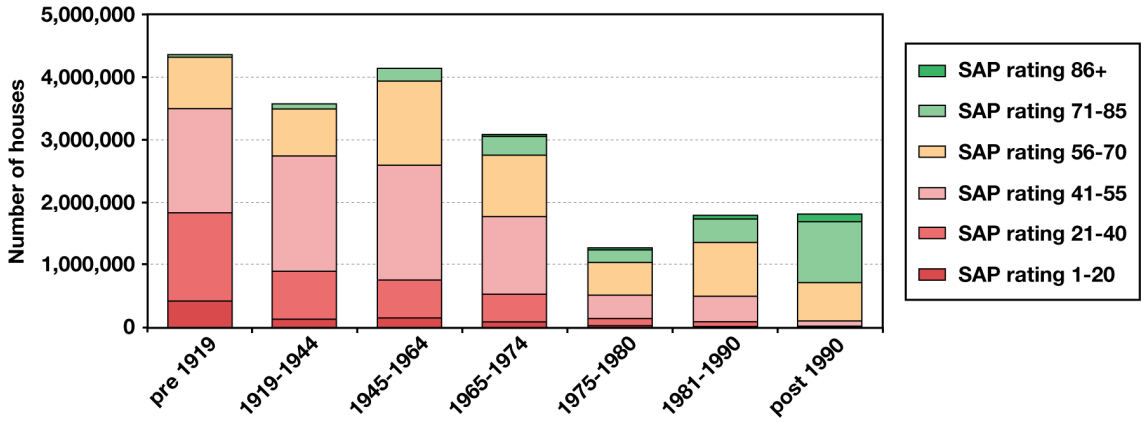

Figure 2.3 *SAP ratings of the English housing stock (Generated using data from CLG 2006).*

As seen, many of the highest SAP ratings can be found in the post 1990 stock due to the enforcement of the Building Regulations. Approximately 60 % of buildings constructed

after 1990 have SAP ratings over 70. In contrast, the highest concentrations of the lowest SAP ratings can be found in the older pre-1919 stock, demonstrating a large correlation between age and energy performance. Around 40 % of pre-1919 homes have SAP ratings from 1-40 (Roberts, 2008a).

A proposed target for 2050 is to raise the average SAP rating of the UK building stock to 80, in line with today's modern building standards (Roberts, 2008a). Comparatively, the national average SAP rating is much lower, being 52.1 in 2006 (BERR, 2008). There is also a variation in energy performance with tenure. The average SAP rating across social housing is 57, whereas the average across the private sector is 47 (Ravetz, 2008). This can be attributed to higher rates of loft and cavity wall insulation in the social sector due to government interventions such as 'Warm Front' and 'Decent Homes', aiming to lower fuel bills and improve the internal condition of homes. By comparison, private sector landlords have little incentive to invest in the energy efficiency of their properties, given that it is the tenants who benefit from lower fuel bills (CLG, 2006; UKGBC, 2008). The introduction of Energy Performance Certificates (EPCs) in 2007 may serve to help this challenge by providing information on the current energy rating of a dwelling to potential buyers or tenants (EEPH, 2010). Nonetheless, this issue remains a major barrier since many properties in the private sector are amongst the lowest in terms of thermal efficiency (CLG, 2006).

2.1.5 Hard-to-treat homes

Hard-to-treat homes are defined as dwellings which possess solid walls, no loft space to insulate, no connection to the gas network or are high-rise. Consequently, these dwellings cannot be upgraded easily or cost effectively using conventional retrofit measures such as cavity wall insulation, loft insulation and modern gas central heating systems. Approximately 10.3 million homes are classed as hard-to-treat across the UK, equivalent to 40 % of the existing housing stock (BRE, 2008). Up to 9 million of these are in England, 6.5 million of which possess solid walls. 1.5 million have no loft space, 0.4 million are high rise and 2.7 million are off the gas grid. This is shown in Table 2.2.

Table 2.2 *Hard-to-treat homes in the UK (Generated using data from BRE 2008).*

	England	Scotland	Wales	N. Ireland	All UK
Total dwellings	21m	2.3m	1.3m	0.7m	25.3m
Solid wall homes	6.5m	0.7m	0.2m	0.1m	7.5m
Homes with no loft	1.5m	unknown	unknown	unknown	~2m
High rise dwellings	0.4m	0.5m	unknown	unknown	~1.5m
Homes off the gas grid	2.7m	0.3m	0.2m	0.5m	3.7m
Total hard-to-treat	9m	0.7m	0.3m	0.5m	10.3m

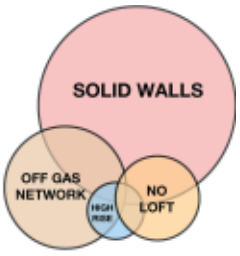

According to Beaumont (2007), more than 66 % of hard-to-treat households are in fuel poverty. A household is said to be in fuel poverty if its occupants need to spend more than 10 % of their income to afford adequate energy services, for heating, lighting, cooking etc in their home (Boardman *et al.* 2005). In addition, dwellings that contain both solid walls and are off the gas grid possess some of the lowest SAP ratings in the UK, with a mean score of 25. Nearly 84 % of these properties are in the private sector. By comparison, Beaumont (2007) states that high rise dwellings which are on the gas network typically perform much better, with SAP ratings averaging at around 60, nearly 10 points above the national average, due to their smaller size and significantly reduced area of exposed walls, resulting in smaller heat losses.

Regarding low-rise properties off the gas network, Beaumont (2007) states that these are particularly common in rural areas, where inaccessibility and a low density housing makes it unattractive for gas companies to build supply networks. Comparatively, safety considerations in high rise flats often means that a piped gas supply is not installed (Beaumont, 2007). Dwellings classed as hard-to-treat for having no space for loft insulation typically refer to those with flat, mansard or chalet roofs built before 1990. High rise flats with over 6 stories are viewed as the most difficult to treat. Developments built from 1950-1970 have some of the largest heating difficulties due to poor physical condition, low maintenance and a lack of gas supply (Beaumont, 2007).

According to Beaumont (2007) it is theoretically possible to internally insulate all solid walled properties in the UK, but there are restrictions on external wall insulation, since it changes the external appearance of a dwelling and planning permission often prohibits its application on listed dwellings or those in conservation areas. According to Boardman *et al.* (2005) and Beaumont (2007), approximately 300,000 dwellings in the UK are listed, and a further 1.2 million are in conservation areas, representing about a quarter of all pre-1919 dwellings. In addition to this, installing external insulation on high rise flats may be problematic if the walls are structurally unsound, or if all owners / leaseholders do not all agree to change the external appearance. By comparison, when internally insulating, individual flats could be improved on a room-per-room basis. There are possible cost reductions through economies of scale, if an entire high-rise block is over clad in a single installation.

2.1.6 Demolition argument

In light of a lack of strategies to improve the state of the UK housing stock, in 2005, Boardman *et al.* (2005) published a report, commissioned by the Environmental Change Institute to provide a strategy for raising the national SAP ratings and meeting

our 60 % carbon reduction target. In addition to refurbishing the existing building stock to high standards with 100 % high performance glazing, 100 % loft insulation, 100 % cavity wall insulation and 15 % solid wall insulation, demolition and rebuilding the worst performing stock also featured on the agenda. It was said that 3.2 million of the most 'leaky' pre-1919 terraced houses would need to be removed to meet our targets by 2050 (Boardman *et al.* 2005).

Ravetz (2008), states that the older, worst performing stock should be seen as a resource rather than a problem, since they have the largest scope for improvements through energy efficient refurbishments. Moreover Power (2008) argues that because demolition can be very time consuming, costly and disruptive to the environment, it is likely to provoke much opposition within local communities, government and industry.

Another argument against the conclusions by Boardman *et al.* (2005) was that 0 % of floors and only 15 % of solid walls were taken in the scenario. Challenging these figures, an analysis by Johnston *et al.* (2005) predicted whether or not the 60 % carbon reduction was possible without demolition. It concluded that through the use of conventional insulation measures alone, a 37-61 % reduction in CO_2 emissions could be achieved, based on 'business as usual' and a stringent demand reduction scenario dependant on higher uptakes of solid wall insulation. Johnston *et al.* (2005) predicted that an 80 % reduction would be possible, but only through reduced demand combined with electrically powered heating systems supported by a decarbonised grid.

Evidently, there may be an opportunity to achieve the 60-80 % carbon reduction without any demolition and rebuild. However, full employment of conventional measures is imperative, alongside improvements to energy generation and supply.

2.1.7 Energy savings from retrofit measures

Shorrock *et al.* (2005) published a comprehensive report for the BRE (Building Research Establishment) analysing the scope for carbon reductions in the UK housing stock. Focusing primarily on individual insulation measures for a typical three bedroom semi-detached house, the study aimed to calculate the energy, carbon and cost savings of conventional retrofit solutions, in addition to forecasting potential further energy savings through an analysis of current uptake trends. Information was calculated based on the BREDEM energy model, which has been continually developed since the 1980s to consider both the physical characteristics of a dwelling and lifestyles of occupants. BREDEM also underpins the SAP calculations in the Building Regulations (BRE, 1997). Figure 2.4 shows the calculated annual energy (kWh/year) and CO_2 savings ($kgCO_2$/year) from conventional retrofit measures (Shorrock *et al.* 2005).

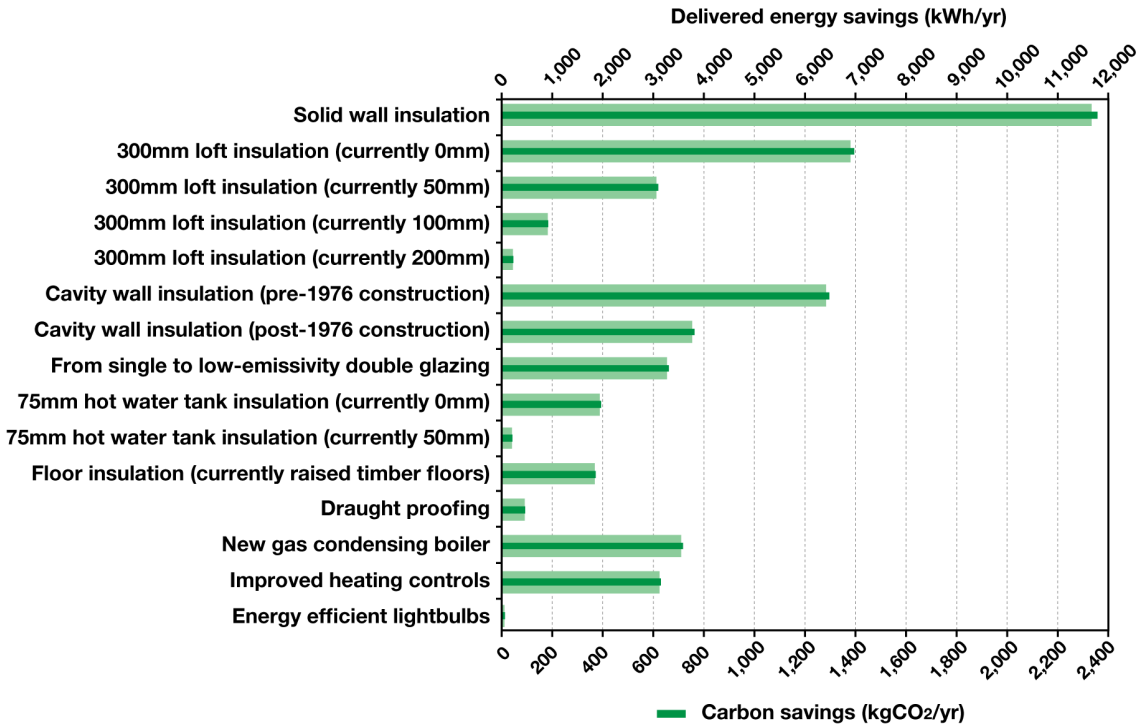

Figure 2.4 *Predicted energy and CO_2 savings from conventional retrofit measures applied to a typical semi-detached house (Generated using data from Shorrock et al. 2005).*

As expected, some measures provide significantly more benefit than others. A much larger saving can be experienced when insulating a solid wall in comparison to a cavity wall, since the baseline U-value is generally lower, and the level of insulation installed is not restricted to the cavity width. The distinction between cavity wall insulation savings in pre and post-1976 construction is due to a change in construction practices from brick-brick cavity wall construction to brick-block cavity walls around this time. Predicted savings from loft insulation and hot water cylinder lagging provide diminishing returns depending on how much insulation is already present. As existing insulation levels approach 300mm and 50mm respectively, the savings become so small that they are not worthwhile. Roberts (2008a), states that cavity wall insulation can reduce heat loss through walls by up to 40 %. Furthermore when insulating the walls and roofs of un-insulated older buildings to post-1990 standards, then a 50-80 % reduction in heat loss through these elements can be achieved (Roberts, 2008a). Determining the actual savings requires knowledge of how much heat was originally being lost through the fabric. This must be assessed on a case-by-case basis.

2.1.8 Cost-effectiveness of retrofit measures

A large social barrier against retrofits is the perception that the capital cost of installation will not be recovered within a reasonable payback period (UKGBC, 2008).

Addressing this issue Shorrock *et al.* (2005) compare the capital costs of each retrofit measure against the estimated energy savings obtained from a reduced heating bill. The data is shown in Table 2.3. The methodology assumes that no grant was made available and 30 % of the energy savings were taken back by the homeowner for increased thermal comfort. Payback calculations assume annual fuel price rises and discount interest rates are at equal percentages, resulting in a simple return on investment calculation.

Table 2.3 *Economic analysis of measures (Generated using data from Shorrock et al. 2005).*

	Capital cost (£)	Annual saving (£/yr)	Measure lifespan (yrs)	Simple ROI (£)	Payback period yrs)
Solid wall insulation	3272	145.85	30	1104	22.4
300mm loft insulation (currently 0mm)	273	86.22	30	2314	3.2
300mm loft insulation (currently 50mm)	254	38.21	30	892	6.6
300mm loft insulation (currently 100mm)	211	11.26	30	127	18.7
300mm loft insulation (currently 200mm)	170	2.70	30	-89	63.0
Cavity wall insulation (pre-1976 construction)	325	80.13	40	2880	4.1
Cavity wall insulation (post-1976 construction)	325	47.10	40	1559	6.9
From single to low-emissivity double glazing	4,000	40.81	20	-3184	98.0
75mm hot water tank insulation (currently 0mm)	20	28.75	15	411	0.7
75mm hot water tank insulation (currently 50mm)	20	2.97	15	25	6.7
Floor insulation (currently raised timber floors)	1,000	32.75	30	-18	30.5
Draught proofing	110	5.67	10	-53	19.4
New gas condensing boiler	300	45.48	12	246	6.6
Improved heating controls	250	57.38	12	439	4.4
Energy efficient lightbulbs	85	21.16	6	42	4.0

Going someway to justify social concerns over refurbishment costs, analysis of the data above suggests that draught proofing, floor insulation, and loft insulation (with over 150 mm of insulation already in place) are marginally uneconomic. Comparatively, the payback for solid wall insulation is over 20 years. Double glazing shows an extremely poor financial return on investment since the energy savings alone do not justify the capital investment. The remainder of conventional retrofitting measures do show positive returns of investment, with the largest benefit occurring from filling cavity walls within pre-1976 stock. Insulating a loft which previously had no insulation appears to provide the shortest payback at just over 3 years, far shorter than double glazing at 98 years.

2.1.9 Energy efficiency uptake trends

Another analysis drawn from Shorrock *et al.* (2005) relates to the current uptake of conventional retrofit products and future forecasts. For double glazing and condensing

boilers these figures are based on "all that is economically and technically possible". Here it can be seen that certain retrofitting measures have more scope for installation than others. Note that projections for solid wall insulation were not available in Shorrock *et al.* (2005). However, a similar forecast from EEPH (2008), based on the industry's current capacity of 15,000-20,000 installations per year has been added. This data is shown below in Figure 2.5.

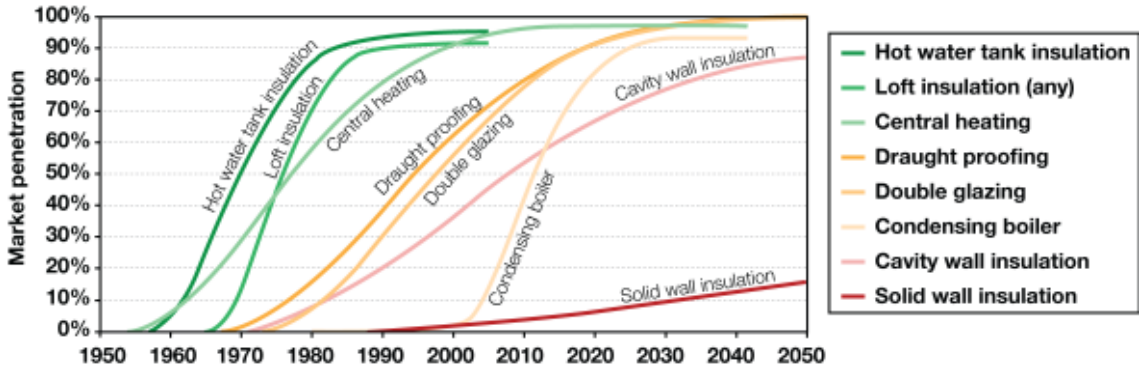

Figure 2.5 *Uptake of measures (Adapted from EEPH 2008 and Shorrock et al. 2005).*

Looking at cavity wall insulation, evidently there is still much potential for walls to be filled in the UK. Likewise, Roberts (2008a), states that 60% of UK domestic houses had unfilled cavity walls in 2004. Regarding double glazing, despite the high capital costs, levels are expected to reach saturation over the coming decades since all new glazing renovations must achieve a minimum centre pane U-value of 1.2 W/m² K or an overall U-value of 1.8 W/m² K, except for in rare specific circumstances such as listed building status. Furthermore, considering uptakes of loft insulation have levelled off, there is considerable scope to ensure that all lofts have above 100mm of insulation.

An additional factor raised by both Ravetz (2008) and Roberts (2008a) is that many homes have first generation retrofits in need of renewal. Ravetz (2008) claims that the deterioration of many post-war retrofits such as double glazing, plumbing and electrics are clearly visible in modern homes, however there are barriers to improvements due to the capital cost of investment and the disruption of refurbishment. Roberts (2008a) believes the main issue regarding first generation double glazing is the high U-values of 3-4 W/m² K, due to poorly insulated frames and narrow air gaps. Subsequently, comparing these heat losses against modern double glazed units with U-values down to 1.2 W/m² K would show considerable differences in thermal performance.

In relation to solid wall insulation, Shorrock *et al.* (2005) states that uptakes seem unlikely to reach saturation over the next few decades due to its current slow uptake and high capital costs, which must be reduced to around £ 2500 (for the whole house)

for the procedure to become marginally cost effective. Roberts (2008a), argues that solid wall insulation should be viewed as an untapped opportunity rather than a barrier since large energy savings can still be made. According to the EEPH (2008), even at the upper limit of the industry's installation capacity, only 15 % of solid walled properties will be insulated by 2050.

Concerning floor insulation, Shorrock *et al.* (2005) argues that uptake will remain slow since the procedure is generally only carried out when a floor needs repair anyway. Similarly, Roberts (2008a) states that floor insulation is disruptive and is only likely to be economically viable during a comprehensive refurbishment of the floor.

Taking an alternate perspective on these issues, Power (2008) argues that there should be more effort from the government to realise the potential for energy savings from the 10 million homes in the UK requiring solid wall insulation. Similarly, Power (2008) believes floor insulation needs to be considered within energy efficiency programmes, since over 10 million homes have un-insulated raised timber floors and the technology is available for improvement.

2.1.10 Government incentive programmes

Government incentive schemes represent a key driver for reducing CO_2 emissions in the housing sector (EEPH, 2010). Several schemes focus on renewable energy installations. These include the Renewable Energy Strategy (RES), Micro-generation Certification Scheme (MCS), Renewable Heat Incentive (RHI) and Feed in Tariffs (FITs). Alternatively, the government's Boiler Scrappage Scheme, launched in 2010, but now closed, funded over 100,000 new boilers across England. Regarding fabric efficiency, there are a number of government incentive schemes in place. Primarily, these focus on installing low cost, non-disruptive measures such as cavity wall insulation and loft insulation, targeting underprivileged households mainly in the social housing sector. However, wider schemes have also been set into motion, encouraging energy suppliers, electricity generators and private investors to provide grants to cover the upfront cost of refurbishments, reaching also into the owner occupied and private sector. A summary of fabric efficiency schemes is given below:

Carbon Emissions Reduction Target (CERT)

During 2008-2011, CERT operated as one of the UK's principal energy efficiency mechanisms. This scheme required all domestic energy suppliers with a customer base exceeding 250,000 to achieve reduction targets for the amount of CO_2 emitted by their customers (equivalent to the total emissions from approximately 700,000 homes each

year). At least two thirds of this target must be achieved through professionally installed insulation measures and 40 % of retrofitting activities should be focused on a priority group of vulnerable households consisting of low income homes, pensioners over the age of 70 and households on disability benefits. In its first 2 years CERT resulted in approximately 1.4 million cavity walls and 1.1 million lofts being insulated. In addition, over 200 million low energy light bulbs have been delivered, 2000 ground source heat pumps installed and 30,000 solid walled properties have been upgraded through either internal or external wall insulation (DECC 2010b).

Community Energy Saving Programme (CESP)

CESP is a retrofitting scheme funded through an obligation on energy suppliers, and for the first time, electricity generators. This scheme provides funding to community partnership groups, housing associations and local authorities to improve energy efficiency in low income and hard-to-treat homes. CESP promotes a 'whole house' approach to refurbishment, aiming to treat as many properties as possible in a house-by-house or street-by-street approach (EEPH, 2008). Between October 2009 and December 2012, CESP funded approximately 100 community schemes, benefitting around 90,000 homes.

In an evaluation of CESP by the DECC (2011), it was claimed that 81 % of scheme submissions included external solid wall insulation and 65 % had boiler replacements with new heating controls. Key challenges during the retrofit process included weather related issues, planning delays for solid wall insulation, cash flow problems due to retrospective payments from energy suppliers, gaining access to eligible households and dealing with resentment from non-eligible householders. In a survey following the retrofitting process, 75 % of occupants agreed that their homes felt warmer and were easier to heat to adequate levels. However just 25 %, said they had seen a decrease in their heating bills and 11 % said their heating bills had increased. According to the DECC (2011), this was largely influenced by rising energy prices.

Decent Homes

In 2000, the government made a commitment to bring all public sector dwellings in England to a basic standard of decency by 2010 through its Decent Homes programme. This placed a responsibility on local authorities, registered social landlords and, to a limited extent, private sector landlords to eliminate the backlog of repairs throughout their stock. In order for a property to meet the Decent Homes standard it must (i) be free of Category 1 Housing Health and Safety Rating Hazards (HHSRH), which covers an assessment of dampness, excessive cold/heat, security, hygiene, sanitation,

structural integrity, accident risk, asbestos etc (ii) be in a reasonable state of repair, (iii) have reasonably modern facilities and services, and (iv) provide a reasonable degree of thermal comfort.

According to the National Audit office (2010), at the start of the programme there were 1.6 million 'non-decent' homes in the social sector, representing 39 % of all social housing. By 2010, over a million houses had been treated, reducing the percentage of non-decent homes in the social sector to 14.5 %, falling short of the original target. Across the entire English stock, it is estimated that 5.9 million dwellings (26 % of homes) failed to meet the Decent Homes standard in 2010, compared to 7.7 million in 2006. The primary reasons for failing were not achieving the HHSRH assessment, followed by not providing adequate levels of thermal comfort (CLG, 2012). In 2010, private rented dwellings had the highest percentage of non-decent homes at 37 %, followed by the owner occupied sector at 25 %.

The average cost to make a home decent is approximately £ 3,600 to £ 10,500 depending on the age and type of property (CLG, 2006). In order to meet the thermal comfort standard a home must have an efficient heating system, cavity wall insulation (where possible) and a minimum of 200 mm loft insulation. Currently several local authorities and housing associations are in the process of adopting a new 'Decent Homes Plus' standard. This typically includes additional measures such as double glazing (except when restricted by planning), full heating controls with an energy efficient boiler, draught proofing, energy efficient doors, and energy efficient lighting in all communal areas, improved sound insulation and a modern kitchen and bathroom.

Warm Front

Warm Front is a government funded scheme providing heating and insulation grants to vulnerable owner occupied and private rented households with SAP ratings of 55 (energy performance certificate band D) or below. Qualifying households must be on income support, income-related employment and support allowance, state pension credit or Job Seekers Allowance. Housing Association or local authority tenants do not qualify. Grants up to £ 3,500 are available for measures such as loft insulation, cavity insulation, draught proofing, hot water tank insulation and new gas, electric or liquid petroleum gas (LPG) heating systems. Alternatively, grants up to £ 6,000 may be allocated where oil central heating and other alternative technologies are required. The scheme is only available in England and it is managed by Carillion Energy Services (formerly Eaga). Equivalent schemes are the Home Energy Efficiency Scheme (HEES) in Wales and the Warm Deal in Scotland.

In a report by the National Audit Office (2009), since the scheme began in 2000, more than 2 million homes had been treated through Warm Front funding by 2009, costing approximately £ 2.2 billion. In a satisfaction survey, 75 % of customers were 'highly satisfied' by the quality of the work done and 84 % would recommend the service to a friend or relative. On average, Eaga estimated that the work done would reduce a household's energy bill by £ 300 a year (depending on the measures installed). A key criticism of the scheme is that applicants are assessed on a 'first come, first served' basis, yet nearly 75 % of households who qualified were not necessarily in fuel poverty. In addition, it was criticised that the scheme lacked a full range of measures such as external wall insulation, meaning it was unable to address hard-to-treat households (National Audit Office, 2009).

Green Deal

From October 2012, the Green Deal will be the key mechanism for improving the energy efficiency of domestic buildings in the UK. In this programme, bill payers will be able to obtain energy efficiency improvements without having to pay for the upfront costs of retrofit works (DECC 2010c). Instead, capital will be privately financed, through consortia made up of banks, consumer and business groups, local authorities etc, as well as the investor community, who recoup their investment through an instalment charge on the consumer's energy bill. The overarching 'golden rule' principle is that the estimated savings on energy bills must be equal to, or greater than, the costs attached to the energy bill. Unlike a conventional loan, the loan repayments remain attached to the property, rather than the bill payer (who may move into a different property before the repayments are complete). Its remit also covers non domestic buildings.

Supporting Green Deal, the government plans to have smart meters installed in every home by 2020. These meters are anticipated to provide customers and energy suppliers with more information on electricity and gas usage, as well as acting as the prime mechanism for governing the claimed bill savings through the Green Deal. All measures installed through Green Deal must be recommended and approved by an accredited advisor, and installed through an accredited installer. The majority of loans are expected to be provided by industry led consortium consisting of 19 blue-chip companies called the Green Deal Finance Company, supported by the Green Investment Bank. Functioning alongside Green Deal, an Energy Company Obligation (ECO) is scheduled to replace CERT and CESP, to provide additional financing to support vulnerable low income households and hard-to-treat properties.

2.1.11 Barriers to energy efficiency

According to Roberts (2008a) and Power (2008), there are a number of conventional cost effective retrofit measures yet to be implemented throughout the UK housing stock and many older homes have vast potential for reduced energy consumption. However, Lowe and Oreszczyn (2008) and Ravetz (2008) claim that a large proportion of cost-effective measures have already been employed, yet significant energy savings are still to be experienced. In addition, both Olivier (2001) and Lowe and Oreszczyn (2008) argue that actual energy performance of the UK building stock may be significantly lower than previously assumed.

Difficulty meeting Building Regulations

In a report by Olivier (2001), it was argued that the official figures for U-values are optimistic and not achieved in practice. This is because actual U-values are often found to be higher than expected when measured in-situ, due to errors found in the quality of construction, as well as thermal bridges and gaps in insulation. According to Hamza and Greenwood (2008), Building Regulations do improve design teams' abilities to meet energy targets, however, many within the industry express concern about uncertainties and difficulties with compliance. Lowe and Oreszczyn (2008) claim that little is known regarding the actual impact of updates to the Building Regulations due to a lack of monitoring following construction. Similarly, Olivier (2001) states there has been no evaluation of the 1982, 1990 or 1995 building regulations since there is no individual or legal binding body to assess energy performance after work is completed.

Too much focus on zero carbon targets

Taking a top-down approach, Lowe and Oreszczyn (2008) believe that many issues hindering the progress of energy efficiency relate to ill-advised policies from the government causing debate within industry. Lowe and Oreszczyn (2008), claim that the government is putting too much pressure on the industry to achieve zero carbon targets, particularly in new build, without fully understanding the complications surrounding fabric improvements in existing homes. Lowe and Oreszczyn (2008) propose that too much investment is being spent on expensive renewable technologies without fully understanding the importance of maximising the performance of the building fabric.

Discrepancies between predicted and actual savings

Hong *et al.* (2006) published a paper looking at the impact of energy efficient refurbishments on the space heating fuel consumption of English dwellings. Here, the

performance of 1,372 properties treated through the Warm Front scheme were analysed before and after a conventional retrofit with cavity wall insulation, loft insulation and a new central heating system. The aim of the study was to lower energy consumption to alleviate low income houses from fuel poverty, along with raising thermal comfort standards to modern levels. Prior to installation, theoretical calculations suggested that cavity wall insulation and loft insulation would save 49 % of fuel consumption, however actual monitoring following the refurbishment showed that only 10-17 % energy savings were achieved.

Conclusions from this study suggest that the refurbishment did raise thermal comfort standards and homes were cheaper to heat, however the expected energy savings were not achieved. Furthermore, Hong *et al.* (2006) claimed that large uncertainties related to the impact of thermal bridges, gaps in insulation and the occupants using more heating following the refurbishment. For example, thermal imaging on a sample of 72 dwellings showed that 20 % of cavity wall areas and 13 % of the loft areas lacked insulation. The introduction of the new gas central heating systems, although more efficient, had no significant impact on reducing fuel consumption due to the occupants increasing the internal temperatures of their home following the refurbishment.

Increased use of heating following refurbishment

This issue of thermal comfort 'take-back' was also reported by Bell and Lowe (2000) in a study analysing the savings of energy efficient refurbishments on four similar sized semi-detached houses. The aim of the study was to confirm that significant energy savings could be gained from conventional 1980s retrofit technologies. Following an extensive two-week energy monitoring period, a 47 % reduction in energy consumption was observed, proving that significant savings could be achieved from conventional retrofit measures. However, this value was 40 % lower than their predicted calculations, which Bell and Lowe (2000) suggested was mostly due to people's behaviour and raised thermal comfort take-back from the new heating systems.

Understandably it is difficult to determine how people will react following an energy efficient refurbishment. Additionally since thermal comfort is largely a subjective matter there will be much variation between different households and tenure. Providing instantaneous feedback on fuel usage and internal temperatures via home energy monitors may serve to help this issue. According to Darby (2006) a 5-15 % energy saving is possible from direct feedback, but there is a lack of evidence to support these savings over the long term.

Socio-economic status of household

According to Binggeli (2003) and Roberts (2008a), before the introduction of gas powered central heating systems in the 1970s, most people preferred indoor temperatures at 20 °C, and would wear more clothes during winter to prevent paying high energy costs. By comparison, nowadays people have developed a thermal comfort preference of 23-25 °C, which tends to be satisfied through higher quantities of energy consumed for heating (Binggeli, 2003; Roberts, 2008a). Both Clinch and Healy (2001), and Milne and Boardman (2000), claim that a large proportion of the thermal comfort take-back relates to the socio-economic status of the household prior to the refurbishment. In a paper discussing the effect of energy efficiency in low-income homes, Milne and Boardman (2000) found that low income houses originally heated to 14.5 °C, experience just 50 % of the expected energy savings, whereas slightly higher income homes originally heated to 16.5 °C tended to experience 70 % of the expected energy savings, due to a lower thermal comfort take-back. Clinch and Healy (2001) believe there is a lack of studies looking at take-backs in high income homes. Here it would be expected that dwellings would see a greater reduction in their energy bills since the home is likely to already be heated to reasonable levels.

Additional barriers within society

Ravetz (2008) claims that many people do not view energy efficient refurbishments as a high priority when updating their homes. Major barriers are the perceived hassle of installation, upfront costs, uncertainties over lower fuel bills and a lack of knowledge over payback periods (UKGBC, 2008). Power (2008) states that energy efficient refurbishment is undervalued by communities. People seem to prefer amenities such as new kitchens, bathrooms, central heating, and general repairs, instead of energy efficient refurbishments since the social gains are more obvious (Bell and Lowe, 2000). Ravetz (2008) forecasts that technological shifts threaten to counter the efforts of energy efficiency. For example more homes will become increasingly diverse in their use of energy with more appliances, lighting and domestic air conditioning.

Insulation causing overheating

Looking to the future, it may become apparent that climate change causes people's thermal comfort needs to adapt to higher temperatures or conversely require more cooling (Ravetz, 2008; Roberts, 2008b). At present little attention is given to issues such as the impacts of overheating in older buildings, security risks for opening windows or the impact of appliance heat gains with technological developments. These

would be interesting to study, however it would rely heavily on predictions, which are difficult to quantify (Ravetz, 2008; Roberts, 2008b).

Within a study related to the effects of climate change on building energy consumption, Holmes and Hacker (2007), modelled a medium-high climate change scenario to determine the impact of raised temperatures on energy consumption. Here it was argued that although there is plentiful data to predict the impact of climate change, there has been limited focus on how significant this will be in relation to thermal comfort adaptation and operational energy consumption throughout the lifespan of a building. Trends from the study revealed that buildings are expected to have higher cooling loads in the summer and lower heating loads in the winter. Both Holmes and Hacker (2007), and Ravetz (2008) predict this will lead to greater overall energy expenditure in buildings that require active cooling. In addition more homeowners are likely to retrofit air conditioning systems or buy portable air conditioning units for their homes, which too would raise consumption.

2.1.12 Passivhaus refurbishment

A large wealth of experience exists within the German retrofit market due to their implementation of the Passivhaus standard within new and existing homes (Lowe and Oreszczyn, 2008; Bell and Lowe, 2000). Core principles of a Passivhaus rely upon the design and specification of super insulation and highly airtight fabric, combined with whole house mechanical ventilation with heat recovery (MVHR). Using this approach, a building has minimal heat losses through the fabric, and is supplied with permanent fresh air and regulated humidity, with no uncomfortable draughts. A Passivhaus must have a total heating demand of 15 kWh/m^2/year or less, or 25 kWh/m^2/year or less if it is a retrofit. By comparison, the average heating consumption for the existing UK building stock is 180 kWh/m^2/year, 100 kWh/m^2/year when renovated and 50-60 kWh/m^2/year if it is a new build (Boonstra, 2005).

An example of a German Passivhaus retrofit is the 'Zukunft Haus Pilot Programme' that ran from 2003-2005. Here, 915 homes, mostly rented flats built pre-1978, were renovated in Eastern and Western Germany with high levels of insulation, external / internal cladding, triple glazing, efficient heating/energy systems, whole house heat recovery and south facing balconies where possible. Overall an 80 % reduction in energy consumption throughout the households was achieved, which was twice as effective as the German building standards (Power, 2008). In 2007, the German Federal Government announced that all German pre-1984 homes should reach this

standard by 2020, through a system of loans, tax incentives and grants, resulting in vast incentives for energy efficient refurbishment (Power, 2008)

A summary of the Passivhaus standards, compared to 2010 UK Building Regulations (for new builds) is shown in Table 2.4. Bell and Lowe (2000) and Lowe and Oreszczyn (2008) argue that there is a need to transfer this knowledge into the UK housing stock so that the UK construction industry will be better equipped at improving the standard of existing houses and meeting the requirements of new building regulations. This will require the transfer of Passivhaus components, installation procedures and more training within the construction industry to inform workers on how to properly meet Passivhaus standards during refurbishment (Lowe and Oreszczyn, 2008).

Table 2.4 *UK Building Regulations and Passivhaus guidelines (Generated from BRE 2011).*

	UK New Build (2010)	**Passivhaus Standard**
Walls, roof and floor	Limiting U-values of 0.25-0.30 W/m^{2}K	U-value should not exceed 0.15 W/m^{2}K
Windows and openings	Typically 1.8-2.2 W/m^{2}K	U-value should not exceed 0.8 W/m^{2}K, with solar heat gain co-efficient of 50%
Orientation and shading	Sometimes considered, but often overlooked in the design process.	Passive solar design principles are followed where applicable
Air tightness	Designed air permeability of 7-10 m^3/m^2 h @ 50 Pa	Designed air permeability of <1m^3/m^2 h @ 50 Pa
Mechanical ventilation with heat recovery (MVHR)	Typically not considered as buildings do not achieve good enough air permeability values (trickle vents, extract fans or stack ventilation used instead)	Incoming fresh air is pre-heated to >5°C. Ducts can run underground to exchange heat with soils. Exhausted Heat recovery efficiency is 85%.
Lighting and appliances	Low energy lighting and C+ rated appliances	Low energy lighting and A+ rated appliances are essential
Total heating demand	~ 55 kWh/m^2/year	15 kWh/m^2/year (new build) 25 kWh/m^2/year (retrofit)

The UK's first certified domestic Passivhaus retrofit was completed in March 2011. It is a solid walled mid-terrace house at 100 Princedale Road in Holland Park, West London. The house was located in a conservation area, so external insulation and new glazing was restricted. Consequently, measures implemented included internal insulation with an air-tight barrier, custom built triple glazed windows to imitate traditional single glazed sash windows, an MVHR and solar thermal collectors for water heating. The newly refurbished property has no gas boiler or radiators. According to Borgstein *et al.* (2011), energy savings of 89 % are projected, equivalent to £ 910 saved a year on fuel bills. Over the next two years, the efficiency and comfort levels of the home will be monitored. This project was funded through the 'Retrofit for the Future' competition, launched by the Technology Strategy Board in March 2009.

2.1.13 Energy efficiency of the non domestic building stock

According to Ravetz (2008) and Lowe and Oreszczyn (2008), the UK's non domestic building sector presents just as large a problem, if not worse in terms of energy efficiency and retrofitting compared to housing. According to Roberts (2008a) about half of the energy use in the non domestic sector is for space heating, and most is for commercial offices, education and retail. According to Roberts (2008a), most large offices have high heating and cooling profiles due to their ageing building fabrics and/or high proportion of glazing, combined with inefficient HVAC (heating, ventilation and air conditioning) systems with poor controls, low occupancy awareness, high heat gains and electrical loads from artificial lighting and equipment. As a result, compared to other sectors, offices possess a higher than average consumption for heating, and double the average for cooling and ventilation (Roberts, 2008a).

Detailed information regarding the type, condition and energy efficiency of the non domestic building stock is yet to be compiled (Ravetz, 2008). Instead, national surveys focus on rateable values, floor space and the number of properties per region. Figure 2.6 displays a profile of the English office stock, segmented by age and region, based on the available data (CLG, 2004b). According to Ravetz (2008), the national floor space of offices has increased by 6 % since 1998, resulting in a total of 597 million square meters by 2007. Visibly, like much of the English housing stock, the largest construction band for commercial offices is pre-1940. The highest concentration is in London, followed by the North West and South East.

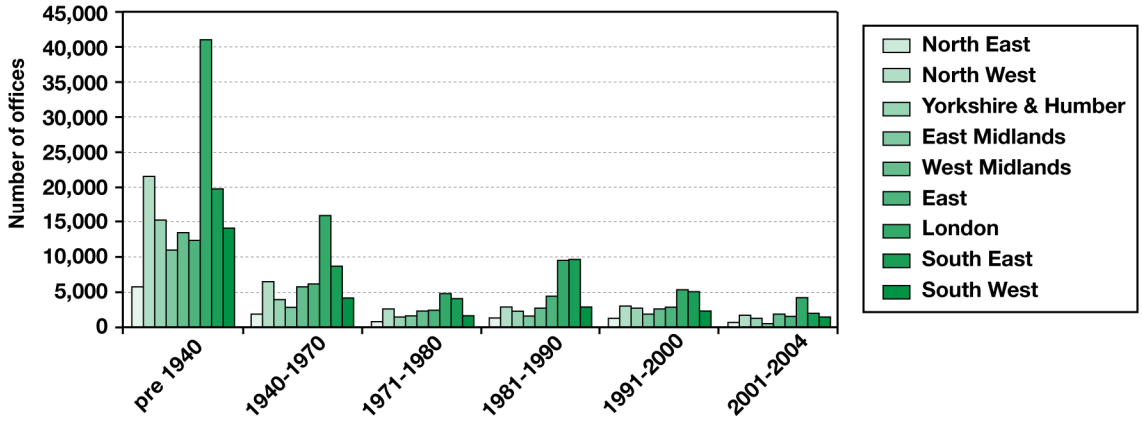

Figure 2.6 *English commercial office stock (Generated using data from CLG 2004b).*

It can be expected that older properties will have lower energy efficiencies since these were constructed before the implementation of modern Building Regulations. The lack of information regarding the energy performance of the UK office stock suggests that the non domestic sector receives much less attention from government when seeking to

improve the energy efficiency of the UK's existing building stock. Ravetz (2008) believes the lack of statistics is due to the non domestic sector being on the business side of the economy where government is tentative to intervene. According to Lowe and Oreszczyn (2008) the weak research base can be attributed to a lack of funding, noting that in 1998 and also 2005, government funding for construction industry research dropped by 70 % compared with the previous years.

Energy Performance Certificates (EPCs)

From October 2008, all non domestic properties to be constructed, refurbished, sold or rented in the UK must be accompanied by an Energy Performance Certificate (EPC). These certificates display the building's predicted energy consumption expressed on a scale from A (very efficient) to G (very in-efficient), as well as advice on how to make cost effective improvements to the building to make it more efficient. EPCs can only be produced by accredited energy assessors. Primarily, EPCs are calculated using the SBEM (Simplified Building Energy Model) methodology. SBEM provides an evaluation of a building's monthly energy use and CO_2 emissions based upon its geometry, zoning, construction, as well as HVAC and lighting equipment (CLG, 2010). Note that SBEM does not aim to predict the *actual* energy consumption of a building; instead its purpose is solely to ensure design compliance with Building Regulations. As a consequence, electricity use for small power (e.g. desktop computers, printers, laptops etc), catering, external lighting and lifts are excluded (Menezes *et al.* 2011).

Display Energy Certificates (DECs)

Also from October 2008, all public buildings (e.g. schools, universities, hospitals, local authority offices, leisure centres, libraries etc) with a total floor area over 1000 m^2 must be accompanied by a Display Energy Certificate (DEC). DECs are similar to EPCs providing an energy rating of the building from A to G, where A is very efficient and G is the least efficient. The primary difference is that DECs are based on the building's metered energy use over a period of 12 months. As with EPCs, a DEC must be prepared by an accredited energy assessor and the certificate must be accompanied by an advisory report recommending energy performance improvements. Once produced, a DEC is valid for 12 months and must be updated annually. According to guidance by CLG (2008), an affected organisation must display the DEC in a prominent place, which is clearly visible to the public. Its purpose is to raise awareness of energy use and to inform visitors to public buildings of the energy use of a building (CLG, 2008).

2.1.14 Environmental impact of refurbishments

The environmental impact of refurbishment, in particular the embodied energy and embodied CO_2 produced through raw material acquisition, component manufacture, transport to site and the onsite construction/retrofit process, is an area of research which is often overlooked. Over the lifecycle of a building, it is estimated that these 'cradle-to-site' embodied impacts account for about 10-20 % of a buildings total energy consumption (SETAC, 2003). Conversely, for low energy, high efficiency buildings, this phase of the building's lifecycle can have a much greater significance representing around 40-75 % of the total lifetime energy consumption (SETAC, 2003; Smil, 2008).

According to Ravetz (2008), the embodied energy required to construct a new building may be up to 10 times more intensive than refurbishment, due to the offsite impacts of construction. Power (2008) claims that the embodied energy required to build a new house is 4-8 times more intensive than a refurbishment to modern standards. These issues were also studied by the Empty Homes Agency (EHA), who demonstrated how comprehensive refurbishment generates about 15 tonnes of embodied CO_2, in comparison to demolition and rebuild which used closer to 50 tonnes of embodied CO_2. According to EHA (2008), the energy consumption of an average UK home is responsible for 5-6 tonnes of CO_2 every year, two thirds of which could be saved by adopting simple energy efficiency measures.

Figure 2.7 illustrates the typical embodied and operational energy costs for an office that has been involved in three major refurbishments at 25 years, 50 years and 100 years into its lifecycle, according to Yohanis and Norton (2002). As shown, operational energy steadily accumulates throughout the lifecycle of a building, whereas the embodied energy builds up in increasingly energy intensive phases.

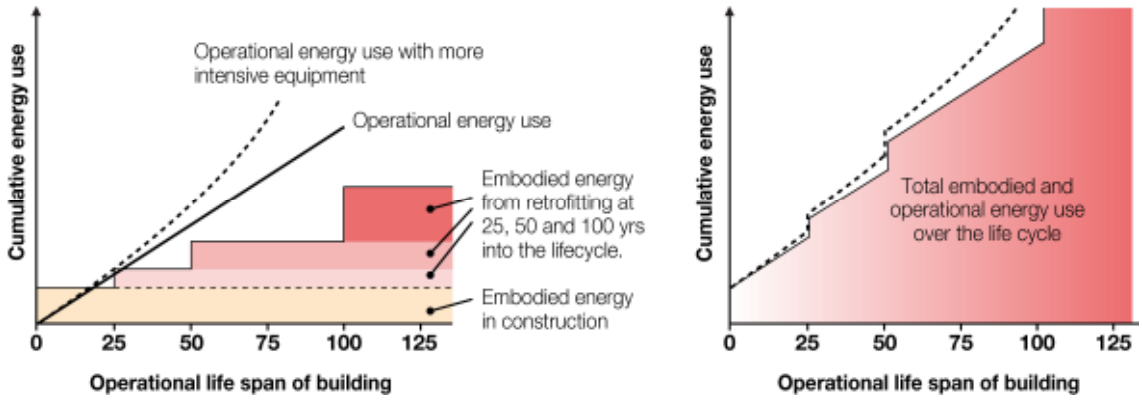

Figure 2.7 *Illustrative embodied and operational energy costs in the life cycle of an office refurbished at 25, 50 and 100 year intervals (Adapted from Yohanis and Norton, 2002).*

Not shown in Figure 2.7 is the potential for operational savings following each retrofit. According to Harris (1999), there is a significant lack of studies concerning the actual embodied energy within refurbishments, particularly those measures designed for energy efficiency. According to Schmidt *et al.* (2004), in a typical application, the in-use savings from insulation are over 100 times the embodied impact of production and disposal. In contrast, Harris (1999) claims that when the thickness of loft insulation is increased beyond 200 mm, the embodied energy threatens to outweigh the operational energy savings. Weir and Muneer (1998) found modern glazing systems have a particularly high embodied energy up to 1500 kWh/m^2, which could take 10-30 years to provide a positive energy contribution.

2.2 Advances in Retrofit Technologies

A number of conventional retrofit solutions are available to improve the thermal performance of existing buildings. These technologies are likely to continue being selected based upon their cost, practicality and specific performance. However, there are limits to the actual energy savings that can be achieved and several barriers to their successful implementation. At present, a number of new technologies are under development to refurbish buildings to higher energy standards. This scoping sub-chapter aims to outline the supporting evidence and key issues surrounding each technology to establish where a contribution to knowledge can be made.

2.2.1 Solid wall insulation

It should be noted that solid wall insulation is still considered as a relatively new technology in the UK retrofit market. According to the EEPH (2009), the solid wall insulation market suffers from low public awareness of the available options and their respective benefits. In addition, the EEPH (2009) claim that the UK needs a major skills and training programme to support the delivery of solid wall insulation and that it is difficult to envisage the installation rate of solid wall insulation increasing without stronger incentive schemes, active promotion and technological innovation.

The solid wall insulation sector can be split into six specific product types, as detailed in Table 2.5. Typical U-values obtained through solid wall insulation range from 1.6 W/m^{2}K for internal flexible lining, to 0.35 W/m^2 K for external cladding (EEPH, 2009). Flexible thermal linings to reduce mould growth are referred to as 'insulated wallpaper'. Common forms of external cladding consist of expanded polystyrene or polyurethane insulation, adhesively bonded and pinned over existing brickwork, with a durable wet render finish. U-values down to 0.1 W/m^2 K can be obtained by increasing

insulation thicknesses up to 300 mm. In general it is not cost effective, or practical to obtain U-values below this figure.

Table 2.5 *Product types within the solid wall insulation sector (Generated from EEPH 2009).*

	Specific product types	Detailed description
External insulation	Wet rendered	An insulation layer, plus a protective layer of render with decorative finish
	Dry cladding systems	Dry cladding fixed to the outside of a building
Internal insulation	Spray applied insulation	Spray applied polyurethane foam applied between previously erected timber or metal studwork and then covered with plasterboard can be fixed to the foam with dabs or a bonded plaster and finish can be applied directly to the foam
	Internal rigid thermal board	Rigid thermal laminated board made of insulation backed plasterboard
	Built up internal systems	Built up systems use insulation held in place using a studwork frame
Insulated wallpaper	Internal flexible linings	Supplied on rolls, typically one metre wide. The material is made from latex and has a fibreglass face that allows it to be decorated

2.2.2 Air leakage barriers

At present, a number of manufacturers supplying airtight retrofit technologies are emerging in the UK construction market, such as those shown in Figure 2.8. Air infiltration and leakage, caused by the uncontrolled movement of air into and out of the building envelope is a major source of energy loss in existing buildings, accounting for approximately 20 % of space heating consumption (Bell and Lowe, 2000). Adverse effects include condensation and mould growth when moist outside air condenses on cold surfaces inside the building. Additionally, unwanted air movement can cause undesirable draughts and internal temperatures, impacting thermal comfort and air conditioning loads if the building is mechanically ventilated (Sadineni *et al.* 2011).

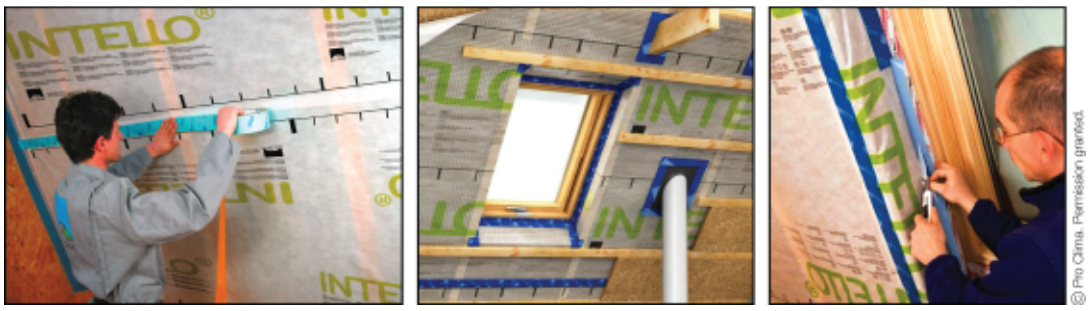

Figure 2.8 *Examples of air leakage barriers and tapes*

Sealing gaps and cracks in the building fabric improves energy efficiency by minimising infiltration. At a basic level, this is achieved by draught proofing windows and doors, and sealing additional openings such as the loft hatches and chimneys if applicable. By

comparison, when aiming to achieve more stringent air tightness standards, such as those set in Passivhaus construction, a far more rigorous approach is required. Here, the building requires a continuous, impermeable, durable air tight barrier, consisting of a combination of interconnected membranes, tapes and flexible sealed joints. All junctions around the windows, external doors as well as the roof, floor and walls must be sealed and air tight sleeves must be applied to all external service penetrations.

If aiming to achieve Passivhaus air tightness, the key challenge is to ensure these technologies are applied consistently and appropriately by a skilled and knowledgeable workforce, following a defined air tightness strategy, which deals with all complicated junctions and partitions. In addition, all new-build and retrofit Passivhaus projects must also incorporate certified windows and doors with airtight seals and locks. Mechanical ventilation is essential to provide adequate ventilation rates.

2.2.3 Vacuum insulation panels

According to Roberts (2008a), the need to reduce insulation thickness is likely to become more important as Building Regulations become more stringent. Addressing this issue, vacuum insulation panels (VIP), shown in Figure 2.9, are an emerging retrofit technology offering 5-10 times better thermal performance than conventional insulation panels, at a fraction of the thickness (Roberts, 2008a; Simmler and Brunner, 2005). The panels consist of micro-porous structure sealed inside a vacuum envelope. Typically, VIP are 250-500 mm² and 20 mm thick, and can be retrofitted to buildings in a variety of applications, such as internal wall and floor insulation (Cremers 2005).

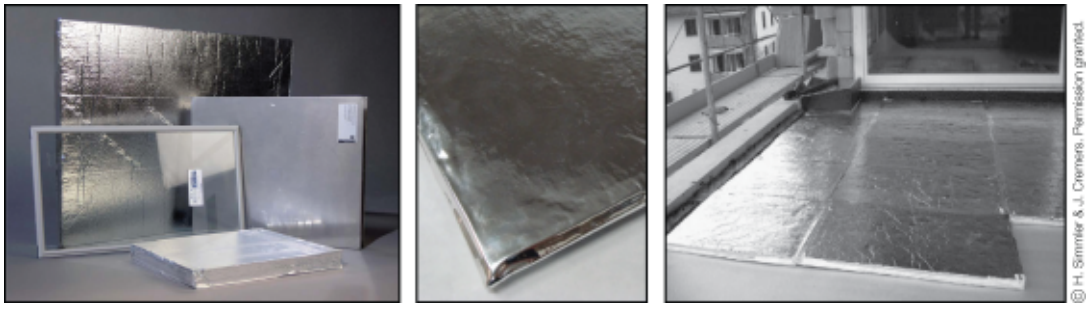

Figure 2.9 *Examples of vacuum insulation products.*

At present, the service life of VIP is uncertain. Simmler and Brunner (2005) claim that VIP needs to retain thermal performance for around 30-50 years to be a viable building fabric component. Roberts (2008a) states that VIP are delicate compared to conventional construction materials and care must be taken during storage, transport and installation to avoid damage. The main sources of defects occur at the edges, corners and seals. According to Simmler and Brunner (2005), retaining a long term

vacuum is a key issue, since it is understood that pressure changes from water and gas penetration are weak points of VIP. Currently, accurate measurements of thermal behaviour are difficult to obtain since no method exists to measure internal pressure changes of installed panels. Simmler and Brunner (2005) believe that more data from actual installations of VIP is required to establish service life.

2.2.4 Emerging glazing technologies

According to construction industry research by Purple (2007), the retrofit market for double glazing in Britain has been erratic over the last few years with the sector approaching maturity following strong growth throughout the 1990s. Despite this, an estimated 9.5 million units are replaced each year and the market value is approximately £ 3.8 billion (Purple 2007).

The main drivers for innovation in the glazing sector are greater energy efficiency, security, aesthetics, thermal comfort and cost (MTP 2007). The current focus is to develop products that combine the lowest possible U-value with a relatively high light transmission and G-value (solar heat gain coefficient). By minimising the U-value this ensures that heat loss is minimised. In contrast a relatively high light transmission and G-value will ensure that the glazing does not block out all the useful natural light and solar energy, whilst also reducing the risk of overheating problems.

According to MTP (2007), the introduction of Window Energy Ratings (WER) to the 2010 Building Regulations are expected to be a key driver in future product development within the glazing sector. The WER evaluates the performance of a glazing system on a scale from A-G (where A is the most efficient and G is the least efficient), considering the whole energy balance of the window, based upon the U-value and G-value of the glass as well as heat losses through the frame. All new glazing installed in existing buildings must have a certified WER of Band-C or above. As a consequence, manufacturers are increasingly focused upon improving the overall performance of glass coatings, window frames, glazing configurations, gas fills and spacer bar technologies to improve the energy efficiency of their products. Alongside these developments, several alternative glazing systems are emerging within the market. Summarised from MTP (2007), these innovations are described below:

Gas filled glazing

Typically, the space between the panes of glass in a conventional double glazing unit is filled with air or nitrogen. Replacing this medium with a more viscous gas can slow the rate of convection currents between the top and bottom of the glazing to minimise heat

loss. The 2002 Building Regulations promoted the use of argon gas in windows for improved energy performance. Subsequently, argon filled glazing is now common within the UK glazing market. More recently, due to the WER, krypton gas has been encouraged due to its increased molecular weight, resulting in an improved energy performance over argon. These units were available from 2006. In general, krypton filled units are more expensive than argon filled units (MTP, 2007).

Triple glazing

According to Roberts (2008a), windows typically represent the worst performing element of a building, with 4-10 times higher heat-loss coefficients compared to the walls, roof and floor. Triple glazing is now common in the German housing market, yet its use in the UK is limited. Manz *et al.* (2006) state that centre pane U-values of triple glazing can be as low as 0.5-0.6 $W/m^2 K$, however, a key issue with triple glazing is cost effectiveness, since the added costs, compared to double glazing are unlikely to justify the energy savings in today's market. An additional factor with triple glazing is the added weight of the glass. Schultz and Jensen (2008) claim the extra pane adds 33 % more weight to the frame.

Super windows

Shown in Figure 2.10, 'super windows' are glazing systems incorporating up to 5 panes of glass, a high performance spacer bar, coatings and a noble gas filling (MTP, 2007).

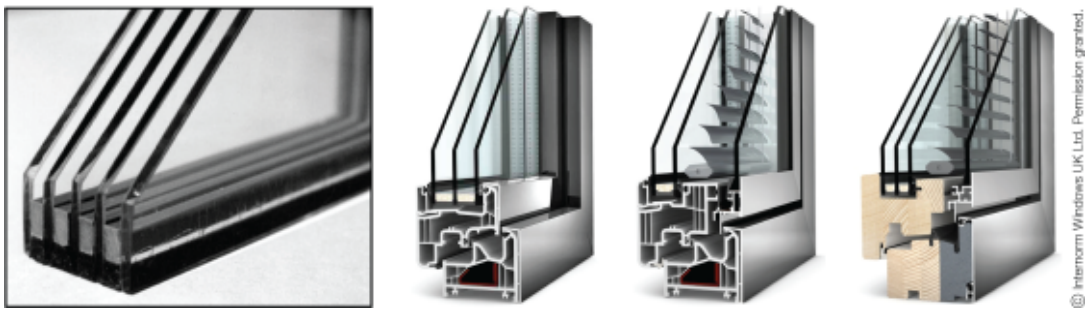

Figure 2.10 *Examples of 'super windows'.*

Typically, these super windows will possess low-emissivity coatings on their inner surfaces, and a coated film is suspended in between these panes. Some units also possess solar reflective blinds between the panes to direct solar radiation and glare. Understandably, these units have very high thermal resistance, but increasing the number of panes and coatings also reduces the useful solar gains, as well as increasing cost and weight (MTP, 2007).

Vacuum glazing

Vacuum glazing typically consists of two panes of glass, held 0.5 mm apart under vacuum with small pillars between the panes to maintain structural performance. Creating a vacuum within a glazing unit is the optimum scenario for reducing convection and conduction. According to Schultz and Jensen (2008), the U-value of vacuum double glazing is in the same range as triple glazing. Conversely, Bahaj *et al.* (2008) claims that vacuumed triple glazing can achieve U-values as low as 0.2 $W/m^2 K$.

To date, the market for vacuum glazing is largely underdeveloped and products are mainly in the prototype stage (MTP 2007). Slim profile vacuum glazing, with a similar thickness to single glazing is available for refurbishing listed buildings, since the single glazed sash windows can be upgraded whilst retaining the original frames (Roberts, 2008a). Currently, most units in the UK are sourced from abroad and cost approximately £ 500/m^2.

Key issues with vacuum glazing are structural pressure, vibrations, window clarity and thermal bridges at the edges. Units must remain completely air tight over a 20-30 year lifespan in order to justify their high capital costs. According to Roberts (2008b), wind and vibration can compromise the integrity of vacuum glazing. Schultz and Jensen (2008) identify edge sealing as a barrier to vacuum glazing. Here, there is a large risk of thermal bridges through air leakage if the frames are not completely airtight. Bahaj *et al.* (2008), state that little research has been established to determine the lifetime of vacuum glazing. This is difficult since there has been a lack of case studies analysing long term performance.

2.2.5 Alternatives to new glazing

According to Mintel (2007), the retrofit market for curtains, shutters and blinds in Britain is worth £ 1.1 billion, split £ 640 million, £ 445 million and £ 23 million respectively, and has been increasing in recent years. During 2004-2006, sales of curtains increased steadily by 2 %, whereas sales of shutters and blinds have increased by 44 % and 66 % respectively. According to Mintel (2007), the increased sales of blinds and shutters were largely due to changes in aesthetic trends, the desire to maximise internal space (in place of large curtains), and a gradually increasing awareness of energy conservation. Sales of specialised insulating products such as thermal blinds, shutters or curtains represent a small proportion of the retrofit market. However, with increased media coverage and more information regarding the energy savings of these products, Mintel (2007) predicts that their uptake could increase significantly.

In-situ performance of curtains, shutters and blinds

In a report for Historic Scotland by Baker (2008), it was argued that there is a significant lack of information concerning the actual thermal performance of conventional retrofit measures applied to single glazing. To address this, Baker (2008) carried out a series of in-situ tests in an environmental chamber to evaluate the U-values of various retrofit measures such as curtains, blinds and shutters applied to single glazing. Prior to testing, the window was draft sealed to reduce air leakage. This procedure reduced the air leakage by 86 % and improved the measured U-value from 4.5 W/m² K to 4.2 W/m² K. Following the tests, the single glazing was replaced with modern double glazing (a slim-profile unit containing a krypton-xenon gas fill) for comparison. The measured centre-pane U-values from this experimentation are shown in Figure 2.11. The estimated uncertainty was ±0.3 W/m²K.

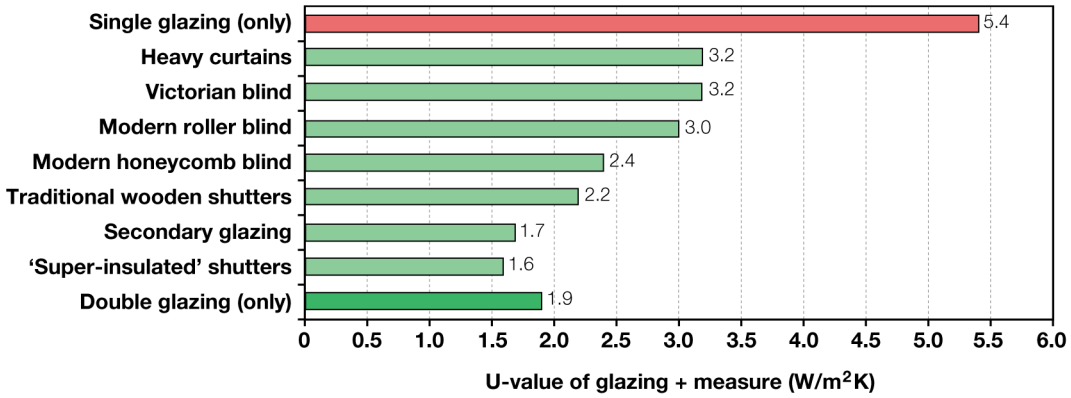

Figure 2.11 *In-situ U-value of glazing renovation measures tested by Baker (2008).*

According to Baker's (2008) findings, all measures improved the U-value of the single glazed window. The most effective solution was a custom-built prototype consisting of a set of wooden shutters, lined with a 9 mm blanket of Spacetherm™, a super insulating aerogel fabric. This one-off prototype achieved a centre pane U-value of 1.6 W/m² K reducing 60 % of the overall heat loss. Additional readings across the surface of this prototype revealed further reductions in heat loss of up to 80 % and a U-value of 0.7 W/m² K. The second most effective solution was secondary glazing, followed by traditional wooden shutters, then the modern roller blind. Heavy curtains were found to reduce the least amount of heat loss, but still provided a significant improvement over the existing single glazing.

Images of the single glazing, the makeup of the modified shutters and the appearance of these shutters once retrofitted are shown in Figure 2.12. As shown, the product blocks out all of the natural light and the insulation is not consistently applied across the surface of the wooden shutter.

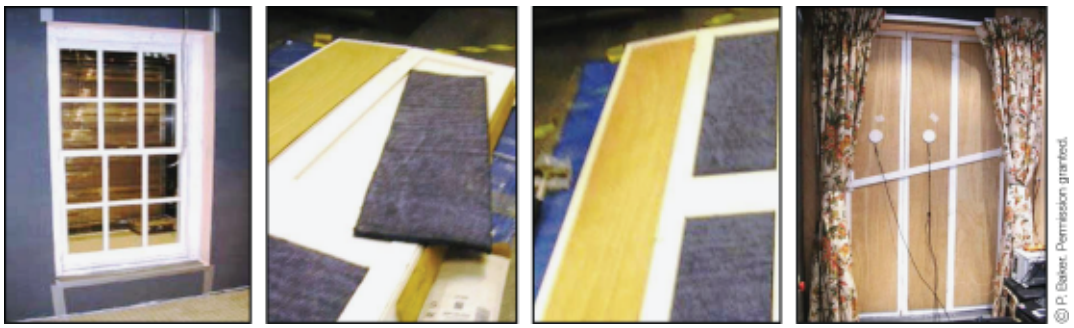

Figure 2.12 *Photographs of the super-insulating aerogel shutters tested by Baker (2008).*

According to Baker (2008), through manufacturing a properly designed shutter, the entire product could achieve 80 % reduction in heat loss equivalent to a U-value of 0.7 W/m² K. If so, this would far exceed the performance of modern double glazing and even rival some new and innovative glazing technologies.

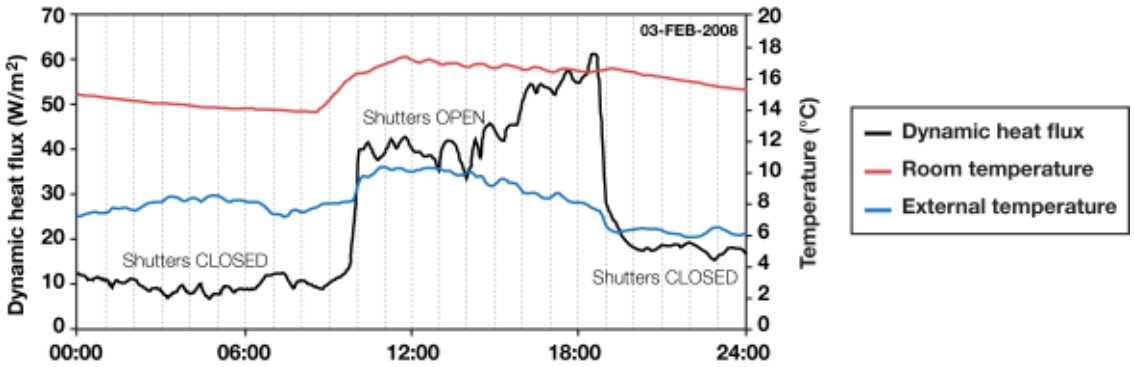

Figure 2.13 *Dynamic heat flux opening and closing the shutters measured by Baker (2008).*

Building on from these findings, Baker (2008) studied the in-situ performance of the insulated shutter in an office in Scotland during the winter period. Occupants were asked to open/close the shutter as normal. The recorded heat flux, internal temperature and external temperatures are illustrated in Figure 2.13. As shown, the heat flux through the glazing increases considerably when the shutters are open. Following personal communication on 30th March 2010, P. Baker stated that there were currently no plans to develop this prototype further.

Movable insulation

A detailed overview of movable insulation solutions aiming to reduce heating and cooling losses through windows, glass doors, skylights, greenhouses and solar hot water heaters is provided in the book 'Movable insulation' by Langdon (1980). Three such solutions are shown in Figure 2.14.

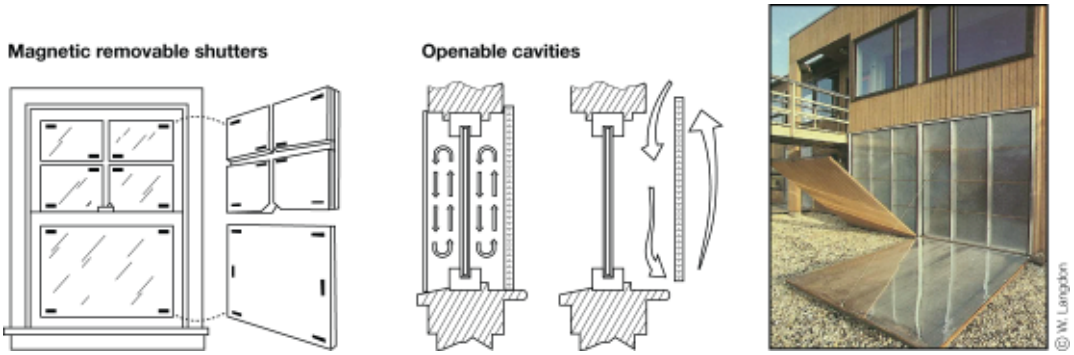

Figure 2.14 *Examples of movable insulation solutions.*

Here, a dynamic U-value is achieved through movable facade components that give an inherent degree of variable performance depending on their position and build-up. According to Langdon (1980), movable insulation is particularly useful if a house is utilising passive solar heating, since movable insulation allows a building to respond to the outside environment, by sometimes allowing energy flow into a dwelling and other times preventing energy transfer between the inside and outside, thus optimising both winter and summer efficiency.

2.2.6 Translucent insulation materials

There is scope to develop new retrofit technologies using translucent insulation materials (TIMs). These materials, shown in Figure 2.15, can perform a similar function to opaque insulation, yet they have the ability to transmit daylight and solar energy, reducing the need for artificial light and heating. TIMs transmit heat, mainly through conduction and radiation, as heat transfer by convection is usually suppressed (Kaushika and Sumathy, 2003).

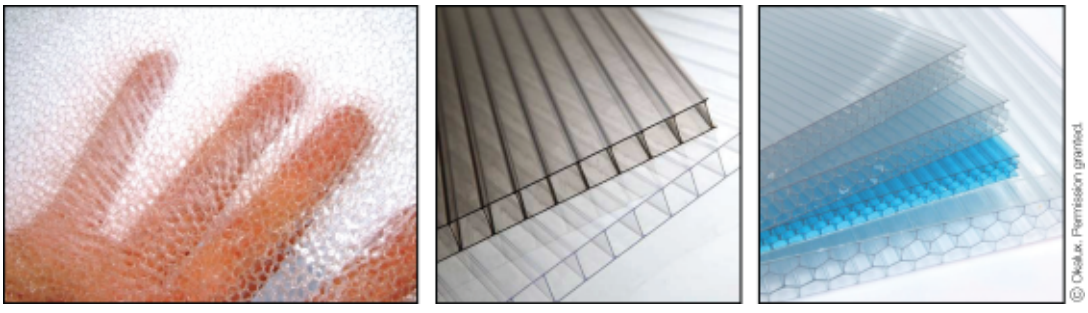

Figure 2.15 *Examples of translucent insulation materials.*

Since the late 1970s, considerable research has been undertaken to increase awareness of translucent insulation materials and demonstrate their enhanced performance over opaque and glazed elements in solar renovation projects (IEA, 1999; Voss, 2000; Dalenbäck, 1996). Honeycomb translucent insulation was first developed in the 1960s

to enhance the insulation of glazing systems with minimal loss to light transmission (Hollands, 1965). Over the past 25 years, TIMs have been applied to windows, skylights, walls, roofs and high-performance solar collectors (Dolley *et al.* 1994, Kaushika and Sumathy, 2003). The thermal and optical properties of a TIM depend on the material, its structure, thickness, quality and uniformity. TIMs typically consist of either glass or plastic arranged in a honeycomb, capillary or closed cell construction. Depending on the macro structure of a TIM, its arrangement can be classified as 'absorber perpendicular', 'absorber parallel', 'cavity' or 'quasi-homogeneous'. These four types and their typical materials are illustrated in Figure 2.16.

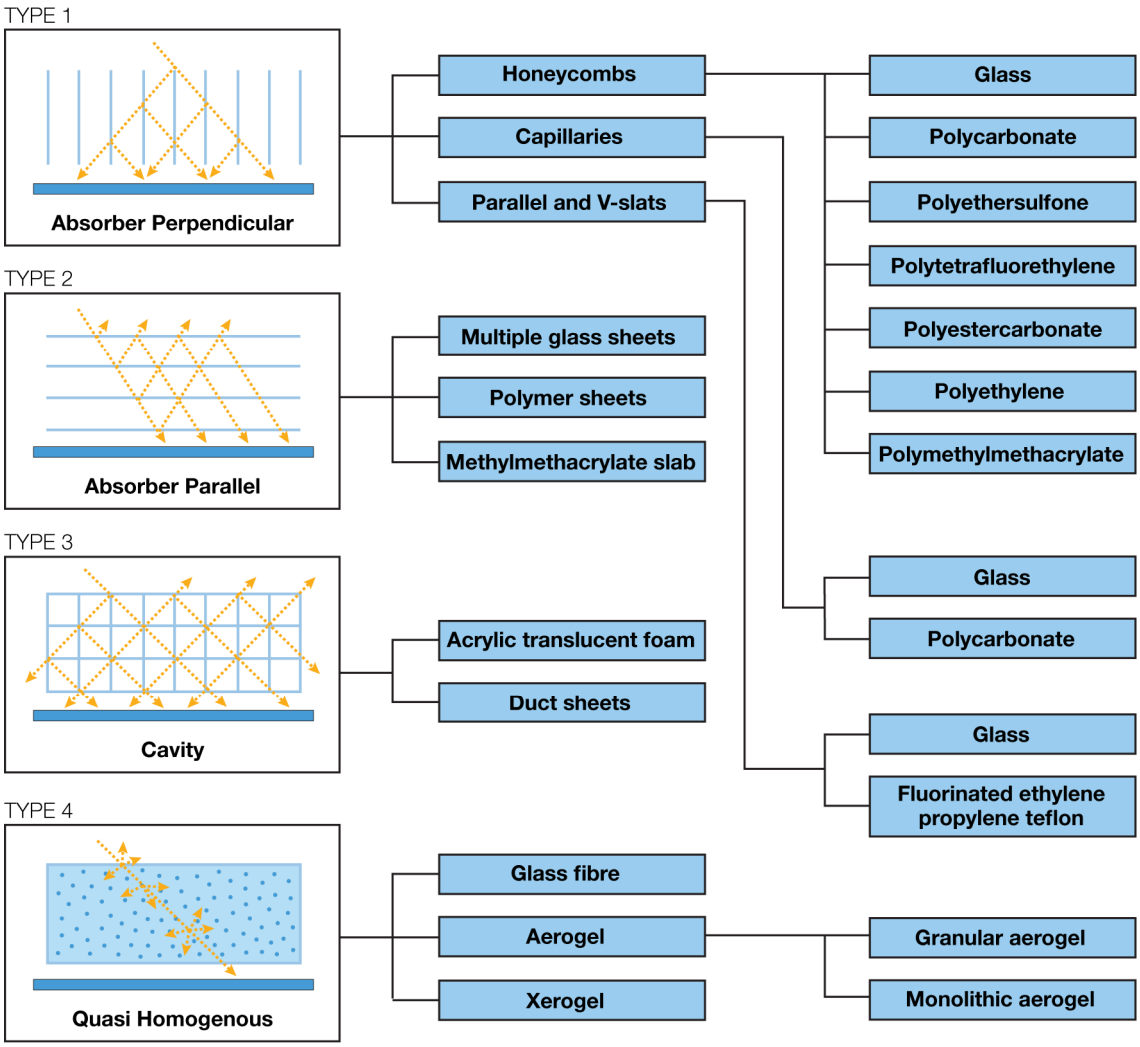

Figure 2.16 *Translucent insulation typologies (Adapted from Wong et al. 2007).*

Translucent insulation in glazing

TIM glazing consists of glass or plastic capillaries or honeycomb structures sandwiched between two glass panes. These systems diffuse light well, while reducing glare and shadowing (Lien *et al.* 1997). Commercial products such as Okalux™ and Arel™ glazing

can exhibit low U-values with high solar and light transmittance. According to Hutchins and Platzer (1996), 40 mm thick Okalux™ capillary glazing, and 50 mm thick Arel™ honeycomb glazing can achieve U-values of 1.36 W/m² K, comparable to modern gas filled double glazing. Alternatively, 80 and 100 mm thick systems can achieve U-values of 0.8 W/m² K, respectively, comparable to modern triple glazing.

According to Robinson and Hutchins (1994), the application of TIM glazing tends to be limited to skylights, atriums and commercial/industrial facades as the geometric structure of TIMs tends to restrict a clear view outside. TIMs appear most transparent when viewed directly on, yet opaque when viewed at an angle. In order to increase visible transmission, it is important to increase capillary size, reduce the thickness or view the TIM from a distance (Lien *et al.* 1997). According to Hutchins and Platzer (1996), normal light transmittance through honeycomb and capillary TIM glazing is 78 and 84 %, respectively. By comparison, normal light transmission through standard double glazing was similar at 81 %. Low-emissivity gas filled double and triple glazing units can be lower at 66 and 63 %, respectively (Hutchins and Platzer, 1996).

Translucent insulation in solar collectors

According to Kaushika and Sumathy (2003) and Wong *et al.* (2007) the most well documented application of TIM is in flat plate collectors for solar air or solar water heating. These systems heat air or water when irradiated by the sun. They can be integrated into buildings in a variety of ways, some of which are shown in Figure 2.17.

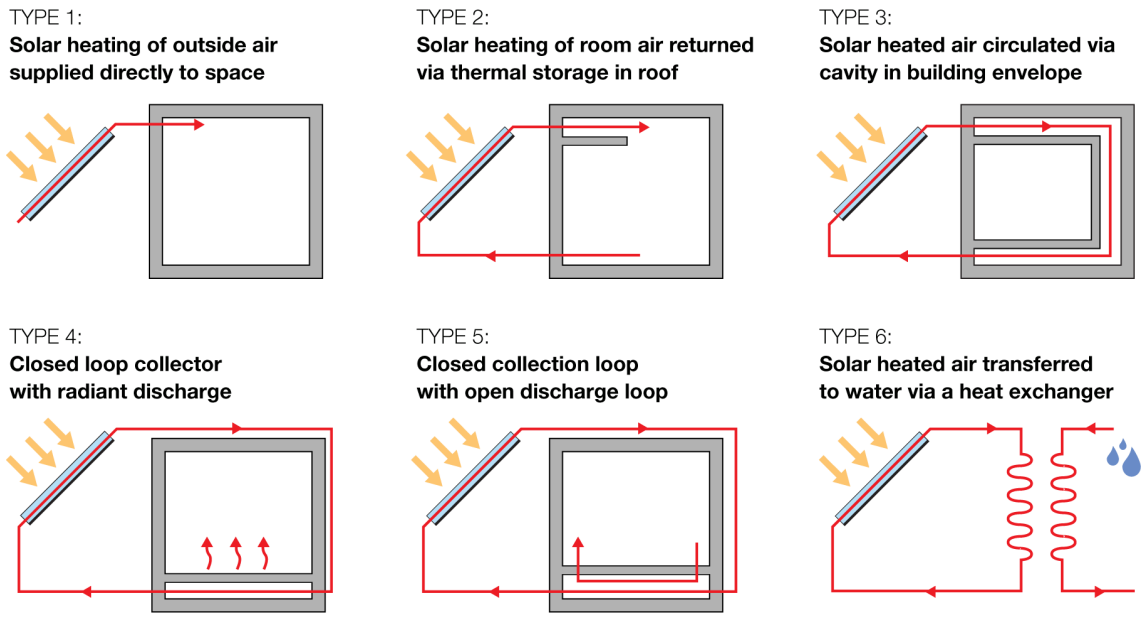

Figure 2.17 *Solar air collector typologies (Adapted from Hastings and Mørck 2000).*

Systems consist of a south facing TIM cover, which transmits solar energy whilst reducing convection and radiation losses to the atmosphere, and a black solar absorbing surface to transfer absorbed energy to a fluid (Hastings and Mørck, 2000; Duffie and Beckman, 2006).

When integrated into the roof or façade of a dwelling, a solar air heater is ideal for preheating the ambient or return air in a mechanically ventilated dwelling (Hastings and Mørck, 2000). Rommel and Wagner (1992) demonstrated how flat plate solar air collectors containing 50-100 mm polycarbonate honeycomb layers function well at lower temperature applications between 40-80 °C. Higher working temperatures of up to 260 °C can be achieved using glass capillaries, whereas plastic covers are susceptible to melting at temperatures above 120 °C.

Schmidt *et al.* (1988) and Kaushika and Reddy (1999) both constructed small scale solar water heaters containing TIM covers in place of conventional glazing. Solar conversion efficiencies up to 63 % and storage tank temperatures of 50-60 °C were attained, indicating that the systems would be an effective preheater. Authors commented that the TIM was found to minimise the risk of freezing whilst also obtaining solar fractions that outperformed some conventional domestic hot water systems.

Zhang *et al.* (2009) investigated the impact of honeycomb diameter and thickness on collector performance. Six flat plate solar air collector prototypes with grooved absorber plates were constructed, where 5 contained honeycomb covers of varying geometries and a single glazed system was used as a control. Experimental results demonstrated that smaller honeycomb thicknesses lead to larger outlet temperatures, yet varying the diameter had little impact. All honeycomb systems outperformed the single glazed collector. A 12 °C outlet temperature difference was observed between the best performing TIM prototype and the control.

Translucent insulation in Trombe walls

Trombe walls (visualised in Figure 2.18) are a type of solar heated collector storage wall invented by Edward Morse in 1881, then later popularised by the French engineer Felix Trombe and architect Jacques Michel in the 1970s (Michel and Trombe, 1971). The passive solar energy system consists of a thermally massive south facing concrete wall, painted black and covered with a sheet of glass with a cavity behind, which is heated up by incoming solar radiation. This captured heat can either be used straight away by venting the warm air inside, or later, by letting it permeate and warm up the concrete wall so that occupants can benefit from it in the evening.

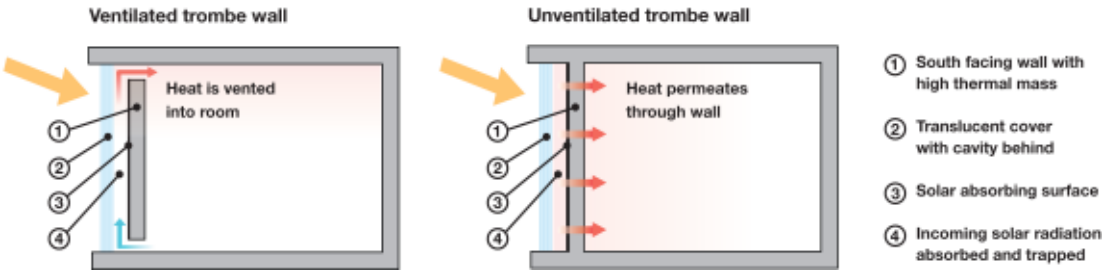

Figure 2.18 *Ventilated and unventilated Trombe walls (Adapted from IEA 1999).*

Several studies characterise the steady state performance, computer simulation techniques and in-situ performance of glazed Trombe walls, such as Monsen *et al.* (1982), Ellis (1995) and Burek and Habeb (2007) respectively. By comparison, Peuportier and Michel (1995), Athienitis and Ramadan (1999) and Suehrcke *et al.* (2004), amongst others, demonstrate that in this application, TIMs such as glass, plastic honeycombs and flat or corrugated polycarbonate sheets can provide significant energy savings when retrofitted to residential and commercial properties. For example, in a comparative study of six houses in France, Peuportier and Michel (1995) found that honeycomb TIMs can increase the efficiency of conventional solar air collectors and Trombe walls by 25 % and 50 % respectively.

A selection of TIM Trombe wall projects compiled by Peurortier *et al.* (2000) is displayed in Table 2.6. Many of these installations were conducted during the 1980s and 1990s by the Fraunhofer-Institute for Solar Energy Systems in Freiburg, southern Germany and through the International Energy Agency's Solar Heating and Cooling programme, established in 1977.

Table 2.6 *TIM Trombe wall installations (Generated from Peurortier et al. 2000).*

Year	Country	Location	Building type	TIM	Type	Area (m²)
1983	Denmark	Freiburg, Merzhausen	1-Family house	Capillary	Passive wall	12
1988	Switzerland	Ardon	Semi-detached house	Aerogel	Passive wall	120
1988	Denmark	Munchen, Grasweg	Bungalow	Honeycomb	Passive wall	40
1988	Denmark	Freiburg, Sauter	Office building	Honeycomb	Passive wall	31
1989	Denmark	Freiburg, Sonnenackerweg	8-Family house	Honeycomb	Passive wall	120
1989	Denmark	Düsseldorf, Hellerhof	Terrace house	Honeycomb	Passive wall	4*22
1990	Great Britain	Glasgow, Strathclyde	Student residential	Honeycomb	Passive wall	1000
1990	Denmark	Freiburg, Tiengen	Semi-detached house	Honeycomb	Passive wall	70
1991	Denmark	Freiburg, Tiengen	Semi-detached house	Aerogel	Passive wall	70
1991	Denmark	Kloster, Windberg	Residential building	Capillary	Passive wall	150
1992	Denmark	Freiburg, Christaweg	Self sufficient solar house	Capillary	Passive wall	80
1992	Denmark	DLR Köln Porz	Crew-training centre	Capillary	Passive wall	900
1993	Denmark	Leipzig, Wahren	School building	Capillary	Passive wall	330
1994	Denmark	Freiburg, Villa Tennheim	Residential building	Capillary	Passive wall	100

One project listed in Table 2.6 is the "Self Sufficient Solar House" in Freiburg (shown in the left photograph of Figure 2.19. Here, the entire dwelling's heating, electricity and hot water demand is met through Passivhaus design, photovoltaic panels for electricity generation, and an 80 m² passive TIM Trombe wall. Trombe wall cavity temperatures up to 70 °C, and temperature lags of 11 hours were predicted in a simulation study by Stahl *et al.* (1994). According to the results of a 3-year monitoring study by Voss *et al.* (1996), the property's space heating requirement was found to be almost zero and only necessary in extreme winter periods. The overall solar conversion efficiency of the Trombe wall was 47 % with average internal temperatures ranging from 16-28 °C. A mechanical shade was used to reduce summertime overheating (Voss *et al.* 1996).

Figure 2.19 *Self sufficient solar house (left) and Strathclyde University (right).*

The world's largest TIM / Trombe wall installation is at Strathclyde University in Glasgow, Scotland, shown in the right photograph of Figure 2.19 (Porteous and Macgregor, 2005). Here, 1040 m² of translucent insulation applied in glazing and Trombe wall applications has been installed over four separate student accommodation blocks serving 376 students. According to a 3-year monitoring study by Twidell *et al.* (1994), the south facade of the building provides a net energy gain throughout the year, providing up to 20 % of the buildings heating even during the mid-winter season. According to monitoring data, the internal temperature in the occupied common rooms was always in the range of 22-26 °C in winter. Available internal temperature data for unoccupied bedrooms with no auxiliary heating was not observed to drop below 18 °C. Overall student satisfaction was very high (with 91 % satisfied or very satisfied). During the summer, peak Trombe wall cavity temperatures of 50 °C were observed. Automated roller blinds serve to prevent overheating.

According to Peurortier *et al.* (2000), a well installed Trombe wall incorporating translucent insulation can save heating energy by up to 150 kWh/m² each heating period. Supporting this, Dolley *et al.* (1994) used a test cell to monitor the thermal

performance of a polycarbonate honeycomb TIM system retrofitted to a southern wall. Extrapolating the results, the study predicted that the annual space heating requirement would be reduced by 150 kWh/year in a typical pre-1930s UK solid walled dwelling, or 40 kWh/year in a super insulated home for every m² of TIM installed. Without shading, the hours of overheating (above 27 °C) were raised from 4 to 31 for properties with solid walls, and from 320 to 784 for super insulated homes.

Drivers and barriers

One of the main advantages of using TIM instead of single or multiple glazed covers is the considerable weight reduction, which can play an important factor in retrofit applications. Despite this, significant implementation of outdoor solar energy systems incorporating TIM has been slow. Platzer and Goetzberger (2004) estimated that over 15,000 m² of TIM had been installed across 85 buildings throughout Germany, Austria and Switzerland, indicating that the market was promising, but not satisfactory.

Platzer and Goetzberger (2004) and Wong *et al.* (2007) claim that commercial uptake of TIMs has been slow due to perceived high-investment costs and small number of payback studies. Peuportier *et al.* (2000) state that production quality must improve to reduce imperfections such as rough or melted edges, which can hinder clarity. In contrast, Kaushika and Sumathy (2003) state that considerable progress has been made to improve the quality and reduce the cost of manufacturing translucent insulation. Although capital costs to manufacture a fully functional TIM cladding system with solar control can reach € 600–1000/m², TIM glazing systems can have costs as low as € 24/m² (Kaushika and Sumathy, 2003; Wong *et al.* 2007). On the basis of this lower cost, Wong *et al.* (2007), calculated a 3–4-year payback period for an industrial production facility in Salzgitter, Germany, renovated with 7500 m² of TIM glazing costing € 180,000 with annual maintenance costs of € 7200. It is unclear whether these payback periods can be directly transferred to the domestic or commercial sector due to likely differences in design quality. Nonetheless, this payback period is significantly less than solid wall insulation and new double glazing.

Some of the key barriers include a lack of product development guides, imperfections in honeycomb or capillary TIMs, the low working temperatures of plastics and the potential for overheating when too much solar radiation is absorbed (Platzer and Goetzberger, 2004; Wong *et al.* 2007). Further to this, Wong *et al.* (2007) states that the high investment cost of TIM, shading devices and control measures has presented barriers to widespread implementation. Conversely, Wong *et al.* (2007), claim that, with improved design guidance combined with more information on the capital cost

and payback periods of TIM in use, there will be increasing evidence to outweigh the barriers currently hindering market growth, especially as fuel prices increase in future, reducing payback periods.

Cutting edge research

Cutting edge research into TIM products focuses on developing systems using quasi-homogenous silica aerogel (Bynum, 2001; Roberts, 2008a and 2008b; Baetens *et al.* 2011). This lightweight, nano-porous material is the only known solid with an excellent combination of high solar and light transmittance and low thermal conductance (Schultz and Jensen, 2008). According to Bahaj *et al.* (2008), aerogel glazing is often portrayed as the 'holy grail' of future glazing technology, offering potential to achieve U-values as low as 0.1 W/m² K, as well as high-solar energy and daylight transmittance of approximately 90 % (Bahaj *et al.* 2008; Schultz and Jensen, 2008).

Figure 2.20 displays the thermal conductivity of silica aerogel, compared to various TIMs and insulation products. As shown, silica aerogel has the lowest thermal conductivity of any material, ranging from 0.018 W/m K for granular silica aerogel to 0.004 W/m K for evacuated monolithic silica aerogel (Cabot, 2011; Yokogawa, 2005). Only vacuum technology has a thermal conductivity of the same order of magnitude (Zimmerman and Bertschinger, 2001).

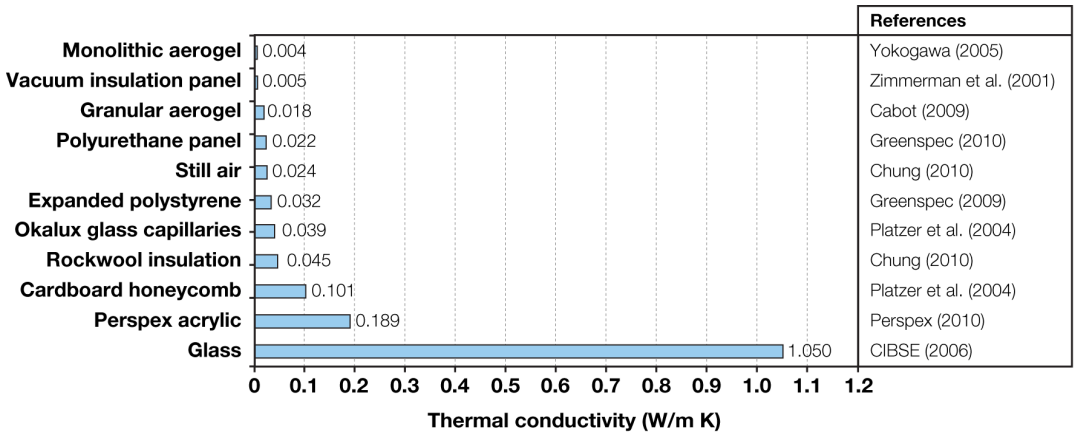

Figure 2.20 *Thermal conductivities of insulation (Generated from assorted references).*

According to Eames (2008), extensive research has been carried out to develop and characterise sealed vacuum technology. As such, Eames (2008) believes that the technology can easily be implemented into refurbishments. By comparison Bahaj *et al.* (2008) state that aerogel insulation is a promising technology, but it is stubbornly in the research and development phase. Similarly, Hrubesh (1998), Schultz and Jensen

(2008) and Roberts (2008b) claim that aerogel is a promising material, yet to realise its full potential in building applications.

The remainder of this literature review will focus on the use of aerogel insulation as a potential driver for new product development. This is due to the material's low thermal conductivity, and the scope for in-situ testing in a variety of retrofit applications. The translucent and insulating nature of this material means that it can be used to reduce the need for both heating and lighting in buildings.

2.3 Silica Aerogel Review

2.3.1 Background

Aerogels are synthetic low-density materials with unique physical properties. They are formed by removing the liquid from a gel under special drying conditions, bypassing the shrinkage and cracking experienced during ambient evaporation. This creates a three-dimensional nano-porous structure, containing 80-99.8 % air (Smirnova, 2002; Yokogawa, 2005). Due to their high porosity, aerogels exhibit the highest known insulation value of any solid, whilst being highly translucent to light and solar radiation (Schwertfeger *et al.* 1998; Platzer, 1987). Aerogels are often cited as a promising material for translucent insulation applications (Van-Bommel and De-Hann, 1995; Bynum, 2001; Soleimani-Dorcheh and Abbasi, 2008). The material can be produced in monolithic or granular form, as shown in Figure 2.21.

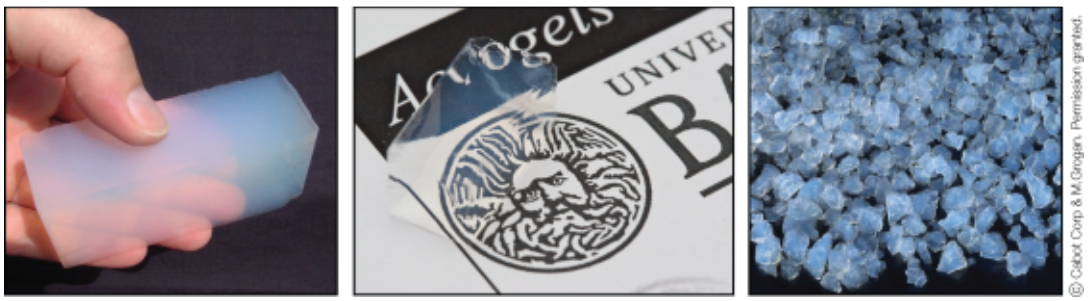

Figure 2.21 *Translucent monolithic aerogel (left), transparent monolithic aerogel (centre), and translucent aerogel granules (right).*

Aerogels were first reported by physicist Samuel Stephens Kistler in the early 1930's. Kistler (1931) aimed to test the hypothesis that "liquid inside a jelly can be replaced by a gas with little or no shrinkage".

Kistler's three-step experiment began by preparing a porous 'sol-gel' (a rigid body containing continuous solid and liquid networks) using sodium silicate and hydrochloric acid. This 'hydrogel' (where the liquid in the pores is water) was then soaked in alcohol several times over a 1-2 week period to strengthen the gel, causing the water inside the pores to be displaced. The resultant 'alcogel' (pores containing alcohol) was dried inside an autoclave using supercritical drying, whereby the temperature and pressure of the autoclave were simultaneously raised to 270 ^{o}C and 100 bar, causing the alcohol to become supercritical (i.e. it begins to vaporise without completely changing phase due to the high pressure). As a result, the alcohol gains properties of both a liquid and a gas, eliminating surface tension inside the gel and enabling the fluid inside the pores to drain out without collapsing the solid structure.

The newly formed 'aerogel' (pores containing air), could be safely handled when cool. The material possessed a low density and was opalescent. Kistler (1933) stated that numerous other materials had been successfully prepared, and that aerogels could be made from practically any material. Nowadays, silica aerogel is still the best-known and most widely prepared aerogel (Steiner and Walker, 2010).

2.3.2 Thermal properties

Aerogel is a super insulation material, since its thermal conductivity is lower than still air (Yokogawa, 2005). The total thermal conductivity of porous insulation depends on the amount of heat transfer through convection in the pores, conduction through the solid and pores, as well as radiation (Yokogawa, 2005; Ashby *et al.* 2009). This relationship is shown in Equation [2.1]:

$$k_{total} = k_{convection} + k_{solid\ conduction} + k_{gas\ conduction} + k_{radiation} \quad [2.1]$$

Typically, pores within conventional insulation are over 1 mm wide, allowing gas molecules to move freely and transfer thermal energy by convection (Yokogawa, 2005). By comparison, pores within aerogel can be as small as 20-40 nm (Soleimani-Dorcheh and Abbasi, 2008), being smaller than the mean-free path of air at 60-100 nm (i.e. the average distance between air molecules at normal atmospheric pressure). As a result, individual air molecules within the pores have no space to transfer thermal energy by convection (Yokogawa, 2005; Smirnova, 2002).

Conduction through the solid structure and air molecules within aerogel is also minimal. With little space for convection, air molecules constantly collide with the walls of the pores, suppressing gas conduction (Ashby *et al.* 2009). Furthermore, as aerogel

only contains 0.1-5 % silica and the thermal conductivity of air is very low, heat transfer is minimal (Bynum, 2001). Conduction in the gas will diminish with any decreases in pressure (Ashby *et al.* 2009). A vacuum inside the pores results in the best insulating properties. Yokogawa (2005) measured thermal conductivities of 0.004 W/m K (ten times better than conventional insulation) using this technique.

The amount of radiative heat transfer through aerogel is dependent on the intensity and wavelength of the thermal radiation, the optical properties of the material, the size and shape of its pores and the overall thickness (Ashby *et al.* 2009; Smirnova, 2002). At ambient temperature the nanosized pores and particles provide effective attenuation of infrared thermal radiation due to high levels of absorption and reflection (Zhu *et al.* 2007). According to Hartmann *et al.* (1987), radiative heat transfer at ambient temperature accounts for 10-15 % of the total thermal conductivity through aerogel.

2.3.3 Optical properties

The optical and infrared properties of silica aerogel have been well documented (Platzer, 1987; Fricke and Tillotson, 1997). It is a translucent insulation material that effectively transmits solar light, but blocks thermal infrared radiation (Fricke and Tillotson, 1997). The material exhibits high translucency, often accompanied by a slight bluish haze (Bynum, 2001). This can be attributed to 'Rayleigh scattering', an optical phenomenon that occurs when light scatters off particles smaller than the wavelength of light, where shorter wavelengths in the blue spectrum are most easily scattered.

Figure 2.22 displays the solar radiation spectrum of ultraviolet (UV), visible light and infrared radiation in the atmosphere. Figure 2.23 displays respective transmission levels through silica aerogel.

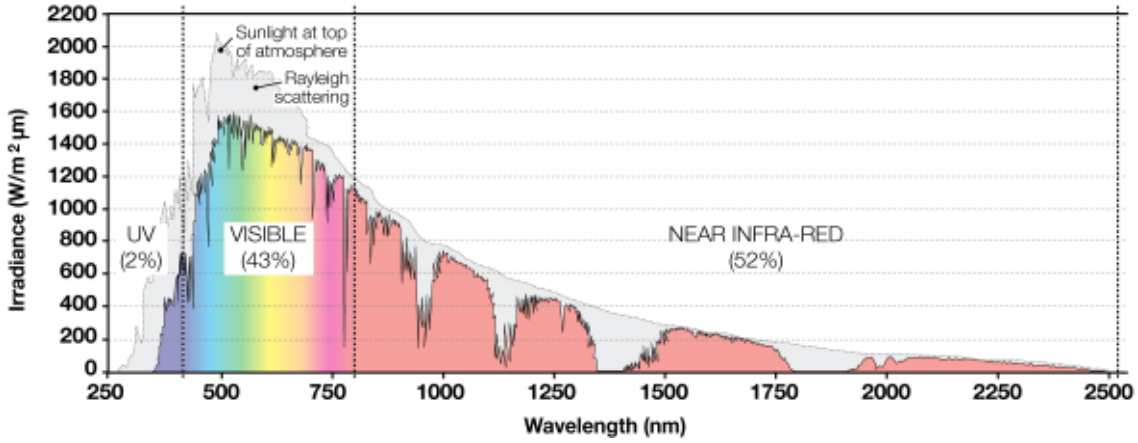

Figure 2.22 *Solar spectral irradiance (Adapted from Duffie and Beckman 2006).*

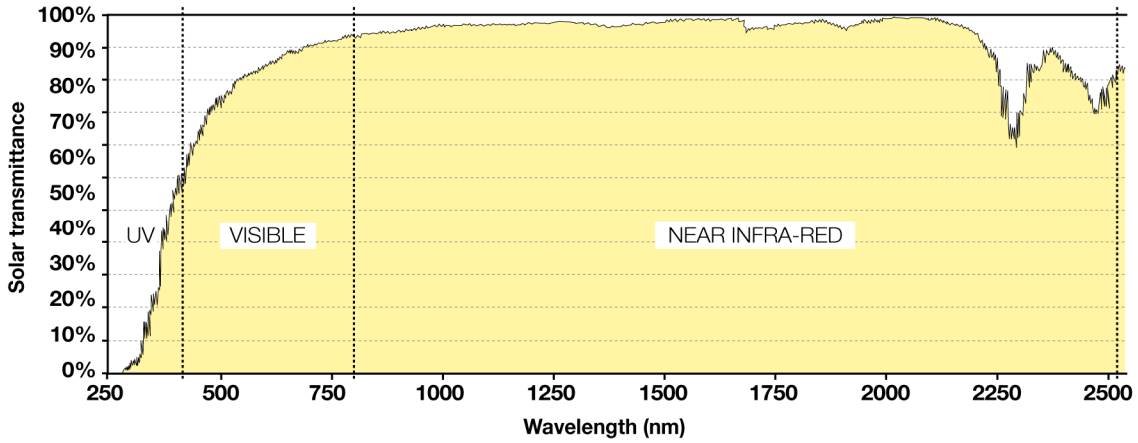

Figure 2.23 *Shortwave transmission through silica aerogel (Adapted from MMG 2004).*

Towards the blue and UV spectral region, absorption is low and transmission levels are reduced due to scattering effects (Smirnova, 2002; MMG, 2004). As seen, in Figure 2.23, transmission levels increase for longer wavelengths of visible light and are high across the near-infrared spectrum, highlighting the materials potential to transmit heat in solar energy applications.

2.3.4 Manufacturing process

A diagram showing the different ways aerogel can be produced is displayed in Figure 2.24. The process has three steps: gel preparation, ageing and drying. Drying takes place through either high temperature supercritical drying (HTSCD), low temperature supercritical drying (LTSCD) or ambient pressure drying (APD):

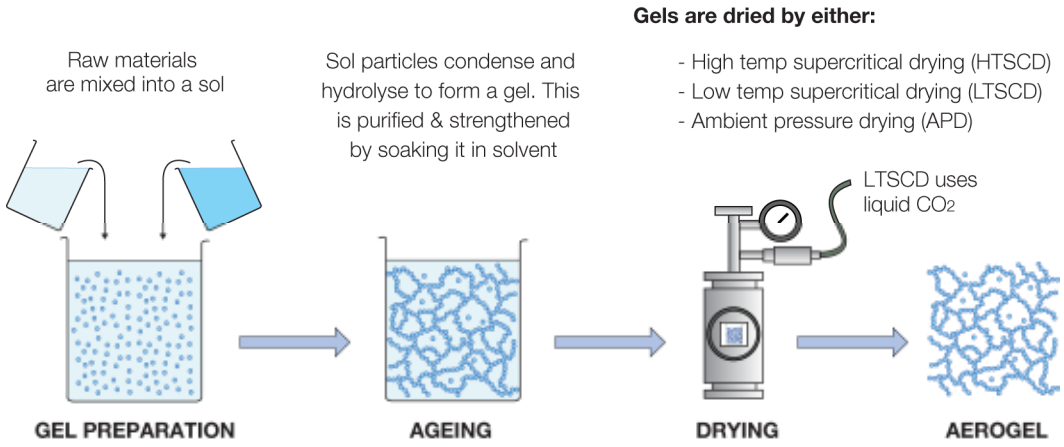

Figure 2.24 *Aerogel production (Adapted from Hüsing and Schubert 2005).*

Before mid 1980's, risks associated with supercritical drying of alcohol were major obstacles to high volume aerogel production (Duer and Svendsen, 1998; Wong *et al.*

2007). Improvements in the manufacturing processes have yielded more cost effective aerogels that are economic to produce on a commercial scale (Deshpande *et al.* 1992; Van-Bommel and De-Hann, 1995; Schwertfeger *et al.* 1998; Ashby *et al.* 2009). The material is produced in monolithic form in laboratories and is available commercially in granular form. Properties such as density, conductivity and hydrophobicity can be optimised through additives (Steiner and Walker, 2010).

Gel preparation

The most common technique for gel preparation involves reacting a silicon precursor, such as sodium silicate (known as 'water-glass'), tetramethoxysilane (TMOS) or tetraethoxysilane (TEOS) with water in a solvent such as ethanol or methanol at ambient temperatures and pressures (Steiner and Walker, 2010), forming silica nanoparticles. Gelation occurs when enough silica nanoparticles agglomerate to form a continuous network spanning throughout the entire volume of sol.

Ageing

Once a silica gel is prepared, it must be given time to age using a solvent exchange process. This is achieved by soaking the gel within a pure organic solvent, usually methanol, ethanol or acetone for up to 24 hours. During this process, solvent diffuses into the pores of the gel in place of any water and impurities. The process, strengthens the gel network, increases transparency and prevents cracking during drying. The solvent is replaced each time equilibrium in concentration is reached. Typically, this step is repeated 3-4 times (Steiner and Walker, 2010).

High temperature supercritical drying (HTSCD)

This process was first used by Kistler (1931) to dry aerogel. Drying relies upon heating and pressurising the wet-gel to ~240 °C at ~ 100 bars, i.e. the conditions that transform alcohol into a supercritical fluid (shown in the phase diagram in Figure 2.25).

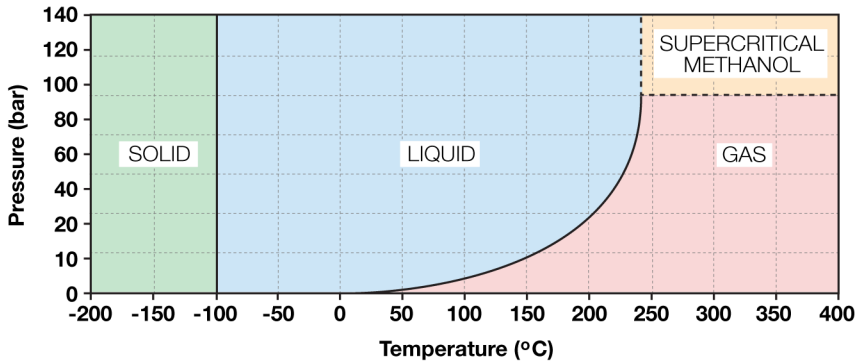

Figure 2.25 *Methanol phase diagram (Adapted from Soleimani-Dorcheh and Abbasi 2008).*

Gels formed using HTSCD have high optical quality and low thermal conductivity. However, the process can be dangerous if proper safety precautions are not taken. In 1984, the Airglass laboratory in Sweden was destroyed due to an autoclave leaking out 1000 litres of methanol at 260 °C and 80 bar (Smirnova, 2002).

Low temperature supercritical drying (LTSCD)

This method of drying was suggested by Tewari *et al.* (1985). Here, solvent inside a wet gel is replaced with a liquid possessing a critical point closer to ambient temperature. Liquid CO_2 was found to be practical, as it is non-flammable and has a low critical point of 31.1 °C and 72.8 bars, as shown in Figure 2.26. Drying can therefore take place at 40 °C, compared to 270 °C, making the process more viable for commercial production. Van-Bommel and De-Hann (1995) developed the technique further showing that supercritical CO_2 could be substituted instead of liquid CO_2 prior to drying.

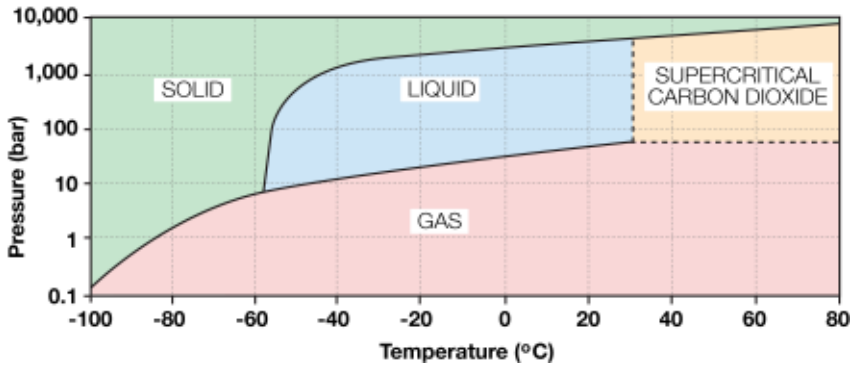

Figure 2.26 *CO_2 phase diagram (Adapted from Soleimani-Dorcheh and Abbasi 2008).*

Ambient pressure drying (APD)

This process (also called 'subcritical drying') emerged in mid 1990s. The process involves chemically modifying the surface of a wet-gel so that it becomes hydrophobic prior to drying. When dried ambiently, the gel partially collapses but re-expand to 85 % of its original volume, since the internal network does not stick together (Schwertfeger *et al.* 1998; Steiner and Walker, 2010). This 'springback effect', was first reported by Desphande *et al.* (1992). Schwertfeger *et al.* (1998), developed the process further enabling low cost water-glass to be used in the gel preparation phase.

The costs involved in ambient pressure drying, are substantially lower than supercritical methods due to simpler technology, lower energy costs and less potential hazards (Smirnova, 2002). Gels dried by ambient pressure drying are typically 50-80 % denser than supercritically dried aerogels, thus are less translucent but mechanically

stronger (Steiner and Walker, 2010). They have a slightly lower surface area, but retain low thermal conductivities of 0.010-0.018 W/m K (Schwertfeger *et al.* 1998).

2.3.5 Product development progress

Commercial applications

The largest manufacturer of translucent aerogel granules is Cabot Corporation. In 2001, Cabot Corporation patented a commercialised process for manufacturing aerogel granules using ambient pressure drying, licensing their product as Lumira™ (formerly Nanogel™). Shown in the left diagram of Figure 2.27, Lumira™ consists of 1-5 mm translucent hydrophobic silica aerogel granules, which are completely moisture and mildew resistant (Cabot, 2004). The granules are produced by spraying the wet-gel with water-glass and sulphuric acid prior to drying forming small spheres that are ambiently dried (Zhu *et al.* 2007). Cabot's production facility in Frankfurt, Germany, can produce about 10,000 tonnes of Lumira™ per year (Werner and Brand, 2010).

Figure 2.27 *Lumira™ aerogel granules (left) and Spaceloft™ aerogel blankets (right).*

Cabot Corporation's Lumira™ has been used in a variety of applications. Suppliers such as Kalwall, Okalux, Lexan, Pilkington and Xtralite have used Lumira™ inside glass, lightweight polycarbonate and glass-reinforced-polyester (GRP) glazing units, skylights and structural building panels, as shown in Figure 2.28.

Figure 2.28 *Encapsulated granular aerogel used in commercial facade systems.*

In contrast, Birdair Inc have used Lumira™ to develop Tensotherm™, a translucent tensile roof membrane containing granular aerogel sandwiched between two layers of Teflon™ fabric. Rockwool Ltd have launched Aerowool™, a thin composite consisting of mineral wool and Lumira™ for interior wall insulation. Cabot Corporation has also used Lumira™ granules as loose fill cavity wall insulation (Cabot, 2011).

One of Cabot Corporation's major competitors in the aerogel insulation market is Aspen Aerogel. In 2001, Aspen Aerogel developed a novel flexible aerogel composite by casting silica gel onto a fibrous batting, which is then dried using supercritical CO_2. Shown earlier in the right side of Figure 2.27, this aerogel is used in products such as Spaceloft™ and Spacetherm™. These flexible blankets have been used to upgrade interior and exterior walls, window frames, floors and roofs of commercial, residential and institutional buildings. Other silica aerogel manufacturers include Airglass in Sweden, BASF in Germany and Thermalux in the USA. Airglass have produced monolithic slabs of aerogel up to 600 x 600 x 10 mm. BASF sells hydrophobic aerogel in granular and powder form. Thermalux produces opaque aerogels (Zhu *et al.* 2007).

Research into monolithic aerogel glazing

To date, several small-scale prototypes have been constructed to characterise the performance of monolithic silica aerogel in glazing. Samples are sandwiched between glass and evacuated to protect the aerogel from tension and moisture, as most aerogels are brittle and hydrophilic (unless waterproofed during manufacture) they degrade in contact with water (Zhu *et al.* 2007). Shown in Figure 2.29, the largest prototype was a 1.2 m^2 window, developed by Schultz and Jensen (2008), consisting of four 55 cm × 55 cm × 15 mm monolithic tiles fitted into an evacuated sealed framing unit.

Figure 2.29 *Aerogel glazing prototypes produced by Schultz and Jensen (2008).*

The prototype developed by Schultz and Jensen (2008) achieved a centre pane U-value of 0.66 W/m² K and an overall U-value of 0.72 W/m² K (measured using a hot box), indicating that thermal bridging at the edges was small. The direct solar transmittance was 75–76 % and the normal transmittance in the visible spectrum was 85–90 %. In a similar study, Duer and Svendsen (1998) measured the performance of five different monolithic aerogel slabs, produced at different laboratories, ranging in thickness from 7-12 mm. Centre pane U-values of glazed samples ranged from 0.41-0.47 W/m² K. Solar and visual transmittance ranged from 74-78 % and from 71-73 %, respectively.

Despite its impressive combination of thermal and optical properties, monolithic silica aerogel is yet to penetrate the commercial glazing market. According to Rubin and Lampert (1983), the cost, long processing time of aerogel, difficulty in manufacturing uniform samples and lack of adequate protection from tension and moisture were key barriers hindering progress. Duer and Svendsen (1998) and Bahaj *et al.* (2008) state that further work is required to improve clarity of samples if they are to replace conventional windows.

A key issue is that the nanostructure of silica aerogel scatters transmitted light resulting in a hazy view. Schultz and Jensen (2008) claim that through improved heat treatment techniques, the Airglass AB plant is capable of producing aerogel tiles with parallel and smooth surfaces, resulting in undistorted views when shielded from direct solar radiation. However, when exposed to non-perpendicular solar radiation, visual distortion still occurs. According to Jensen *et al.* (2004), Schultz *et al.* (2005) and Schultz and Jensen (2008), aerogel glazing is an excellent option for large areas of north-facing facades, enabling a net energy gain during the heating season. Through developments in edge sealing techniques, units are anticipated to have a lifespan of 20–25 years without degradation (Schultz and Jensen, 2008).

Research into granular aerogel glazing

The use of granular aerogel in glazing for energy conservation offers an alternative solution to monolithic aerogel which is cheaper, more robust and easier to produce on a commercial scale (Fricke *et al.* 1987). Systems should not be considered as a direct replacement for transparent windows, as the granules restrict the clear view outside. Instead, this material offers potential to achieve low U-values, enhanced light scattering and drastically reduced sound transmission in areas where an outside view is not essential (Wittwer, 1992).

According to Fricke *et al.* (1987), in general, monolithic aerogel systems are better understood than the granular fillings. The in-situ performance of granular aerogel

glazing was originally investigated by Wittwer (1992). U-values from 1.1 to 1.3 W/m² K were measured for 20 mm thick glazing units filled with granules ranging from 1 to 9 mm in diameter. Smaller granules perform better thermally, as less heat is conducted through air gaps between granules. Optically, the larger aerogel granules permitted more light and solar transmission.

More recently, Reim *et al.* (2002; 2005) have measured and modelled the performance of granular aerogels encapsulated inside a 10 mm twin-wall plastic panel, sandwiched between two glass panes with an insulated gas filling. The twin-wall panel was selected to prevent granules from settling over time, creating a thermal bridge along the top edge. U-values as low as 0.37–0.56 W/m² K were calculated for prototypes containing krypton/argon gas fillings. Without the glass cover panes, the solar and light transmission was 88 and 85 %, respectively. Using a thermal model in a German climate, Reim *et al.* (2002) calculated the energetic benefit of granular aerogel glazing to be comparable to triple glazing. Results demonstrated that granular aerogel glazing could reduce the risk of overheating on southern and east/west facades. On north-facing facades, the energetic balance of aerogel glazing was significantly better than triple glazing due to improved heat retention.

Research into granular aerogel shutters

This literature review identified a single study assessing the performance of granular aerogel applied to existing windows in a retrofit application. In this study, Schultz (1993) constructed three 600 x 600 x 20 mm translucent insulating shutters using acrylic panels filled with granular aerogel, as shown in Figure 2.30.

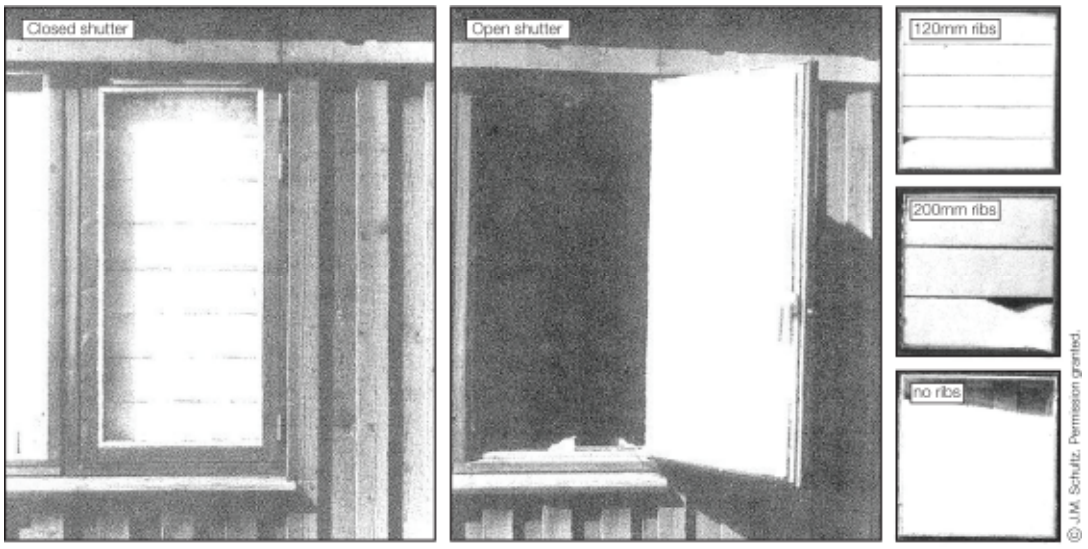

Figure 2.30 *Insulating shutters containing granular aerogel built by Schultz (1993).*

Each panel incorporated a different internal ribbed construction and was fixed to the inside frame of a south facing double glazed window within a test building at the Technical University of Denmark. Monitoring consisted of in-situ U-value and solar transmission testing, followed by a two year photographic study investigating the impact of moisture ingress and granule settling with the shutters taken down and exposed the outdoor Danish climate. The aerogel had a conductivity of 0.029 W/m K (opposed to 0.018 W/m K, which is now commercially available).

Schultz (1993) calculated that the shutters would improve the U-value of a double glazed window from 2.86 W/m^2 K to 1.01 W/m^2 K. By comparison, the lowest measured U-value was 1.68 W/m^2 K. According to Schultz (1993), this large discrepancy was due to the product not fully covering the window frame. The reduction in solar transmission was not found to be detrimental, changing from 0.75 to 0.45. Long term settling of the granules was observed in all three prototypes, but was found to be most significant in the panel with no internal ribs, reducing the thermal performance by approximately 20 %. Moisture ingress was also observed in all cases; as the aerogel was not water-proof it degraded over time, turning white and reducing solar transmission by 3 %.

According to Schultz (1993), the results of this study indicated that insulating shutters with granular aerogel are an attractive alternative to traditional shutters, providing an equivalent heat loss coefficient from half the thickness. Regarding future development, Schultz (1993) stated that an optimum shutter design should cover the whole window area including the fixed part of the frame, use hydrophobic granular aerogel to prevent degradation from moisture ingress and have rib spacing below 120 mm to prevent any air gaps forming along the top of the shutter.

According to Schultz (1993), key benefits of a granular aerogel shutter would be its ease of handling, non-load bearing burden on existing windows and the ability to remain in front of a window for the whole of the heating season, due to its high solar transmission of approximately 50 %. Regarding monolithic aerogel, Schultz (1993) states this will always be too expensive to apply to insulating shutters. Adding to this, Schultz (1993) states that monolithic aerogel shutters are likely to incur an “irritating distortion” as the view outside would not be fully transparent, opposed to granular aerogel shutters which would act as a source of diffused light.

Research into Aerogel Solar collectors

This literature review found no examples of granular or monolithic aerogel applied to flat plate solar air heaters and only a few studies exist assessing the aerogel applied to solar water collectors.

Svendsen (1992) constructed a 1.4 m^2 flat plate solar water collector prototype incorporating monolithic silica aerogel. The design consisted of black copper absorber sheet integrated with black copper tubes, sandwiched between monolithic silica aerogel tiles (evacuated to 0.1 bar) at the top, back and edges of the absorber to eliminate cold bridges. All of the aerogel tiles were nominally 60 x 60 x 2 cm, had a solar transmission of 0.9 and were produced by Airglass Ltd. Svendsen (1992) commented that difficulty in producing and drying the aerogel tiles caused imperfections causing condensation which may have negatively affected results. Nonetheless, controlled testing inside a solar chamber demonstrated that the prototype could achieve 60-80 % efficiencies.

Supporting calculations by Svendsen (1992) demonstrated that the prototype could generate up to 700 kWh/m^2/year, twice as high as commercial flat plate collectors. Svendsen (1992) simulated the performance of collectors with 15, 20 and 25 mm aerogel thicknesses. The highest annual energy saving was predicted for the 25 mm collector, but Svendsen (1992) commented that the 20 mm collector would yield equally satisfactory results. Further improvements to efficiency were claimed to be possible by utilising ground reflected as well as direct solar radiation.

According to Svendsen (1992), the main advantage of aerogel was its ability to provide high efficiency, due to its low heat losses and high ability to utilise solar irradiance as low as 90 W/m^2, compared to 240 W/m^2 for conventional glazed solar thermal collectors. The author commented that the quality of the aerogel available was acceptable, but the material must be mass produced for it to be of commercial interest.

Further modelling by Nordgaard and Beckman (1992) assessed the performance of monolithic silica aerogel in solar collectors for water heating. In particular, the study assessed the distribution of direct, scattered, and absorbed solar radiation in monolithic silica aerogel tiles of different thicknesses. Top loss coefficients of 1.0-2.25 W/m^2 K for 10 mm thick covers, 0.5-1.5 W/m^2 K for 20 mm thick covers and 0.25-1.0 W/m^2 K for 40 mm covers were calculated across a range of absorber plate temperatures. According to Nordgaard and Beckman (1992) the total transmittance of a 20 mm thick monolithic silica aerogel tile equals that of single glass pane, and increasing the thickness to 45 mm reduces total solar transmittance to 0.72, approximately equivalent to double glazing.

Simulations by Nordgaard and Beckman (1992), compared the performance of a typical glazed collector to the monolithic silica aerogel collector designed by Svendsen (1992). According to Nordgaard and Beckman (1992), the reduction in solar transmittance compared to a single glass pane is more than compensated by the reduction in heat

losses, providing efficiencies of more than 60 % and increasing the yearly gain by as much as 41 %. Nordgaard and Beckman (1992) commented that monolithic silica aerogel collectors could be particularly applicable for large district heating networks, but the lack of commercial availability and the high capital cost are significant barriers Conversely, if monolithic silica aerogel was mass produced and the collectors were fully developed, it is expected that the collector will be a significant breakthrough for solar heating systems.

Regarding granular aerogel, although no prototype testing studies were found, Ortjohann (2001) predicted that super-insulating solar thermal collectors could be produced using granular aerogel sandwiched inside an evacuated collector design. The main benefit would be its low weight, ease of handling and ability to provide an efficient collector design without an optimised absorber technology. Conversely, the main disadvantage would be the difficulty in maintaining the long-life of the vacuum technology (Ortjohann, 2001). Countering this, the performance of granular aerogel without a vacuum has been investigated by Reim *et al.* (2005). It was claimed that their glazing prototype with solar transmittance of 65 %, possessed high potential for use in insulated solar walls, with 40 % less heat loss than conventional glass solar collectors, without the need for an evacuated product.

Research into Aerogel Trombe walls

The potential use of monolithic or granular aerogel applied to passive solar Trombe walls has been discussed by Fricke *et al.* (1987), Fricke (1988; 1992), Caps and Fricke (1989), Fricke and Tilotson (1997) and Peurortier *et al.* (2000). This system would consist of a thermally massive black-painted brick wall, over which would be translucent insulation consisting of monolithic or granular silica aerogel between two protective glass panes (Fricke, 1992). Most of the produced heat would be transferred into the house. To prevent overheating, a shading device would be necessary.

There are two examples of large non-evacuated granular Aerogel Trombe walls mentioned in academic literature, both installed on semi-detached houses. However, there is little detailed information regarding the cost, architectural integration or in-situ thermal performance of these installations. According to Fricke and Tilotson (1992) a “convincing example” was a 120 m^2 system installed on two-family household in Ardon, Switzerland in 1989, constructed for a lower cost than conventional insulation. Here, the energy consumption for heating was found to be exceptionally low at about 300 litres of oil per year, equivalent to approximately 3500 kWh/year (compared to the average UK household gas consumption of 16,000 kWh/year (BERR,

2007)). A second example was a 70 m² system installed in Freiburg-Tiengen, Germany in 1991. No supporting literature could be found regarding this system.

In 2007, a prototype of an Aerogel Trombe wall was designed and constructed as part of the US Department of Energy's 'Solar Decathlon' project: a biennial event challenging teams to design, build, and operate solar powered houses that are cost-effective, energy-efficient, affordable and attractive. The prototype, shown in Figure 2.31, was designed by W. Colson, Senior Vice President of Hunter Douglas Inc. and was constructed in collaboration with a team of researchers from Massachusetts Institute of Technology, USA, lead by K. Keville.

Figure 2.31 *The Hunter Douglas Solar Decathlon house incorporating a Trombe wall containing granular aerogel and glass blocks filled with water.*

The south facing aerogel Trombe wall, named the "Hunter Douglas Solar Window" consists of 112 modular acrylic blocks, each containing a 1-inch layer of encapsulated granular aerogel in-front of a 2.5 inch layer of encased water. According to a press release from Hunter Douglas (2007), this encased water-base thermal mass layer heats up to approximately 100 degrees Fahrenheit (~38 °C) on cold sunny days in winter and the aerogel prevents heat loss to outside, while the interior thermal mass slowly releases its heat to the dwelling over a 24-36 hour period. When the product was used as the sole heating source over the course of two winters, the resultant internal temperature of the dwelling was 21 °C for 90% of the time, with some supplemental heat required for the remaining 10%.

Beyond information in press releases, this literature review found no peer reviewed studies or empirical monitoring data evaluating the in-situ performance of this prototype. In 2007, W. Colson registered the US Patent 8082916 "Solar heating blocks" for the design of the double compartment acrylic blocks, containing water and a translucent insulating material, such as aerogel, for use in assembling solar heating panels in the walls of buildings (Colson, 2007). According to personal communication with W. Colson on 20th July 2012, a technical paper on this product is being prepared.

Commenting on monolithic aerogel, modelling by Caps and Fricke (1989) finds that a Trombe wall containing a 15 mm thick layer of evacuated monolithic silica aerogel between double glazing cover achieves minimal solar heat losses compared to conventional TIM due to its high solar transmission of 50-60 % and low U-value of 0.5 W/m² K. However, Caps and Fricke (1989) state conventional TIMs are technically simpler as the evacuated system would also require a durable vacuum-tight metal rim.

2.3.6 Environmental impact assessment

According to Lawrence Berkeley Laboratory, the production and use of silica aerogel is environmentally benign, the product is non-toxic, non-flammable and can be easily recycled (MMG, 2004). Conversely, according to manufacturing studies, silica aerogel requires reasonably toxic chemicals, diffusion-controlled processes that consume a lot of solvent and, depending on the drying process, high-pressure vessels running for a long time (Soleimani-Dorcheh and Abbasi 2008; Steiner and Walker, 2010).

At present, the only data on embodied energy and CO_2 of silica aerogel comes from Aspen Aerogel opaque insulation blankets. Shown in Figure 2.32, its production energy is 53.9 MJ/kg and its CO_2 burden is 4.3 $kgCO_2/kg$.

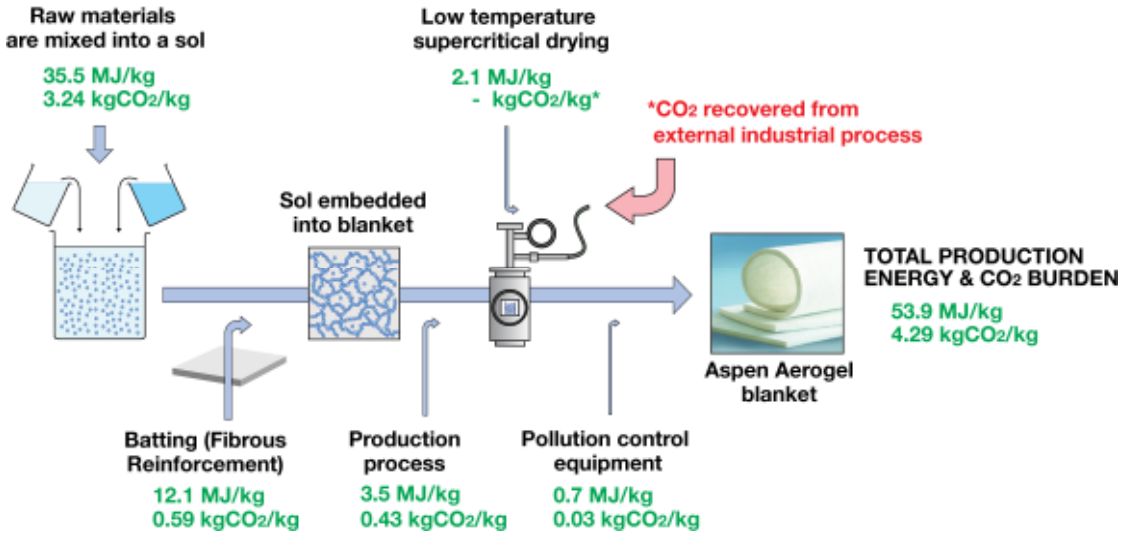

Figure 2.32 *Production energy & CO_2 in Spaceloft™ (Adapted from Aspen Aerogel 2011).*

Allocation of these values across the production line was obtained from personal communication on with G. Berry (Technical advisor at Proctor Group Ltd; UK suppliers of Aspen Aerogel Spacetherm™ blankets) on 25th September 2009. Note that Aspen Aerogel does not disclose the amount of CO_2 required during supercritical extraction, highlighting a need for further investigation. According to Aspen Aerogel, this CO_2 is a recycled waste product recovered from ethanol and ammonia production plants.

To date there has been no peer-reviewed life cycle assessment (LCA) of aerogel conducted to the ISO 14000 standards. Both Cabot Corporation and Aspen Aerogel received a 'Silver' Cradle-to-Cradle environmental award from McDonough Braungart Design Chemistry (MBDC) for their aerogel production. MBDC claim to evaluate a products complete formulation, energy use, water use and recycling potential when assessing environmental impacts (MBDC, 2008). Unfortunately, the detail behind the data collection and interpretation stages forming these studies is confidential, making it difficult to assess the rigour and validity of the results. According to GBA (2007), the MBDC Cradle-to-Cradle programme does not undergo third party certification, thus does not comply with the ISO 14000 standards for life cycle assessment.

According to the University of Bath's 'Inventory of Carbon and Energy' produced by Hammond and Jones (2008), the production energy and CO_2 burden associated with natural insulation materials such as hempcrete and wood fibreboards ranges from 3.5-26.8 MJ/kg and 0.2-1.7 $kgCO_2/kg$ respectively. Mineral-based insulations such as rock wool and glass mineral wool are typically higher ranging from 16.6-38.8 MJ/kg and 1.1-1.4 $kgCO_2/kg$ respectively. Oil derived insulations such as Phenolic foam and expanded polystyrene typically have the highest production energy and CO_2 burden ranging from 70-98.3 MJ/kg and 2.5-3 $kgCO_2/kg$, respectively. Figure 2.33 and Figure 2.34 normalise these figures for the production energy and CO_2 burden and compare them against available data for granular aerogel and aerogel blankets.

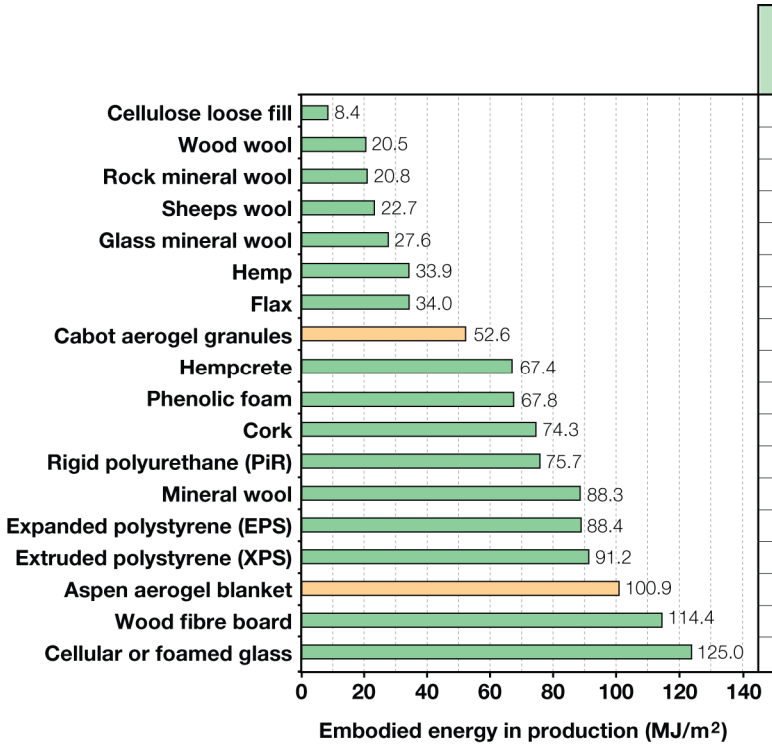

	Embodied energy (MJ/kg)	Thermal conductivity (W/m K)	Density (kg/m³)
Cellulose loose fill	6.7	0.039	32
Wood wool	10.8	0.038	50
Rock mineral wool	18.3	0.036	32
Sheeps wool	23.2	0.039	25
Glass mineral wool	38.8	0.036	20
Hemp	21.8	0.039	40
Flax	26.8	0.039	33
Cabot aerogel granules	41.8	0.018	70
Hempcrete	3.5	0.070	275
Phenolic foam	70	0.022	45
Cork	15.0	0.044	113
Rigid polyurethane (PiR)	86.6	0.025	35
Mineral wool	16.6	0.038	140
Expanded polystyrene (EPS)	98.3	0.036	25
Extruded polystyrene (XPS)	95.0	0.032	30
Aspen aerogel blanket	53.9	0.013	144
Wood fibre board	13.0	0.044	200
Cellular or foamed glass	26.5	0.043	110

Figure 2.33 *Embodied energy data for insulation (Generated from assorted references).*

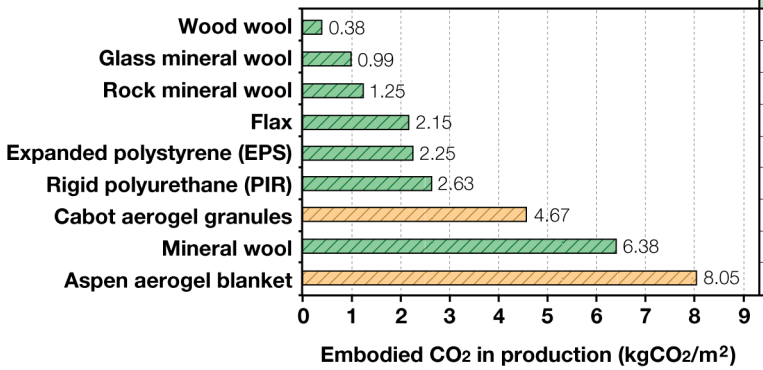

Embodied CO_2 ($kgCO_2/kg$)	Thermal conductivity (W/m K)	Density (kg/m^3)
0.2	0.038	50
1.4	0.036	20
1.1	0.036	32
1.7	0.039	33
2.5	0.036	25
3.0	0.025	35
3.7	0.018	70
1.2	0.038	140
4.3	0.013	144

Figure 2.34 *Embodied CO2 data for insulation (Generated from assorted references).*

Note that the functional unit is based upon the thickness and density of insulation, per m^2, required to achieve an R-value of 1 m^2 K/W, based on guidance by CEPMC (2000) and Schmidt *et al.* (2004). Data for Cabot Corporation's aerogel granules are based upon the impacts of the Aspen Aerogel blankets shown in Figure 2.32, but without the impact of the batting affiliated to the production of the opaque blanket and with adjusted values for density and thermal conductivity.

As shown in Figure 2.33 and Figure 2.34, the embodied energy of Aspen Aerogel's blanket is considerable compared to conventional insulation materials, despite its impressive insulation properties. To a certain degree this is influenced by the high density of the material at 144 kg/m^3, due to the fibrous battling. However, the estimated impact for Cabot's granular aerogel is also high (partly due to the higher conductivity of the granules), considering that it is less dense at 70 kg/m^3. These findings imply that aerogel may have a relatively high environmental impact, despite its impressive thermal performance. Note that available data for double-glazing indicates that production energy and CO_2 burden can be much higher at 360-5470 MJ/m^2 and 18-279 $kgCO_2/m^2$, depending on the frame type and gas fill. Nonetheless, as these figures are relatively high, compared to conventional insulation, it demonstrates that a full environmental assessment may be required to justify the performance of energy aerogel based retrofit technologies.

2.4 Conclusion

This literature review was split into three sub-chapters, investigating the UK retrofit challenge, emerging retrofit technologies and ultimately focusing on silica aerogel as a promising material for further research in line with the objectives of this thesis.

Millions of existing buildings across the UK have obsolete existing windows and/or 'hard-to-treat' solid brick walls that are difficult to improve cost effectively. There is a strong correlation between the age of the UK building stock and its thermal efficiency as Building Regulations setting standards for insulation were only enforced after 1976. Poor quality construction, thermal comfort take-back and a lack of monitoring following refurbishments pose a serious threat to obtaining real, long term energy savings. Success has been achieved in Germany through the adoption of the Passivhaus standard in new and existing homes. However, without the appropriate construction skills and easy access to cost effective components, it will be difficult for this standard to become practical in the UK, particularly due to the complexities associated with achieving such high air tightness levels in old, leaky buildings. The significance of embodied energy over the life cycle of refurbished buildings and retrofit products needs to be better understood. The existing building stock should be viewed as a resource rather than a challenge.

Translucent insulation materials are an underdeveloped area of research, with potential to reduce energy consumption for heating and artificial lighting in existing buildings. Over the past 25 years, translucent insulation has been applied to windows, walls, skylights, roofs and high-performance solar collectors, yet the market penetration is not satisfactory. It is claimed that with improved design guidance combined with more information on the capital cost and payback periods in use, there will be increasing evidence to outweigh the barriers currently hindering market growth, especially as fuel prices increase in future, reducing pay back periods.

Cutting edge research in translucent insulation focuses on product development utilising silica aerogel insulation. This unique nano-porous material has the lowest thermal conductivity of any solid, whilst being highly translucent to light and solar radiation. Solid tiles of monolithic silica aerogel can be produced in laboratories, but the high cost, long processing time and difficulty manufacturing uniform samples protected from tension and moisture are key barriers hindering market growth. By comparison, mass produced aerogel granules available to the construction industry can achieve similar low thermal conductivities and high translucency, whilst being more robust and cheaper to produce on a commercial scale.

To date, the in-situ performance of granular aerogel in several novel applications has not yet been fully established. Moreover, the environmental impact of silica aerogel production is unclear. Specifically, three research gaps have been identified:

- **RESEARCH GAP 1:** There is a lack of studies assessing the predicted and in-situ performance or payback period of a translucent retrofit solution, incorporating granular aerogel to improve the thermal performance of existing single glazed windows without blocking out all of the useful natural light

- **RESEARCH GAP 2:** There is a lack of publically available life cycle assessments of the silica aerogel following the ISO 14000 standards, despite many solvents being used in its production, often accompanied by intensive drying processes, which may consume large amounts of energy and CO_2.

- **RESEARCH GAP 3:** There is a lack of studies assessing the predicted and in-situ performance or payback period of an active solar air collector incorporating granular aerogel into the cover, retrofitted to the external south facing wall of a property to provide insulation and solar heated warm air.

In line with the objectives of this thesis, the first research gap will be addressed via a pilot study to verify technical performance of granular aerogel in a proof-of-principle prototype. The second research gap will be addressed through a streamlined life cycle assessment of silica aerogel to verify the environmental performance of the material. The third research gap will be addressed by designing a fully functional prototype with its technical and environmental performance verified. Addressing each research gap individually provides three contributions to knowledge under the category of "*empirical work which has not been done before covering scientific measurement and/or engineering development*" (Francis 1976; Phillips and Pugh, 1992).

It should also be noted that the literature review identified scope to investigate issues such as the technical and economic challenges associated with deep retrofitting and the Passivhaus Standard. In addition, the literature review identified scope to undertake analysis to facilitate further research into the development of passive solar Trombe walls incorporating granular aerogel and their variable performance applied to different building types across the UK. Both of these areas are addressed in two further studies in this thesis (in Chapters 5 and 7 respectively) and are motivated by live project work undertaken with the sponsor company during this EngD.

Chapter 3

IMPROVING THE THERMAL PERFORMANCE OF EXISTING WINDOWS USING TRANSLUCENT GRANULAR AEROGEL

Abstract

This chapter contains a pilot study assessing the potential for translucent granular aerogel to be retrofitted over single glazed windows to reduce heat loss without blocking out all of the useful natural light and solar radiation. In-situ U-value and light transmission testing of 6 mm and 10 mm thick prototype panels consisting of clear twin-wall polycarbonate sheets filled with granular aerogel was carried out and validated with steady state calculations. The core contribution to knowledge from this study is that an 80 % reduction in the rate of heat loss is possible without detrimental reductions in light transmission. Payback calculations accounting for the inevitable thermal bridging from openable domestic retrofit solutions such as roller shutters or pop-in secondary glazing suggest that a return on investment between 3.5 and 9.5 years is possible if products are consistently used over the heating season. A further case study in this chapter covers a parametric assessment of heating, cooling and day lighting loads in offices with different glazing types. Preliminary findings indicate that a translucent aerogel shutter, which operates automatically, retrofitted to a single glazed or first generation double glazed office, can meet or exceed the performance of new triple glazing across all facade orientations.

3.1 Introduction

This study aims to provide in-situ U-value and light transmission measurements, validated with theoretical calculations to verify the thermal, optical and financial performance of a novel translucent retrofit solution incorporating granular aerogel to improve the thermal performance of existing windows. Illustrated in Figure 3.1, granular aerogel has potential to be encapsulated inside clear plastic or glass casings in a variety of novel retrofit solutions such as sliding, hinged or roller shutters, airtight Venetian blinds or 'pop-in' secondary glazing.

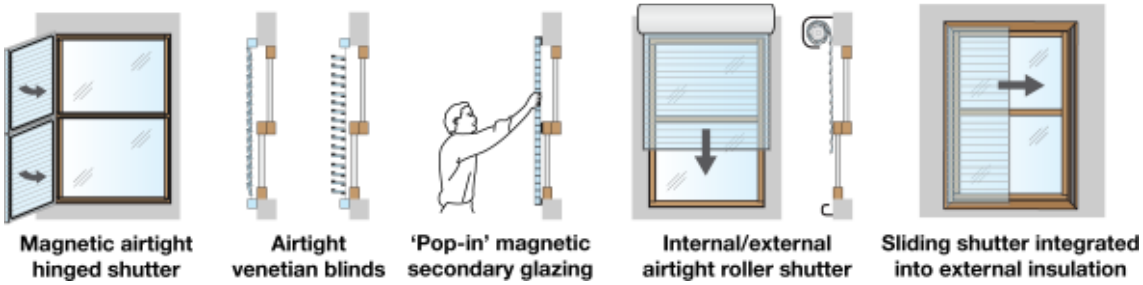

Figure 3.1 *Concepts to improve existing windows using encapsulated granular aerogel.*

As granular aerogel does not permit a clear view outside, solutions that can be closed during the early evenings/night, but drawn out of the way when required, may increase the widespread applicability across the housing stock. Alternatively, in applications where the outside view is not essential, e.g. non domestic buildings, then secondary glazing systems containing granular aerogel could be developed.

3.1.1 Motivation

A single study was identified in the literature review assessing the performance of granular aerogel shutters applied to existing windows. Here, Schultz (1993) constructed three prototypes, measuring their U-value and solar transmission, as well the long term resistance to weathering and settling. The prototypes improved the in-situ U-value of an existing double glazed window from 2.86 W/m^2 K to 1.68 W/m^2 K, whilst reducing solar transmission from 0.75 to 0.45. According to Schultz (1993), the results indicated that insulating shutters with granular aerogel are an attractive alternative to traditional shutters, providing an equivalent heat loss coefficient from half the thickness.

There are several motivations meriting a new study in this area. For example, in Schultz's research, the granular aerogel had a conductivity of 0.029 W/m K, compared to 0.018 W/m K, which is now commercially available. Furthermore, the prototypes were tested on an existing double glazed window in a Danish climate (not single glazing

in the UK). There was also a large discrepancy between the predicted and in-situ U-values. Basic improvements include retrofitting the prototypes over the entire window frame and reducing internal rib spacing to reduce settling of the granular aerogel.

An influential study from the literature review was a series of in-situ U-value tests carried out by Baker (2008) to establish the thermal performance of retrofit solutions such as curtains, blinds and shutters retrofitted to single glazed windows. The best thermal performance was obtained from a custom made prototype consisting of wooden shutters lined with 9 mm thick strips of Spacetherm™, an opaque aerogel fabric. When retrofitted to the single glazed window, this prototype reduced heat losses by 60 %, but it blocked out all of the natural light. Baker (2008) concluded that an 80 % reduction in heat loss would be possible by designing a purpose built solution.

3.1.2 Market assessment

The primary market for aerogel based glazing renovation products is anticipated to be existing homes containing single glazed windows, particularly if new glazing cannot be financially justified or installed due to planning restrictions. Figure 3.2 illustrates the distribution of single glazed homes across England.

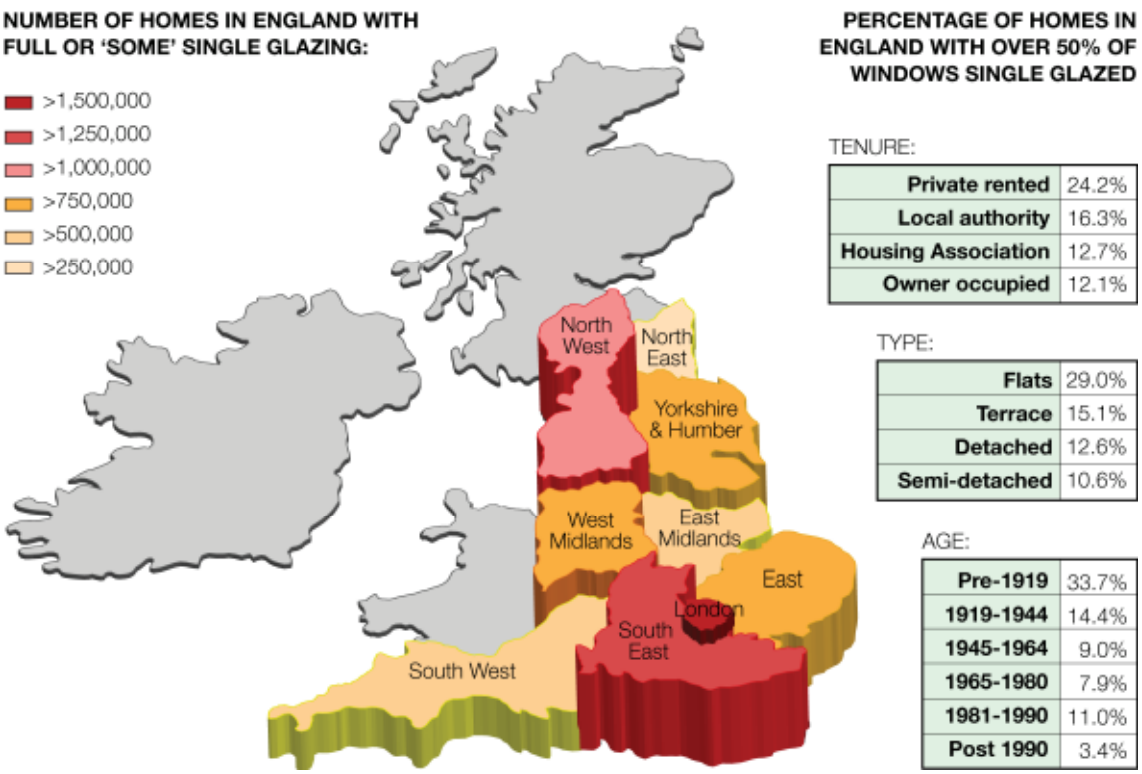

Figure 3.2 *Number of homes in England with single glazed windows by region, age, type and tenure (Generated using data from Utley and Shorrock 2008 and GGF 2009).*

According to GGF (2009), approximately 3.1 million homes in England possess full single glazing and a further 5.3 million homes possess 'some' single glazed windows. Up to 300,000 of these dwellings are listed and 1.2 million are in conservation areas (Boardman *et al.* 2005). The three regions with the most single glazing are London with 1.5 million single glazed homes, the South-East with 1.3 million and the North-West with 1.1 million homes. According to Utley and Shorrock (2008), across the UK, 34 % of homes constructed before 1919, 29 % of flats and 24 % of private rented dwellings still have over half of their windows single glazed.

According to Shorrock *et al.* (2005), new double glazing is not cost effective, with financial paybacks lasting far longer than a predicted twenty year product lifespan. Despite this, the market for new glazing in the UK is approaching maturity following strong growth throughout the 1990s (Purple, 2007). Furthermore, levels are expected to reach saturation over the coming decades (Shorrock *et al.* 2005). However, as Figure 3.3 illustrates, it is important to note that nearly 12 million homes had double glazing installed by 1992, which has now exceeded its anticipated twenty year product lifespan. It is these first generation double glazed units which have high U-values of 3-4 W/m² K, due to poorly insulated frames and narrow 6 mm air gaps. According to Building Regulations Part L1B: Conservation of Fuel and Power in Existing Buildings, all glazing renovations must achieve an overall U-value of 1.8 W/m² K, or centre pane U-value of 1.2 W/m² K (HM Government, 2010).

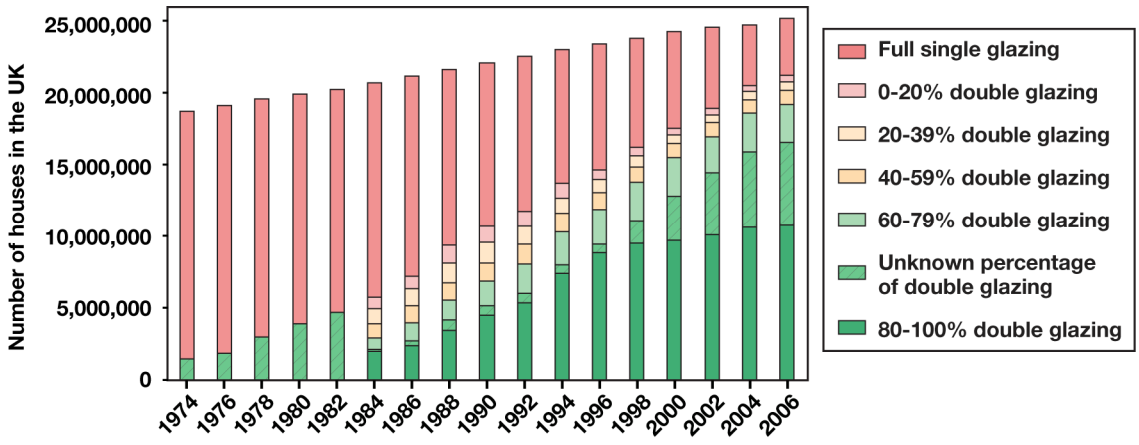

Figure 3.3 *Glazing types in the UK (Generated using data from Utley and Shorrock 2008).*

The commercial office stock is another sector where translucent insulation solutions may be appropriate. As the majority of offices in England were constructed pre-1940, a large proportion are expected to have full single glazing or first generation double glazing. Automated shutters or secondary glazing systems aimed at this sector could cover large areas of the façade where a clear view is not necessary. These could be

particularly effective when combined with control systems to optimise operation, allowing for these products to open or close to gain the best balance between seasonal heating, cooling and lighting energy consumption. Understandably, widespread applicability will require solutions to have a lower capital cost than new glazing.

3.2 Methodology

In the following experiment, two prototype panel thicknesses were compared, using an unmodified window as a control. During the testing phase, the prototypes were permanently fixed to the inside pane of an existing window creating a reasonable airtight seal to represent the best operational scenario. Twin-wall polycarbonate was anticipated to be the most appropriate medium for encapsulating granular aerogel as the panel is lightweight, has a high impact resistance and the twin-wall channels prevent the granules settling over time. Payback calculations based on the measured U-values were carried out to assess the impact of the inevitable thermal bridging that would occur when openable solutions are introduced.

In-situ testing took place during February–March 2010. The prototypes were set up in a high occupancy office in Central London heated by conventional radiators. The candidate window was single glazed, north facing, well shaded and had metal frames. The glazing was away from draughty doors and the radiator beneath the window was switched off. The glazing area contained eight panes of glass, each measuring 540 × 680 mm. Three adjacent panes were used during testing.

Note that solar transmission was not measured during this experiment and testing took place in a north facing window. According to Klems and Keller (1988), the effects of solar gain can limit the accuracy of in-situ U-value measurements. If a south facing window was selected, then exposure to direct solar radiation could result in a net energy gain. Based on commercially available data for polycarbonate sheets filled with aerogel granules, solar transmission is anticipated to be ±5 % of the measured light transmission (Cabot and Roda, 2010).

The reason why in-situ testing was selected over laboratory testing was to gain a representation of the performance of the prototype under real conditions. According to Martin and Watson (1990) although laboratory testing allows extremely accurate measurements, it is difficult to account for the variation in wind, temperature and diffuse sky radiation, which can have a significant impact on the performance of a translucent insulation material.

Prototype description

Figure 3.4 illustrates the arrangement of both prototype panels and the control. Each prototype consisted of a clear twin-wall polycarbonate panel manually filled with 3 mm diameter granules of translucent aerogel manufactured by Cabot Corporation. One panel had a thickness of 6 mm and the other was 10 mm thick. Prior to filling, both polycarbonate panels were cut to fit neatly over the candidate glazing area. Once filled, they were sealed around the edges and securely attached to the internal face of the window frame using duct tape. A 15 mm air gap was created between the panels and the existing glazing. A measure of air tightness was not taken.

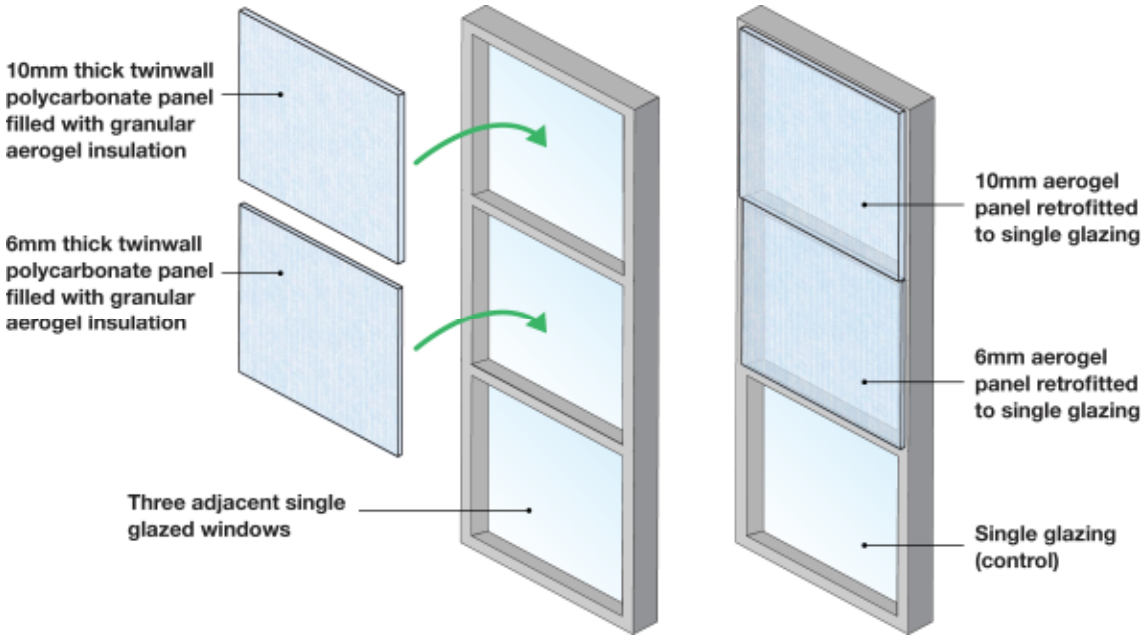

Figure 3.4 *Schematic diagram of the 6 mm aerogel panel, 10 mm aerogel panel and the control. Prototype panels were manually filled and fitted to the single glazed window.*

U-value measurement equipment

A schematic diagram of the equipment used to measure the in-situ U-values is shown in Figure 3.5. Figure 3.6 displays photographs of the experiment once set up.

Heat flux was monitored using Peltier modules thermally bonded to the centre of both prototypes and the control. A Peltier module is a preassembled semiconductor device, comprising of P-type and N-type junctions, layered between two metal plates. Typically, these devices are used for their ability to become hot or cold when voltage passes through them. Reversing this function, the devices can generate a voltage when heat is induced across the plates. The voltage generated by this 'Peltier effect' corresponds to a heat flux when multiplied by a calibration factor (Haruyama, 2001).

Temperature difference was monitored using seven K-type thermocouples. External temperature was monitored by positioning one thermocouple outside an adjacent openable window, which was shut afterwards. Ambient internal temperature was monitored using three thermocouples pointing towards the indoor space by the centre of both prototypes and the control. Three additional thermocouples were also used to monitor the internal surface temperatures for a robust monitoring process.

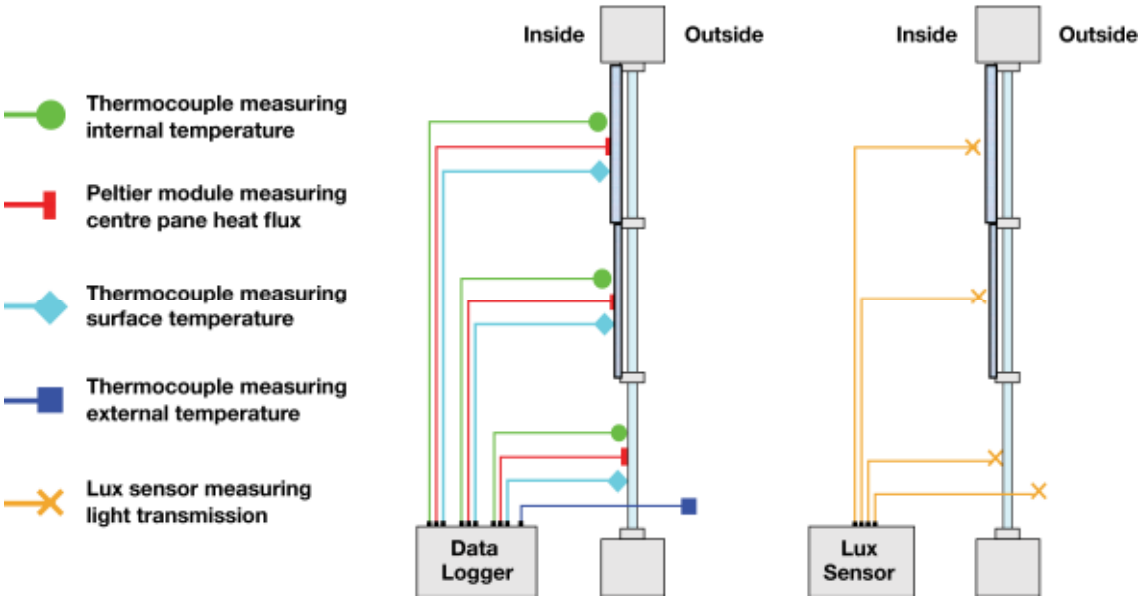

Figure 3.5 *Thermal monitoring equipment (left) and optical monitoring equipment (right).*

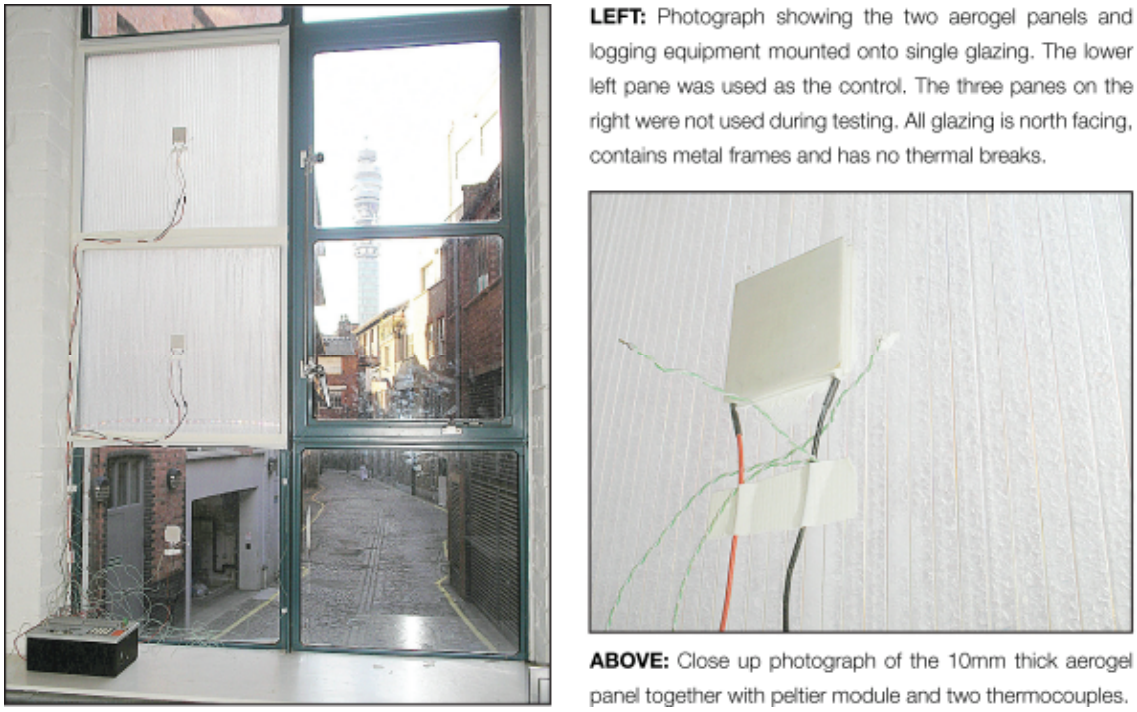

LEFT: Photograph showing the two aerogel panels and logging equipment mounted onto single glazing. The lower left pane was used as the control. The three panes on the right were not used during testing. All glazing is north facing, contains metal frames and has no thermal breaks.

ABOVE: Close up photograph of the 10mm thick aerogel panel together with peltier module and two thermocouples.

Figure 3.6 *Photograph showing the installed prototype panels and monitoring equipment.*

All sensors were connected to a CR23X micro logger (data sheet available from Campbell Scientific, 2005). The data logger recorded values every 5 minutes.

Light transmission equipment

Light transmission was measured by positioning lux sensors at the points marked in the right-hand diagram in Figure 3.5. Readings were taken in a range of outdoor conditions, i.e. cloudy, sunny and during rain to represent different levels of day lighting. Internal readings were taken by holding the lux sensor approximately 5 cm away from the centre of each prototype panel and the control. Outdoor readings were taken by positioning the lux sensor outside of the adjacent openable window.

It is important that internal and external lux readings beside both prototype panels and the control be taken simultaneously as outdoor conditions can vary. In this experiment, only one sensor was available; thus results have an inherent degree of inconsistency relative to one another due to minor delays (of a few seconds) between tests.

3.3 Steady State Calculations

The steady state U-value of both prototypes retrofitted to an existing single glazed window was calculated using Equation [3.1]:

$$U = 1 / (R_{\text{external surface}} + R_{\text{single glazing}} + R_{\text{air gap}} + R_{\text{aerogel panel}} + R_{\text{internal surface}}) \qquad [3.1]$$

This U-value calculation was undertaken using the mean thermal resistance (R-value) of each layer, considering their upper and lower limits. The thermal resistances of the internal surface, external surface and the air gap were calculated in accordance with BS EN ISO 6946:2007. The air gap was treated as an unventilated air layer, with upper and lower limits accounting for the combined heat transfer coefficients for convective and long wave radiation. The centre pane thermal resistance of the single glazing was calculated by dividing the measured thickness of the glass (4 mm) by an upper limit of 1.05 W/mK (CIBSE, 2006) and lower limit 0.96 W/mK (Chung, 20107) for its thermal conductivity.

Data regarding the U-values of both aerogel panels was obtained from personal communication on 25th March 2010 with R. Lowe from Xtralite Ltd, a UK based company that supplies polycarbonate panels filled with aerogel granules, mainly in rooflight applications. The lower limit (i.e. best performance) for these U-values was based on the industrial recommendation, and the higher limit (i.e. worst performance)

was based on a 15 % reduction in thermal performance, accounting for the manual filling process. This higher limit was selected based upon a measured test, which took place with P. Baker at Glasgow Caledonian University on 30 March 2010, comparing the thermal conductivities of a manually filled and industrial filled aerogel panel.

Table 3.1 displays the upper, lower and mean thermal resistances for each layer within the prototypes and control. An emissivity range of 0.89–0.95 was used when calculating the upper and lower range of internal surface resistances for the control (Bynum, 2001; CIBSE, 2006), compared with a range of 0.8–0.9 for the prototype panels (Mitchell, 2000; Jones and Rudlin, 2006).

Table 3.1 *Calculated thermal resistances for the prototype panel layers and control.*

	R-value (m^2 K/W)		
	Worst case	**Best case**	**Mean**
External surface	0.0205	0.0621	0.0413
Single glazing	0.0038	0.0042	0.0040
15mm air gap	0.1790	0.2342	0.2066
6mm aerogel panel	0.2339	0.2752	0.2566
10mm aerogel panel	0.4404	0.5181	0.4793
Internal surface (prototypes)	0.1313	0.1811	0.1562
Internal surface (control)	0.1211	0.1548	0.1380

Table 3.2 displays the calculated U-values at the centre pane of both prototypes and the control. According to calculations, the 6 mm aerogel panel yields a mean U-value of 1.54 W/m² K and the 10 mm aerogel panel yields a mean U-value of 1.15 W/m² K. By comparison, the control has a much higher mean U-value of 5.70 W/m² K.

Table 3.2 *Calculated U-values for the prototypes and control.*

	U-value (W/m^2K)		
	Worst case	**Best case**	**Mean**
Control	6.88	4.52	5.70
6mm aerogel panel	1.76	1.32	1.54
10mm aerogel panel	1.29	1.00	1.15

3.3.1 Predicted annual heat loss

The estimated annual heat loss through a 1 m² single glazed window retrofitted with each prototype was calculated based on the simple heat loss Equation [3.2]:

$$\text{Fabric Heat Loss} = \text{U-Value} \times \text{Area} \times \text{Temperature Difference} \qquad [3.2]$$

Calculations were performed using hourly external temperature data from the CIBSE TRY weather file for London (CIBSE, 2008). Assuming the product is being used in a

domestic application, the annual heating profile was assumed to operate at 21 °C, all year round, with a night time setback of 18 °C operating between 10 pm and 7 am. Four different product usage profiles were calculated to represent how each aerogel panel might perform if adapted into an openable insulation solution, which would incur inevitable thermal bridges when left open.

Profile 1 sets a baseline for heat loss calculations; it assumes that the single glazing is un-insulated all year round and no benefit is gained. Comparatively, Profiles 2–4 assume that the prototypes are consistently used from 1st October to 31st May, the months where approximately 90 % of the degree days for London Thames Valley occur (Vesma, 2009). Profile 2 assumes that the window is insulated from 10 pm to 7 am. Profile 3 assumes that the window is insulated for longer times from 6 pm to 8 am. Profile 4 assumes that the prototype is permanently insulating all day and night, thus behaving like secondary glazing. Figure 3.7 displays the estimated annual heat loss for each of the usage profiles modelled.

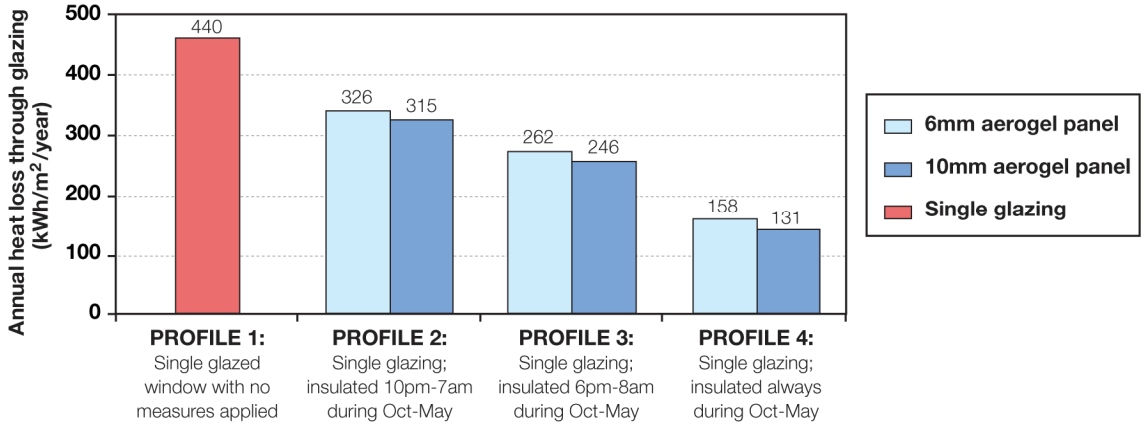

Figure 3.7 *Predicted annual heat loss through a single glazed window retrofitted with each prototype. Four operational scenarios illustrate the dependence of energy savings on product usage. Outside of the defined heating season it is assumed that the window is un-insulated.*

According to the steady state calculations, both prototypes have large potential to improve the thermal performance of single glazing, cutting between 65 and 70 % of the annual heat losses when permanently used over the heating season. Understandably, when considering openable insulation solutions, the degree of energy savings is highly dependent on how often the product is used. Preliminary calculations suggest that an openable solution can limit annual energy savings to 25–45 %. However, by using the product earlier in the evening and later in the morning, a higher proportion of heat losses can be reduced.

Beyond product usage, note that the actual savings are also dependant on the internal temperature set point. Furthermore, if a similar study was carried out in another region, or country, then the heating demand and subsequent heat loss could vary significantly.

3.3.2 Predicted impact on light transmission

According to Cabot (2009), light transmission through granular aerogel decreases by 20 % each time its thickness increases by 10 mm, as visualised in Figure 3.8. As shown, 6 mm of aerogel is predicted to permit 88 % of light transmission and 10 mm of aerogel permits 80 %.

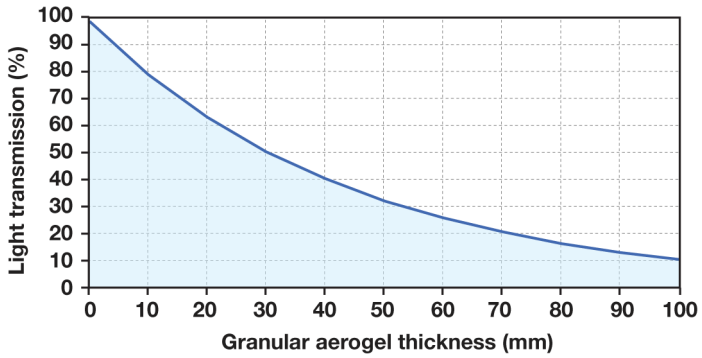

Figure 3.8 *Light transmission through granular aerogel (Generated from Cabot 2009).*

To calculate the light transmission of the entire system, the single glazing and the polycarbonate panels must also be considered. CIBSE (2006) states that light transmission through single glazing, including the effects of dirt is 80 %. C&A Supplies (2009) state that a 6 mm polycarbonate panel allows 85 % light transmission and 10 mm panels allow 80 %. Multiplying the corresponding values together, the theoretical total light transmission through the 6 mm aerogel panel and 10 mm aerogel panel is 60 and 51 %, respectively.

3.4 In-Situ Results

Figure 3.9 displays the external temperature and three ambient internal temperatures logged during the in-situ test period from 20 February 2010 to 1 March 2010. Over the 10 days, the average external temperature was 7.4 °C with a maximum of 12.5 °C and minimum of 2.1 °C. The average internal temperatures adjacent to the control, 6 mm aerogel panel and 10 mm aerogel were 19.3, 20.0 and 20.1 °C, respectively. The average surface temperature of the control was 14.3 °C, whereas the 6 mm and 10 mm aerogel panels were several degrees warmer at 17.6 and 18.3 °C, respectively.

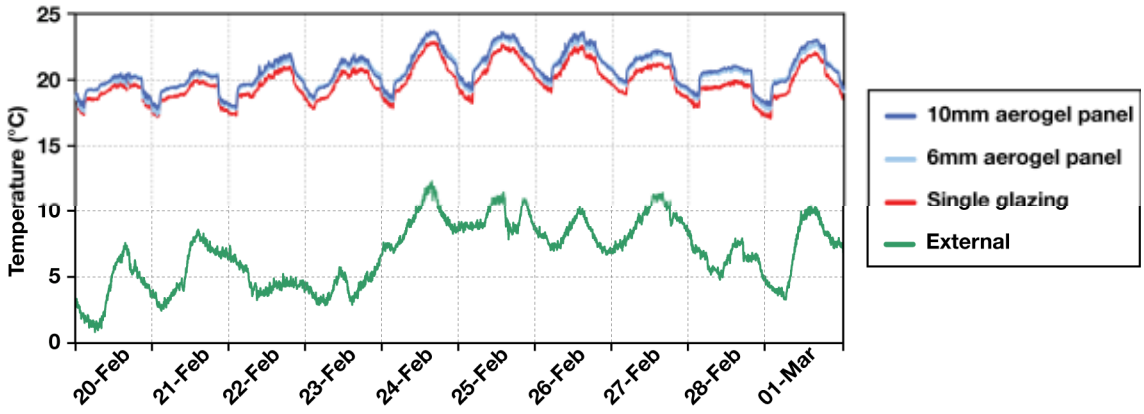

Figure 3.9 *Measured external and internal air temperature adjacent to the prototype panels and control. Of the three internal readings, the 10 mm aerogel panel was consistently the warmest, closely followed by the 6 mm aerogel panel, then the control.*

3.4.1 Heat flux

Figure 3.10 shows the induced heat flux from the Peltier modules. As expected, heat flux through the control was significantly larger than the heat flux through both prototypes. Studying the relative performance compared with that of the control, the 6 mm aerogel panel reduced heat flux by approximately 73 % and the 10 mm aerogel panel by approximately 80 %. Calibration of these units occurred on 14 December 2009 at Glasgow Caledonian University. Initial testing has shown the accuracy to be within 1 % for heat flux measured with a temperature difference of 20 °C.

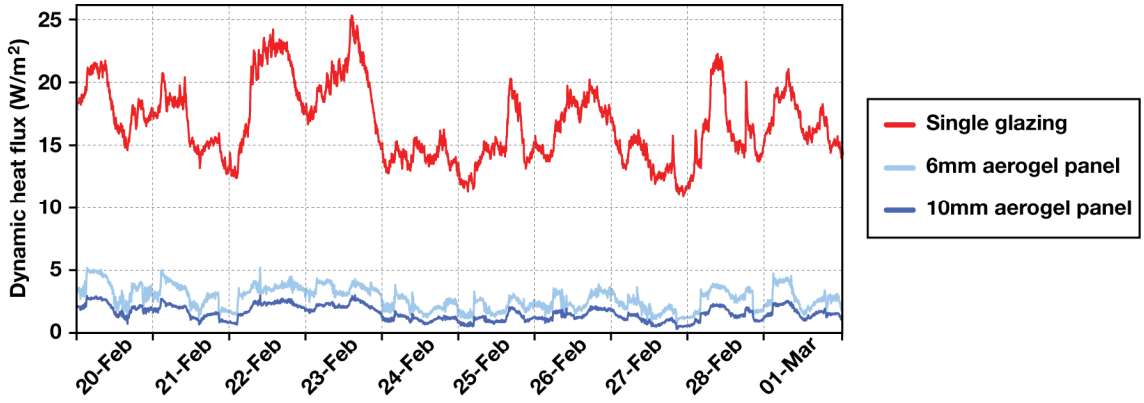

Figure 3.10 *Measured centre pane heat flux through the prototype panels and control during in-situ testing. Heat flux through the control was significantly large compared with readings through the prototypes. Heat flux through the 10 mm aerogel panel was consistently the lowest of the three readings.*

3.4.2 U-values

According to Cheeseman *et al.* (2007), instantaneous calculation of a U-value based on heat flux and temperature difference does not provide an accurate measurement of

thermal transmission due to the effects of time lag. This is especially true for higher insulating materials. In response, Cheeseman *et al.* (2007) states that dynamic U-value can be rationalised by calculating the cumulative average of the results over time. This is demonstrated in Figure 3.11.

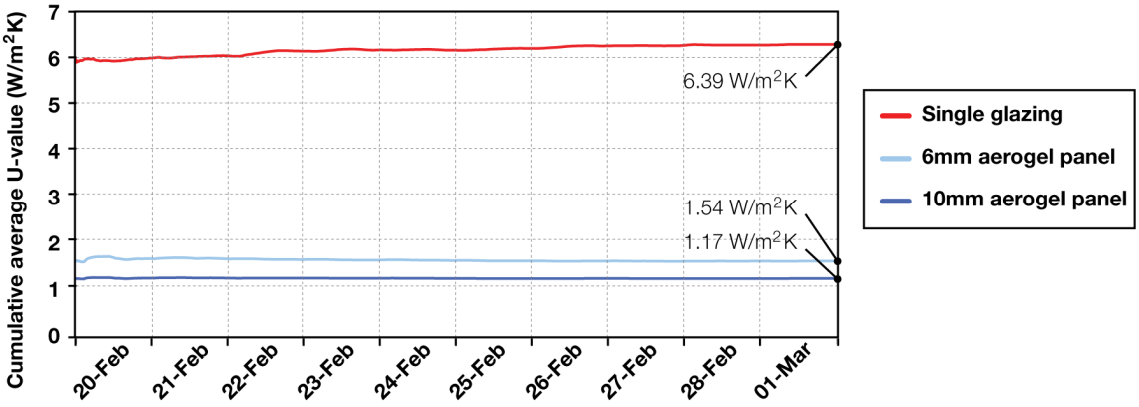

Figure 3.11 *Cumulative average U-values for the prototype panels and control calculated from the in-situ heat flux and temperature difference.*

By applying a cumulative average formula, dynamic U-values for both prototypes appear to approach steady state in 3-5 days of testing. The control took approximately 7 days. According to results, the control has a U-value of 6.39 W/m² K and the U-value of the 6 mm and 10 mm aerogel panels was 1.54 W/m² K and 1.17 W/m² K respectively.

3.4.3 Light transmission

Figure 3.12 displays the measured lux levels at five intervals throughout March 2010. Readings were taken during various external conditions. In all cases, results show that the control allows more light transmission than both prototypes. Light transmission reduced slightly more in the 10 mm aerogel panel than in the 6 mm aerogel panel.

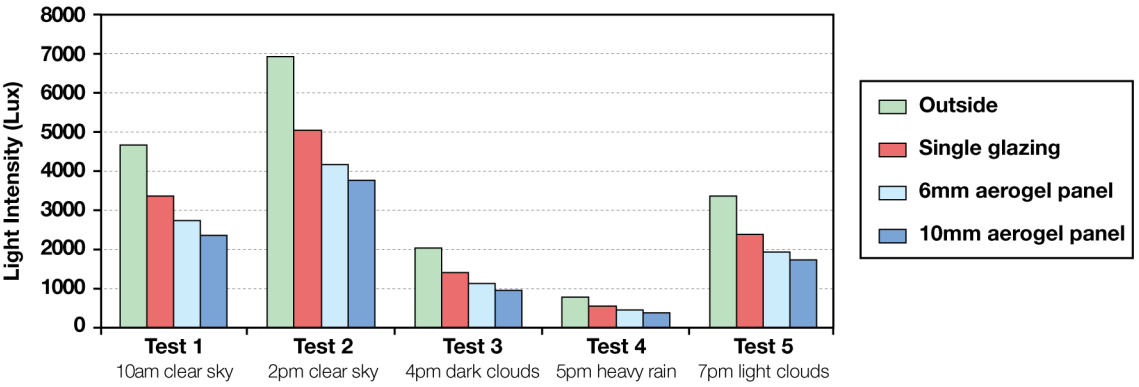

Figure 3.12 *Measured light intensity outside compared with internal readings adjacent to the prototype panels during five time intervals/weather conditions.*

Figure 3.13 aggregates the lux readings as a percentage. As expected, the percentage of allowable light transmission across each test was not identical. Inconsistencies may be caused by delays when using the lux meter, dirt on windows, ridges in the polycarbonate panels or variations in the aerogel granules. The average light transmission through the 6 mm aerogel panel, 10 mm aerogel panel and the control was 58, 51 and 73 %, respectively.

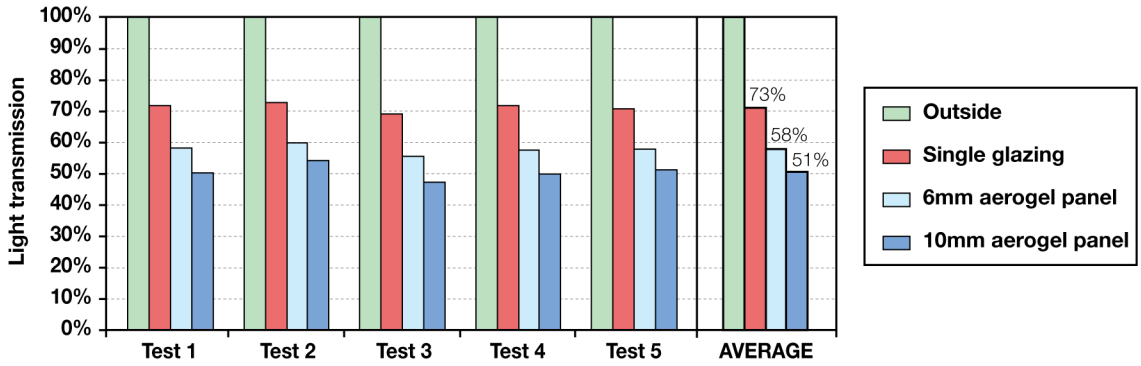

Figure 3.13 *Measured light transmissions from the five test periods aggregated as a percentage. An average across all tests is shown to the right.*

3.5 Discussion

Experimentation has demonstrated the impressive thermal performance of granular aerogel in a glazing application. Based on in-situ heat flux measurements, a 10 mm aerogel panel has been shown to reduce the rate of heat loss through glazing by 80 % without detrimental impacts on light transmission. Shown in Figure 3.14, both the predicted and in-situ U-values are in close agreement. Measured uncertainty for the in-situ U-values based upon equipment accuracy and the differences between internal air & surface temperature readings is 19.3% and 14.6% for the 6mm and 10mm thick aerogel panels respectively. Table 3.3 summarises the in-situ test results.

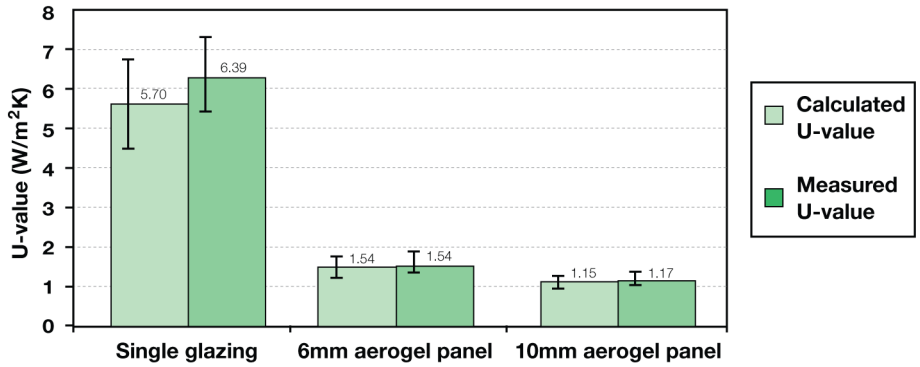

Figure 3.14 *Comparing the calculated and measured U-values.*

Table 3.3 *Summary of in-situ testing results.*

	Thermal performance		Optical performance	
	Measured U-value	Reduction in heat loss	Measured transmission	Reduction in light
Control	6.39 W/m²K	-	73%	-
6mm aerogel panel	1.54 W/m²K	74%	58%	22%
10mm aerogel panel	1.17 W/m²K	80%	51%	31%

Figure 3.15 displays a theoretical payback calculation for the 10 mm aerogel panel retrofitted to a single glazed window in a gas heated home. The model utilises a net present value equation with a discounted interest rate of 3.5 % (HM Treasury, 2003). Annual energy savings from heating were calculated using a baseline temperature of 21 °C with an 18 °C night time setback between 10 pm and 7 am. In-situ U-values were applied to the operational profiles described in Section 3.3.1, to account for openable insulation solutions. A unit cost of £ 0.04/kWh was used to represent the cost of gas. A conventional gas condensing boiler with a winter efficiency of 84 % was selected to represent the heating system within a typical UK home (GGF, 2009; DECC, 2010a). £ 55/m² was taken as the initial capital cost of the retrofit measure. This cost consisted of a 10 mm thick 1 m² twin-wall polycarbonate priced £ 10 (C&A Supplies, 2009), 8 litres of granular aerogel costing approximately € 4/litre and a 50 % mark up to cover additional costs such as airtight fixtures and installation. The cost of granular aerogel was obtained by personal communication with E. Ruiz of Cabot on 20th March 2009.

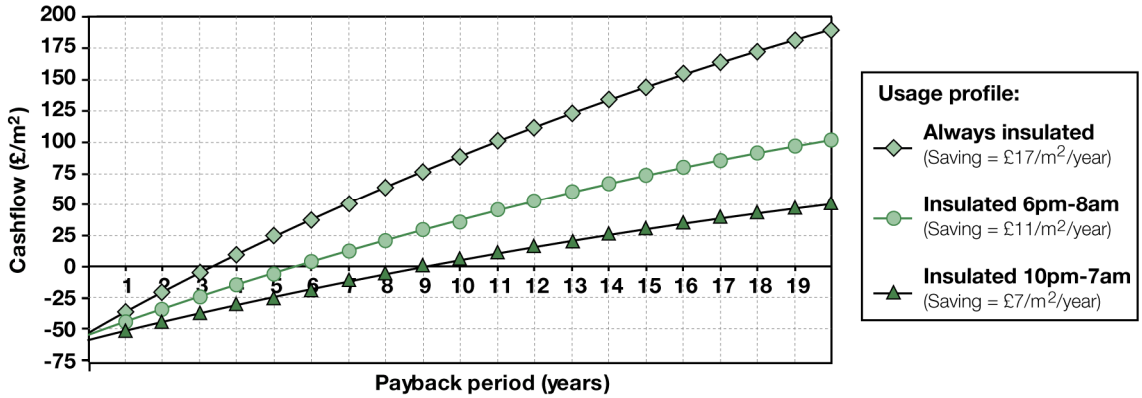

Figure 3.15 *Payback calculations for 10 mm aerogel panel retrofitted to single glazing.*

According to calculations, the 10 mm aerogel panel could payback between 3.5 and 9.5 years, providing a positive return on investment of £ 42–185/m² over a twenty year product lifespan. These results are promising, considering that new double and triple glazing does not provide a payback to a homeowner. Note that the 9.5 year payback calculation assumes that the window is only insulated between 10 pm and 7 am, when the heating profile is set back to 18 °C. A 5.8 year payback is calculated if the window is

insulated for longer from 6 pm to 8 am. Shorter paybacks are expected if the capital cost was driven down by the economies of scale associated with mass production. Furthermore, as this model does not account for potential increases in energy prices, this could reduce payback periods further. The true payback period is highly dependent on actual temperatures both inside and outside, as well as how consistently the product is used over the heating season. If developed into an openable insulation solution, which is not used consistently, this could limit the cost effectiveness significantly.

According to in-situ testing, the 10 mm aerogel panel was capable of achieving the Building Regulations centre pane U-value target of 1.2 $W/m^2 K$, without evacuating the panel or inserting a noble gas filling, demonstrating that granular aerogel can be used to achieve modern building standards at minimal costs. Future development should seek to maintain this performance, while developing suitable forms and airtight attachment methods tailored towards the needs of different occupants and building types. For openable solutions, efforts should be made to educate users on how to operate products effectively or develop products with control systems, such as automatic roller or sliding shutters to ensure maximum benefit can be gained.

It is envisaged that openable translucent insulation solutions for bedrooms and living rooms may be the most widely accepted products across the housing stock. Alternatively, skylights and windows with limited outside views are anticipated to be most suitable for secondary glazing solutions. Modular, removable products may be particularly suited towards tenants living in privately rented accommodation, especially if landlords are unwilling to pay for energy efficiency measures themselves. Internal solutions aiming to improve the windows in homes limited by planning restrictions may only be suitable if incorporated adequately. Bathroom windows may not be suitable due to potential condensation risks.

3.6 Further Modelling Applied to Offices

To evaluate the potential annual energy savings from translucent automated aerogel shutters retrofitted to offices with single or first generation double glazing, compared to new double or triple glazing, a parametric assessment of heating, cooling and day lighting was conducted using IES dynamic thermal modelling software. Shown in Figure 3.16, 24 offices were modelled, consisting of 6 glazing profiles modelled on north, south, east and west orientations. Each office zone has a 10m x 10m floor area, is fully glazed on one facade and has a thermal buffer above, below and around the perimeter to isolate heat transfer to the exposed glazing area.

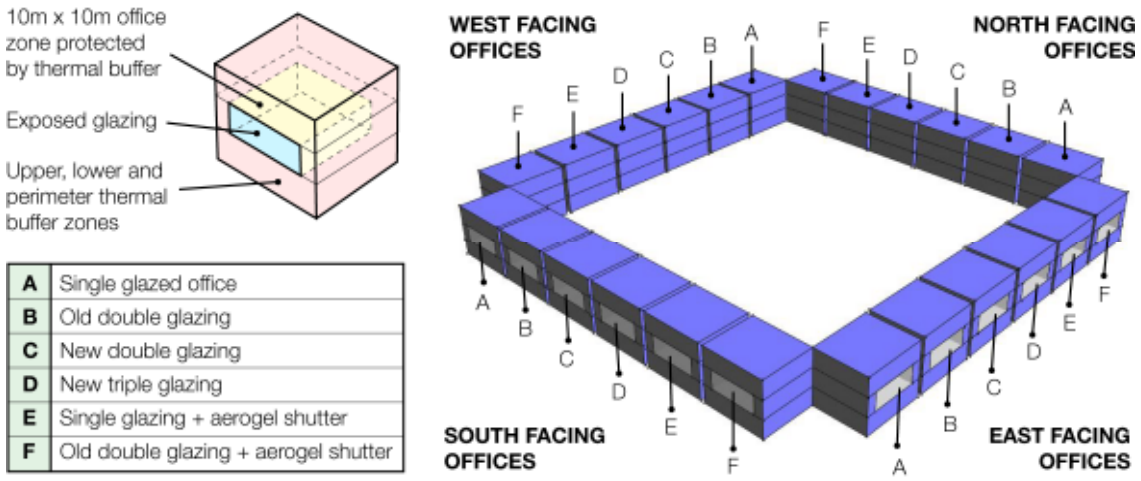

Figure 3.16 *Thermal model developed for the parametric glazing assessment.*

The U-value of single glazing, first generation double glazing, new double glazing and new triple glazing were assumed to be 5.7, 2.8, 1.8 and 0.8 W/m² K respectively. Corresponding G-values and light transmission percentages were assumed to be 0.85, 0.8, 0.7 and 0.5, then 75 %, 65 %, 70 % and 50 % respectively. The U-value and light transmission of single glazing retrofitted with aerogel shutters is taken as 1.17 W/m² K and 51 % (based on in-situ testing for the 10 mm shutter) with an estimated G-value of 0.51. For first generation double glazing retrofitted with aerogel shutters an estimated U-value of 0.95 W/m² K and light transmission of 45 % was used based on steady state calculation with an estimated G-value of 0.45.

Energy consumption for heating and cooling were assumed to operate continuously between 8 am and 6 pm, with 21.1 °C and 23.9 °C setpoints respectively. A load of 12 W/m² for fluorescent lighting with automatic dimmers that reduce energy consumption to 25 % when indoor day lighting is above 500 lux was assumed. Internal gains from people (12 W/m²) and equipment (10 W/m²) were included. Infiltration was 0.25 L/s/m². The CIBSE TRY weather file for London, UK was used.

Figure 3.17 - Figure 3.20 display the predicted annual heating, cooling and lighting loads, in kWh per m² of floor area for the 24 offices analysed. In each figure, the first six results represent the total annual energy consumption obtained directly from the individual 100 m² office zones. The final two load columns are interpolated from the two single glazed and first generation double glazed models, respectively, with and without aerogel shutters, to represent the potential annual energy savings from an automated openable solution, based on the glazing profile which provides the minimum combined heating and cooling load at every hour of the year.

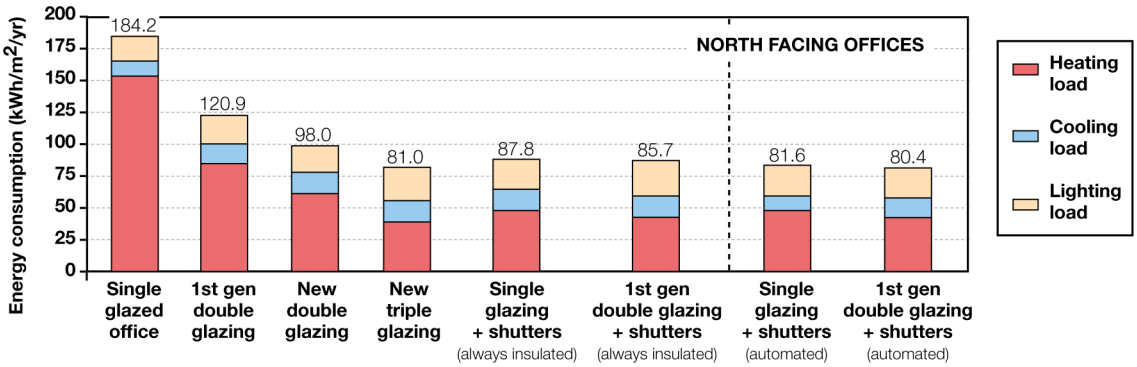

Figure 3.17 *Predicted annual loads for NORTH facing offices.*

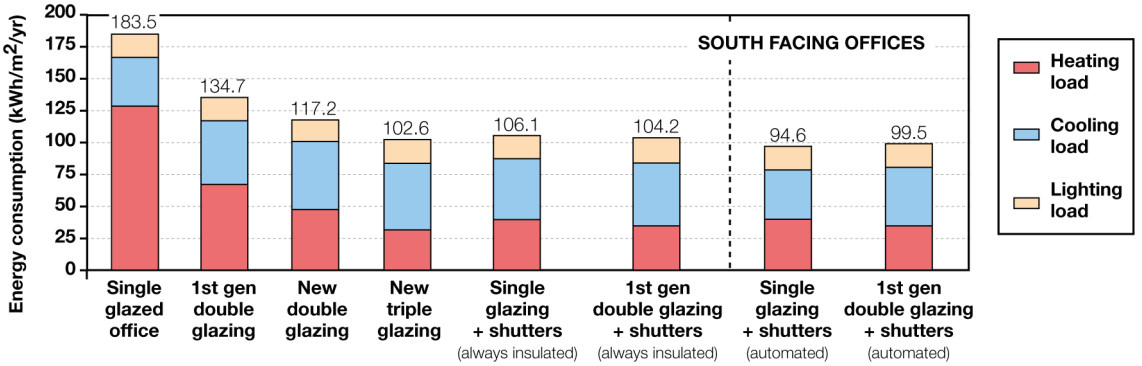

Figure 3.18 *Predicted annual loads for SOUTH facing offices.*

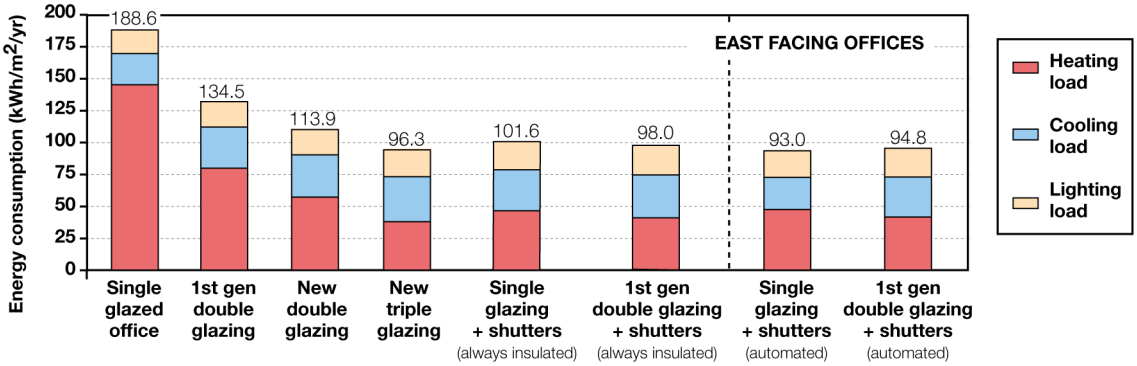

Figure 3.19 *Predicted annual loads for EAST facing offices.*

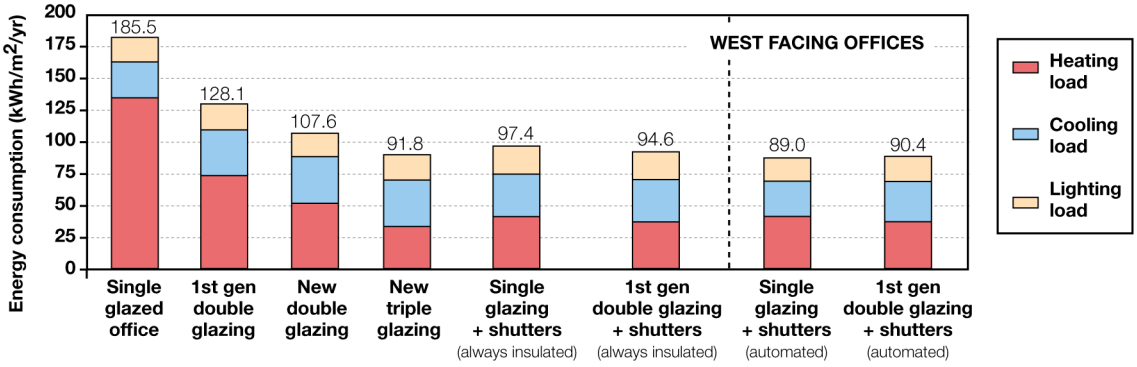

Figure 3.20 *Predicted annual loads for WEST facing offices.*

When analysing the results obtained directly from the thermal models, the single glazed office has the largest annual heating load and the triple glazed office has the smallest, driven primarily by the glazing U-values, as well as the G-values in winter. By comparison, the largest cooling load, driven by solar and internal gains is observed on the south facing triple glazed office, due to its low U-value and G-value, followed by the new double glazed office. Lighting loads are relatively similar in each scenario, with the lowest found in the single glazed offices due to its high light transmission.

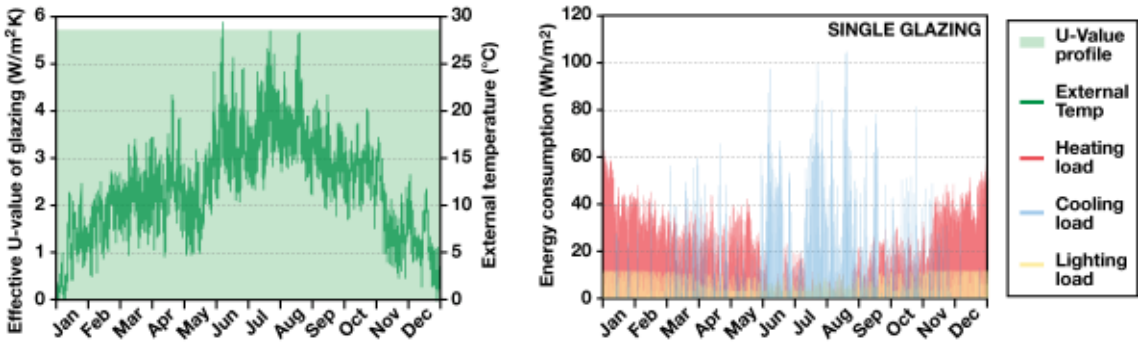

Figure 3.21 *Static U-value profile and annual loads for the south facing single glazed office.*

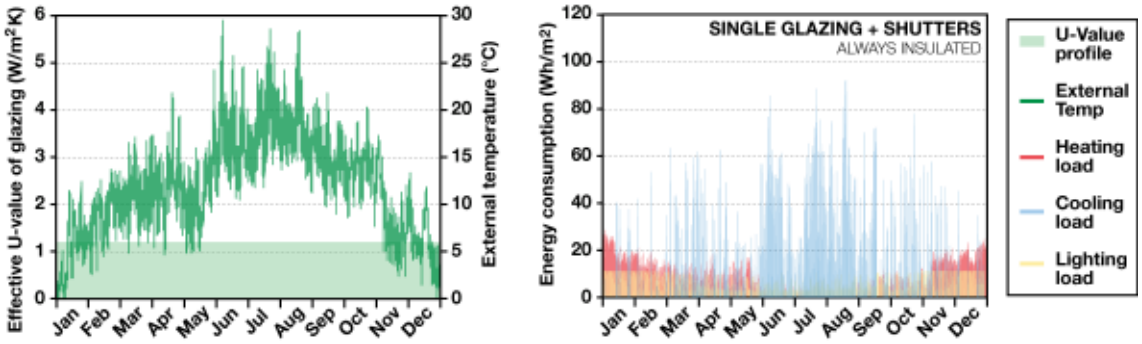

Figure 3.22 *Static U-value profile and annual loads for the south facing single glazed office retrofitted with aerogel shutters closed permanently throughout the year.*

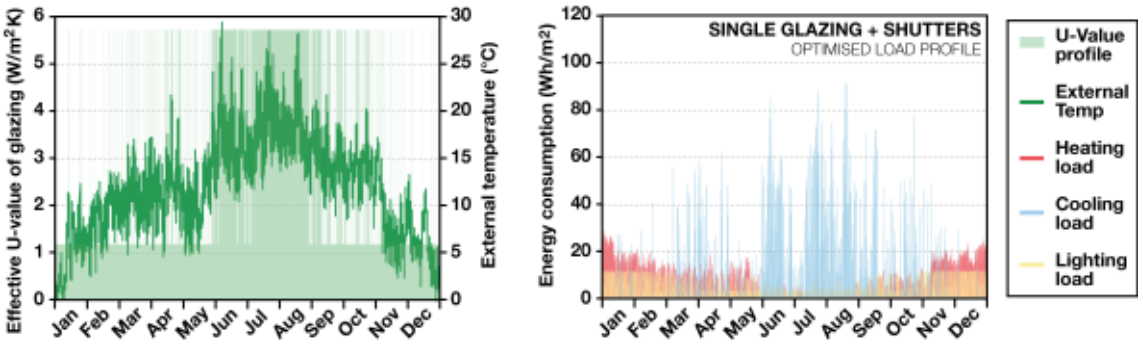

Figure 3.23 *Dynamic U-value profile and annual loads for the south facing single glazed office retrofitted with aerogel shutters which open and close automatically.*

The single glazed and first generation double glazed offices with aerogel shutters *always* retrofitted provide total annual energy consumption which outperforms new double glazing across all four orientations, but does not exceed new triple glazing. By comparison, across all orientations the two interpolated results for single glazing and first generation double glazing, fitted with movable automated shutters, provide a total annual energy consumption which matches the performance of triple glazing on the north facade and exceeds it on the east or west facades. The south facade in particular, demonstrates the greatest potential savings over triple glazing.

Figure 3.21 to Figure 3.23 show the U-value profile and external temperature alongside the hourly loads corresponding to the single glazed office, the single glazed office always insulated with shutters and the single glazed office fitted with automated shutters. As shown, in Figure 3.23, by automatically opening and closing the shutters when beneficial, it is theoretically possible to significantly reduce both heating and cooling loads.

When assessing the aforementioned results, note that the loads presented are for mechanically ventilated offices with all windows closed in summertime. If openable, then the cooling loads could be reduced by a certain degree through natural ventilation. Nonetheless, the theoretical minimum heating profile would still be valid. The costs incurred for a fully automated shutter may outweigh the potential benefit. An alternate approach would be to have a manually operated system which can be opened during summertime when the external temperature is cooler than internal temperature, yet closed again if the temperature difference switches. During winter, the shutters may be manually opened on mild days, when it is beneficial to increase solar transmittance. The increase in lighting load when the glazing is insulated with translucent shutters was not found to be detrimental.

3.7 Conclusion

This chapter has presented novel in-situ test results and predicted annual energy performance calculations related to translucent aerogel ‘shutters’ in domestic and non domestic building applications. The core contribution to knowledge arising from this study is that translucent granular aerogel retrofitted over an existing single glazed window can reduce the rate of heat loss by 80 %, without detrimental reductions in light transmission; predicted payback periods of 3.5-9.5 years are possible depending on product use.

The results of this study support Baker's (2008) hypothesis that an 80 % reduction in heat loss through single glazing is achievable by designing a purpose built retrofit solution containing aerogel. As Baker tested the performance of wooden shutters lined with strips of opaque aerogel fabric, the novel feature obtained from this follow up study is that by utilising translucent aerogel granules, a lightweight product containing a consistent layer of insulation can be produced, which does not block out all of the useful natural light.

Compared to research by Schultz (1993), the results serve to verify the thermal, optical and financial performance of commercially available granular aerogel applied to single glazing in a UK climate. Design improvements include use of hydrophobic aerogel to avoid thermal degradation, the use of closely spaced internal ribs to reduce the settling and retrofitting the prototype over the entire window frame to achieve optimum performance. These improvements are anticipated to increase the applicability for granular aerogel across both the domestic and commercial glazing market.

Payback calculations indicate that granular aerogel is capable of providing cost effective energy savings within the product's lifespan, even if an openable solution is introduced. Note that payback periods can be significantly increased if an openable solution is not operated consistently throughout the heating season. Nonetheless, provided that capital costs of installed systems are kept low, translucent retrofit solutions for glazing could provide an attractive investment over new double or triple glazing, with equivalent thermal performance.

A parametric investigation of automated translucent aerogel 'shutters' in office buildings has demonstrated that this product can meet or exceed the performance of new triple glazing when retrofitted to single glazing on all orientations, with even greater savings achieved when retrofitted over first generation double glazed units. Control systems to automate and optimise the performance would function based on the temperature measurements between inside and outside of the office space. The capital cost of such controls should not outweigh the operational savings.

If taken forward to the next stage of product development, a key issue to consider would be how to design solutions that accommodate occupant behaviour to ensure it can be installed and used in the most cost effective way. A thorough understanding of design conflicts is required to enable development to be targeted towards the most appropriate shapes, sizes and types of windows across different types of buildings. Furthermore, it would be important to develop solutions that are aesthetically pleasing and respectful of physical or planning constraints.

Chapter 4

STREAMLINED LIFE CYCLE ASSESSMENT OF TRANSPARENT SILICA AEROGEL MADE BY SUPERCRITICAL DRYING

Abstract

This chapter contains a streamlined life cycle assessment (LCA) of silica aerogel following the ISO 14000 standards. Prior to this investigation there was no publically available LCA of this material conducted to the ISO 14000 standards, despite many solvents used in production, often accompanied by intensive drying processes, which may consume large amounts of energy and CO_2. Primary data for this 'cradle-to-factory gate' study, such as the mass of raw materials and electricity usage was collected for silica aerogel made by low and high temperature supercritical drying. Findings were compared against the predicted operational savings arising from retrofitting translucent aerogel panels to a single glazed window to upgrade its thermal performance. Results should be treated as a conservative estimate as the aerogel is produced in a laboratory which has not been developed for mass manufacture or refined to reduce its environmental impact. Furthermore, the samples are small and assumptions to upscale the manufacturing volume occur without major changes to production steps or equipment used. Despite these factors, parity between the CO_2 burden and CO_2 savings is achieved in less than 2 years, indicating that silica aerogel can provide a measurable environmental benefit. Further savings are quantified by refining the economies of scale.

4.1 Introduction

This chapter summarises the findings of a streamlined life cycle assessment (LCA) conducted to investigate the environmental impact of silica aerogel production. To facilitate this study an independent collaboration was built with M.Grogan at the University of Bath's Department of Physics. During this collaboration, Grogan was conducting a PhD focused on the use of aerogels in fibre optics, involving manufacturing small samples of aerogel in a laboratory to optimise their transparency. With permission from Grogan and his supervisor (T. Birks), an experiment was set up to manufacture small aerogel samples whilst measuring the amount of raw materials and electricity consumed during the production process. All samples were prepared jointly with Grogan in a facility at Bath University, which had not been refined to reduce its environmental impact. All work conducted for the LCA thereafter was carried out independently, with Grogan only providing advice regarding suitable scaling assumptions to represent mass manufacture.

4.1.1 Motivation

This thesis takes a systematic approach to improving UK building fabrics considering both operational savings and embodied impacts; a critical balance that is typically ignored. Several innovative technologies have been developed to satisfy the growing demand for energy efficient buildings. Finding a balance between insulation thickness, cost and in-situ performance is essential. Above all, technologies must provide a measurable benefit over their life cycle i.e. the in-use savings must not be outweighed by manufacture, transport and end-of-life impacts.

The literature review found no publically available life cycle assessments of the silica aerogel production process following the ISO 14000 standards. To be compliant with ISO 14000 standards, an LCA must have a clearly defined goal, scope and functional unit. Furthermore, all assumptions, data collection processes and interpretation steps must be transparent and the findings must be approved via an independent third party peer review.

Currently, the two major manufacturers of aerogel, Aspen Aerogel and Cabot Corporation, have had an LCA of their production processes conducted as part of the Cradle-to-Cradle certification scheme. Key outputs of the process include figures for the production energy and CO_2 burden. According to MBDC (2008) both manufacturers received a 'Silver' environmental award. However, full details concerning the scope, methodology and assumptions made are confidential. According to GBA (2007), the

Cradle-to-Cradle certification scheme does not undergo third party review, thus does not comply with ISO 14000 standards.

Many solvents are used in the production of silica aerogel, often accompanied by intensive drying processes, which may consume large amounts of energy and CO_2. Compared to conventional insulation, figures for the Aspen Aerogel production energy and CO_2 burden are relatively high, even when taking their product's improved thermal performance into account. This is concerning, especially since Aspen Aerogel do not disclose the amount of CO_2 used during drying. Further investigation is essential to justify the environmental benefits of aerogel.

4.2 Streamlined Life Cycle Assessment

Life cycle assessment (LCA) is a process by which the environmental impacts associated with a product can be quantified over its life cycle from 'cradle-to-grave'. To date there has been no peer reviewed LCA of aerogel meeting the ISO 14000 standards. This study addresses this by conducting a streamlined LCA following BS EN ISO 14044:2006: "Environmental Management: Life Cycle Assessment: Requirements and Guidelines". Findings have undergone a third party review being published in the peer reviewed *Applied Energy* Journal.

4.2.1 Goal

The aim of this study was to establish the CO_2 burden and production energy associated with two different methods of silica aerogel manufacture. Data was compared against the predicted CO_2 and energy savings when retrofitting aerogel to building fabrics in-situ. The purpose of this investigation was to identify whether the production costs of silica aerogel can be recovered by its operational savings within a realistic product lifespan. The study also served to provide a unique comparison between two of the three known methods of aerogel production.

The intended audience for this study includes environmental engineers, architects, materials scientists and product designers. Results are intended to be publicly available. It is anticipated that results may be compared against the life cycle impacts of conventional and emerging building fabric technologies. All comparisons must recognise that the results of this study were based on a laboratory experiment, scaled-up to produce 1 m^3 volumes. Scaling assumptions must be treated as conservative estimates for commercial production due to the lack of information from industry

concerning the actual economies and efficiencies of scale associated with the mass production of aerogel.

4.2.2 Scope

This study is a 'cradle-to-factory gate' assessment. Primary data was collected for two methods of aerogel production. Secondary data was used to account for the energy use and CO_2 burden from extracting raw materials, as well as the carbon intensity of the electricity grid. The impact of transport (of raw materials / finished products) and end of life processing (e.g. product re-use, recycling, landfill etc) were omitted. However, their potential impacts are discussed.

At the University of Bath, high transparency aerogels are being produced using both low and high temperature supercritical drying (LTSCD and HTSCD) for research into optical applications. Utilising their experience in aerogel production, two production experiments were conducted, monitoring the CO_2 and energy usage associated with manufacturing small samples of silica aerogel using both drying techniques. It should be noted that there is a third method for aerogel production, via ambient pressure drying. Currently the group does not produce aerogels in this way.

The results of this study should be treated as a conservative estimate for the production cost of aerogel. The processes developed at the University of Bath have not been developed or refined for mass manufacture. As such, no recycling of solvents or CO_2 occurs. Furthermore, just 40ml of aerogel is produced during each production run. The aerogels are monolithic (not granular) and have a high optical quality. Scaling assumptions to upscale the manufacturing volume, without major changes to production steps or equipment must be treated with caution.

The functional units for this investigation are: (i) energy use (kWh) and (ii) CO_2 burden ($kgCO_2$), required to produce 1 m^3 of aerogel. Results are compared against the operational energy and CO_2 savings arising from retrofitting a 10 mm thick, 1 m^2 twin-wall polycarbonate panel filled with aerogel granules to a single glazed window. The predicted performance of this product over a 15 year lifespan was estimated based upon the results of in-situ testing and steady state calculations for annual energy savings per m^2 of glazing (presented in Chapter 3).

4.3 Data Collection

Data collection was split across three stages: Gel preparation, ageing and drying. Gel preparation took place during April 2010. Following this, gels were aged in solvent for 3

weeks, and then supercritically dried. Figure 4.1 displays the system boundary for both methods of aerogel manufacture studied. Monitoring procedures and omitted factors are outlined.

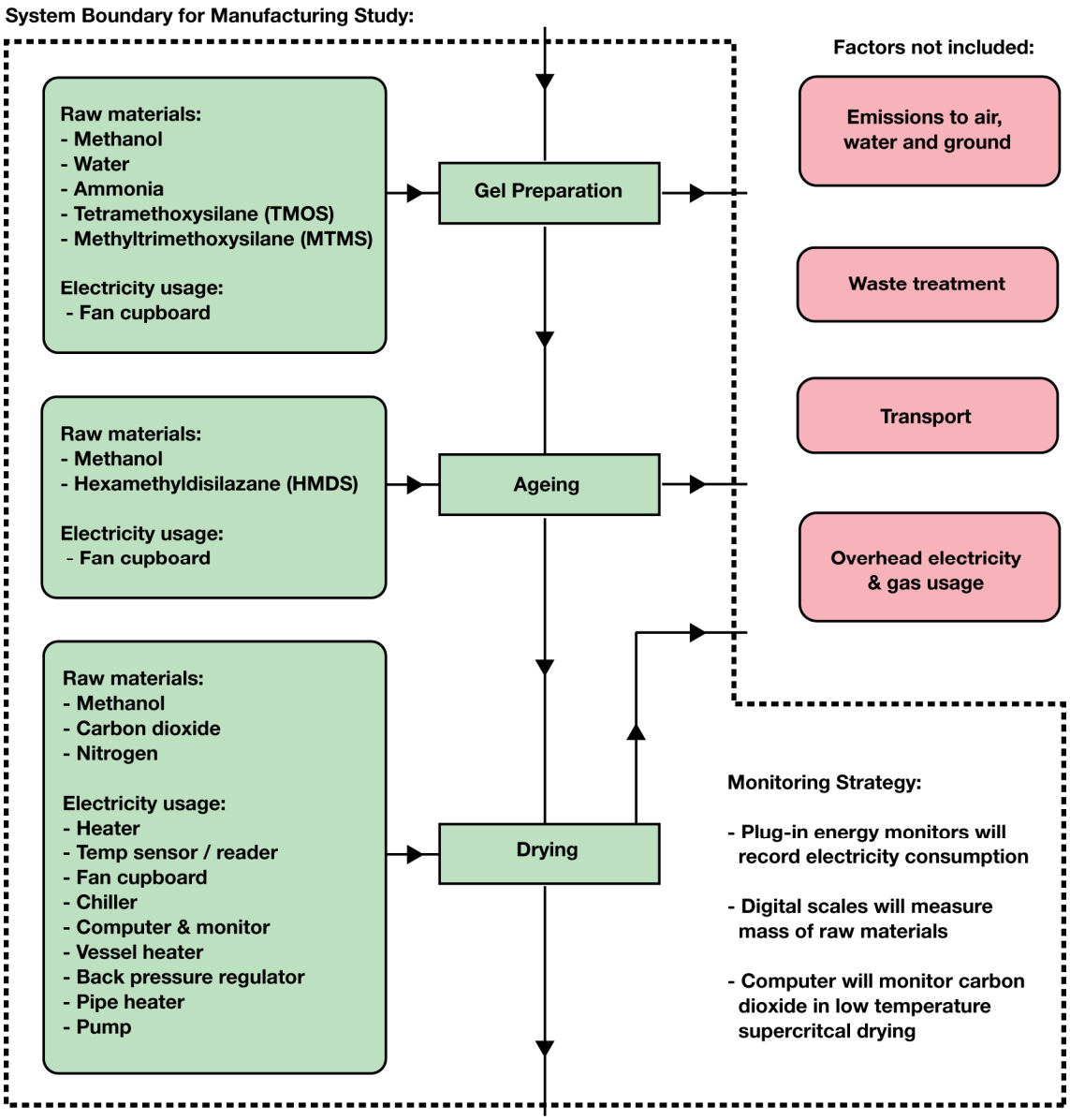

Figure 4.1 *System boundary and monitoring strategy for the production experiment.*

4.3.1 Gel preparation

The first stage of aerogel production involved mixing the chemicals together at the correct proportions inside a ventilated fume cupboard (shown in Figure 4.2). Approximately 40 ml of solution was prepared for both drying methods. The HTSCD samples were prepared in 4 glass test tubes, and the LTSCD samples were prepared in 18 smaller plastic cuvettes. Approximately 10-12 minutes after the raw ingredients were mixed the samples became rigid alcogels.

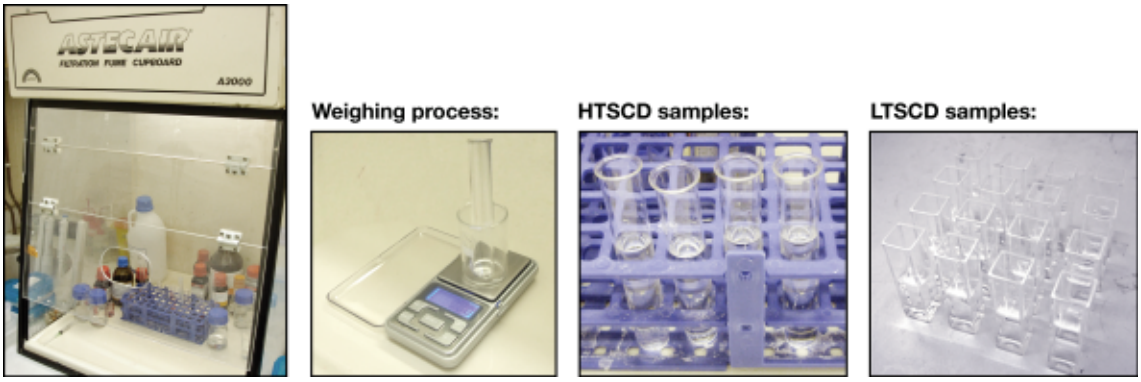

Figure 4.2 *Fume cupboard, digital scales and alcogel samples.*

The mass of all raw ingredients was measured using digital scales and the electricity use of the fume cupboard was logged using an 'Eco-Eye Plug-in Energy Monitor', displaying the rate of energy use (W) and the total energy use (kWh).

Table 4.1 and Table 4.2 show the respective data collection inventories for the HTSCD and LTSCD samples. All gel samples were prepared and weighed by the research engineer with supervision from M.Grogan. Note that gel preparation time (and consequent electricity use) was higher than normal due to time spent weighing each ingredient on the digital scales.

Table 4.1 *Data collection inventory for HTSCD gel preparation.*

Raw materials used in gel preparation (HTSCD)	**Volume (ml)**	**Mass (g)**	**Material supplier**
Tetramethoxysilane	14.4	14.64	Fisher
Methyltrimethoxysilane	1.6	1.36	Alfa Aesar
Methanol	16	12.52	Fisher
Analytical reagent grade water	8	8.00	Fisher
Ammonia 2M	0.016	0.014	Sigma Aldrich
Electrical equipment	**Running time (h)**	**Total kWh**	**Equipment supplier**
Fan cupboard	00:43	0.063	Astec

Table 4.2 *Data collection inventory for LTSCD gel preparation.*

Raw materials used in gel preparation (LTSCD)	**Volume (ml)**	**Mass (g)**	**Material supplier**
Tetramethoxysilane	16.2	16.56	Fisher
Methanol	16.2	12.96	Fisher
Analytical reagent grade water	8.1	8.10	Fisher
Ammonia 2M	0.072	0.062	Sigma Aldrich
Electrical equipment	**Running time (h)**	**Total kWh**	**Equipment supplier**
Fan cupboard	01:20	0.112	Astec

4.3.2 Ageing

Following gel preparation, 2 ml of methanol was added to each sample and they were covered with Parafilm to prevent shrinkage from ambient drying. Over the next 3 weeks, the gels were fully immersed in several solvent baths (by M.Grogan) within the sealed plastic containers. During this step, all unreacted water diffused out from the gel, and the network had time to strengthen. In total, the HTSCD samples went through two solvent exchanges during the ageing process. The LTSCD samples went through five, where the fourth included a surface modification to make the gel hydrophobic. All saturated aging solvents were disposed into waste containers sent to the university waste management facility. Table 4.3 and Table 4.4 display the respective data collection inventories.

Table 4.3 *Data collection inventory for HTSCD ageing process.*

Raw materials used in ageing (HTSCD)	**Volume (ml)**	**Mass (g)**	**Material supplier**
Methanol - covering samples	8	6.33	Fisher
Methanol - 1st exchange	125	98.88	Fisher
Methanol - 2nd exchange	125	98.88	Fisher
Electrical equipment	**Running time (h)**	**Total kWh**	**Equipment supplier**
Fan cupboard	00:10	0.014	Astec

Table 4.4 *Data collection inventory for LTSCD ageing process.*

Raw materials used in ageing (LTSCD)	**Volume (ml)**	**Mass (g)**	**Material supplier**
Methanol - covering samples	36	28.48	Fisher
Methanol - 1st exchange	250	197.75	Fisher
Methanol - 2nd exchange	250	197.75	Fisher
Methanol - 3rd exchange	200	158.20	Fisher
Hexamethyldisilazane - 4th exchange	40	30.96	Sigma Aldrich
Methanol - 4th exchange	160	126.56	Fisher
Methanol - 5th exchange	200	158.20	Fisher
Electrical equipment	**Running time (h)**	**Total kWh**	**Equipment supplier**
Fan cupboard	00:35	0.049	Astec

4.3.3 High temperature supercritical drying

Figure 4.3 displays the equipment used and monitored during HTSCD. The process utilised an autoclave with a 1-litre capacity, connected to an electric heater and temperature sensor. A nitrogen bottle was connected prior to drying to create an inert atmosphere within the autoclave and check that the seals were capable of withstanding supercritical pressures. During supercritical drying, temperature was controlled by

manually entering set-points on the heater controller and pressure was controlled using a needle valve. Excess solvent was drained into a container as pressure was released.

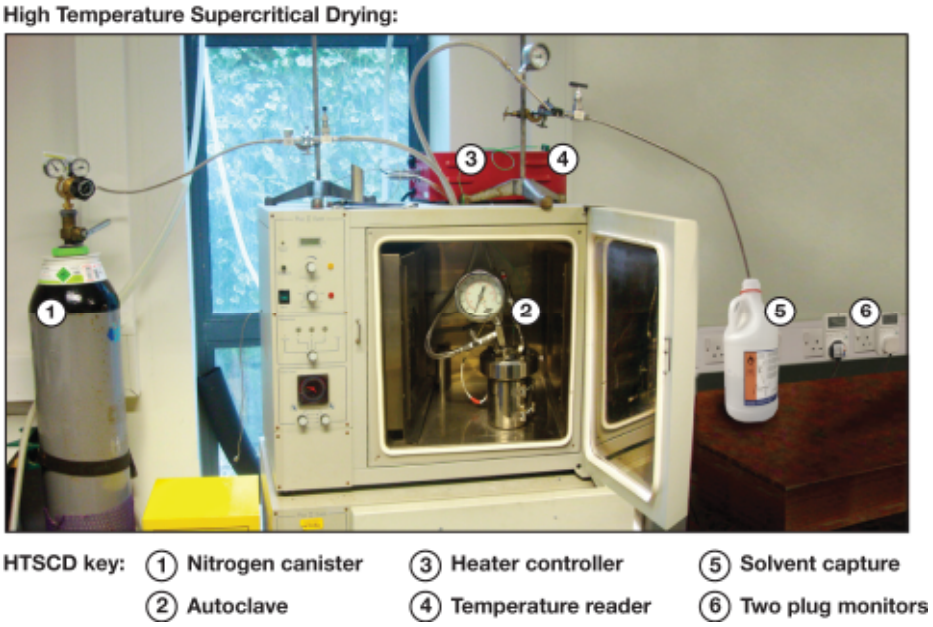

Figure 4.3 *Photograph of equipment used in HTSCD.*

To begin, the 4 gel samples (still inside the test tubes) were placed inside the autoclave with 400 ml of methanol. Two steel bars were then inserted to displace some of the unused volume, as shown in Figure 4.4. The autoclave was then sealed and filled with regulated nitrogen to 100 bar to check the chamber integrity. After 5 minutes, the nitrogen flow was disconnected and autoclave pressure was dropped to 10 bar.

Figure 4.4 *Closed HTSCD autoclave (left), view inside autoclave (right).*

Figure 4.5 shows the temperatures and pressures during HTSCD. The heater was programmed to a set point of 75 °C. Temperatures were raised 25 °C every 10 minutes until reaching 250 °C. Between 95-110 minutes, the set point was gradually increased to 280 °C. During this time, the pressure was allowed to rise to 100 bar, and then carefully controlled to stay at this level. At 120 minutes, solvent was manually drained out of the autoclave causing the pressure to fall. 15 minutes later, the heater set point was reduced to 100 °C and the unit was switched off. The autoclave was then left to cool for 100 minutes, after which the aerogel could be removed. Approximately 95 % of waste solvent was recovered and disposed via the university's waste management facility.

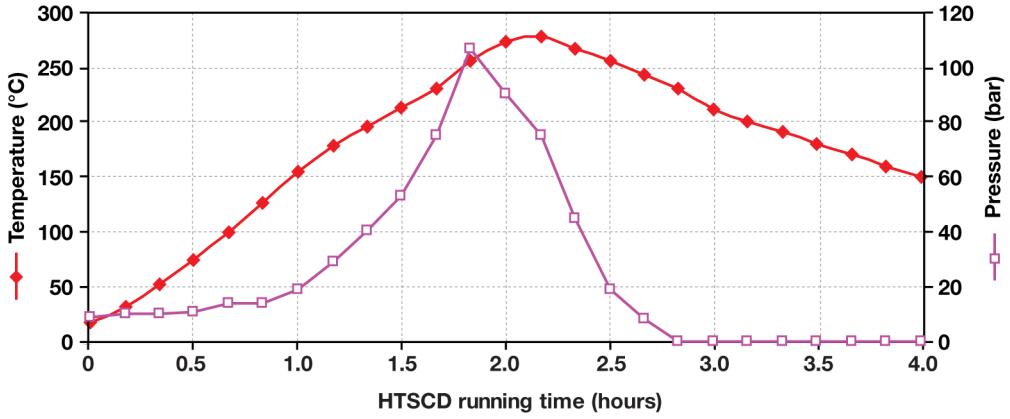

Figure 4.5 *Temperature and pressure profile during HTSCD.*

According to Grogan, although the fluid in this process exceeded the critical point of methanol by ~40 °C and ~25 bar, previous experience has indicated that if the pressure and temperature do not reach at least these values, the aerogel will be cracked and more shrunken. Grogan attributes this to excess water causing a change in the critical point of the pore fluid, requiring a higher temperature and pressure to reach supercritical conditions. Table 4.5 displays the data inventory for the HTSCD process.

Table 4.5 *Data collection inventory for HTSCD.*

Raw materials used in drying (HTSCD)	**Volume (ml)**	**Mass (g)**	**Material supplier**
Methanol	400	316.4	Fisher
Nitrogen - (N_2 at 100 bar 296 K)	~500	0.057	BOC gases
Electrical equipment	**Running time (h)**	**Total kWh**	**Equipment supplier**
Heater	02:15	0.882	SciMed
Temperature sensor	04:00	0.013	RS

During the supercritical drying process, two plug-in electricity monitors were used to record the total kWh consumed by the heater and temperature sensor. The total energy

use of the process was 0.895 kWh. The mass of nitrogen used was calculated using the formula n=PV/RT. Here n= quantity of nitrogen consumed (moles), P = Pressure (bar), V = volume (litres), R = universal gas constant (0.0832), and T = temperature (Kelvin).

4.3.4 Low temperature supercritical drying

Figure 4.6 shows the equipment used and monitored during LTSCD. The process utilised a 1-litre capacity autoclave with a window for viewing supercritical extraction. The autoclave was connected to a liquid CO_2 canister, chiller, pipe heater, pump and vessel heater. A backpressure regulator controlled the outflow of CO_2 and depressurisation rate of the autoclave. The entire process, including the flow rate of liquid CO_2 was controlled by a computer.

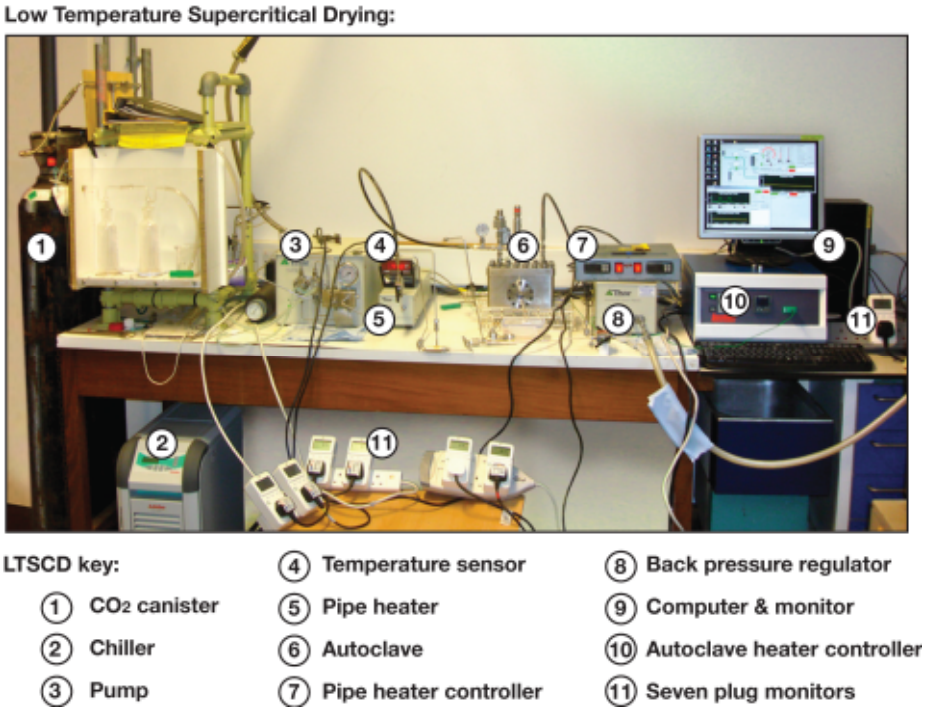

Figure 4.6 *Photograph of equipment used in LTSCD.*

To prepare the autoclave for supercritical drying, the 18 gel samples (removed from the cuvettes) were placed inside the autoclave filling approximately 5-10 % of the usable space (shown in Figure 4.7). 200ml of methanol was added to prevent the samples from cracking during the drying process. Following this, the autoclave was sealed and liquid CO_2 flowed in until in equilibrium with the bottle pressure (~55 bar). Prior to entering the autoclave, the liquid CO_2 was chilled to 0 ^{o}C. A dual-piston pump increases the CO_2 pressure to 100 bar, flowing through a pipe heater at 45 ^{o}C into the autoclave.

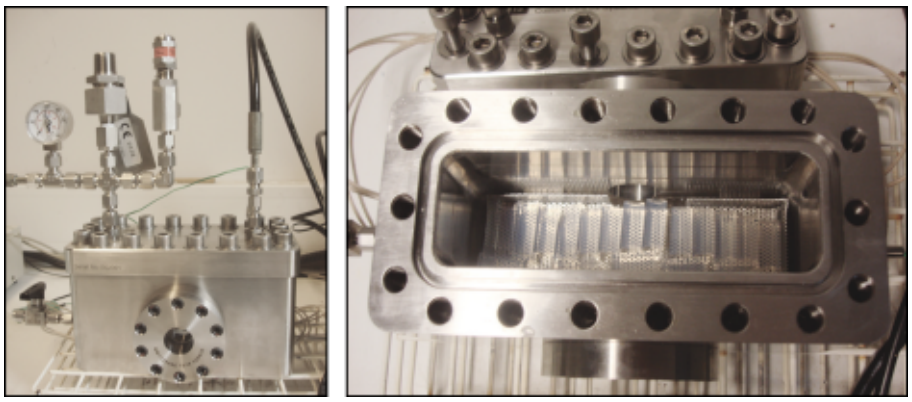

Figure 4.7 *Closed LTSCD autoclave (left), view inside autoclave (right).*

Figure 4.8 shows photographs taken through the window of the autoclave as liquid CO_2 entered and submerged the gel.

Figure 4.8 *Liquid CO_2 entering autoclave (photos taken at 0-30 minutes into drying).*

Figure 4.9 shows the temperature and pressure profile during LTSCD. Once supercritical conditions were reached, a vessel heater maintained the supercritical temperature at 45 °C, for approximately 4 hours. When depressurisation occurred, the chiller was switched off. As pressure dropped below 50 bar, the pipe heater and vessel heater were also switched off. Once cooled, the autoclave was opened and the aerogel could be removed.

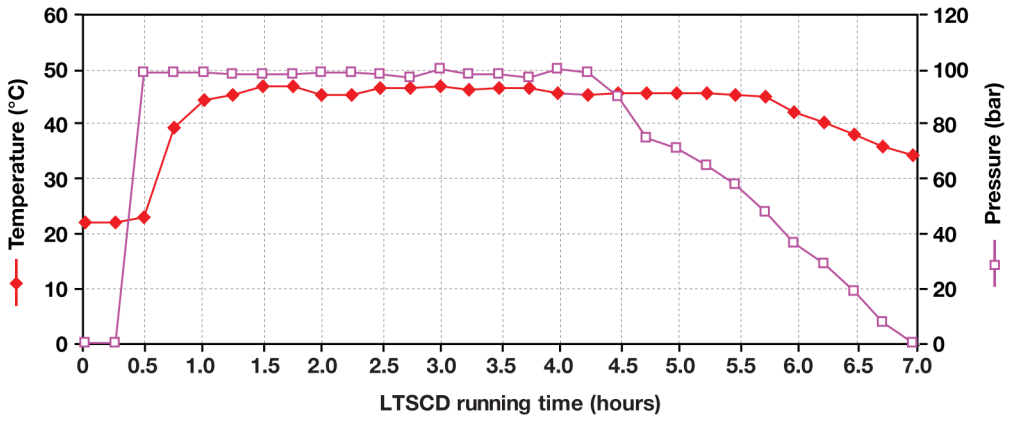

Figure 4.9 *Temperature and pressure profile during LTSCD.*

Throughout LTSCD, no recycling of CO_2 occurred. Instead, all excess CO_2 was trailed through a pipe out of a nearby window. The total duration of CO_2 flow was 4 hours, 20 minutes. Figure 4.10 shows the flow rate, monitored by a computer during the drying process. The total amount of CO_2 used was 4.538 kg, split across four main cycles. This value was verified by weighing the CO_2 bottles using mechanical scales before and after supercritical drying.

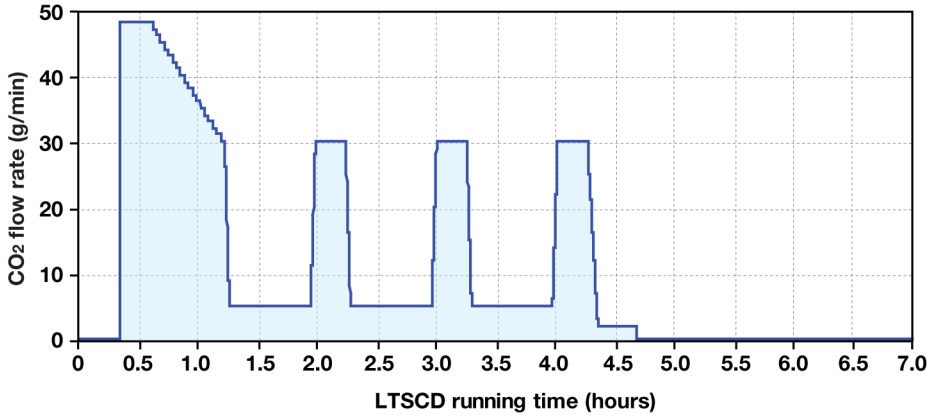

Figure 4.10 *CO_2 flow rate and pressure profile during the LTSCD.*

During LTSCD, seven plug-in electricity monitors were used to record the energy use of each piece of equipment. The total energy use was 3.063 kWh. The chiller (which cooled the CO_2 before entering the autoclave) accounted for over half of the total energy use, using 1.629 kWh. The computer with monitor had the second largest energy use accounting for 0.641 kWh. Table 4.6 displays the data collection inventory for the entire LTSCD process.

Table 4.6 *Data collection inventory for LTSCD.*

Raw materials used in drying (LTSCD)	**Volume (ml)**	**Mass (g)**	**Material supplier**
Methanol	200	158.2	Fisher
Carbon dioxide	-	4,538	BOC gases
Electrical equipment	**Running time (h)**	**Total kWh**	**Equipment supplier**
Chiller	04:30	1.629	Thar
Computer and monitor	07:00	0.641	Dell
Vessel heater	05:45	0.206	Syrris and Lenton
Back pressure regulator	07:00	0.200	Thar
Pipe heater	05:45	0.185	Thar and SciMed
Pump	07:00	0.180	Thar
Temperature sensor	07:00	0.022	RS

4.4 Aerogel Properties

Figure 4.11 and Figure 4.12 show photographs of the aerogel samples produced from HTSCD and LTSCD respectively:

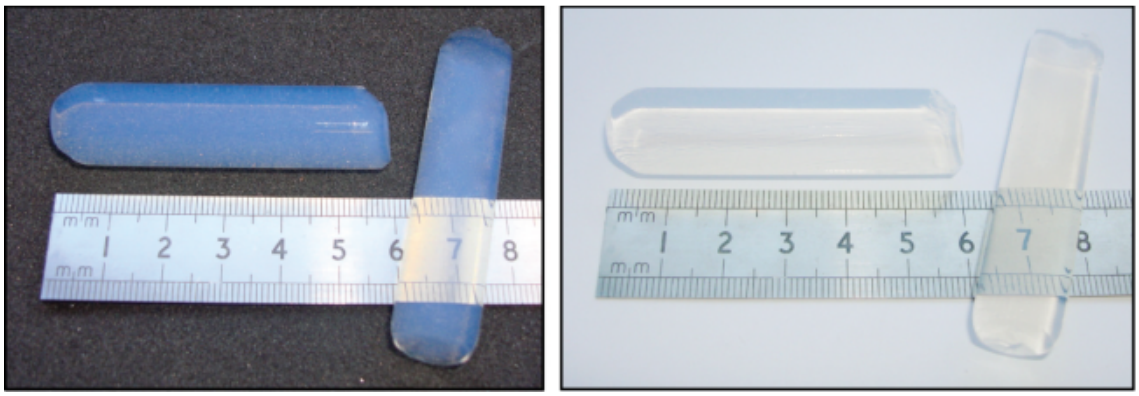

Figure 4.11 *Two aerogel samples produced through HTSCD.*

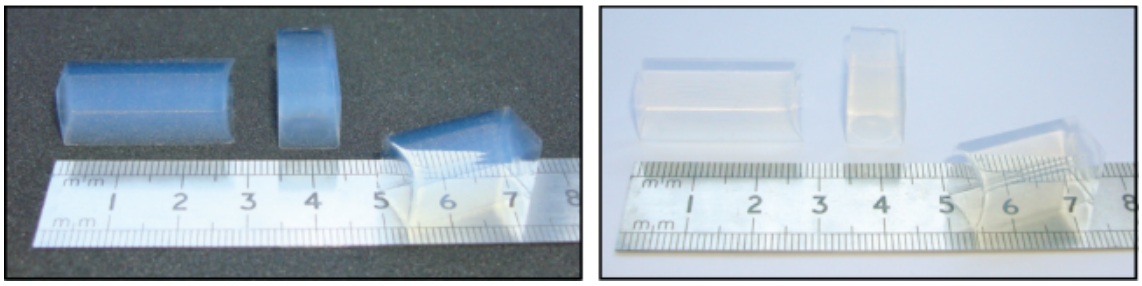

Figure 4.12 *Two aerogel samples produced through LTSCD.*

The samples had good optical quality and no internal cracks. They could be handled with care, but were fragile at the edges. They appear blue against a dark background and yellow against a light background. This is due to different wavelengths of light being transmitted, absorbed and reflected by the nanosized pores due to Rayleigh scattering (Fricke and Tillotson, 1997).

To assess the properties of the aerogel made in a lab compared to industrially produced aerogel, a scanning electron microscopy (SEM) was used to investigate the general topography of the LTSCD and HTSCD samples alongside ambiently dried translucent granular aerogel produced industrially by Cabot Corporation. All samples were fractured prior to investigation. The industrial granules were fractured by crushing them against the viewing plate. The HTSCD and LTSCD aerogel samples were fractured by cutting them with a scalpel. All samples were brittle.

Figure 4.13 displays low magnification SEM images of the three aerogels showing their fracture conditions. As shown, the surface of all three samples appeared smooth and it was not possible to see individual pores or particles, indicating that these features are on a nanoscale. Micro-cracks and beach marks were clearly visible across the surface of each sample where fracturing occurred. This fracturing characteristic implied that the lab samples should have similar properties to industrially produced aerogel.

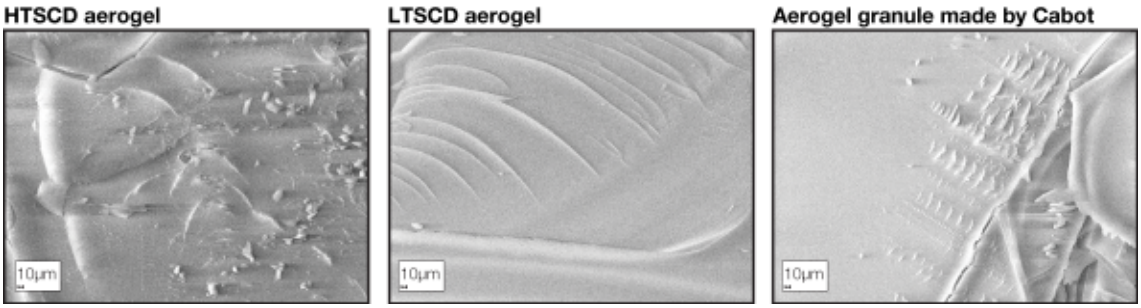

Figure 4.13 *Scanning electron microscopy showing the surface characteristics of three different aerogel samples at 500x magnification. HTSCD aerogel (left). LTSCD aerogel (centre), Ambient dried translucent granular aerogel produced industrially by Cabot Corporation (right).*

4.5 Inventory Analysis

Figure 4.14 displays the production energy and CO_2 burden associated with making 40 ml of aerogel via LTSCD and HTSCD.

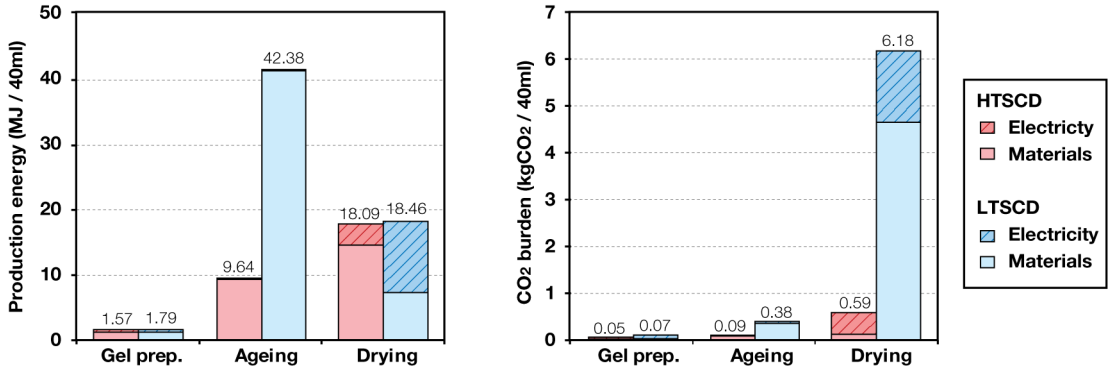

Figure 4.14 *Production impact associated with making 40ml aerogel via HTSCD and LTSCD. Left graph compares production energy. Right graph compares CO_2 burden.*

For each raw material and electrical usage, the production energy and CO_2 burden were calculated based upon the following assumptions: The energy and CO_2 spent to produce methanol was used to represent the impact of all chemicals. Methanol accounted for

~96 % of all chemicals used in both processes. An energy cost of 47 MJ/kg and CO_2 burden of 0.4 $kgCO_2$/kg was used for pure methanol manufacture (Neelis *et al.* 2005; Berge, 2009). This reference also contains a methanol combustion value of 30 MJ/kg, which was not included (Berge, 2009). The impacts of nitrogen and water use were also disregarded. A carbon factor of 0.517 $kgCO_2$/kWh was assumed for grid electricity in the UK (DECC, 2010a).

The total production energy associated with HTSCD was 29.3 MJ/40ml. The total production energy associated with LTSCD was higher at 62.6 MJ/40ml. Regarding the total CO_2 burden, HTSCD was accountable for 0.73 $kgCO_2$/40 ml. LTSCD was higher at 6.64 $kgCO_2$/40 ml. The methanol used during ageing had the most significant impact on the total production energy. The liquid CO_2 consumed during LTSCD had the most significant impact on total CO_2 burden.

4.6 Impact Assessment

To attain the functional unit, M.Grogan considered several ways in which both laboratory scale processes could be optimised to create 1 m^3 (1000 litres) of aerogel without major changes to equipment or manufacturing steps. These changes were:

(i) The maximum batch size during gel preparation could be expanded to 1-litre without different stirring mechanisms.

(ii) The gel preparation time could be reduced to 20 minutes (as weighing ingredients during data collection prolonged the process).

(iii) The amount of solvent used during ageing could be reduced, as the least amount of solvent required for aging is an identical volume to that of the gel. On this basis, 4 soaks are required for HTSCD and 7 soaks are required for LTSCD to completely remove the water before supercritical drying. This was calculated from tolerances of 0.16 % water for HTSCD and 0.00128 % water for LTSCD, the same water % used to successfully make gels in this study.

(iv) It was estimated that both 1-litre autoclaves could be filled with up to 500 ml of gel without changing the equipment, making drying 12.5 times more efficient.

Applying each change still meant that 1000 batches of gel would have to be prepared and aged, then supercritically dried over 2000 cycles, to produce 1 m^3 of aerogel. The resultant production energy and CO_2 burden arising from these scaled batches is shown in Figure 4.15.

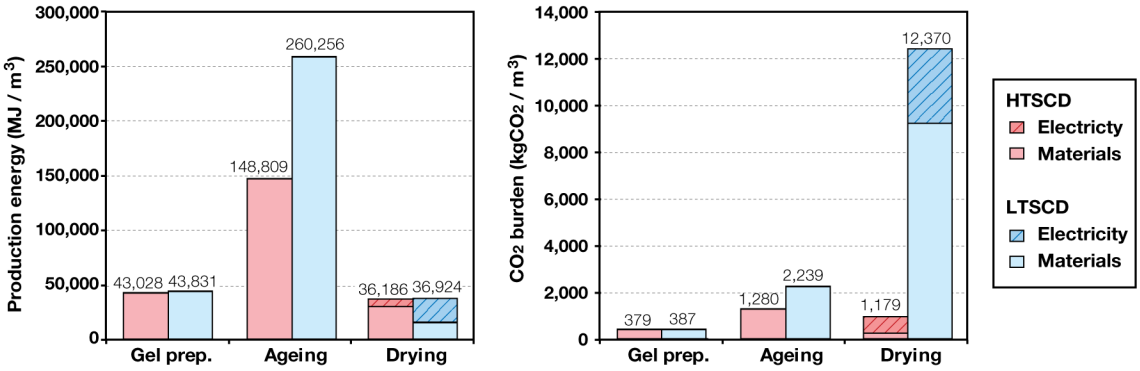

Figure 4.15 *Scaled production impact for making 1m³ aerogel via HTSCD and LTSCD. Left graph compares production energy. Right graph compares CO_2 burden.*

4.7 Interpretation

Prior to this investigation, in-situ testing (presented in Chapter 3) found that retrofitting a 10 mm thick, 1 m² twin-wall polycarbonate panel filled with aerogel granules to single glazing could reduce the rate of heat loss by 80 %. If adapted into removable secondary glazing, fitted permanently from 1st October - 31st May in a gas heated home in London, UK, then annual energy savings of approximately 400 kWh/year, per m² of glazing are predicted, equivalent to 1440 MJ/m²/year and 80 $kgCO_2/m^2$/year, assuming the house is heated to 21 °C all year round with an 18 °C night-time set back, a baseline glazing U-value of 6.39 W/m² K, boiler efficiency of 84 % and gas carbon factor of 0.198 $kgCO_2$/kWh (DECC, 2010a). Taking a wall thickness of 0.5 mm for the polycarbonate panel, approximately 0.008 m³/m² of granular aerogel is required to fill this prototype. Figure 4.16 displays the predicted production energy and CO_2 burden arising from manufacturing this volume of aerogel. Values are compared against the material's estimated operational savings over a 15-year product lifespan.

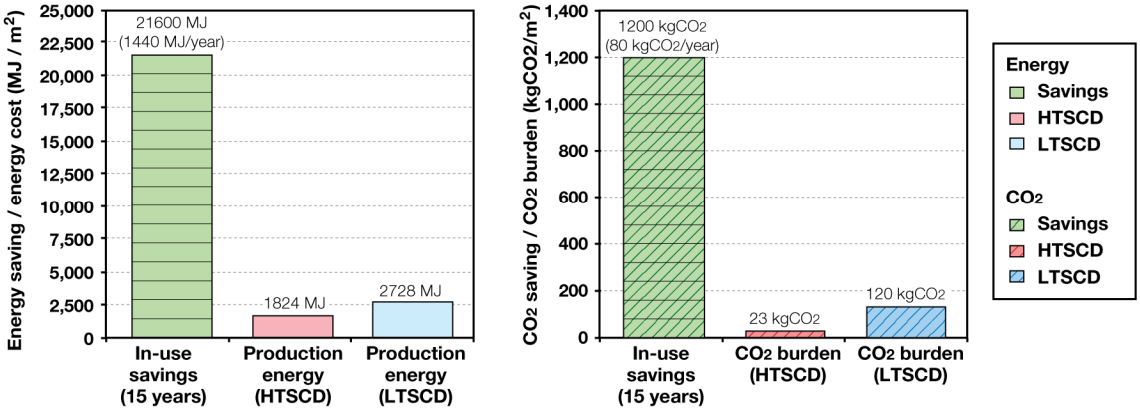

Figure 4.16 *Production costs of aerogel vs. in-use savings over product lifespan. Left graph compares production energy. Right graph compares CO_2 burden.*

Results show that aerogel can provide a positive energy and CO_2 contribution within 0.3-1.9 years. Aerogel produced by HTSCD can recover its production energy within 1.3 years and its CO_2 burden within 0.3 years. Meanwhile, aerogel produced by LTSCD can recover its production energy within 1.9 years and its CO_2 burden within 1.5 years.

4.7.1 Transport and end of life processing

Two factors omitted in this comparison were transport (of raw materials / finished products) and the impact of end of life processing (e.g. product re-use, recycling, landfill etc). Transport can be complicated to assess since it is unclear where a system boundary should be drawn in a global economy. A full sensitivity analysis should consider the type of vehicle, transport distance and loading etc. Contrarily, end of life processing can be difficult to assess since it is uncertain what might happen to products at the end of their usable lifespan.

According to the University of Bath, presumably, aerogel would just be crushed and disposed of at the end of its life in the same way as sand or rocks, since the material consists of amorphous silica, which is not carcinogenic. Conversely, provided the aerogel has not been contaminated during its incorporation into a building, the thermal and optical properties are not expected to degrade and the material can be re-used again, resulting in further operational savings.

According to the Cambridge Eco Selector, a comprehensive materials selection tool developed by Granta Design (2012) with Cambridge University, transporting 1 kg of insulation 100 km by ship and 300 km using a 32 ton truck accounts for just 0.15 MJ and landfill accounts for 0.2 MJ. As such, these factors are not expected to have a significant impact on the interpretation of results.

4.8 Limitations

A significant factor affecting the accuracy of this study is the differences between laboratory and industrial scale aerogel manufacture. Currently, scaling assumptions used to produce a 1 m^3 volume of aerogel do not accurately represent the energy use and CO_2 burden that would result from producing this volume industrially. This issue is difficult to resolve, due to the lack of information from industry concerning the actual economies and efficiencies of scale associated with mass production of aerogel. As such, the interpretation of these results should be treated as conservative estimates, used to provide judgement as to whether silica aerogel is a good environmental technology or not. Primary sources of discrepancy are given below:

Laboratory production scaling

The laboratory process was scaled with no major changes to equipment or production steps. The maximum batch size for gel preparation and drying was restricted to 1 litre and 0.5 litres respectively. This meant 1000 batches of gel would have to be separately prepared and dried over 2000 cycles to produce 1 m^3 of aerogel. This is unrealistic in the context of commercial production. Larger batch sizes or continuous production would result in far greater efficiencies.

CO_2 recycling

In the laboratory study, no recycling of CO_2 occurred. A total of 4.5 kg of CO_2 was used to dry 40 ml of aerogel using LTSCD. This mass was directly scaled by 2000 times to produce 1 m^3 of aerogel. This scaling factor could be eliminated if CO_2 recycling had occurred. According to Aspen Aerogel, all CO_2 is recycled at their production facility.

Energy recovery

No recycling or energy recovery from solvents occurred. The energy used to produce methanol was taken as 47 MJ/kg. The material has a combustion value of 30 MJ/kg, which was not included in the impact assessment. When producing aerogel on a mass scale, it can be assumed that solvents would be recycled/re-used or burnt for energy recovery. If recycled, then less methanol would need to be used. If the energy were recovered, this would result in the life cycle energy use in producing methanol being reduced to 17 MJ/kg.

Production quality

The aerogel manufactured for this study were solid, crack free and possessed high optical quality. Scaling assumptions predicted that 4-7 solvent exchanges were required to reproduce the high quality aerogel from the laboratory study. These exchanges aimed to purify the gels and completely remove the water to prevent cracking. Manufacturing granules with lower optical quality could mean that fewer solvent exchanges would be required, and less control would be needed to prevent cracking. Additionally, thinner granules require less time in the supercritical drying equipment as the time taken to remove the solvent scales with the square of the thickness.

Equipment efficiency

The electrical equipment used in the study could be more efficient. The chiller used the largest amount of electricity during LTSCD. This unit was large and not been

appropriately sized for its function. In industry, issues such as this would be corrected for cost savings, resulting in reductions in overall energy and CO_2 usage.

Fuel supply

Within industry, all (or some) of the production plant could be run by gas fuelled equipment in place of electricity. If this was the case then the CO_2 emissions factor could be reduced from 0.517 $kgCO_2/kWh$ to 0.198 $kgCO_2/kWh$.

4.9 Industrial Economies of Scale

When the results generated in this experiment are compared to the corresponding benchmarks for Aspen Aerogel's Spaceloft insulation, the laboratory scale production energy and CO_2 burden values, per m^3, are 28-42x and 4.4-23x larger, respectively, than industrial benchmarks. Note that the lower value in each of these ranges represents the magnitude of difference for HTSCD aerogel and the higher value represents LTSCD aerogel. In addition, note that the production energy and CO_2 burden, per m^3, for Spaceloft is 8139 MJ/m^3 and 648 $kgCO_2/m^3$ respectively, generated by multiplying the products impacts, per kg, by its nominal density of 151 kg/m^3 (Aspen Aerogel, 2010).

In an effort to understand (and bridge the gap) between laboratory scale and industrial scale manufacture, Figure 4.17 demonstrates how altering the scaling assumptions can significantly reduce this discrepancy.

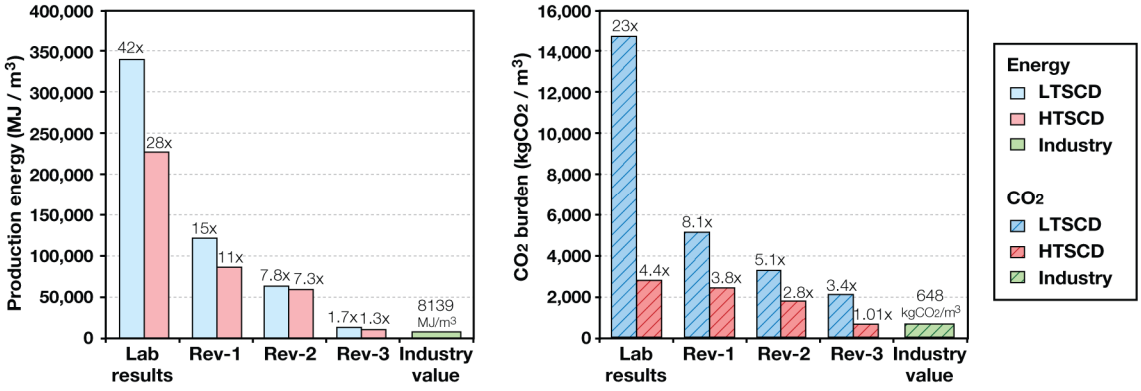

Figure 4.17 *Scaling revisions to bridge discrepancies between laboratory and industrial production. Left graph compares production energy. Right graph compares CO_2 burden. Bars are labelled showing the magnitude of difference compared to industry benchmarks.*

Firstly, in Revision 1, the batch size for gel preparation and drying was increased to 1000 litres enabling $1m^3$ of aerogel to be manufactured over one production run (as

opposed to preparing 0.5 litres of gel 2000 times, followed by drying 1 litre of gel 1000 times). To facilitate this change, it was assumed that electricity use is scaled up by 1000, 100 kg of CO_2 is used during drying for LTSCD and that all methanol usage in both manufacturing methods is combusted for energy recovery. The culmination of this revision causes the magnitude of difference to reduce to 11-15x and 3.8-8.1x respectively for production energy and CO_2 burden.

Going further, Revision 2, assumes that two solvent exchanges for HTSCD and three for LTSCD are carried out and that the chiller efficiency in LTSCD is increased by 80 %. This causes the production energy and CO_2 burden discrepancy to be reduced further to 7.3-7.8x and 2.8-5.1x respectively.

Following this, Revision 3 assumes that all CO_2 used during drying for LTSCD and all methanol used in both processes is recovered/recycled (thus eliminating the impact). This causes the difference to reduce to 1.3-1.7x for the embodied energy and 1.01-3.4x for the embodied CO_2.

Final figures for the production energy and CO_2 burden are 12,523 MJ/m^3 and 1,950 $kgCO_2/m^3$ for aerogel made by low temperature supercritical drying, and 10,230 MJ/m^3 and 651 $kgCO_2/m^3$ for aerogel made by high temperature supercritical drying.

4.10 Conclusion

The aim of this study was to investigate whether the use of aerogel as an insulation technology for the building sector provides a measurable environmental benefit over its life cycle. Two methods of aerogel production were investigated to compile a data inventory for this assessment. For each, the production energy and CO_2 burden was quantified and scaled up to produce a 1 m^3 volume of aerogel. The impact was then compared against the operational savings over 15 years, arising from retrofitting translucent aerogel to single glazing.

The core contribution to knowledge in this novel life cycle study is that aerogel produced by LTSCD and HTSCD could recover its production cost within 0.3-1.9 years. These findings are well within the predicted lifespan of building products containing aerogel. The LTSCD method of aerogel manufacture had the longest environmental payback. This was largely due to LTSCD having a higher amount of solvent use during the ageing process and because supercritical drying required more energy intensive equipment, whilst also directly consuming CO_2.

The environmental impact of both manufacturing techniques could be reduced if larger batches were produced, more energy efficient equipment were used and/or if recycling or energy recovery of solvents took place. The greatest improvements are expected from LTSCD, since there is an opportunity to recycle the CO_2 used during drying. If the desire is to produce granular aerogel, there may also be opportunities to reduce the amount of solvents used, which account for a significant proportion of the total production energy.

It should be emphasised that the true economies and efficiencies of scale associated with mass production are unclear due to a lack of information regarding commercial manufacturing of aerogel. Despite these factors, results have demonstrated that aerogel can provide a measurable benefit over its life cycle. Furthermore, an analysis of the scaling assumptions has shown that the discrepancies between laboratory and industrial scale manufacture can be significantly reduced to provide more realistic figures for production energy and CO_2 burden.

Based on the results, following industrial scaling, values of 12,523 MJ/m^3 and 1,950 $kgCO_2/m^3$ would be recommended for the production energy and CO_2 burden of silica aerogel made by low temperature supercritical drying. Respective figures for aerogel made by high temperature super critical drying are 10,230 MJ/m^3 and 651 $kgCO_2/m^3$. Note that there is still a need for a publically available LCA of aerogel made by ambient pressure drying.

Promising results have been observed when comparing the environmental impact of aerogel production to the in-use savings from aerogel in a glazing application. A similar comparative assessment could be carried out if analysing aerogel in a different application, such as solar Trombe walls or solar air collectors, for example. If undertaken, the impact of additional materials, such as the polycarbonate panel or any framing components should also be considered.

Chapter 5

RETROFIT FOR THE FUTURE: A 'NEAR PASSIVHAUS' WHOLE HOUSE REFURBISHMENT INCORPORATING AEROGEL

Abstract

This chapter contains a case study of a whole house refurbishment, which took place as part of the 'Retrofit for the Future' programme; a competition challenging teams to develop innovative refurbishment strategies with potential to reduce 80 % of CO_2 emissions in low-rise social housing. A four bedroom 'hard-to-treat' property in South-East London is transformed into a six bedroom super-insulated home. Numerous retrofit technologies were implemented, including external insulation, triple glazing, mechanical ventilation with heat recovery, photovoltaic panels for electricity generation and a solar thermal collector to preheat the hot water supply. The design team aspired to obtain the German "Passivhaus standard", but this was not achieved due to difficulties achieving the required air tightness targets on-site. Nonetheless, the air tightness is 3 times better than UK new build standard and a number of valuable experiential lessons were learnt. Aerogel has been applied successfully to a hard-to-treat area of the ground floor, a custom-built external plant room door and in an innovative solar air collector integrated into the external insulation on the south façade, preheating the air in the mechanical ventilation system (refer to Chapter 6 for details of the predicted and in-situ performance of this 'Aerogel Solar Collector'). Ongoing research after this EngD will include a two year whole house energy monitoring programme with residents in-situ.

5.1 Introduction

'Retrofit for the Future' was a government funded competition launched by the Technology Strategy Board (TSB) in March 2009. The aim of the competition was to develop a host of innovative and scalable whole house refurbishment strategies with potential to reduce 80 % of CO_2 emissions in low-rise social housing. Following an open call for applications, the competition was split into two phases. In 'Phase 1', £ 20,000 was awarded to teams to undertake a technical assessment of their property's baseline primary energy use and CO_2 emissions, supported by a detailed 'whole house' design proposal. In 'Phase 2', £ 150,000 was awarded to undertake on-site retrofit works, supported by a 2 year monitoring programme.

In total, 86 teams across the UK were shortlisted and awarded funding to implement their strategies onto occupied houses. Amongst these was a collaboration consisting of Buro Happold, Gallions Housing Association, Fraser Brown MacKenna (FBM) Architects, Martin-Arnold Associate surveyors and Axis Europe contractors. Gallions manage over 5,600 properties within six London boroughs. Included in this remit are approximately 4,000 hard-to-treat properties and 2,200 pre-cast concrete properties in the Thamesmead Estate in South-East London, where this project took place.

5.1.1 Retrofit house

Figure 5.1 displays a photo of the property selected for the retrofit. The property was a three-storey, four bedroom, pre-cast concrete end terrace house in the Thamesmead Estate, typical of the local area. Key features included a large south facing concrete wall, a mixture of single-glazed and old double-glazed windows, unused ground-floor garages (too narrow for modern cars) and an open-air walkway along the first floor. The property is sited within a unit of five terraced houses.

Figure 5.1 *Photographs of the South-West and North-East elevations prior to retrofit works.*

5.1.2 Thamesmead estate

The Thamesmead estate was constructed during the 1960s using the 'French Balency System' technique (Figure 5.2). This large panel construction method was first used in Ireland and Great Britain during 1949. Structures consist of pre-cast concrete walls integrated with plumbing, gas district heating pipework and ventilation ducts combined with in-situ concrete floors containing electrical wiring, also providing a connection to a district heating network. These 'functional units' avoided the need for complex joints providing numerous advantages in terms of cost, speed, flexibility of planning and number of man hours required (Power, 2000).

Figure 5.2 *Historic photographs of the Thamesmead estate being constructed.*

Thamesmead has been in need of regeneration for many years. When built, the large scale approach to urban planning encouraged large, bold units, such as three storey terraced houses and large tower blocks, all with some form of outdoor space. Nowadays however, the estate suffers from anti-social behaviour due to a combination of high unemployment, a lack of community surveillance and numerous alleyways created by ground floor garages and walkways. After the energy crisis, the district heating supply was disconnected. In addition, the stock is inadequately insulated, hard-to-treat and prone to moisture-related problems such as condensation, rising damp and mould growth made worse by insufficient heating and fuel poverty.

5.1.3 Existing plans and sections

Within Gallions' archives, a number of historic plans and sections were found for dwellings in Thamesmead. However, none were of suitable visual quality, to provide sufficient details of the build-up and dimensions. Addressing this issue, updated floor plans, shown in Figure 5.3 were produced by Martin-Arnold Associates. A typical section through an external Balency System wall and floor plate, based on large panel system construction reports by BRE (1986; 1987; 1989) is illustrated in Figure 5.4 (drawn by S.Craig, facade engineer at Buro Happold).

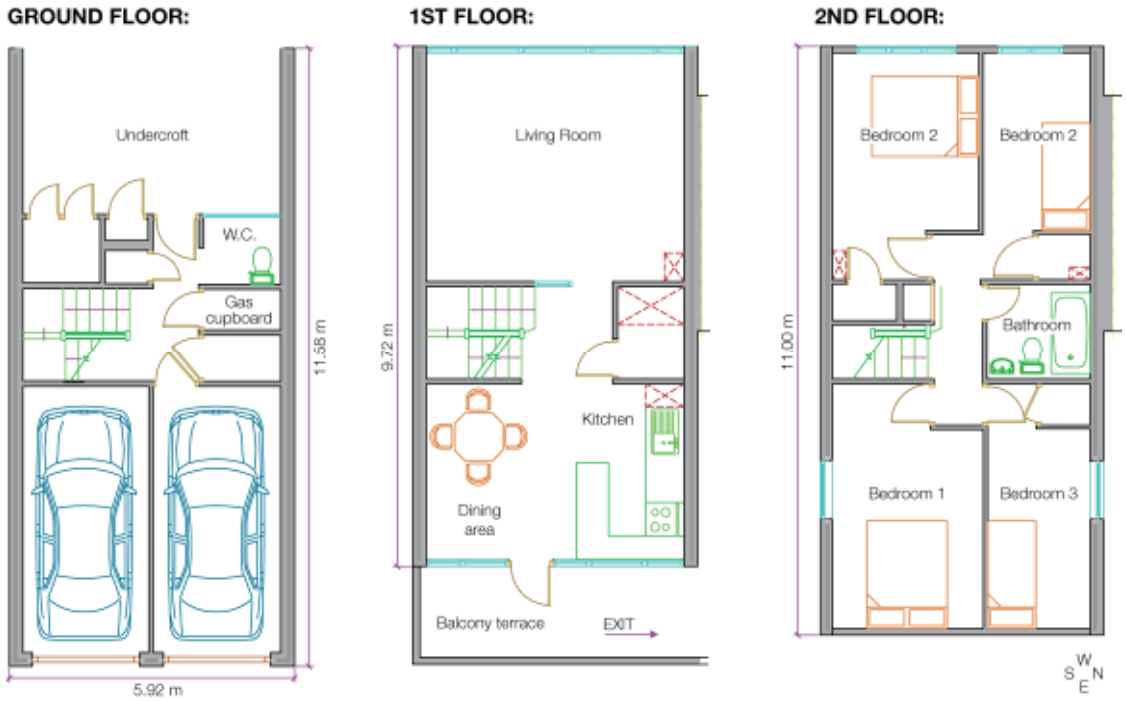

Figure 5.3 *Floor plans of the property*

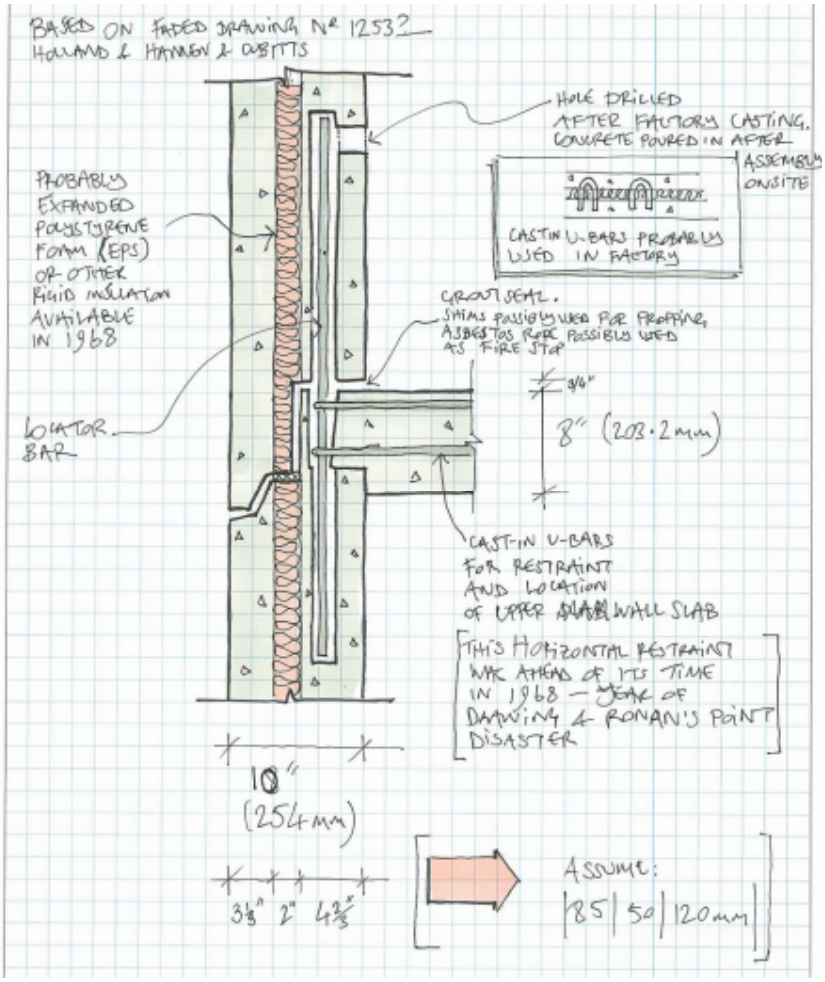

Figure 5.4 *Estimated build-up of Balency system external walls.*

5.2 Baseline Performance

To investigate the baseline performance of the property, thermal imaging, in-situ value testing and SAP modelling was carried out independently by the research engineer. Findings are summarised in the next three sections, respectively.

5.2.1 Pre-retrofit thermal imaging

Figure 5.5 and Figure 5.6 display two thermal images taken prior to retrofit works began. All images are focused around a top floor bedroom on the dwellings north-east elevation, heated to 30 °C by a 2 kW thermostatically controlled heater. Figure 5.5 displays the bedroom's exposed asbestos wall and overhanging floor. Figure 5.6 focuses on the partition wall between the bedroom and a 'link house' next door which was not being retrofitted. During testing the external temperature was 12 °C. Note that images were taken during the daytime, meaning there was some residual heat on the building's exterior due to solar gain.

Figure 5.5 *Thermal image of the asbestos wall and overhanging bedroom.*

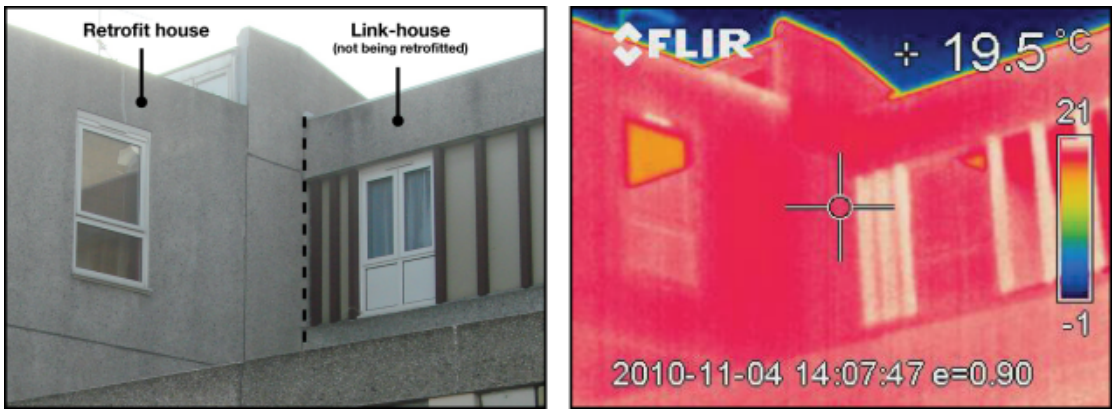

Figure 5.6 *Thermal image of the partition wall between the retrofit house and link house.*

Despite uncertainty due to the residual heat, Figure 5.5 shows that the asbestos panelling on the north wall performs poorly in relation to the pre-cast concrete construction present in the walls and overhanging floor. There is little/no distinction between the retrofit house and the other houses on the estate (shown in the background of Figure 5.5). Similarly, Figure 5.6 shows little distinction between the thermal performance of the dwelling and link house next door (not being retrofitted), which would be expected in the post-retrofit thermal assessment.

5.2.2 In-situ U-value testing

In November 2010 a series of in-situ U-value tests were conducted to measure the actual U-value of the walls, roof and an overhanging floor before extensive retrofit work began. Figure 5.7 shows the arrangement of monitoring equipment, highlighting the room and elements that were monitored. Testing lasted for 10 days.

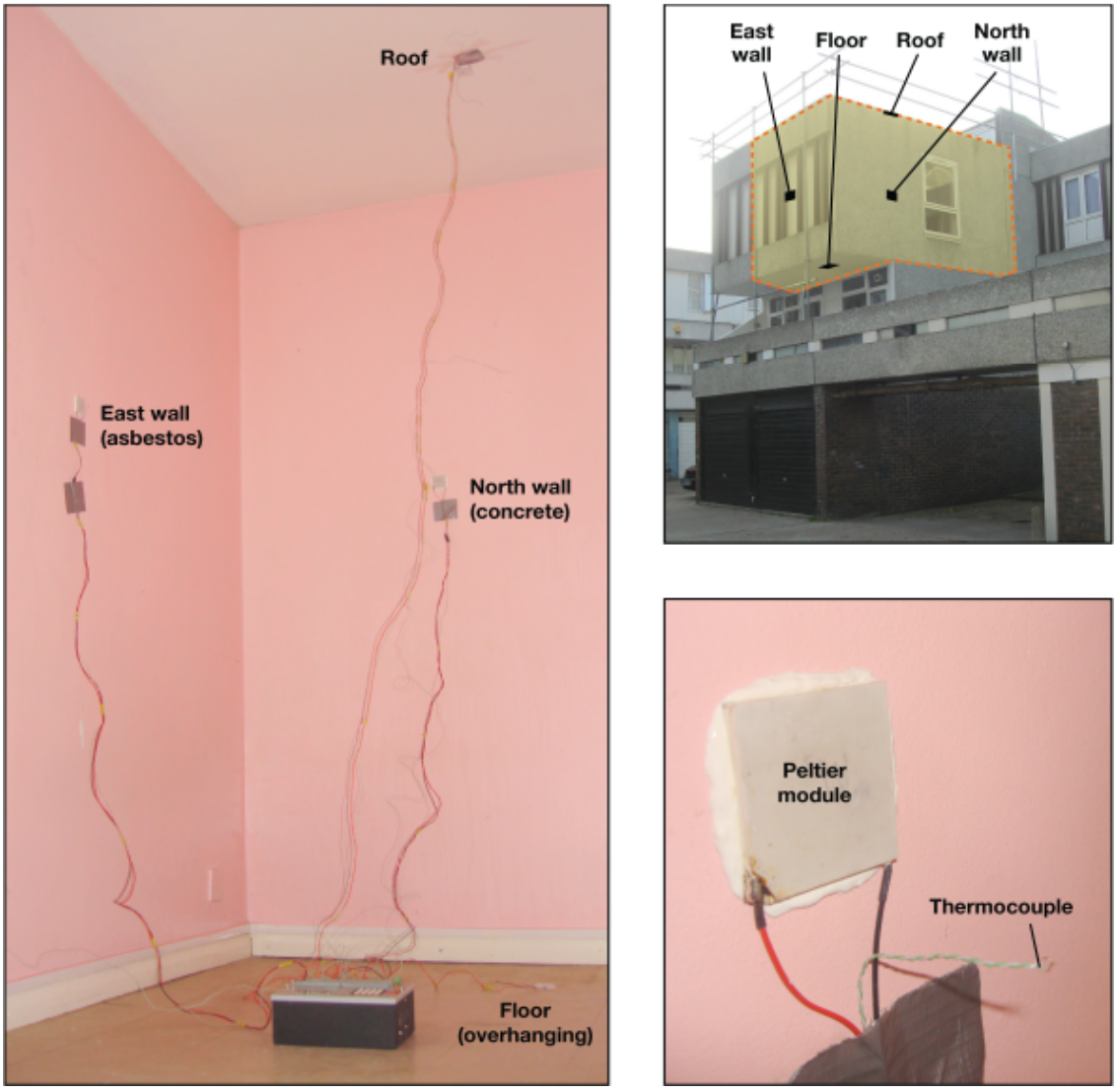

Figure 5.7 *In-situ U-value testing on the retrofit house.*

All tests were conducted in the top floor bedroom heated by the 2 kW thermostatically controlled heater. As the U-value = heat flux / temperature difference, in-situ monitoring consisted of heat flux measurements through each element, internal air temperature measurements besides each element and an external air temperature measurement, monitored using a thermocouple trailed out of a nearby window. Temperature monitoring was conducted using K-type thermocouples. Heat flux was measured using peltier modules, calibrated in December 2009, thermally bonded to each internal surface. All equipment was wired into a CR23X micro logger.

Predicted U-values

Table 5.1 displays theoretical U-values for each element. Calculations were performed using IES Virtual Environment software, following the EN-ISO U-value methodology. Note that two build-ups were calculated for the east wall and roof respectively, to account for possible construction differences due to inconsistent roof insulation and the external timber beams on the east wall. Insulation thickness assumptions were based on an intrusive survey.

Table 5.1 *U-value calculations for Balency system construction.*

	Construction layers (inside to out)	Thickness (m)	Conductivity (W/m K)	U-value (W/m^2 K)
NORTH WALL: Balency system	Gypsum plasterboard	0.010	0.420	**0.847**
	Concrete inner leaf	0.110	1.700	
	Expanded polystyrene insulation	0.035	0.040	
	Concrete outer leaf	0.080	1.700	
EAST WALL: Asbestos section	Plasterboard	0.010	0.160	**2.271**
	Cavity	0.030	-	
	Asbestos board	0.010	0.360	
EAST WALL: Asbestos & timber section	Plasterboard	0.010	0.160	**0.908**
	Cavity	0.030	-	
	Asbestos board	0.010	0.360	
	Timber	0.080	0.121	
ROOF: No insulation	Plasterboard	0.010	0.160	**1.701**
	Cavity	0.100	-	
	Timber joists	0.020	0.121	
	Asphalt	0.020	0.500	
ROOF: With insulation	Plasterboard	0.010	0.160	**0.748**
	Cavity	0.100	-	
	Glass fibre insulation	0.030	0.040	
	Timber joists	0.020	0.121	
	Asphalt	0.020	0.500	
FLOOR: Overhanging	Timber	0.080	0.121	**1.015**
	Concrete outer leaf	0.140	1.130	

External temperature

Figure 5.8 displays the internal and external temperatures monitored during in situ testing. Note that for a three day period during the test, the electric heater switched

itself off (as the manual feed electricity meter ran out of credit). Raw data during this period was omitted (indicated in the graphs by the dashed line), as there was an insufficient temperature difference to undertake U-value calculations. As shown, external temperature during the useful test period varied from 3-12 °C. Internal temperature measurements were coolest by the floor ranging from 22-25 °C, compared to 32-36 °C measured by the walls and roof. This could be partially attributed to the heat in the space rising as well as the exposed concrete floor.

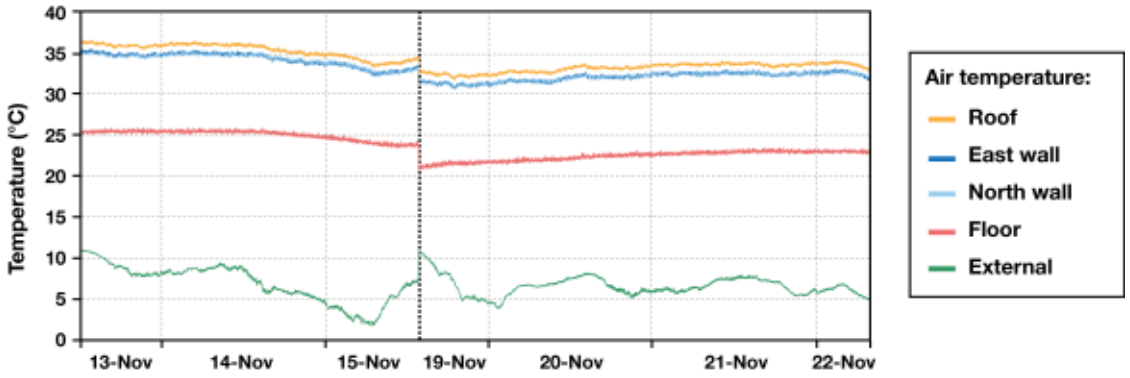

Figure 5.8 *Internal and external air temperatures measurements during in-situ testing.*

Heat flux

Figure 5.9 displays the monitored heat flux through each element following calibration. The largest heat flux was observed through the roof and lowest was found through the floor, closely followed by the east and north walls.

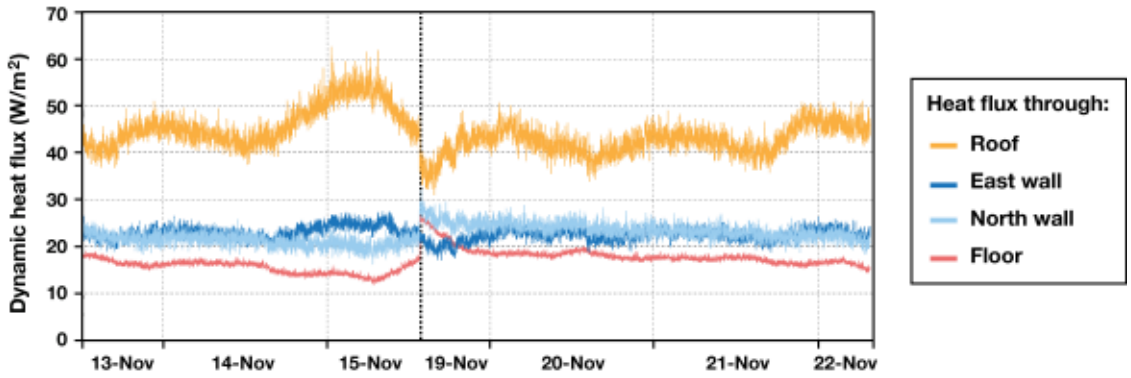

Figure 5.9 *Dynamic heat flux through the peltier modules mounted to each element.*

In-situ U-values

Figure 5.10 displays the cumulative average U-value over time for each element. Values stabilised after 3.5 days of continuous testing. Measured U-values were 1.61 W/m² K for the roof, 1.07 W/m² K for the floor, 0.89 W/m² K for the north wall, and 0.88 W/m² K for the east wall.

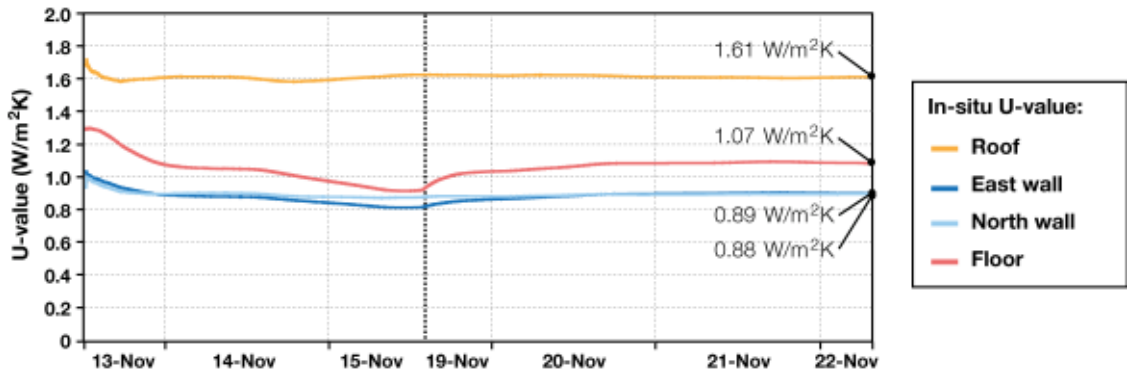

Figure 5.10 *Cumulative average U-value for each element.*

Summary of U-value testing

A comparison between the predicted and measured U-values is displayed in Figure 5.11. Mean values for the in-situ measurements were within ±6 % of predictions (assuming the roof section had no insulation and the heat flux sensor on the east wall was positioned over an asbestos panel with a timber beam behind it). Note that an uncertainty up to ±14.7% has been calculated for the predicted U-values based upon the upper and lower limit of their thermal conductivities. Furthermore, an uncertainty of ±13.2% was calculated for the in-situ U-values, based upon the equipment accuracies and the difference between internal air & surface temperature measurements.

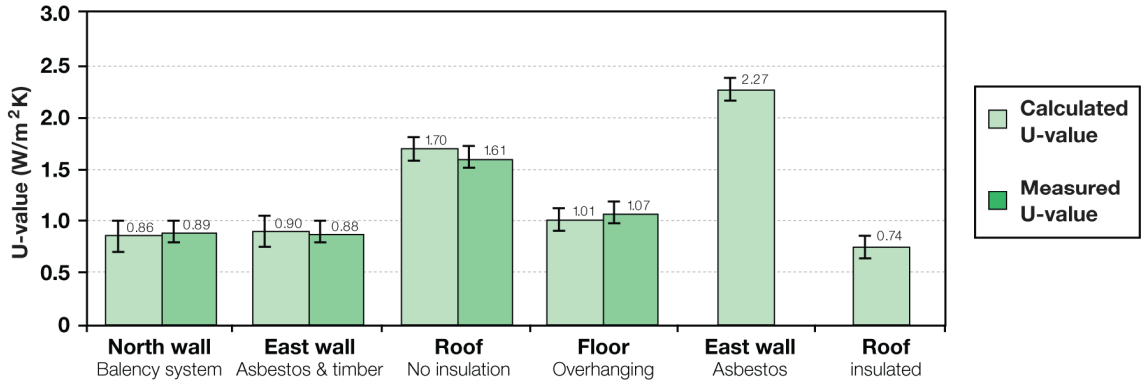

Figure 5.11 *Predicted and measured U-values.*

It was assumed the measured U-value of the north wall could be used to represent all pre-insulated external Balency walls in the thermal model and that a weighted U-value based on the proportion of timber beams would be the most appropriate solution for dealing with the asbestos walls. The floor U-value provides a useful indication of how the exposed overhang performs. However, this U-value could not be used to represent the ground floor, as the U-value and temperature profile would be different. The measured U-value of the roof indicates that the patchy insulation provides little benefit.

5.2.3 Baseline CO_2 emissions

An assessment of the dwelling's baseline CO_2 emissions was conducted using the Standard Assessment Procedure (SAP) using IES Virtual Environment supported by JPA Designer SAP calculation tool and a whole house SAP extension spreadsheet provided by the TSB to account for lighting (currently limited by regulation), cooking equipment and appliances. Both IES and JPA are Building Regulation compliant SAP software. In particular, they can implement the guidance laid down in SAP 2009 to provide an industry accepted prediction of dwelling emissions rate.

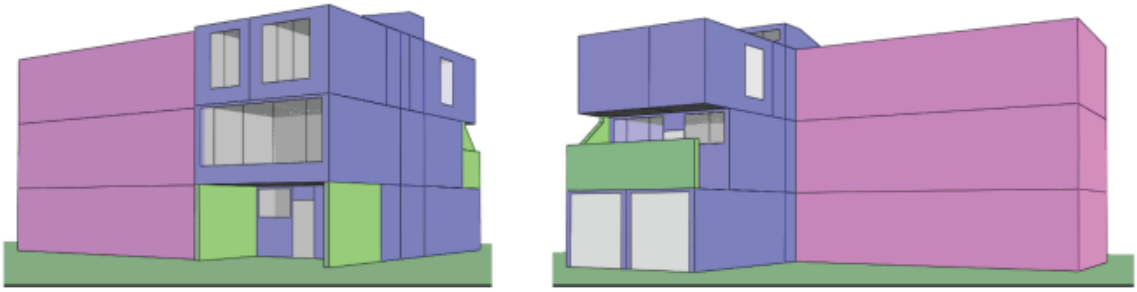

Figure 5.12 *Baseline geometry built to represent the existing house prior to any retrofit work. Left image shows the rear entrance through the garden. Right image shows the double garage and front entrance through the first floor walkway.*

Figure 5.12 displays the baseline geometry of the property created using IES. Assumptions regarding the baseline fabric and services were obtained through in-situ U-value data, walkthrough surveys and information provided by Gallions Housing Association. The baseline air-tightness of the property was 9.1 m^3/m^2 hr @ 50Pa, as measured by BSRIA Ltd (appointed by the TSB to provide monitoring support) on the 19th of April 2010.

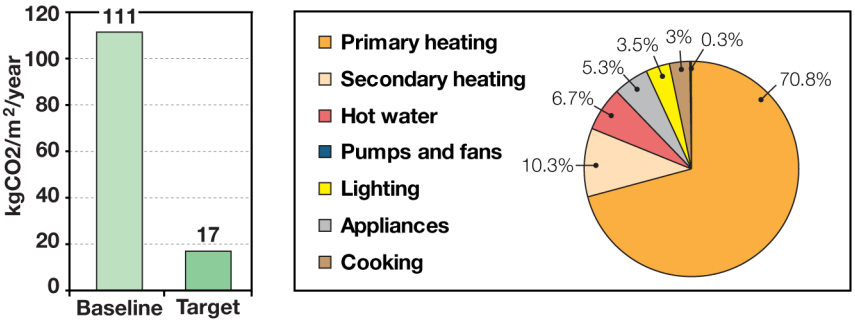

Figure 5.13 *Analysis of the dwelling's baseline CO_2 emissions.*

The dwelling's baseline CO_2 emissions was 111 $kgCO_2/m^2$/year, equivalent to a SAP rating and band of 34(F). The distribution of these emissions is displayed in Figure

5.13. Approximately 70 % arose from the primary space heating system consisting of an old gas boiler and radiators, 10 % were allocated to secondary heating (i.e. electric heaters) and hot water usage, appliances, lighting and cooking equipment each consumed between 3-7 % of the dwelling's total CO_2 emissions. Note that small power consumption is not included in the SAP calculation process.

5.3 Retrofit Strategy

The development and refinement of the whole house retrofit strategy arose from several months of meetings between Buro Happold, FBM architects and Martin-Arnold Associates. After lengthy discussions it was agreed by all parties to aim for the German Passivhaus standard for thermal bridge free insulation and high air-tightness. This strategy was encouraged by Gallions from an early stage in the design process. At the time, no UK domestic property had been retrofitted to this standard. To support this, Gallions appointed C.Boonstra, Director of Trecodome BV as an external Passivhaus consultant to undertake preliminary Passivhaus calculations.

In order to achieve the required maximum space heating demand of 25 kWh/m²/year for retrofits, Passivhaus guidance specifies that all external walls, roofs and floors should achieve a maximum U-value of 0.15 W/m² K. All glazed elements and external doors should achieve a maximum U-value of 0.8 W/m² K. Supporting this approach would be external cladding, triple glazing, whole house mechanical ventilation with heat recovery (MVHR), photovoltaic (PV) panels for electricity generation, solar thermal collectors for domestic hot water preheating and a conventional gas boiler to meet peak heating demands. To minimise air leakage, Passivhaus certified tapes, adhesives and sleeves would be required.

As a means to eliminate thermal bridging from the roof, garage space and balcony walkways, FBM proposed to flatten the roof and transform the garage space and balcony into usable internal space. This extension would provide space for roof-based renewable technologies and convert the property from a four to a six bedroom house, providing a larger living room and kitchen diner. Although this extension was not part of TSB funding, Gallions were keen to develop the solution, as it would provide a retrofitting approach to convert their existing stock into extended family houses. FBM used Revit Architecture, to model the existing building and the proposed layouts, as shown in Figure 5.14 and Figure 5.15 respectively. According to FBM, this level of detail would not normally be required for such as small project. However, it ensured that in 3D, no cold bridges or poor junctions were missed before the air tests could take place.

Figure 5.14 *3D model of the house pre-retrofit (Image provided by FBM architects).*

Figure 5.15 *3D model of the house post-retrofit (Image provided by FBM architects).*

Key tasks undertaken by the research engineer during this design phase included SAP calculations to verify the % reduction in CO_2 emissions, product development research with aerogel and cost effectiveness calculations for each major retrofit measure. This work is summarised in the following three sections.

5.3.1 Baseline CO_2 emissions

Preliminary validation of the proposed retrofit strategy was undertaken through further SAP modelling using IES, supported by JPA and the TSB's whole house SAP extension spreadsheet. Alongside the updated building services and fabric properties, a new geometry was produced in line with architectural plans to convert the 4 bedroom property into a 6 bedroom property. This revised geometry, shown in Figure 5.16, reduced the area of the exposed thermal envelope, whilst increasing the floor area.

Figure 5.16 *Updated geometry following architectural changes. Left image shows the new kitchen extension on the ground floor. Right image shows the new living room on the 1st floor.*

Figure 5.17 displays the predicted CO_2 emissions of the dwelling, per m^2, as each retrofit measure is added sequentially. 'Baseline' emissions refer to the CO_2 emissions calculated during Section 5.2.3, whereas 'Architectural changes' refers to the baseline CO_2 emissions of the revised geometry with an increased floor area.

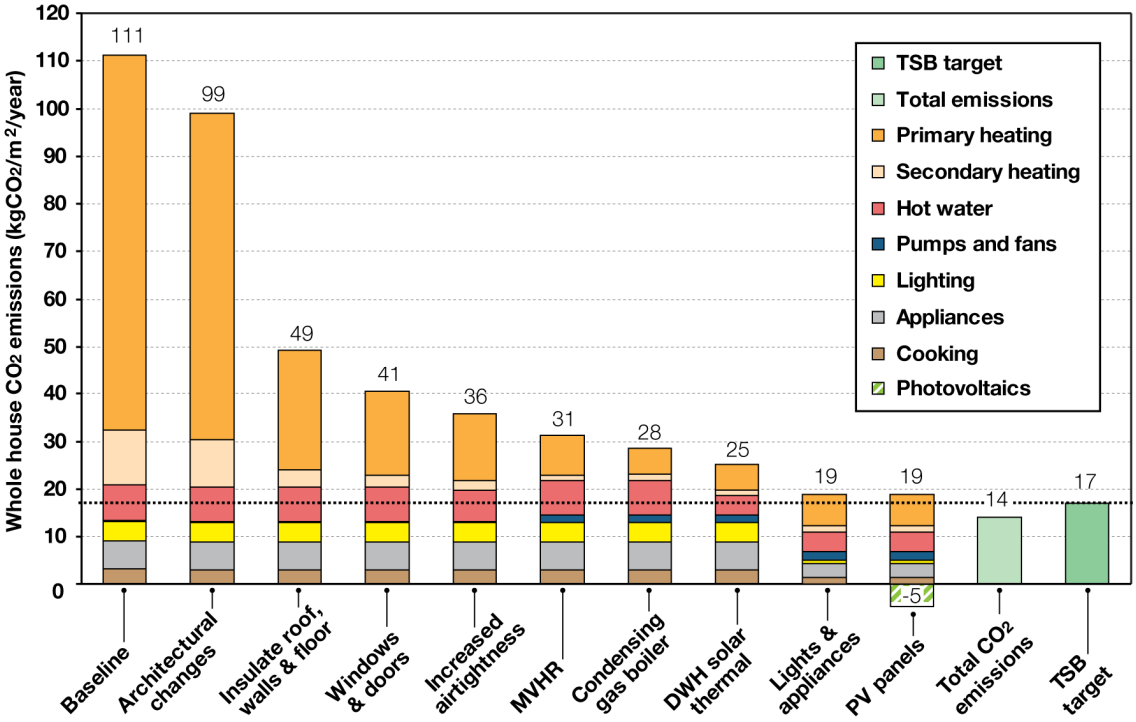

Figure 5.17 *Extended SAP calculations to achieve TSB target.*

Architectural changes reduced the dwelling's overall CO_2 emissions from 111 to 99 $kgCO_2/m^2/year$. Insulating the walls, roof and floor reduced this to 49 $kgCO_2/m^2/year$ and improving the glazing and air-tightness reduced this further to 36 $kgCO_2/m^2/year$. Beyond this point, services improvements have a diminishing impact, demonstrating that it would be difficult to achieve the TSB target of 17 $kgCO_2/m^2/year$ without renewable generation. Based on the available roof area, with ten PV panels generating

2.3 kWp, the overall dwelling's CO_2 emissions are reduced to 14 $kgCO_2/m^2$/year. Table 5.2 displays the key inputs and outputs from SAP modelling during this process.

Table 5.2 *Modelling parameters and outputs from energy modelling.*

		Baseline performance of existing property	Modelled performance of refurbished property
Total floor area	m^2	154.23	174.90
Total volume	m^3	396.55	448.81
INPUTS: Fabric performance			
Walls	W/m^2K	0.89 (measured)	0.1
Roof	W/m^2K	1.61 (measured)	0.1
Floor	W/m^2K	1.07 (measured)	0.15
Windows	W/m^2K	2.8	0.8
Skylights	W/m^2K	5.7	n/a
Entrance doors	W/m^2K	2.8	0.73
Other doors	W/m^2K	5.7 (garage)	0.62 (plant room)
Air change rate	m^3/m^2hr @50Pa	9.1 (measured)	1.0
INPUTS: Heating, hot water & electrical systems			
Primary heating	-	Old gas boiler (65% efficient + radiators)	MVHR (92% efficient, SFP 0.85 W/l/s) Gas condensing boiler
Secondary heating	-	Electric heaters	(90.1% efficient + radiators)
Heating controls	-	Room thermostat	Room thermostats with time and temperature controls
Domestic hot water	-	Instantaneous water heating at point of use (electric immersion)	500 litre tank fed by $3m^2$ solar thermal and boiler top up
Electricity generation	-	n/a	PV panels (2.30 kWp)
Lighting	-	Tungsten	100% CFL
Appliances and cooking	-	C-rated	A-rated
OUTPUTS: SAP calculations			
Total fabric heat losses	W/K	504.44	116.46
Ventilation heat losses	W/K	92.02	22.69
Heat loss coefficient	W/K	596.46	139.15
Heat loss parameter	W/m^2K	3.88	0.80
SAP rating	-	34	92
SAP band	-	F	A
OUTPUTS: Extended SAP calculations			
Fuel costs	£/year	1896.47*	351.17*
Primary energy	kWh/m^2/year	681.38*	88.49*
CO_2 emissions	$kgCO_2$/year	111.10*	14.03*

*Note that all values are modelling predictions ONLY and do not represent actual consumption figures to be assessed post-occupancy

As SAP does not accurately account for Passivhaus construction detailing, the building fabric was also modelled (by C. Boonstra) using the PHPP (the Passive House Planning Package) tool. Within this model, a preliminary heating demand of 25 kWh/m^2/year was achieved meeting the Passivhaus certification requirements for retrofit properties. The verification of this value following on-site air tightness is discussed in Section 5.5.

5.3.2 Innovation with aerogel

Due to the research engineer's vested interest in aerogel insulation, the design team were keen to engage in new product development opportunities with this material. To facilitate this process, a product development meeting, chaired by the research

engineer, was set up on 27th July 2010 with R.Lowe, Technical Services Manager at Xtralite Ltd (aerogel rooflight suppliers), J.Richings, Technical Director of Permarock Products Ltd (external cladding suppliers), S. Craig, Buro Happold Facade engineer and M. Montgomery, Gallions Investment Planning Manager.

Concepts to upgrade windows

Prior to this meeting, several concepts had been independently generated by the research engineer. Shown in Figure 5.18, they included airtight external shutters, internal pop-in/magnetic shutters, and fabric based aerogel 'net curtains'. Reversible, 'heat-collecting' shutters containing aerogel and phase change material were identified as a promising concept to insulate windows whilst absorbing/releasing solar energy.

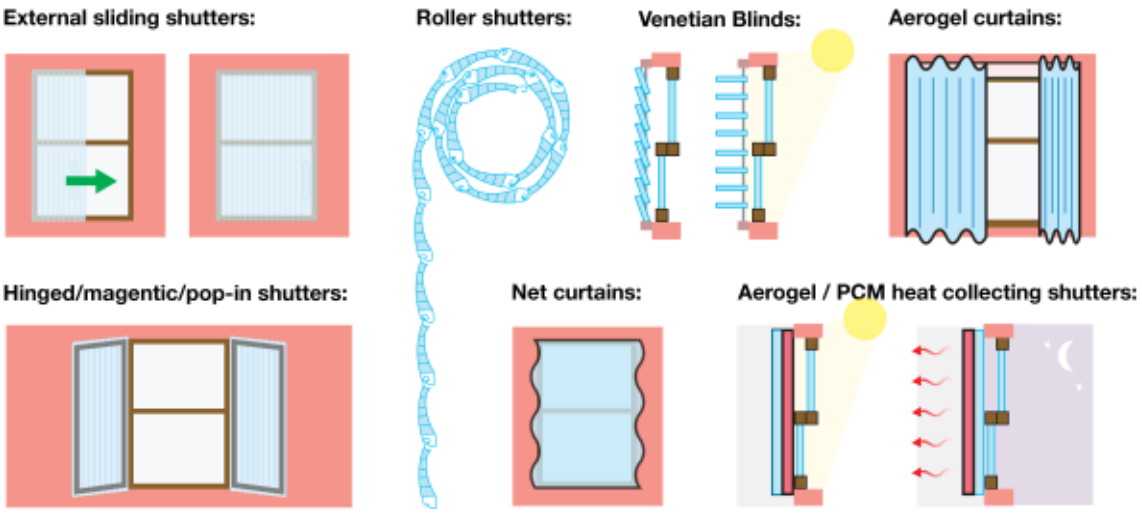

Figure 5.18 *Concepts to improve existing windows using aerogel.*

Following a review of each concept, R. Lowe sketched out the most viable options Xtralite Ltd could manufacture and install. Proposed concepts were simple sliding screens, bi-fold shutters and sliding shutters, illustrated in Figure 5.19.

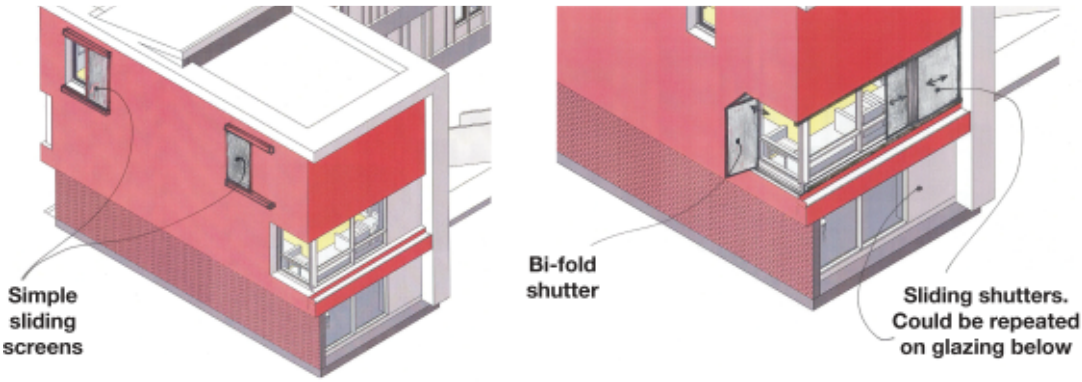

Figure 5.19 *Concepts for movable aerogel shutters (drawn by R.Lowe, Xtralite Ltd).*

These concepts were eventually rejected following M. Montgomery's concerns that energy savings were heavily reliant upon occupant usage. In addition, a team consensus was that these products might have hindered Passivhaus certification as insulation/air tightness targets may have been difficult if retaining the existing glazing.

Concepts to upgrade walls

Moving on, all parties were keen to retrofit aerogel into a solar wall application, due to the absence of moving parts and the dwelling's large south-facing wall.

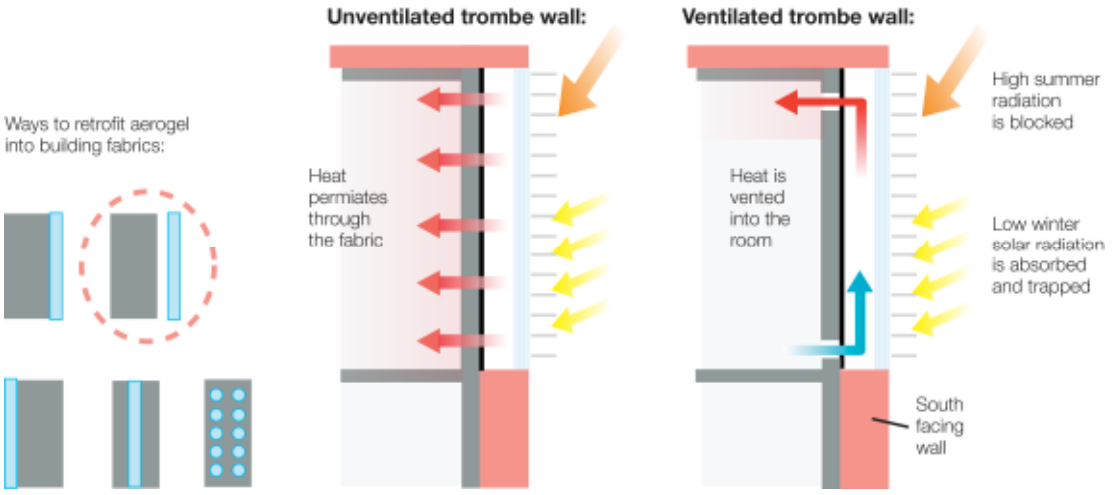

Figure 5.20 *Concepts to improve existing walls using aerogel.*

Figure 5.20 displays the preliminary concept to retrofit aerogel into a Trombe wall application. Further discussion, led this passive concept to be adapted into an active flat plate collector feeding warm air into the MVHR, as visualised in Figure 5.21.

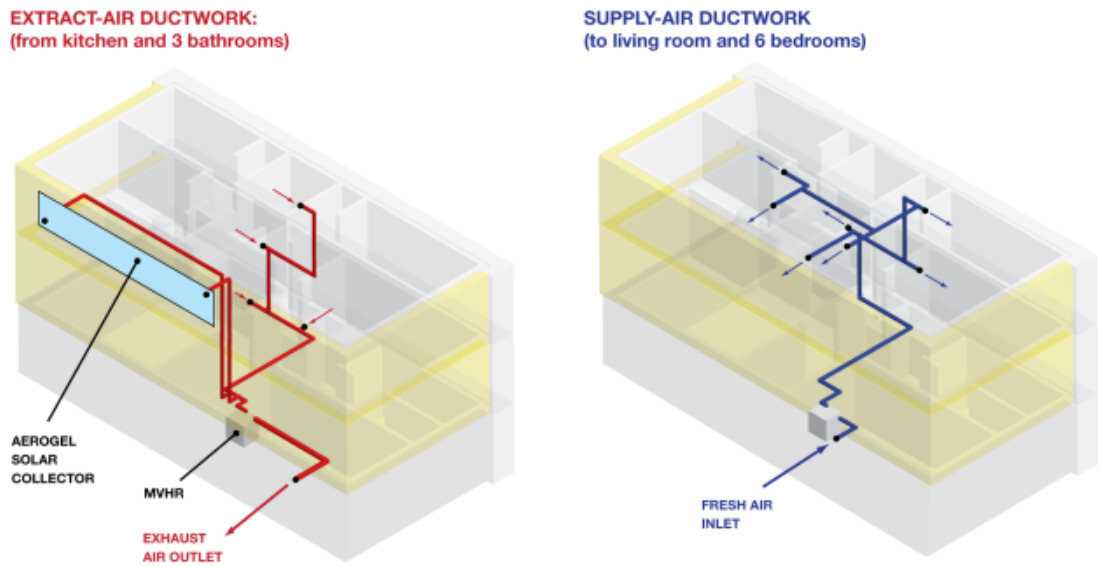

Figure 5.21 *Aerogel Solar Collector concept showing connection to MVHR.*

On-going development (and eventual installation) of this 'Aerogel Solar Collector' took place following several further product development meetings chaired by the research engineer, held with R. Lowe, J. Richings and C.Biggs the Technical Director of Nuaire Ltd (MVHR suppliers). A detailed case study of this prototype including the construction stages, predicted and in-situ performance can be found in Chapter 6.

Concepts to upgrade floors

A second approved application of aerogel was the integration of opaque Spacetherm™ blankets over a hard-to-treat area of the ground floor. Illustrated in Figure 5.22, the dwelling's ground floor had three different slab heights; all of which were difficult to insulate to a U-value of 0.15 W/m² K whilst retaining a floor-to-ceiling height of 2.3 m.

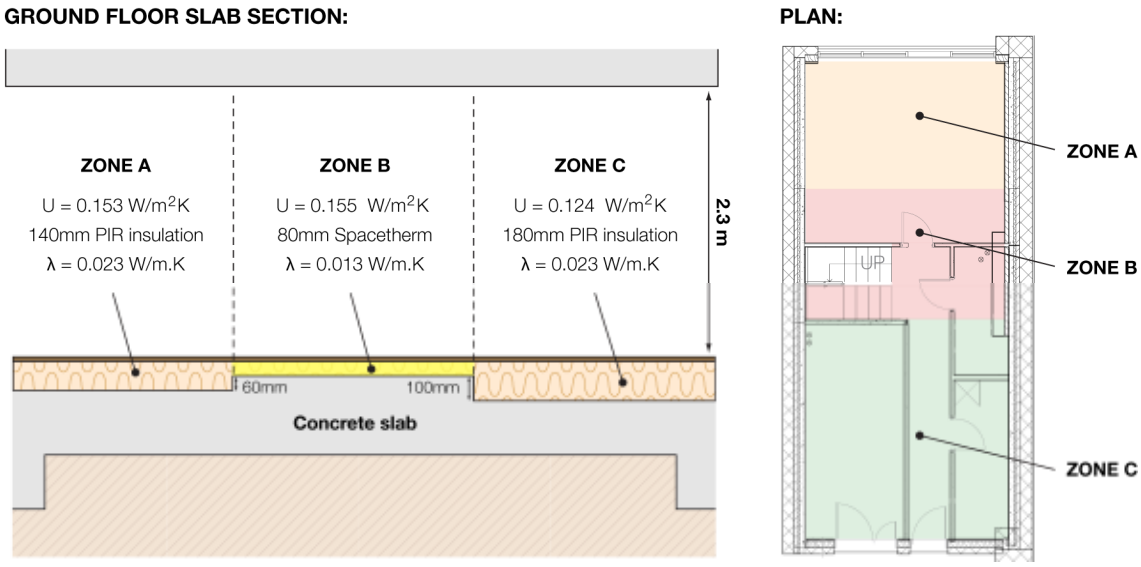

Figure 5.22 *Insulation thicknesses specified for the ground floor.*

In 'Zone A' and 'Zone C' high performance polyurethane insulation (PIR), with a conductivity of 0.023 W/m K could achieve a suitable U-value, within the spatial limits. However, in 'Zone B', 80 mm of Spacetherm™ aerogel insulation with a conductivity of 0.013 W/m K was the only suitable material to achieve the necessary U-value (without excavating the floor). Opaque Spacetherm™ aerogel blankets are manufactured by Aspen Aerogel and supplied to the UK market by Proctor Group Ltd.

Concepts to upgrade external doors

For the entrance of the property, a Passivhaus certified door with an overall U-value of 0.8 W/m² K supplied by Internorm UK was specified costing £ 4,800. Due to the high costs associated with this product the design team were keen to explore ways in which

Passivhaus performance could be achieved on an external plant room door through a lower cost solution.

On 28th September 2010, a collaboration was built between the research engineer and S.Proctor, Spacetherm™ Team Manager at Proctor Group Ltd. S.Proctor had been developing a custom made door incorporating Spacetherm™ insulation in partnership with Winkhaus lock manufacturers. A prototype had only been installed at S.Proctor's house in Scotland and nowhere else in the UK. Theoretical data from S. Proctor showed a U-Value for a 50 mm thick door below 0.65 W/m² K. Taking this concept forward, S.Proctor agreed to install a custom-made prototype of a double-leaf plant room door, incorporating aerogel at a capital of £ 1,800 including installation. The predicted and in-situ U-value of this 'Spacetherm™ Aerogel Door' is detailed in Section 5.7.

5.3.3 Cost effectiveness of measures

During the design phase, an optional assessment set by the TSB in Phase 1 was to estimate the cost effectiveness of measures one-by-one from a common base in terms of the "*£ spent / tonne CO_2 saved over lifetime*". Excluding the Aerogel Solar Collector, which was not modelled in SAP, Figure 5.23 displays the percentage CO_2 reduction of each major retrofit measure, calculated through thermal modelling using IES and JPA. Note that savings from individual heating and insulation measures have been normalised to account for the discrepancies in predicted performance that occur when measures are added in combination. Furthermore, savings from the MVHR were calculated in combination with improved air tightness (1 m³/m² hr @ 50 Pa) as the product would be unable to recover and supply heat efficiently if the ventilation losses are too high, resulting in a negative contribution to space heating.

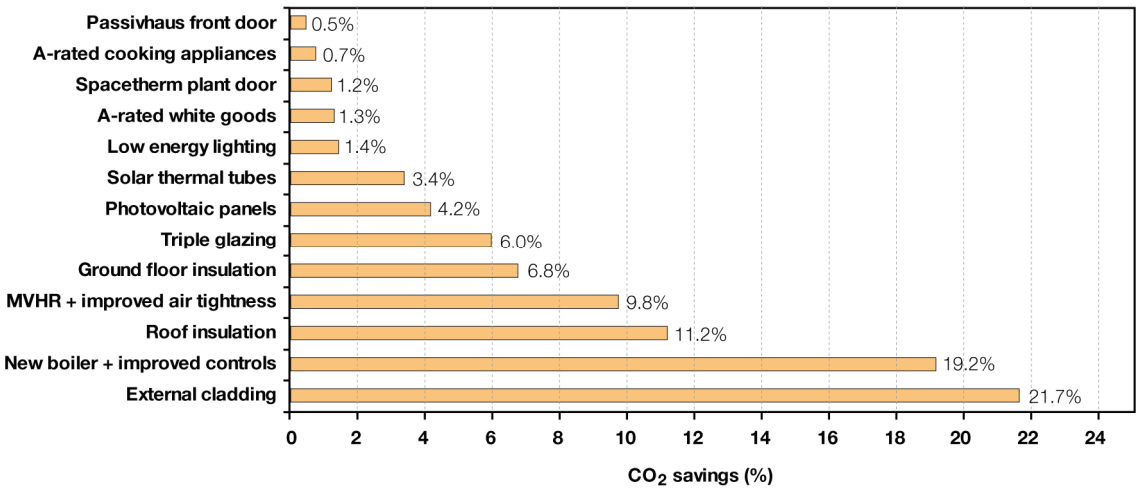

Figure 5.23 *Predicted primary energy and CO_2 savings for each retrofit measure.*

According to thermal modelling calculations, external cladding reduces the largest percentage of CO_2 emissions (21.7%), closely followed by the new gas-condensing boiler with improved heating controls (19.2%). Roof insulation, the MVHR, ground floor insulation and new triple glazing were each estimated to save between 6–11% of CO_2 emissions, respectively. The photovoltaic panels and solar thermal collector were estimated to save 4.2% and 3.4%, respectively. Understandably, due to the small area in comparison to the rest of the building fabric, the entrance door improvement saves the least amount of CO_2. In contrast, the larger double-leaf Spacetherm™ Aerogel Door with improved U-value is predicted to save slightly more CO_2 emissions. Lighting and appliances also fall short compared to the large-scale insulation measures.

Figure 5.24 displays the estimated capital cost of each measure based on information provided by Martin-Arnold Associates. As shown, the largest capital cost was the external cladding at £ 20,500 (costing ~£140/m² of façade area), followed by the triple glazing at £ 17,500 (costing ~£500/m² of glazing area). The PV panels with inverter cost £ 12,000. The solar thermal collector and hot water cylinder cost £ 7,200. The roof renewal cost £ 6,000. The MVHR cost £ 5,150. The Passivhaus door and the new gas-condensing boiler both cost £ 4,500. Ground floor insulation was £ 4,475 (of which £ 3,500 was the Spacetherm™ blankets). The Spacetherm™ Aerogel door was £ 1,800.

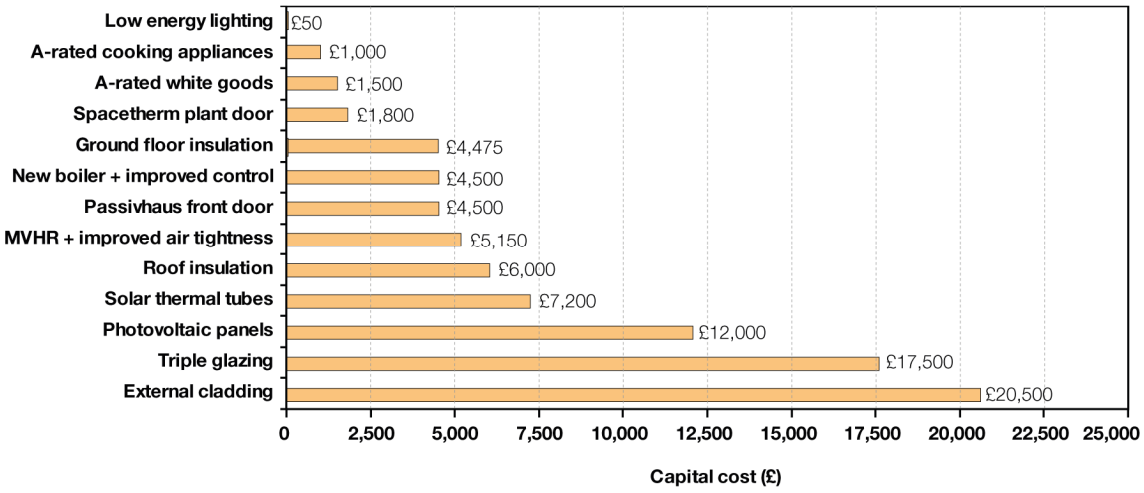

Figure 5.24 *Predicted fuel bill savings for each retrofit measure.*

Figure 5.25 displays the calculated cost effectiveness of measures in terms of £ spent / tonne CO_2 saved over lifetime. The Passivhaus certified front door was found to be the least cost effective measure due to its high capital cost and low CO_2 savings over the lifespan (20 years), followed by the triple glazing, PV panels and cooking appliances. The high capital cost of the external cladding, ground floor insulation and roof insulation performed well, despite the high capital costs due to their large CO2 savings

and long assumed lifespans (40 years). Low energy lighting provided the most favourable cost effectiveness (based on the assumption that it would last for 8 years). The new gas condensing boiler and heating controls was found to be the second most cost effective measure, due to its relatively low cost to install and large CO_2 savings.

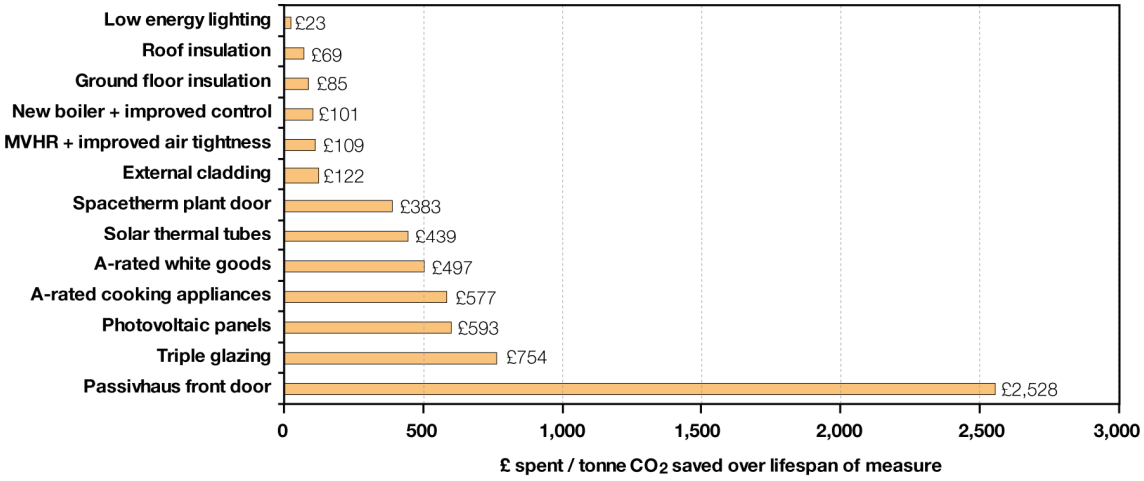

Figure 5.25 *Cost effectiveness of measures in £ spent / tonne CO_2 saved over lifetime.*

5.4 Summary of On-Site Retrofit Works

All major on-site retrofit works ran from November 2010 to October 2011. By March 2012, the property was commissioned and handed over to Gallions.

The lead contractor during the on-site retrofit process was Axis Europe Ltd. It should be noted that Axis, like most UK contractors, had no prior experience working on a retrofit project aiming to achieve Passivhaus certification. Throughout the project, the role of project management and quantity surveying was led by Martin-Arnold Associates. All plans, sections and elevations for the planning application and on-site works, including Passivhaus detailing, were produced by FBM architects.

Buro Happold's role, lead internally by the research engineer, included producing schematics for major heating and hot water elements as well as the ventilation system. Schematics for the PV panels and solar thermal collectors were produced by their respective sub-contractors. The research engineer led the system sizing and (with support from C.Biggs of Nuaire Ltd) the control strategy for the Aerogel Solar Collector. All monitoring equipment for this prototype, together with a whole house package of monitoring equipment to meet the TSB funding requirements was specified by the research engineer and installed by BSRIA Ltd.

Following planning approval, existing residents were re-housed on a permanent basis to leave the property unoccupied. Scaffolding was erected to facilitate measures such as external cladding, triple glazing and roof renewal. Demolition works, including removal of the first floor balcony were undertaken to facilitate the architect's plans to convert for a six bedroom property. Redundant services such as the old boiler, pipe work, radiators were removed. Openings for the new triple glazing and ventilation ductwork were cut. All asbestos panelling was removed.

Air tightness briefing

At the beginning of on-site works, Axis' site manager was briefed by FBM architects on the importance and application of the air-tight technologies that had been specified. Shown in Figure 5.26, these products include (i) Tescon Tape for corners and edges in timber construction, (ii) Contega tape for connections to unplastered walls, (iii) Unitape for sealing of overlaps (iv) Orcon F adhesive, for joints and seals between tapes and (v) Unitape sleeves (available in a wide range of diameters for sealing of service pipes, duct work penetrations etc). At the time of briefing, Axis' site manager was confident on their application and had support from FBM if queries arose.

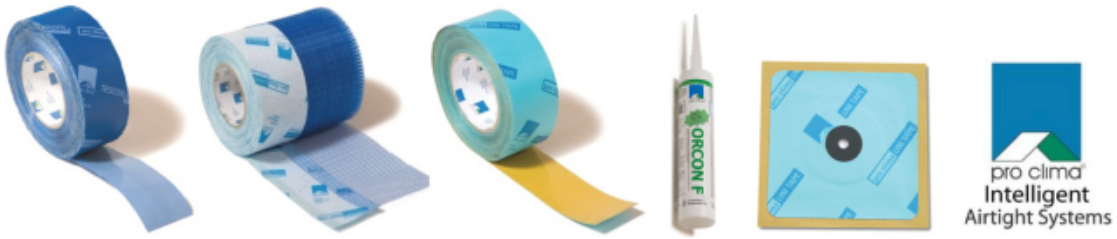

Figure 5.26 *Pro Clima airtight tapes. From left to right, the products are: Tescon tape, Contega tape, Unitape, Orcon F adhesive and Unitape sleeves.*

Roof renewal

The first major task undertaken was the removal of the existing roof and skylights to create an airtight, insulated and reinforced flat roof with parapet. Shown in Figure 5.27, new timber joists were constructed and the surface was insulated and lined with a continuous airtight roof membrane and 300 mm of Celotex polyurethane insulation to achieve a U-value of 0.1 W/m^2 K. To minimise penetrations, a core was created for services cables and pipes, sealed using airtight sleeves beneath the insulation layer. A man-safe system fixed directly through the insulation layer with thermally broken screws was attached. A drainage hole, connected to a downpipe was also created, but this did not penetrate through the insulation layer.

Figure 5.27 *Steps taken during roof renewal.*

Triple glazing

For the glazing, Nordan UK's 'N-tech' triple glazing was specified throughout the property. These Passivhaus certified units possess an overall U-value of 0.7 W/m² K and solar g-value of 0.5. All existing windows were removed and timber boxes to reduce thermal bridging were created to house the new units. With the exception of the top floor bedrooms, all rooms would possess a new glazing layout in line with the architect's plans. In particular, stud walls were created to house a large area of glazing in the living room, newly extended over the 1st floor walkway (shown in Figure 5.28). A new kitchen on the ground floor would also contain floor-to-ceiling glazing and a triple glazed door leading into the garden. During installation, all glazing units were manually lifted into place, fixed to the timber frames and sealed around the perimeter using airtight tapes. Solar control blinds were fitted to all windows following installation.

Figure 5.28 *New triple glazing (with an internal view from the living room).*

External doors

Figure 5.29 shows the Spacetherm™ Aerogel Door and the Passivhaus certified door respectively. During installation both products were sealed around the perimeter using airtight tapes. Following removal of the garage door, a new stud wall was created for the Spacetherm™ Aerogel Door, manufactured and installed by Proctor Group Ltd. During normal day-to-day usage, Gallions specified that this door would be locked as it contained access to the MVHR unit, solar thermal cylinder, PV inverter and monitoring hub. Despite its high capital cost, the Passivhaus entrance door did not contain a letterbox, so an external box needed to be fitted to the rear gate in the garden.

Figure 5.29 *Spacetherm™ plant room door and Passivhaus entrance door.*

Ground floor

To seal the ground floor, airtight tapes and membranes were applied to the internal perimeter of the building (shown in Figure 5.30). In Zones A and C, polyurethane insulation was cut and quickly installed. In Zone B, eights 10 mm thick layers of Spacetherm™ insulation blankets had to be manually cut and layered by contractors. According to Axis, these blankets produced a lot of dust when handling and were difficult to cut manually. According to Proctor Group Ltd, encapsulated sheets were offered to the contractor which could have resolved these issues (but at extra cost).

Figure 5.30 *Ground floor insulation. PIR in left image. Spacetherm in central & right image.*

Heating system

The 'Potterton Promax System 12 kW HE Plus A Efficiency boiler' shown in Figure 5.31 was installed to provide space heating during peak winter conditions as well as top-up for the domestic hot water cylinder. The system provides zoned time and temperature controlled heating, through the use of thermostatic radiator valves and thermostats on each floor. Small radiators were provided in each room. Where the boiler flue penetrates through the building fabric to the outside, an airtight sleeve was used.

Figure 5.31 *Boiler flue, boiler room and radiators.*

Mechanical ventilation

For the ventilation system, the MRXBOX95B-WH1 unit with rigid ductwork supplied by Nuaire Ltd was installed (see Figure 5.32). The MVHR unit recovers heat at 90 % efficiency, with a specific fan power of 0.76 W/L/s. The system runs continuously. An automatic summer bypass switch operates when external temperature exceeds 20 °C. All internal doors were undercut by 10 mm to provide additional internal ventilation.

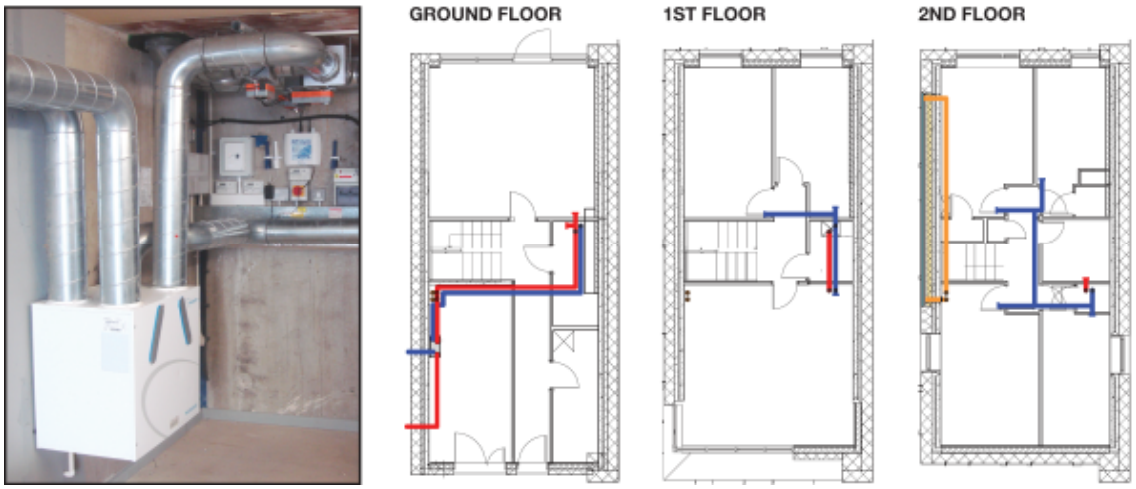

Figure 5.32 *MVHR system in the plant room and supply/extract schematic for the house.*

External insulation

External cladding (shown in Figure 5.33) was installed by Permarock Product's Ltd approved installers. To achieve a U-value of 0.15 W/m² K, a 300 mm layer of expanded polystyrene insulation was bonded with adhesives and pinned in place. A mineral insulation firebreak was incorporated between the 1st and 2nd floor of the property. All joints between blocks were sealed with expanding foam. The perimeters of windows were sealed with screed and mesh to Permarock Product's approved details.

Figure 5.33 *External insulation during and after installation.*

External rendering

Shown in Figure 5.34, the external finish of the building combines a bright yellow render with white detailing on the partition wall, parapet and north elevation. Bespoke extruded metallic fins designed by FBM were later added to the render to add character. The ground floor contains a grey pebbledash finish.

Figure 5.34 *External rendering (garden entrance and southern aspect).*

Photovoltaic panels

Ten PV panels generating 2.30 kWp, tilted at 25◦ and spaced adequately apart to avoid overshadowing at a 15◦ solar angle were installed by PV systems Ltd. Shown in Figure 5.35, all panels were bolted to a 'Lo-Pro' aluminium support system weighted down by concrete slabs to avoid penetrating through the insulation layer. All cabling was fed through the pre-cut services core. An inverter converts direct current generated by the panels into alternating current delivered to the property and electrical grid.

Figure 5.35 *Photovoltaic panels on the roof and the inverter in the plant room.*

Solar thermal collector

Shown in Figure 5.36, a single 3 m² Thermomax DF100 vacuum tube solar thermal collector, ballasted to the roof, was installed by Future Heating Ltd as a preheat for the domestic hot water system. The system was sized to provide a 40 % solar fraction. A 500 litre dual coil cylinder (with 255 litres of dedicated solar storage) was also installed in the plant room. The tubes lie flat on the roof and were manually rotated to 25◦

Figure 5.36 *Solar thermal collector on the roof and the hot water cylinder in the plant room.*

Whole house monitoring equipment

As part of the TSB's funding requirements, all teams were required to install a package of whole house monitoring equipment to provide real-time performance data on all renewable technology, internal and external environmental conditions as well as gas, electricity and water consumption. All data can be accessed wirelessly and was supplied by BSRIA Ltd and Orsis Ltd, the two companies in-charge of hosting the TSB's monitoring data. A selection of the equipment installed is shown in Figure 5.37.

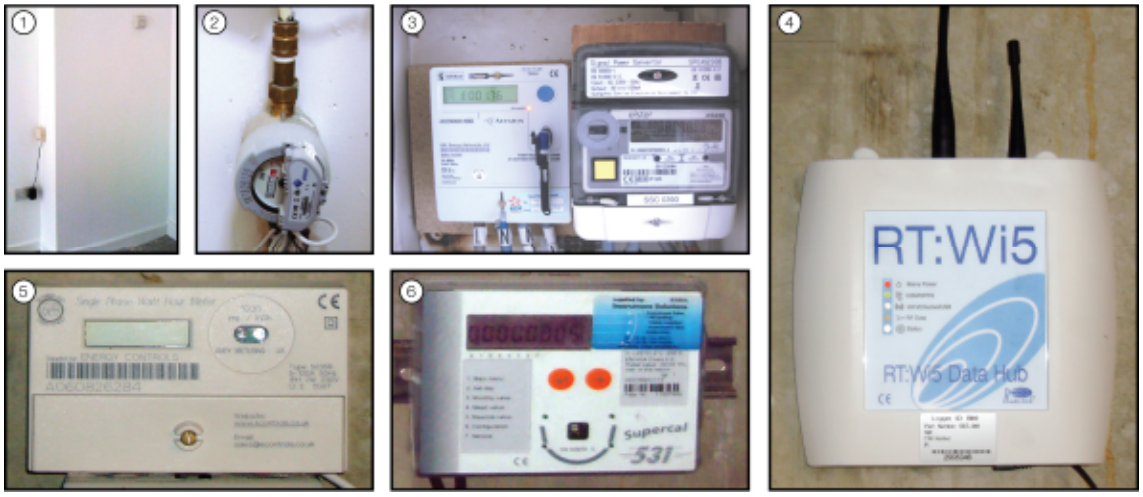

Figure 5.37 *CO2 sensor, water meter, electric meter, GPRS hub, power meter, heat meter*

Inside the dwelling are three temperature/humidity sensors measuring internal conditions in the living room and two bedrooms on the 2nd floor. There is also a CO_2 sensor in the living room to provide a measure of air quality. In a kitchen cupboard are smart meters measuring gas and electricity consumption. The electricity meter has also been configured to capture the amount of electricity exported to the grid. A water meter is also fitted. On the roof of the property are two pyranometers (shown in Figure 5.38) measuring solar radiation; one is tilted at the same angle as the PV panels, the other is tilted horizontally to capture solar radiation hitting the Aerogel Solar Collector.

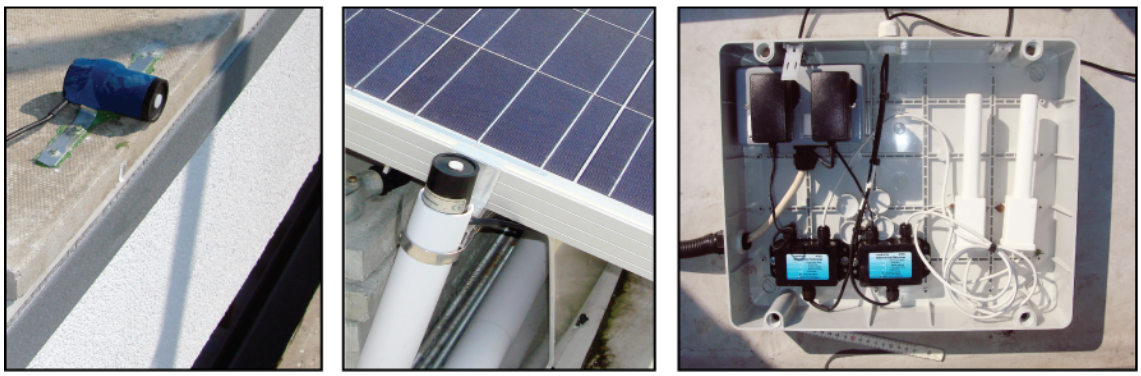

Figure 5.38 *Two pyranometers and the power supply on the roof.*

Also monitoring the Aerogel Solar Collector are 8 temperature/humidity sensors (see Chapter 6 for more detailed information). In the plant room are three single phase power meters. One measures the electricity generated by the PV panels. The other two measure the power consumption of the MVHR and pumps for the solar thermal system. A heat flux meter also measures the heat output of the solar thermal collectors. Also in the plant room are two temperature and humidity sensors inside the supply and extract ductwork for the MVHR. All sensors have transmitters that wirelessly connect to a GPRS data hub.

It should be noted that all monitoring data collected for this retrofit is accessible to the research community via the Technology Strategy Board. Also, since August 2011, the research engineer has compiled all raw data for internal / external temperatures and solar radiation into monthly spreadsheets for further analysis (see Appendices). After June 2013, the house will have been occupied for 12 months. At this point, gas, electricity and water use and renewable energy generation can be usefully analysed.

Completed retrofit house

Two photographs of the completed retrofit property are shown in Figure 5.39. Tasks before handover included commissioning of the monitoring equipment, domestic hot water system, PV panels, air flow rates for the mechanical ventilation system and control system for the Aerogel Solar Collector.

Figure 5.39 *Photographs of the completed retrofit house.*

5.5 Passivhaus Assessment

The main shortfall of this project was that Passivhaus compliance was not achieved due to the air tightness target not being met. The lowest air tightness level measured during this project was 3.6 m^3/m^2 hr @ 50 Pa. Figure 5.40 compares this output with the predicted space heating demands modelled in PHPP at 0.6 and 1.0 air changes. As shown, both the 0.6 and 1.0 air changes would have provided a theoretical space heating demand under of 25 kWh/m^2/year or less. However, at 3.6 air changes, the predicted space heating demand is 32 kWh/m^2/year, falling short of the target.

	Applied:	Monthly Method	Applied:	Monthly Method	Applied:	Monthly Method
Specific Space Heat Demand:	23	kWh/(m^2a)	25	kWh/(m^2a)	32	kWh/(m^2a)
Pressurization Test Result:	0.6	h^{-1}	1.0	h^{-1}	3.6	h^{-1}
	PASS		PASS		FAIL	

Figure 5.40 *Modelled space heating demands for Passivhaus compliance.*

Several months of on-site meetings were spent identifying all of the possible reasons why Passivhaus levels of air tightness were not achieved. These meetings recommended that smoke testing be conducted and that intrusive investigations be carried out by Axis to inspect the quality of all air-tight tapes and membranes behind elements such as the glazing, external doors, roof and ground floor perimeter as well as all major mechanical services penetrations.

Figure 5.41 *Main sources of air leakage identified during smoke testing.*

Smoke testing (conducted in June 2011), shown in Figure 5.41, revealed that the partition wall, roof and parts of the ground floor perimeter were the main sources of air leakage during construction. Intrusive surveys revealed that a number of measures were installed without proper consideration for air tightness, e.g. external lighting was fitted without air-tight sleeves, the sills on window frames were installed without proper use of tapes (since these sills arrived after the windows were installed), and a lower cost roof membrane with no air tightness credentials was ordered by the

contractors irrespective of the architect's original specification. Leakage was also found inside the Aerogel Solar Collector due to imperfections in sealing the frame.

Attempts to improve air-tightness, such as re-sealing the Aerogel Solar Collector, applying air tight sleeves to all services penetrations, re-sealing the glazing, internal roof and ground floor perimeter was carried out by Axis, but no significant improvement in the dwelling's overall air tightness was achieved. Eventually it was agreed by all that the costs to expose the partition wall and external roof membrane would be too great to justify obtaining Passivhaus compliance (which was outside of the TSB's original project briefing). It is important to note that despite the issues experienced, the air-tightness levels are 3 times better than the current UK new-build standard of 10 m^3/m^2 hr @ 50 Pa.

5.6 Thermal Imaging

To investigate possible thermal bridges, a post-retrofit thermal imaging survey was carried out during the early morning of 15th March 2012 by M. Montgomery of Gallions with the research engineer present. During the assessment, the whole property was heated using boiler-fed radiators. External temperature was 3-5 °C. Monitored living room temperatures were 17-18 °C. Monitored bedroom temperatures were 23.5 °C. External relative humidity was 96-92 %. Internal relative humidity in the living room and bedroom were 45 % and 37 % respectively.

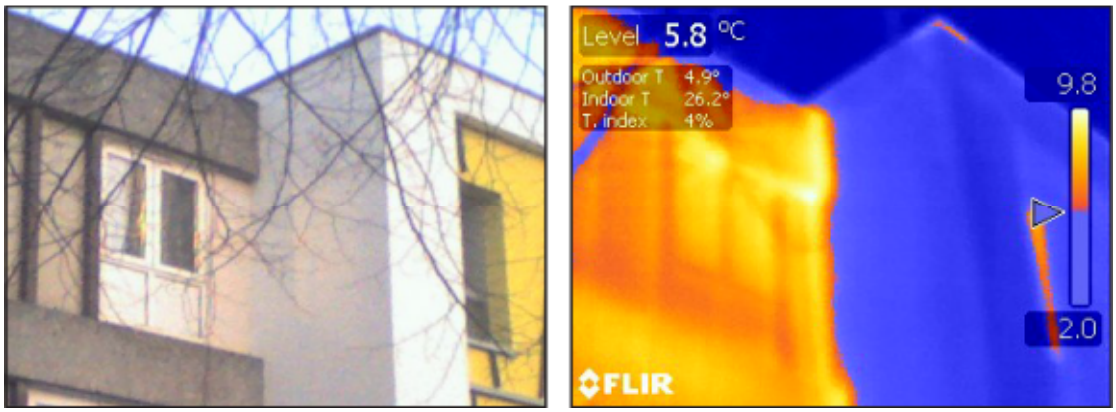

Figure 5.42 *Thermal image showing the partition wall (top) on the north-west elevation.*

Figure 5.42 displays the partition wall on the north-west elevation. As shown, where the retrofit house and link-house meet, there is not a clean divide between fabric heat losses. Consequently, this is believed to be one area where thermal bridging or air leakage may have occurred. Figure 5.43 displays a further thermal image of this

partition wall, focusing on the mid-section. As shown, heat loss appears to be most significant where the facade meets the floor and ceiling slabs.

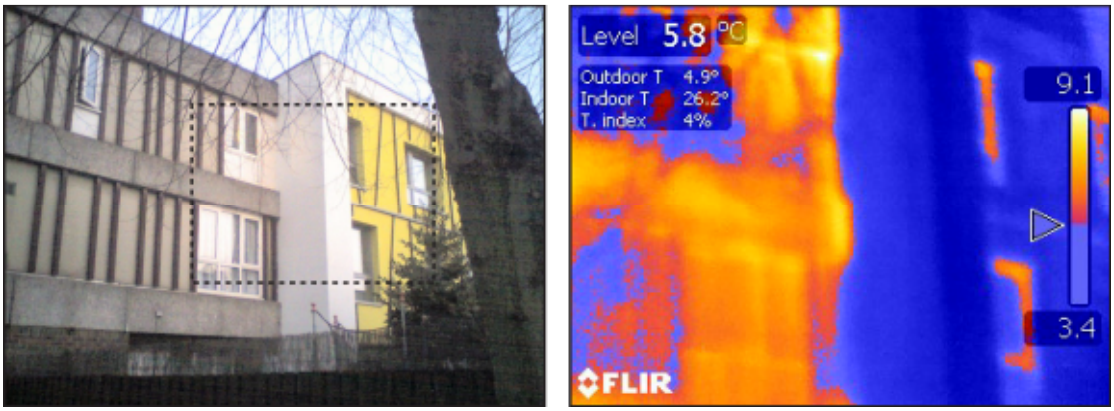

Figure 5.43 *Thermal image showing the partition wall (middle) on the north-west elevation.*

Figure 5.44 displays a series of thermal images taken of the partition wall on the other side of the property between the retrofit house and the link house. No major unexpected thermal bridges can be seen on the partition wall. The link-house next door is significantly less insulated, resulting in far higher heat losses through the fabric. Heat loss from the boiler flue and flue gas is visible, but believed to be normal.

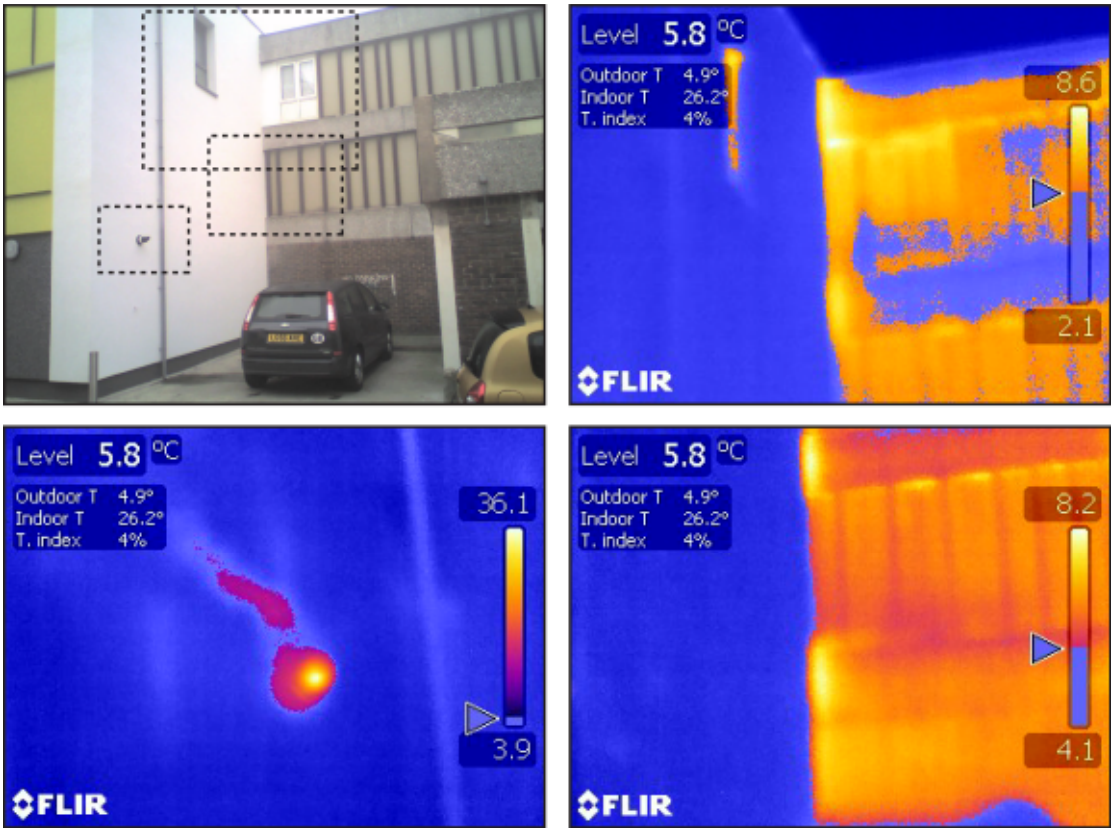

Figure 5.44 *Thermal image showing partition wall and boiler flue on north-east elevation.*

When assessing the living room glazing on the south-east elevation, shown in Figure 5.45, no major unexpected thermal bridges can be seen. The warm area in the bottom left corner of the image is the exhaust air from the MVHR.

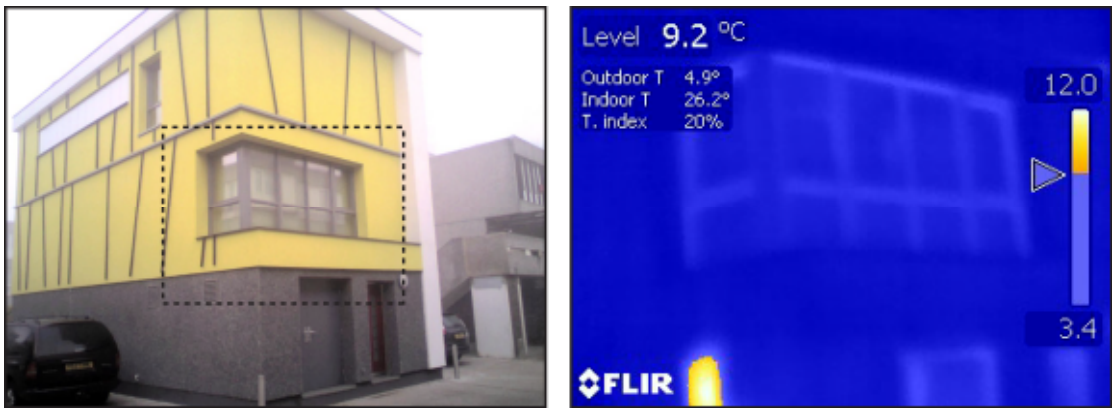

Figure 5.45 *Thermal image of living room and MVHR exhaust on south-east elevation.*

Figure 5.46 displays a thermal image of the rear bedroom windows on the west elevation. Compared to the living room windows, visible heat loss though the frames can be seen, which is possibly due to higher internal temperatures observed in these rooms from the monitoring data. As shown, the link-house in the background is clearly illuminated, demonstrating significant improvements in thermal performance through retrofit works.

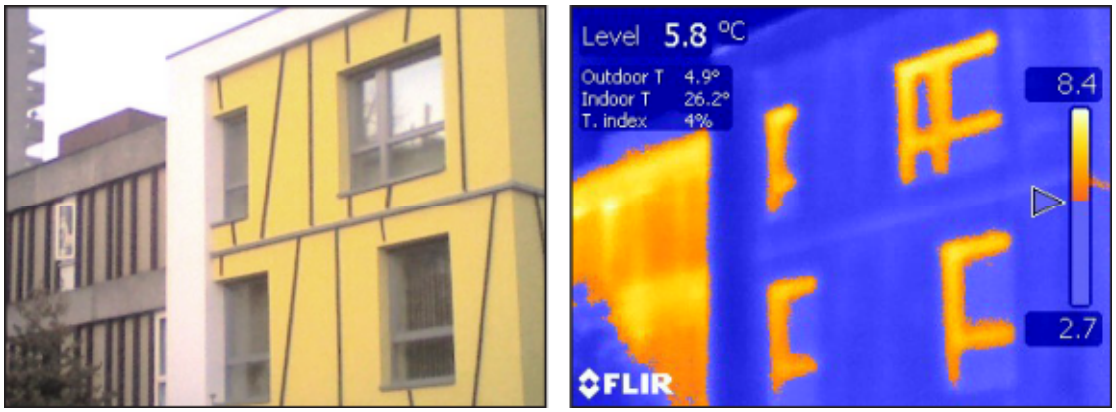

Figure 5.46 *Thermal image showing glazing and link-house on the west elevation.*

5.7 Thermal Assessment of the Aerogel Door

In November 2011, an experiment was conducted to measure the in-situ U-value of the Spacetherm™ Aerogel Door for the first time. As with previous in-situ U-value testing, experimentation involved measuring the heat flux through the door (shown in Figure 5.47), as well as the internal and external temperatures. The dynamic U-value was

calculated by dividing the heat flux by the temperature difference. To rationalise this figure, a cumulative average U-value over time was calculated.

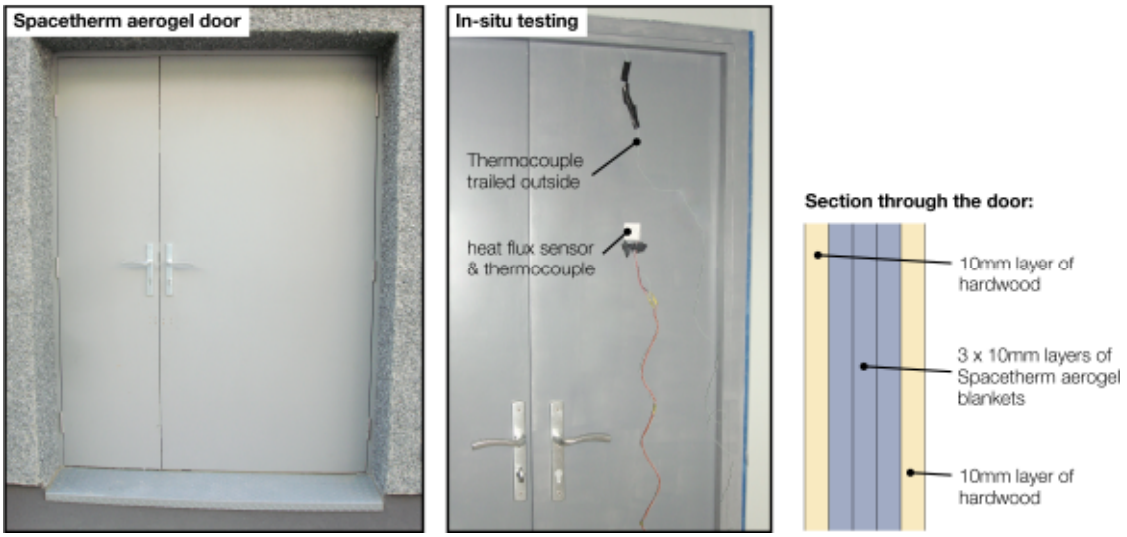

Figure 5.47 *Outside view of the Spacetherm™ door & internal view with the heat flux sensor.*

Predicted U-value

Table 5.3 displays the thickness, predicted thermal conductivity and R-value for each layer within a section of the Spacetherm™ Aerogel Door (visualised in the right of Figure 5.47). Excluding framing, the door's theoretical U-value is 0.384 W/m² K.

Table 5.3 *U-value calculations for the Spacetherm™ door.*

Construction layers	Thickness (m)	Conductivity (W/m K)	R-value (m² K/W)	U-value (W/m² K)
Inner surface	-	-	0.1300	-
Hardwood	0.01	0.160	0.0625	-
Spacetherm	0.03	0.013	2.3077	-
Hardwood	0.01	0.160	0.0625	-
Outer surface	-	-	0.0400	-
		TOTAL	**2.60**	**0.384**

In-situ U-value

Figure 5.48 displays the dynamic and cumulative average U-value generated during in-situ testing. During the test period, outside temperatures ranged from 5.1-10.5 °C and the internal temperature beside the door remained fairly stable from 18.9-19.6 °C. The induced heat flux (following calibration) ranged from 3-7 W/m², peaking during the coldest periods. Five minute data was collected for approximately 72 hours. As shown, the cumulative average U-value remains relatively stable after 1.5 days of testing,

converging at 0.389 W/m² K. The uncertainty of this U-value based upon the different results obtained from internal air & surface temperature measurements is 15.5%.

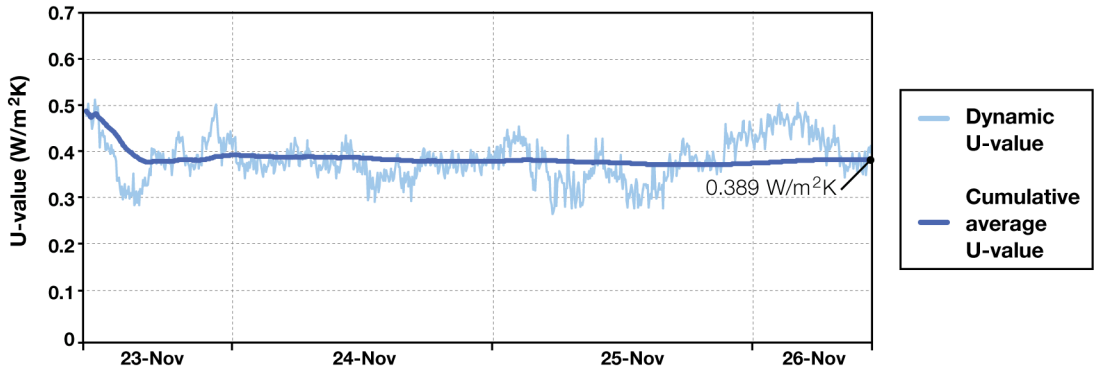

Figure 5.48 *In-situ U-value measurement.*

Summary of U-value testing

The predicted and in-situ U-value of the Spacetherm™ Aerogel Door correlate well demonstrating the impressive thermal properties of this product. Take note, that this experiment and calculations do not take the framing into account. When included, the manufacturers claim that the overall U-value of the door is predicted to increase to 0.65 W/m² K. Nonetheless, these findings are promising, indicating that a Passivhaus level of performance can be achieved based on a central U-value measurement.

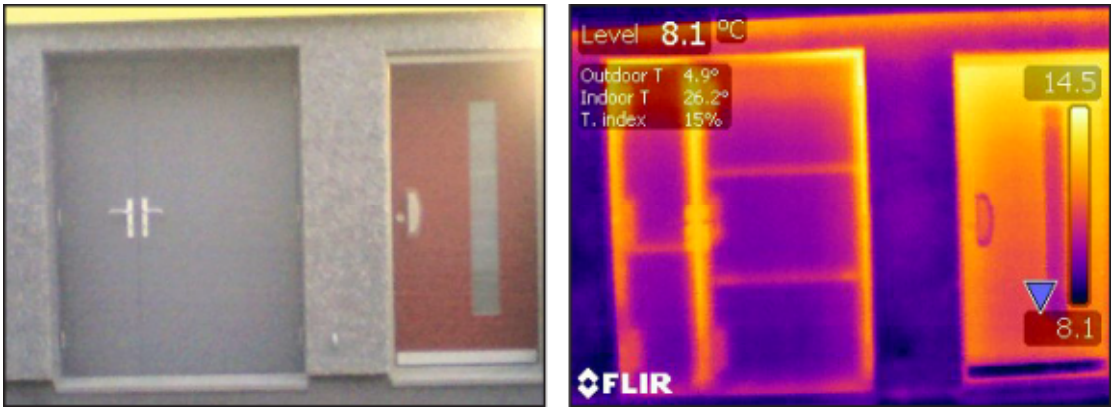

Figure 5.49 *Thermal image of the Spacetherm™ door & Passivhaus door on east elevation.*

Figure 5.49 displays a thermal image of the Aerogel Door next to the Passivhaus entrance door. As shown, the Aerogel Door appears cooler than the Passivhaus door, indicating that it is retaining more heat. However, note that heat loss between layers of aerogel board and framing are clearly visible, as is the split line between the double leaf door and the locking mechanism, indicating scope to reduce heat losses further.

5.8 Project Review and Conclusion

On 6th December 2011, a post-retrofit project review meeting was held between Buro Happold, Gallions, Axis, Martin-Arnold Associates and FBM architects. The aim of this meeting was to evaluate the retrofit project programme, the total costs incurred, the lessons learnt from Passivhaus as well as the key project successes.

The meeting was chaired by Jim Martin (Senior Partner at Martin-Arnold Associates) and the research engineer. In attendance was Chris Francis (Gallions, Head of Asset Management), Ian Beckett (Gallions, Director of Development and Regeneration), David Cramption (Axis Europe, Senior Divisional Manager), Tunji Awe (Axis Europe, Cost and Programmes Manager), Stephen Mitchell (Martin-Arnold Associates, project management and quantity surveying) and Balaji Thangavel (FBM architects).

5.8.1 Project programme and total costs

The original sum forecasted by Martin-Arnold Associates for this retrofit project was £ 268,795. Of this, £ 127,500 was TSB funding (after VAT) to cover 'energy efficient' improvements such as insulation, heating systems and renewable technologies. A further £ 141,295 would be funded by Gallions to cover 'rational' and 'decent homes' improvements such as the roof renewal, internal demolition works, new kitchen and bathroom and new wiring etc.

By comparison, the final cost incurred on this project was £ 330,770. This was £ 63,707 higher than the original forecasted sum, equivalent to a 45 % increase in costs for the Gallions funded element. Most elements of this increase in costs can be attributed to improvement works requested by Gallions, time delays on-site incurred by Axis, or additional costs resulting from the attempt to obtain Passivhaus compliance.

In June 2011, following smoke testing, the site manager for this project was dismissed by Axis for poor performance and severely overrunning from the original programme of works. Following this departure, there was a lack of senior management overseeing and coordinating works. This led to a slow-down of on-site works, resulting in the situation where the property was very close to completion for several months before the final hand-over date.

In the meeting, Axis accepted that these issues should have been picked up earlier by the contractors as part of their supervisory work. Axis also agreed that programme of works was not well coordinated by the contractor, works took place out of sequence and that updates to the original programme were infrequent and lacked detail. In addition, Axis recognised that better appreciation and understanding of the Passivhaus standard

by the site manager, particularly during extensive fabric improvements could have been sought to avoid much of the corrective work and time delays.

Gallions recognised that it should have enforced a better internal reporting process to monitor the delivery, timing and costs associated with of this project. Gallions originally treated the scheme as an extension to its Asset Management improvement programme, but it would have been better handled as a special project with a more formalised approval process.

As an individual project, the cost of retrofit works was very high when compared to a standard refurbishment cost. As specialist elements of the work become more common within the UK supply chain, the cost associated with the procurement and installation of these elements are expected to become more economical. Additionally, specialist works would benefit from economies of scale if they were undertaken to multi-dwelling properties, where collective benefits could be obtained in the installation of additional insulation and renewable energy solutions. Nonetheless, for the Gallions' funded element of this the project, they have received:

- A fully refurbished property and two additional bed spaces.
- A better understanding of how this type of property can be dealt with in future.
- A leading example of current low carbon technology, including the innovative use of solar energy used to preheat incoming cold air into the building.

5.8.2 Lessons learnt from Passivhaus

The ability to meet the strict air-tightness levels required of a Passivhaus dwelling proved to be the most challenging issue faced on site. The level of detailing and quality of workmanship required to achieve this on a refurbishment project (something not ever achieved in the UK before the project commenced) was much more difficult than anticipated by the design team and contractors. Poor understanding of the air-tightness principles by the contractor's site team and a lack of quality control meant abortive works were a regular feature on site.

There was some debate during the course of the works as to the air tightness of the concrete. It should be noted that concrete made under factory conditions can be treated as an air tight material. The main area of air leakage was through the party wall into the adjoining property and over the top of the party wall through the party roof structure. This was only discovered during a smoke test following two failed air tightness tests. The smoke test showed that practically all of the air leakage was into the adjoining

building. However, by this time in the project, it was too late to address the party wall and make it air tight.

To avoid this issue in future projects, the most straight forward solution would either be to externally insulate the entire row of houses, thus eliminating the challenge of insulating the partition wall. Alternatively, a continuous internal air-tight membrane would be recommended to create an unbroken barrier at the partition wall and the floor/roof slab edge. To support this discussion the research engineer developed *10 lessons learnt*, which the design team agreed were important to re-visit if attempting a Passivhaus project again:

1. There should be an understanding at the outset that Passivhaus cannot be applied to all retrofit projects due to the disruption and technical challenge.

2. Before adopting Passivhaus, the project team should be fully trained on the work methodologies required to achieve certification. Specifically air-tightness.

3. Passivhaus projects greatly benefit from the services of a contractor with specialist expertise as the process requires a step change in build quality.

4. It is beneficial to smoke test before retrofit works commences, as this will identify the key elements to be addressed. Party walls are a particular problem.

5. To avoid remedial works, all airtight tapes/barriers and services penetrations must be properly sequenced before the glazing and insulation is installed.

6. Allow plenty of time for specialist items such as triple glazing, external doors & the MVHR, since the UK market for Passivhaus compliant products is currently underdeveloped.

7. Do not cover up the materials and joints forming the air-tight barrier until the installation quality has been inspected and the air tightness has been verified.

8. Agree contractual 'hold-points' for air-tightness and smoke testing to take place after all significant fabric upgrades. Review the programme and costs at each stage of the project.

9. Having an 'Air Tightness Champion' on-site full/part time that understands and can predict the problems and associated with refurbishment is an advantage.

10. Proper onsite training and inductions of all sub-contractor site staff is essential before they are allowed on site to avoid uncertainty of Passivhaus requirements.

5.8.3 Key project successes

Despite the high cost and difficulties involved in this project, the design process and lessons learnt have implications across the whole housing stock and construction industry, in terms of (i) how to retrofit to achieve 'deep' reductions in CO_2 emissions, and also (ii) the step-change required by industry to meet the technical challenge, in terms of understanding, organisation and skills.

Passivhaus experience

Through this project the design team and contractors have gained invaluable experience in the design, modelling, construction and evaluation of Passivhaus retrofits. Despite on-site difficulties, the air permeability achieved is far better than UK new build standard. Consequently, thermal comfort is expected to be greatly improved and heating bills are expected to be minimal. Dampness and condensation problems have been treated, thus improving quality of life for occupants.

Support from local council

Through this process, a close working relationship was developed with Bexley's planners and Building Control. Bexley have been very impressed with Gallions' investment in energy conservation and the approach to dealing with high demand for larger family accommodation particularly from multigenerational families living together. The building represents a major success in reducing fuel poverty. The architectural makeover could represent a change to the perception of the buildings in the Thamesmead estate.

Roll-out potential

Lessons learnt through this project provide valuable information going forward to help others achieve the right balance between energy efficiency and cost. If aiming to roll-out a deep retrofitting strategy across the entire Thamesmead estate, or the nation's stock of hard-to-treat solid walled dwellings, for which there are 6.6 million homes, an adapted retrofit strategy based on the lessons learnt, SAP modelling and cost effectiveness analysis from this project would be recommended. Instead of aiming to meet an 80 % reduction in CO_2 emissions, a 40-60 % reduction would be more cost effective. This approach would require insulation to the walls and roof, combined with new glazing, efficient heating systems and new low energy lighting and appliances. Improvements to air tightness would be advised, but not to the strict level of Passivhaus compliance. Renewable generation would only be recommended if the savings can be financially justified through government incentives.

Post-occupancy evaluation

Over the next two years, a package of wireless monitoring equipment will capture important information such as the internal temperature and CO_2 levels within the house, power consumption of the MVHR, energy generation of the PV panels and solar water heater, as well as the total consumption of gas, electricity and water. A roof mounted solar radiation sensor, combined with temperature and humidity sensors inside the collector Aerogel Solar Collector cavity and MVHR ductwork provide a unique insight into this system's performance.

A 7 person family only moved into this property in June 2012, consequently no long term utility data to verify the predicted cut in CO_2 emissions can be presented in this thesis. Ultimately, the long term success of this project from a CO_2 savings and occupant perspective, will rely heavily on their comfort and satisfaction levels, combined with how well they engage with new technologies and conserve energy at home. Following the monitoring period this building will add significantly to the knowledge and understanding of low carbon technology in residential property going forward. Interviews with the occupants will be held to facilitate this process.

Innovation

Several innovative concepts and products incorporating aerogel insulation have been developed and tested as part of this project, providing some valuable insights into this material. Applying aerogel to the ground floor, proved to be one of least cost effective and troublesome measures to install on this retrofit process. Evidently, the material is an effective insulator for hard-to-treat zones, but it must be applied in practical thicknesses and applications for it to be a viable cost effective retrofit solution. By comparison, the Spacetherm™ Aerogel Door, developed by Proctor Group Ltd was found to be an effective alternative to expensive, heavy and thick Passivhaus doors, designed to achieve U-values of 0.8 $W/m^2 K$ or less. Prior to this installation, the product had not been installed on any other English properties. The total cost of this product including installation was nearly 3 times lower than the Passivhaus door.

Other emerging products utilised in this retrofit include the 'Lo-Pro' framing system for supporting PV panels on flat roofs without penetrating through the insulation; the use of air-tight technologies, external cladding and triple glazing, which are still relatively new to the UK construction market; and also the monitoring equipment, which the electrical sub-contractors initially knew little about.

Full details of the main innovation, the 'Aerogel Solar Collector' preheating the air in the mechanical ventilation system can be found in the next chapter.

Chapter 6

PREDICTED & IN-SITU PERFORMANCE OF A SOLAR AIR COLLECTOR INCORPORATING A GRANULAR AEROGEL COVER

Abstract

In this chapter, the in-situ performance of a 5.4 m^2 solar air collector containing granular aerogel is simulated and tested. The collector was incorporated into the external insulation of a mechanically ventilated end terrace house, recently refurbished in London, UK. During the 7-day in-situ test period, peak outlet temperatures up to 45 °C were observed and validated to within 5% of their predicted values. Resultant supply and internal air temperatures peaked at 25-30 °C and 21-22 °C respectively. Peak efficiencies of 22-36 % were calculated based on the proposed design across a range of cover types. Estimated outputs ranged from 118-166 kWh/m^2/year for collectors with different thickness granular aerogel covers, compared to 110 kWh/m^2/year for a single glazed collector, 140 kWh/m^2/year for a double glazed collector and 202 kWh/m^2/year for a collector incorporating high performance monolithic aerogel. Financial payback periods of 9-16 years were calculated across all cover types. Using a streamlined life cycle assessment, a CO_2 burden payback of 0-2 years was predicted comparing the impact of the raw materials in the framing, cover and absorber, to the predicted energy savings for each system. An efficiency of up to 60 % and a financial payback period as low as 4.5 years was predicted for an optimised collector incorporating a 10 mm thick granular aerogel cover.

Nomenclature

A_c	Collector area (m²)
A_d	Exposed area of ductwork (m²)
C_p	Specific heat capacity (J/kg K)
D_h	Hydraulic diameter (m)
F_R	Heat removal factor
F'	Collector efficiency factor
F''	Collector flow factor
H	Collector height (m)
H'	Average cavity height
h_c	Convection coefficient (W/m² K)
h_r	Radiation coefficient (W/m² K)
h_w	Wind coefficient (W/m² K)
k	Thermal conductivity (W/m K)
L	Cube root of house volume (m)
$\dot{m}$	Mass flow rate (kg/s)
Nu	Nusselt number
Pr	Prandtl number
Q_U	Useful energy (W)
R	Thermal resistance (m² K/W)
Re	Reynolds number
S	Solar irradiance (W/m²)
T_a	Ambient temperature (°C)
T_{inside}	Inside temperature of house (°C)
T_i	Collector inlet temperature (°C)
T_{fm}	Mean fluid temperature (°C)
T_L	Average temperature of air lost to the environment (°C)
T_o	Collector outlet temperature (°C)
T_{pm}	Mean plate temperature (°C)
U_{Back}	Back heat loss coefficient (W/m² K)
U_d	Loss coefficient of duct (W/m² K)
U_{front}	Front heat loss coefficient (W/m² K)
U_L	Overall heat loss coefficient (W/m² K)
v_w	Wind velocity (m/s)
V	Total volume of dwelling (m³)
W	Collector width (m)

Greek letters

α	Plate absorptance
β	Collector tilt (◦)
ε	Emissivity
η_1	Instantaneous efficiency
μ	Dynamic viscosity (kg/m s)
ρ	Density (kg/m³)
σ	Stefan-Boltzmann constant (W/m² K⁴)
τ	Cover transmission

Subscripts

Used in emissivity calculations, radiation and convection heat transfer coefficients and outlet temperature validation:

1	Inner surface of collector cover
2	Absorber plate
3	Inner surface of back insulation
i	Inlet
o	Outlet

6.1 Introduction

The following chapter investigates the thermal performance, financial payback period and life cycle impact of a solar air collector incorporating a granular aerogel. In-situ testing took place in a dwelling, recently refurbished as part of the Technology Strategy Board's 'Retrofit for the Future' competition. The house is a three-storey 1960s pre-cast concrete end terrace, in South-East London, UK, with a large south facing wall, ideal to test new solar energy technologies. Through refurbishment works, the property has been transformed from a four to a six bedroom house, super-insulated with external cladding (U-value 0.1 W/m² K), triple glazing (U-value 0.8 W/m² K, G-value 0.5) and high levels of air tightness (3.5 m³/m² h @ 50 Pa). Fresh air is provided by a mechanical ventilation system with heat recovery (MVHR). PV panels and vacuum tube collectors provide renewable electricity and water heating.

The 6 x 0.9 metre solar collector prototype has been incorporated into the property's external insulation on the south facade. It provides a free source of heating to the property by elevating the temperature of the extract air used to indirectly preheat the supply air for the MVHR. Basic components consist of (i) a cover, translucent to solar radiation whilst reducing convection and radiation losses (ii) a black perforated solar absorbing sheet inside a cavity, (iii) back insulation to reduce conduction losses, and (iv), insulated ducts to transfer the air into the house. A novel feature of this prototype is its highly insulated translucent cover, consisting of a 40 mm multi-wall polycarbonate panel filled with high performance aerogel granules. This 40 mm thick granular aerogel cover was selected to minimise the front heat loss coefficient of the collector as the prototype was originally being incorporated into a house aspiring to meet Passivhaus insulation levels. This cover is predicted to reduce heat losses significantly through the collector compared to traditional glazed systems, whilst allowing sufficient solar transmission for heat collection.

6.1.1 Motivation

Across the UK, there are approximately 7.5 million 'hard-to-treat' dwellings with solid walls, 6 million of which are not listed or in conservation areas (Beaumont, 2007; BRE, 2008). According to Roberts (2008a), solid wall insulation should be viewed as an untapped opportunity rather than a barrier for improving the performance of these homes, since large energy savings can still be made. However, the EEPH (2009) state that it is difficult to envisage the installation rate of solid wall insulation increasing without stronger incentive schemes, active promotion and technological innovation.

Innovation in the form of solar air collectors or solar Trombe walls incorporated into external insulation schemes could provide a novel approach to utilising the nation's stock of undervalued solid walled dwellings as well as increasing awareness for solid wall insulation technologies. The literature review indentified a lack of in situ studies of solar air collectors incorporating granular aerogel. This study seeks to contribute to this field, motivated by the lower cost and increased functionality of granular aerogel over monolithic aerogel, supported by its recent emergence within the construction sector.

The concept of a Trombe wall incorporating a monolithic aerogel cover encapsulated within double-glazing was originally proposed by Fricke (1988). According to modelling by Caps and Fricke (1989), a 15 mm thick monolithic aerogel cover, sandwiched between double glazing, then evacuated, could achieve minimal solar heat losses compared to conventional glass or translucent honeycomb covers due to its high solar transmission of 50–60 % and low U-value of 0.5 W/m² K.

By comparison, Svendsen (1992) constructed a 1.4 m² flat plate collector prototype incorporating monolithic aerogel for water heating, with measured efficiencies of 60–80 %, indicating that the prototype could generate up to 700 kWh/m²/year, being twice as efficient as commercial flat plate collectors. Modelling by Nordgaard and Beckman (1992) verified this performance, demonstrating that the reduction in solar transmittance compared to a single glass pane is more than compensated by the reduction in heat losses, achieving efficiencies of more than 60 %.

Ortjohann (2001) predicted that super-insulating solar thermal collectors could be produced using granular aerogel sandwiched inside an evacuated collector design. The main benefit would be its low weight, ease of handling and ability to provide an efficient collector design without an optimised absorber technology. Conversely, the main disadvantage would be the difficulty in maintaining a vacuum throughout the life-span of the product (Ortjohann, 2001).

Countering this, the performance of granular aerogel without a vacuum has been investigated by Wittwer (1992) achieving U-values of 1.1 to 1.3 W/m² K from 20 mm thick samples encapsulated within double glazing. Meanwhile, Reim *et al.* (2005) achieved even lower U-values of 0.4 W/m² K for 20 mm thick plastic panels filled with granular aerogel, sandwiched between two glass panes with krypton and argon gas fillings. According to Reim *et al.* (2005) without the glass panes (and gas fillings), the solar transmittance of their prototype was 65 %, indicating high potential for use in insulated solar walls, with 40 % less heat losses than conventional glass solar collectors.

6.2 Prototype Description

A schematic diagram of the 'Aerogel Solar Collector' constructed for this study, together with an outline of the monitoring equipment, is shown in Figure 6.1. The prototype is a flat plate solar air heater incorporated into an MVHR system running in continuous operation. Air extracted from the kitchen and bathrooms is fed into the solar collector cavity, where it is heated by incoming solar irradiance. This heat is then used to provide additional energy to indirectly heat the incoming fresh air supply to the property's living room and bedrooms. Automatic flow and bypass controls maintain comfortable internal temperatures all year round, with radiators providing top-up heating to meet peak winter demand when necessary.

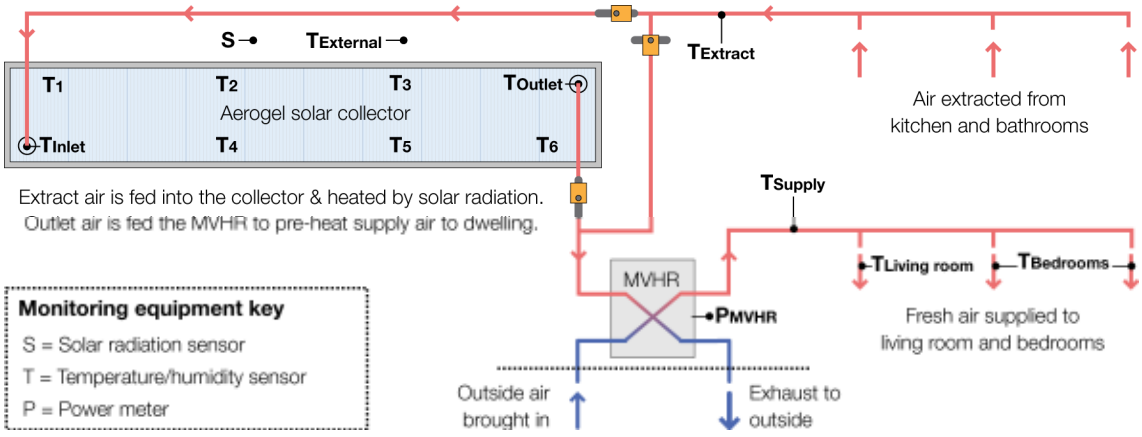

Figure 6.1 *Schematic of the Aerogel Solar Collector and monitoring equipment.*

6.2.1 Roles and responsibilities

It is worth emphasising that the development of this concept into a fully functional prototype was primarily led by the research engineer, but it would not have been possible without the full support of a collaborative process supported by the client and several industrial partners. The main responsibilities of the research engineer included product development, management, chairing all design meetings, building all industrial collaborations, undertaking preliminary system sizing using a steady state calculation model (outlined in Sections 6.3 and 6.4), producing all technical drawings used on-site by the contractors, as well as overseeing the specification of the control system, monitoring equipment installations and air flow commissioning.

Key partners included: C.Biggs (Technical Director of Nuaire Ltd), whose expertise focused on the MVHR integration, including the selection of controls and the absorber sheet as well as sizing the cavity; J.Richings (Technical Director of Permarock Products Ltd), whose expertise focused on the external cladding integration, including the timber

frame design and a fire break around the perimeter; R.Lowe (Technical Services Manager at Xtralite Ltd), whose expertise focused on the aerogel framing system, including technical advice on suitable fixings and aerogel panel properties.

M.Montomergy, (Investment Planning Manager for Gallions Housing Association) was also influential in the preliminary sizing of product, desiring a large prototype to be constructed, which would be visible to the wider community. All monitoring equipment was specified by the research engineer and installed by BSRIA Ltd with support from A.Gilbert (Instrument Solutions Rental Manager at BSRIA Ltd). All controls were installed by MD Electrical, Axis' electrical sub-contractor. Commissioning of the air flows was undertaken by H.Hall (of Andrew Reid & Partners LLP).

6.2.2 Detailed design

A floor plan showing the location of the Aerogel Solar Collector on the south facing 2nd floor wall is shown in Figure 6.2. Note that the collector has been integrated into the exhaust side of the mechanical ventilation system (opposed to directly heating air on the supply side), due to Gallions Housing Association not wanting to pass the dwellings fresh air supply through a prototype which had not been tested before. The collector is located at high level, spanning along the top floor of the south wall, avoiding overshadowing from surrounding buildings.

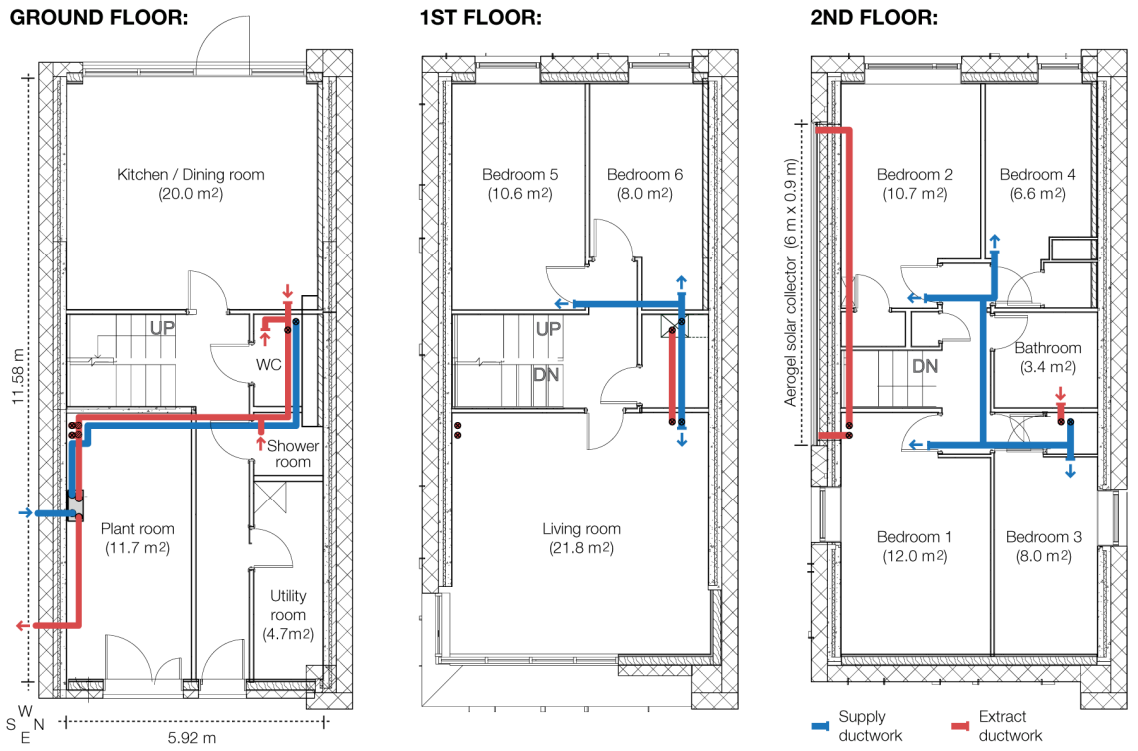

Figure 6.2 *Layout diagram of the house showing the Aerogel Solar Collector and the location of supply and extract ductwork in the mechanical ventilation system.*

Figure 6.3 contains a section through the inlet of the Aerogel Solar Collector. Key features include an aluminium support system, a timber frame painted black, an absorber in the centre of the cavity, back insulation and a fire break.

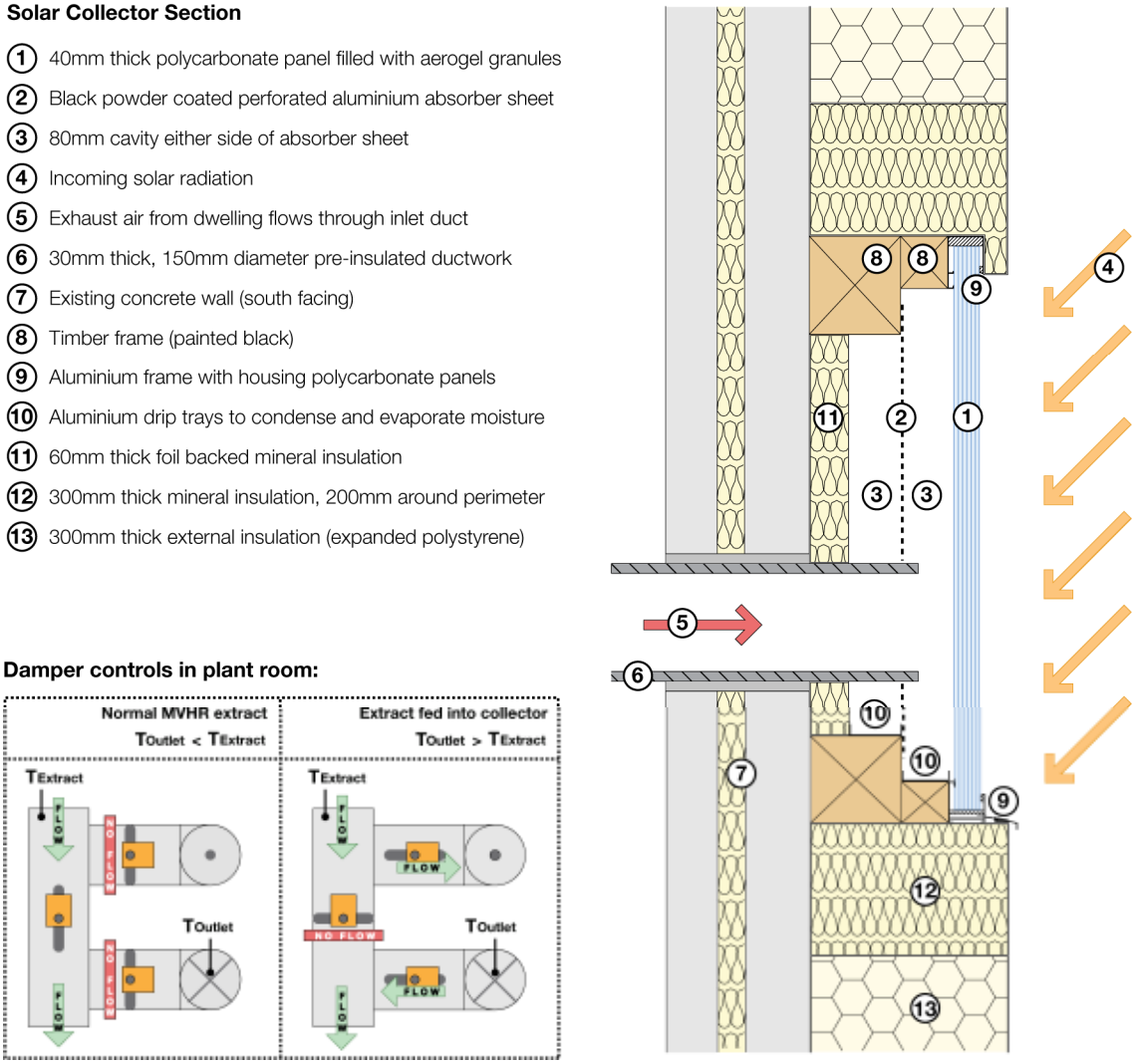

Figure 6.3 *Section through the inlet duct of the Aerogel Solar Collector.*

6.2.3 Construction steps

Figure 6.4 to Figure 6.10, show the key steps taken to construct the Aerogel Solar Collector. Shown in Figure 6.4, the collector consists of a 6 m x 0.9 m timber frame fixed directly to the outside of the dwelling's existing concrete wall, which had been screeded flat. Two 150 mm diameter holes were diamond cut through the external wall, in the bottom left and top right corners of the collector to facilitate the inlet and outlet respectively. Screwed to the front of the timber is an aluminium framing system provided by Xtralite Ltd to support the cover system. 200 mm of mineral insulation was inserted around the perimeter of the frame to act as a fire break.

Figure 6.4 *Solar collector frame.*

Directing air to and from the solar collector are spans of 150 mm diameter pre-insulated ducts (shown in the two right diagrams of Figure 6.5). These ducts are the 'HR-WTW pre-insulated Duct System' supplied from Ubbink. They are vapour resistant and can be used in temperature ranges of –40 °C to +100 °C. All exposed ductwork in the dwelling was boxed in following installation. Warm air from the collector outlet runs vertically down to a plant room on the ground floor.

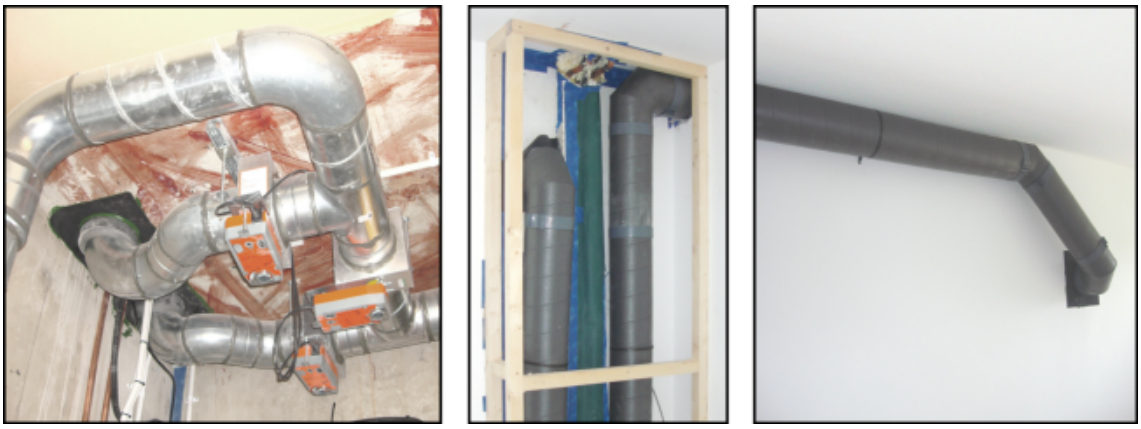

Figure 6.5 *Damper and ductwork arrangement.*

Inside the plant room is an arrangement of three dampers (shown in the left of Figure 6.5), to direct air flow. These dampers operate simultaneously based on a changeover relay provided by a temperature differential electronic thermostat, supplied by Titan Products Ltd. This control unit is wired to a thermistor located in the solar collector outlet (shown in the right of Figure 6.6), and another in the exhaust air ductwork (from the kitchen and bathrooms) in the plant room. The changeover relay directs air into the collector when the outlet temperature is 5 °C greater than the exhaust temperature. Note that the MVHR also has a summer bypass function (independent of the three control dampers) which activates when the outside air temperature exceeds 20 °C.

Also, shown in Figure 6.6, the inside of the collector was insulated with 50 mm of foil backed mineral insulation to reduce heat transfer from the inside of the collector to the adjacent bedrooms as well as reflect incoming solar radiation to the rear side of the absorber sheet. Two aluminium drip trays were bonded to the inside edges of the timber frame to allow any moisture build up inside the collector, either side of the absorber, to condense and vaporise.

Figure 6.6 *Collector showing the foil backed insulation and thermistor in the outlet duct.*

The absorber consists of three black powder coated perforated aluminium sheets, supplied by APW Ltd, fixed side-by-side spanning across the width of the collector. Each sheet is 1 mm thick and contains 4.7 mm diameter perforations at 8 mm pitches, creating a 40 % open area. Shown in Figure 6.7, the sheet fitted on the inlet side of the collector has a pre-cut hole enabling the inlet ductwork to penetrate through so that incoming air passes over its surface. When fitted, there is an 80 mm cavity either side.

Figure 6.7 *Absorber sheet and photo of installation showing drip trays and sensors.*

Shown in Figure 6.7 and Figure 6.8, during the installation of the absorber sheets, eight temperature/humidity sensors, with wireless radio transmitters were fixed to the

absorber sheet at high and low level to monitor the profile across the collector. All transmitters were fixed to the front of the absorber sheet to obtain the clearest signal down to a data hub in the plant room. Each sensor head is located behind the absorber sheet and contains a plastic shield to protect against direct solar irradiance without disrupting airflow.

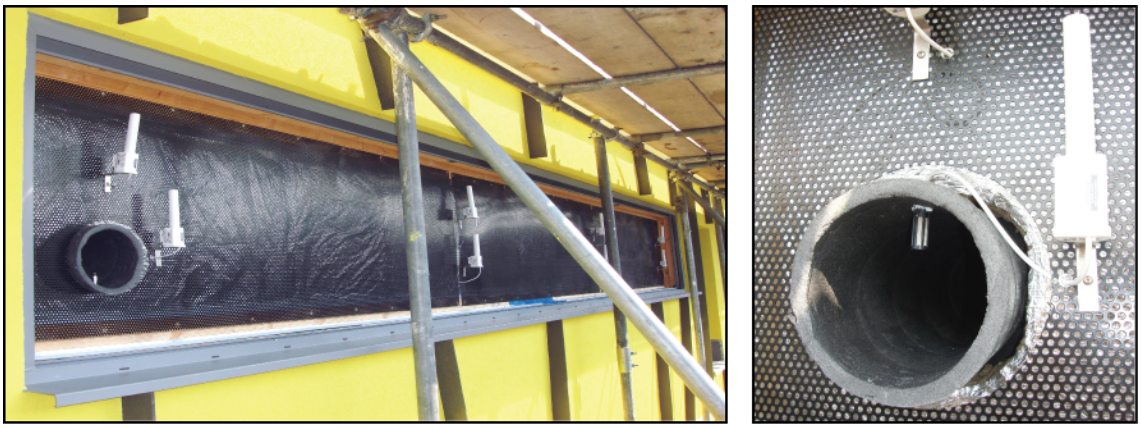

Figure 6.8 *Installation of the absorber sheets and temperature/humidity sensor at the inlet.*

Four additional temperature/humidity sensors were installed in the supply and extract MVHR ductwork, as well as the living room and a north facing bedroom (Bedroom 3 in Figure 6.2). A pyranometer mounted horizontally on the edge of the roof measures the intensity of solar irradiance hitting the solar wall. A power meter on the MVHR measures the electricity used by the fans. All sensors provide 5-minute pulsed outputs.

The final step in constructing the solar collector was to seal the system by installing the aerogel panels inside the collector frame. Shown in Figure 6.9, the panels consist of 40 mm thick multi-wall polycarbonate panels, which manually clip together to create a reasonable air tight seal. Twelve panels were installed inside the aluminium frame.

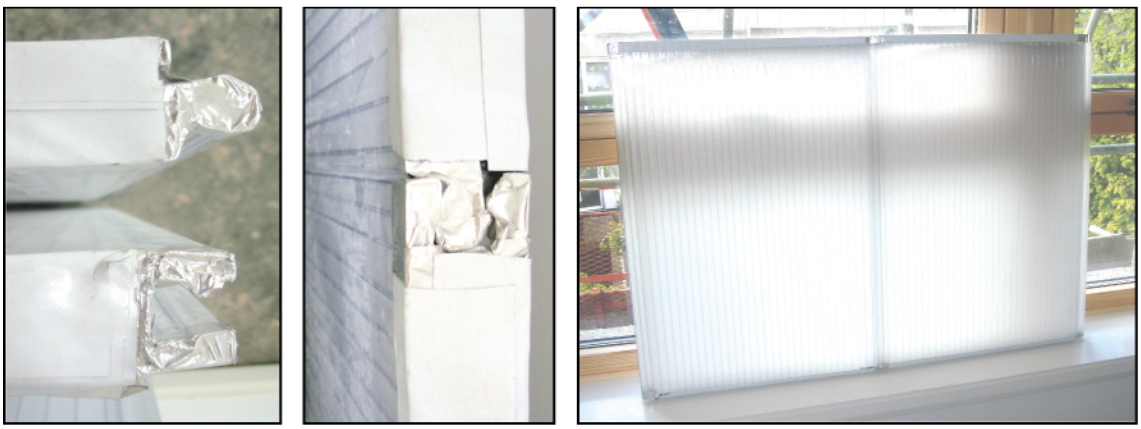

Figure 6.9 *Polycarbonate panels filled with granular aerogel (prior to installation).*

A photograph of the constructed Aerogel Solar Collector is shown in Figure 6.10. Each polycarbonate panel was manufactured to include additives for flame resistance and UV stabilisation, making them suitable for outdoor use and capable of withstanding temperatures up to 150 °C without warping. They have Class 1 approval and a EuroClass (B-s1, d0) fire rating, also when filled with aerogel (Cabot and Roda, 2010).

Figure 6.10 *South-east elevation of the retrofit house.*

Take note that the 40 mm cover thickness was selected to enable the prototype to achieve an overall U-value below the Passivhaus target of 0.8 W/m² K for glazed openings (BRE, 2010). This was important to the design team as the prototype was being integrated into the external cladding scheme, as opposed to being a stand-alone solar air collector mounted at roof level. This thickness was also preferred by the client over thinner covers, since it would enable a larger prototype to be constructed, more visible to the wider community, without increased risk of overheating inside the dwelling. In Section 6.4.1, thermal modelling demonstrates how the operational efficiency can be improved using thinner granular aerogel covers with higher solar transmittance, but worse U-values.

6.3 Calculation Methodology

Duffie and Beckman (2006) provide one of the most comprehensive and widely cited resources for predicting the performance of solar energy technologies. With the exception of the overall heat loss coefficient (U_L) and collector efficiency factor (F') equations derived by Parker (1981), this reference provides the foundation for the following methodology used to predict the performance of the Aerogel Solar Collector.

Energy balance equation

The steady state thermal performance of a flat-plate collector can be calculated from Equation [6.1], taking account of thermal and optical losses to determine the distribution of incident solar irradiance into useful energy gain (Q_U).

$$Q_U = A_C F_R [S(\tau\alpha) - U_L(T_i - T_a)] \qquad [6.1]$$

A_C is the aperture area of the collector. F_R, refers to a plate efficiency or 'heat removal factor'. S is the total solar irradiance on the collector surface. τ is the cover transmittance. α is the absorptance of the absorber plate. U_L is the overall heat loss coefficient. T_i is the inlet fluid temperature. T_a is the ambient temperature outside.

Collector heat losses

The overall heat loss coefficient (U_L) depends upon heat losses through the front and back of the collector, convection and radiation exchanges inside the cavity and heat losses due to wind. Figure 6.11 illustrates these parameters within a one-dimensional section of the Aerogel Solar Collector.

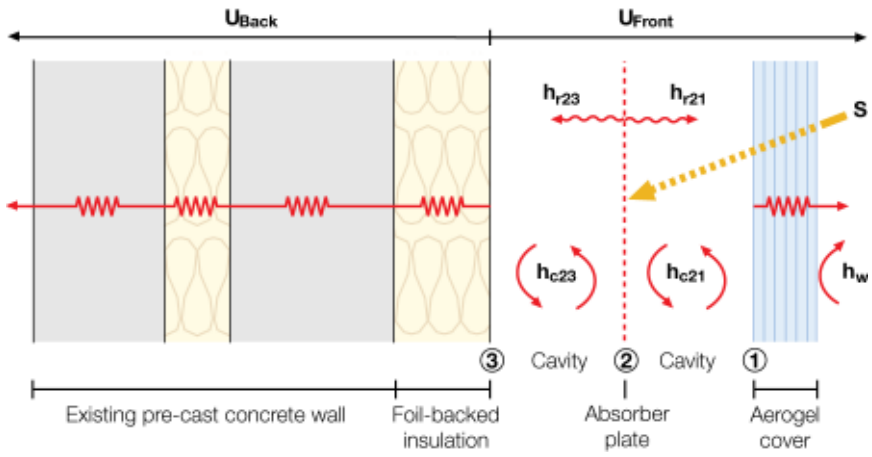

Figure 6.11 *Energy balance through solar collector.*

In this figure, h_w is the wind heat transfer coefficient, h_r and h_c are radiation and convection coefficients respectively, where the subscripts 1,2 and 3 correspond to the

inner surface of the collector, the absorber plate, and the inner surface of the back insulation, respectively. U_{Front} and U_{Back} are the thermal transmittances through the respective layers.

Duffie and Beckman (2006) derive the loss coefficients for a variety of solar air collector layouts. However, the literature does not cover solar air collectors with airflow on both sides of the absorber sheet. Addressing this issue, Parker (1981) determined that the overall heat loss coefficient for this arrangement can be calculated using Equation [6.2].

$$U_L = \{4h_{c21}h_{c23}U_{Back}U_{Front} + 2h_{r21}[(h_{c21}+h_{c23})(h_{r23}U_{Front}+U_{Back}U_{Front}+h_{r23}U_{Back}) + h_{c21}h_{c23}U_{Front}] + 2h_{r23}U_{Back}[h_{c21}h_{c23}+h_{c21}U_{Front}+h_{c23}U_{Front}] + h_{c21}U_{Front}[h_{c21}(2h_{r23}+h_{r21}) + h_{r23}Q + h_{c21}U_{Back}[h_{c21}(h_{r23}+2h_{c23}) + h_{r21}Q]\}/D \quad [6.2]$$

Where:

$$D = \{2h_{c21}h_{c23}P + 2h_{c23}U_{Back}U_{Front} + h_{r21}[Q(h_{c21}+h_{r23}+U_{Back}) + h_{c21}h_{r23}] + h_{r23}Q(h_{c21}+U_{Front})\}$$

$$P = h_{c21} + U_{Back} + U_{Front}$$

$$Q = h_{c21} + 2h_{c23}$$

Radiation coefficients

The radiation heat transfer coefficients between the absorber plate and the collector (h_{r21}) and the absorber plate to the back insulation (h_{r23}) can be found using Equations [6.3] and [6.4] respectively.

$$h_{r21} = \frac{4\sigma T_{fm}^{\ 3}}{(1/\varepsilon_1)+(1/\varepsilon_2)-1} \quad [6.3]$$

$$h_{r23} = \frac{4\sigma T_{fm}^{\ 3}}{(1/\varepsilon_2)+(1/\varepsilon_3)-1} \quad [6.4]$$

Here, ε is the surface emissivity and T_{fm} is the mean fluid temperature, expressed in Kelvin. σ is the Stefan Boltzmann constant. Note that $T_{fm,}$ the mean fluid temperature, must be estimated at this stage, but can be corrected later using an iterative calculation (Duffie and Beckman, 2006).

Convection coefficients

The convection heat transfer coefficients can be calculated using Equation [6.5].

$$h_c = Nu\,(k / D_h) \qquad [6.5]$$

k is the thermal conductivity of air at the estimated mean fluid temperature. D_h is the hydraulic diameter of the air gap (two times the thickness). Nu refers to the Nusselt number, dependant on whether the flow regime is turbulent or laminar based on the Reynolds number, found using Equation [6.6].

$$Re = \frac{2\dot{m}}{H'\mu} \qquad [6.6]$$

μ is the dynamic viscosity. $\dot{m}$ is the mass flow rate. H' is the height of the cavity. When Re<2300 the fluid is laminar and Equation [6.7] should be used to calculate Nu, whereas if Re>2300, then the fluid should be treated as turbulent and Equation [6.8] is used.

$$Nu_{laminar} = 4.9 + \left[\frac{0.0606(RePr\,D_h / H')^{1.2}}{1 + 0.909(RePr\,D_h / H')^{0.7}\,Pr^{0.17}}\right] \qquad [6.7]$$

$$Nu_{turbulent} = 0.0158Re^{0.8} \qquad [6.8]$$

Pr is the Prandtl number, calculated from Equation [6.9], where C_p is the specific heat capacity of the fluid (air) inside the collector.

$$Pr = \frac{\mu Cp}{k} \qquad [6.9]$$

Front heat losses

Front heat losses through a single cover (U_{Front}) can be calculated with Equation [6.10].

$$U_{Front} = \left[\frac{C}{T_{pm}}\left(\frac{T_{pm} - T_a}{1+f}\right)^e + \frac{1}{h_w}\right]^{-1} + \frac{\sigma(T_{pm} + T_a)(T_{pm}^2 + T_a^2)}{(\varepsilon_2 + 0.00591h_w)^{-1} + \left(\frac{1 + f + 0.133\varepsilon_2}{\varepsilon_1}\right) - 1} \qquad [6.10]$$

Where:

$$f = 1.07866\,(1 + 0.089h_w - 0.1166h_w\varepsilon_p)$$

$$C = 520\,(1 - 0.00005\beta^2)$$

$$e = 0.430\,(1 - 100 / T_{pm})$$

ε_1 and ε_2 are the emissivity of the cover and absorber plate respectively. T_a and T_{pm} correspond to ambient and mean plate temperature, respectively, expressed in Kelvin. T_{pm} must be estimated at this stage, but will be corrected later using an iterative calculation. h_w is the wind heat transfer coefficient. β is the collector tilt in degrees.

Wind coefficient

The wind heat loss coefficient, h_w, accounting for free and forced convection, can be calculated using Equation [6.11].

$$h_w = \max\left(5, \frac{8.6 v_w^{0.6}}{L^{0.4}}\right) \quad [6.11]$$

Here, v_w is the wind velocity and L is the cube root of the dwelling volume. According to Duffie and Beckman (2006), a minimum value of 5 W/m² K occurs in vertical solar collectors under still conditions.

Back losses

Thermal losses through the back of the collector are calculated using Equation [6.12].

$$U_{Back} = \frac{1}{\sum_{i-1}^{i=n} R_i} \quad [6.12]$$

Here, $\sum_{i-1}^{i=n} R_i$ is the sum of the thermal resistances of the insulation layers. For the Aerogel Solar Collector, these layers consist of the back insulation inside the collector, as well as the thermal resistance and internal surface resistance of the existing wall.

Heat removal factor

The heat removal factor (F_R) is a ratio between the actual useful energy gain of the collector to the maximum possible useful energy gain, obtained by setting the mean plate temperature to the inlet temperature so that heat losses are minimised. F_R is the product of two design constants: the collector efficiency factor (F') and a collector flow factor (F''), as shown in Equation [6.13].

$$F_R = F'F'' \quad [6.13]$$

Collector efficiency factor

According to Parker (1981), for solar air collectors with flow on both sides of the absorber plate, the collector efficiency factor (F') can be calculated using Equation [6.14], where the values of D, P (and Q) are given earlier in Equation [6.2].

$$F' = D/\{2h_{c21}h_{c23}P + 2h_{c23}U_{Back}U_{Front} + h_{r21}[(h_{c21} + h_{r23})(P + 2h_{c23}) + U_{Back}(2h_{c23} + U_{Front}) + h_{c21}h_{r23}] + h_{r23}[h_{c21}(P + 2h_{c23}) + 2h_{c23}U_{Front} + U_{Back}U_{Front}]\} \quad [6.14]$$

Collector flow factor

The collector flow factor (F") can be calculated from Equation [6.15]. Here $\frac{\dot{m}Cp}{A_C U_L F'}$ can be defined as the 'dimensionless collector mass flow rate'.

$$F'' = \frac{\dot{m}Cp}{A_C U_L F'}\left[1 - \exp\left(-\frac{A_C U_L F'}{\dot{m}Cp}\right)\right] \quad [6.15]$$

Mean fluid temperature

At this stage, it is possible to calculate Q_u, using Equation [6.1]. In turn, the mean fluid temperature can be calculated using Equation [6.16]:

$$T_{fm} = T_i + \frac{Q_U / A_C}{F_R U_L}(1 - F'') \quad [6.16]$$

In Equations [6.3] and [6.4], T_{fm} was estimated. As such, the recalculated value should be fed back into the original equations. According to Duffie and Beckman (2006), typically 2-3 iterations provide sufficiently accurate values. Alternatively, computer packages can automate iteration loops updating values dependant on fluid properties such as density, specific heat capacity, thermal conductivity, dynamic viscosity and the Prandtl number.

Mean plate temperature

Similarly, the mean plate temperature can be calculated using Equation [6.17]. Again, the recalculated value should be fed back into the original equations, using an iterative process.

$$T_{pm} = T_i + \frac{Q_U / A_C}{F_R U_L}(1 - F_R) \quad [6.17]$$

Outlet temperature

The basic method of measuring collector performance is to expose it to solar irradiance and measure the inlet and outlet temperatures and the fluid flow rate. The useful gain can then be calculated using Equation [6.18]:

$$Q_U = \dot{m}\,Cp\,(T_o - T_i) \quad [6.18]$$

Rearranging this equation in terms of the outlet temperature (T_o) gives Equation [6.19]:

$$T_o = T_i + \frac{Q_U}{\dot{m}Cp} \quad [6.19]$$

Ductwork heat losses

Heat losses in the ductwork leaving a solar collector can be significant (Duffie and Beckman, 2006). The temperature drop (ΔT_o) from ductwork can be calculated using Equation [6.20]:

$$\Delta T_o = \frac{U_d A_d (T_o T_{inside})}{\dot{m}Cp} \quad [6.20]$$

T_{inside} is the internal temperature, assuming ductwork runs internally through the building. A_d is the exposed area of the ductwork where thermal losses occur. U_d is the heat loss coefficient of the ducting.

Instantaneous efficiency of collector

Instantaneous efficiency can be calculated using Equation [6.21]:

$$\eta_1 = \frac{Q_U}{A_C S} = F_R(\tau\alpha) - \frac{F_R U_L (T_i - T_a)}{S} \quad [6.21]$$

MVHR supply temperature

The resultant supply air temperature leaving an MVHR, following indirect heat exchange with the exhaust air can be calculated using Equation [6.22], where η_{MVHR} is the efficiency of the MVHR heat exchanger and T_o is the outlet temperature of the collector, adjusted to account for ductwork heat losses:

$$T_s = T_a + [\eta_{MVHR} (T_o - T_a)] \quad [6.22]$$

6.4 Steady State Model

Table 6.1 displays the interface of a steady state model created to characterise the Aerogel Solar Collector. Key inputs include the collector make-up and dimensions, the weather conditions and the inlet fluid properties. Key outputs include the overall efficiency, collector efficiency factor, overall heat loss parameter and heat removal factor, as well as the outlet temperature and useful energy before/after passing through the ductwork leading to the MVHR. The model includes an iteration loop to correct initial estimations for the mean plate temperature and mean fluid temperature. The

model also calculates resultant supply air temperature leaving the MVHR based on the efficiency of the heat exchanger. Values can be compared to the baseline supply temperature without the solar collector.

Table 6.1 *Input and output parameters of the steady state model.*

CHARACTERISE CONSTRUCTION LAYERS

				Aerogel panel	Air gap (front)	Black aluminium	Air gap (back)	Foil-backed insulation	Concrete inner-leaf	EPS insulation	Concrete outer-leaf	Inner surface
1	Thickness	x	m	0.040	0.080	0.001	0.080	0.060	0.080	0.035	0.105	-
2	Conductivity	k	W/m K	0.022	-	250	-	0.035	1.701	0.040	1.701	-
3	Resistance	R	m^2 K/W	1.85	-	0	-	1.71	0.05	0.88	0.06	0.13
4	U-value	U	W/m^2 K	0.54	-	250000	-	0.58	21.26	1.14	16.20	7.69
5	Emissivity	ε	-	0.91	-	0.70	-	0.10	-	-	-	-

CHARACTERISE WEATHER

				Input
6	Ambient temperature	Ta	°C	7.5
7	Incident radiation	S	W/m^2	500
8	Wind velocity	v_w	m/s	5

CHARACTERISE FLAT PLATE COLLECTOR

				Input
9	Width	W	m	6.0
10	Height	H	m	0.9
11	Tilt	β	°	90
12	Cover transmittance	τ	-	0.46
13	Plate absorptance	α	-	0.54
14	Mean plate temperature	T_{pm}	°C	34.61
15	Mean fluid temperature	T_{fm}	°C	34.18

CHARACTERISE HEAT TRANSFER FLUID

				Input
16	Mass flow rate	$\dot{m}$	kg/s	0.043
17	Inlet air temperature	T_i	°C	23
18	Average cavity height	H'	m	0.687
19	Density	ρ	kg/m^3	1.1655
20	Specific heat capacity	Cp	J kg K	1006.5
21	Thermal conductivity	k	W/m K	0.02645
22	Dynamic viscosity	μ	kg/m s	1.86E-05
23	Prantl number	Pr	-	0.705

CHARACTERISE DWELLING

				Input
24	Total volume	V	m^3	400
25	Internal temperature	Tinside	°C	21

CHARACTERISE OUTLET DUCTWORK

				Input
26	Duct diameter	D	m	0.15
27	Duct length	L	m	10
28	Insulation thickness	Δx	m	0.03
29	Insulation conductivity	k	W/m K	0.035

CHARACTERISE MVHR

				Input
30	Heat exchanger efficiency	η_{MVHR}	%	90

CALCULATIONS

				Output
31	Stephan-Botlzman constant	σ	-	5.67E-08
32	Hydraulic diameter	Dh	m	0.16
33	Reynolds number	Re	-	6748
34	Flow regime?		-	Turbulent
35	Nusselt number	Nu	-	
36	Laminar flow calculation		-	n/a
37	Turbulent flow calculation		-	18.28
38		Selection:	-	18.28
39	Wind coefficient	h_w	W/m^2 K	10.16
40	Convection coefficient	h_{c21}	W/m^2 K	3.02
41	Convection coefficient	h_{c23}	W/m^2 K	3.02
42	Radiation coefficient	h_{r21}	W/m^2 K	4.30
43	Radiation coefficient	h_{r23}	W/m^2 K	0.65
44	Back losses	U_b	W/m^2 K	0.35
45	Front losses	U_f	W/m^2 K	0.47
46	Overall losses	U_L	W/m^2 K	0.78
47	Collector efficiency factor	F'	-	0.96
48	Capacitance rate	-	-	10.62
49	Collector flow factor	F''	-	0.95
50	Heat removal factor	F_R	-	0.92
51	Area of outlet ductwork	Ao	m^2	4.71
52	Loss coefficient of ductwork	U_d	W/m^2 K	1.17
53	Temperature drop from ducts	T_d	°C	1.89

PREDICTED PERFORMANCE

				Output
54	Useful energy	Q_u	W	555.90
55	Outlet temperature	T_o	°C	35.84
56	Mean plate temperature	T_{pm}	°C	34.61
57	Mean fluid temperature	T_{fm}	°C	34.18
58	Instantaneous efficiency	η_1	%	0.21
	Effect of ductwork leaving collector			
59	Useful energy	Q_u	W	474.29
60	Outlet temperature	T_o	°C	33.96
	Supply temperature to house			
61	Basecase (no solar collector)	T_s	°C	21.45
62	Supply temp with solar collector	T_s	°C	31.31

When characterising the collector, the model assumes heat flow through the cover and back is one-dimensional, and construction properties are independent of temperature. Edge losses and the effects of dust, dirt and moisture are not considered. The collector is assumed to be completely airtight. Air properties are dependent on the mean fluid temperature inside the collector. Perforations in the double sided absorber plate (exposed area of 40 %) are accounted for by reducing plate absorption to (α x 0.6). The

average wind velocity is taken as 5 m/s. To account for the thickness of the granular aerogel cover, its thermal resistance is added in series to the front heat loss coefficient.

6.4.1 Cover efficiency investigation

To investigate the efficiency of different solar collector covers, Table 6.2 displays the predicted heat removal factor, overall heat loss parameter and collector efficiency factor, based upon the U-value and total solar transmittance (TST) of four multi-wall polycarbonate panels filled with granular aerogel at 10, 16, 25 and 40 mm thicknesses (Lexan, 2011). Values are benchmarked against properties of single glazing, double glazing and a double glazed cover encapsulating a 15 mm layer of high performance monolithic silica aerogel (Schultz *et al.* 2008).

Table 6.2 *Design parameters for different collector covers calculated from the U-value and total solar transmittance (TST).*

Collector cover type	U-value	TST	F_R	U_L	F'
Single glazing	5.70	0.85	0.63	4.36	0.78
Double glazing	2.80	0.80	0.74	2.71	0.85
10mm granular aerogel	1.48	0.70	0.86	1.31	0.93
16mm granular aerogel	0.97	0.62	0.89	1.06	0.94
25mm granular aerogel	0.62	0.61	0.91	0.84	0.96
40mm granular aerogel	0.54	0.46	0.92	0.78	0.96
15mm monolithic aerogel	0.66	0.75	0.91	0.87	0.96

As shown, the single glazed cover has the highest solar transmittance at 0.85, however, its U-value is also the highest at 5.7 W/m² K. Conversely, the 40 mm granular aerogel cover has the lowest solar transmittance at 0.46, but also the lowest U-value at 0.54 W/m² K. The monolithic aerogel cover retains good properties for both, with its high solar transmittance of 0.75 and low U-value of 0.66 W/m² K. Regarding U_L, F_R and F', it is evident that the cover's U-value has a large influence on the overall collector losses U_L. Similarly, the collector efficiency factor and heat removal factor, representing the ability of the collector to retain heat, are strong functions of the cover's U-value. Conversely, TST has a less significant impact on U_L, F_R and F'. It should be noted, however, that higher transmittance increases the mean plate and fluid temperatures, resulting in higher radiation and convection heat transfer coefficients, increasing the overall losses.

According to Hastings and Mørck (2000), efficiency curves for closed loop solar air collectors should be produced as a function of the outlet and ambient temperature in the form $(T_o-T_a)/S$. Based on this approach, Figure 6.12 displays the overall efficiency of each collector cover, when incorporated into the 6 x 0.9 metre solar air collector

designed for this study. Outlet temperatures and efficiencies are calculated for ambient temperatures ranging from -10 °C to +20 °C. Solar irradiance and wind speed are 500 W/m² and 5 m/s respectively. The inlet air temperature is taken as 23 °C with a mass flow rate of 0.043 kg/s (based on an extract airflow rate of 37 L/s for a house with one kitchen and three bathrooms).

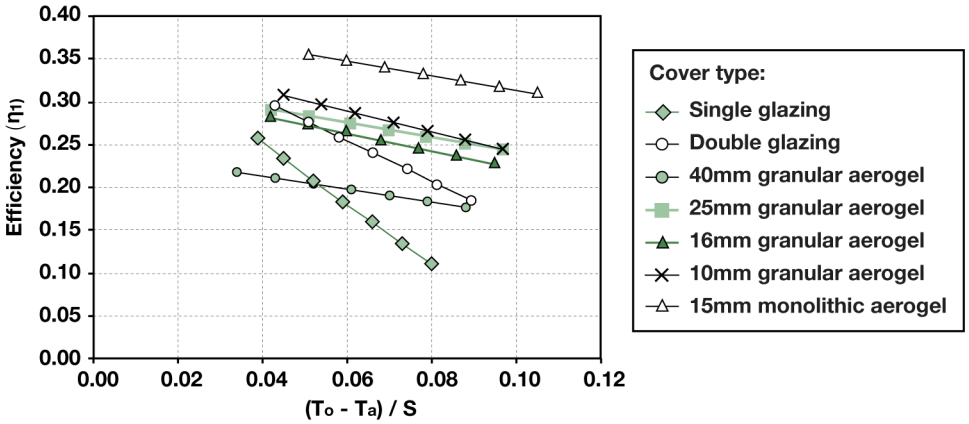

Figure 6.12 *Efficiency curves for different solar collector covers.*

According to the efficiency calculations, the solar collector containing monolithic aerogel operates at the highest efficiency, peaking at 36 % when ambient temperature is set to 20 °C. Alternatively, the 10 mm thick cover is the best performing granular aerogel system, with peak efficiencies of 31 %, followed by the 25 mm and 16 mm thickness covers at 29 %. The 40 mm cover performs less favourable with a peak efficiency of 22 %. Interestingly the single glazed cover provides a higher efficiency than this system, when ambient temperature is between 10-20 °C. However, when ambient temperature drops below this value, the 40 mm cover provides a higher efficiency due to its improved heat retention properties, evident from the shallower gradient as seen on all of the aerogel collectors. Similarly, the double glazed collector has a higher efficiency than the 16 mm and 25 mm granular aerogel covers at ambient temperatures above 20 °C, but below this temperature its efficiency is lower.

Figure 6.13 displays the predicted collector efficiencies at different mass flow rates. In each calculation, solar irradiance, wind speed and inlet temperatures are assumed to be 500 W/m², 5 m/s and 23 °C respectively. An ambient temperature of 7.5 °C was selected to represent the average external temperature during October 1st – May 31st, the months when approximately 90 % of the degree-days for London Thames Valley occur (Vesma, 2009), calculated using hourly weather data from the CIBSE TRY London weather file (CIBSE, 2008).

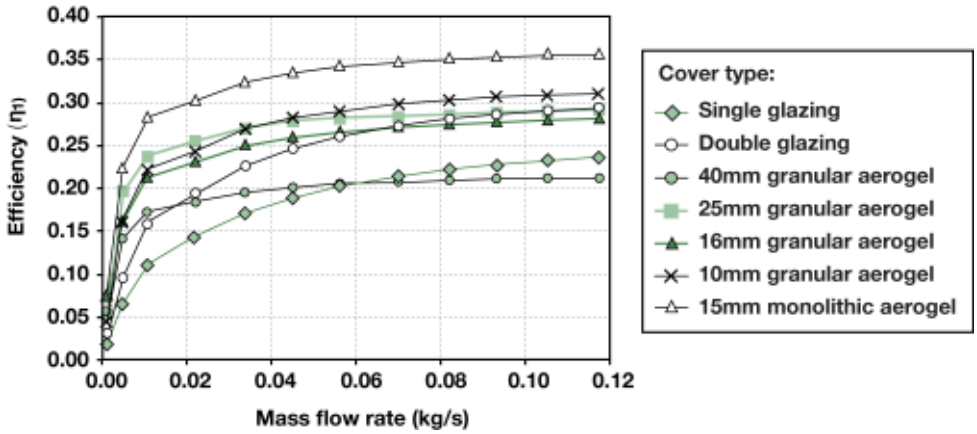

Figure 6.13 *Efficiency curves at different mass flow rates.*

As shown, higher efficiencies occur at higher mass flow rates due to the mean temperature of the collector being lower, resulting in less heat losses. Again, there are conditions when the single glazed collector outperforms the 40 mm granular aerogel system. In this instance, mass flow rates above 0.050 kg/s result in the single glazed collector operating at a higher efficiency. Similarly, the double glazed collector operates at a higher efficiency than the 16 mm granular aerogel system at mass flow rates above 0.065 kg/s. By comparison, the 10 mm cover provides a higher efficiency than both glazed collectors. The 15 mm monolithic aerogel covers possess significantly higher operating efficiencies across all flow rates investigated.

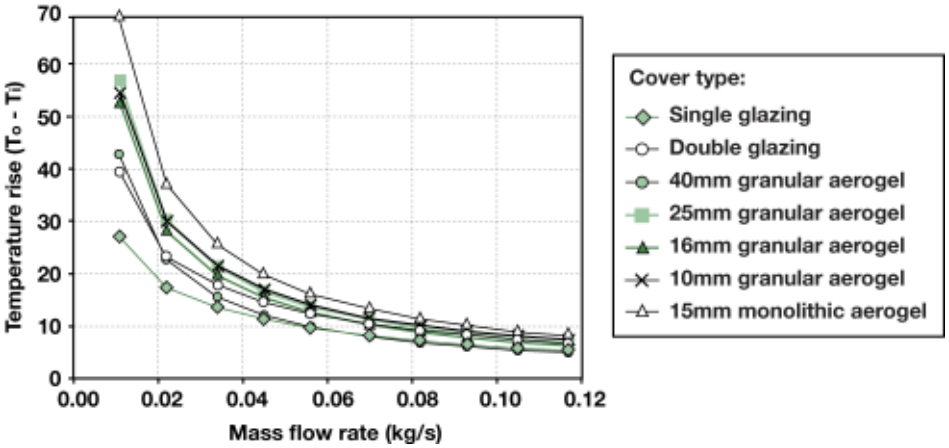

Figure 6.14 *Temperature rise across each collector surface.*

Figure 6.14 displays the predicted temperature rise across the collectors at different mass flow rates. As shown, an increasing mass flow rate reduces the outlet temperature of each collector. At the lowest mass flow rate modelled, temperature rises of 28-70 °C degrees are predicted across all collectors. Conversely, at a mass flow rate of 0.043 kg/s, as modelled in Figure 6.12, temperature rises of 12-20 °C degrees are predicted.

In each case, the monolithic aerogel cover provides the highest temperature rise, whereas the single glazed cover achieves the lowest, until mass flow rates are increased above 0.050 kg/s. Note that some temperatures such as those predicted for the 10 mm and 25 mm granular aerogel collectors appear to almost follow each other, despite their differing efficiencies, particularly at higher mass flow rates. However, upon close inspection, comparing the values with Figure 6.13 demonstrates a good correlation between both sets of results accounting for convergence at higher mass flow rates.

When analysing the efficiencies in Figure 6.12 and Figure 6.13, note that these values are strongly influenced by the tilt angle of the collector, the inlet air temperature as well as the open area of the absorber sheet, all of which are not optimised in this system. As such, if efficiencies are compared to typical solar air collectors, such as those found in Hastings and Mørck (2000), the values appear low. For example, a glazed collector with a plane black painted absorber, with flow on both sides can operate at efficiencies of 15-45 % at different mass flow rates (Hastings and Mørck, 2000), compared to 23 - 32 % for the 10 mm granular aerogel collector. Countering this, if ambient air is fed into the cavity and the plate absorption coefficient is increased to 0.9, the steady state model gives operational efficiencies from 40 – 60 % for the 10 mm granular aerogel collector across the range of mass flow rates. This indicates that granular aerogel can be used in high performance collector design, comparable to the results of Nordgaard and Beckman (1992) and Svendsen (1992), and hypotheses of Ortjohann (2001) and Reim *et al.* (2005).

6.5 In-Situ Performance

In-situ monitoring of the Aerogel Solar Collector took place in a controlled test under cool sunny conditions from 14th-20th October 2011 following commissioning of air flow rates in the dwelling. During monitoring, the building was largely unoccupied, except for periods during the 18th-20th October, when internal construction works took place, resulting in the MVHR fan 'boosting' whenever PIR sensors detected movement in the kitchen or bathrooms. No auxiliary heating was used. During testing, the blinds were closed in the living room to minimise passive solar gains.

When analysing in-situ results, note that commissioning of air flow rates revealed significant discrepancies between air flow and static pressure measurements upstream of the collector (measured by the inlet) and downstream of the collector (measured at plant room level). At 100 % fan speed ('boost' operation) the air flow downstream of the collector was 83 L/s (static pressure -104 Pa), whereas upstream of the collector the air

flow rate was 37 L/s (static pressure of -39 Pa). Similarly at 50 % fan speed ('normal' operation) the air flow downstream of the collector was 54 L/s (static pressure -48 Pa), whereas upstream of the collector the air flow rate was 28 L/s (static pressure -18 Pa). In addition, at 50 % fan speed an air flow rate of 34.5 L/s was measured upstream of the collector prior to the damper arrangement, indicating that 6.5 L/s was passing through the dampers rather than being directed up towards the solar collector inlet. These pressure drops and air flow reductions were later isolated and attributed to air infiltration through drainage holes running along the bottom edge of the aluminium frame, in addition to control damper blades not sealing perfectly. Nonetheless, despite these issues, promising results were observed during the monitoring phase, as follows.

6.5.1 Inlet and outlet temperature

Figure 6.15 displays the monitored inlet and outlet temperatures inside the solar collector compared to external temperature and solar irradiance.

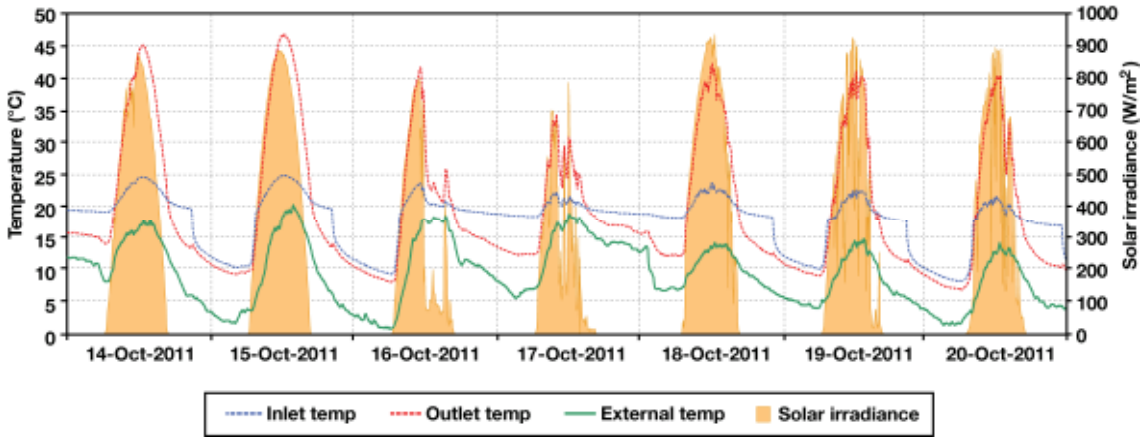

Figure 6.15 *Measured inlet and outlet temperature inside the collector cavity, compared to external temperature and solar radiation during the 7 day test period.*

During the 7 day test period the average external temperature was 9.7 °C, with a maximum of 20.5 °C occurring during the 15th October and minimum of 1.2 °C that night. Irradiance levels were high for the majority of the testing phase, with mostly sunny weather conditions. Minimal cloud coverage was observed on the 19th and 20th October, resulting in fluctuations in irradiance levels throughout the day and slightly lower daytime external temperatures. Meanwhile, relatively high cloud cover was observed between early afternoon on the 16th and early morning on 18th October. Significantly higher night time external temperatures of approximately 6-7 °C were observed during this period, when compared to average night-time temperatures of 2-3 °C during clear nights. A maximum irradiance of 940 W/m² occurred on the 18th

October at 12:40 hrs. Peak outlet temperatures ranged from 34.5 °C, measured at 10:00 hrs on 17th October (a day with relatively high cloud cover) to 46.8 °C, measured at 12:30 hrs on 15th October (a clear sunny day).

Other points of interest in Figure 6.15 is that the inlet temperature increases by up to 5 °C during the daytime, most probably due to heat gain inside the cavity. Alternatively, the sharp decreases in the inlet and outlet temperatures during the nights demonstrate that air leakages during no flow conditions have a significant impact on collector performance. Nonetheless, an average buffer of 7 °C is found between the collector and the outside air. During the nights of the 16-17th October, it is evident that the control dampers remained open, indicating that the temperature difference for the damper changeover relay could be reduced to improve the system efficiency.

6.5.2 Supply, extract and room temperatures

Figure 6.16 displays the temperature profile of the extracted air from the kitchen and bathrooms (fed into the collector) and supply air (fed to the living room and bedrooms following indirect heat exchange between the outside air and collector outlet).

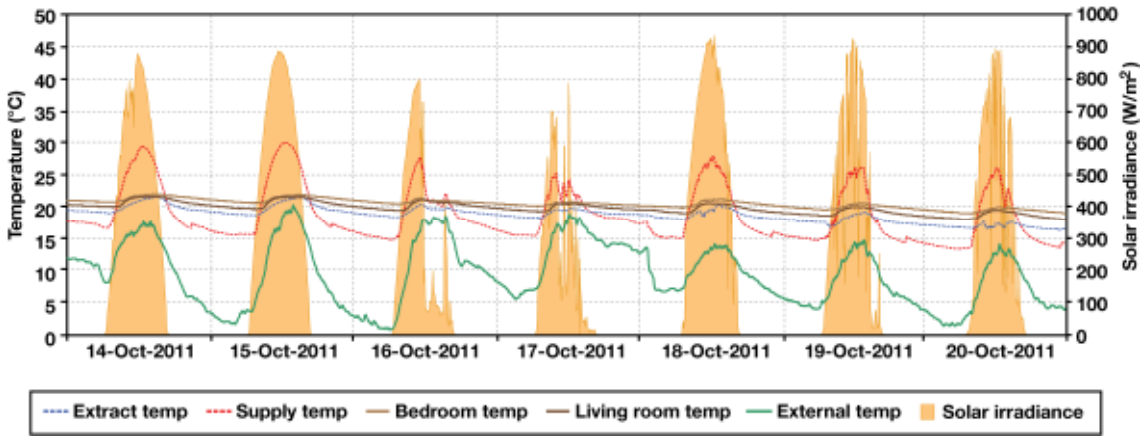

Figure 6.16 *Measured supply and extract temperatures, compared to the living room and north facing bedroom temperature (and external temperature and solar radiation).*

Peak supply temperatures measured inside the duct leaving the plant room of 25-30 °C were observed during the test period. At this time, peak internal temperatures of 21.5 °C and 21.9 °C were monitored in the living room and bedroom respectively, indicating that the collector is capable of raising the temperature of the dwelling to comfortable levels without overheating. Comparing the living room and a north facing bedrooms temperature to the extract temperature showed maximum temperature increases of 2.7-3.0 °C, respectively indicating a notable difference in the zones supplied by warm air.

When analysing Figure 6.16, monitored data demonstrates that the north facing bedroom is continuously warmer than the living room. During the night time, the living room is typically 1-2 °C cooler than the bedroom. As morning approaches, the living room temperature slowly increases to reach the bedroom temperature at around noon, then dropping again towards the late evening. This behaviour is understandable since the floor area of the bedroom is 8 m² making it easier to heat, compared to the living room at 21 m². In addition, as the living room contains large areas of glazing on the south and east facades, compared to the north facing bedroom with a single window, this is expected to contribute significantly to overnight heat losses. One discrepancy that is difficult to isolate is the 1 °C difference observed during the daytimes of the 18th-20th October, compared to the 14th-17th October. It is thought this discrepancy is caused by workers in the house those days walking in and out of the living room during testing without closing doors, resulting in cooler air from the un-heated spaces circulating in that space. By comparison, little activity was expected in the bedroom on those days.

6.5.3 Temperature profile through the collector

Figure 6.17 displays the temperature profile through the solar collector cavity, based on the eight temperature measurements taken behind the absorber sheet (at points marked earlier in Figure 6.1). Values are displayed for the 15th October, a clear sunny day, as well as the 18th October which was mostly clear, except for some scattered clouds in the evening.

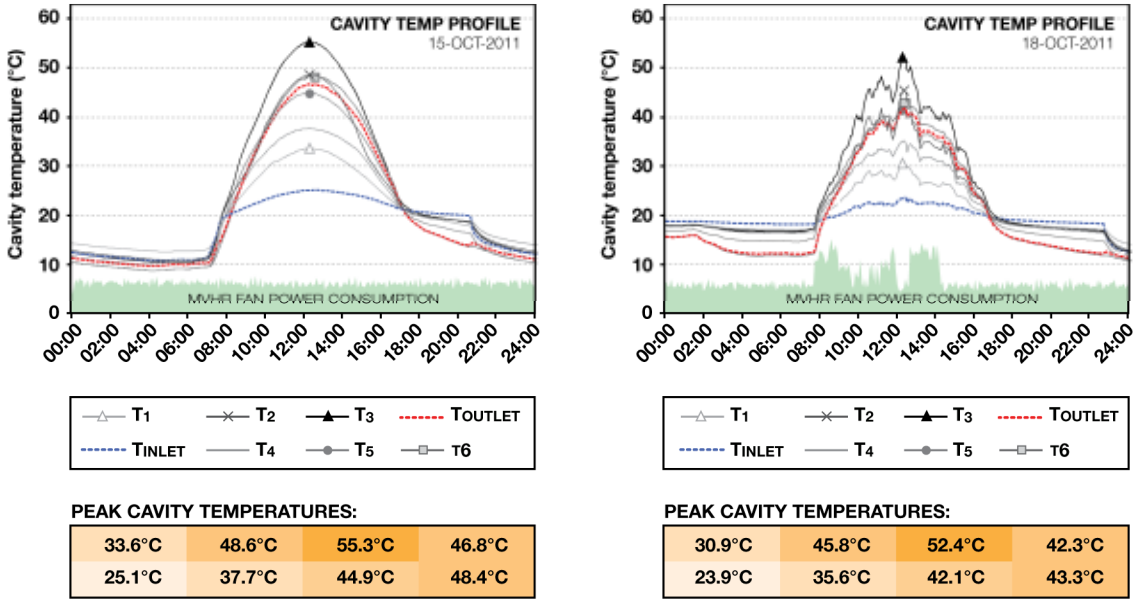

Figure 6.17 *Temperature profiles through the solar collector cavity. Left graph shows 15th October with the MVHR fan running in 'normal' operation. Right graph shows 18th October with the MVHR in 'boost' mode at various points in the day.*

As shown, there is a significant difference between the two sets of data. This is largely because the dwelling was occupied during the 18th October and occupancy sensors repeatedly activated the 'boost' on the MVHR, effectively doubling the mass flow rate through the solar collector at various points throughout the day.

An indication of when boosting occurred can be established by analysing the peaks in the MVHR power use (shown at the base of each graph). As shown, sustained periods of boosting during the 18th October occurred from 7:45-9:30 hrs, at 11:45-12:00 hrs and from 12:30-2:15 hrs. As a result, sharp temperature drops of up to 10 °C are observed. However, the collector quickly heats up again once 'normal' flow is resumed. By comparison, the temperature profile through the cavity on the 15th October follows a much smoother profile, with readings along the top edge being the higher than their lower counterparts. On both days, there is evidence of a 'hot spot' in the top central right zone of the cavity (T_3), up to 10 °C hotter than the outlet in peak conditions. A similar 'hot spot' was reported by the Danish Technical Institute in a study of connectable solar collectors. Here, Jensen and Bosanac (2002) claimed that the most likely cause was a less even distribution of air flow over that area.

6.6 Validation

In order to validate the steady state model and design parameters presented in the cover efficiency investigation, Figure 6.18 displays the predicted vs. measured outlet temperatures for the 15th and 18th October. In each case, outlet temperatures are calculated based on in-situ data for external temperature, irradiance and the inlet fluid temperature. Average mass flow rates of 0.048 kg/s and 0.073 kg/s are applied for the MVHR under 'normal' and 'boost' operation respectively (calculated based on average air flow rates of 41 L/s and 60 L/s in the commissioning report).

The impact of air infiltration and leakages has been accounted for by following a methodology to correct Q_U, proposed by Bernier and Plett (1988). According to Bernier and Plett (1988), for collectors under negative pressure, inward infiltration can be calculated using Equation [6.23].

$$Q_U = \dot{m}_{average} Cp(T_o - T_i) - (\dot{m}_o - \dot{m}_i) Cp(T_i - T_a) \quad [6.23]$$

Conversely, for collectors under positive pressure (or no flow conditions), outward leakages can be accounted for using Equation [6.24].

$$Q_U = \dot{m}_{average} Cp(T_o - T_i) - (\dot{m}_i - \dot{m}_o) Cp(T_L - T_a) \quad [6.24]$$

In each equation, $\dot{m}_o$ and $\dot{m}_i$ refer to the measured mass flow rates at the inlet and outlet of the collector, respectively. T_L is the average temperature of air lost to the environment, estimated using $(T_i+T_o)/2$, where T_o is based on an initial estimate, corrected using an iteration loop.

In order to validate the collector outlet temperatures, it was first necessary to determine a reduction factor for leakages/infiltration, since the drop in mass flow rate was not just caused though leaks inside the collector. It was also caused through air passing through the damper blades, thus not going through the collector. Based on commissioning (at 50 % fan speed), it was established that just 47.5 L/s (of the total 54 L/s) was extracted from the collector as 6.5 L/s was passing through the dampers. Of this 47.5 L/s, only 28 L/s was measured upstream of the collector inlet, indicating that 19.5 L/s could be attributed to infiltration. Consequently, the impact of infiltration accounted for in the validation process could be reduced by 25 %. Next, it was then necessary to identify the times at which air was flowing through the collector, compared to no-flow conditions. This was determined by assessing the temperature difference between the outlet temperature and the extract temperature from the house (based upon the control strategy outlined in Section 6.2.3).

Following these steps, for each line of 5 minute experimental data, Qu is calculated assuming either a predicted 'leakage in' or 'leakage out'. The outlet temperature is then determined for each time period.

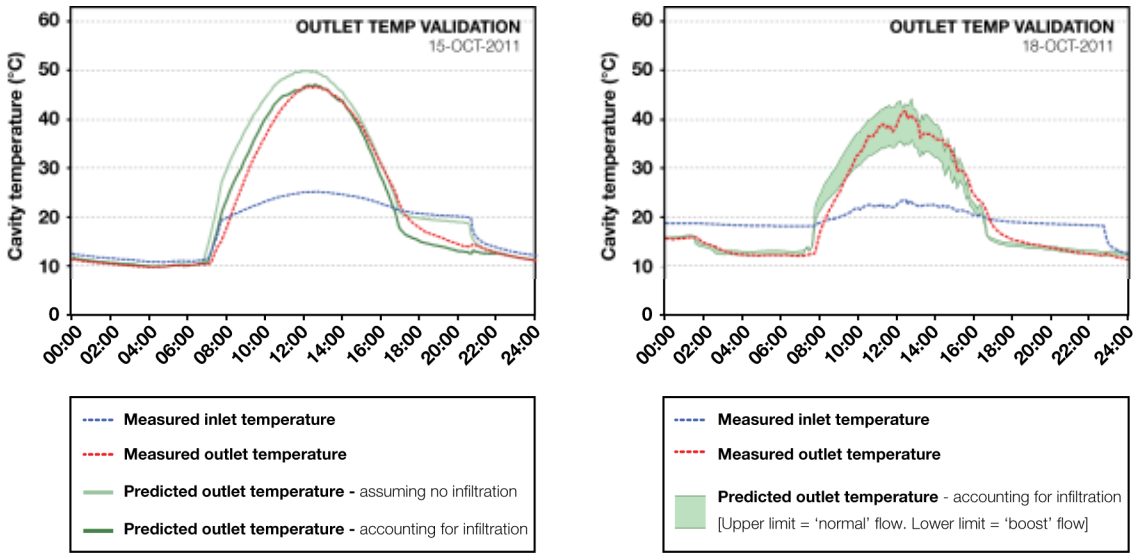

Figure 6.18 *Predicted vs. In-situ outlet temperatures. Left graph shows 15th October, where the predictions assume the collector is perfectly sealed and also taking leakage into account. Right graph shows 18th October where the outlet temperature is predicted at 'normal' and 'boost' flow rates.*

Predicted outlet temperatures for the 15th October are calculated assuming the collector is perfectly sealed and also accounting for infiltration. As shown in the lefthand graph in Figure 6.18, the peak outlet temperature is overestimated by approximately 4-5 °C if the collector is assumed to be perfectly sealed. Furthermore, during the evening/night, the predicted outlet temperature closely follows the inlet temperature profile, since losses are assumed to be minimal. By comparison, if leakages are accounted for, the peak outlet temperature closely matches the measured value and evening/night time losses correlate much better with the measured outlet temperature. A discrepancy inherent to both calculations due to their steady state nature is the temperature lag experienced during the morning as the collector begins to heat and during the evening as it cools. Nonetheless, if Q_U is calculated from the predicted outlet temperature taking losses into account, energy output is found to be within 5 % of the measured value.

For October 18th, the predicted outlet temperature (taking losses into account) is calculated with an upper and lower limit to account for the MVHR switching between 'normal' and 'boost' mode respectively. As shown, in the righthand graph in Figure 6.18, the measured outlet temperature is within the allowable limits of the two flow rates modelled. Again there is a discrepancy due to lag inside the collector, not accounted for in the steady state model. Nonetheless, with the air leakages accounted for, the predicted and measured outlet temperatures correlate reasonably well.

6.7 Discussion

This study has demonstrated that incorporating granular aerogel into flat plate solar air collectors can result in improved working efficiencies over conventional glazed systems. Due to the issues regarding fragility, manufacturing difficulties, availability and the perceived higher cost of monolithic aerogel, encapsulated granular aerogel can be viewed as the preferred cover material to develop novel solar technologies such as solar air heaters, solar water heaters, and solar Trombe walls.

6.7.1 Predicted annual energy savings

Although in-situ results were based on a collector with a 40 mm granular aerogel cover, the reasonable correlation between predicted and measured performance has gone some way towards verifying the design parameters calculated in the cover efficiency investigation. As a result, Figure 6.19 displays the predicted annual energy output for comparative solar air collectors with different cover types. Climate data is generated from annual hourly irradiance (on a south facing vertical surface) and external temperature data generated using the CIBSE TRY London weather file (CIBSE, 2008).

All calculations assume a constant inlet temperature of 23 °C and mass flow rate of 0.048 kg/s. In each case, collectors are assumed to be built completely air tight. To isolate the benefits of the collector from the standard MVHR operation, calculations only count the energy output if the collector outlet temperature is higher than the inlet temperature. Alternatively, the MVHRs summer bypass function is assumed to be operational, discounting the energy output if the external temperature exceeds 20 °C. All calculated outputs are reduced by 5 % to account for discrepancies observed in the steady state model.

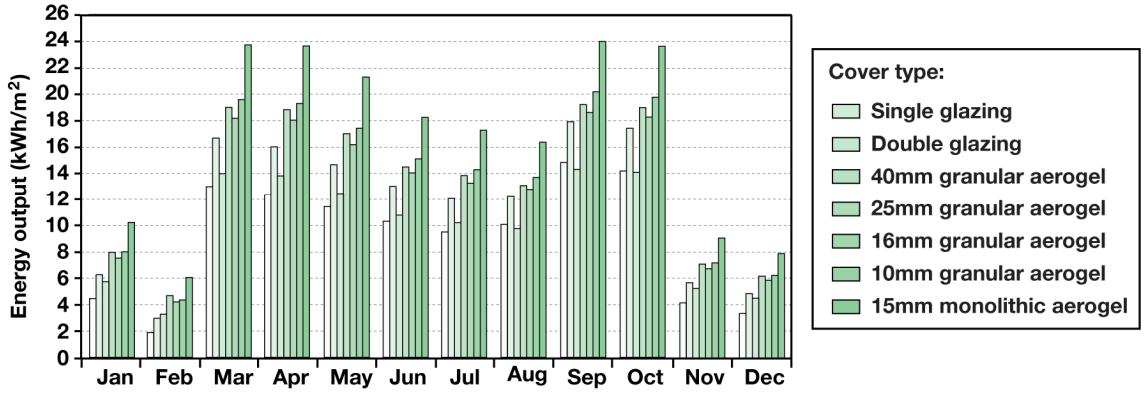

Figure 6.19 *Predicted annual energy output for solar collector types.*

Predicted annual energy outputs range from 110 kWh/m²/year for the single glazed collector to 202 kWh/m²/year for the monolithic aerogel cover. Energy outputs for the granular aerogel systems are 118 kWh/m²/year with the 40 mm cover, 161 kWh/m²/year with the 25 mm cover, 154 kWh/m²/year with the 16 mm cover and 166 kWh/m²/year with the 10 mm cover. The double glazed collector has a predicted energy output of 140 kWh/m²/year. For each case, the largest savings are estimated during the midseason, when heating is required and incident radiation levels are high. By comparison, benefits can be obtained even during the coldest months.

6.7.2 Payback calculations

Utilising these annual energy outputs, Figure 6.20 displays a predicted payback curve for each collector type. To avoid uncertainties regarding fabric performance, auxilary heating systems and occupancy usage, which must be dealt with on a case-by-case basis, payback calculations assume that the collector output is offsetting an automated electric heating coil in an MVHR system.

The baseline cost of electricity is assumed to be £ 0.12/kWh, with a 6 % annual fuel price inflation rate and 2 % discount interest rate applied. The capital costs for each cover type is based on sales costs obtained through personal communication with R.

Lowe from Xtralite Ltd on 1st November 2011. These costs were £ 190/m², £ 160/m², £ 143/m² and £ 100/m² for the 40, 25 16 and 10 mm thick polycarbonate panels filled with granular aerogel, respectively. The single and double glazed covers were estimated at £ 60/m² and £ 120/m², respectively. A speculative cost of £ 350/m² was given to the 15 mm monolithic aerogel cover (not available commercially). Based on this investigation an additional cost of £ 120/m² was applied to account for the timber and aluminium framing as well as the perforated absorber sheet.

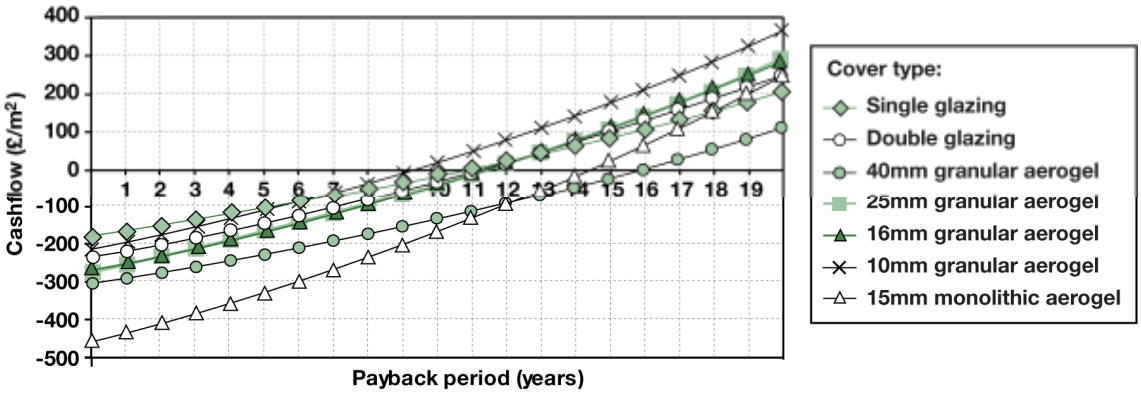

Figure 6.20 *Predicted payback periods for solar collector types.*

According to the payback calculations, all solar collectors provide a return on investment within 9-16 years. The fastest payback is obtained from the 10 mm granular aerogel system, followed by the 25 mm and 16 mm systems and both conventional glazed collectors with 11 year estimated payback periods. Interestingly, the 40 mm granular aerogel system and the monolithic aerogel collector have longer payback periods at 14 and 16 years, respectively. Evidently, if future systems are designed with granular aerogel it is unnecessary to utilise cover thicknesses above 25 mm unless the solar transmittance can be improved. Furthermore, if it becomes commercially available, the cost of a monolithic aerogel must be considerably less than estimated here for it to be cost effective.

The aforementioned payback calculations (per m² of collector) do not include the fixed cost of controls, which were £ 40 for the temperature differential electronic thermostat with thermistors, and £ 510 for the three dampers with spring return actuators. An additional cost of £ 120 incurred for the 'optional summer bypass' on the MVHR was not included. If all of these costs are taken into account then payback periods (for a 5.4 m² collector) increase from to 9-16 years to 14-21 years across all solar collector types. Alternatively, if it is assumed that just one damper with spring return actuator is used to control air flow and the MVHR summer bypass switch was specified independently of the solar collector (thus not included in the payback calculation), then payback

periods can be reduced to 10-17 years, which is more acceptable. Countering these costs, if it were assumed that solar air collectors were eligible to the £ 0.085/kWh generation tariff under the governments Renewable Heat Incentive (RHI, 2011), which domestic hot water solar thermal panels currently obtain, then paybacks can be reduced to 7-13 years. Evidently, even with the cost of controls included, it is possible to develop an economically viable technology.

If the collector had an 'optimised design' as described earlier, with a 10 mm thick cover, ambient air fed into the cavity and overall plate absorption of 0.9, then the predicted annual energy output for this system is 355 kWh/m²/year. Predicted payback periods for this optimised system are as low as 4.5 years.

6.8 Streamlined Life Cycle Assessment

Figure 6.21 displays the system boundary for a streamlined LCA conducted to investigate whether each solar collector can provide a measurable environment benefit over its life cycle. As shown, the study compares the energy and CO_2 burden associated with raw material acquisition and manufacture, to the respective operational savings from the solar air collector energy output. Factors excluded from the investigation include transport, on-site installation, maintenance and end-of-life processing. Additional omitted factors include the energy use of the MVHR fan (as this is running irrespective of the solar air collector) and the production impacts associated with ductwork and controls.

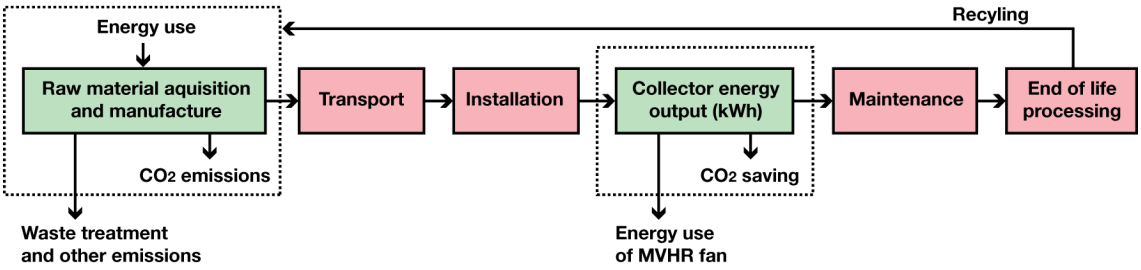

Figure 6.21 *System boundary for the streamlined LCA*

Table 6.3 displays the inventory developed for the production assessment. For each component the initial amount of material used (either by mass or volume) is estimated based on the technical drawings produced for the 6 x 0.9 meter collector. The total impact is then divided by 5.4 to generate m² impacts. All aluminium and timber framing is considered to be consistent for each of the different cover types analysed. The single and double glazed collectors assume that the polycarbonate and granular

aerogel covers are replaced by glass panes. The monolithic aerogel cover assumes the cover is replaced by a 15 mm aerogel layer, encapsulated between two glass panes. For each thickness of granular aerogel covers, the multiwall polycarbonate panels are assumed to be completely filled with aerogel, taking each channel to have a 1 mm wall thickness. Data for the mass of each polycarbonate panel, per m^2, is based on manufacturer data from C&A Supplies (2009).

Table 6.3 *LCA inventory. For all components the initial volume or mass is based on the amount of material used to construct a 6 x 0.9 meter collector. The total impact is divided by 5.4 to generate m^2 impacts.*

		Production energy			CO_2 burden		
Aerogel	**Volume (m^3)**	**MJ/m^3**	**MJ**	**MJ/m^2**	**$kgCO_2/m^3$**	**$kgCO_2$**	**$kgCO_2/m^2$**
Granular aerogel inside 10mm cover	0.0432	10230	441.9	81.8	651	28.1	5.2
Granular aerogel inside 16mm cover	0.0702	10230	718.1	133.0	651	45.7	8.5
Granular aerogel inside 25mm cover	0.1080	10230	1104.8	204.6	651	70.3	13.0
Granular aerogel inside 40mm cover	0.1782	10230	1823.0	337.6	651	116.0	21.5
15mm monolithic aerogel layer	0.0810	12523	1014.4	187.8	1950	158.0	29.3
Polycarbonate	**Mass (kg)**	**MJ/kg**	**MJ**	**MJ/m^2**	**$kgCO_2/kg$**	**$kgCO_2$**	**$kgCO_2/m^2$**
10mm thick 2-wall polycarbonate panel	9.2	112.9	1036.4	191.9	6	55.1	10.2
16mm thick 3-wall polycarbonate panel	14.6	112.9	1646.1	304.8	6	87.5	16.2
25mm thick 5-wall polycarbonate panel	17.8	112.9	2011.9	372.6	6	106.9	19.8
40mm thick 7-wall polycarbonate panel	22.7	112.9	2560.6	474.2	6	136.1	25.2
Glass							
Single glass cover	40.5	15	607.5	112.5	0.85	34.4	6.4
Double glass cover	81.0	15	1215.0	225.0	0.85	68.9	12.8
Aluminium (recycled)							
Cover framing	15.9	34.1	543.1	100.6	1.98	31.5	5.8
Absorber sheets	4.2	27.8	117.2	21.7	1.67	7.0	1.3
Drip trays	5.7	27.8	157.5	29.2	1.67	9.5	1.8
Mineral insulation							
Inside cavity	5.1	16.8	85.1	15.8	1.05	5.3	1.0
Collector perimeter	21.0	1.05	22.1	4.1	1.05	22.1	4.1
Timber							
Collector framing	170.4	7.4	1261.0	233.5	0.45	76.7	14.2

To support the earlier work in this thesis, the production energy (MJ/m^3) and CO_2 burden ($kgCO_2/m^3$) associated with granular and monolithic aerogel production are based on the experimental data generated from the streamlined life cycle assessment presented earlier in Chapter 4. Figures for high temperature supercritical drying (HTSCD) are used to represent granular aerogel production. Conversely, figures for low temperature supercritical drying (LTSCD) are used to represent monolithic aerogel production. In each case, the impacts taking industrial economies of scale are used (referred to as 'Rev-3' in the earlier study). Note that in reality, the granular aerogel is manufactured through Cabot Corporation's ambient pressure drying process, for which there is no industrial benchmark available. Consequently, by allocating HTSCD to

granular aerogel and LTSCD to monolithic aerogel, this assumes that the monolithic aerogel is the more intensive to produce.

For all other materials (glass, polycarbonate, aluminium, timber and mineral insulation), assumptions for the production energy (MJ/kg) and CO_2 burden ($kgCO_2/kg$) were obtained from Hammond and Jones (2008). Note that all aluminium components are assumed to be manufactured from recycled material. According to EEA (2011), more than 90 % of the aluminium used across the European building and construction sector is recycled. If virgin aluminium was used, this would have a significant impact on the interpretation of this study, since the production energy and CO_2 burden of each component would be 7.5 and 6.8 times more intensive respectively (Hammond and Jones, 2008).

Figure 6.22 displays the calculated production energy and CO_2 burden associated with manufacturing each solar collector type.

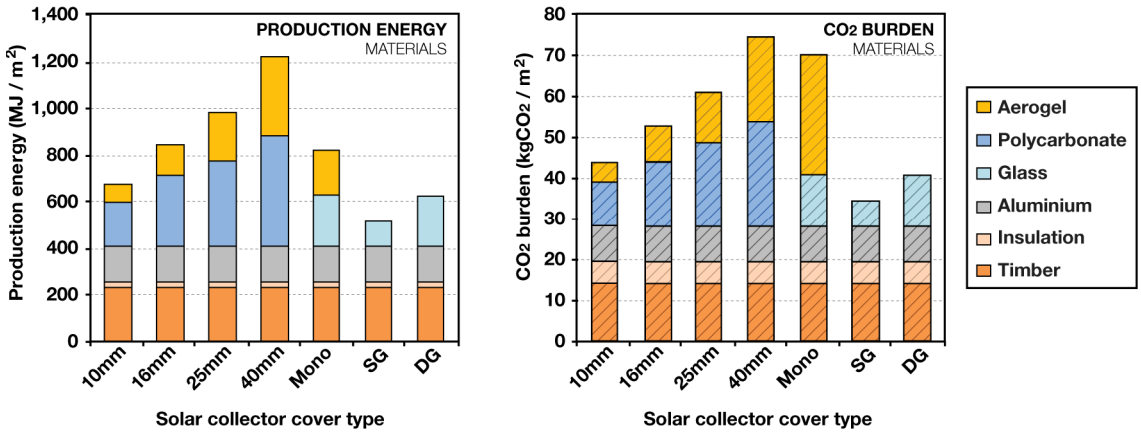

Figure 6.22 *Production impact associated with manufacturing each solar collector. Left graph compares production energy. Right graph compares CO_2 burden.*

As shown, the single glazed collector is found to have the smallest impact across all of the covers analysed. Conversely, the collector with the 40 mm thick cover polycarbonate cover filled with granular aerogel has the largest impact, closely followed by the monolithic aerogel cover in terms of CO_2 burden, or the 25 mm cover in terms of production energy. For each of the granular aerogel systems, it is the polycarbonate which is the most intensive material in the cover. Nevertheless, the aerogel is found to be a significant factor in the materials overall impacts, accounting for 12-28 % of the collectors total production energy and 12-29 % of the CO_2 burden across the range of granular aerogel covers. For the monolithic aerogel cover, the aerogel accounts for 23 % and 42 % of the total production energy and CO_2 burden respectively.

To put these values into perspective, Figure 6.23 compares the total production impacts for each collector to the energy output (in MJ) predicted over a 15 year period and the corresponding CO_2 saving (assuming an electrical grid intensity of 0.517 $kgCO_2/kWh$).

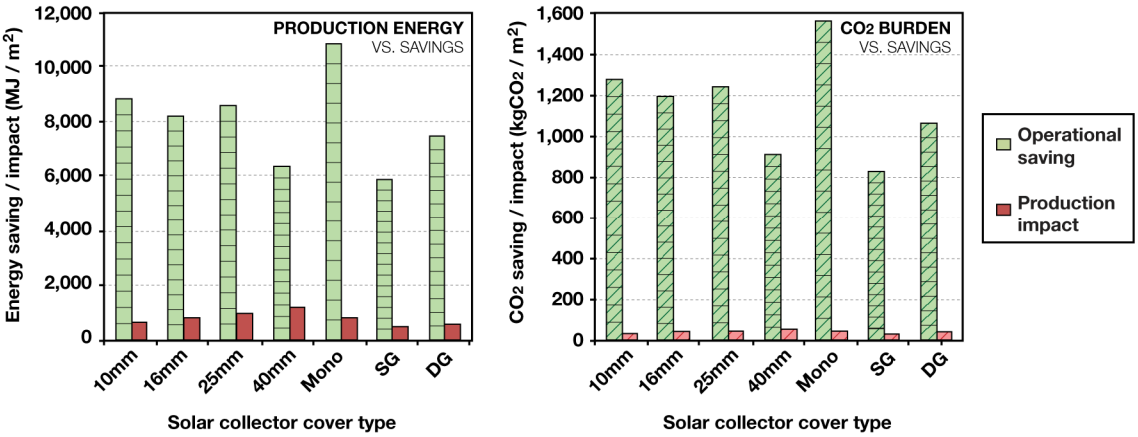

Figure 6.23 *Production costs of each collector vs. in-use savings over product lifespan. Left graph compares production energy. Right graph compares CO_2 burden.*

As shown, for each collector, the predicted savings outweigh the production impacts several times over during the life span. The shortest payback in terms of production energy comes from the 10 mm granular aerogel collector and monolithic silica aerogel collector at 1.1 years, followed by the single and double glazed collectors at 1.3 years, then the 16, 25 and 40 mm granular aerogel covers 1.5, 1.7 and 2.9 years respectively. By comparison, the shortest payback in terms of the CO_2 burden is the 10 mm granular aerogel collector and monolithic silica aerogel collector at 0.45 years, followed by the 16 mm, double glazed, 25 mm and single glazed collectors at 0.56-0.61 years respectively, and the 40 mm granular aerogel collector at 0.87 years.

6.9 Conclusion

This study has demonstrated that a solar air collector containing a translucent granular aerogel cover can function well in a domestic solar heating application and payback its environmental impact in a short operational timescale. During the validated test period, despite air leakages / infiltration, the prototype successfully raised the temperature of the extract air in a mechanically ventilated dwelling up to 45 °C, providing additional energy to preheat the supply air up to 30 °C. Resultant internal temperatures of 21-22 °C indicate that the prototype will play an important role in maintaining comfortable living conditions throughout the heating season.

Long term evaluation of the Aerogel Solar Collector is currently being conducted as part of a two year monitoring scheme. The property has been occupied by a 7 person family, since 12th June 2012. Preliminary monitoring data captured for the Aerogel Solar Collector from 1st November 2011 – 31st October 2012 can be found in the Appendices.

During the monitoring period, a stagnation point of 58.8 °C was observed during February 2nd when the MVHR was switched off during a sunny afternoon. However, once operational, an outlet temperature of 43.9 °C was measured for this month at 1 pm on February 25th. At this time, MVHR supply and living room temperatures were 28.9 °C and 23.5 °C, respectively, whilst outside air temperature was 13.8 °C. Through May-September, there was some evidence of overheating with peak living room and bedroom temperatures exceeding 26 °C, whilst outside air temperatures are above 30 °C. The minimum internal temperature was 10.3 °C at night on February 11th when the dwelling was unoccupied and external temperature was below zero. The average internal temperature over the entire dataset was 20.9 °C for the living room and bedroom. Little/no auxiliary energy for heating is expected.

Take note that the majority of leakage inside the solar collector was addressed by Axis in early February 2012. Figure 6.24 shows a thermal image of the system taken during an early morning in March 2012. As shown, the insulation provided by the 40 mm thick aerogel cover (and the 50 mm foil backed mineral insulation supplied by Rockwool Ltd inside the cavity), achieves a similar standard to the 300 mm external cladding. There is still evidence of minor frame heat loss by the inlet and the top edge of the outlet, but this is not proving to be detrimental in the preliminary long term monitoring.

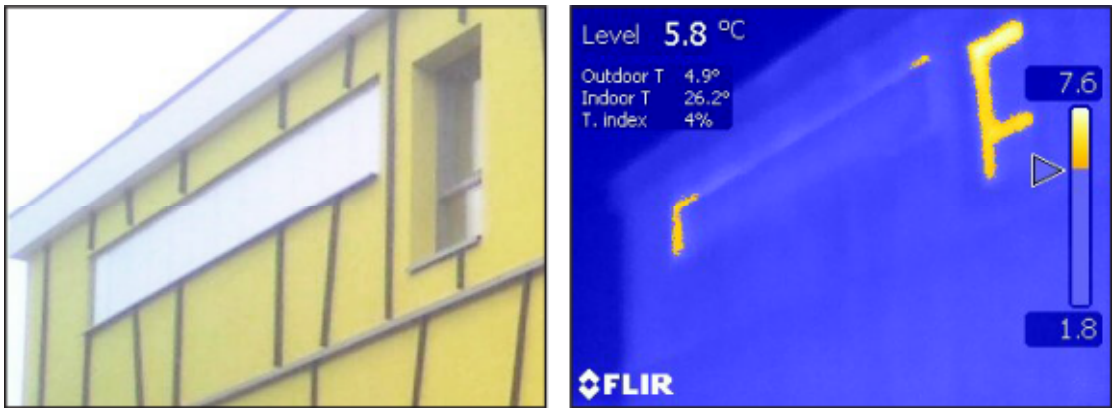

Figure 6.24 *Thermal image showing Aerogel Solar Collector on south elevation.*

On-going monitoring will seek to quantify the contributions provided by the solar collector against the property's total gas and electricity consumption, whilst being

benchmarked against other renewable technologies. The overall aim of the refurbishment is to reduce the property's baseline CO_2 emissions by 80 %.

At the start of this project, the team were keen to use this house as a novel test-rig for new technologies. Consequently, one factor that is yet to be established is the long term durability of this prototype compared to conventional glazed solar collectors. Under normal usage as a facade component for day lighting, the aerogel filled polycarbonate panels and aluminium support systems would possess a 15 year warranty against yellowing, light transmission and thermal degradation (Cabot and Roda, 2010). Alone, the aerogel granules are not expected to degrade during the foreseeable life of the solar collector. In addition, since silica is inert, the aerogel can last the life of a structure and be recycled when the building is decommissioned (Cabot and Roda, 2010).

Key areas where degradation may occur include the seals, connections and fixtures supporting the cover system and framing, due to expansion and contraction of components during summertime, general wear from wind and rain exposure, and moisture build-up inside the cavity. A further issue is the integrity of the MVHR, bypass controls and dampers in the plant room. It is imperative that this product be systematically evaluated over its operational lifespan. If developed into a market ready solution, a minimum lifespan of 15 years would be required to justify the life cycle costs.

Take note that the prototype reported in this study was incorporated into the 'extract' side of the mechanical ventilation system due the design team not wanting to pass the dwelling's fresh air supply through a prototype which had not been tested before. Consequently, there are opportunities to improve the overall efficiency of this system by passing ambient air into the cavity and by connecting it directly to the supply air side. Furthermore, the plate absorption coefficient could feasibly be increased to 0.9. Applying these changes to the steady state model gives operational efficiencies of up to 60 % for a 10 mm granular aerogel collector, comparable to the results of Nordgaard and Beckman (1992) and Svendsen (1992), and hypotheses of Ortjohann (2001) and Reim *et al.* (2005). The predicted annual energy output for this system is 355 kWh/m^2/year with a payback as low as 4.5 years.

Further efficiency improvements could be achieved through incorporating thermal storage into the cavity or by connecting the collector outlet to an air-water heat exchanger during the summertime to avoid wasting heat. There is a need to refurbish our existing building stock to achieve energy efficiency standards, going beyond the limitations of conventional measures. Findings from this study aim to contribute towards this challenge.

Chapter 7

PRELIMINARY THERMAL MODELLING OF PASSIVE TROMBE WALLS INCORPORATING AEROGEL

Abstract

This chapter contains two thermal modelling studies investigating the performance of granular aerogel applied to passive solar Trombe walls. In the first study, the predicted energy savings and financial payback period of an 8 m^2 Trombe wall incorporating a 10 mm thick granular aerogel cover is compared against the performance of a single glazed Trombe wall in a new detached house with high thermal mass. Results demonstrate that the Aerogel Trombe wall is capable of reducing the building's annual heat load by 26 % with a minimum payback period of 7.5 years, compared to an energy saving of 18 % and a 9 year payback for the glazed system. In the second study, a parametric thermal modelling assessment is conducted considering four different areas of Aerogel Trombe wall, retrofitted to four different house types built to six notional construction standards. Calculated energy savings range from 183 kWh/m^2/year for an 8 m^2 system retrofitted to a solid walled detached house, to 62 kWh/m^2/year for a 32 m^2 system retrofitted to a super insulated flat. Predicted energy savings from Trombe walls up to 24 m^2 are found to exceed the energy savings from external insulation across all house types and constructions. Small areas of Trombe wall can provide a useful energy contribution without creating a significant overheating risk. If larger areas are to be installed, then detailed calculations would be recommended to assess and mitigate potential overheating issues.

Nomenclature

A_r	Trombe wall area (m^2)
C_b	Thermal storage capacity of building (MJ/K)
C_p	Specific heat capacity of wall (KJ/kg K)
DD	Degree day hours (h K)
f	Solar fraction
f_i	Fraction of monthly load supply by solar energy
I_{TC}	Hourly critical irradiance level (W/m^2)
k	Thermal conductivity of wall (W/m K)
K_T	Monthly average daily clearness index
L_A	Auxiliary energy requirement for the month (GJ)
L_{ad}	Monthly building heat load without the Trombe wall (GJ)
L_w	Monthly heat loss with zero glazing transmittance (GJ)
N	Number of days in a month
R_n	Ratio of irradiance on a tilted surface to horizontal surface at noon
$\overline{R}$	Ratio of monthly average daily irradiance on tilted to horizontal surface
r_{tn}	Ratio of irradiance at solar noon to daily irradiance on a horizontal surface
$\overline{S}$	Monthly average absorbed solar irradiance (MJ/m^2)
S_b	Thermal storage capacity of building for a month (GJ)
S_w	Thermal storage capacity of Trombe wall for a month (GJ)
$\overline{T}_a$	Monthly average ambient temperature (°C)
T_b	Baseline temperature for degree-days (°C)
ΔT_b	Allowable temperature swing between low and high thermostat settings (°C)
$\overline{T}_i$	Monthly average inner wall temperature (°C)
T_r	Room temperature at low thermostat setting (°C)
$\overline{T}_w$	Monthly average outer wall temperature (°C)
ΔT_w	Half temperature difference between inside and outside wall (°C)
Δt	Inner and outer wall temperature difference (°C); seconds in 24 hours
Q_D	Energy dump in zero capacitance system (GJ)
Q_i	Heat gain across Trombe wall (GJ)
Q_u	Useful energy from Trombe wall (GJ)
Q_n	Net heat transfer into rooms through Trombe wall (GJ)
$(UA)_{ad}$	Building heat loss coefficient (W/K)
U_i	Loss coefficient between inner wall and air inside room (W/m^2 K)
U_k	Conductance from outer wall to room (W/m^2 K)
U_w	Trombe wall heat loss coefficient (W/m^2 K)
x	Wall thickness (m)
X_c	Critical irradiance ratio
Y	Storage dump ratio

Greek Symbols

ρ	Density of the wall (kg/m^3)
$\bar{\phi}$	Monthly average daily un-utilizability
$(\tau\alpha)$	Transmittance-absorptance product

7.1 Introduction

This chapter contains the results of two preliminary thermal modelling studies investigating the predicted thermal performance of passive Trombe walls incorporating translucent granular aerogel. Trombe walls are a type of solar heated collector storage wall, consisting of a south-facing element (typically glass), an internal concrete wall and a cavity, heated up by incoming solar irradiance. This captured heat can either be used straight away by venting the warm air inside, or later, by letting it permeate and warm up the concrete wall so that occupants can benefit from it in the evening.

In the first study, the thermal performance of an 8 m^2 Trombe wall incorporating a 10 mm thick polycarbonate cover filled granular aerogel is predicted. A comparable system was recently incorporated into a new detached pilot-house in East Hampshire, UK, being developed as the part of the upcoming "Whitehill Bordon Eco-town". The decision to develop this 'Aerogel Trombe Wall' arose through consultation between Buro Happold Ltd and East Hampshire Council, during a preliminary feasibility meeting on 31/03/2010. The design and construction phases of this project have since been handled by Riches Hawley Mikhail (RHM) Architects and Robinson Associate Engineers. With permission from the client and the design team, the performance of this prototype has been modelled for this EngD. However, no monitoring data is available yet to validate the results.

The calculation methodology for this investigation feeds into a second study, containing a parametric assessment of different Aerogel Trombe wall areas, retrofitted to a range of house types built to varying construction standards. This work builds on modelling by Dolley *et al.* (1994) who predicted the performance of different areas of Trombe walls incorporating honeycomb translucent insulation, retrofitted to a detached house if built with solid brick walls, un-filled cavity walls, to the 1976 and 1990 Building Regulations, as well as 'super-insulation' standards. Going beyond the approach by Dolley *et al.* (1994), new elements include predictions for semi-detached houses, flats and terrace houses, theoretical payback calculations for each system, and a comparison of the energy savings compared to conventional insulation.

7.2 Calculation Methodology

According to Duffie and Beckman (2006, p750), the thermal performance of passive Trombe walls can be calculated using the 'Un-Utilizability Design Method' developed by Monsen *et al.* (1982). The methodology assumes that the fraction of solar energy collected by a Trombe wall converted into useful heat, i.e. the utilizability, is based upon the actual thermal storage capacity of a building and its Trombe wall, to the ratio of energy that would be dumped in a zero capacitance building that can store no energy. Calculations are done monthly, with a key result being the annual amount of auxiliary energy needed to heat the passively designed building. Building loads are calculated using a simple degree-day method, using the baseline heat loss coefficient of the building calculated by the designer (Duffie and Beckman, 2006).

The methodology assumes that the Trombe wall is unventilated and that heat transfer through the wall is linear. This creates a simple resistance network (shown in the left diagram of Figure 7.1) to enable straightforward calculation of the net heat transfer through the wall into the indoor spaces. Monsen *et al.* (1982) claim that these assumptions are valid for all reasonable system designs, i.e. the energy storage of the wall is less than the heating load of a single winter's day. According to Monsen *et al.* (1982), the methodology allows users to parametrically assess a large range of design options, such as cover types, solar absorptance properties, different baseline building heat losses as well as high and low temperature set-points.

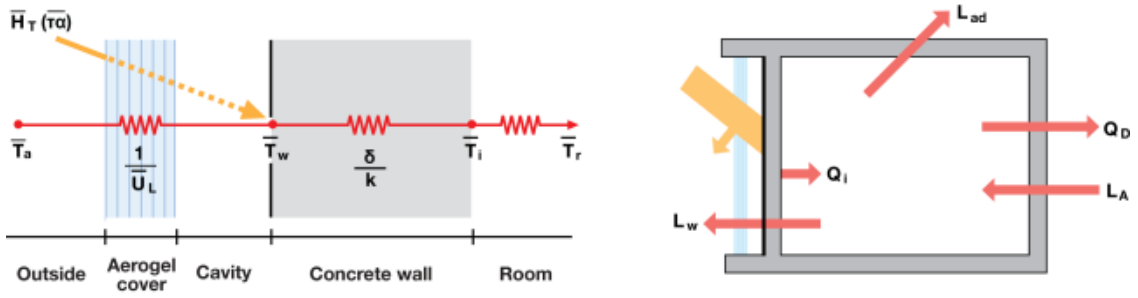

Figure 7.1 *Monthly average resistance network (Right) and energy flows (Left) for the Aerogel Trombe wall (Adapted from Monsen et al. 1982 and Duffie and Beckman 2006).*

The methodology used in this study is based on the formulas developed by Monsen *et al.* (1982), more recently published by Duffie and Beckman (2006). These formula are presented over the next 5 pages. Note that in several instances the methodology refers to additional formula to manually calculate figures for monthly-average solar irradiance such as ratios of beam and diffuse irradiance as well as estimated cloud-cover dependant on the site latitude/longitude. These solar irradiance formula are

omitted from this methodology, since the values can also be derived from online climate data, such as NASA's "Surface Meteorology and Solar Energy Data Set", integrated into software such as RETScreen International.

Load calculations

The right diagram of Figure 7.1 shows the main monthly energy flows considered in the Un-Utilizability Design Method. L_A, is the monthly requirement for auxiliary energy for a building with a Trombe wall. L_w is the monthly heat loss through the Trombe wall assuming no solar irradiance is absorbed. L_{ad} is the monthly heat load that occurs with no heat transfer through the Trombe wall. Q_i is the net heat gain through the Trombe wall. Q_D is the energy dump that would occur in a zero capacitance system. Loads L_{ad} and L_w can be determined from Equations [7.1] and [7.2] respectively:

$$L_{ad} = (UA)_{ad}(DD) \qquad [7.1]$$

$$L_w = U_w A_r (DD) \qquad [7.2]$$

Here, $(UA)_{ad}$ is the building heat loss coefficient. DD is total monthly degree day hours. A_r and U_w correspond to the area and heat loss coefficient of the Trombe wall. U_w is calculated from Equation [7.3]:

$$U_w = \frac{1}{\frac{1}{\overline{U}_L} + \frac{1}{U_i} + \frac{x}{k}} \qquad [7.3]$$

Here, $\overline{U}_L$ is the average heat loss coefficient from the outer wall surface through the Trombe wall cover to the ambient air. According to Duffie and Beckman (2006) it can be conceptually derived in the same way as the front heat loss coefficient for flat plate solar collectors (see Equation 6.10). U_i is the heat transfer coefficient between the inner wall surface and the air in the adjacent room to the Trombe wall. x and k correspond to the thickness and conductivity of the wall.

Net heat transfer through Trombe wall

Q_n, the net heat transfer into rooms through the Trombe wall, can be calculated using Equation [7.4]:

$$Q_n = U_k A_r (\overline{T}_w - T_r) \Delta t N \qquad [7.4]$$

Here, U_k is the conductance from the outer surface of the wall to the room, calculated from Equation [7.5]. $\overline{T}_w$ is the monthly average outer wall temperature, calculated from

Equation [7.6], where $\overline{T}_a$ is the monthly mean ambient temperature. T_r is the room temperature at its low thermostat setting. N represents the number of days in the month. Δt is the temperature difference between the outer and inner wall surface, where $\overline{T}_i$, the inner wall surface temperature, is calculated from Equation [7.7] which assumes linear heat transfer. $\overline{S}$ refers to the monthly average absorbed solar irradiance (see Duffie and Beckman 2006, p 239).

$$U_k = \frac{U_i k}{k + U_i \delta} \qquad [7.5]$$

$$\overline{T}_w = \frac{\overline{S} + \left(U_k T_r + \overline{U}_L \overline{T}_a\right)\Delta t}{\left(U_k + \overline{U}_L\right)\Delta t} \qquad [7.6]$$

$$\overline{T}_i = T_r - \frac{U_L}{U_i}\left(T_r - \overline{T}_w\right) \qquad [7.7]$$

Energy dump

The excess heat that enters a building through its Trombe wall, but does not contribute towards reducing the auxiliary energy load, is referred to as 'dumped energy'. This is concept is visualised in Figure 7.2, which shows a theoretical operational sequence for a Trombe wall in a zero capacitance building where all solar gain that exceeds the instantaneous auxiliary energy load is dumped. As shown, any incident irradiance below the critical radiation level is useful and any energy above must be dumped.

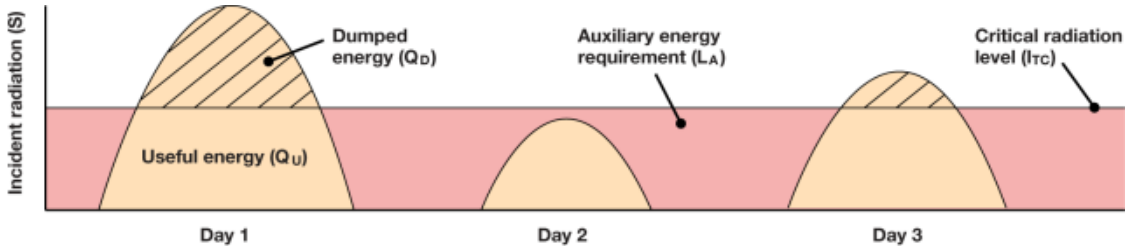

Figure 7.2 *Dumped, useful and auxiliary energy for a zero capacitance Trombe wall (Adapted from Duffie and Beckman 2006, p745).*

The monthly energy dump that would occur in a zero capacitance system can be calculated from Equation [7.8]:

$$Q_D = \frac{U_k A_r \overline{S}\ N\overline{\Phi}}{U_L + \overline{U}_k} \qquad [7.8]$$

Here, $\bar{\phi}$ refers to the monthly average daily utilizability, which can be calculated from Equation [7.9]:

$$\bar{\Phi} = \exp\left\{\left[a + b\left(\frac{R_n}{\bar{R}}\right)\right]\left[\bar{X}_c + c\bar{X}_c^2\right]\right\} \quad [7.9]$$

Where:

$$a = 2.943 - 9.271\bar{K}_T + 4.031\bar{K}_T^2$$

$$b = -4.345 + 8.853\bar{K}_T - 3.602\bar{K}_T^2$$

$$c = -0.170 - 0.306\bar{K}_T + 2.9361\bar{K}_T^2$$

$\bar{K}_T$ refers to the average daily clearness index on the Trombe wall surface; $\bar{R}$ is the ratio of the monthly average daily total irradiance on a tilted surface to that on a horizontal surface; R_n is the ratio of irradiance on a tilted surface to that of a horizontal surface at solar noon (see Duffie and Beckman 2006, p77, p109 and p136 respectively for these solar irradiance formulae). $\bar{X}_c$ refers to the monthly average critical irradiance ratio, which can be calculated from Equation [7.10]:

$$\bar{X}_c = \frac{I_{TC}}{r_{t,n}R_n\bar{H}} \quad [7.10]$$

Here, $\bar{H}$ is the monthly average daily total solar irradiance on a horizontal surface, which can be obtained from meteorological data such as those found in Duffie and Beckman (2006), p843-881. $r_{t,n}$ is the ratio of irradiance at solar noon to daily total irradiance on a horizontal surface (see Duffie and Beckman 2006, p89). I_{TC} refers to the hourly critical irradiance level, which makes the energy dump zero. This is calculated using Equation [7.11]:

$$I_{TC} = \frac{1}{(\overline{\tau\alpha})A_r}\left[(UA)_{ad}\left(\frac{U_L}{U_k} + 1\right)\frac{T_b - \bar{T}_a}{T_r - \bar{T}_a} + U_L A_r\right](T_r - \bar{T}_a) \quad [7.11]$$

Here, T_b is the baseline temperature for which degree days were calculated. $(\overline{\tau\alpha})$ is the monthly average transmittance-absorptance product, which can be calculated from Equation [7.12], where $\bar{H}_T$ is the monthly average daily total solar irradiance on a tilted plane (see Duffie and Beckman 2006, p109).

$$\overline{(\tau\alpha)} = \frac{\overline{S}}{\overline{H_T}} = \frac{\overline{S}}{\overline{H}.\overline{R}} \qquad [7.12]$$

Storage-dump ratio

The storage dump ratio, Y, is the ratio between the theoretical energy dump in a zero capacitance building to the actual storage capacity of the building, S_b, and the Trombe wall, S_w. It is calculated using Equation [7.13]:

$$Y = \frac{S_b + 0.047(S_w)}{Q_D} \qquad [7.13]$$

The storage capacity of the wall is slightly weighted compared to the building, indicating that heat stored in the building is more effective than heat stored in the Trombe wall. This is because thermal storage in the building or wall raises the temperature of components, leading to increased heat losses; the thermal resistance of the building will generally be greater than that of the wall; and also because the temperature difference between the building and ambient air is ordinarily smaller than the temperature difference between the Trombe wall and ambient air (Monsen *et al*, 1982). To calculate S_b and S_w, Equation [7.14] and [7.15] can be used respectively:

$$S_b = C_b(\Delta T_b)N \qquad [7.14]$$

$$S_w = \frac{\rho C_p \delta^2}{2k\Delta t} Q_i \qquad [7.15]$$

Here, C_b and C_p correspond to the effective thermal storage capacity of the building and specific heat capacity of the wall. ΔT_b is the allowable temperature swing between the building's low and high thermostat settings. ρ is the density of the wall. Δt refers to the number of seconds in 24 hours (86400 seconds). Q_i is the heat gain across the Trombe wall, calculated from Equation [7.16]:

$$Q_i = \frac{2kA_r}{\delta}(\Delta T_w)\Delta tN \qquad [7.16]$$

In the above equation, again Δt refers to the number of seconds in 24 hours. ΔT_w is half of the temperature difference between the inside and outside wall surfaces.

Solar fraction

The solar fraction, i.e. the proportion of the buildings energy load, which is met by the net energy gain from the Trombe wall, can be calculated from Equation [7.17]:

$$f = \min\{P f_i + 0.88(1-P)[1-\exp(-1.26 f_i)], 1\} \quad [7.17]$$

Where:

$$P = [1-\exp(-0.144Y)]^{0.53}$$

Here, f_i is the fraction of the monthly load supply by solar energy, which can be calculated from Equation [7.18]:

$$f_i = \frac{L_w + Q_i}{L_{ad} + L_w} \quad [7.18]$$

Auxiliary energy requirement

The final step is to calculate the buildings auxiliary energy requirement for the month, L_A. This is calculated from Equation [7.19]:

$$L_A = (L_{ad} + L_w)(1-f) \quad [7.19]$$

Once L_A is known, the energy savings, i.e. the useful energy from the Trombe wall, can be determined by subtracting the auxiliary energy requirement from the building heat load without the Trombe wall, as shown in Equation [7.20]:

$$Q_u = L_{ad} - L_A \quad [7.20]$$

7.3 Trombe Wall Case Study

In the following study, the predicted auxiliary energy requirement of a dwelling containing an 8 m² Trombe wall incorporating a 10 mm thick granular aerogel cover is assessed. Results are compared against the predicted annual heating load with a conventional single glazed Trombe wall.

7.3.1 Baseline model

The property used for this analysis is a highly insulated three bedroom detached house, located in Whitehill Borden, East Hampshire. It possesses high levels of glazing on the south façade and thermally massive walls. The proposed location for the Trombe wall is on the South elevation, stretching over the ground and first floor.

Figure 7.3, displays a thermal model of the dwelling, constructed using IES Virtual Environment software. Note that the Trombe wall has been included in this figure as a

visual aid only and its properties were not included in the baseline thermal modelling assessment. Furthermore, all geometry and construction materials for the Trombe wall and dwelling are based on the RHM architect's and Robinson Associate engineer's *preliminary* drawings and design specification provided to the research engineer on 20/04/2011. These have been updated since this modelling study took place.

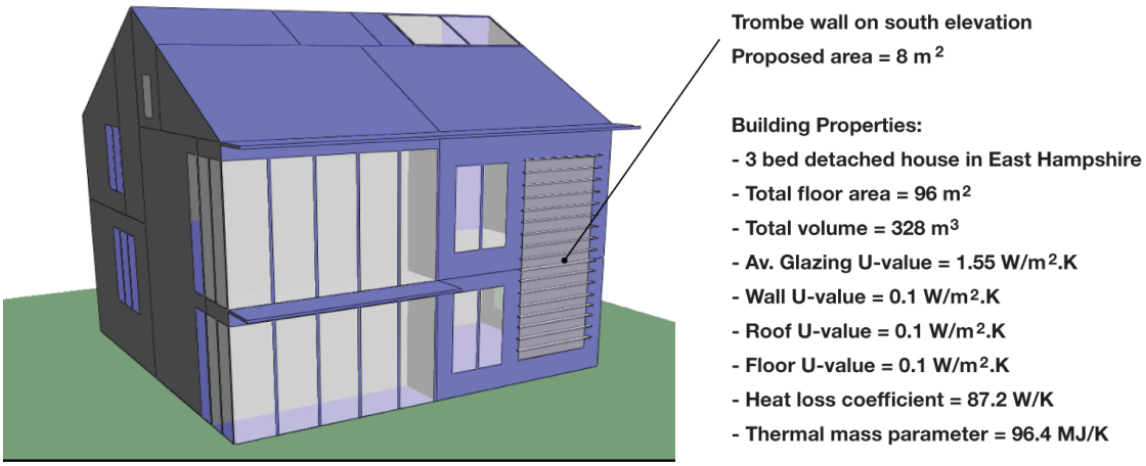

Figure 7.3 *Thermal model of house and Trombe wall.*

Construction parameters representing the dwelling's effective thermal capacitance and heat loss parameter were obtained through a SAP assessment of the thermal model. Assuming 400 mm dense concrete (2015 kg/m^3) combined with insulation to achieve U-values of 0.1 W/m^2 K for the walls, roof and floor and an average U-value of 1.55 W/m^2 K for the glazing, an overall effective thermal capacitance and heat loss parameter of 96.4 MJ/K and 87.2 W/K were calculated respectively. This heat loss parameter is four times better than the average detached house in the UK at 342 W/K (Utley and Shorrock, 2008).

7.3.2 Trombe wall performance

In order to calculate and compare the performance of a granular aerogel and single glazed Trombe wall to the baseline performance of the dwelling, a steady state model was created. This model generates monthly-average figures for a building's heating load, with and without the Trombe wall, the system solar fraction, average cavity temperatures, critical irradiance levels and net energy gain. Monthly-average heat loads and solar fraction can also be evaluated in terms of the actual thermal capacity of the building and Trombe wall or in the theoretical 'zero' or 'infinite' capacity scenarios.

Understandably, the depth of this tool is limited by the 'monthly-average' figures it produces. Consequently, detailed information regarding peak temperatures and the

time/day they occur, as well as information regarding thermal lags cannot be assessed. Nonetheless, the flexibility of the input process enables parameters such as different Trombe wall compositions, site locations, areas and dwelling construction properties, to be promptly compared and evaluated.

To represent the dwelling in this scenario, monthly-average data for solar irradiance, ambient temperature and degree-days was obtained for a site in the nearby town of Farnborough, North-East Hampshire, using the NASA climate dataset found in RETscreen International. The dwelling is assumed to have a minimum allowable inside temperature of 18 °C and an allowable temperature swing of 6 °C.

The concrete wall in the Trombe wall was assigned a thickness of 400 mm, density of 2105 kg/m^3, conductivity of 1.7 W/m K, heat capacity of 0.95 kJ/kg K and channel depth of 160 mm between the outer wall surface and inner surface of the cover. The solar transmission and U-value of the single glazed cover was taken as 0.85 and 5.7 W/m^2 K respectively, whereas the solar transmission and U-value of the 10 mm aerogel cover was taken as 0.7 and 1.48 W/m^2 K respectively (Lexan, 2011). Based on these properties, Table 7.1 and Table 7.2 display the key results from the steady state modelling for the granular aerogel and single glazed Trombe walls respectively.

Table 7.1 *Predicted performance of the 8 m^2 Aerogel Trombe wall.*

AEROGEL TROMBE WALL (8m^2)		Jan	Feb	Mar	Apr	May	Jun	Jul	Aug	Sep	Oct	Nov	Dec	TOTAL
Average external temperature	°C	5.3	5.1	7.1	8.7	12.4	15.2	17.4	17.2	14.4	11.1	7.4	5.3	-
Degree days	-	394	361	338	279	174	84	19	25	108	214	318	394	-
Baseline building heat losses	kWh	911	836	782	645	402	194	43	57	250	495	736	911	6262
Average solar radiation (horizontal)	kWh/m^2/day	0.77	1.39	2.34	3.59	4.57	4.84	4.8	4.23	2.86	1.73	0.96	0.6	-
Average absorbed solar radiation	kWh/m^2/day	0.98	1.28	1.45	1.56	1.56	1.51	1.55	1.66	1.54	1.45	1.17	0.81	-
Net energy gain through Trombe wall	kWh	71	110	166	198	220	237	258	265	231	197	116	42	2111
Dumped energy	kWh	0	0	0	0	0	43	215	207	0	0	0	0	465
Solar fraction	%	8	13	21	31	55	100	100	100	92	40	16	5	-
Auxiliary heating requirement	kWh	840	726	616	447	181	0	0	0	19	297	620	869	4616

Table 7.2 *Predicted performance of the 8 m^2 single glazed Trombe wall.*

SINGLE GLAZED TROMBE WALL (8m^2)		Jan	Feb	Mar	Apr	May	Jun	Jul	Aug	Sep	Oct	Nov	Dec	TOTAL
Average external temperature	°C	5.3	5.1	7.1	8.7	12.4	15.2	17.4	17.2	14.4	11.1	7.4	5.3	-
Degree days	-	394	361	338	279	174	84	19	25	108	214	318	394	-
Baseline building heat losses	kWh	911	836	782	645	402	194	43	57	250	495	736	911	6262
Average solar radiation (horizontal)	kWh/m^2/day	0.77	1.39	2.34	3.59	4.57	4.84	4.8	4.23	2.86	1.73	0.96	0.6	-
Average absorbed solar radiation	kWh/m^2/day	1.19	1.56	1.76	1.89	1.90	1.83	1.89	2.02	1.87	1.76	1.42	0.99	-
Net energy gain through Trombe wall	kWh	25	58	102	131	157	176	197	202	170	136	66	3	1422
Dumped energy	kWh	0	0	0	0	0	0	154	145	0	0	0	0	299
Solar fraction	%	3	7	13	20	39	91	100	100	68	27	9	0	-
Auxiliary heating requirement	kWh	886	778	679	515	245	18	0	0	80	359	670	908	5139

Energy contribution

Figure 7.4 and Figure 7.5 display the predicted monthly reduction in auxiliary energy for heating with the Aerogel Trombe wall and single glazed Trombe wall installed, respectively, alongside the estimated 'energy dump' i.e. the cooling load, which must be mitigated through shading, passive ventilation or active cooling.

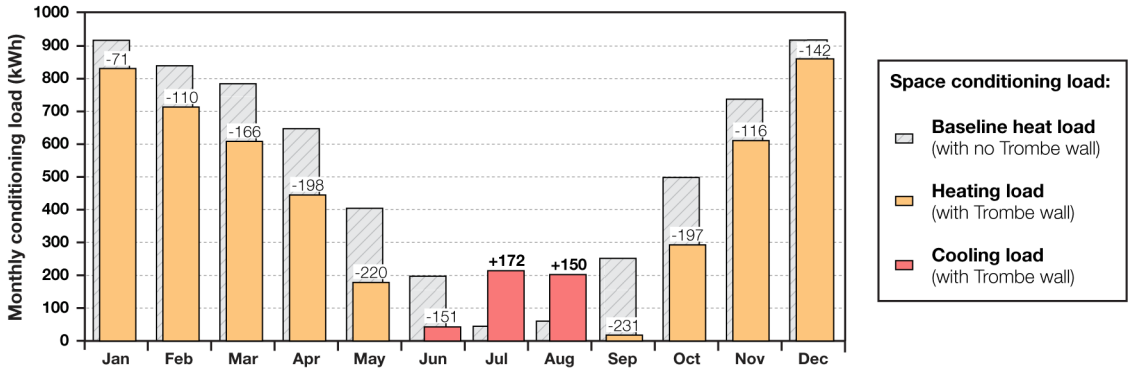

Figure 7.4 *Space conditioning load with Aerogel Trombe wall.*

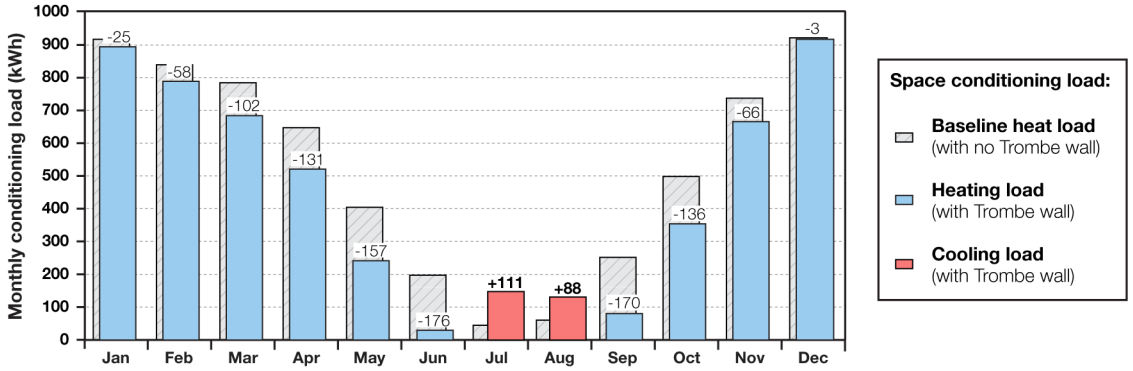

Figure 7.5 *Space conditioning load with single glazed Trombe wall.*

As shown, with the Aerogel Trombe wall the space conditioning load is reduced in all months except July and August (despite some cooling required in June). Overall, the baseline heat load is reduced by 26 % from 6262 kWh/year to 4616 kWh/year, with 465 kWh/year of excess heat generated. Similarly, the single glazed Trombe wall reduces space conditioning in all months except July and August, but energy contribution is minimal during peak winter months. With this system, the theoretical baseline heat load is reduced by 18 % from 6262 kWh/year to 5139 kWh/year, with 299 kWh/year of unwanted energy generated.

Per m² of installed area, focusing on heating only, the Aerogel Trombe wall saves 206 kWh/m²/year compared 140 kWh/m²/year for the single glazed system. Accounting for energy dump, these figures drop to 148 and 108 kWh/m²/year respectively.

Solar fraction

Figure 7.6 and Figure 7.7 display the monthly solar fractions for the Aerogel Trombe wall and single glazed Trombe wall respectively, based on the actual capacitance of the building and wall, compared to 'infinite' and 'zero' capacitance systems.

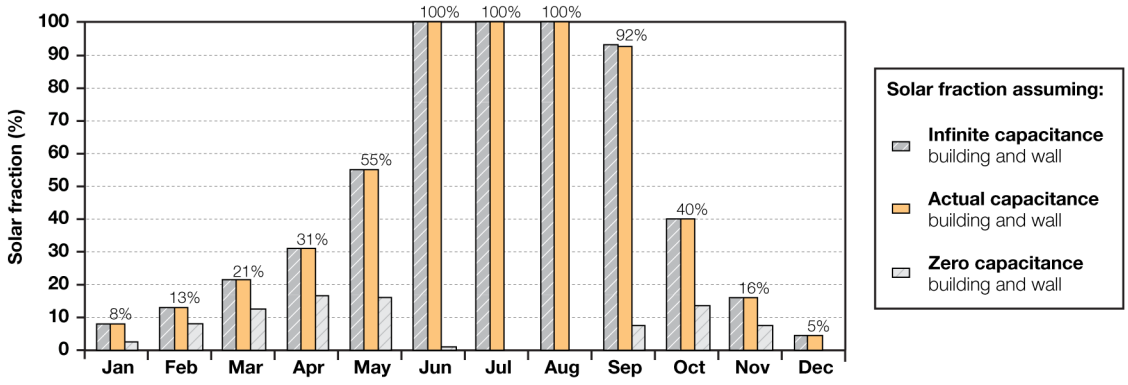

Figure 7.6 *Monthly solar fraction of the Aerogel Trombe wall.*

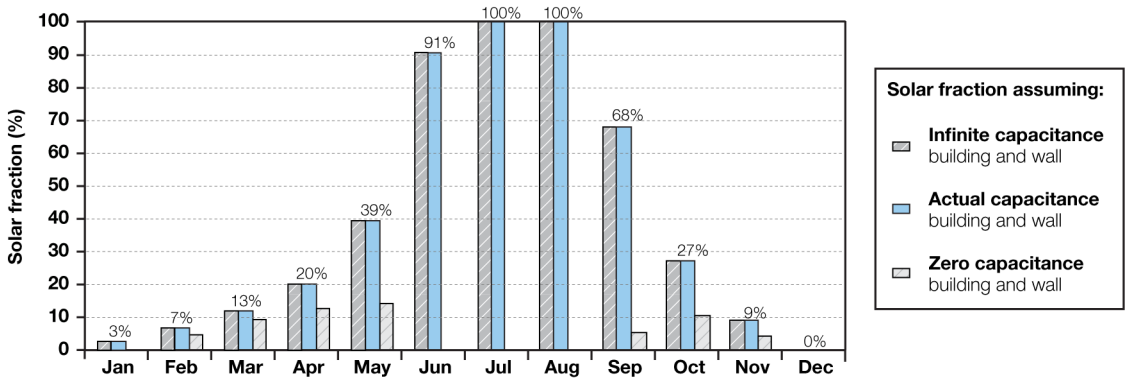

Figure 7.7 *Monthly solar fraction of the Single glazed Trombe wall.*

According to the calculations, for both Trombe walls, the solar fraction based on the actual capacitance of the building and Trombe wall, closely resembles that of an 'infinite' thermal capacitance system. This demonstrates that the high capacitance dwelling combined with the thermally massive concrete wall functions well, taking full advantage of the incoming solar irradiance.

By comparison, if the Trombe wall and building is assumed to have little/no ability to store and retain heat i.e. if the building were a lightweight structure or if the solar storage wall was highly insulated with a low thermal conductivity, this would reduce the Trombe walls effectiveness. As shown, the solar fraction is reduced considerably throughout all months and is at nullified during the summer months since no heat can be stored and utilised throughout the evenings to early morning.

Payback calculation

A preliminary payback calculation for both Trombe walls is displayed in Figure 7.8. The return on investment for two heating options is assessed: an electrical heating system and 91 % efficient gas boiler. Based on Chapter 6, a cost of £ 60/m² and £ 100/m² was assigned for the single glazed cover and 10 mm thick granular aerogel cover. A further £ 120/m² was applied for the timber, aluminium framing and a brise-soleil shading grill (instead of the perforated absorber sheet). It is assumed that energy dump is mitigated by passive ventilation and by the shading grill blocking high summer sun. Discount interest rates and fuel price increase rates were set to 2 % and 6 % respectively. Baseline gas and electricity prices were assumed to be 0.04 p/kWh and 0.12 p/kWh.

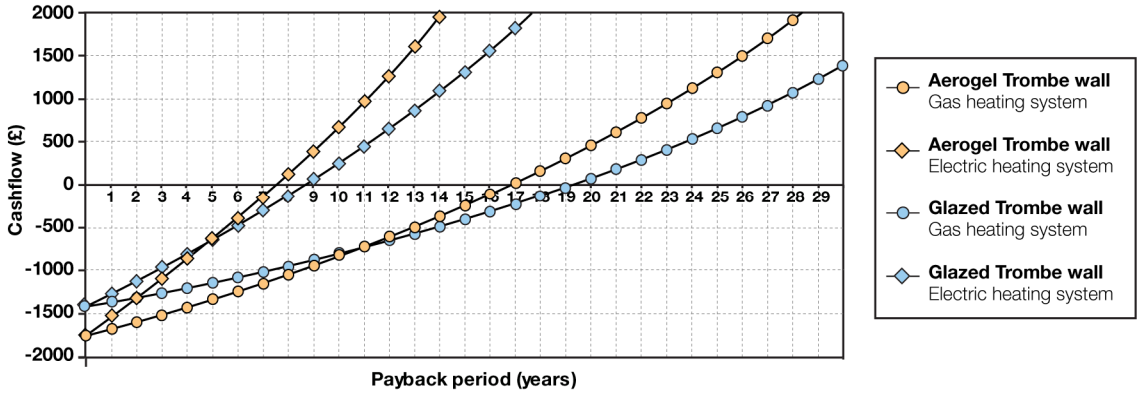

Figure 7.8 *Predicted payback calculation for Trombe wall.*

According to the financial model, if gas is used as the primary heating fuel, then a 17 year payback is predicted for the Aerogel Trombe wall compared to 19.5 years for the single glazed system. By comparison, if electricity is used, corresponding paybacks reduce to 7.5 years and 9 years.

Summary of findings

Results presented in this section will need to undergo experimental validation as part of future research. Due to limited involvement in the development of the Aerogel Trombe wall at the Whitehill Bordon site, note that the actual system and dwelling's dimensions and materials may differ significantly to the final installed system. Nonetheless, preliminary modelling has demonstrated that passive Trombe walls incorporated into the design of low-energy buildings can provide a positive energy contribution. Results indicate that replacing the conventional single glazed cover in the Trombe wall with a 10 mm thick granular aerogel cover can provide improved performance, despite the reduction in solar transmission and increased cooling load. Initial payback calculations shown here suggest that granular aerogel can reduce the payback period by 2-3 years, compared to traditional single glazed Trombe walls.

7.4 Parametric Trombe Wall Assessment

In the previous study, the Trombe walls investigated were incorporated into a new dwelling possessing a high thermal capacitance and thermally massive concrete storage wall to take full advantage of the system. By comparison, if this product was to be developed into a *retrofit* solution, fitted directly to the outside of existing buildings, built to varying insulation levels, then the performance may vary significantly.

Taking this forward, this second study contains a parametric thermal modelling assessment of different Trombe wall areas retrofitted directly to the outside of a range of house types and construction standards. This works builds on an extrapolation study by Dolley *et al.* (1994) who estimated the thermal performance of different translucent honeycomb Trombe wall areas retrofitted to a theoretical detached house, built with solid walls, un-filled cavity walls, to 1976 and 1990 Building Regulations standards as well as to 'super-insulation' standards (equivalent to 2010 Building Regulations).

Baseline housing stock performance

The first step in this parametric assessment involved generating representative heat loss parameters for different house types and insulation standards. This was achieved by conducting a series of SAP assessments on the Whitehill Bordon detached house geometry, followed by extrapolating results to generate equivalent heat loss parameters for different house types.

According to Utley and Shorrock (2008), the average heat loss parameter for detached houses in the UK is 342 W/K. By comparison, a baseline heat loss parameter of 469W/K was calculated for the detached house geometry assuming a solid brick wall construction. When modelled with unfilled cavity walls the heat loss parameter was 388W/K. When constructed to the 1976, 1990 and 2010 Building Regulations this reduced to 292W/K, 206W/K and 132W/K respectively. When modelled as a 'super-insulated' property with Passivhaus U-values and air tightness levels the heat loss parameter was 67 W/K.

Excluding results for the 'super-insulated' and 2010 Building Regulations property (as they only represent around 1 % of the UK's existing stock), the average heat loss parameter calculated from the SAP assessments was 339 W/K, correlating very well with data from Utley and Shorrock (2008). As a result, it was assumed that the generated values could be directly scaled across different house types.

According to Utley and Shorrock (2008), the national average heat loss parameter for semi-detached houses, terrace houses and flats is 264 W/K, 235 W/K, and 167 W/K

respectively (Utley and Shorrock, 2008). Table 7.3 displays the scaled heat loss parameters for each house type, with an outline of the different fabric assumptions.

Table 7.3 *Extrapolated heat loss parameters used in the parametric assessment.*

		Extrapolated heat loss parameters (W/K)			
Construction type	**Assumed U-value and air permeability**	**Detached**	**Semi Detached**	**Terrace**	**Flat**
Solid wall	Walls (2.16), Glazing (5.7), Roof (1.7), Floor (1.0) Air permeability = 15	469	362	322	229
Unfilled cavity wall	Walls (1.24), Glazing (5.7), Roof (1.7), Floor (1.0) Air permeability = 15	388	300	267	190
1976 Building Regs	Walls (0.76), Glazing (5.7), Roof (0.6), Floor (1.0) Air permeability = 15	292	225	200	142
1990 Building Regs	Walls (0.45), Glazing (3.3), Roof (0.25), Floor (0.45) Air permeability = 10	206	159	141	100
2010 Building Regs	Walls (0.25), Glazing (2.0), Roof (0.16), Floor (0.25) Air permeability = 10	132	102	90	64
Super insulated	Walls (0.15), Glazing (0.8), Roof (0.15), Floor (0.15) Air permeability = 1	67	52	46	33

Data processing & limitations

Table 7.4 to Table 7.7 display the predicted annual space heating consumption for each dwelling type and construction standard with 0, 8, 16, 24 or 32 m² areas of Trombe wall installed on their south facade. In each case, it was assumed in the steady state model that a Trombe wall incorporating a 10 mm granular aerogel cover is retrofitted directly to the outside of the dwelling's existing wall (i.e. brick with/without insulation and a cavity), as opposed to an 'optimised' concrete storage wall, which would require more disruptive retrofit works to install.

Results are tabulated using a similar approach to Dolley *et al.* (1994), with figures for predicted annual energy savings given in kWh/year and in kWh/m²/year, whereby m² refers to the installed area of the Trombe wall (not m² of floor area). Similarly to Dolley *et al.* (1994), it is assumed that the Trombe wall possesses no shading system or summertime ventilation. Energy dump is given opposed to hours of overheating per year, provided by Dolley *et al.* (1994). Illustrations beneath each table display the Trombe wall energy savings (per m² of installed area) and the annual solar fraction (%).

Similarly to the first study, note that these preliminary results should only be treated as indicative values, which have not been validated experimentally in this application. Once validated, it is anticipated that this data could be used as preliminary design guidance to assist designers in sizing Trombe walls, dependant on house type and insulation level. However, at this stage, predicted annual heating load and energy savings for each house type / construction standard are intended solely for comparative purposes, as opposed to providing accurate information.

Table 7.4 *Results for detached houses*

Construction			Area of Trombe wall installed (m^2)				
			0	8	16	24	32
Solid wall	Annual space heating consumption	kWh/year	30,431	28,968	27,700	26,647	25,655
	Net energy gain from Trombe wall	kWh/year		1,463	2,925	4,388	5,850
	Useful energy from Trombe wall	kWh/year		1,463	2,731	3,784	4,776
	Excess energy from Trombe wall	kWh/year		0	194	604	1,074
	Savings per m^2 of Trombe wall	kWh/m^2/year		183	171	158	149
	Annual solar fraction	%		4.8%	9.0%	12.4%	15.7%
Unfilled cavity wall	Annual space heating consumption	kWh/year	25,215	23,813	22,701	21,710	20,774
	Net energy gain from Trombe wall	kWh/year		1,453	2,906	4,359	5,812
	Useful energy from Trombe wall	kWh/year		1,402	2,514	3,505	4,441
	Excess energy from Trombe wall	kWh/year		51	392	854	1,371
	Savings per m^2 of Trombe wall	kWh/m^2/year		175	157	146	139
	Annual solar fraction	%		5.6%	10.0%	13.9%	17.6%
1976 Building Regulations	Annual space heating consumption	kWh/year	18,940	17,694	16,722	15,829	14,994
	Net energy gain from Trombe wall	kWh/year		1,361	2,722	4,084	5,445
	Useful energy from Trombe wall	kWh/year		1,246	2,219	3,111	3,947
	Excess energy from Trombe wall	kWh/year		115	504	973	1,498
	Savings per m^2 of Trombe wall	kWh/m^2/year		156	139	130	123
	Annual solar fraction	%		6.6%	11.7%	16.4%	20.8%
1990 Building Regulations	Annual space heating consumption	kWh/year	13,348	12,312	11,505	10,754	10,058
	Net energy gain from Trombe wall	kWh/year		1,182	2,365	3,547	4,729
	Useful energy from Trombe wall	kWh/year		1,036	1,843	2,594	3,290
	Excess energy from Trombe wall	kWh/year		146	522	953	1,439
	Savings per m^2 of Trombe wall	kWh/m^2/year		130	115	108	103
	Annual solar fraction	%		7.8%	13.8%	19.4%	24.7%
2010 Building Regulations	Annual space heating consumption	kWh/year	8,561	7,785	7,169	6,595	6,069
	Net energy gain from Trombe wall	kWh/year		922	1,845	2,767	3,689
	Useful energy from Trombe wall	kWh/year		776	1,392	1,966	2,491
	Excess energy from Trombe wall	kWh/year		146	453	801	1,198
	Savings per m^2 of Trombe wall	kWh/m^2/year		97	87	82	78
	Annual solar fraction	%		9.1%	16.3%	23.0%	29.1%
Super insulated	Annual space heating consumption	kWh/year	4,358	3,819	3,374	2,986	2,672
	Net energy gain from Trombe wall	kWh/year		683	1,366	2,049	2,732
	Useful energy from Trombe wall	kWh/year		539	985	1,373	1,687
	Excess energy from Trombe wall	kWh/year		144	381	677	1,046
	Savings per m^2 of Trombe wall	kWh/m^2/year		67	62	57	53
	Annual solar fraction	%		12.4%	22.6%	31.5%	38.7%

ENERGY SAVINGS (per m^2 of Trombe wall)

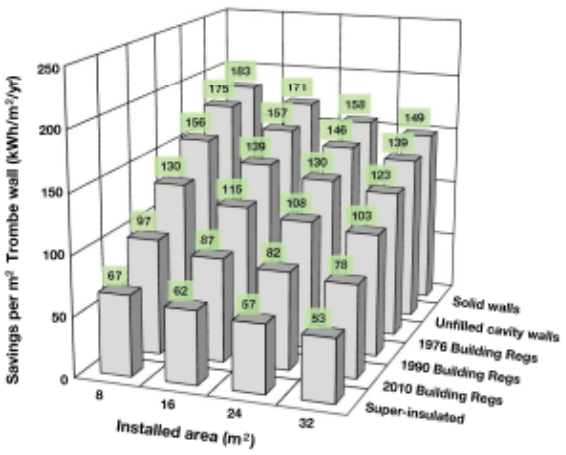

SOLAR FRACTION

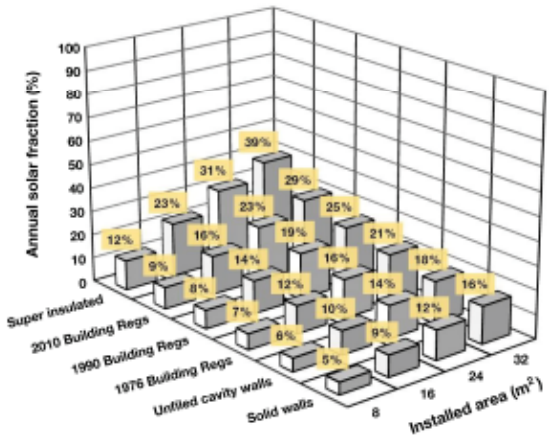

Table 7.5 *Results for semi-detached houses*

Construction			Area of Trombe wall installed (m^2)				
			0	8	16	24	32
Solid wall	Annual space heating consumption	kWh/year	23,492	22,029	20,890	19,871	18,927
	Net energy gain from Trombe wall	kWh/year		1,463	2925	4,388	5,850
	Useful energy from Trombe wall	kWh/year		1,463	2602	3,622	4,565
	Excess energy from Trombe wall	kWh/year		0	323	766	1,285
	Savings per m^2 of Trombe wall	kWh/m^2/year		183	163	151	143
	Annual solar fraction	%		6.2%	11.1%	15.4%	19.4%
Unfilled cavity wall	Annual space heating consumption	kWh/year	19,463	18,096	17,058	16,097	15,208
	Net energy gain from Trombe wall	kWh/year		1,453	2,906	4,359	5,812
	Useful energy from Trombe wall	kWh/year		1,367	2,405	3,366	4,254
	Excess energy from Trombe wall	kWh/year		86	501	993	1,558
	Savings per m^2 of Trombe wall	kWh/m^2/year		171	150	140	133
	Annual solar fraction	%		7.0%	12.4%	17.3%	21.9%
1976 Building Regulations	Annual space heating consumption	kWh/year	14,627	13,423	12,494	11,633	10,844
	Net energy gain from Trombe wall	kWh/year		1,361	2,722	4,084	5,445
	Useful energy from Trombe wall	kWh/year		1,204	2,133	2,994	3,783
	Excess energy from Trombe wall	kWh/year		157	590	1,089	1,662
	Savings per m^2 of Trombe wall	kWh/m^2/year		151	133	125	118
	Annual solar fraction	%		8.2%	14.6%	20.5%	25.9%
1990 Building Regulations	Annual space heating consumption	kWh/year	10,306	9,314	8,528	7,805	7,171
	Net energy gain from Trombe wall	kWh/year		1,182	2,365	3,547	4,729
	Useful energy from Trombe wall	kWh/year		992	1,778	2,500	3,135
	Excess energy from Trombe wall	kWh/year		191	587	1,047	1,594
	Savings per m^2 of Trombe wall	kWh/m^2/year		124	111	104	98
	Annual solar fraction	%		9.6%	17.3%	24.3%	30.4%
2010 Building Regulations	Annual space heating consumption	kWh/year	6,602	5,858	5,254	4,708	4,256
	Net energy gain from Trombe wall	kWh/year		922	1,845	2,767	3,689
	Useful energy from Trombe wall	kWh/year		743	1,348	1,894	2,346
	Excess energy from Trombe wall	kWh/year		179	497	873	1,344
	Savings per m^2 of Trombe wall	kWh/m^2/year		93	84	79	73
	Annual solar fraction	%		11.3%	20.4%	28.7%	35.5%
Super insulated	Annual space heating consumption	kWh/year	3,361	2,839	2,408	2,076	1,796
	Net energy gain from Trombe wall	kWh/year		683	1,366	2,049	2,732
	Useful energy from Trombe wall	kWh/year		522	952	1,285	1,565
	Excess energy from Trombe wall	kWh/year		161	414	764	1,167
	Savings per m^2 of Trombe wall	kWh/m^2/year		65	60	54	49
	Annual solar fraction	%		15.5%	28.3%	38.2%	46.6%

ENERGY SAVINGS (per m^2 of Trombe wall)

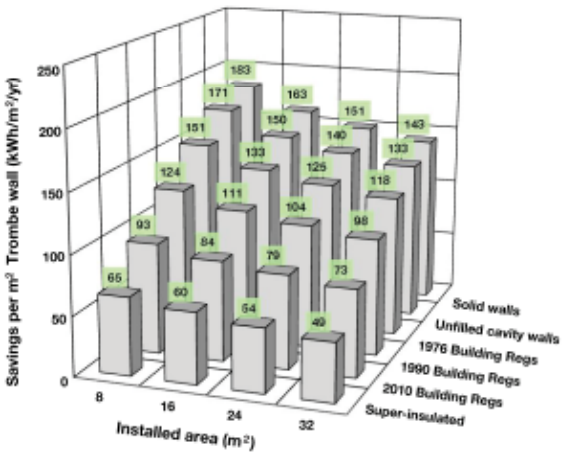

SOLAR FRACTION

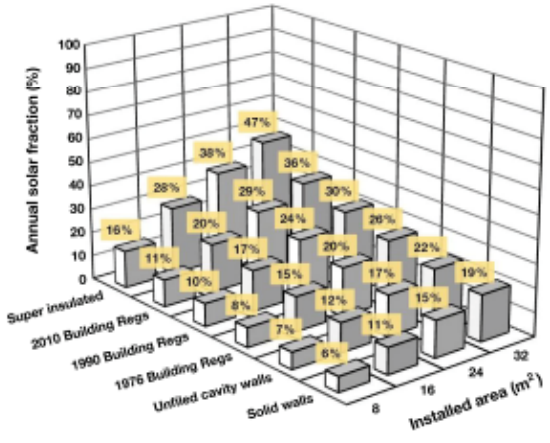

Table 7.6 *Results for terrace houses*

Construction			Area of Trombe wall installed (m^2)				
			0	8	16	24	32
Solid wall	Annual space heating consumption	kWh/year	20,912	19,449	18,361	17,359	16,441
	Net energy gain from Trombe wall	kWh/year		1,463	2,925	4,388	5,850
	Useful energy from Trombe wall	kWh/year		1,463	2,551	3,553	4,471
	Excess energy from Trombe wall	kWh/year		0	374	835	1,379
	Savings per m^2 of Trombe wall	kWh/m^2/year		183	159	148	140
	Annual solar fraction	%		7.0%	12.2%	17.0%	21.4%
Unfilled cavity wall	Annual space heating consumption	kWh/year	17,325	15,982	14,963	14,019	13,154
	Net energy gain from Trombe wall	kWh/year		1,453	2,906	4,359	5,812
	Useful energy from Trombe wall	kWh/year		1,343	2,362	3,306	4,171
	Excess energy from Trombe wall	kWh/year		110	544	1,053	1,642
	Savings per m^2 of Trombe wall	kWh/m^2/year		168	148	138	130
	Annual solar fraction	%		7.7%	13.6%	19.1%	24.1%
1976 Building Regulations	Annual space heating consumption	kWh/year	13,020	11,843	10,922	10,077	9,320
	Net energy gain from Trombe wall	kWh/year		1,361	2,722	4,084	5,445
	Useful energy from Trombe wall	kWh/year		1,177	2,098	2,943	3,700
	Excess energy from Trombe wall	kWh/year		184	624	1,141	1,745
	Savings per m^2 of Trombe wall	kWh/m^2/year		147	131	123	116
	Annual solar fraction	%		9.0%	16.1%	22.6%	28.4%
1990 Building Regulations	Annual space heating consumption	kWh/year	9,174	8,201	7,422	6,715	6,126
	Net energy gain from Trombe wall	kWh/year		1,182	2,365	3,547	4729
	Useful energy from Trombe wall	kWh/year		972	1,752	2,458	3048
	Excess energy from Trombe wall	kWh/year		210	613	1,089	1,682
	Savings per m^2 of Trombe wall	kWh/m^2/year		122	109	102	95
	Annual solar fraction	%		10.6%	19.1%	26.8%	33.2%
2010 Building Regulations	Annual space heating consumption	kWh/year	5,877	5,146	4,547	4,031	3,614
	Net energy gain from Trombe wall	kWh/year		922	1,845	2,767	3,689
	Useful energy from Trombe wall	kWh/year		731	1,329	1,846	2,263
	Excess energy from Trombe wall	kWh/year		191	515	921	1,427
	Savings per m^2 of Trombe wall	kWh/m^2/year		91	83	77	71
	Annual solar fraction	%		12.4%	22.6%	31.4%	38.5%
Super insulated	Annual space heating consumption	kWh/year	2,992	2,476	2,061	1,748	1,479
	Net energy gain from Trombe wall	kWh/year		683	1,366	2,049	2,732
	Useful energy from Trombe wall	kWh/year		515	931	1,244	1,513
	Excess energy from Trombe wall	kWh/year		168	435	805	1,220
	Savings per m^2 of Trombe wall	kWh/m^2/year		64	58	52	47
	Annual solar fraction	%		17.2%	31.1%	41.6%	50.6%

ENERGY SAVINGS (per m^2 of Trombe wall)

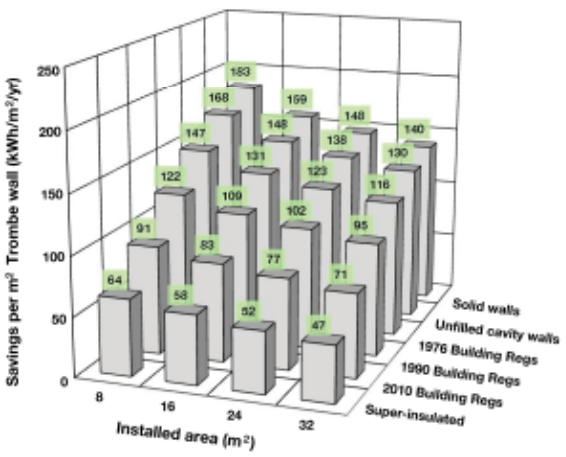

SOLAR FRACTION

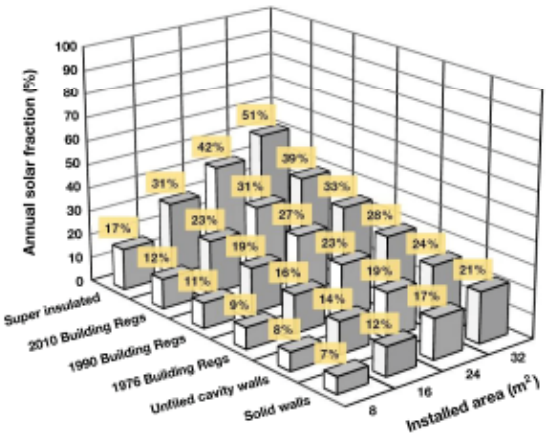

Table 7.7 *Results for flats*

Construction			Area of Trombe wall installed (m²)				
			0	8	16	24	32
Solid wall	Annual space heating consumption	kWh/year	14,861	13,495	12,443	11,502	10,735
	Net energy gain from Trombe wall	kWh/year		1,463	2,925	4,388	5,850
	Useful energy from Trombe wall	kWh/year		1,366	2,418	3,359	4,125
	Excess energy from Trombe wall	kWh/year		96	507	1,029	1,725
	Savings per m² of Trombe wall	kWh/m²/year		171	151	140	129
	Annual solar fraction	%		9.2%	16.3%	22.6%	27.8%
Unfilled cavity wall	Annual space heating consumption	kWh/year	12,312	11,054	10,064	9,178	8,460
	Net energy gain from Trombe wall	kWh/year		1,453	2,906	4,359	5,812
	Useful energy from Trombe wall	kWh/year		1,258	2,248	3,134	3,852
	Excess energy from Trombe wall	kWh/year		195	658	1,225	1,960
	Savings per m² of Trombe wall	kWh/m²/year		157	140	131	120
	Annual solar fraction	%		10.2%	18.3%	25.5%	31.3%
1976 Building Regulations	Annual space heating consumption	kWh/year	9,253	8,140	7,249	6,491	5,884
	Net energy gain from Trombe wall	kWh/year		1,361	2,722	4,084	5,445
	Useful energy from Trombe wall	kWh/year		1,113	2,004	2,761	3,369
	Excess energy from Trombe wall	kWh/year		249	719	1,322	2,076
	Savings per m² of Trombe wall	kWh/m²/year		139	125	115	105
	Annual solar fraction	%		12.0%	21.7%	29.8%	36.4%
1990 Building Regulations	Annual space heating consumption	kWh/year	6,519	5,593	4,842	4,243	3,769
	Net energy gain from Trombe wall	kWh/year		1,182	2,365	3,547	4,729
	Useful energy from Trombe wall	kWh/year		926	1,678	2,276	2,750
	Excess energy from Trombe wall	kWh/year		256	687	1,271	1,979
	Savings per m² of Trombe wall	kWh/m²/year		116	105	95	86
	Annual solar fraction	%		14.2%	25.7%	34.9%	42.2%
2010 Building Regulations	Annual space heating consumption	kWh/year	4,176	3,475	2,914	2,492	2,132
	Net energy gain from Trombe wall	kWh/year		922	1,845	2,767	3,689
	Useful energy from Trombe wall	kWh/year		701	1,262	1,685	2,044
	Excess energy from Trombe wall	kWh/year		222	583	1,083	1,645
	Savings per m² of Trombe wall	kWh/m²/year		88	79	70	64
	Annual solar fraction	%		16.8%	30.2%	40.3%	48.9%
Super insulated	Annual space heating consumption	kWh/year	2,126	1,627	1,272	1,002	799
	Net energy gain from Trombe wall	kWh/year		683	1,366	2,049	2,732
	Useful energy from Trombe wall	kWh/year		499	854	1,124	1,327
	Excess energy from Trombe wall	kWh/year		184	512	926	1,405
	Savings per m² of Trombe wall	kWh/m²/year		62	53	47	41
	Annual solar fraction	%		23.5%	40.2%	52.8%	62.4%

ENERGY SAVINGS (per m² of Trombe wall)

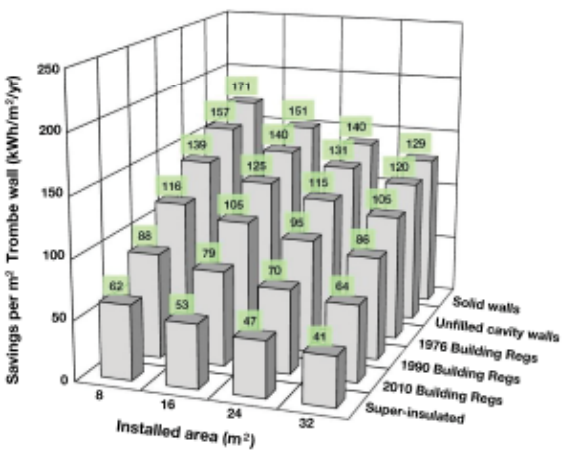

SOLAR FRACTION

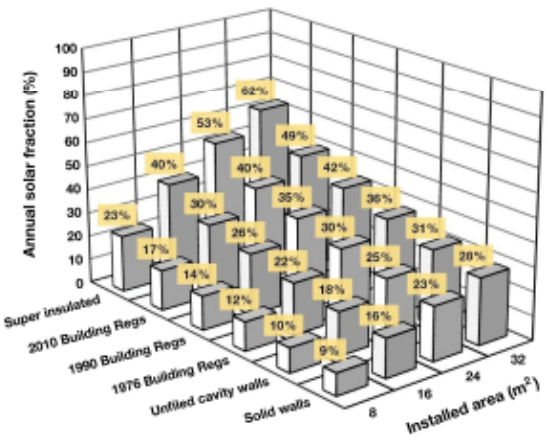

7.5 Discussion

The preliminary results of the parametric modelling study provide a useful insight into how the performance of the Aerogel Trombe wall may vary when retrofitted to different notional house types and constructions. For example, it is possible to see how utilisation and energy savings per m² reduce as larger areas of Trombe wall are specified and when systems are installed onto more highly insulated buildings. By comparison, as the installed Trombe wall area increases and the propertys' baseline heating demand reduces, annual solar fractions naturally increase. Evidently, the proportion of useful vs. wasted energy should be taken into account, to avoid over sizing a Trombe wall, especially on highly insulated dwellings.

In detached homes, predicted energy savings range from 183 kWh/m²/year for an 8 m² Trombe wall retrofitted to a solid walled property, to 64 kWh/m²/year for a 32 m² Trombe wall retrofitted to a property built in 2010. Similar findings were observed by Dolley *et al.* (1994) when analysing a Trombe wall incorporating a 100 mm thick translucent honeycomb cover (with U-value of 0.8 W/m² K and solar transmittance of 48 %). Here, energy savings were 153 kWh/m²/year for 8 m² system installed on a solid walled detached house, compared to 35 kWh/m²/year for a 32 m² system installed on a detached house built to 2010 Building Regulations. Evidently, figures generated by Dolley *et al.* (1994) are slightly lower than the values calculated in this parametric investigation. This could be due to lower solar transmittance of the 100 mm honeycomb cover, compared to the 10 mm granular aerogel cover at 70 %.

Payback calculation

Figure 7.9 displays a payback curve based on the energy savings per m² from all Trombe walls modelled in the parametric assessment. The estimated capital cost of each Trombe wall is taken as £ 220/m² (assuming £ 100/m² for the aerogel cover, and another £ 120/m² for the framing and a shading system). The baseline cost of electricity and gas is assumed to be £ 0.12/kWh and £ 0.04/kWh respectively, with a 6 % annual fuel price inflation rate and 2 % discount interest rate applied.

The two bands correspond to payback periods for gas and electrically heated homes respectively. In each case, the upper limit of the band (providing the shortest payback), represents the predicted payback period for 8 m² Trombe wall on a solid walled detached property. Conversely, the lower limit (providing the longest payback period) represents the predicted payback for 32 m² of Trombe wall installed on a super insulated flat. All values between these limits represent the paybacks for the remaining house types and Trombe wall areas.

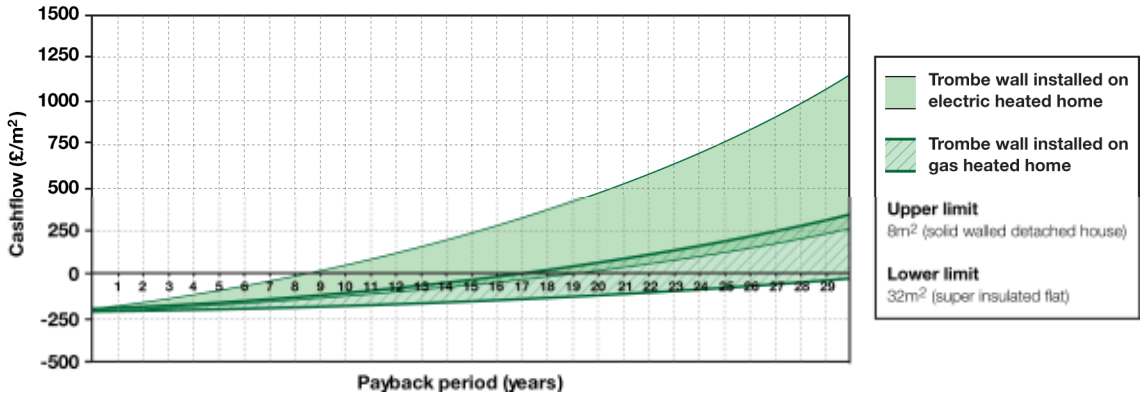

Figure 7.9 *Payback curve based on energy savings from the parametric assessment.*

Predicted payback periods for the different Trombe wall installations range from 8-19 years in electrically heated homes, or 17-35 years in gas heated homes. Evidently, the product may only be a viable retrofit option in electric heated homes or gas heated homes with little/no insulation. Countering this however, as these payback periods are similar to those calculated by Shorrock *et al.* (2008) for external insulation, if a dwelling is being overclad, it may be viable to incorporate a Trombe wall into the design if there is a suitable free area of south facade.

External insulation comparison

To investigate if a Trombe wall provides a greater energy saving, per m², compared to conventional insulation, Figure 7.10 illustrates the predicted energy savings from the Trombe wall vs. the predicted energy savings through external insulation. The degree-day calculation assumes that the building operates an 18 hour heating schedule on the days when heating is required (i.e. maximising the need for insulation) and it is assumed that 1 m² of external wall area is upgraded to a U-value of 0.15 W/m² K. Upper and lower limits on the Trombe wall energy savings, represent the maximum and minimum predicted savings from the detached house and flats respectively.

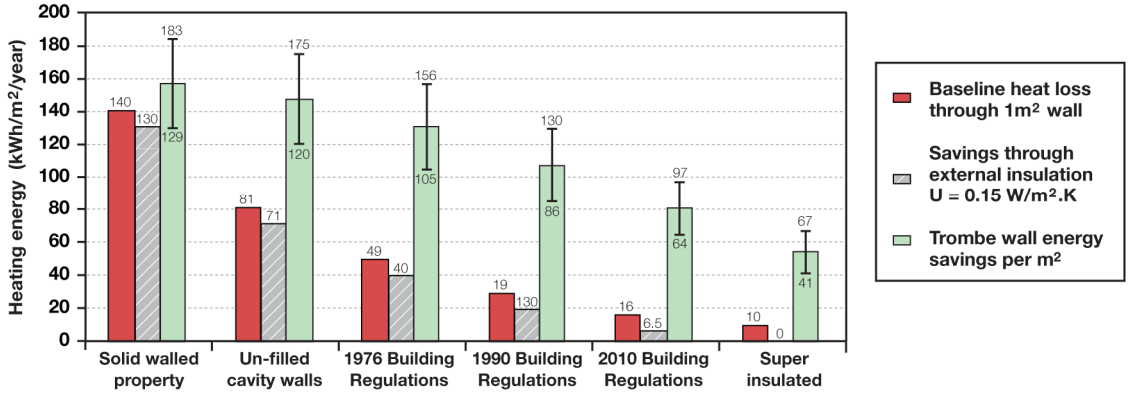

Figure 7.10 *Energy savings from external insulation vs. energy savings from a Trombe wall.*

In all cases (with the exception of 32 m² of Trombe wall on a solid walled flat) the Trombe wall energy savings exceed the predicted energy savings through external insulation, indicating that an Aerogel Trombe wall can be used as a stand-alone system or incorporated into an external cladding scheme to enhance its overall benefit. Evidently, as properties are built to better insulation standards, the energy savings from insulation diminish at a greater rate than the predicted Trombe wall energy savings. The greatest potential for increased energy savings is observed within un-filled cavity wall properties and dwellings built to 1976-1990 Building Regulations.

7.6 Conclusion

This chapter aimed to serve as a preliminary evaluation into the thermal performance of aerogel applied to passive solar Trombe walls. Findings support the hypothesis of Dolley *et al.* (1994) that Trombe walls incorporating translucent insulation can outperform glazed Trombe walls and conventional external insulation.

Modelling found that an 8 m² Aerogel Trombe wall applied to a new, thermally massive building could save up to 26 % of the annual heat load with a minimum payback period of 7.5 years, compared to 18 % annual savings and 9 year payback for a glazed system. Applied in a direct retrofit application, predicted energy savings range from 183 kWh/m²/year for an 8 m² Trombe wall retrofitted to a solid walled detached house, to 62 kWh/m²/year for a 32 m² Trombe wall retrofitted to a super insulated flat.

Evidently, the performance of Trombe walls is highly reliant upon the storage capacity of the building and wall it is applied to. In certain circumstances, payback periods can be long, especially if systems are oversized or not installed on appropriate dwellings. The greatest energy savings can be obtained when applied to a wall with a thermal mass since the heat generated can be fully utilised throughout the evening-morning. By comparison, if applied in a retrofit application, then older solid walled properties or properties with un-filled cavity walls can provide large energy savings.

Preliminary modelling has found that a small area of Trombe wall can provide a useful energy contribution without creating a significant overheating risk. If larger areas are to be installed, then detailed calculations would be recommended to assess the potential overheating issues. Static shading grills to cut high summer sun, combined with passive vents at the top and bottom of the wall would be recommended to regulate overheating without active cooling. It is likely that the most appropriate application for Aerogel Trombe walls would be in 'deep' retrofits, particularly if incorporated alongside an external cladding scheme to enhance its benefit.

Chapter 8

CONCLUSIONS & FURTHER WORK

8.1 Conclusions

The core objective of this thesis was to design, build and test novel environmentally responsible retrofit technologies with potential to reduce demand for heating and/or artificial lighting in existing buildings. This has been achieved through the development of two working prototypes incorporating translucent granular aerogel insulation in novel applications and a streamlined life cycle assessment verifying the material's production impact. Each study addresses an important research gap associated with the use and environmental assessment of silica aerogel. Three contributions to knowledge in the resulting studies are achieved, all of which have been published in peer reviewed scientific journal papers.

The proof-of-principle prototype incorporating granular aerogel built to improve the thermal performance of existing glazing without blocking out all of the useful natural light demonstrates that it is possible to meet Building Regulations requirements for glazing renovation U-values in a cost effective manner, without replacement windows. This is important as a large portion of the existing UK building stock has single glazed or first generation double glazed windows, where improvements are limited by the long payback periods of new glazing, low incentives for private landlords or planning restrictions in listed buildings and conservation areas. There is scope to develop the prototype further into a range of translucent products, such as pop-in secondary glazing, sliding shutters or roller blinds capable of fitting to a wide range of window types and sizes. If operated effectively by users or automated controls, these products could achieve significant reductions in energy consumption for heating and cooling, without detrimental impact on the artificial lighting loads.

Applied to external south facing walls, granular aerogel can be used to insulate as well as harness free solar energy for heating, making better use of the nation's stock of un-insulated solid walled properties. The prototype built for this research demonstrates that a small area of a solar air collector integrated into the external insulation of a hard-to-treat property, preheating the air in a mechanical ventilation system, can provide a significant source of free warm air heating, enabling the property to retain comfortable

living conditions without the need for auxiliary heating throughout most of the year. Despite not achieving Passivhaus certification in the whole house retrofit, the prototype was capable of achieving a Passivhaus U-value whilst also boosting the supply air temperatures from the heat recovery system. As such, this system may be well suited as a Passivhaus component, most applicable for properties aiming to achieve 'deep' reductions in CO_2 emissions beyond the limits of conventional measures. It should be noted that there are opportunities to improve the efficiency of this prototype further through an optimised absorber, collector tilt angle, integrating thermal storage into the cavity, ensuring air tight construction or connecting the system to an air-water heat exchanger to make best use of excess heat in summertime.

The Retrofit for the Future project was an influential case study affecting the final outcomes and experience gained during this Engineering Doctorate. Many valuable lessons were learnt related to building fabric assessments, project planning, quality control, design detailing and whole house retrofitting, particularly due to adopting the Passivhaus Standard. Due to the high capital costs and time taken to complete this project, it is expected that this level of deep retrofitting would not appropriate in the current UK retrofit market. Primarily this is due to the level of disruption, technical challenge, UK skills shortage and lack of cost effective Passivhaus certified components. However, it should be noted that the aim of this retrofit competition was to reduce theoretical operational CO_2 emissions by 80 %, going far beyond the limitations of conventional retrofitting approaches, which was successfully achieved. On-going monitoring will seek to validate these predictions. Ultimately the success of this project will rely heavily on the occupants' satisfaction level, combined with how well they engage with the new technologies and conserve energy at home.

The application of opaque aerogel blankets into a hard-to-treat area of the retrofit property's ground floor as well as the innovative custom-built external plant room door, demonstrate the potential for silica aerogel to be used in a number of different applications suitable for retrofitting into existing buildings. Evidently, the material proved to be expensive to apply to the ground floor (at 80 mm thickness) and feedback from contractors was that it was difficult to cut & install. However, it should be noted that this was the only material capable of meeting a Passivhaus U-value, without excavating the ground floor. Applied to an external door, just 30 mm of aerogel blankets provided a central measured U-value better than a Passivhaus certified front door & at a lower capital cost, despite being a larger door. This preliminary evaluation is particularly promising, indicating that this product could be an appropriate alternative for expensive and thick Passivhaus certified doors.

The concept of passive Trombe walls incorporating granular aerogel may prove to be more applicable across the existing UK housing stock, compared to solar air collectors as they do not rely on mechanical ventilation. Preliminary thermal modelling has demonstrated that granular aerogel can enhance the performance of single glazed Trombe walls and that optimum performance can be achieved when integrating these systems into dwellings with high thermal mass. Alternatively, preliminary parametric modelling of Aerogel Trombe walls on existing buildings, demonstrates that these systems can provide high energy savings, per m^2, particularly on older buildings with solid brick walls, comparable to external insulation. In contrast, small Trombe walls areas can provide significant solar fractions, particularly on more insulated dwellings with lower heating requirements.

Streamlined life cycle assessment has proved to be an invaluable tool to verify the environmental performance of the built prototypes following a systematic approach, which considers both operational savings and embodied impacts; a critical balance that is typically ignored. Findings have demonstrated that the energy use and CO_2 burden in aerogel manufacture can be quickly recovered by the operational savings obtained from both retrofit technologies, despite conservative scaling to represent mass production. Studies like this will become increasingly important as Building Regulations become more stringent, resulting in lower operational energy use, increasing the significance of embodied energy and CO_2 over the life cycle of buildings. Silica aerogel is a unique material, with potential for many applications in new insulation products. Innovative materials such as this should not be overlooked in the effort to reduce the life cycle CO_2 emissions across our existing building stock.

8.2 Further Work

At the end of this doctorate there are several opportunities to apply the findings of this thesis by developing concepts, undertaking original research studies and/or carrying out further monitoring experiments. Five such studies have been listed below:

(i) **Product development and user testing of translucent aerogel shutters**
The aim of this study would be to develop the concept of translucent aerogel 'shutters' into a suite of working, fully certified prototypes suitable for commercialisation. Original research studies could include user testing of manually operated or automated solutions. Engineering development would

be required to select the most appropriate fixtures to enable the product to be retrofitted to a wide variety of window shapes and sizes.

(ii) **Long term monitoring of the Aerogel Solar Collector**

The aim of this study would be to evaluate the long term performance of the Aerogel Solar Collector installed at the retrofit house. Original research could include an assessment of the predicted vs. actual annual energy savings based on the outlet temperature and auxiliary heating used in the occupied dwelling. Further studies could include an analysis of moisture in the cavity, the effectiveness of flow and bypass controls to mitigate overheating and a study of the impact of stagnation on system integrity.

(iii) **Long term monitoring of the Retrofit for the Future project**

The aim of this study would be to evaluate the long term energy savings achieved in the Retrofit for the Future case study. Original research could include a thermal comfort and occupancy satisfaction study and/or validation of each technology's predicted vs. actual performance. Annual fuel bill savings could be compared to the occupants' previous energy usage to verify if an 80 % reduction in household CO_2 emissions is achieved.

(iv) **In-situ testing and validation of Trombe walls incorporating aerogel**

The aim of this study would be to validate the thermal performance of a Trombe wall incorporating granular aerogel through in-situ monitoring and dynamic thermal modelling. The prototype currently being installed at the Whitehill Bordon eco-town could be the subject of this investigation. Original research studies could include an overheating assessment, annual solar fraction evaluation and financial payback evaluation based on the energy savings and actual cost of components.

(v) **Life cycle assessment of aerogel made by ambient pressure drying**

The aim of this study would be to undertake a full life cycle assessment of silica aerogel granules made by ambient pressure drying. Original research studies could include estimating the embodied energy and embodied CO_2, compared to figures for high and low temperature supercritical drying presented in this thesis. Taking this assessment further, the study could include wider LCA indicators such as human toxicity, photochemical ozone creation, global warming, acidification and eutrophication potential.

8.3 Restatement of Thesis and Contributions

The following statement summarises the key argument in this thesis, based on the evidence in the three contributions to knowledge and two supporting studies.

> *When applied appropriately in translucent insulation applications, granular aerogel can be a cost effective and environmentally sustainable material suitable for retrofitting into existing buildings to achieve deep reductions in energy consumption for heating, without detrimental impact in natural lighting or solar transmission.*

The three contributions to knowledge in this thesis are:

(i) **Study investigating the steady state & in-situ performance of translucent granular aerogel retrofitted to an existing single glazed window.** During in-situ testing a 10 mm thick prototype reduced the rate of heat loss through single glazing by 80 % without detrimental reductions in light transmission. Payback periods of 3.5-9.5 years are predicted depending on use. Study published in the *International Journal of Sustainable Engineering*.

(ii) **Streamlined life cycle assessment (LCA) of transparent silica aerogel made by supercritical drying following the ISO 14000 standards.** Silica aerogel was made using two of the three known aerogel production methods in a laboratory which had not been refined for mass manufacture. Despite this, the production energy and CO_2 burden from silica aerogel manufacture can be recovered within 0-2 years when retrofitted to buildings in a glazing application. Study published in the *Applied Energy* Journal.

(iii) **Study investigating the steady state & in-situ performance of a solar air collector incorporating granular aerogel in the cover, preheating air in a mechanical ventilation system with heat recovery in a domestic property.** During in-situ testing, peak outlet temperatures up to 45 °C were observed and validated to within 5 % of predictions, preheating the dwelling's fresh air supply up to 30 °C, facilitating internal temperatures of 21-22 °C without auxiliary heating. The predicted financial and CO_2 payback for a range of cover thicknesses is 7-13 years and 0-1 years, respectively. An efficiency up to 60 % and a financial payback of 4.5 years is predicted with an optimised design incorporating a 10 mm thick granular aerogel cover. Study published in the *Energy and Buildings* Journal.

References

Ashby M, Ferreira P and Schodek D. 2009. *Nanomaterials, nanotechnologies and design – an introduction for engineers and architects*, 1st edition, Butterworth-Heinemann, Oxford, UK

Aspen Aerogel. 2010. *Nanotechnology at work*, http://www.aerogel.com/

Aspen Aerogel. 2011. *Spaceloft data sheet*, http://www.aerogel.com/products/pdf/Spaceloft_DS.pdf

Athienitis AK and Ramadan H. 1999. Numerical model of a building with transparent insulation, *Solar Energy*, Vol. 67 (1-3), pp. 101-109

Baetens R, Petter-Jelle B and Gustavsend A. 2011. Aerogel insulation for building applications- a state-of-the-art review, *Energy and Buildings,* Vol. 43 (4), pp. 761-769

Bahaj ABS, James PAB, Jentsch MF. 2008. Potential of emerging glazing technologies for highly glazed buildings in hot arid climates, *Energy and Buildings*, Vol. 40 (5), pp. 720-731

Baker P. 2008. *Improving the thermal performance of traditional windows*, Glasgow Caledonian University, Historic Scotland, http://www.historic-scotland.gov.uk/thermal-windows.pdf

Barraclough T. 2012. *The risk of summer overheating in energy efficiency retrofitted UK domestic properties*, MSc Dissertation, School of Computing and Technology, University of East London, UK

Beaumont A. 2007. *Hard-to-treat homes in England*, W07 - housing regeneration and maintenance, Building Research Establishment, Watford, UK, http://www.enhr2007rotterdam.nl/documents/W07_paper_Beaumont.pdf [16/03/2010]

Bell M and Lowe R, 2000. Energy efficient modernisation of housing - a UK case study, *Energy and Buildings*, Vol. 32 (3), pp. 267-280

Berge B. 2009. *The ecology of building materials*, 2nd edition, Architectural press, Oxford, UK

Bernier MA and Plett EG. 1988. Thermal performance representation and testing of air solar collectors, *Solar Energy Engineering*, Vol.110, pp. 74-81.

BERR. 2007. *Energy trends - December 2007*, Department for Business Enterprise & Regulatory Reform http://www.berr.gov.uk/files/file43304.pdf [08/05/2012]

BERR. 2008. *Energy consumption in the United Kingdom - domestic data tables*, Table 3.5 - SAP rating 1970-2006, http://www.berr.gov.uk/whatwedo/energy/statistics/publications/ecuk/page17658.html

Binggeli C, 2003**.** *Building systems for interior designers*, 1st edition, John Wiley & Sons, New Jersey, USA

Boardman B, Darby S, Killip G, Hinnels M, Jardine C and Palmer J. 2005. *40% house*, University of Oxford, Environmental Change Institute, Oxford, UK, http://www.eci.ox.ac.uk/research/energy/downloads/40house/40house.pdf [20/11/2008]

Boonstra C. 2005. *European passive house in the UK?* Resource 05- low carbon technology showcase, Building Research Establishment, Watford, UK, http://www.resource05.co.uk/presentations/day1/chiel%20boonstra.pdf [12/03/2012]

Borgstein EH, Pakenham TJC and Raja AM. 2011. *Low energy retrofit of solid walled terraced dwellings*, CIBSE technical symposium, 6th-7th Sept 2011, Demontfort University, Leicester, UK

BRE. 1986. *Bison large panel system dwellings - construction details*, Hotchkiss AR and Edwards MJ, Building Research Establishment, BRE press, Watford, UK

BRE. 1987. *Reema large panel system dwellings - construction details*, Hotchkiss AR and Edwards MJ, Building Research Establishment, BRE press, Watford, UK

BRE. 1989. *Improving the habitability of large panel system dwellings*, Cornish JP, Hendson G, Uglow CE, Stephen RK and Sanders CH, Building Research Establishment, BRE press, Watford, UK

BRE. 1997. *Domestic energy report (bredem)* - general information leaflet 31, Building Research Establishment, BRE press, Watford, UK

BRE. 2008. *A study of hard-to-treat homes using the English house condition survey*, Part 1 – dwelling and household characteristics of hard-to-treat homes, Building Research Establishment, BRE press, Watford, UK

BRE. 2010. *Passivhaus primer*, Building Research Establishment, BRE press, Watford, UK http://www.passivhaus.org.uk/filelibrary/passivhaus%20standards/bre_passivhaus_primer.pdf [12/01/2012]

BSI. 2006a. BS EN ISO 14044-2006 *Environmental management - life cycle assessment - requirements and guidelines*, British Standards Institution, London, UK

BSI. 2007. BS EN ISO 6946-2007 *Building components and building elements - thermal resistance and thermal transmittance - calculation method*, British Standards Institution, London, UK

Bynum RT. 2001. *Insulation handbook*, 1st edition, Mcgraw-Hill, New York, USA

C&A Supplies. 2009. *Polycarbonate sheets* [online], http://www.casupply.co.uk/acatalog/polycarbonate_sheeting.html [07/04/2009]

Cabot. 2004. Cabot Nanogel promises unmatched energy savings - revolutionary insulating material makes the best window, wall and skylight products better, *Pigment & Resin Technology*, Vol. 33(6), pp. 345

Cabot and Roda. 2010. *Façade systems with Nanogel*, Cabot Corporation & Roda, http://www.cabot-corp.com/wcm/download/en-us/ae/facade%20systems%20roda.pdf [01/11/2010]

Cabot. 2011. *Cabot Nanogel aerogel- aerogel for insulation, daylighting and additives*, http://www.cabot-corp.com/aerogel/ [18/02/2011]

Campbell Scientific. 2005. *CR23X specifications*, http://s.campbellsci.com/documents/us/product-brochures/s_cr23x.pdf [18/05/2010]

Caps R and Fricke J. 1989. Fibrous insulations with transparent cover for passive use of solar energy, *Thermophysics,* Vol. 10 (2), pp. 493-504.

CEPMC. 2000. *Guidance for the provision of environmental information on construction products, council for European producers of materials for construction*, Council for European producers of materials for construction, Brussels, Belgium

Cheeseman B, Mavroulidou M, Maidment G, Smith M and Potter N. 2007. *Developing an in-situ post construction quality control methodology to ensure better energy efficiency of buildings*, Proceedings of the 10th international conference on environmental science and technology, 5th-7th Sept 2007, Greece

Chung DL, 2010. *Composite materials- functional materials for modern technologies*, 2nd edition, Springer, New York, USA

CIBSE. 2006. *Environmental design - CIBSE guide A*, 7th edition, CIBSE publications department, Chartered institution of building services engineers London, UK

CIBSE. 2008. *TRY hourly weather data set – London*, test reference year from 1983-2004 data sets, Chartered institution of building services engineers London, UK http://www.cibse.org/ [08/11/2010]

CLG. 2001. *English house condition survey - supporting tables*, profile of the stock, table a1.3 dwelling type by age category, Department for communities and local government, West Yorkshire, UK http://www.communities.gov.uk/archived/general-content/housing/224506/englishhouse/ [01/06/2009]

CLG. 2003. *English house condition survey – 2003 regional report*- supplementary tables, Department for communities and local government, West Yorkshire, UK http://www.communities.gov.uk/documents/housing/xls/152975.xls [10/06/2009]

CLG. 2004a. *English house condition survey 2004 - annual report*, Decent homes and decent place, Department for communities and local government, West Yorkshire, UK

CLG. 2004b. *Age of commercial and industrial stock - local authority level 2004* (England and Wales), table 2.1 number of hereditaments by region and age for each bulk class, Department for communities and local government, http://www.communities.gov.uk/archived/publications/planningandbuilding/ageindustrialstock

CLG. 2006. *Review of sustainability of existing buildings*, Department for communities and local government, http://www.communities.gov.uk/documents/planningandbuilding/pdf/154500.pdf

CLG. 2008. *Improving the energy efficiency of our buildings - a guide to display energy certificates and advisory reports for public buildings*, Department for communities and local government, http://www.communities.gov.uk/documents/planningandbuilding/pdf/20.pdf [12/03/2012]

CLG. 2010. *A technical manual for SBEM – UK volume*, Department for communities and local government, http://www.ncm.bre.co.uk/filelibrary/sbem_technical_manual_v3.5.a_01mar10.pdf [12/03/2012]

CLG. 2012. *English housing survey - headline report 2010-2011*, Department for communities and local government, http://www.communities.gov.uk/documents/statistics/pdf/2084179.pdf [09/03/2012]

Climate Change Act. 2008. *Carbon targeting and budgeting*, Chapter 27, Part 1 - the target for 2050, her Majesty's stationery office limited, London, UK

Clinch JP and Healy JD. 2001. Cost benefit analysis of domestic energy efficiency, *Energy Policy*, Vol. 29 (2), pp. 113-124

Colson W. 2007. US Patent 8082916, *Solar heating blocks*, filed April 5th 2007 http://www.google.com/patents/us8082916

Cremers J. 2005. Applications of vacuum insulation systems in the building envelope: technological, structural and architectural aspects, PhD thesis, Technical University of Munich, http://mediatum2.ub.tum.de/node?id=601020 [09/08/2012]

Dalenbäck JO. 1996. Solar energy in building renovation, *Energy and Buildings*, Vol. 24 (1), pp. 39-50

Darby S. 2006**.** *The effectiveness of feedback on energy consumption*, Environmental change institute, University of Oxford, UK, http://www.eci.ox.ac.uk/research/energy/downloads/smart-metering-report.pdf [05/08/2010]

DECC. 2010a. *SAP 2009*, version 9.90 (may 2010), the government's standard assessment procedure for energy rating of dwellings, Department of Energy and Climate Change, BRE Presss, Watford, UK, http://www.bre.co.uk/filelibrary/sap/2009/sap-2009_9-90.pdf [30/05/2010]

DECC. 2010b. *Paving the way for a Green Deal: Extending the carbon emissions reduction target supplier obligation to December 2012,* [09/03/2012]

DECC. 2010c. *The green deal – a summary of the government's proposals*, Department of Energy and Climate Change, http://www.decc.gov.uk/assets/decc/legislation/energybill/1010-green-deal-summary-proposals.pdf [09/03/2012]

DECC. 2011. *Evaluation of the community energy saving programme*, Department of Energy and Climate Change, Cag, Ipsos Mori & the BRE, http://www.decc.gov.uk/assets/decc/11/funding-support/3342-evaluation-of-the-community-energy-saving-programm.pdf [08/03/2012]

Deshpande R, Hua DW, Smith DM and Brinker JC. 1992. Pore structure evolution in silica gel during aging/drying, III effects of surface tension, *Non-Crystalline Solids*, Vol. 144, pp. 32-44

Dolley P, Martin C and Watson M. 1994. Performance of walls clad with transparent insulation material in realistic operation, *Building and Environment*, Vol. 29 (1), pp. 83-88

Dowson M, Harrison D, Craig S and Gill Z. 2011. Improving the thermal performance of single-glazed windows using translucent granular aerogel, *International Journal of Sustainable Engineering*, Vol. 4, pp. 266-280

Dowson M, Grogan M, Birks T, Harrison D and Craig S. 2011. Streamlined life cycle assessment of transparent silica aerogel made by supercritical drying, *Applied Energy*, Vol. 97, pp. 396-404

Dowson M, Pegg I, Harrison D and Dehouche Z. 2012. Predicted and in situ performance of a solar air collector incorporating a translucent granular aerogel cover, *Energy and Buildings*, Vol. 49, pp. 173-187

Dowson M, Poole A, Harrison D and Susman G. 2012. Domestic UK retrofit challenge: Barriers, incentives and current performance leading into the Green Deal, *Energy Policy,* Vol. 50, pp. 294-305

Duer K and Svendsen S. 1998. Monolithic silica aerogel in super insulating glazings, *Solar Energy*, Vol. 63 (4), pp. 259-267

Duffie JA and Beckman WA. 2006. *Solar engineering of thermal processes*, 3rd edition, John Wiley & Sons inc, New Jersey, USA

EEPH. 2008. *The insulation industry, working in partnership with government to insulate the existing housing stock by 2050*, Energy efficient partnership for housing

EEPH. 2009. *Solid wall insulation supply chain review*- Purple market research for the EEPH and the Energy Saving Trust, Energy efficient partnership for housing, http://itsacoastthing.com/pdf/solid%20wall%20insulaton%20chain%20review.pdf [04/03/2012]

EEPH. 2010. *2050 roadmap for energy efficiency and low carbon housing*. Summary report of evidence base. Draft for discussion, Energy efficient partnership for housing, Sept 2010

EEA. 2011. *Recycling* [online], European Aluminium Association, http://www.alueurope.eu/ [18/11/2011]

EHA. 2008. *New tricks with old bricks*, Empty homes agency, London, UK, http://www.emptyhomes.com/documents/publications/reports/new%20tricks%20with%20old%20bricks%20-%20final%2012-03-081.pdf [10/02/2009]

Eames PC. 2008. Vacuum glazing- current performance & future prospects, *Vacuum*, Vol. 82 (7), pp. 717–722

Francis JRD. 1976. Supervision and Examination of Higher Degree Students, Bulletin of the University of London, 31, 3 - 6

Fricke J, Caps R, Büttner D, Heinemann U, Hümmer E and Kadur A. 1987. Thermal loss coefficients of monolithic and granular aerogel systems, *Solar Energy Materials*, Vol.16 (1-3), pp. 267-274

Fricke J. 1988**.** Aerogels, *Scientific American*, Vol. 258 (5), pp. 92-97

Fricke J. 1992. Aerogels and their applications, *Non-Crystalline Solids, Vol. 147+148, pp. 356-362*

Fricke J and Tillotson T. 1997. Aerogels- production, characterization and applications, *Thin Solid Films*, Vol.297 (1-2), pp. 212-223

GBA. 2007. *Green building product certification and labelling systems*, Green Building Alliance, http://www.pa-greenbuildingproducts.org/green_product_labeling.aspx [06/08/2009]

GGF. 2009. *Carbon calculator*, Glass and Glazing Federation, http://www.ggf.org.uk/carboncalculator.aspx [10/06/2009]

Granta Design. 2012. *Eco audit tool*, http://www.grantadesign.com/products/ecoselector/ [1/8/2012]

Greenspec. 2010. *Materials - embodied energy* [online], accessed, http://www.greenspec.co.uk/html/materials/embodied_energy.html [7/2/2010]

Hammond G and Jones C. 2008. *Inventory of carbon and energy (ice)*, Version 1.6a, University of Bath, UK, http://www.persona.uk.com/bexhill/core_docs/cd-09/cd-09-45.pdf [02/02/2010]

Hamza N and Greenwood D. 2008. Energy conservation regulations- impacts on design and procurement of low energy buildings, *Building and Environment*, Vol.44 (5), pp. 929-936

Harris DJ. 1999. A quantitative approach to the assessment of the environmental impact of building materials, *Building and Environment*, Vol.34 (6), pp. 751-758

Hartmann J, Rubin M and Arasteh D. 1987. *Thermal and solar optical properties of silica aerogel for use in insulated windows*, Proceedings of the 12th annual passive solar conference, June 12th-16th, Portland, Oregon, USA

Haruyama. 2001. Performance of peltier elements as a cryogenic heat flux sensor at temperatures down to 60k, *Cryogenics*, Vol. 41, pp. 335-339

Hastings R and Mørck O. 2000. *Solar air systems – a design handbook*, 1st edition, Jame & James Ltd, London, UK

HM Government. 2010. *Conservation of fuel and power approved document L1b*, the Building Regulations 2000, 2010 edition, NBS, Riba enterprises, London, UK

HM Treasury. 2003. *The green book- appraisal and evaluation in central government*, Treasury Guidance, The Stationary Office, London, UK

Hollands KGT. 1965. Honeycomb devices in flat-plate solar collectors, *Solar Energy*, Vol. 9 (3), pp. 159-164

Holmes MJ and Hacker JN. 2007. Climate change, thermal comfort and energy- meeting the design challenges of the 21st century, *Energy and Buildings*, Vol. 29 (7), pp. 802-814

Hong SH, Oreszczyn T and Ridley I. 2006. The impact of energy efficient refurbishment on the space heating and fuel consumption in English dwellings, *Energy and Buildings*, Vol. 38 (10), pp. 1171-1181

Hrubesh LW. 1998. Aerogel applications, *Non-Crystalline Solids*, Vol. 225, pp. 335-342

Hunter Douglas. 2007. *Warm light wall system chosen for zero energy home*, Press release on 02/10/2007 by Office News Wire, http://www.officenewswire.com/4746

Hunter Douglas. 2008. G*reen R&D- Hunter Douglas warm light wall,* Press release on 26/02/2008 by Eco Home Magazine, http://www.ecohomemagazine.com/alternative-energy/green-rd-hunter-douglas-warm-light-wall.aspx

Hüsing N and Schubert U. 2005. *Aerogels*, Institute for inorganic chemicals, Vienna University of Technology, Austria, http://www.wiley-vch.de/vch/software/ullmann/pdf/aerogels.pdf [11/01/2010]

Hutchins MG and Platzer WJ. 1996. The thermal performance of advanced glazing materials, *Renewable Energy*, Vol. 8 (1-4) pp. 540-545

IEA. 1999. *Solar renovation concepts and systems*, A report of task 20 subtask F, Solar Heating and Cooling Programme, International Energy Agency

Jensen SØ and Bosanac M. 2002. *Connectable solar air collectors*, SEC-R-22, Solar Energy Centre Denmark, Danish Technological Institute, Denmark

Jensen KI, Schultz JM and Kristiansen FH. 2004. Development of windows based on highly insulating aerogel glazings, *Non-Crystalline Solids*, Vol. 350, pp.351–357

Johnston D, Lowe RJ and Bell M. 2005. An exploration of the technical feasibility of achieving CO_2 emission reductions in excess of 60% within the UK housing stock by the year 2050, *Energy Policy*, Vol. 33 (13), pp. 1643-1659

Jones I and Rudlin J. 2006. *Process monitoring methods in laser welding of plastics*, proceedings of the 2nd international conference on joining plastics, national physical laboratory, 25th-26th April 2006, London, UK, pp. 233

Kaushika ND and Reddy KS. 1999. Thermal design and field experiment of transparent honeycomb insulated integrated-collector-storage solar water heater, *Applied Thermal Engineering*, Vol. 19 (2), pp. 145-161.

Kaushika ND and Sumathy K. 2003. Solar transparent insulation materials- a review, *Renewable and Sustainable Energy Reviews*, Vol. 7 (4), pp. 317-351

Killip G. 2005. *Built fabric & building regulations*, background material F, 40% house project, Environmental Change Institute, University of Oxford, UK, http://www.eci.ox.ac.uk/research/energy/downloads/40house/background_doc_f.pdf [02/05/2012]

Kistler S. 1931. Coherent expanded aerogels and jellies, *Nature*, Vol. 127 (3211), pp. 741

Klems J and Keller H. 1988. *In-situ measurements of fenestration u-values and overall thermal performance*, Lawrence Berkeley Laboratory, California, USA

Langdon W, 1980. Movable Insulation: A guide to reducing heating and cooling losses through the windows in your home, ISBN 0878572988, Rodale Press, Emmaus, Pa, USA

Lexan. 2011. *Polycarbonate filled with Nanogel* [online], Amerilux, Lexan, http://www.ameriluxinternational.com/html/architectdata/nanogel/documents/nanogeldata.pdf [28/02/2011]

Lien A, Hestnes A and Aschehoug Ø. 1997. The use of transparent insulation in low energy dwellings in cold climates, *Solar Energy*, Vol. 59 (1-3), pp. 27-35

Lowe R and Oreszczyn T. 2008. Regulatory standards and barriers to improved performance for housing, *Energy Policy*, Vol. 36 (12), pp. 4475-4481

Manz H, Brunner S and Wullschleger L. 2006. Triple vacuum glazing- heat transfer and basic mechanical design constraints, *Solar Energy*, Vol. 80 (12), pp. 1632-1642

MBDC. 2008. *Cradle to cradle certification program*, Version 2.1.1, Mcdonough Braungart Design Chemistry, Charlottesville, USA, http://www.epea.com/documents/outline_certificationv2_1_1.pdf [18/02/2010]

Menezes A, Cripps A, Bouchlaghem D and Buswell R. 2011. Predicted vs. actual energy performance of non domestic buildings- using post occupancy evaluation data to reduce the performance gap, *Applied Energy*, Vol 97, pp. 355-364

Michel J and Trombe F, 1971. French Patent Anvar Trombe Michel BF 7123778, filed June 29th, 1971

Milne G and Boardman B. 2000. Making cold homes warmer - the effect of energy efficiency improvements in low-income homes, *Energy Policy*, Vol. 28 (6-7), pp. 411-424

Mintel. 2007. *Curtains up for Britain's window shutters and blinds market*, Press release, Mintel oxygen reports, http://www.marketresearchworld.net/index2.php?option=com_content&do_pdf=1&id=1166 [14/07/2009]

Mitchell M. 2000. *Design and micro-fabrication of a molded polycarbonate continuous flow polymerase chain reaction device*, PhD thesis, Department of Mechanical Engineering, Louisiana State University, Louisiana, USA

MMG. 2004. *White paper - silica aerogels*, Microstructured Materials Group, Lawrence Berkeley Laboratory, California, USA, http://www.sps.aero/key_comspace_articles/tsa-009_white_paper_silica_aerogels.pdf [28/08/2010]

Monsen WA, Klein SA and Beckman WA. 1982. The un-utilizability design method for collector storage walls, *Solar Energy*, Vol. 25 (5), pp. 421-429

MTP. 2007. *Innovative glazing* - supporting UK government policy on sustainable products, Market Transformation Programme, https://www.pauljervis.net/filemgmt/visit.php?lid=197 [14/07/2009]

Muthesius S. 1984. *The English terraced house*, 1st edition, Yale University Press, New Haven, USA

National Auditing Office. 2009. *The warm front scheme*, report by the controller and auditing general, HC 126 session 2008-2009, The Stationary Office, London, UK, http://www.nao.org.uk/publications/0809/the_warm_front_scheme.aspx [09/03/2010]

National Auditing Office. 2010. *The decent homes programme*, report by the controller and auditing general, hc 212 session 2009-2010, The Stationary Office, London, UK, http://www.nao.org.uk/publications/0910/the_decent_homes_programme.aspx [09/03/2010]

Neelis M, Patel M, Gielen D and Blok K. 2005. Modelling CO_2 emissions from non-energy use with the non-energy use emission accounting tables (neat) model, *Resources Conservation and Recycling*, Vol. 45 (3), pp. 226-250

Nordgaard A and Beckman WA. 1992. Modelling of flat-plate collectors based on monolithic silica aerogel, *Solar Energy*, Vol.49 (5), pp. 387-402

Olivier D. 2001. *Building in ignorance- demolishing complacency, improving the energy performance of 21st century homes*, EEASOX and ACE, Herefordshire, UK

Ortjohann J. 2001. *Granular aerogel for the use in solar thermal collectors*, ISES 2001 solar world congress, Adelaide, South Australia

Parker BF. 1981. Derivation of efficiency & loss factors for solar air heaters, *Solar Energy*, Vol. 26 (1), pp 27-32

Perspex. 2010. *Perspex for glazing*- PXTD 236, http://www.qdplastics.co.uk/assests/docs/acrylic/perspex_glazing236.pdf [18/05/2010]

Peuportier B and Michel J. 1995. Comparative analysis of active and passive solar heating systems with transparent insulation, *Solar Energy*, Vol. 54 (1), pp. 13-18

Peuportier B, Kohler N, Lewis O, Tombazis A and Voss K. 2000. *Education of architects in solar energy and environment*, Section 3.1 - advanced glazing and transparent insulation, http://www.cenerg.ensmp.fr/ease/advanced_glazing.pdf [15/10/2010]

Phillips EM and Pugh DS. 1994. How to get a PhD - a handbook for students and their supervisors, 2nd Edition, Open University Press

Platzer WJ. 1987. Solar transmission of transparent insulation material, *Solar Energy Materials*, Vol. 16 (1-3), pp. 275-287

Platzer WJ and Goetzberger A. 2004. *Recent advances in transparent insulation technology*, transparent insulation - TI8, Fraunhofer-Institute for Solar Energy Systems, Freiburg, Germany

Porteous C and Macgregor K. 2005. *Solar architecture in cool climates*, Earthscan, London, UK

Power S. 2000. The development of the Ballymun housing scheme, Dublin 1965-1969, *Irish Geography*, Vol. 33 (2), pp. 199-212

Power A. 2008. Does demolition or refurbishment of old and inefficient homes help to increase our environmental, social and economic viability? *Energy Policy*, Vol. 36 (12), pp. 4487-4501

Purple. 2007. *Trade sector profiles*, UK domestic glazing sector, http://www.eeph.org.uk/uploads/documents/partnership/est%20glazing%20sector%20profile%20june%202007%20final2.pdf [26/03/2012]

Ravetz J. 2008. State of the stock - what do we know about existing buildings and their future prospects? *Energy Policy*, Vol. 36 (12), pp. 4462-4470

Reim M, Beck A, Körner W, Petricevic R, Glora M, Weth M, Schliermann T, Fricke J, Schmidt C and Pötter F. 2002. Highly insulating aerogel glazing for solar energy usage, *Solar Energy*, Vol.72 (1), pp. 21-29

Reim M, Körner W, Manara J, Korder S, Arduini-Schuster M, Ebert H, Fricke J. 2005. Silica aerogel granulate material for thermal insulation and daylighting, *Solar Energy*, Vol. 79, pp. 131-139

RHI. 2011. *Tariff level tables*, Renewable Heat Incentive, http://www.rhincentive.co.uk/ [28/11/2011]

Roberts S. 2008a. Altering existing buildings in the UK, *Energy Policy*, Vol. 36 (12), pp. 4482-4486

Roberts S. 2008b. Effects of climate change on the built environment, *Energy Policy*, Vol. 36 (12), pp. 4552-4557

Robinson PD and Hutchins MG. 1994. Advanced glazing technology for low energy buildings in the UK, *Renewable Energy*, Vol. 5 (1), pp. 298-309

Rommel M and Wagner A. 1992. Application of transparent insulation materials in improved flat-plate collectors and integrated collector storage system, *Solar Energy*, Vol.49 (5), pp. 371-380

Rubin M and Lampert CM. 1983. Transparent silica aerogels for window insulation, *Solar Energy Materials*, Vol.7 (4), pp. 393-400

Sadineni SB, Madala S and Boehm RF. 2011. Passive building energy savings- a review of building envelope components, *Renewable and Sustainable Energy Reviews*, Vol. 15 (8), pp. 3617-3631

Schmidt CH, Goetzberger A and Schmid J. 1988. Test results and evaluation of integrated collector storage systems with transparent insulation, *Solar Energy*, Vol. 41 (5), pp. 487-494.

Schmidt A, Jenson A, Clausen A, Kamstrup O and Postlethwaite D. 2004. A comparative life cycle assessment of building insulation products made of stone wool, paper wool and flax - Part 1, *LCA Case Studies*, Vol. 9 (1), pp. 53-66

Schultz JM. 1993. Insulating shutters with granular aerogel, Thermal insulation laboratory, Report No. 242, Technical University of Denmark, Denmark

Schultz JM, Jensen KI and Kristiansen FH. 2005. Super insulating aerogel glazing, *Solar Energy Materials & Solar Cells*, Vol. 89 (2-3), pp. 275-285

Schultz JM and Jensen KI. 2008. Evacuated aerogel glazings, *Vacuum*, Vol. 82 (7), pp. 723-729

Schwertfeger F, Frank D and Schmidt M. 1998. Hydrophobic waterglass based aerogels without solvent exchange or supercritical drying, *Non-Crystalline Solids*, Vol. 225, pp. 24-29

SETAC. 2003. *Lifecycle assessment in building and construction - a state-of-the-art report*, Society of environmental technology and chemistry, 1st edition, SETAC Press, USA

Shorrock L, Henderson J and Utley J. 2005. *Reducing carbon emissions from the UK housing stock*, http://projects.bre.co.uk/pdf_files/br480reducingcarbonemissionsfromukhousing.pdf [20/11/2008]

Simmler H and Brunner S. 2005. Vacuum insulation panels for building application - basic properties, ageing mechanisms and service life, *Energy and Buildings*, Vol. 37 (11), pp. 1122-1131

Smil V. 2008. *Energy in nature and society - general energetics of complex systems*, 1st edition, MIT press, Cambridge, UK

Smirnova I. 2002. *Synthesis of silica aerogels and their application as a drug delivery system*, approved dissertation for the doctorate of engineering, faculty III - process sciences, Technical University of Berlin, Berlin, Germany

Soleimani-Dorcheh A and Abbasi MH. 2008. Silica aerogel - synthesis, properties and characterization, *Materials Processing Technology*, Vol. 199 (1-3), pp. 10-26

Steiner S and Walker W. 2010. *open source nanotech* [online], http://www.aerogel.org/ [11/01/2010]

Suehrcke H, Daldehog D, Harris JA, Lowe RW. 2004. Heat transfer across corrugated sheets and honeycomb transparent insulation, *Solar Energy*, Vol. 76 (1-3), pp. 351-358

Svendsen S. 1992. Solar collector with monolithic silica aerogel, *Non-Crystalline Solids*, Vol. 145, pp. 240-243

Tewari PH, Hunt AJ and Lofftus KD. 1985. Ambient-temperature supercritical drying of transparent silica aerogels, *Material Letters*, Vol. 3 (9-10), pp. 363-367

Twidell JW, Johnstone C, Zuhdy B and Scott A. 1994. Strathclyde University's passive solar, low-energy, residences with transparent insulation, *Solar Energy*, Vol. 52 (1), pp.85-99

UKGBC. 2008. *Low carbon existing homes*, United Kingdom Green Building Council, London, UK, http://www.ukgbc.org/site/document/download/?document_id=371 [20/11/2008]

Utley J and Shorrock LD. 2008. *Domestic energy fact-file 2008*, Building Research Establishment, BRE press, Watford, UK, http://www.bre.co.uk/filelibrary/pdf/rpts/fact_file_2008.pdf [10/02/2010]

Van-Bommel MJ, De-Haan AB. 1995. Drying of silica aerogel with supercritical carbon dioxide, *Non-Crystalline Solids*, Vol. 186, pp. 78-82

Vesma. 2009. UK degree day figures, http://www.vesma.com/ddd/index.html [10/06/2009]

Voss K. 2000. Solar energy in building renovation – results and experience of international demonstration buildings, *Energy and Buildings*, Vol. 32 (3), pp. 291-302

Weir G and Muneer T. 1998. Energy and environmental impact of double glazed windows, *Energy Conversion*, Vol. 39 (3-4), pp. 243-256

Werner M and Brand L. 2010. *Aerogels* [online], general sector reports, chemistry and materials, http://www.observatorynano.eu/project/filesystem/files/wp2_chemistrymaterials_focusreport_aerogels_29_04_2010.pdf [20/01/2011]

Wittwer V. 1992. Development of aerogel windows, *Non-Crystalline Solids*, Vol. 145, pp. 233-236

Wong IL, Eames PC and Perera RS. 2007. A review of transparent insulation systems and the evaluation of payback period for building applications, *Solar Energy*, Vol. 81 (9), pp. 1058-1071

Yohanis YG and Norton B. 2002. Lifecycle operational and embodied energy for a generic single-storey office building in the UK, *Energy*, Vol. 27 (1), pp. 77-92

Yokogawa H. 2005. *Handbook of sol-gel science & technology*, Volume 2, Chapter 13 - thermal conductivity of silica aerogels, Sumio Sakka (editor), Kluwer Academic Publishers, New York, USA

Zhang Z, Zuo R, Li P, Su W. 2009. Thermal performance of solar air collector with transparent honeycomb made of glass tube, *Science in China Series E*, Vol. 52 (8), pp. 2323-2329

Zhu Q, Li Y, Qui Z. 2007. *Research progress on aerogels as transparent insulation materials*, International Conference on Power Engineering, Oct 23rd -27th, Hangzhou, China, Vol. 1, pp. 1117 - 1121

Zimmerman M and Bertschinger H. 2001. High performance thermal insulation systems- vacuum insulation products (vip), International Energy Agency, Duebendorf, Switzerland, pp. 8

Appendices

Energy Policy 50 (2012) 294–305

Contents lists available at SciVerse ScienceDirect

Energy Policy

journal homepage: www.elsevier.com/locate/enpol

Domestic UK retrofit challenge: Barriers, incentives and current performance leading into the Green Deal

Mark Dowson [a,b,*], Adam Poole [b], David Harrison [a], Gideon Susman [b]

[a] School of Engineering and Design, Brunel University, London, UB8 3PH, UK
[b] Buro Happold Ltd, 17 Newman Street, London, W1T 1PD, UK

HIGHLIGHTS

- CERT, CESP, Decent homes and Warm Front have not targeted the full extent of private and social homes.
- There is a risk that Green Deal will fail due to low consumer appeal and low incentives for investors.
- Up to half of the predicted energy savings from whole house retrofits may not be achieved in practice.
- Passivhaus is identified as best practice for retrofit, yet there is a lack of skills and components.
- Embodied energy in materials and components must be better understood to achieve life cycle savings.

ARTICLE INFO

Article history:
Received 22 March 2012
Accepted 11 July 2012
Available online 16 August 2012

Keywords:
Hard-to-treat homes
Green Deal
Passivhaus

ABSTRACT

This paper reviews the thermal performance of the existing UK housing stock, the main fabric efficiency incentive schemes and the barriers to obtaining deep energy and CO_2 savings throughout the stock. The UK faces a major challenge to improve the thermal performance of its existing housing stock. Millions of dwellings possess 'hard-to-treat' solid walls and have glazing which is not cost effective to improve. A range of fabric efficiency incentive schemes exist, but many do not target the full range of private and social housing. From now on, the Green Deal will be the UK's key energy efficiency policy. However, the scheme is forecasted to have low consumer appeal and low incentives for investors. Moreover, calculated Green Deal loan repayments will be reliant upon estimated energy savings, yet it is claimed that retrofit measures may only be half as effective as anticipated due to a lack of monitoring, poor quality installation and the increased use of heating following refurbishment. Looking to Germany, there has been success through the Passivhaus standard, but the UK currently lacks appropriate skills and cost effective components to replicate this approach. In addition, the embodied energy in retrofit products and materials threatens to counter operational savings.

1. Introduction

The thermal performance of our existing building stock must improve significantly for the UK to meet its target to reduce CO_2 emissions by 80%, against the 1990 baseline by 2050 (Climate Change Act, 2008). In 2008, the country's 26 million dwellings were estimated to be responsible for 27% of all UK CO_2 emissions (Utley and Shorrock, 2008). According to recent forecasts, 75–85% of the current UK building stock will still be in use by 2050 (Power, 2008; Ravetz, 2008). This is a major issue, since millions of these properties contain poorly performing solid walls, single glazing and uninsulated roofs/floors responsible for a significant amount of wasted heat. These features can be expensive and disruptive to improve, furthermore, improvement can be limited by available space and planning restrictions (Beaumont, 2007; EEPH, 2008). There is scope to retrofit these buildings to make deep cuts in CO_2 emissions, but effective implementation is no trivial task. Solutions must account for the variety in age, size, quality, composition, function and social value of the existing building stock, as well as the different needs, expectations and budgets of homes owners and occupiers.

2. Survey of English housing stock

The English Housing Survey is a national survey commissioned by the Department for Communities and Local Government to monitor the age, type, tenure and condition of the English housing stock. Approximately 6200 houses undergo physical inspections annually by qualified surveyors with findings extrapolated to

* Corresponding author. Tel.: +44 07706 260523, +44 02079 279700.
E-mail addresses: mark.dowson@burohappold.com, darkmowson@hotmail.com (M. Dowson), adam.poole@burohappold.com (A. Poole), david.harrison@brunel.ac.uk (D. Harrison), gideon.susman@burohappold.com (G. Susman).

0301-4215/$ - see front matter © 2012 Elsevier Ltd. All rights reserved.
http://dx.doi.org/10.1016/j.enpol.2012.07.019

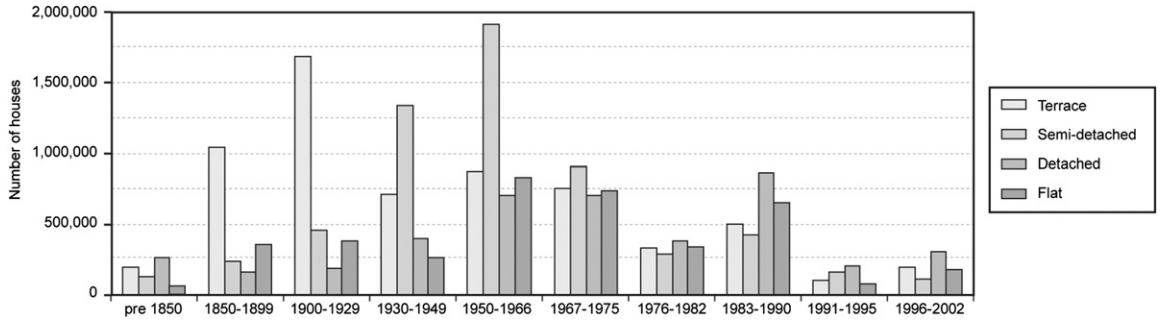

Fig. 1. Profile of the UK Housing stock by age and type.

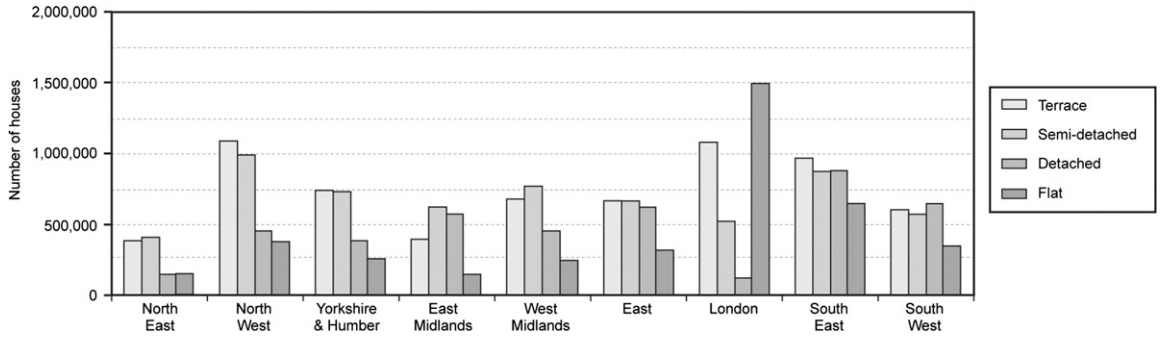

Fig. 2. English housing stock, dwelling type by region.

represent the 20.4 million dwellings, which make up the English housing stock (CLG, 2012). Fig. 1 displays a profile based on statistical data from CLG (2001), segmenting the housing stock by age and type, across each major construction period. As shown, England contains millions of Victorian and Edwardian terraced houses, post-war semi-detached houses and flats built during the 1960s. Building Regulations were only enforced after 1976, setting minimum standards for insulation. As a result solid walls, un-filled cavity walls, single glazing, un-insulated roofs and un-insulated floors were common construction features before this time.

Increasing housing demand, as well as the availability of construction materials and machinery over the past century, has led to distinctive types of dwellings across the English housing stock (Beaumont 2007). Fig. 2 displays a regional stock profile segmented by house type generated using statistics from CLG (2003). As shown, London has a particularly high proportion of flats and terraced houses, whereas Northern regions tend to have higher concentrations of terraced houses and semi-detached houses.

3. History of UK Building Regulations

The thermal efficiency of the UK building stock is governed through the Building Regulations. The UKs first mandatory Building Regulations were enforced in Scotland in 1964. England and Wales soon followed with separate regulations in 1966, as did Northern Ireland in 1967 (Killip, 2005). Each of these regulations was produced largely in response to public health issues rather than a need to improve the energy efficiency of dwellings. Only following the 1973 energy crisis were these standards later revised in 1976 to provide minimum *U*-value standards to limit the heat losses through the walls, roof and floors in new dwellings. Table 1 lists the historic minimum *U*-values and air permeability targets for compliance with Building Regulations for England and Wales from 1976 to 2006, generated using numeric data from Killip (2005). As shown, continual revisions to Building Regulations have caused *U*-value targets for all new buildings to become increasingly stringent. However, it should be noted that *U*-value requirements for exposed walls only imply the presence of full cavity wall insulation in new buildings registered after 1995. Furthermore, minimum *U*-values for windows were only raised beyond single glazing standards by 1990. Additional measures such as eliminating thermal bridges and limiting air permeability to reduce heat losses through infiltration also occurred as part of the 1990 Building Regulations.

Table 1
Historic *U*-values & air permeability targets in the building regulations.

Building Regulations	Exposed walls (W/m^2 K)	Roof (W/m^2 K)	Floor (W/m^2 K)	Windows (W/m^2 K)	Air permeability (m^3/m^2h @ 50Pa)
1976	1.0	0.6	n/a	n/a	n/a
1982	0.6	0.35	n/a	n/a	n/a
1990	0.45	0.25	0.45	3.3	10
1995	0.45	0.25	0.35	3.3	10
2000	0.35	0.25	0.25	2.2	10
2006	0.35	0.16–0.25	0.25	2.0–2.2	10

From 2006, Part L1A of the Building Regulations for England and Wales required all new dwellings to demonstrate design compliance using the Standard Assessment Procedure (SAP). SAP is a government approved calculation method, which estimates a dwellings CO_2 emissions, in kg CO_2/m^2/year, based upon the design *U*-values, air tightness level, efficiency of space heating, lighting and hot water systems, as well as pumps/fans and any savings from renewable technologies. For Part L1A compliance, the calculated Dwelling Emission Rate (DER) must demonstrate a 25% improvement over a Target Emission Rate (TER) calculated from

a notional building constructed to 2002 standards. In 2010, compliance levels were raised to a 25% reduction over a notional building constructed to 2006 standards. For 2013, Building regulations (under consultation) are expected to raise compliance levels further to a 44% reduction over 2006 standards. Future revisions are anticipated to set 'zero carbon' then 'net carbon' targets for all developers, resulting in an increasing need for well insulated building fabrics and efficient systems, with more reliance on renewable technologies. Currently, SAP only deals with 'regulated' loads, excluding energy use and CO_2 emissions associated with small power plug loads. Moreover SAP, currently does not allow variations in household size, heating patterns or geographic location, although all of these are expected to be introduced into SAP in connection with its use in support of the government's new Green Deal.

4. Thermal efficiency of existing housing

An output of the SAP calculation is a rating from 1 to 100, which provides an indication of the overall efficiency of a dwelling. Larger scores represent higher efficiencies and lower running costs. For existing buildings, the SAP rating can be calculated from a reduced SAP method (RdSAP) based upon an on-site survey, which considers the dwelling's size, construction characteristics, thermal insulation levels, annual running costs as well as the installed heating and hot water systems and lighting type (DECC, 2010a). Fig. 3 displays a representation of the SAP ratings across the stock, based upon the findings of the English Housing Survey, presented in CLG (2006). As seen, many of the highest SAP ratings can be found in the post 1990 stock due to the enforcement of the Building Regulations. Approximately 60% of buildings constructed after 1990 have SAP ratings over 70. In contrast, the highest concentrations of the lowest SAP ratings can be found in the older pre-1919 stock, demonstrating a large correlation between age and energy performance. Around 40% of pre-1919 homes have SAP ratings from 1 to 40 (Roberts, 2008a).

A proposed target for 2050 is to raise the average SAP rating of the UK building stock to 80, in line with today's modern building standards (Roberts, 2008a). Comparatively, the national average SAP rating is much lower, being 52.1 in 2006 (BERR, 2008). Apart from age, there is also a correlation between energy performance and tenure. The average SAP rating across social housing is 57, whereas the average across the private sector is 47 (Ravetz, 2008). This can be attributed to higher rates of loft and cavity wall insulation in the social sector due to government interventions such as 'Warm front' and 'Decent homes', aiming to lower fuel bills and improve the internal condition of homes. By comparison, private sector landlords have little incentive to invest in the energy efficiency of their properties, given that it is the tenants who benefit from lower fuel bills (CLG, 2006, UKGBC, 2008). The introduction of Energy Performance Certificates (EPCs) in 2007 may serve to help this challenge by providing information on the current energy rating of a dwelling to potential buyers or tenants (EEPH, 2010). Nonetheless, this issue remains a major barrier since many properties in the private sector are amongst the lowest in terms of thermal efficiency (CLG, 2006).

5. "Hard-to-treat" homes

"Hard-to-treat" homes are defined as dwellings which possess solid walls, no loft space to insulate, no connection to the gas network or are high-rise. Consequently, these dwellings cannot be upgraded easily or cost effectively using conventional measures such as cavity wall insulation, loft insulation and modern gas central heating. According to the BRE (2008), there are approximately 10.3 million hard-to-treat homes across the UK, equivalent to 40% of the existing housing stock. Nine million of these are in England, 6.5 million of which possess solid walls. 1.5 million have no loft space, 0.4 million are high rise and 2.7 million are off the gas grid. These statistics, from BRE (2008), are shown in Table 2, with their distribution illustrated in Fig. 4.

According to Beaumont (2007), more than 66% of hard-to-treat households are in fuel poverty. A household is said to be in fuel poverty if its occupants need to spend more than 10% of their

Table 2
The number of hard-to-treat homes in the UK.

	England (m)	Scotland (m)	Wales (m)	N. Ireland (m)	Total (m)
Total number of dwellings	21	2.3	1.3	0.7	25.3
Solid walls	6.5	0.7	0.1	0.1	7.5
No loft space	1.5	unknown	unknown	unknown	~2
High rise	0.4	0.5	unknown	unknown	~1.5
Off gas grid	2.7	0.3	0.5	0.5	2.7
Total hard-to-treat dwellings	9	0.7	0.5	0.5	~10.3

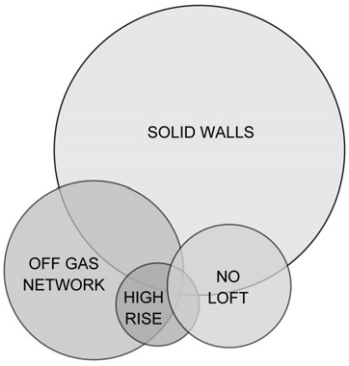

Fig. 4. The distribution of hard-to-treat homes in the UK.

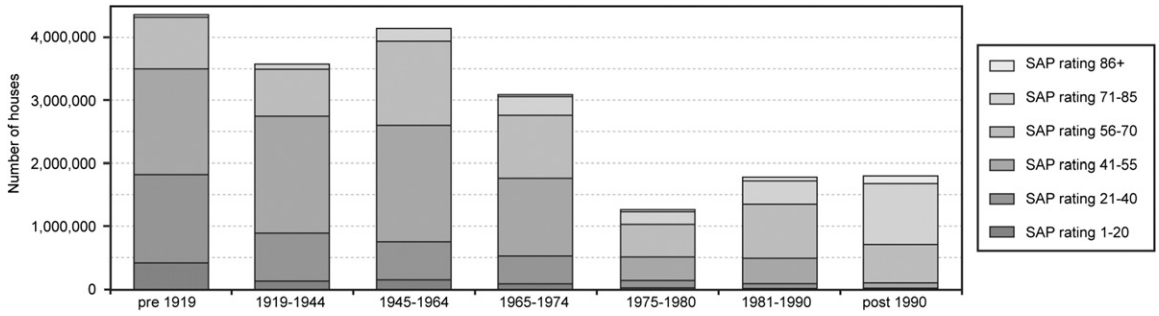

Fig. 3. SAP ratings across the English housing stock.

income to afford adequate energy services, for heating, lighting, cooking in their home (Boardman et al., 2005). In addition, dwellings that contain both solid walls and are off the gas grid possess some of the lowest SAP ratings in the UK, with a mean score of 25. Nearly 84% of these properties are in the private sector. By comparison, Beaumont (2007) states that high rise dwellings which are on the gas network typically perform much better, with SAP ratings averaging at around 60, nearly 10 points above the national average, due to their smaller size and significantly reduced area of exposed walls, resulting in smaller heat losses.

Regarding low-rise properties that are off the gas network, Beaumont (2007) states that these are particularly common in rural areas, where inaccessibility and a low urban density makes it unattractive for gas companies to build supply networks. Comparatively, safety considerations in high rise flats often means that a piped gas supply is not installed (Beaumont, 2007). Hard-to-treat dwellings with no space for loft insulation typically refer to those with flat, mansard or chalet roofs built before 1990. High rise flats with at least 6 stories are typically viewed as the most difficult to treat. In particular, developments built from 1950 to 1970 have some of the largest heating difficulties due to poor physical condition, low maintenance and a lack of gas supply (Beaumont, 2007).

According to Beaumont (2007) it is theoretically possible to internally insulate all solid walled properties in the UK, but there are restrictions on external wall insulation, since it changes the external appearance of a dwelling and planning permission prohibits its application on listed dwellings or those in conservation areas. According to Beaumont (2007) and Boardman et al. (2005), approximately 300,000 dwellings in the UK are listed, and a further 1.2 million are in conservation areas, representing about a quarter of all pre-1919 dwellings. In addition, installing external insulation on high rise flats may be problematic if the walls are structurally unsound, or if all owners/leaseholders do not all agree to change the external appearance. Alternatively, when internally insulating, individual flats could be improved on a room-per-room basis. It should be noted, that there are possible cost reductions through economies of scale, if an entire high-rise block is over clad in a single installation.

According to Boardman (2007), at least 800,000 of the most 'leaky' pre-1919 homes must be removed to meet the 2050 CO_2 reduction target. In contrast, Ravetz (2008), states that the older, worst performing stock should be seen as a resource rather than a problem, since they have the largest scope for improvements through energy efficient refurbishments. Moreover, Power (2008) argues that because demolition can be very time consuming, costly and disruptive to the environment, it is likely to promote much opposition within local communities, government and industry.

6. Energy savings from conventional retrofit measures

Shorrock et al. (2005) published a study for the Building Research Establishment analysing the scope for CO_2 reductions in the UK housing stock. Focusing on insulation measures for a typical 3-bedroom semi-detached house, the study calculated the energy, CO_2 and cost savings of conventional retrofit solutions, calculated based on the BREDEM energy model, which has been continually developed since the 1980s to consider both the physical characteristics of a dwelling and lifestyles of occupants. BREDEM also underpins the SAP calculations in the Building Regulations. Fig. 5 shows the calculated annual energy and CO_2 savings from conventional retrofit measures, generated using numeric data from Shorrock et al. (2005).

As expected, some measures provide significantly more benefit than others. A much larger saving can be experienced when insulating a solid wall in comparison to a cavity wall, since the baseline *U*-value is generally lower, and the level of insulation installed is not restricted to the cavity width. The distinction between cavity wall insulation savings in pre and post-1976 construction is due to a change in construction practices from brick–brick cavity wall construction to brick–block cavity walls

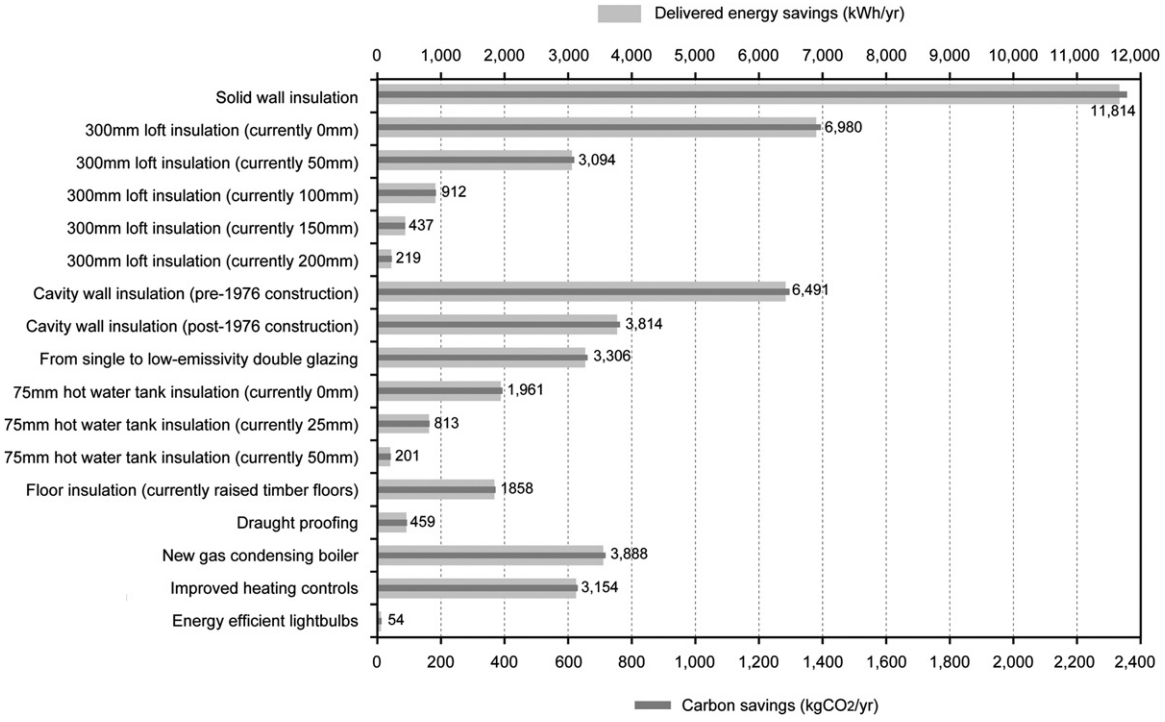

Fig. 5. Predicted delivered energy and CO_2 savings from conventional retrofit measures applied to a typical semi-detached house.

around this time. Predicted savings from loft insulation and hot water cylinder lagging provide diminishing returns depending on how much insulation is already present. As existing insulation levels approach 300 mm and 50 mm, respectively, the savings become so small that they are not worthwhile.

Roberts (2008a) states that cavity wall insulation can reduce heat loss through walls by up to 40% and when insulating the walls and roofs of un-insulated older buildings to post-1990 standards, then a 50–80% reduction in heat loss through these elements can be achieved. Determining the actual savings requires knowledge of how much heat was originally being lost through the fabric. This must be assessed on a case-by-case basis.

7. Cost-effectiveness of conventional retrofit measures

Shorrock et al. (2005) published figures for the capital cost of different retrofit measures against the estimated energy savings obtained from a reduced heating bill. This data is shown below in Table 3. The methodology assumes that no grant was made available and 30% of the energy savings were taken back by the homeowner for increased thermal comfort. Payback calculations assume annual fuel price rises and discount interest rates are at equal percentages, resulting in a simple return on investment calculation.

Analysis suggests that draught proofing, floor insulation, and loft insulation (with over 150 mm of insulation already in place) are marginally uneconomic. Comparatively, double glazing shows an extremely poor financial return on investment since the payback period far exceeds the predicted product lifespan and the energy savings alone do not justify the capital investment. The remainder of conventional retrofitting measures do show positive returns of investment, with the largest benefit occurring from filling cavity walls within pre-1976 stock. Insulating a loft which previously had no insulation appears to provide the shortest payback at just over 3 years, far shorter than double glazing at 98 years.

8. Energy efficiency uptake trends

Another analysis from Shorrock et al. (2005) relates to the current uptake of conventional retrofit products and future forecasts. For double glazing and gas condensing boilers these figures are based on "all that is economically and technically possible". Here it can be seen that certain retrofitting measures have more scope for installation than others. Note that projections for solid wall insulation were not available in Shorrock et al. (2005). However, a similar forecast from EEPH (2008), based on the industry's current capacity of 15,000–20,000 installations per year has been added. This data, generated from both sources is shown in Fig. 6.

Looking at cavity wall insulation, evidently there is still much potential for walls to be filled in the UK. Likewise, Roberts (2008a), states that 60% of UK domestic houses had unfilled cavity walls in 2004. Regarding double glazing, despite the high capital costs, levels are expected to reach saturation over the coming decades since all new glazing renovations must achieve a minimum centre pane U-value of 1.2 $W/m^2 K$ or an overall U-value of 1.8 $W/m^2 K$, except for in rare specific circumstances such as listed building status. Furthermore, considering uptakes of loft insulation have levelled off, there is considerable scope to ensure that all lofts have above 100 mm of insulation.

An additional factor raised by both Ravetz (2008) and Roberts (2008a) is that many homes have first generation retrofits in need of renewal. Ravetz (2008) claims that the deterioration of many post-war retrofits such as double glazing, plumbing and electrics are clearly visible in modern homes, however there are barriers to improvements due to the capital cost of investment and the hassle of refurbishment. Roberts (2008a) believes the main issue regarding first generation double glazing is the high U-values of 3–4 $W/m^2 K$, due to poorly insulated frames and narrow air gaps. Comparing these heat losses against modern double glazed units with U-values down to 1.2 $W/m^2 K$ would show considerable differences in thermal performance.

Regarding solid wall insulation, Shorrock et al. (2005) states that uptakes seem unlikely to reach saturation over the next few decades due to its slow uptake and high capital costs, which must be reduced to around £2500 (for the whole house) for the procedure to become marginally cost effective. Roberts (2008a), argues that solid wall insulation should be viewed as an untapped opportunity rather than a barrier since large energy savings can still be made. According to EEPH (2008), even at the upper limit of the industry's installation capacity only 15% of solid walled homes will be insulated by 2050.

Shorrock et al. (2005) argues that floor insulation uptake will remain slow since the procedure is generally only carried out when a floor needs repair. Similarly, Roberts (2008a) states that floor insulation is disruptive and is only likely to be economically viable during a comprehensive refurbishment of the floor.

Table 3
Capital cost, energy savings and simple payback period for conventional retrofit measures applied to a typical 3-bedroom semi-detached house.

Retrofit measure	Capital Cost (£)	Annual savings (£/yr)	Measure lifespan (yrs)	Lifetime saving (£)	Simple R.O.I. (£)	Payback period (yrs)
Solid wall insulation	3272	145.6	30	4376	1104	22.4
300 mm loft insulation (currently 0 mm)	273	86.2	30	2587	2314	3.2
300 mm loft insulation (currently 50 mm)	254	38.2	30	1146	892	6.6
300 mm loft insulation (currently 100 mm)	211	11.3	30	338	127	18.7
300 mm loft insulation (currently 150 mm)	199	5.4	30	162	−37	36.9
300 mm loft insulation (currently 200 mm)	170	2.7	30	81	−89	63.0
Cavity wall insulation (pre-1976 construction)	325	80.1	40	3205	2880	4.1
Cavity wall insulation (post-1976 construction)	325	47.1	40	1884	1559	6.9
From single to low-e double glazing	4000	40.8	20	816	−3184	98.0
75 mm DHW tank insulation (currently 0 mm)	20	28.8	15	431	411	0.7
75 mm DHW tank insulation (currently 25 mm)	20	12.0	15	180	160	1.7
75 mm DHW tank insulation (currently 50 mm)	20	3.0	15	45	25	6.7
Raised timber floor insulation	1000	32.8	30	983	−18	30.5
Draught proofing	110	5.7	10	57	−53	19.4
New gas condensing boiler	300	45.5	12	546	246	6.6
Improved heating controls	250	57.4	12	689	439	4.4
Energy efficient light bulbs	85	21.2	6	127	42	4.0

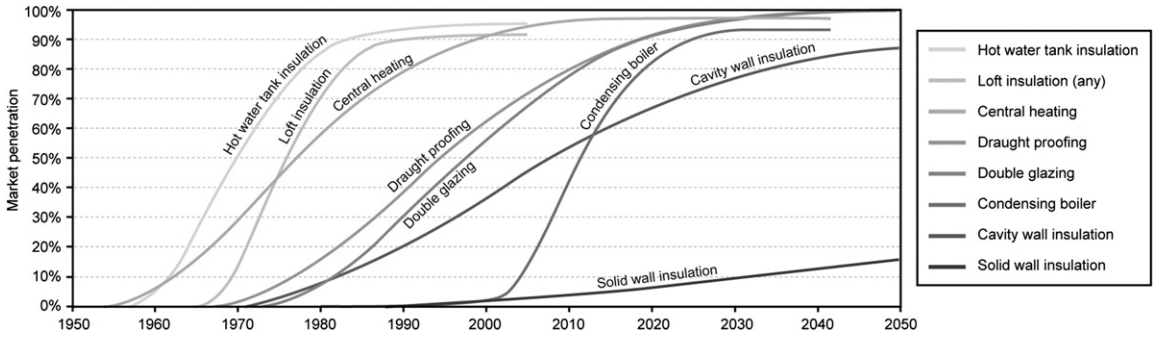

Fig. 6. Market penetration of conventional energy efficiency measures.

Taking an alternate perspective, Power (2008) argues that there should be more effort from the government to realise the potential for energy savings from the 10 million homes in the UK requiring solid wall insulation. Similarly, Power (2008) believes floor insulation needs to be considered within renewal programmes, since 10 million homes have un-insulated raised timber floors and the technology is available for improvement.

9. Government incentive programmes

Government incentive schemes represent a key driver for reducing CO_2 emissions in the housing sector (EEPH, 2010). Several focus on renewable energy, including the Renewable Energy Strategy (RES), Micro-generation Certification Scheme (MCS), Renewable Heat Incentive (RHI) and Feed in Tariffs (FITS). Alternatively, the government's Boiler Scrappage Scheme, launched in 2010, but now closed, funded over 100,000 new boilers across England. Regarding fabric efficiency, primarily these focus on installing low cost, non-disruptive measures such as cavity wall insulation and loft insulation, targeting underprivileged households mainly in the social housing sector. However, wider schemes have been set into motion, encouraging energy suppliers, electricity generators and private investors to provide grants to cover the upfront cost of refurbishments, reaching also into the owner occupied and private sector. A summary of fabric efficiency schemes is given below:

9.1. Carbon emissions reduction target (CERT)

During 2008–2011, CERT operated as one of the UK's principal energy efficiency mechanisms. This scheme required all domestic energy suppliers with a customer base exceeding 250,000 to achieve reduction targets for the amount of CO_2 emitted by their customers (equivalent to the total emissions from approximately 700,000 homes each year). At least two thirds of this target must be achieved through professionally installed insulation measures and 40% should be focused on a priority group of vulnerable households consisting of low income homes, pensioners over the age of 70 and households on disability benefits. In its first 2 years CERT resulted in approximately 1.4 million cavity walls and 1.1 million lofts being insulated. In addition, over 200 million low energy light bulbs have been delivered, 2000 ground source heat pumps installed and 30,000 solid walled properties have been upgraded through either internal or external wall insulation (DECC, 2010b).

9.2. Community energy saving programme (CESP)

CESP is a retrofitting scheme funded through an obligation on energy suppliers, and for the first time, electricity generators. This scheme provides funding to community partnership groups, housing associations and local authorities to improve energy efficiency in low income and hard-to-treat homes. CESP promotes a 'whole house' approach, aiming to treat as many properties as possible in a house-by-house or street-by-street approach (EEPH, 2008). Between October 2009 and December 2012, CESP funded approximately 100 community schemes, benefitting around 90,000 homes. According to DECC (2011), 81% of scheme submissions included external solid wall insulation and 65% had boiler replacements with new heating controls. Key challenges during installation included weather related issues, planning delays for solid wall insulation, cash flow problems due to retrospective payments from energy suppliers, gaining access to eligible households and dealing with resentment from non-eligible householders. In a post retrofit survey, 75% of occupants agreed their homes felt warmer and were easier to heat to adequate levels. Just 25% said they had seen a decrease in their heating bills and 11% said their heating bills had increased. According to DECC (2011), this was influenced by rising energy prices.

9.3. Decent homes

In 2000, the government made a commitment to bring all public sector dwellings in England to a basic standard of decency by 2010 through its Decent homes programme. This placed a responsibility on local authorities, registered social landlords and, to a limited extent, private sector landlords to eliminate the backlog of repairs throughout their stock. For a property to meet the Decent homes standard it must (i) be free of Category 1 Housing Health and Safety Rating Hazards (HHSRH), which covers an assessment of dampness, excessive cold/heat, security, hygiene, sanitation, structural integrity, accident risk, asbestos etc (ii) be in a reasonable state of repair, (iii) have reasonably modern facilities and services, and (iv) provide a reasonable degree of thermal comfort.

According to the National Audit Office (2010), at the start of the programme there were 1.6 million 'non-decent' homes in the social sector, representing 39% of all social housing. By 2010, over a million houses had been treated, reducing the percentage of non-decent homes in the social sector to 14.5%, falling short of the original target. Across the entire English stock, it is estimated that 5.9 million dwellings (26% of homes) failed to meet the Decent homes standard in 2010, compared to 7.7 million in 2006. The primary reasons for failing were not achieving the HHSRH assessment, followed by not providing adequate levels of thermal comfort (CLG, 2012). In 2010, private rented dwellings had the highest percentage of non-decent homes at 37%, followed by the owner occupied sector at 25%.

According to CLG (2006), the average cost to make a home decent is approximately £3600–£10,500 depending on the age and type of property. In order to meet the thermal comfort

standard a home must have an efficient heating system, cavity wall insulation (where possible) and a minimum of 200 mm loft insulation. Currently several local authorities and housing associations are in the process of adopting a new 'Decent homes Plus' standard. This typically includes additional measures such as double glazing (except when restricted by planning), full heating controls with an energy efficient boiler, draught proofing, energy efficient doors, and energy efficient lighting in all communal areas, improved sound insulation and a modern kitchen and bathroom.

9.4. Warm Front

Warm Front is a government funded scheme providing heating and insulation grants to vulnerable owner occupied and private rented households with SAP ratings of 55 (energy performance certificate band D) or below. Qualifying households must be on income support, income-related employment and support allowance, state pension credit or Job Seekers Allowance. Housing Association or local authority tenants do not qualify. Grants up to £3500 are available for measures such as loft insulation, cavity insulation, draught proofing, hot water tank insulation and new gas, electric or liquid petroleum gas (LPG) heating systems. Up to £6000 may be allocated where oil central heating and other alternative technologies are required. The scheme is only available in England and it is managed by Carillion Energy Services (formerly Eaga). Equivalent schemes are the Home Energy Efficiency Scheme (HEES) in Wales and the Warm Deal in Scotland.

In a report by the National Audit Office (2009), since the scheme began in 2000, more than 2 million homes had been treated through Warm Front funding by 2009, costing approximately £2.2 billion. In a satisfaction survey, 75% of customers were 'highly satisfied' by the quality of the work done and 84% would recommend the service to a friend or relative. Eaga estimated that the work done would reduce a household's energy bill by £300 a year (depending on the measures installed). A key criticism of the scheme was that applicants are assessed on a "first come, first served" basis, yet nearly 75% of households who qualified were not necessarily in fuel poverty. In addition, it was criticised that the scheme lacked a full range of measures such as external wall insulation, meaning it was unable to address hard-to-treat households (National Audit Office, 2009).

9.5. Green Deal

From October 2012, the Green Deal will be the key mechanism for improving the energy efficiency of domestic buildings in the UK. In this programme, bill payers will be able to obtain energy efficiency improvements without having to pay for the upfront costs of retrofit works (DECC, 2010c). Instead, capital will be privately financed, through consortia made up of banks, consumer and business groups, local authorities etc, as well as the investor community, who recoup their investment through an instalment charge on the consumer's energy bill. The overarching 'golden rule' principle is that the estimated savings on energy bills must be equal to, or greater than, the costs attached to the energy bill. Unlike a conventional loan, the loan repayments remain attached to the property, rather than the bill payer (who may move into a different property before the repayments are complete). Its remit also covers non-domestic buildings.

Supporting Green Deal, the government plans to have smart meters installed in every home by 2020. These meters are anticipated to provide customers and energy suppliers with more information on electricity and gas usage, as well as acting as the prime mechanism for governing the claimed bill savings through the Green Deal. All measures installed through Green Deal must be recommended and approved by an accredited advisor, and installed through an accredited installer. The majority of loans are expected to be provided by industry led consortium consisting of 19 blue-chip companies called the Green Deal Finance Company, supported by the Green Investment Bank. Functioning alongside Green Deal, an Energy Company Obligation (ECO) is scheduled to replace CERT and CESP, to provide additional financing to support vulnerable low income households and hard-to-treat properties.

10. Green Deal criticism

During the launch of Green Deal, the Energy and Climate Change Secretary announced a "third industrial revolution: a green revolution", one that would allow the most inefficient households to save £550 per year on their fuel bills, increase the number of jobs in the insulation industry from 27,000 to 250,000 and reduce nationwide spending on gas by up to £2.5 billion per year (Huhne, 2010). Whilst being an elegant idea, there are many who believe this simply will not be achieved, due to a number of fundamental issues such as low consumer appeal and investor incentives. These issues, plus others are described below:

10.1. Consumer appeal

As the Green Deal does not offer subsidies for retrofit works, it is feared this shift will make energy efficiency improvements less attractive to consumers, causing the number of homes being insulated to plummet (Gardiner, 2012). According to DECC, annual cavity wall insulation installations are predicted to drop by 67% from 510,000 to 170,000 homes per year. For loft insulation, levels are predicted to drop by 93% from over 1 million to 70,000 homes per year. Early 2011 trials for the Green Deal, including Affinity Sutton's "Future Fit project" and the B&Q loft clearance service in the London borough of Sutton have not been encouraging. The Future Fit project offered to pay for the upfront cost of energy efficiency improvements through a financing mechanism resembling Green Deal. However, take-up rates from advertising were just 4.8%, and of those who took part 23% dropped out during the lead up to retrofit works (McCann, 2011). In contrast, B&Q provided a 40% grant and offered to clear out a homeowner's loft in order to install insulation. Out of 400 household who expressed an interest, 126 agreed to an energy audit and only 66 went ahead with any insulation (Withers, 2011). The primary reason for the 60 homeowners not pursuing the grant following the energy audit was that they were sceptical regarding the levels of long-term energy savings that would be achieved (Withers, 2011).

10.2. Investor incentives

Recently, we have been investigating the financial attractiveness of large-scale Green Deal investments by developing a series of retrofit assessment tools to facilitate strategic business modelling/'war-gaming' workshops. When trialled internally, we assumed that each finance provider (acting as either a bank, retailer or energy company) would be looking to obtain an internal rate of return of up to 11–15% due to the unknown risks attached with Green Deal. To date, we have found that it is difficult to make the Green Deal attractive as a way to make money (although we do recognise that it can appeal to companies who are in a position to provide finance for reasons other than an internal rate of return). Our modelling has also shown that it becomes more difficult to achieve a return on investment if a property does not fall under the category of "most in-efficient", e.g., if it has a C-rated boiler as opposed to an F-rated boiler.

We therefore expect investors to segment the Green Deal market and target households that offer the best returns. Only limited profiling is possible, but Green Deal companies may have to spend money on data mining and marketing to facilitate the most profitable opportunities. Further to this, our modelling has shown that the recent cut in tariff rates to renewable energy measures, maintenance costs (if included in the contract) and the upfront cost of energy audits (if not passed onto the bill payer) can prolong the investment periods detrimentally.

10.3. Technical issues

The Golden Rule was established to protect consumers and investors from over extending themselves financially. However, it could in fact be restricting the level of CO_2 savings obtainable from whole house retrofitting, because it limits the size of a Green Deal loan to the amount that can be repaid by savings generated. Paradoxically, meeting the Golden Rule will be problematic because it is a difficult to accurately predict the annual energy savings from different retrofit packages without fully understanding the technical performance of the building and the energy usage patterns of its inhabitants, including any re-bound effect with improved comfort conditions. Lainé (2012) expressed concern that the current RdSAP engine, used to facilitate Green Deal assessments, will not recommend cavity wall insulation if the existing *U*-value is below 0.6 W/m^2 K, despite the opportunity to implement low-cost insulation to achieve a *U*-value of 0.35 W/m^2 K. This would mean that up to 2.3 million cavity-walled homes built since 1983 could be given incorrect advice and would not be able to use Green Deal to finance the work (Lainé, 2012).

Those in fuel poverty, a fifth of all households, look to be ignored by the scheme. If a household struggles to pay for fuel, it will be in a weak position to raise a Green Deal for building improvements. There are also problems with multiple-occupancy buildings and whether everyone needs to agree before the building fabric can be improved. It should be noted as well that the effect of a 'Green Deal' on a property's value and ease of re-sell is unknown. The Green Deal is innovative in how it attaches the loan to the building rather than the occupier but the market implications of this are untested.

11. Further barriers to energy efficiency

According to Power (2008) and Roberts (2008a), there are a number of conventional cost effective measures yet to be implemented throughout the UK housing stock and many older homes have vast potential for reduced energy consumption. However, Lowe and Oreszczyn (2008) and Ravetz (2008) claim that a large proportion of cost-effective measures have already been employed, yet significant energy savings are still to be experienced. As a result, both Olivier (2001) and Lowe and Oreszczyn (2008) argue that actual energy performance of the UK building stock may be significantly lower than previously assumed.

11.1. Difficulty meeting Building Regulations

In a report by Olivier (2001), it was argued that the official figures for *U*-values are optimistic and not achieved in practice. This is because actual *U*-values are often found to be higher than expected when measured in-situ, due to errors in the quality of construction, as well as thermal bridges and gaps in insulation. According to Hamza and Greenwood (2008), Building regulations do improve design teams' abilities to meet energy targets, however, many within the industry express concern about uncertainties and difficulties with compliance. Lowe and Oreszczyn (2008) claim that little is known regarding the actual impact of updates to the Building Regulations due to a lack of monitoring following construction. Similarly, Olivier (2001) states there has been no evaluation of the 1982, 1990 or 1995 Building Regulations since there is no individual or legal binding body to assess energy performance after on-site retrofitting work is complete.

11.2. Too much focus on zero carbon targets

Taking a top-down approach, Lowe and Oreszczyn (2008) believe that many issues hindering the progress of energy efficiency relate to ill-advised policies from the government causing debate within industry. Lowe and Oreszczyn (2008), claim that the government is putting too much pressure on the industry to achieve zero carbon targets, particularly in new build, without fully understanding the complications surrounding fabric improvements in existing homes. Lowe and Oreszczyn (2008) propose that too much investment is being spent on expensive renewable technologies without fully understanding the importance of maximising the performance of the building fabric.

11.3. Discrepancies between predicted and actual savings

Hong et al. (2006) published a paper looking at the impact of energy efficient refurbishments on the space heating fuel consumption of English dwellings. Here, the performance of 1372 properties treated through the Warm Front scheme were analysed before and after a conventional retrofit with cavity wall insulation, loft insulation and a new central heating system. The aim was to lower energy consumption to alleviate low income houses from fuel poverty, along with raising thermal comfort standards to modern levels. Prior to installation, theoretical calculations suggested that cavity wall insulation and loft insulation would save 49% of fuel consumption, however actual monitoring following the refurbishment showed that only 10–17% energy savings were achieved.

Conclusions were that the refurbishment did raise thermal comfort standards and homes were cheaper to heat, however the expected energy savings were not achieved (Hong et al., 2006). Regarding the complexities of achieving actual energy savings, Hong et al. (2006) claimed that large uncertainties related to the impacts of thermal bridges, gaps in insulation and the occupants using more heating following the refurbishment. Thermal imaging on a sample of 72 dwellings showed that 20% of cavity wall areas and 13% of the loft areas lacked insulation. It was revealed that the introduction of the new heating system resulted in 35% of savings being taken back to raise thermal comfort in the home.

11.4. Increased use of heating following refurbishment

This issue of thermal comfort 'take-back' was reported by Bell and Lowe (2000) in a study analysing the savings of energy efficient refurbishments on four similar sized semi-detached houses. The aim was to confirm that significant savings could be gained from conventional 1980s retrofit technologies. Following an extensive two-week energy monitoring period, a 47% reduction in energy consumption was observed, proving that significant savings could be achieved from conventional retrofit measures. However, this was 40% lower than their predictions, which Bell and Lowe (2000) suggested was mostly due to people's behaviour and thermal comfort take-back from the new heating systems.

11.5. Socio-economic status of household

According to Binggeli (2003) and Roberts (2008a), before the introduction of gas powered central heating systems in the 1970s, most people preferred indoor temperatures at 20 °C or less, and would wear more clothes during winter to prevent paying high energy costs. By comparison, nowadays people have developed thermal comfort preferences of 23–25 °C, which tends to be satisfied through higher quantities of energy consumed for heating (Binggeli, 2003; Roberts 2008a). Both Clinch and Healy (2000), and Milne and Boardman (2000), claim a large proportion of this take-back relates to the socio-economic status of the household prior to the refurbishment. Milne and Boardman (2000) found that low income houses originally heated to 14.5 °C, experience energy savings that are only 50% of those anticipated, whereas slightly higher income homes originally heated to 16.5 °C tended to experience 70% of the anticipated energy savings, due to a lower thermal comfort take-back. Clinch and Healy (2000) believe there is a lack of studies looking at take-backs in high income homes. Here it would be expected that dwellings would see greater energy bill savings since the home is likely to already be heated to reasonable levels.

11.6. Additional barriers within society

Ravetz (2008) claims that many people do not view energy efficient refurbishments as a high priority when updating their homes. Major barriers are the perceived hassle of installation, upfront costs, uncertainties over lower fuel bills and a lack of knowledge over payback periods (UKGBC, 2008). Power (2008) states that energy efficient refurbishment is undervalued by communities. People seem to prefer amenities such as new kitchens, bathrooms, central heating, and general repairs, instead of energy efficient refurbishments since the social gains are more obvious (Bell and Lowe, 2000). Ravetz (2008) forecasts that technological shifts threaten to counter the efforts of energy efficiency. For example more homes will become increasingly diverse in their use of energy with more appliances, lighting and domestic air conditioning.

11.7. Insulation causing overheating

Looking to the future, it may become apparent that climate change causes people's thermal comfort needs to adapt to higher temperatures or conversely require more cooling (Ravetz, 2008; Roberts, 2008b). At present little attention is given to issues such as the impacts of overheating in older buildings, security risks for opening windows or analysis of appliance heat gains with technological developments. These would be interesting to study, however it would rely heavily on predictions, which are difficult to quantify (Ravetz, 2008; Roberts, 2008b). Both Holmes and Hacker (2007), and Ravetz (2008) predict this will lead to greater overall energy expenditure in buildings that require active cooling. In addition more homeowners are likely to retrofit air conditioning units or buy portable air conditioning systems for their homes, which too would raise consumption.

12. Passivhaus refurbishment

A large wealth of experience exists with the German retrofit market due to their implementation of the Passivhaus standard within new and existing homes (Bell and Lowe, 2000; Lowe and Oreszczyn, 2008). Core principles of a Passivhaus rely upon the design and specification of super insulation and highly airtight fabric, combined with whole house mechanical ventilation with heat recovery (WHMVHR). Using this approach, a building has minimal fabric heat losses, and is supplied with permanent fresh air and regulated humidity, with no uncomfortable draughts. A Passivhaus must have a total heating demand of 15 kW h/m^2/year or less, or 25 kW h/m^2/year or less if it is a retrofit. By comparison, the average heating consumption for the existing UK building stock is 180 kW h/m^2/year, 100 kW h/m^2/year when renovated and 50–60 kW h/m^2/year if it is a new build (Boonstra, 2005).

An example of a German Passivhaus retrofit project is the 'Zukunft Haus Pilot Programme' that ran from 2003 to 2005. Here, 915 homes, mostly rented flats built pre-1978, were renovated in Eastern and Western Germany with high levels of insulation, external/ internal cladding, triple glazing, efficient heating and energy systems, whole house heat recovery and south facing balconies where possible. Overall an 80% reduction in energy consumption throughout the households was achieved, which was twice as effective as the German building standards (Power, 2008). In 2007, the German Federal Government announced that all German pre-1984 homes should reach this standard by 2020, through a system of loans, tax incentives and grants, resulting in vast incentives for energy efficient refurbishment (Power, 2008).

A summary of Passivhaus standards compared to 2010 new build Building Regulations, according to BRE (2011) is shown in Table 4. A key challenge with Passivhaus is achieving the required air tightness target of < 1 m^3/m^2 h^{-1} @ 50Pa, as it requires a predefined air tightness strategy, which deals with all junctions and partitions through impermeable and durable air tight barriers, interconnected membranes, tapes and flexible sealed joints. Bell and Lowe (2000) and Lowe and Oreszczyn (2008) argue that there is a need to transfer this knowledge into the UK housing stock so that the UK construction industry will be better equipped at improving the standard of existing houses and meeting the requirements of new Building Regulations. This will require the transfer of components, installation procedures and training

Table 4
England and Wales Building Regulations (HM government, 2010) compared to the Passivhaus standard.

	2010 England and Wales Building Regulations Part L1A	German Passivhaus standard
Walls, roof and floor	Limiting *U*-values of 0.25–0.3 W/m^2 K	*U*-value should not exceed 0.15 W/m^2 K
Windows and openings	Typically 1.8-2.2 W/m^2 K	*U*-value should not exceed 0.8 W/m^2 K with solar heat gain coefficient of 0.5
Orientation and shading	Sometimes considered, but often overlooked in the design process	Passive solar design principles are followed
Air tightness	Design air change rate of 7–10 m^3/m^{2}h @50Pa	Design air change rate of < 1 m^3/m^2 h @50Pa
Whole house heat recovery	Typically not considered as buildings do not achieve air change rates below 3 m^3/m^2 h @50Pa	Incoming fresh air is pre-heated to > 5C. Exhausted heat recovery efficiency is at least 85%.
Lighting and appliances	Low energy lighting and C+ rated appliances	Low energy lighting and A+ rated appliances are required
Total heating demand	$\sim$55 kW h/m^2/year	< 15 kW h/m^2/year (new build) < 25 kW h/m^2/year (retrofit)

methods within the construction industry to inform workers on how to properly meet Passivhaus standards during refurbishment (Lowe and Oreszczyn, 2008).

The UK's first certified domestic Passivhaus retrofit was completed in March 2011. It is a solid walled mid-terrace house at 100 Princedale Road in Holland Park, West London. The house was located in a conservation area, so external insulation and new glazing was restricted. Consequently, measures implemented included internal insulation with an air-tight barrier, custom built triple glazed windows to imitate traditional single glazed sash windows, a WHMVHR system and solar thermal collectors for water heating. The newly refurbished property has no gas boiler or radiators. According to Borgstein et al. (2011), energy savings of 89% are projected, equivalent to £910 saved a year on fuel bills. This project was funded through the 'Retrofit for the Future' competition, launched by the Technology Strategy Board in March 2009. This competition provided 86 winning teams with £150,000 to upgrade existing social homes in the UK, challenging them to reduce CO_2 emissions by 80%.

13. Environmental impact of refurbishments

The environmental impact of refurbishment, in particular the embodied energy and embodied CO_2 produced through raw material acquisition, component manufacture, transport to site and the onsite construction/retrofit process, is an area of research which is often overlooked. Over the lifecycle of a building, it is estimated that these 'cradle-to-site' embodied impacts account for about 10–20% of a building's total energy consumption (SETAC, 2003). Conversely, for low energy, high efficiency buildings, this phase of the building's lifecycle can have a much greater significance representing around 40–75% of the total lifetime consumption of energy (SETAC, 2003; Smil, 2008).

According to Ravetz (2008), the embodied energy required to construct a new building may be up to 10 times more intensive than refurbishment, due to the offsite impacts of construction and transport. Power (2008) claims that the embodied energy required to build new homes is 4–8 times more intensive than a refurbishment to modern standards. These issues were also studied by the Empty Homes Agency, who demonstrated how comprehensive refurbishment generates about 15 t of embodied CO_2, in comparison to demolition and rebuild which used closer to 50 t of embodied CO_2. According to EHA (2008), the energy consumption of an average UK home is responsible for 5–6 t of CO_2 every year, two thirds of which could be saved through simple energy efficiency measures.

Over the life cycle, the fabric and services in a building will be adapted, maintained and renewed several times, resulting in recurring embodied energy cost. According to Cole and Kernan (1996) as well as Yohanis and Norton (2002), the recurring embodied energy for buildings with a short lifespan tends to be less than the initial embodied energy in construction; yet for buildings with life spans up to 100 years, this embodied energy can be 2–3 times greater than the impacts of the construction phase. Fig. 7 illustrates the typical embodied and operational energy costs for an office that has been involved in three major refurbishments at 25 years, 50 years and 100 years into its buildings lifecycle, according to estimations by Yohanis and Norton (2002). As shown, operational energy steadily accumulates throughout the lifecycle of a building, whereas the embodied energy builds up in increasingly energy intensive phases.

Not shown in Fig. 7 is the potential for operational savings following each retrofit. According to Harris (1999), there is a significant lack of studies concerning the actual embodied energy within refurbishments, particularly those measures designed for energy efficiency. According to Schmidt et al. (2004), in a typical application, the in-use savings from insulation are over 100 times the embodied impact of production and disposal. In contrast, Harris (1999) claims that when the thickness of loft insulation is increased beyond 200 mm, the embodied energy threatens to outweigh the operational energy savings. Weir and Muneer (1998) found modern glazing systems have a particularly high embodied energy up to 1500 kW h/m^2, which could take 10–30 years to provide a positive energy contribution.

14. Conclusion

The aim of this paper was to (i) review the thermal performance of the existing UK housing stock (ii) assess the energy savings, financial payback and uptake trends associated with different retrofit measures, (iii) review the key outcomes of the various fabric efficiency incentives, and (iv), understand the key barriers to obtaining deep energy and CO_2 savings throughout the stock.

There is a strong correlation between the age and tenure characteristics of dwellings and their thermal efficiency, due to historic updates to Building Regulations and a lack of incentives aimed at private landlords. Millions of homes in the UK are classed as hard-to-treat. It is essential that these properties be viewed as an opportunity to reduce CO_2 emissions, since they represent some of the worst performing homes with the most potential for thermal improvement. However, many of these properties, particularly those with solid walls, will not be insulated by 2050 without stronger incentive schemes, active promotion and technological innovation.

Evidently, some measures such as double glazing have a particularly long financial payback period which threatens to counter

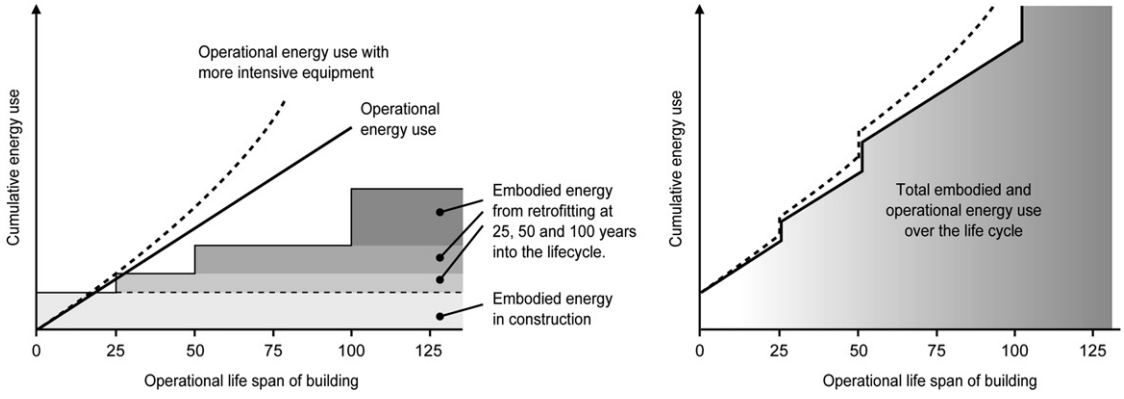

Fig. 7. Illustrative embodied and operational energy costs in the life cycle of an office building refurbished at 25, 50 and 100 year intervals.

their benefits. As millions of homes still contain single glazing or have first generation double glazing in need of improvement, careful consideration needs to be given when deciding to upgrade these units. Equally, the high capital cost of solid wall insulation is one of the many barriers preventing its widespread implementation. Opportunities to externally insulate multiple dwellings simultaneously should be sought to benefit from economies of scale.

From now on, the Green Deal is scheduled to be the UK's main energy efficiency scheme. However, there is risk this scheme will fail to meets its targets, particularly due to low consumer appeal and low investor incentives. To meet the 2050 CO_2 reduction target, it is imperative that the Green Deal targets and improves the performance of all households and not just those which are easy to treat using conventional measures. This will require more information to the bill payer, such as realistic projections for long-term fuel reductions, more transparency regarding the benefits and disruption of different retrofit packages and more information about the wider implications of the scheme such as how it impacts fuel poverty, household value and re-saleability.

We have found that strategic war-gaming exercises can be a useful tool to evaluate preliminary investment scenarios for the Green Deal. Better access to housing stock, capital cost and energy savings data at a local level, combined with more clarity on marketing, administration and energy assessment costs will help to improve the accuracy of this process. Evidently, more attention needs to be given to areas of the housing stock which are less cost effective to improve. Poor quality construction, thermal comfort take-back and a lack of monitoring following refurbishments pose a serious threat to obtaining real, long-term energy savings. This could be particularly problematic for the Green Deal, with its 'golden rule' financing mechanism, based heavily on predicted savings rather than actual fuel bill savings.

It should be noted that success has been achieved in Germany through their adoption of the Passivhaus standard in both new and existing homes. Over the next few years it can be expected that a handful of certified Passivhaus retrofits will emerge in the UK. However, without the appropriate construction skills and easy access to cost effective components, it will be difficult for this standard to become practical in the UK, particularly due to the complexities associated with achieving such high air tightness levels in old, leaky dwellings.

The significance of embodied energy over the life cycle of buildings being refurbished is an area which also needs to be better understood. Measures such as double glazing, have a particularly high embodied energy, which threatens to counter their installed benefit. The full extent of materials, on-site processes and transport during refurbishment are areas that need to be carefully audited. There is a risk, in particular when undertaking a deep retrofit, that the sum of this embodied energy will not be recovered for many years after the works have been undertaken.

Acknowledgements

The corresponding author would like to thank the EPSRC, Brunel University, Buro Happold Ltd for funding this research. This study forms part of a wider research project focused on product development and life cycle assessment of novel retrofit technologies incorporating silica aerogel insulation (see Dowson et al. 2011a, 2011b and 2012).

References

Beaumont, A., 2007. Hard-to-Treat homes in England, W07- Housing Regeneration and Maintenance, International Conference 25th-28th June, Sustainable Urban Area, Rotterdam 2007, Building Research Establishment, Watford, UK.

Bell, M., Lowe, R., 2000. Energy efficient modernisation of housing—A UK case study. Energy and Buildings 32, 267–280.

BERR—Department for Business Enterprise & Regulatory Reform., 2008. Energy consumption in the United Kingdom—domestic data tables, Table 3.5—SAP rating 1970-2006, Available from: 〈http://www.berr.gov.uk/whatwedo/energy/statistics/publications/ecuk/page17658.html〉.

Binggeli, C., 2003. Building Systems for Interior Designers, Firstst ed. John Wiley & Sons, New Jersey, USA.

BRE, 2008. A Study of Hard-to-treat Homes Using the English House Condition Survey. Part 1—Dwelling and Household Characteristics of Hard-to-treat Homes. Building Research Establishment, Watford, UK - Building Research Establishment.

BRE - Building Research Establishment., 2011. Passivhaus standard, Available from: 〈http://www.passivhaus.org.uk〉.

Boardman, B., Darby, S., Killip, G., Hinnels, M., Jardine, C., Palmer, J., 2005. 40% House, University of Oxford. Environmental Change Institute, Oxford, UK.

Boardman, B., 2007. Home Truths: A Low-Carbon Strategy to Reduce UK Housing Emissions by 80% by 2050. University of Oxford, Environmental Change Institute, Oxford, UK.

Boonstra, C., 2005. European Passive House in the UK? Chiel Boonstra, Trecodome, Resource 05 Low Carbon Technology Showcase, 13th–15th September 2005. Building Research Establishment, Watford, UK.

Borgstein, E.H., Pakenham, T.J.C., Raja, A.M., 2011. Low Energy Retrofit of Solid Walled Terraced Dwellings, Green Tomato Energy Ltd, CIBSE Technical Symposium, 6th–7th September 2011. DeMontfort University, Leicester, UK.

CLG—Communities And Local Government., 2001. English House Condition Survey—supporting tables, profile of the stock, Table A1.3 dwelling type by age category, Available from: 〈http://www.communities.gov.uk/archived/general-content/housing/224506/englishhouse/〉.

CLG—Communities and Local Government., 2003. Regional report: supplementary tables, Available from: 〈http://www.communities.gov.uk/documents/housing/xls/152975.xls〉.

CLG, 2006. Review of Sustainability of Existing Buildings, the Energy Efficiency of Dwellings—Initial Analysis. CLG Publications, West Yorkshire, UK - Communities and Local Government.

CLG—Communities and Local Government., 2012. English Housing Survey, Headline Report 2010-2011, CLG Publications, London, UK.

Climate ChangeAct, 2008. Carbon Targeting and Budgeting, Chapter 27, Part 1—The Target for 2050. Her Majesty's Stationery Office Limited, London, UK.

Clinch, J., Healy, J., 2000. Cost benefit analysis of domestic energy efficiency. Energy Policy 29, 113–124.

Cole, R., Kernan, P., 1996. Lifecycle energy use in office buildings. Building and Environment 31, 307–317.

DECC, 2010a. SAP 2009: Version 9.90 (May 2010), The Government's Standard Assessment Procedure for Energy Rating of Dwellings. BRE Press, Watford, UK - Department of Energy and Climate Change.

DECC—Department of Energy and Climate Change., 2010b. Paving the way for a Green Deal: Extending the Carbon Emissions Reduction Target Supplier Obligation to December 2012, Crown Copyright, URN 10D/711.

DECC—Department of Energy and Climate Change., 2010c. The Green Deal—A Summary of the Government's Proposals, Crown Copyright. Ref 10D/996.

DECC—Department of Energy and Climate Change., 2011. Evaluation of the Community Energy Saving Programme—A Report on the Findings from the Process and Householder Experience Research Streams, CAG Consultants, Ipsos MORI and the BRE.

Dowson, M., Harrison, D., Craig, S., Gill, Z., 2011a. Improving the thermal performance of single-glazed windows using translucent granular aerogel. International Journal of Sustainable Engineering 4, 266–280.

Dowson, M., Grogan, M., Birks, T., Harrison, D., Craig, S., 2011b. Streamlined life cycle assessment of transparent silica aerogel made by supercritical drying. Applied Energy 97, 396–404.

Dowson, M., Pegg, I., Harrison, D., Dehouche, Z., 2012. Predicted and in situ performance of a solar air collector incorporating a translucent granular aerogel cover. Energy and Buildings 49, 173–187.

EEPH, 2008. The Insulation Industry, Working in Partnership With Government to Insulate the Existing Housing Stock by 2050. EEPH publications, London, UK - Energy Efficient Partnership for Housing.

EEPH—Energy Efficient Partnership for Housing., 2010. 2050 Roadmap for Energy Efficiency and Low Carbon Housing. Summary Report of Evidence Base. Draft for Discussion. Purple Market research and EEPH. September 2010.

EHA, 2008. New Tricks with Old Bricks. Empty Homes Agency Ltd, London, UK - Empty Homes Agency.

Gardiner J., Is the Green Deal heading for failure?, *Building,* 13 January 2012, Available from: 〈http://www.building.co.uk/is-the-green-deal-heading-for-failure?/5030176.article〉.

Hamza, N., Greenwood, D., 2008. Energy conservation regulations: impacts on design and procurement of low energy buildings. Building and Environment 4, 929–936.

Harris, D., 1999. A quantitative approach to the assessment of the environmental impact of building materials. Building and Environment 34, 51–758.

HM Government, 2010. The Building Regulations, Part L1A: Conservation of Fuel and Power in New Dwellings, 2010 edition, NBS, RIBA Enterprises Ltd.

Holmes, J., Hacker, J., 2007. Climate change, thermal comfort and energy: meeting the design challenges of the 21st century. Energy and Buildings 39, 802–814.

Hong, S., Oreszczyn, T., Ridley, I., 2006. The impact of energy efficient refurbishment on the space heating and fuel consumption in English dwellings. Energy and Buildings 38, 1171–1181.

Huhne C., 2010. Green growth: the transition to a sustainable economy, Speech to LSE, 02 November 2010, Available from: 〈http://www.decc.gov.uk/en/content/cms/news/lse_chspeech/lse_chspeech.aspx〉.
Killip, G., 2005. Built Fabric & Building Regulations, Background Material F: 40% House Project, Environmental Change Institute. University of Oxford, UK.
Lainé, L., 2012. Filling the Gaps: Accuracy of Green Deal Advice for Cavity-Walled Homes. Consumer focus, London, UK.
Lowe, R., Oreszczyn, T., 2008. Regulatory standards and barriers to improved performance for housing. Energy Policy 36, 4475–4481.
McCann K., 2011. Top tips: delivering the Green Deal, Guardian, 24 September 2011, Available from: 〈http://www.guardian.co.uk/housing-network/2011/sep/24/top-tips-green-deal-housing?INTCMP=SRCH〉.
Milne, G., Boardman, B., 2000. Making cold homes warmer—the effect of energy efficiency improvements in low-income homes. Energy Policy 28, 411–424.
National Audit Office., 2009. The Warm Front Scheme, Report by the Controller and Auditing General, HC 126 session 2008–2009, NAO Marketing and Communications Team, the Stationary Office, London, UK.
National Audit Office., 2010. The Decent Homes Programme, Report by the Controller and Auditing General, HC 212 Session 2009–2010, NAO Marketing and Communications Team, The Stationary Office, London, UK.
Olivier, D., 2001. Building in Ignorance: Demolishing Complacency, Improving the Energy Performance of 21st Century Homes, UK. EEASOX and ACE, Herefordshire.
Power, A., 2008. Does demolition or refurbishment of old and inefficient homes help to increase our environmental, social and economic viability? Energy Policy 36, 4487–4501.
Ravetz, J., 2008. State of the stock—what do we know about existing buildings and their future prospects? Energy Policy 36, 4462–4470.
Roberts, S., 2008a. Altering existing buildings in the UK. Energy Policy 36, 4482–4486.
Roberts, S., 2008b. Effects of climate change on the built environment. Energy Policy 36, 4552–4557.
SETAC—The Society of Environmental Technology and Chemistry., 2003. Lifecycle Assessment in Building and Construction—A State-of-the-art Report, 1st Edition, SETAC Press, USA.
Schmidt, A., Jenson, A., Clausen, A., Kamstrup, O., Postlethwaite, D., 2004. A Comparative life cycle assessment of building insulation products made of stone wool, paper wool and flax, part 1: Background, goal and scope, life cycle inventory, impact assessment and interpretation. LCA Case Studies 9, 53–66.
Shorrock, L., Henderson, J., Utley, J., 2005. Reducing Carbon Emissions from the UK Housing Stock. BRE Press, Watford, UK.
Smil, V., 2008. Energy in Nature and Society—General Energetics of Complex Systems, 1st ed. MIT Press, Cambridge, UK.
UKGBC—United Kingdom Green Building Council., 2008. Low Carbon Existing Homes—Report, Supported by Energy Efficient Partnership for Homes, Sustainable Development Commission and Technology Strategy board, London, UK.
Utley, J., Shorrock, L.D., 2008. Domestic Energy Factfile 2008, Building Research Establishment. BRE Press, Watford, UK.
Weir, G., Muneer, T., 1998. Energy and environmental impact of double glazed windows. Energy Conversion 39, 243–256.
Withers I., 2011. Nearly half of householders turn down Green Deal in trial, *Building*, 12 November 2011, Available from: 〈http://www.building.co.uk/sustainability/sustainability-news/nearly-half-of-householders-turn-down-green-deal-in-trial/5023001.article〉.
Yohanis, Y., Norton, B., 2002. Life-cycle operational and embodied energy for a generic single-storey office building in the UK. Energy 27, 77–92.

International Journal of Sustainable Engineering
Vol. 4, No. 3, September 2011, 266–280

Taylor & Francis
Taylor & Francis Group

Improving the thermal performance of single-glazed windows using translucent granular aerogel

Mark Dowson[a,b]*, David Harrison[a], Salmaan Craig[b] and Zachary Gill[b]

[a]*School of Engineering and Design, Brunel University, London, UK;* [b]*Buro Happold Ltd, 17 Newman Street, London W1T 1PD, UK*

(*Received 21 May 2010; final version received 26 January 2011*)

Cost-effective materials, products and installation methods are required to improve the energy efficiency of the UK's existing building stock. The aim of this paper is to assess the potential for high-performance translucent granular aerogel insulation to be retrofitted over single glazing to reduce heat loss without blocking out all of the useful natural light. *In situ* testing of a 10-mm-thick prototype panel, consisting of a clear twin-wall polycarbonate sheet filled with granular aerogel, was carried out and validated with steady-state calculations. Results demonstrate that an 80% reduction in heat loss can be achieved without detrimental reductions in light transmission. Payback calculations accounting for the inevitable thermal bridging from openable solutions such as roller shutters or pop-in secondary glazing suggest that a return on investment between 3.5 and 9.5 years is possible if products are consistently used over the heating season. Granular aerogel is a promising material for improving the thermal performance of existing windows. Future research will seek to map out different ways in which the material can be applied to the existing UK housing stock, identifying which systems offer the greatest potential for widespread CO_2 savings over their life cycle.

Keywords: granular aerogel; translucent insulation; retrofit products; energy-efficient refurbishments

1. Introduction

Reducing demand for heating and lighting in buildings is imperative for the UK to cut 80% of its CO_2 emissions by 2050, in relation to the 1990 baseline (Climate Change Act 2008). In 2008, the country's 26 million dwellings were responsible for 27% of all UK CO_2 emissions (Utley and Shorrock 2008). Non-domestic buildings were accountable for a further 20% (RCEP 2007). It is anticipated that over 80% of the current building stock will still be in use by 2050 (Power 2008, Ravetz 2008). This is a major issue, because millions of these properties contain elements such as solid walls, single glazing and un-insulated floors responsible for a significant amount of wasted heat. These features are expensive and disruptive to improve; furthermore, associated improvements can be limited by available space and planning restrictions (Beaumont 2007, EEPH 2008).

This paper focuses on the potential to improve the performance of glazing in existing buildings. Windows typically lose 4–10 times more heat per square metre, compared with walls, roofs and floors (Roberts 2008). According to Shorrock *et al.* (2005), new double glazing is not cost-effective, with estimated payback periods lasting up to 98 years. In 2006, approximately 3 million dwellings in England contained full single glazing and 5.1 million homes contained 'some' single-glazed windows (CLG 2006). Furthermore, approximately 70% of non-domestic buildings were constructed before double glazing became a legal requirement in 1976 (Roberts 2008). Of the remaining stock, around three quarters contain first generation double-glazed windows installed over 20 years ago (Ravetz 2008, Roberts 2008). These units possess un-insulated frames, deteriorated air seals, narrow air gaps and a high *U*-value (heat loss coefficient) of $3-4\,W/m^2\,K$ that does not meet modern Building Regulations (Roberts 2008).

2. Literature review

A number of innovative glazing technologies were developed to satisfy the growing demand for energy-efficient buildings (Roberts 2008). Super-insulating windows with *U*-values below $1\,W/m^2\,K$ can be achieved in several ways. The current focus is to develop products that combine the lowest possible *U*-value, with a relatively high *G*-value (solar heat gain coefficient) and light transmission, to ensure that heat loss is minimised without blocking out the useful energy and daylight from the sun (MTP 2007). Innovations include low iron glass, selective coatings, insulated gas fillings, insulated frames, triple glazing, vacuum glazing, chromic glass and photovoltaic glazing. Finding a balance between cost and *in situ* performance over the lifespan is essential, particularly for measures that rely on sustaining a vacuum.

According to Baker (2008), there is a lack of *in situ* studies analysing the thermal performance of low-cost

*Corresponding author. Email: mark.dowson@burohappold.com

ISSN 1939-7038 print/ISSN 1939-7046 online

DOI: 10.1080/19397038.2011.558931
http://www.informaworld.com

alternatives to double glazing. In response, Baker (2008) used an environmental chamber to measure the *U*-values of seven different retrofit measures including curtains, blinds, secondary glazing and wooden shutters fitted to single glazing. The single glazing (*U*-value = 5.4 $W/m^2 K$) was then replaced with modern double glazing (*U*-value = 1.9 $W/m^2 K$) for comparison. Baker (2008) found that all measures reduced heat loss, yet most measures blocked out all natural light. The greatest reduction in heat loss came from a custom-made set of wooden shutters lined with 9 mm of Spacetherm™, an opaque insulating blanket embedded with super insulating 'silica aerogel' particles. This one-off prototype achieved a centre pane *U*-value of 1.6 $W/m^2 K$, reducing 60% of the overall heat loss. Baker (2008) concluded that an 80% reduction (equivalent to triple glazing) would be possible by designing a purpose built product.

There is scope to develop new retrofit technologies using transparent insulation materials (TIMs). These materials perform a similar function to opaque insulation, yet they have the ability to transmit daylight and solar energy, reducing the need for artificial light and heating. TIMs transmit heat, mainly through conduction and radiation, as convection is usually suppressed (Kaushika and Sumathy 2003). The thermal and optical properties of a TIM depend on the material, its structure, thickness, quality and uniformity. Depending on the structure of a TIM, its arrangement can be classified as absorber

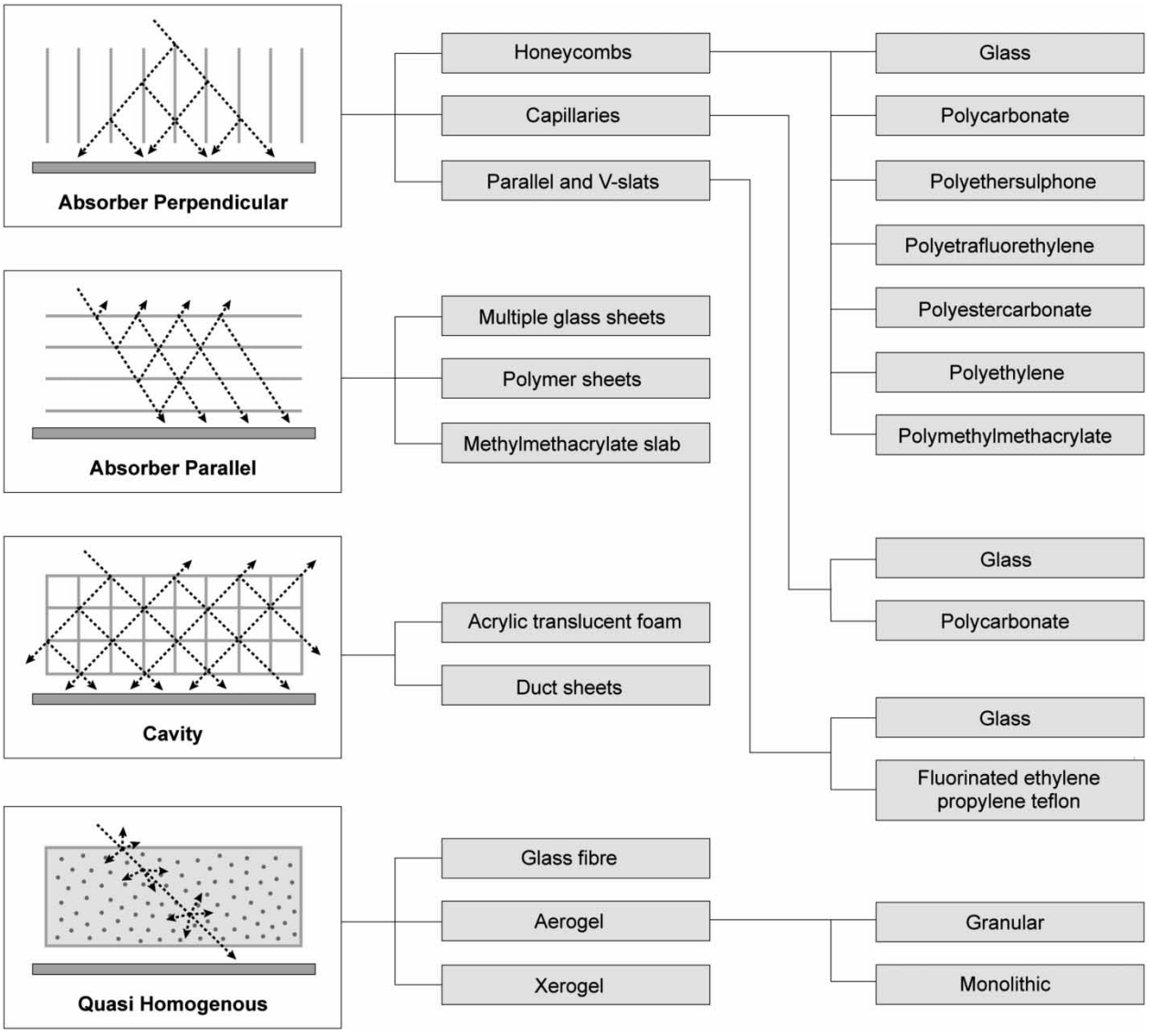

Figure 1. Types of TIMs (adapted from Wong *et al.* 2007). Reprinted from Journal of Solar Energy, 81, L. Wong, P. Eames and R. Perera. A review of transparent insulation systems and the evaluation of payback period for building applications, 1058–1071, © 2007, with permission from Elsevier.

perpendicular, absorber parallel, cavity or quasi-homogeneous. These four types are illustrated in Figure 1. TIMs typically consist of either glass or plastic arranged in a honeycomb, capillary or closed cell construction. Alternatively, granular or monolithic silica aerogel can be used to achieve higher insulation values.

Honeycomb transparent insulation was first developed in the 1960s to enhance the insulation value of glazing systems with minimal loss to light transmission (Hollands 1965). Over the past 25 years, TIMs have been applied to windows, skylights, walls, roofs and high-performance solar collectors (Dolley *et al.* 1994, Kaushika and Sumathy 2003). TIM glazing typically consists of glass or plastic capillaries or honeycomb structures sandwiched between two glass panes. These systems diffuse light well, while reducing glare and shadowing (Lien *et al.* 1997). Commercial products such as Okalux and Arel glazing can exhibit low *U*-values with good solar and light transmittance. According to Hutchins and Platzer (1996), 40-mm-thick Okalux capillary glazing, and 50-mm-thick Arel honeycomb glazing can achieve *U*-values of $1.36\,W/m^2\,K$ – comparable to modern gas filled double glazing. Alternatively, 80- and 100-mm thick systems can achieve *U*-values of $0.8\,W/m^2\,K$, respectively – comparable to modern gas filled triple glazing units.

According to Robinson and Hutchins (1994), the application of TIM glazing tends to be limited to skylights, atriums and commercial/industrial facades as the geometric structure of TIMs tends to restrict a clear view outside. TIMs appear most transparent when viewed directly on, yet opaque when viewed at an angle. In order to increase visible transmission of TIM glazing, it is important to increase capillary size, reduce the thickness or view the TIM from a distance (Lien *et al.* 1997). According to measurements by Hutchins and Platzer (1996), normal light transmittance through honeycomb and capillary TIM glazing is 78 and 84%, respectively. By comparison, normal light transmission through standard double glazing was similar at 81%. Low-emissivity gas-filled double and triple glazing units can be lower at 66 and 63%, respectively (Hutchins and Platzer 1996).

Platzer and Goetzberger (2004) and Wong *et al.* (2007) claim that commercial uptake of TIMs has been slow due to perceived high-investment costs and small number of payback studies. Peuportier *et al.* (2000) state that production quality must improve to reduce imperfections such as rough or melted edges, which can hinder clarity. Comparatively, Kaushika and Sumathy (2003) state that considerable progress has been made to reduce the quality and cost of manufacturing transparent insulation. Although capital costs to manufacture a fully functional TIM cladding system with solar control can reach €600–1000/m^2, TIM glazing systems can have costs as low as €24/m^2 (Kaushika and Sumathy 2003, Wong *et al.* 2007). On the basis of this lower cost, Wong *et al.* (2007), calculated a 3–4-year payback period for an industrial production facility in Salzgitter, Germany, renovated with $7500\,m^2$ of TIM glazing costing €180,000 with annual maintenance costs of €7200. It is unclear whether these payback periods can be directly transferred to the domestic or commercial sector due to probably differences in design quality. Nonetheless, this payback period is significantly less than new double glazing.

State of the art research into TIM glazing focuses on developing systems using transparent silica aerogel. This lightweight, nanoporous material is the only known material with an excellent combination of high solar and light transmittance and low thermal conductance (Schultz and Jenson 2008). According to Bahaj *et al.* (2008), aerogel glazing is often portrayed as the 'holy grail' of future windows, offering potential to achieve *U*-values as low as $0.1\,W/m^2\,K$, as well as high-solar energy and daylight transmittance of approximately 90% (Bahaj *et al.* 2008, Schultz and Jenson 2008). The thermal, optical and infrared properties of silica aerogels are well known (Rubin and Lampert 1983, Platzer 1987, Fricke and Tillotson 1997, Yokogawa 2005). The material effectively transmits solar light while blocking heat transfer by conduction, convection and thermal infrared radiation (Fricke and Tillotson 1997). Silica aerogel has the lowest thermal conductivity of any material, ranging from $0.018\,W/m\,K$ for granular silica aerogel to $0.004\,W/m\,K$ for evacuated monolithic silica aerogel (Yokogawa 2005, Cabot 2009). Figure 2 displays the thermal conductivity of silica aerogel, compared to various TIMs and insulation products. As shown, only vacuum technology has a thermal conductivity of the same order of magnitude as aerogel (Zimmerman and Bertschinger 2001).

To date, several small-scale prototypes have been constructed to characterise the performance of monolithic silica aerogel in glazing. Samples are sandwiched between glass sheets and evacuated to protect the aerogel from tension and moisture, as most aerogels are brittle and hydrophilic meaning that they will degrade in contact with water (Zhu *et al.* 2007, Schultz and Jenson 2008). Duer and Svendsen (1998) measured the performance of five different monolithic aerogel slabs, produced at different laboratories, ranging in thickness from 7 to 12 mm. Centre pane *U*-values of glazed samples ranged from 0.41 to $0.47\,W/m^2\,K$. Solar and visual transmittance ranged from 74 to 78% and from 71 to 73%, respectively. Jensen *et al.* (2004), Schultz *et al.* (2005) and Schultz and Jenson (2008) reported on the performance of monolithic aerogel glazing produced by the Airglass AB plant in Sweden. The largest prototype was a $1.2\,m^2$ window, consisting of four $55\,cm \times 55\,cm \times 15\,mm$ monolithic tiles fitted into an evacuated, sealed framing unit. This prototype achieved a centre pane *U*-value of $0.66\,W/m^2\,K$ (measured in a laboratory), and an overall *U*-value of $0.72\,W/m^2\,K$ (measured using a hot box), indicating that the effect of

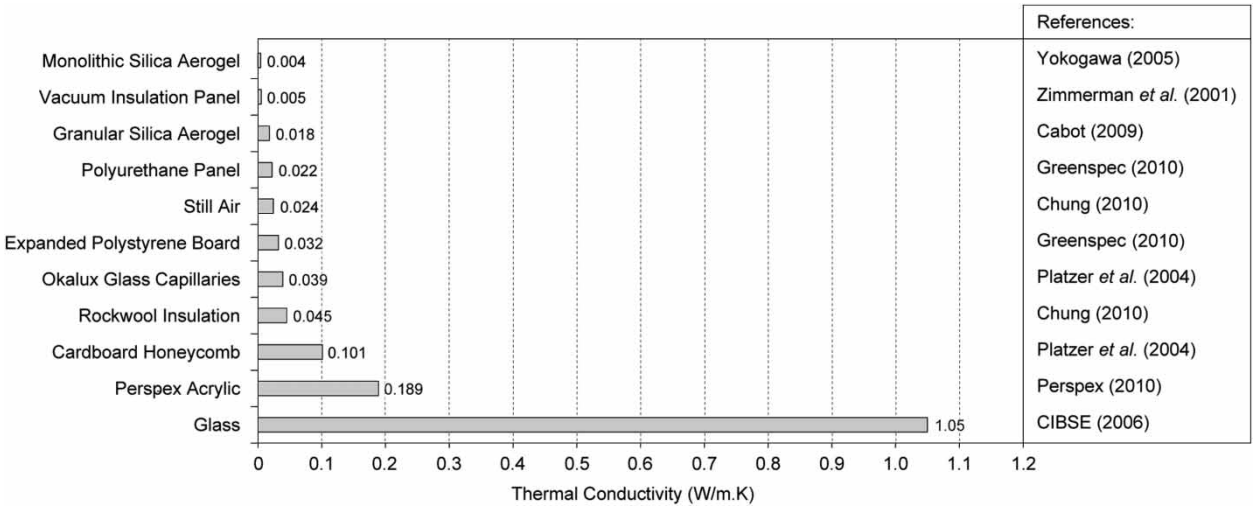

Figure 2. Thermal conductivity of TIMs and insulation products (Zimmerman and Bertschinger 2001, Platzer and Goetzberger 2004, Yokogawa 2005, CIBSE 2006, Cabot 2009, Chung 2010, Greenspec 2010, Perspex 2010).

thermal bridging at the edges was small. The direct solar transmittance was 75–76% and the normal transmittance in the visible spectrum was 85–90%.

Despite its impressive combination of thermal and optical properties, monolithic silica aerogel is yet to penetrate the commercial glazing market. According to Rubin and Lampert (1983), the cost, long processing time of aerogel, difficulty in manufacturing uniform samples and lack of adequate protection from tension and moisture are key barriers hindering progress. Duer and Svendsen (1998) and Bahaj *et al.* (2008) state that further work is required to improve clarity of samples if they are to replace conventional windows. A key issue is that the nanostructure of silica aerogel scatters transmitted light resulting in a hazy view. Schultz and Jenson (2008) claim that through improved heat treatment techniques, the Airglass AB plant is capable of producing aerogel tiles with parallel and smooth surfaces, resulting in undistorted views when shielded from direct solar radiation. However, when exposed to non-perpendicular solar radiation, visual distortion still occurs. According to Jensen *et al.* (2004), Schultz *et al.* (2005) and Schultz and Jenson (2008), aerogel glazing is an excellent option for large areas of north-facing facades, enabling a net energy gain during the heating season. Through developments in edge sealing techniques, units are anticipated to have a lifespan of 20–25 years without degradation (Schultz and Jenson 2008).

The use of granular aerogel in glazing offers an alternative solution to monolithic aerogel which is cheaper, more robust and easier to produce on a commercial scale. Systems should not be considered as a direct replacement for transparent windows, because the granules restrict the clear view outside. Instead, this material offers potential to achieve low *U*-values, enhanced light scattering and drastically reduced sound transmission in areas where an outside view is not essential (Wittwer 1992). The largest manufacturer of aerogel granules is Cabot Corporation who produces Nanogel® 1–5 mm translucent, hydrophobic silica aerogel granules, which are completely moisture and mildew resistant (Cabot 2004). Cabot's production facility in Frankfurt, Germany, can produce about 10,000 tonnes of Nanogel® per year (Werner and Brand 2010). Companies such as Kalwall, Pilkington and Okalux are now using Nanogel® across a wide range of applications (Cabot 2004). Commercial products include filled polycarbonate, glass or glass-reinforced polyester glazing units, skylights and structural building panels.

The performance of granular aerogel glazing was originally investigated by Wittwer (1992). *U*-values from 1.1 to 1.3 $W/m^2 K$ were measured for 20-mm-thick glazing units filled with granules ranging from 1 to 9 mm in diameter. Smaller granules perform better thermally, as less heat is conducted through air gaps between granules. Optically, the larger aerogel granules permitted more light and solar transmission. More recently, Reim *et al.* (2002, 2005) have measured and modelled the performance of granular aerogels encapsulated inside a 10-mm twin-wall plastic sheet, sandwiched between two glass panes with an insulated gas filling. The twin-wall sheet was selected to prevent granules from settling over time, creating a thermal bridge along the top edge. *U*-values as low as 0.37–0.56 $W/m^2 K$ were calculated for prototypes containing krypton/argon gas fillings. Without the glass cover panes, the solar and light transmission was 88 and 85%, respectively. Using a thermal model in a German climate, Reim *et al.* (2002) calculated the energetic benefit of granular aerogel glazing to be comparable to triple

glazing. Results demonstrated that granular aerogel glazing could reduce the risk of overheating on southern and east/west facades. On north-facing facades, the energetic balance of aerogel glazing was significantly better than triple glazing due to improved heat retention.

3. Research contribution

The literature review identified no research papers looking at the potential for TIM to be retrofitted over existing single-glazed windows to reduce heat loss without blocking out all of the useful natural light. There is also a lack of *in situ* studies and payback studies looking at the performance of TIM in use. This paper aims to address these issues, while pursuing the opportunity to develop novel retrofit solutions using granular aerogel. Illustrated in Figure 3, granular aerogel can easily be poured inside plastic or glass casings to develop a host of novel retrofit solutions such as sliding, hinged or roller shutters, airtight Venetian blinds or pop-in secondary glazing. As granular aerogel does not permit a clear view outside, solutions that can be closed during the evenings/night, but drawn out of the way when required, may increase the widespread applicability across the housing stock. Alternatively, in applications where the outside view is not essential, e.g. non-domestic buildings, then secondary glazing systems containing granular aerogel may be more appropriate.

This paper aims to provide new *in situ* measurements, validated with theoretical calculations to estimate the performance of these novel retrofit solutions in use. Specifically, this paper measures the resultant *U*-value and light transmission arising from retrofitting a translucent twin-wall polycarbonate panel filled with granular aerogel over an existing single-glazed window. Two panel thicknesses are tested and compared, using an unmodified window as a control. The panels are permanently fixed over the entire window creating a reasonable airtight seal to represent the best operational scenario. Twin-wall polycarbonate is anticipated to be the most appropriate medium for encapsulating granular aerogel as the panel is lightweight and has a high-impact resistance, and the twin-wall channels prevent the granules settling over time. Payback calculations based on the measured *U*-values are carried out to assess the impact of the inevitable thermal bridging that would occur when openable solutions are introduced.

Note that solar transmission is not measured during the experiments and testing takes place in a north-facing window. According to Klems and Keller (1988), the effects of solar gain can limit the accuracy of *in situ U*-value measurements. If a south-facing window was selected, then exposure to direct solar radiation could result in a net energy gain. On the basis of commercially available data for polycarbonate sheets filled with aerogel granules (not retrofitted over existing glazing), solar transmission is anticipated to be $\pm 5\%$ of the measured light transmission (Cabot 2010). The reason why *in situ* testing was selected over laboratory testing was to gain a representation of the performance of the prototype under real conditions. Although laboratory testing allows extremely accurate measurements, it is difficult to account for the variation in wind, temperature and diffuse sky radiation, which can have a significant impact on a TIMs performance (Martin and Watson 1990).

4. Method

4.1 Testing environment

In situ testing took place during February–March 2010. Prototypes were set up in a high-occupancy office in Central London heated by conventional radiators. The candidate window was single glazed, north facing, well shaded and had metal frames. The glazing was away from draughty doors and a radiator beneath the window was switched off. The glazing area contained eight panes of glass, each measuring 540 mm × 680 mm. Three adjacent panes were used during testing.

4.2 Prototypes

Figure 4 illustrates the arrangement of both prototypes and the control. The two prototypes consist of a twin-wall

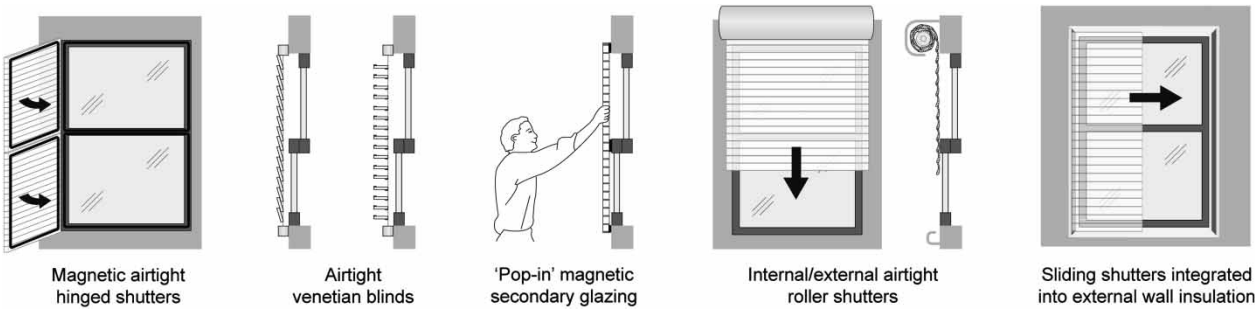

Figure 3. Concepts to improve existing windows using encapsulated granular aerogel.

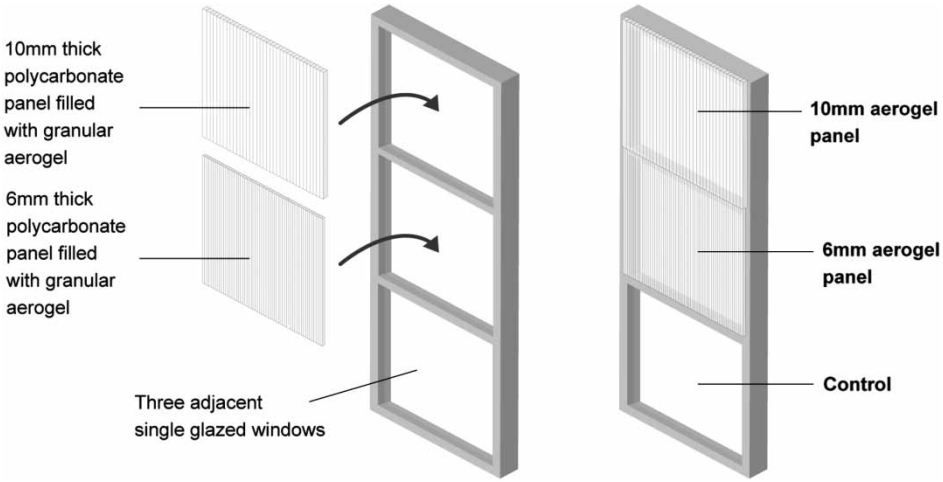

Figure 4. Schematic diagram of the 6-mm aerogel panel, 10-mm aerogel panel and the control.

polycarbonate sheet manually filled with 3-mm-diameter aerogel granules. One of these 'aerogel panels' was 6-mm thick and the other was 10-mm thick. Both prototypes were cut to fit neatly over the candidate window. They were sealed around the edges and securely attached to the internal face of the window frame using duct tape. A 15-mm air gap was created between the panels and the existing glazing. A measure of air tightness was not taken.

4.3 U-value measurements

The layout of equipment used to measure the *in situ U*-values of both prototypes and the control is shown on the left-hand diagram in Figure 5. Figure 6 displays photographs of the experiment once set up. Heat flux and temperature difference were monitored using three Peltier modules and seven K-type thermocouples, connected to a CR23X micro logger – data sheet available from Campbell Scientific (2005). Heat flux, external, internal and surface temperatures were logged every 5 min.

External temperature was monitored by positioning one thermocouple outside an adjacent, openable window, which was shut afterwards. Ambient internal temperature was monitored using three thermocouples pointing towards the indoor space by the centre of both prototypes and the control. Three additional thermocouples were also used to monitor the internal surface temperatures for a robust monitoring process.

Heat flux was monitored using Peltier modules thermally bonded to the centre of both prototypes and the control. A Peltier module is a pre-assembled semiconductor device, comprising of P- and N-type junctions, layered between two metal plates. Typically, these devices are used for their ability to become hot or cold when voltage passes through them. Reversing this function, the devices can generate a voltage when heat is

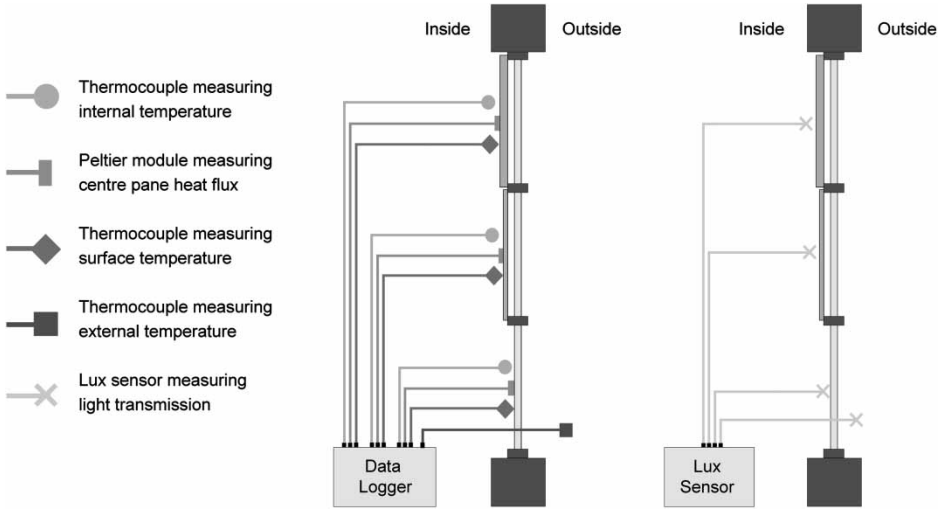

Figure 5. Schematic diagrams of the thermal and optical monitoring equipment.

Left: Photograph showing the two aerogel panels and logging equipment mounted onto single glazing. The bottom left pane of glass was used as the control. The three panes on the right hand side were not used during testing. All glazing is north facing, contains metal frames and has no thermal breaks.

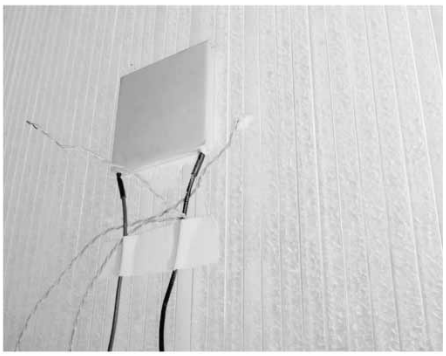

Above: Close-up photograph of the peltier module and two thermocouples mounted to the 10mm thick aerogel panel.

Figure 6. Photograph showing the prototype panels and monitoring equipment.

induced across the plates. The voltage generated by this 'Peltier effect' corresponds to a heat flux when multiplied by a calibration factor (Haruyama 2001).

4.4 Measuring light transmission

Light transmission was measured by positioning lux sensors at the points marked in the right-hand diagram in Figure 5. Readings were taken in a range of outdoor conditions, i.e. cloudy, sunny and during rain to represent different levels of day lighting. Internal readings were taken by holding the lux sensor approximately 5 cm away from the centre of each prototype panel and the control. Outdoor readings were taken by positioning the lux sensor outside of the adjacent operable window.

It is important that internal and external lux readings beside both prototype panels and the control be taken simultaneously as outdoor conditions can vary. For this experiment, only one sensor was available; therefore, results will have an inherent degree of inconsistency relative to one another due to minor delays (of a few seconds) between tests.

5. Steady-state calculations

5.1 U-values

The U-value ($W/m^2 K$) of the prototypes is given by the following equation:

$$U = \frac{1}{R_{\text{external surface}} + R_{\text{single glazing}} + R_{\text{air gap}} + R_{\text{aerogel panel}} + R_{\text{internal surface}}}. \quad (1)$$

The total U-value for each system is calculated from the mean thermal resistance (R-value) of each layer, considering their upper and lower limits. The thermal resistances of the internal surface, external surface and the air gap were calculated in accordance with BS EN ISO 6946:2007. The air gap was treated as an unventilated air layer, with upper and lower limits accounting for the combined heat transfer coefficients for convective and long-wave radiation. The centre pane thermal resistance of the single glazing was calculated by dividing the measured thickness of the glass (4 mm) by an upper limit of 1.05 W/m K (CIBSE 2006, p. 174) and lower limit 0.96 W/m K (Chung 2010, p. 297) for its thermal conductivity.

Data on the thermal resistances for both aerogel panels were obtained from personal communication with R. Lowe (25 March 2010) from Xtralite – a company which supplies polycarbonate panels filled with aerogel granules. The upper limits of the aerogel panels are based on the information provided, and the lower limits are based on a 15% reduction in performance, accounting for the manual filling process. This lower limit was selected based upon a measured test, which took place at Glasgow Caledonian University on 30 March 2010, comparing the thermal conductivities of a manually filled and industrial filled aerogel panel.

Table 1 displays the upper, lower and mean thermal resistances for each layer within the prototypes and control. An emissivity range of 0.89–0.95 was used when calculating the upper and lower range of internal surface resistances for the control (Bynum 2001, p. 249, CIBSE 2006, p. 183), compared with a range of 0.8–0.9 for the prototype panels (Mitchell 2000, p. 24, Jones and Rudlin 2006, p. 223).

Table 2 displays the calculated U-values at the centre pane of both prototype and the control. According to calculations, the 6-mm aerogel panel yields a U-value of

Table 1. Upper, lower and mean thermal resistances for each layer within the prototype panels and control.

	R-value (m^2 K/W)		
Layer	Lower limit	Upper limit	Mean
External surface	0.0205	0.0621	0.0413
Single glazing	0.0038	0.0042	0.0040
15 mm air gap	0.1790	0.2342	0.2066
6 mm aerogel panel	0.2339	0.2752	0.2566
10 mm aerogel panel	0.4404	0.5181	0.4793
Internal surface (prototypes)	0.1313	0.1811	0.1562
Internal surface (control)	0.1211	0.1548	0.1380

Table 2. Calculated *U*-values for the prototype panels and the control.

	U-value (W/m^2 K)		
	Worst case	Best case	Mean
Control	6.88	4.52	5.70
6 mm aerogel panel	1.76	1.32	1.54
10 mm aerogel panel	1.29	1.00	1.15

1.54 W/m^2 K and the 10-mm aerogel panel yields a *U*-value of 1.15 W/m^2 K. By comparison, the control has a much higher *U*-value at 5.70 W/m^2 K.

5.2 Heat loss

Figure 7 displays the estimated annual heat loss through a single-glazed window retrofitted with both prototypes. Calculations were performed using hourly temperature data from the CIBSE TRY weather file for London (CIBSE 2008). The annual heating profile is assumed to operate at 21°C, all year round, with a night-time set-back temperature of 18°C operating between 10 p.m. and 7 a.m. Four different product usage profiles are shown to represent how each aerogel panel might perform if adapted into an openable insulation solution, such as translucent airtight shutters or roller blinds. Profile 1 sets a baseline for heat loss calculations; it assumes that the single glazing is un-insulated all year round and no benefit is gained. Comparatively, Profiles 2–4 assume that the prototypes are consistently used from 1 October to 31 May, the months where approximately 90% of the degree-days for London Thames Valley occur (Vesma 2009). Profile 2 assumes that the window is insulated from 10 am to 7 pm Profile 3 assumes that the window is insulated for longer times from 6 p.m. to 8 a.m. Profile 4 assumes that the prototype is permanently insulating all day and night, thus behaving like secondary glazing.

According to calculations, both prototypes have large potential to improve the thermal performance of single glazing, cutting between 65 and 70% of the annual heat loss when permanently insulating over the heating season. Understandably, when considering openable insulation solutions, the degree of energy savings is highly dependant on how often the product is used. Preliminary calculations suggest that an openable solution can limit annual energy savings to 25–45%. By using the product earlier in the evening and later in the morning, a higher proportion of heat losses can be reduced. Beyond product usage, note that the actual savings are also dependant on the internal baseline temperature. Furthermore, if a similar study was carried out in another region, or country, then the heating demand and subsequent heat loss could vary significantly.

5.3 Light transmission

According to Cabot (2009), light transmission through aerogel decreases by 20% each time its thickness increases by 10 mm. Figure 8 visualises this relationship. As shown,

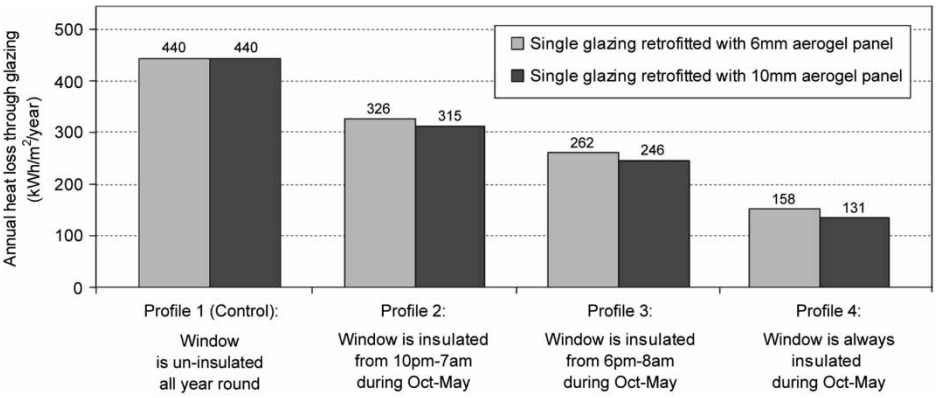

Figure 7. Predicted annual heat losses through a single-glazed window retrofitted with a 6-mm aerogel panel and 10-mm aerogel panel. Four operational scenarios are shown to illustrate the dependence of energy savings on product usage. Outside of the defined heating season, it is assumed that the window is un-insulated.

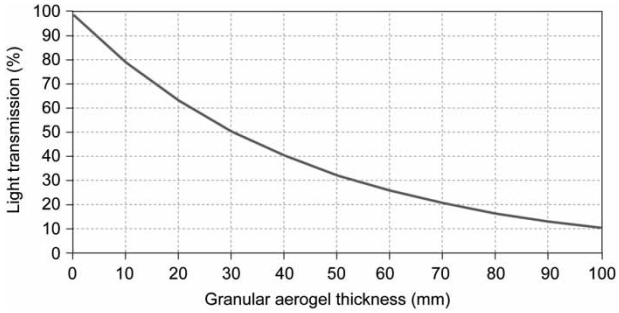

Figure 8. Calculated light transmission through granular aerogel.

6 mm of aerogel allows 88% of light transmission and 10 mm allows 80%.

To calculate the light transmission of the entire system, the single glazing and the polycarbonate panels must also be considered. CIBSE (2006, p. 31) states that light transmission through single glazing, including the effects of dirt is 80%. C&A Supplies (2010) state that a 6-mm polycarbonate panel allows 85% light transmission and 10-mm panels allow 80%. Multiplying the corresponding values together, the theoretical total light transmission through the 6-mm aerogel panel and 10-mm aerogel panel is 60 and 51%, respectively.

6. Results

6.1 Temperature profile

Figure 9 shows the external temperature and three ambient internal temperatures logged from 20 February 2010 to 1 March 2010. Over the 10 days, the average external temperature was 7.4°C with a maximum of 12.5°C and minimum of 2.1°C. The average internal temperatures beside the control, 6 mm aerogel panel and 10 mm aerogel were 19.3, 20.0 and 20.1°C, respectively. The average surface temperature beside the control was 14.3°C, whereas the 6- and 10-mm aerogel panels were several degrees warmer at 17.6 and 18.3°C, respectively.

6.2 Heat flux

Figure 10 shows the induced heat flux from the Peltier modules. Preliminary calibration of these units occurred on 14 December 2009 at Glasgow Caledonian University. Initial testing has shown the accuracy to be within 1% across a heat flux range of 0–20°C. As expected, heat flux

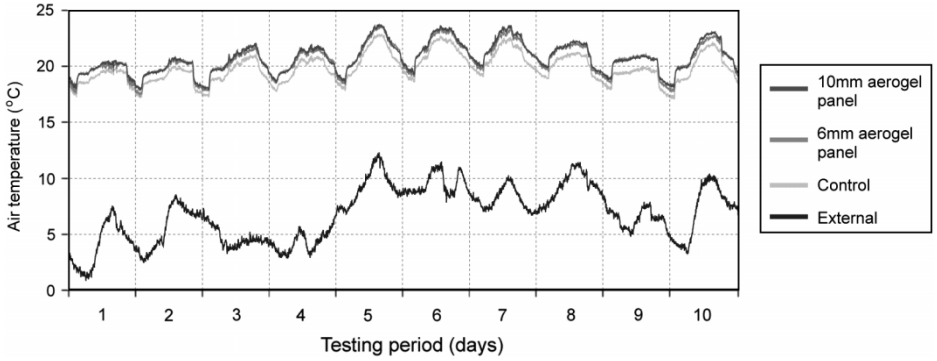

Figure 9. Measured external temperature and three internal air temperatures besides the 6-mm aerogel panel, 10-mm aerogel panel and control during *in situ* testing. Of the three internal readings, the 10-mm aerogel panel was consistently the warmest, closely followed by the 6-mm aerogel panel, then the control.

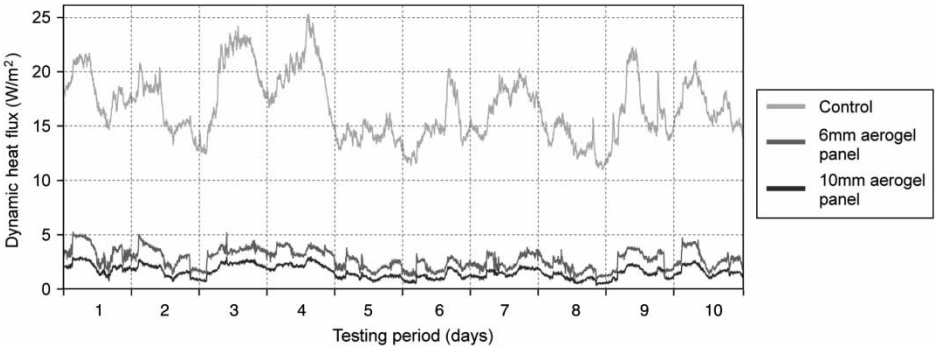

Figure 10. Measured centre pane heat flux through the 6-mm aerogel panel, 10-mm aerogel panel and control during *in situ* testing. Heat flux through the control was significantly large compared with readings through the prototypes. Heat flux through the 10-mm aerogel panel was consistently the lowest of the three readings.

through the control was significantly larger than the heat flux through both prototypes. Studying the relative performance compared with that of the control, we found that the 6-mm aerogel panel reduced heat flux by approximately 73% and the 10-mm aerogel panel by approximately 80%.

6.3 U-values

According to Cheeseman *et al.* (2007), instantaneous calculation of a *U*-value based on heat flux and temperature difference does not provide an accurate measurement of thermal transmission due to the effects of time lag. This is especially true for higher insulating materials. Cheeseman *et al.* (2007) state that a dynamic *in situ U*-value can be rationalised by calculating the cumulative average of the results over time. By applying the cumulative formula, the dynamic *U*-values of both prototypes appear to approach steady state between 3 and 5 days of testing. The control took approximately 7 days. According to the results, the control has a *U*-value of 6.39 $W/m^2 K$, the 6-mm aerogel panel yields a *U*-value of 1.54 $W/m^2 K$ and the 10-mm aerogel panel yields a *U*-value of 1.17 $W/m^2 K$.

6.4 Light transmission

Figure 11 displays the measured light intensities at five time intervals throughout March 2010. Readings were taken during various external conditions. In all cases, results show that the control allows more light transmission, than both prototypes. Light transmission reduced slightly more in the 10-mm aerogel panel than in the 6-mm aerogel panel.

Figure 12 aggregates the lux readings as a percentage. As expected, the percentage of allowable light transmission across each test was not identical. Inconsistencies may be caused by delays when using the lux meter, dirt on windows, ridges in the polycarbonate panels or variations in the aerogel granules. The average light transmission through the 6-mm aerogel panel, 10-mm aerogel panel and the control was 58, 51 and 73%, respectively.

7. Discussion

A summary of results from *in situ* testing is shown in Table 3. The aim of this study was to assess the use of granular aerogel in a novel application and in a real-time environment. Experimentation has demonstrated the impressive thermal performance of this material. On the

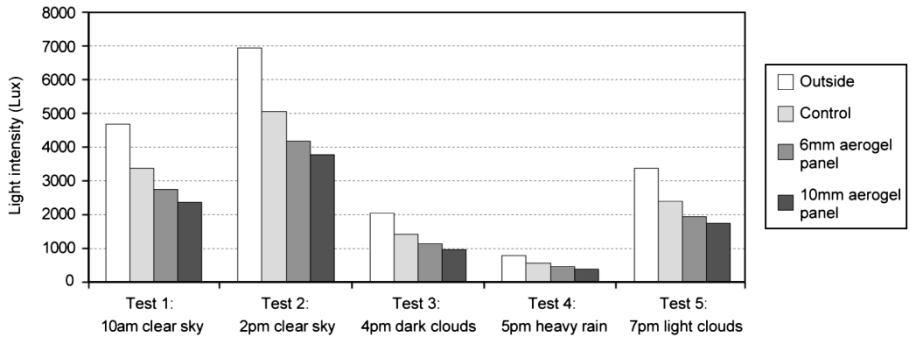

Figure 11. Measured light intensity outside compared with internal readings beside the control, 6-mm aerogel panel and 10-mm aerogel panel during five time intervals/weather conditions. Internal light transmission was consistently highest through the control, followed by 6-mm then by 10-mm aerogel panels, respectively.

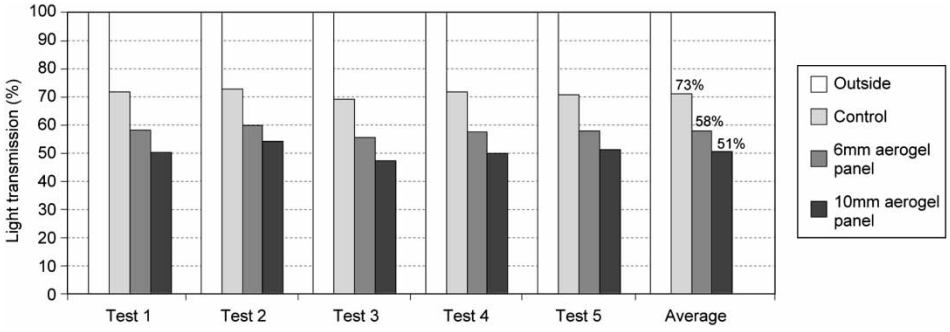

Figure 12. Measured light transmissions from the five test periods aggregated as a percentage. Results show that the proportion of light transmitted through the control and two prototypes compared with the light intensity outside was in close correlation across each test. The average percentage of light transmission is shown to the right.

Table 3. Summary of *in situ* testing results.

	Thermal performance		Optical performance	
	Measured *U*-value ($W/m^2 K$)	Reduction in heat loss (%)	Measured transmission (%)	Reduction in light (%)
Control	6.39	–	73	–
6 mm aerogel panel	1.54	74	58	22
10 mm aerogel panel	1.17	80	51	31

basis of *in situ* heat flux measurements, a 10-mm aerogel panel has been shown to prevent up to 80% of heat loss without detrimental impacts on light transmission. As shown in Figure 13, the measured *U*-values were within the allowable limits of the steady-state calculations, indicating that both sets of results are in close agreement.

Figure 14 displays a theoretical payback model for the 10-mm aerogel panel retrofitted to a single-glazed window in a gas-heated home. The model utilises a net present value equation with a discounted interest rate of 3.5% (HM Treasury 2003). Annual energy savings from heating were calculated using a baseline temperature of 21°C with an 18°C night-time set-back between 10 p.m. and 7 a.m. *Insitu U*-values were applied to the operational profiles described in Section 5.2, to account for openable insulation solutions. A unit cost of £0.04/kWh was used to represent the cost of gas. A conventional gas-condensing boiler with a winter efficiency of 84% was selected to represent the heating system within a typical UK home (GGF 2009, DECC 2010). £55/m^2 was taken as the initial capital cost of the retrofit measure. This cost consisted of a $10\,mm \times 1\,m^2$ twin-wall polycarbonate priced £10 (C&A Supplies 2010), 8 l of granular aerogel costing approximately €4/l and a 50% mark-up to cover additional costs such as airtight fixtures and installation. The cost of granular aerogel was obtained by personal communication with E. Ruiz (20 March 2009) of Cabot Corporation.

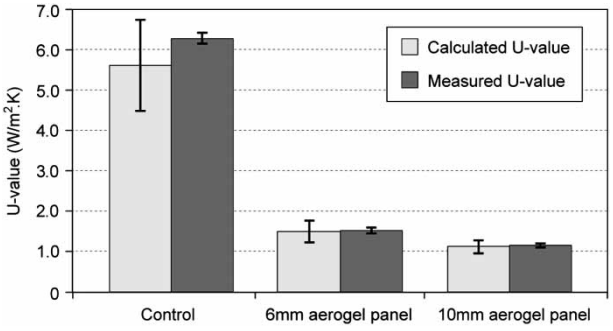

Figure 13. Comparing the calculated and measured *U*-values.

According to the payback calculations, the 10-mm aerogel panel could payback between 3.5 and 9.5 years, providing a positive return on investment of £42–185/m^2 over a 20-year product lifespan. These results are promising, especially when considering that new double and triple glazing does not provide a payback to a homeowner. Note that the 9.5 year payback calculation assumes that the window is only insulated between 10 pm. and 7 am, when the heating profile is set back to 18°C. A 5.8-year payback is calculated if the window is insulated for longer times from 6 pm to 8 am. Shorter paybacks could be expected if the capital cost of the product was driven down by the economies of scale associated with mass production. Furthermore, as this model does not account for potential increases in energy prices, this could reduce payback periods further. It is important to realise,

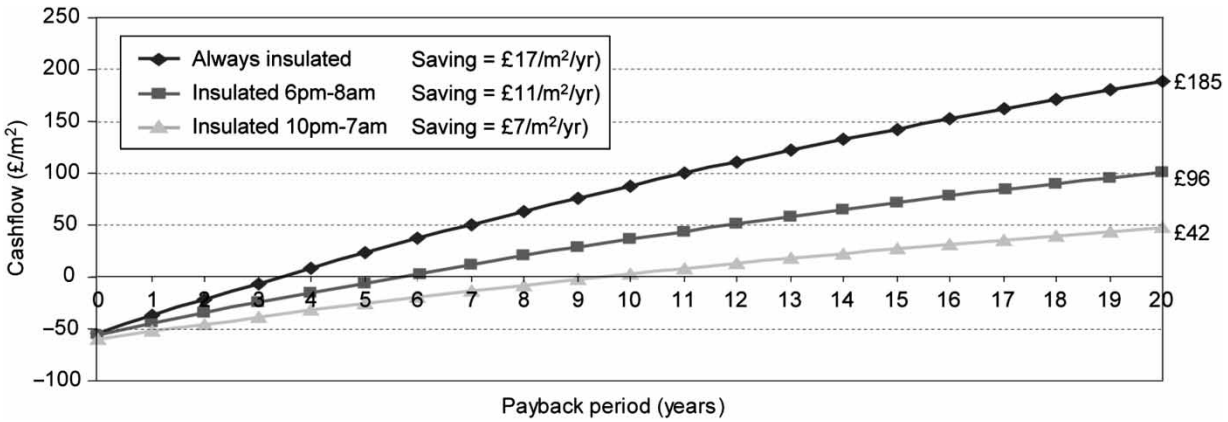

Figure 14. Payback calculations for 10-mm aerogel panel retrofitted to single glazing.

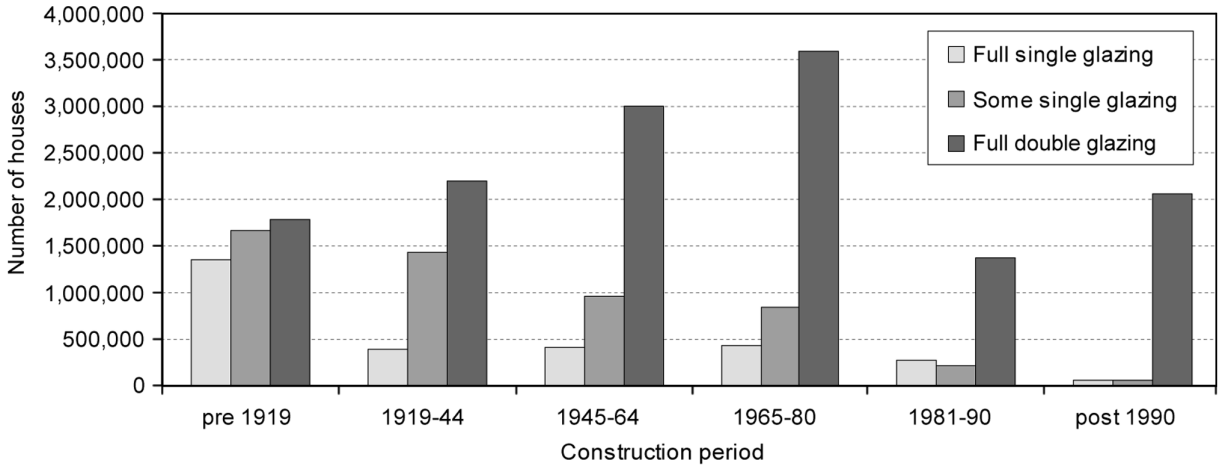

Figure 15. The distribution of glazing types across the English housing stock by construction period (generated from CLG 2006).

however, that the true payback period is highly dependant on actual temperatures both inside and outside, as well as how consistently the product is used over the heating season. If developed into an openable insulation solution, which is not used consistently, this could limit the cost-effectiveness significantly.

Building Regulations Part L1B states that new glazed elements must achieve a centre pane *U*-value of 1.2 $W/m^2 K$ in order to meet refurbishment standards (HM Government 2010, p. 19). According to this study, the 10-mm aerogel panel was capable of achieving this target without evacuating the panel or inserting a noble gas filling, demonstrating that granular aerogel can be used to achieve modern building standards at minimal costs. Future development should seek to maintain this performance, while developing suitable forms and airtight attachment methods tailored towards the needs of different occupants and building types. For openable solutions, efforts should be made to educate users on how to operate products effectively or develop products with control systems, such as automatic roller or sliding shutters to ensure maximum benefit can be gained.

Figure 15 shows the distribution of glazing types across the English housing stock by construction period. As seen, pre-1919 homes have the largest distribution of full single glazing. Additionally, a significant amount of homes constructed before the 1980s still have 'some' single-glazed windows. According to the English Housing Survey (CLG 2010), private rented homes, dwellings in London and the South East and in village/city centres or isolated rural areas are the most likely properties to contain single glazing. It is envisaged that openable translucent insulation solutions for bedrooms and living rooms may be the most widely accepted products across these houses. Alternatively, skylights and windows with limited outside views are anticipated to be most suitable for secondary glazing solutions. Modular, removable products may be particularly suited towards tenants living in privately

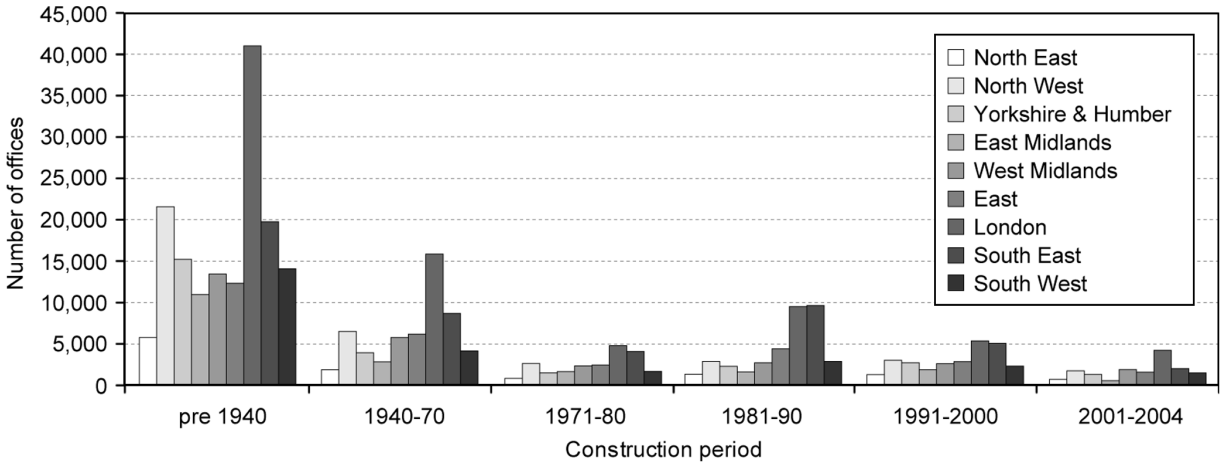

Figure 16. English office stock segmented by construction period and location (generated from CLG 2004).

rented accommodation, especially if landlords are unwilling to pay for energy efficiency measures themselves. Internal solutions aiming to improve the windows in homes limited by planning restrictions may only be suitable if incorporated adequately. Bathroom windows may not be suitable due to potential condensation risks.

The commercial office stock may be another sector where translucent insulation solutions are equally or more appropriate. As shown in Figure 16, the majority of offices in England were constructed pre-1940, thus are very likely to have single-glazed windows. Secondary glazing solutions aimed at this sector could cover large areas of the façade where a clear view is not necessary. Alternatively, roller shutters, airtight blinds or sliding screens could be particularly effective for insulating windows in winter, yet providing a clear view in summer. In order to be widely accepted across the sector, it is essential that suitable day-lighting levels be maintained. Building management system controls could be integrated into openable products to optimise both the thermal and optical performance. Understandably, widespread applicability will require solutions to have a lower capital cost to new glazing systems.

8. Conclusion

The results of this study prove Baker's (2008) hypothesis that an 80% reduction in heat loss through single glazing is achievable by designing a purpose built retrofit solution containing aerogel. Baker (2008) tested the performance of a wooden shutter lined with strips of Spacetherm® – an opaque fibrous insulation containing aerogel particles. This study shows that by utilising translucent aerogel granules, a lightweight product containing a consistent layer of insulation can be produced, which does not block out all of the useful natural light. Compared with previous research investigating the performance of granular aerogel systems, these results provide the first indication of the materials thermal and optical performance when applied to low-cost retrofit solutions seeking to retain existing windows. This knowledge is valuable, because it is anticipated to increase the widespread applicability for granular aerogel across both the domestic and commercial glazing market. Payback calculations indicate that granular aerogel is capable of providing cost-effective energy savings within the product lifespan, even if an openable solution is introduced. Note that payback periods can be significantly increased if an openable solution is not operated consistently throughout the heating season.

Future research will seek to (i) map out all ways in which granular aerogel can be applied to the existing UK building stock to reduce demand for heating and artificial lighting, (ii) investigate which solutions are most widely applicable, considering physical or planning constraints and (iii) identify which systems offer the greatest potential for widespread CO_2 savings over the life cycle. A key issue to consider is how to design solutions that accommodate for occupant behaviour to ensure it can be installed and used in the most cost-effective way. A thorough understanding of design conflicts is required to enable development to be targeted towards the most appropriate shapes, sizes and types of windows across different types of buildings. Aerogel is a unique material, with potential for many applications in new insulation products. Innovative materials such as this should not be overlooked in the effort to reduce CO_2 emissions across our existing building stock.

Acknowledgements

The authors would like to thank the EPSRC, Brunel University and Buro Happold Ltd for funding this research. The authors also thank the reviewers for their constructive comments.

References

Bahaj, A., James, P., and Jentsch, M., 2008. Potential of emerging glazing technologies for highly glazed buildings in hot arid climates. *Journal of Energy and Buildings*, 40, 720–731.

Baker, P, 2008. *Improving the thermal performance of traditional windows [online]*, Glasgow Caledonian University, Historic Scotland, Centre for Research on Indoor Climate & Health. Available from: http://www.historic-scotland.gov.uk/thermal-windows.pdf [Accessed 15 March 2009].

Beaumont, A., 2007. Hard to treat homes in England, W07 – housing regeneration and maintenance [online]. *In*: *International conference 25th–28th June – Sustainable Urban Areas – Rotterdam 2007*, Housing Centre, Building Research Establishment, Watford, UK. Available from: http://www.enhr2007rotterdam.nl/documents/W07_paper_Beaumont.pdf [Accessed 16 March 2010].

British Standards Institution, 2007. *Building components and building elements – thermal resistance and thermal transmittance – calculation method*. London: BSI Group, BS EN ISO 6946:2007.

Bynum, R., 2001. *Insulation handbook*. Chapter 12 – Radiant barriers and reflective insulation, New York: McGraw-Hill.

C&A Supplies Ltd, 2010. *Polycarbonate sheets [online]*, Available from: http://www.casupply.co.uk/acatalog/polycarbonate_sheeting.html [Accessed 20 January 2010].

Cabot Corporation, 2004. Cabot nanogel promises unmatched energy savings – revolutionary insulating material makes the best window, wall and skylight products better. *Journal of Pigment & Resin Technology*, 33 (6), 345.

Cabot Corporation, 2009. *Nanogel translucent aerogel [online]*, Available from: http://www.cabot-corp.com/wcm/download/en-us/ae/New%20EURO%20General%20brochure%20-%20Engl%20073778%20GOOD%20FORMAT.pdf [Accessed 7 April 2009].

Cabot Corporation, 2010. *Façade systems with Nanogel® [online]*, Cabot Corporation & Roda. Available from: http://www.cabot-corp.com/wcm/download/en-us/ae/Facade%20systems%20roda.pdf [Accessed 01 November 2010].

Campbell Scientific, 2005. *CR23X specifications [online]*, Available from: http://www.campbellsci.com/documents/product-brochures/s_cr23x.pdf [Accessed 18 May 2010].

Cheeseman, B., *et al.*, 2007. Developing an *in-situ* post construction quality control methodology to ensure better energy efficiency of buildings. *In*: *Proceedings of the 10th international conference on Environmental Science and Technology*, 5–7 September 2007, Kos Island, Greece.

Chung, D.L., 2010. *Composite materials: functional materials for modern technologies*. 2nd ed. New York: Springer.

CIBSE, 2006. *Environmental design – CIBSE guide A*. 7th ed. London: CIBSE Publications Department, Chartered Institute of Building Services Engineers.

CIBSE, 2008. *CIBSE TRY hourly weather data set – London [online]*, Test reference year from 1983–2004 data sets. Available from http://www.cibse.org/index.cfm?go=publications.view&item=332 [Accessed 08 November 2010].

CLG, 2004. *Age of commercial and industrial stock [online]*, Communities and Local Government. Available from http://www.communities.gov.uk/archived/publications/planningandbuilding/ageindustrialstock [Accessed 10 June 2009].

CLG, 2006. *Summary statistics – insulation and homes [online]*, Communities and Local Government. Available from: http://www.communities.gov.uk/documents/housing/xls/summarystats2006.xls [Accessed 10 June 2009].

CLG, 2010. *English housing survey, household report 2008–2009 [online]*, Communities and Local Government. Available from: http://www.communities.gov.uk/publications/corporate/statistics/ehs200809householdreport [Accessed 05 November 2010].

Climate Change Act, 2008. *Carbon targeting and budgeting, Chapter 27, Part 1 – The target for 2050*. London, UK: Her Majesty's Stationery Office Limited.

DECC, 2010. *The government's standard assessment procedure for energy rating of dwellings* [online], SAP 2009, version 9.90, March 2010, Published by BRE on behalf of Department of Energy and Climate Change, BRE Press, Watford. Available from: http://www.bre.co.uk/filelibrary/SAP/2009/SAP-2009 9-90.pdf [Accessed 30 May 2010].

Dolley, P., Martin, C., and Watson, M., 1994. Performance of walls clad with transparent insulation material in realistic operation. *Journal of Building and Environment*, 29 (1), 83–88.

Duer, K. and Svendsen, S., 1998. Monolithic silica aerogel in super insulating glazings. *Journal of Solar Energy*, 63 (4), 259–267.

EEPH – Energy Efficient Partnership for Housing, 2008. *The insulation industry, working in partnership with government to insulate the existing housing stock by 2050 [online]*, Available from: http://www.eeph.org.uk/uploads/documents/partnership/Insulation%20briefing%20paper%20Final%20v3%2007%2008%2008.pdf [Accessed 10 June 2010].

Fricke, J. and Tillotson, T., 1997. Aerogels: production, characterization and applications. *Journal of Thin Solid Films*, 297, 212–223.

GGF, 2009. *Carbon calculator [online]*, Glass and Glazing Federation. Available from: http://www.ggf.org.uk/carbonCalculator.aspx [Accessed 10 June 2009].

Greenspec, 2010. *Insulation materials compared – oil derived insulation [online]*, Available from: http://www.greenspec.co.uk/html/materials/insulation-oil_derived.html [Accessed 18 May 2010].

Haruyama, 2001. Performance of peltier elements as a cryogenic heat flux sensor at temperatures down to 60K. *Journal of Cryogenics*, 41, 335–339.

HM Government, 2010. *Conservation of fuel and power approved document L1B*. The Building Regulations 2000, 2010 ed. London: NBS, Riba Enterprises.

HM Treasury, 2003. *The green book: appraisal and evaluation in central government*. Treasury Guidance, London: The Stationary Office.

Hollands, K., 1965. Honeycomb devices in flat-plate solar collectors. *Journal of Solar Energy*, 9 (3), 159–164.

Hutchins, M. and Platzer, W., 1996. The thermal performance of advanced glazing materials. *Journal of Renewable Energy*, 8 (1–4), 540–545.

Jensen, K., Schultz, J., and Kristiansen, F., 2004. Development of windows based on highly insulating aerogel glazings. *Journal of Non-Crystalline Solids*, 350, 351–357.

Jones, I. and Rudlin, J., 2006. Process monitoring methods in laser welding of plastics. *In*: *Proceedings of the 2nd international conference on Joining Plastics*. National Physical Laboratory, 25–26 April 2006, London, pp. 233.

Kaushika, N. and Sumathy, K., 2003. Solar transparent insulation materials: a review. *Journal of Renewable and Sustainable Energy Reviews*, 7, 317–351.

Klems, J. and Keller, H., 1988. *In-situ measurements of fenestration U-values and overall thermal performance, windows and daylighting program*. CA: Applied Science Division, Lawrence Berkeley Laboratory.

Lien, A., Hestnes, A., and Aschehoug, Ø., 1997. The use of transparent insulation in low energy dwellings in cold climates. *Journal of Solar Energy*, 59 (1–3), 27–35.

Martin, C. and Watson, M., 1990. *A field test of the performance of an opaque wall clad with transparent insulation material*, Contractor Report, Department of Energy, Renewable Energy. EMC Report to ETSU S1197-P8.

Mitchell, M., 2000. *Design and micro-fabrication of a molded polycarbonate continuous flow polymerase chain reaction device*, Thesis (PhD). Department of Mechanical Engineering, Louisiana State University, USA.

MTP – Market Transformation Programme, 2007. *Innovation BN – innovative glazing; supporting UK Government Policy on sustainable products [online]*, Available from: https://www.pauljervis.net/filemgmt/visit.php?lid=197 [Accessed 14 July 2009].

Perspex, 2010. *Perspex for glazing: PXTD 236 [online]*, Available from: http://www.qdplastics.co.uk/assests/docs/acrylic/perspex_glazing236.pdf [Accessed 18 May 2010].

Peuportier, B., *et al.*, 2000. *Education of architects in solar energy and environment [online]*, Altener Programme of the European Commission, DG TREN, Section 3.1 – advanced glazing and transparent insulation. Available from: http://www.cenerg.ensmp.fr/ease/advanced_glazing.pdf [Accessed 15 October 2010].

Platzer, W., 1987. Solar transmission of transparent insulation material. *Journal of Solar Energy Materials*, 16 (1–3), 275–287.

Platzer, W.J. and Goetzberger, A., 2004. *Recent advances in transparent insulation technology*. Transparent Insulation – TI8, Fraunhofer-Institute for Solar Energy Systems, Freiburg, Germany.

Power, A., 2008. Does demolition or refurbishment of old and inefficient homes help to increase our environmental, social and economic viability? *Journal of Energy Policy*, 36, 4487–4501.

Ravetz, J., 2008. State of the stock – what do we know about existing buildings and their future prospects? *Journal of Energy Policy*, 36, 4462–4470.

RCEP – Royal Comission on Environmenatl Pollution, 2007. *The urban environment – twenty-sixth report*. Norwich: The Stationery Office, 109.

Reim, M., *et al.*, 2002. Highly insulating aerogel glazing for solar energy usage. *Journal of Solar Energy*, 72 (1), 21–29.

Reim, M., *et al.*, 2005. Silica aerogel granulate material for thermal insulation and daylighting. *Journal of Solar Energy*, 79, 131–139.

Roberts, S., 2008. Altering existing buildings in the UK. *Journal of Energy Policy*, 36, 4482–4486.

Robinson, P. and Hutchins, M., 1994. Advanced glazing technology for low energy buildings in the UK. *Journal of Renewable Energy*, 5 (1), 298–309.

Rubin, M. and Lampert, C., 1983. Transparent silica aerogels for window insulation. *Journal of Solar Energy Materials*, 7, 393–400.

Schultz, J., Jensen K., and Kristiansen, F., 2005. Super insulating aerogel glazing. *Journal of Solar Energy Materials & Solar Cells*, 89, 275–285.

Schultz, J. and Jenson, K., 2008. Evacuated aerogel glazings. *Journal of Vacuum*, 82, 723–729.

Shorrock, L., Henderson, J., and Utley, J., 2005. *Reducing carbon emissions from the UK housing stock*. Watford: BRE Press.

Utley, J. and Shorrock, L., 2008. *Domestic energy factfile 2008*. Building Research Establishment, Watford: BRE Press.

Vesma, 2009. *UK monthly and weekly degree day figures [online]*, Available from: http://www.vesma.com/ddd/index.html [Accessed 10 June 2009].

Werner, M. and Brand, L., 2010. *Focus report 2010 – aerogels [online]*, General sector reports, chemistry and materials, ObservatoryNANO, p12. Available from: http://www.observatorynano.eu/project/filesystem/files/WP2_ChemistryMaterials_FocusReport_Aerogels_29_04_2010.pdf [Accessed 20 January 2011].

Wittwer, V., 1992. Development of aerogel windows. *Journal of Non-Crystalline Solids*, 145, 233–236.

Wong, L., Eames, P., and Perera, R., 2007. A review of transparent insulation systems and the evaluation of payback period for building applications. *Journal of Solar Energy*, 81, 1058–1071.

Yokogawa, H., 2005. Handbook of sol-gel science & technology. *In*: S. Sakka, ed. *Chapter 13 – Thermal conductivity of silica aerogels*, Vol. 2. New York: Kluwer Academic Publishers.

Zhu, Q., Li, Y., Qui, Z., 2007. Research progress on aerogels as transparent insulation materials. *In*: *Challenges of power engineering and environment, international conference on Power Engineering*, October 23rd–27th, Hangzhou, China, Vol. 1, pp. 1117–1121.

Zimmerman, M. and Bertschinger, H., 2001. High performance thermal insulation systems: vacuum insulation products (VIP). *In*: *Proceedings of the international conference and workshop EMPA*, 22–24 January 2001, International Energy Agency, Duebendorf, p. 8.

Applied Energy 97 (2012) 396–404

Contents lists available at SciVerse ScienceDirect

Applied Energy

journal homepage: www.elsevier.com/locate/apenergy

Streamlined life cycle assessment of transparent silica aerogel made by supercritical drying

Mark Dowson [a,c,*], Michael Grogan [b], Tim Birks [b], David Harrison [a], Salmaan Craig [c]

[a] School of Engineering and Design, Brunel University, London UB8 3PH, UK
[b] Department of Physics, University of Bath, Bath BA2 7AY, UK
[c] Buro Happold Ltd., 17 Newman Street, London W1T 1PD, UK

ARTICLE INFO

Article history:
Available online 7 December 2011

Keywords:
Silica aerogel
Transparent insulation
Life cycle assessment
LCA
Advanced glazing

ABSTRACT

When developing sustainable building fabric technologies, it is essential that the energy use and CO_2 burden arising from manufacture does not outweigh the respective in-use savings. This study investigates this paradigm by carrying out a streamlined life cycle assessment (LCA) of silica aerogel. This unique, nanoporous translucent insulation material has the lowest thermal conductivity of any solid, retaining up to four times as much heat as conventional insulation, whilst being highly transparent to light and solar radiation. Monolithic silica aerogel has been cited as the 'holy grail' of future glazing technology. Alternatively, translucent granular aerogel is now being produced on a commercial scale. In each case, many solvents are used in production, often accompanied by intensive drying processes, which may consume large amounts of energy and CO_2. To date, there has been no peer-reviewed LCA of this material conducted to the ISO 14000 standard.

Primary data for this 'cradle-to-factory gate' LCA is collected for silica aerogel made by low and high temperature supercritical drying. In both cases, the mass of raw materials and electricity usage for each process is monitored to determine the total energy use and CO_2 burden. Findings are compared against the predicted operational savings arising from retrofitting translucent silica aerogel to a single glazed window to upgrade its thermal performance. Results should be treated as a conservative estimate as the aerogel is produced in a laboratory, which has not been developed for mass manufacture or refined to reduce its environmental impact. Furthermore, the samples are small and assumptions to upscale the manufacturing volume occur without major changes to production steps or equipment used. Despite this, parity between the CO_2 burden and CO_2 savings is achieved in less than 2 years, indicating that silica aerogel can provide a measurable environmental benefit.

1. Introduction

This study forms part of a systematic approach to improving UK building fabrics while considering both embodied impacts and operational savings – a critical balance that is typically ignored. A number of innovative insulation technologies have been developed to satisfy the growing demand for energy efficient buildings. Finding a balance between thickness, cost and in situ performance is essential, particularly for measures that rely on sustaining a vacuum. Above all, however, technologies must provide a measurable benefit over their life cycle i.e. the in-use savings must not be outweighed by the respective energy and CO_2 burden arising from manufacture, transport and end-of-life processing. This study investigates this paradigm by carrying out a streamlined 'cradle-to-factory gate' life cycle assessment (LCA) of transparent silica aerogel following the environmental standard BS EN ISO 14044:2006 [1]. Silica aerogel is an emerging super insulation material, rapidly gaining interest within the new build and refurbishment markets. Despite many solvents being used in silica aerogel production, often accompanied by intensive drying processes, which may consume large amounts of energy and CO_2, there has been no peer-reviewed LCA of this material conducted to date.

1.1. What is aerogel?

Aerogels are synthetic low-density materials with unique physical properties [2]. They are formed by removing the liquid from a gel under special drying conditions, bypassing the shrinkage and cracking experienced during ambient evaporation [3]. This creates a solid three-dimensional nanoporous structure, containing 80–99.8% air [4,5]. Due to their high porosity, aerogels exhibit the lowest thermal conductivity of any solid, whilst being transparent to

* Corresponding author at: Buro Happold Ltd., 17 Newman Street, London W1T 1PD, UK. Tel.: +44 07706 260523; fax: +44 02079 279700.
E-mail address: mark.dowson@burohappold.com (M. Dowson).

0306-2619/$ - see front matter © 2011 Elsevier Ltd. All rights reserved.
doi:10.1016/j.apenergy.2011.11.047

light and solar radiation [6,7]. Aerogels are often cited as a promising material for translucent insulation applications [2–7]. The material can be produced in monolithic or granular form. Commercial products for the building sector include cavity insulation, glazing units and cladding systems containing granular aerogel, along with translucent and opaque insulation boards, blankets and tensile roof membranes embedded with aerogel particles. Alternatively, transparent monolithic silica aerogel has been cited as the 'holy grail' of future glazing technology, with potential to achieve *U*-values as low as 0.1 $W/m^2 K$ [8]. Current research and development into monolithic glazing is limited by the high cost of production, long processing time and difficulty creating large uniform samples with complete transparency [9].

1.2. How is it made?

Aerogels were first reported by Samuel Stephens Kistler in the early 1930s [10]. Kistler aimed to test the hypothesis that "liquid inside a jelly can be replaced by a gas with little or no shrinkage".

Kistler's three-step experiment began by preparing a porous 'sol–gel' (a rigid body containing continuous solid and liquid networks) using sodium silicate and hydrochloric acid. This 'hydrogel' (where the liquid in the pores is water) was then soaked in alcohol several times over a 1–2 week period to strengthen the gel, causing the water inside the pores to be displaced. The resultant 'alcogel' (pores containing alcohol) was dried inside an autoclave using supercritical drying. The temperature and pressure of the autoclave were simultaneously raised to 270 °C and 100 bar, causing the alcohol to become supercritical (i.e. it begins to vaporise without completely changing phase due to the high pressure). As a result, the alcohol gains properties of both a liquid and a gas, eliminating surface tension inside the gel and enabling the fluid inside the pores to drain out without collapsing the solid structure. The newly formed 'aerogel' (pores containing air), could be safely handled when cool. The material possessed a low density and was opalescent. Kistler stated that numerous other materials had been successfully prepared, and that aerogels could be made from practically any material. Nowadays, silica aerogel is still the best-known and most widely prepared aerogel [11].

Up until mid 1980, risks associated with supercritical drying of alcohol were major obstacles to high volume aerogel production [12]. However, improvements in the manufacturing processes have yielded more cost effective aerogels that are economic to produce on a commercial scale [2,6,13,14]. The process has three steps: gel preparation, ageing and drying. Drying takes place through either high temperature supercritical drying (HTSCD), low temperature supercritical drying (LTSCD) or ambient pressure drying.

The most common technique for gel preparation involves reacting a silicon precursor, such as sodium silicate ("water–glass"), tetramethoxysilane (TMOS) or tetraethoxysilane (TEOS) with water in a solvent such as ethanol or methanol at ambient temperatures and pressures [11], forming silica nanoparticles. Gelation occurs when enough silica nanoparticles agglomerate to form a continuous network spanning throughout the entire volume of sol. Once the gel is prepared, it must be aged through a solvent exchange process to strengthen the gel network and prevent cracking during drying. This is achieved by soaking the gel within a pure organic solvent, usually methanol, ethanol or acetone for at least 24 h. The solvent is replaced each time equilibrium in concentration is reached – typically, this step is repeated 3–4 times.

High temperature supercritical drying was originally used by Kistler to dry aerogel. It relies upon heating and pressurising the wet gel to ~240 °C and ~100 bar, i.e. the conditions that transform the alcohol within the gel into a supercritical fluid. The process can be dangerous if proper safety precautions are not taken. In 1984, the Airglass laboratory in Sweden was destroyed due to an autoclave leaking out 1000 L of explosive methanol [11].

Low temperature supercritical drying was developed in the mid 1980s [15]. Here, the solvent inside the wet gel is replaced with liquid CO_2 prior to drying, as it possesses a critical point closer to ambient temperature. Drying therefore takes place at ~40 °C and ~100 bar, making the process more viable for commercial production. To increase the efficiency of production, supercritical CO_2 can be substituted instead of liquid CO_2. CO_2 recycling can also occur [14].

Ambient pressure drying, also called 'subcritical drying' emerged in the mid 1990s [6,13]. This process involves chemically modifying the surface of a wet-gel so that it becomes hydrophobic prior to drying. When dried ambiently, the gel partially collapses but re-expand to 85% of its original volume, since the internal network does not stick together. Gels dried by ambient pressure drying typically have 50–80% denser porosities than supercritically dried aerogels, thus are less transparent but mechanically stronger [11].

1.3. What is its environmental impact?

According to Lawrence Berkeley Laboratory, the production and use of silica aerogels is environmentally benign, the product is non-toxic, non-flammable, and it can be easily recycled [16]. Conversely, according to manufacturing studies, silica aerogel requires reasonably toxic chemicals, diffusion-controlled processes that consume a lot of solvent, and depending on the drying process, high-pressure vessels running for a long time [4,11].

Two major manufactures of silica aerogel are Cabot Corporation and Aspen Aerogels. Cabot produces translucent granules and insulation blankets via ambient pressure drying. Aspen produces opaque insulation boards and blankets embedded with silica aerogel particles via LTSCD. In 2008, both companies received a 'Silver' Cradle-to-Cradle environmental award from McDonough Braungart Design Chemistry (MBDC) for their aerogel production. MBDC claim to evaluate a products complete formulation, energy use, water use and recycling potential when assessing environmental impacts [17]. Unfortunately, data from these studies is confidential, making it difficult to assess the rigour and validity of the results. Moreover, as the MBDC Cradle-to-Cradle programme does not undergo third party certification, it does not comply with the ISO standards for life cycle assessment [18].

At present, the only data on embodied energy and CO_2 of silica aerogel comes from Aspen Aerogels opaque insulation blankets. According to the manufacturers, its production energy is 53.9 MJ/kg and its CO_2 burden is 4.3 $kgCO_2/kg$, excluding CO_2 used for supercritical extraction as it is recovered from external industrial processes. Compared to conventional insulation, these values are reasonably high. According to the University of Bath's Inventory of Carbon and Energy [19], the production energy and CO_2 burden in organic insulation ranges from 3.5 to 26.8 MJ/kg and 0.2 to 1.7 $kgCO_2/kg$, respectively. Contrarily, mineral insulation ranges from 16.6 to 38.8 MJ/kg and 1.1 to 1.4 $kgCO_2/kg$, respectively. Oil derived insulation ranges from 70 to 98.3 MJ/kg and 2.5 to 3 $kgCO_2/kg$. Note that available data for double-glazing indicates that production energy and CO_2 burden can be much higher at 360–5470 MJ/m^2 and 18–279 $kgCO_2/m^2$, depending on the frame type and gas fill. Nonetheless, it is interesting that Aspen do not disclose the amount of CO_2 required during supercritical extraction of their aerogel. According to the manufacturers, this CO_2 is a recycled waste product recovered from ethanol and ammonia production plants. Evidently, the actual amount of CO_2 used is unclear, thus highlighting a need for further investigation.

2. Streamlined LCA

Life cycle assessment (LCA) is a process by which the environmental impacts associated with a product can be quantified over its life cycle from 'cradle-to-grave'. To date there have been no peer-reviewed life cycle assessments of silica aerogel meeting the ISO 14000 standards. This study addresses this issue by conducting a streamlined LCA following BS EN ISO 14044:2006.

2.1. Goal

The aim of this study is to establish the CO_2 and energy costs associated with two different methods for manufacturing silica aerogel. Data will be compared against potential CO_2 and energy savings when retrofitting aerogel to building fabrics in situ. The purpose of this investigation is to identify whether the production costs of silica aerogel can be recovered by its operational savings within a realistic product lifespan. The study will also serve to provide a unique comparison between two (of the three) methods of aerogel production.

The intended audience for this study includes environmental engineers, architects, materials scientists and product designers. Results are intended to be publicly available. It is anticipated that results may be compared against the life cycle impacts of conventional and emerging building fabric technologies. All comparisons must recognise that the results of this study are based on a laboratory experiment, scaled-up to produce 1 m^3 volumes. Scaling assumptions must be treated as conservative estimates for commercial production due to the lack of information from industry concerning the actual economies and efficiencies of scale associated with mass production.

2.2. Scope

This study is a 'cradle-to-factory gate' assessment. Primary data is collected for two methods of aerogel production. Secondary data is used to account for the energy use and CO_2 burden from extracting raw materials, as well as the grid intensity of electricity. The impact of transport (of raw materials/finished products) and end of life processing (e.g. product re-use, recycling, landfill, etc.) are omitted from this study. However, their significance is discussed.

At the University of Bath, aerogels are produced using both low and high temperature supercritical drying for research into optical applications. We made use of their experience in aerogel production to conduct two studies, monitoring the CO_2 and energy usage associated with manufacturing small samples of silica aerogel using both drying techniques. It should be noted that there is a third method for aerogel production, via ambient pressure drying. Currently the group does not produce aerogels in this way.

The results of this study should be treated as a conservative estimate for the production cost of aerogel. The processes developed at the University of Bath have not been developed or refined for mass manufacture. As such, no recycling of solvents or CO_2 occurs. Furthermore, just 40 ml of aerogel is produced during each production run. The aerogels are solid (not granular) and have a high optical quality. Scaling assumptions to upscale the manufacturing volume, without major changes to production steps or equipment must be treated with caution.

The functional unit for this investigation is the energy use (kW h) and CO_2 burden ($kgCO_2$) required to produce 1 m^3 of aerogel. Results are compared against the operational energy and CO_2 savings arising from retrofitting a 1 cm thick, 1 m^2 twin-wall polycarbonate panel filled with aerogel granules to a single glazed window. The predicted

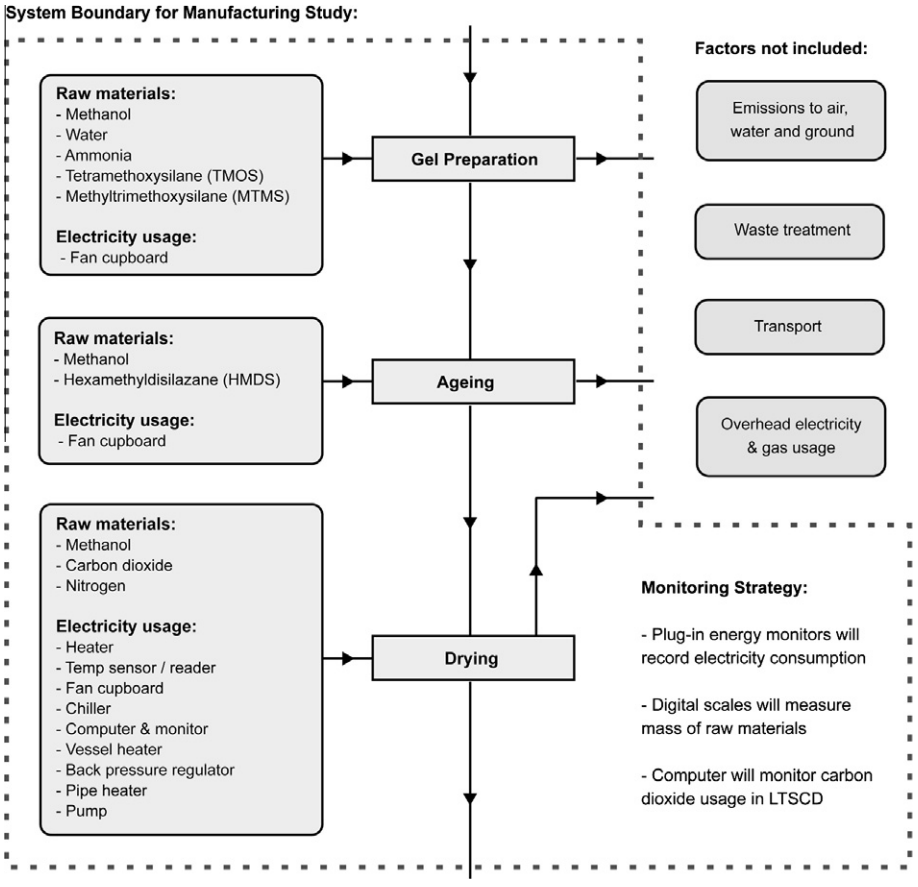

Fig. 1. System boundary and monitoring strategy for manufacturing study.

Table 1
Data collection inventory for HTSCD gel preparation.

Raw materials used in gel preparation (HTSCD)	Volume (ml)	Mass (g)	Material supplier
Tetramethoxysilane	14.4	14.64	Fisher
Methyltrimethoxysilane	1.6	1.36	Alfa Aesar
Methanol	16	12.52	Fisher
Analytical reagent grade water	8	8.00	Fisher
Ammonia 2 M	0.016	0.014	Sigma Aldrich
Electrical equipment:	Running time (h)	Total (kW h)	Equipment supplier
Fan cupboard	00:43	0.063	Astec

Table 2
Data collection inventory for LTSCD gel preparation.

Raw materials used in gel preparation (LTSCD)	Volume (ml)	Mass (g)	Material supplier
Tetramethoxysilane	16.2	16.56	Fisher
Methanol	16.2	12.96	Fisher
Analytical reagent grade water	8.1	8.10	Fisher
Ammonia 2 M	0.072	0.062	Sigma Aldrich
Electrical equipment:	Running time (h)	Total (kW h)	Equipment supplier
Fan cupboard	01:20	0.112	Astec

Table 3
Data collection inventory for HTSCD ageing process.

Raw materials used in ageing (HTSCD)	Volume (ml)	Mass (g)	Material supplier
Methanol – covering samples	8	6.33	Fisher
Methanol – 1st exchange	125	98.88	Fisher
Methanol – 2nd exchange	125	98.88	Fisher
Electrical equipment:	Running time (h)	Total (kW h)	Equipment supplier
Fan cupboard	00:10	0.014	Astec

Table 4
Data collection inventory for LTSCD ageing process.

Raw materials used in ageing (LTSCD)	Volume (ml)	Mass (g)	Material supplier
Methanol – covering samples	36	28.48	Fisher
Methanol – 1st exchange	250	197.75	Fisher
Methanol – 2nd exchange	250	197.75	Fisher
Methanol – 3rd exchange	200	158.20	Fisher
Hexamethyldisilazane – 4th ex	40	30.96	Sigma Aldrich
Methanol – 4th exchange	160	126.56	Fisher
Methanol – 5th exchange	200	158.20	Fisher
Electrical equipment:	Running time (h)	Total (kW h)	Equipment supplier
Fan cupboard	00:35	0.049	Astec

performance of this product over a 15 year lifespan is estimated based upon the results of in situ testing, carried out by the corresponding author prior to this streamlined LCA [20].

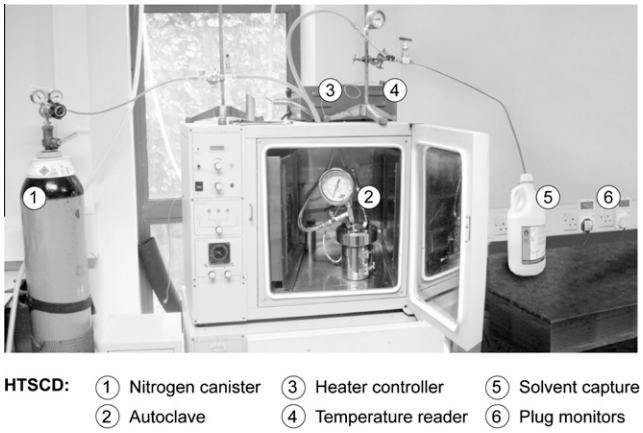

Fig. 2. Equipment for HTSCD.

3. Data collection

Data collection is split across three stages: gel preparation, ageing and drying. Gel preparation took place during April 2010. Following this, gels were aged in solvent for 3 weeks, and then supercritically dried. Fig. 1 displays the system boundary for both methods of aerogel manufacture studied. Monitoring procedures and omitted factors are outlined.

3.1. Gel preparation

The first stage of aerogel production involved mixing the chemicals together at the correct proportions, inside a ventilated fume cupboard. Approximately 40 ml of solution was prepared for both drying methods. The HTSCD samples were prepared in four glass test tubes, and the LTSCD samples were prepared in 18 smaller plastic cuvettes. Approximately 10–12 min after the raw ingredients were mixed the samples became rigid alcogels. The mass of all raw ingredients was measured using digital scales and the electricity use of the fume cupboard was logged using an 'Eco-Eye Plug-in Energy Monitor', displaying the rate of energy use (W) and the total energy use (kW h). Tables 1 and 2 show the respective data collection inventories for the HTSCD and LTSCD samples. Note that gel preparation time, and consequent electricity usage was higher than normal, due to time spent weighing each ingredient on the digital scales.

3.2. Ageing

After gel preparation, 2 ml of methanol was added to each sample to prevent ambient drying and they were covered with Parafilm. Over the next 3 weeks, the gels were fully immersed in several solvent baths within the sealed plastic containers. During this step, all unreacted water diffused out from the gel, and the network had time to strengthen. In total, the HTSCD samples went through two solvent exchanges during the ageing process. The LTSCD samples went through five, where the fourth included a surface modification to make the gel hydrophobic. All saturated ageing solvents were disposed into waste containers sent to the universities waste management facility. Tables 3 and 4 display the respective data collection inventories.

3.3. High temperature supercritical drying

Fig. 2 displays the equipment used and monitored during HTSCD. The process utilises an autoclave with a 1-L capacity, connected to an electric heater and temperature sensor. A nitrogen bottle is connected prior to drying to create an inert atmosphere

within the autoclave and check that the seals are capable of withstanding supercritical pressures. During supercritical drying, the temperature is controlled by manually entering set-points on the heater controller and the pressure is controlled using a needle valve. Excess solvent is drained away into a container as pressure is released.

To begin, the four gel samples (still inside the test tubes) were placed inside the autoclave with 400 ml of methanol. Two steel bars were then inserted to displace some of the unused volume. The autoclave was then sealed and filled with regulated nitrogen to 100 bar to check the integrity of the chamber. After approximately 5 min, the nitrogen flow was disconnected and the pressure inside the autoclave was dropped to 10 bar.

The heater was programmed to a set point of 75 °C. Temperatures were raised 25 °C every 10 min until reaching 250 °C. Between 95 and 110 min, the set point was gradually increased to 280 °C. During this time, the pressure was allowed to rise to 100 bar, and then carefully controlled to stay at this level. At 120 min, solvent was manually drained out of the autoclave causing the pressure to fall. 15 min later, the heater set point was reduced to 100 °C and the unit was switched off. The autoclave was then left to cool for 100 min, after which the aerogel could be removed. 95% of waste solvent was recovered and disposed via the universities waste management facility.

Although the fluid in this process exceeded the critical point of methanol by ~40 °C and ~25 bar, we have noticed that if the pressure and temperature do not reach at least these values, the aerogel will be cracked and more shrunken. We attribute this to excess water causing a change in the critical point of the pore fluid, requiring higher temperature and pressure to reach supercritical conditions.

During the supercritical drying process, two plug-in electricity monitors were used to record the total kW h of the heater and temperature sensor. The total energy use of the process was 0.895 kW h. Table 5 displays the data inventory for the entire HTSCD process. The mass of nitrogen used was calculated using the formula $n = PV/RT$. Here n = quantity of nitrogen consumed (moles), P = pressure (bar), V = volume (L), R = universal gas constant (0.0832), and T = temperature (Kelvin).

3.4. Low temperature supercritical drying

Fig. 3 shows the equipment used and monitored during LTSCD. The process utilises a 1-L capacity autoclave with a window for viewing supercritical extraction. The autoclave is connected to a liquid CO_2 canister, chiller, pipe heater, pump and vessel heater. A backpressure regulator controls the outflow of CO_2 and depressurisation rate of the autoclave. The entire process, including the flow rate of liquid CO_2, is controlled by a computer.

To begin, the 18 gel samples (removed from the cuvettes) were placed inside the autoclave filling approximately 5–10% of the usable space. 200 ml of methanol was added to prevent the samples from cracking during the drying process. Next, the autoclave was sealed and liquid CO_2 flowed in until in equilibrium with the bottle pressure (~55 bar). Prior to entering the autoclave, the liquid CO_2 was chilled to 0 °C. A dual-piston pump increases the CO_2 pressure to 100 bar, flowing through a pipe heater at 45 °C into the autoclave.

Table 5
Data collection inventory for HTSCD.

Raw materials used in drying (HTSCD)	Volume (ml)	Mass (g)	Material supplier
Methanol	400	316.4	Fisher
Nitrogen (N_2 at 100 bar, 296 K)	~500	0.057	BOC gases
Electrical equipment:	**Running time (h)**	**Total (kW h)**	**Equipment supplier**
Heater	02:15	0.882	SciMed
Temperature sensor	04:00	0.013	RS

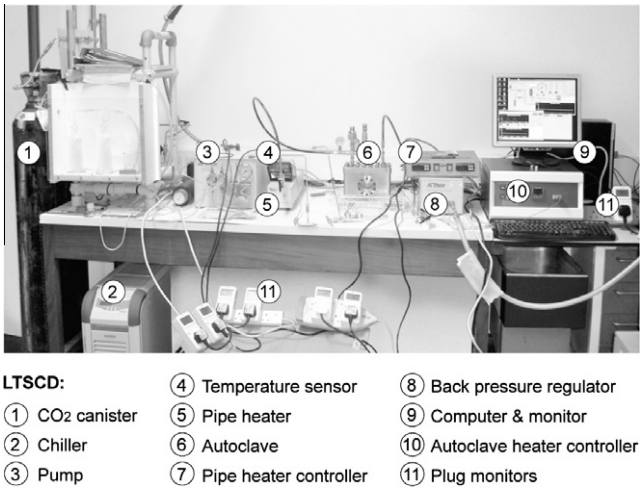

Fig. 3. Equipment for LTSCD.

Fig. 4 shows photographs taken through the window of the autoclave as liquid CO_2 enters and submerges the gel. Once supercritical conditions were reached, a vessel heater maintains the supercritical temperature at 45 °C, for approximately 4 h. When depressurisation occurred, the chiller was switched off. As pressure dropped below 50 bar, the pipe heater and vessel heater were also switched off. Once cooled, the autoclave was opened and the aerogel could be removed.

Throughout LTSCD, no recycling of CO_2 occurred. Instead, all excess CO_2 was trailed through a pipe out of a nearby window. The total duration of CO_2 flow was 4 h, 20 min. The total amount of CO_2 used, monitored by a computer during the drying process, was 4.538 kg, split across four main cycles. This value was verified by weighing the bottles using mechanical scales before and after supercritical drying.

During LTSCD, seven plug-in electricity monitor monitors were used to study the energy use of each piece of equipment. The total energy use was 3.063 kW h. The chiller (which cooled the CO_2 before entering the autoclave) accounted for over half of the total energy use, using 1.629 kW h. The computer with monitor had the second largest energy use accounting for 0.641 kW h. Table 6 displays the data collection inventory for the entire LTSCD process.

4. The aerogel

Fig. 5 shows photographs of the aerogel produced from HTSCD and LTSCD respectively. Samples have good optical quality and no internal cracks. They can be handled with care, but are fragile at the edges. Samples appear blue against a dark background and yellow against a light background. This is due to different wavelengths of light being transmitted, absorbed and reflected by the nanosized pores due to Rayleigh scattering [3].

To assess the properties of the aerogel samples made in a lab compared to industrially produced aerogel, scanning electron microscopy (SEM) was used to investigate the general topography of the LTSCD and HTSCD samples alongside ambiently dried translucent granular aerogel produced industrially by Cabot Corporation. All samples were fractured prior to investigation. The

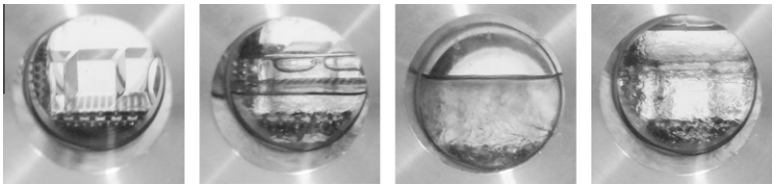

Fig. 4. Liquid CO_2 entering autoclave (photos taken at 0–30 min into drying).

Table 6
Data collection inventory for LTSCD.

Raw materials used in drying (LTSCD)	Volume (ml)	Mass (g)	Material supplier
Methanol	200	158.2	Fisher
Carbon dioxide	–	4538	BOC gases
Electrical equipment:	Running time (h)	Total (kW h)	Equipment supplier
Chiller	04:30	1.629	Thar
Computer & monitor	07:00	0.641	Dell
Vessel heater	05:45	0.206	Syrris & Lenton
Back pressure regulator	07:00	0.200	Thar
Pipe heater	05:45	0.185	Thar & SciMed
Pump	07:00	0.180	Thar
Temperature sensor	07:00	0.022	RS

industrial granules were fractured by crushing them against the viewing plate. The HTSCD and LTSCD aerogel samples were fractured by cutting them with a scalpel. All samples were brittle.

Fig. 6 displays low magnification SEM images of the three aerogels showing their fracture conditions. As shown, the surface of all three samples appeared smooth and it was not possible to see individual pores or particles, indicating that these features are on a nanoscale. Micro-cracks and cleavage marks were clearly visible across the surface of each sample where fracturing occurred. This fracturing characteristic implied that the lab samples should have similar properties to industrially produced aerogel.

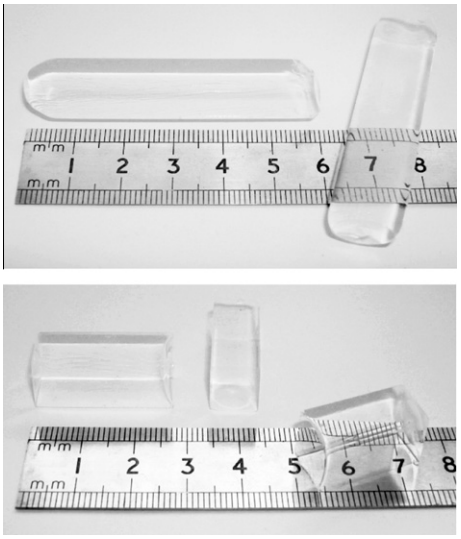

Fig. 5. Aerogel samples produced in the experiment. Top image shows the aerogel produced by HTSCD. Bottom image shows the aerogel produced by LTSCD.

5. Inventory analysis

Fig. 7 displays the production energy and CO_2 burden associated with making 40 ml of aerogel via LTSCD and HTSCD. For each raw material and electrical usage, the production energy and CO_2 burden was calculated, based upon the following assumptions. The energy and CO_2 spent to produce methanol was used to represent the impact of all chemicals. Methanol accounted for ~96% of all chemicals used in both processes. An energy cost of 47 MJ/kg and CO_2 burden of 0.4 $kgCO_2$/kg was used for pure methanol manufacture [21,22]. Note that this reference for methanol also contains a combustion value of 30 MJ/kg, which was not included at this stage [22]. The impacts of nitrogen and water use were also disregarded. A carbon factor of 0.517 $kgCO_2$/kW h was assumed for grid electricity in the UK [23].

The total production energy associated with HTSCD was 29.3 MJ/40 ml. The total production energy associated with LTSCD was higher at 62.6 MJ/40 ml. Regarding the total CO_2 burden, HTSCD was accountable for 0.73 $kgCO_2$/40 ml. LTSCD was higher at 6.64 $kgCO_2$/40 ml. The methanol used during ageing had the most significant impact on the total production energy. The CO_2 consumed during LTSCD had the most significant impact on total CO_2 burden.

6. Impact assessment

To attain the functional unit, we have considered several ways both laboratory scale processes could be optimised to create 1 m^3 (1000 l) of aerogel without major changes to equipment or manufacturing steps. These changes are:

Firstly, the maximum batch size during gel preparation could be expanded to 1-L without different stirring mechanisms. Secondly, gel preparation time could be reduced to 20 min (as weighing ingredients during data collection prolonged the process). Thirdly, the amount of solvent used during ageing could be reduced, as the least amount of solvent required for ageing is an identical volume to that of the gel. On this basis, four soaks are required for HTSCD and seven soaks are required for LTSCD to completely remove the water before supercritical drying. This was calculated from tolerances of 0.16% water for HTSCD and 0.00128% water for LTSCD, the same water% used to successfully make gels in this study. Finally, we estimate that both 1-L autoclaves could be filled with up to 500 ml of gel without changing the equipment, making drying 12.5 times more efficient.

Applying each change still means 1000 batches of gel must be prepared and aged, then supercritically dried over 2000 cycles, to produce 1 m^3 of aerogel. Nonetheless, the production energy and CO_2 burden arising from these scaled batches is shown in Fig. 8.

7. Interpretation

Prior to this investigation, in situ testing found that retrofitting a 1 cm thick, 1 m^2 twin-wall polycarbonate panel filled with aerogel granules to single glazing could reduce heat loss by 80% [20]. If adapted into removable secondary glazing, for example, fitted

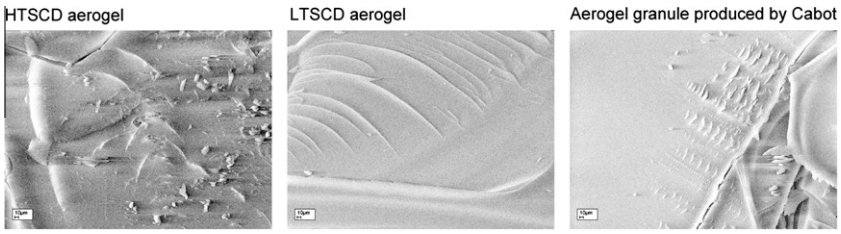

Fig. 6. Scanning electron microscopy showing the surface characteristics of three different aerogel samples at 500× magnification. The left image shows the HTSCD aerogel. The middle image shows the LTSCD aerogel. The right image shows ambiently dried translucent granular aerogel produced industrially by Cabot Corporation.

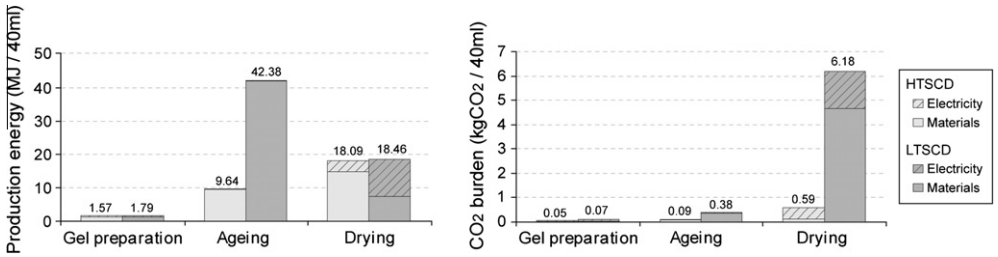

Fig. 7. Production impact associated with making 40 ml aerogel via HTSCD and LTSCD. Left graph compares production energy. Right graph compares CO_2 burden.

permanently from 1st October–31st May in a gas heated home in London, UK, then annual energy savings of approximately 400 kW h/m^2/year are predicted, equivalent to 1440 MJ/m^2/year and 80 kgCO_2/m^2/year (assuming a boiler efficiency of 84%, a gas carbon factor of 0.198 kgCO_2/kW h [23], and that the house is heated to 21 °C all year round with an 18 °C night-time set back). Taking a wall thickness of 0.5 mm, approximately 0.008 m^3/m^2 of granular aerogel was required to fill the twin-wall polycarbonate panel. Fig. 9 displays the predicted energy and CO_2 production cost for these production runs. Values are compared against the material's estimated operational savings over a 15-year product lifespan.

Results show that aerogel can provide a positive energy and CO_2 contribution within 0.3–1.9 years. Aerogel produced by HTSCD can recover its production energy within 1.3 years and its CO_2 burden within 0.3 years. Contrarily, aerogel produced by LTSCD can recover its production energy within 1.9 years and its CO_2 burden within 1.5 years.

Two factors omitted in this comparison were transport (of raw materials/finished products) and the impact of end of life processing (e.g. product re-use, recycling, landfill, etc). Transport can be complicated to assess since it is unclear where a system boundary should be drawn in a global economy. A full sensitivity analysis should consider the type of vehicle, transport distance and loading, etc. Contrarily, end of life processing can be complicated to assess since it is uncertain what might happen to products at the end of their usable lifespan. Presumably, aerogel would just be crushed and disposed of in the same way as sand or rocks, since the material consists of amorphous silica, which is not carcinogenic. Conversely, provided the aerogel has not been contaminated during its incorporation into a building, the thermal and optical properties are not expected to degrade and the material can be re-used again, resulting in further operational savings. According to the Cambridge Eco Selector (a comprehensive materials selection tool developed by Cambridge University), transporting 1 kg of insulation 100 km by ship and 300 km using a 32 ton truck accounts for just 0.15 MJ and landfill accounts for 0.2 MJ. As such, these factors are not expected to have a significant impact on the interpretation of results.

8. Limitations

A significant factor affecting the accuracy of this study is the differences between laboratory and industrial scale aerogel manufacture. Currently, scaling assumptions used to produce a 1 m^3 volume of aerogel, do not accurately represent the energy use and CO_2 burden that would result from producing this volume industrially. This issue is difficult to resolve, due to the lack of information from industry concerning the actual economies and efficiencies of scale associated with mass production of aerogel. As such, the interpretation of these results should be treated as conservative estimates, used to provide judgement as to whether silica aerogel is a good environmental technology or not. Primary sources of discrepancy are given below:

8.1. The laboratory process was scaled with no major changes to equipment or production steps

The maximum batch size for gel preparation and drying was restricted to 1 L and 0.5 L respectively. This meant 1000 batches of gel would have to be separately prepared and dried over

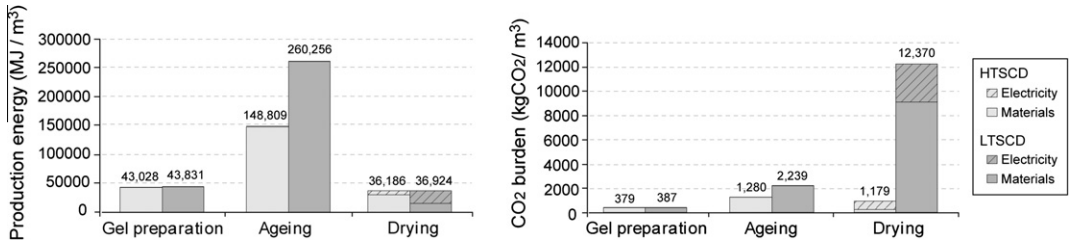

Fig. 8. Scaled production impact for making 1 m^3 aerogel via HTSCD and LTSCD. Left graph compares production energy. Right graph compares CO_2 burden.

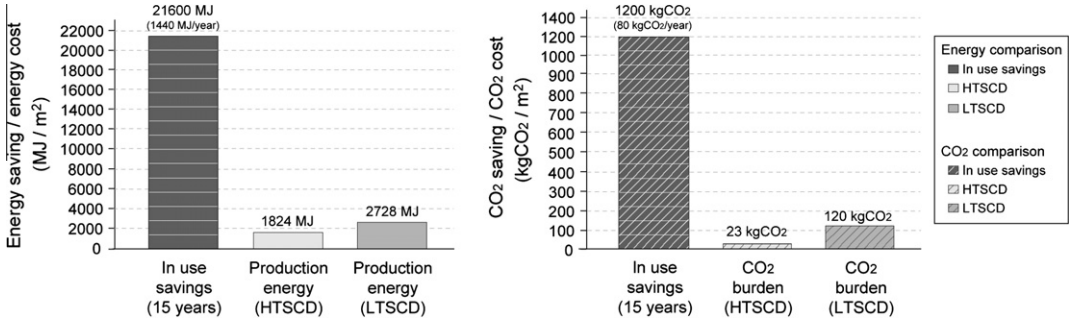

Fig. 9. Production costs of aerogel vs. in-use savings over product lifespan. Left graph compares production energy. Right graph compares CO_2 burden.

2000 cycles to produce 1 m^3 of aerogel. This is unrealistic in the context of commercial production. Larger batch sizes or continuous production would result in far greater efficiencies.

8.2. No recycling of CO_2 occurred

In the laboratory study, 4.5 kg of CO_2 was used to dry 40 ml of aerogel using LTSCD. This mass was directly scaled by 2000 times to produce 1 m^3 of aerogel. This scaling factor could be eliminated if CO_2 recycling had occurred. According to Aspen Aerogels, all CO_2 is recycled at their production facility.

8.3. No recycling or energy recovery from solvents occurred

The energy used to produce methanol was taken as 47 MJ/kg. The material has a combustion value of 30 MJ/kg, which was not included in the impact assessment. When producing aerogel on a mass scale, it can be assumed that solvents would be recycled/re-used or burnt for energy recovery. If recycled, then less methanol would need to be used. If the energy were recovered, this would result in the life cycle energy use in producing methanol being reduced to 17 MJ/kg.

8.4. The aerogels were solid, crack free and possessed high optical quality

Scaling assumptions predicted that 4–7 solvent exchanges were required to reproduce the high quality aerogel from the laboratory study. These exchanges aimed to purify the gels and completely remove the water to prevent cracking. Manufacturing granules with lower optical quality could mean that fewer solvent exchanges are required, and less control is needed to prevent cracking. Additionally, thinner granules require less time in the supercritical drying equipment as the time taken to remove the solvent scales with the square of the thickness.

8.5. Electrical equipment could be more efficient

The chiller used the largest amount of electricity during LTSCD. This unit was large and not been appropriately sized for its function. In industry, issues such as this would be corrected for cost savings, resulting in reductions in overall energy and CO_2 usage.

9. Industrial economies of scale

If we compare the results generated in this experiment to the corresponding benchmarks for Aspen Aerogel's Spaceloft® insulation, we find that our production energy and CO_2 burden, per m^3, is 28–42× and 4.4-23x larger, respectively, than industrial benchmarks. Note that the lower value in each of these ranges represents the magnitude of difference for HTSCD aerogel and the higher value represents LTSCD aerogel. In addition, note that the production energy and CO_2 burden, per m^3, for Spaceloft® is 8139 MJ/m^3 and 648 kgCO_2/m^3 respectively, generated by multiplying the products impacts, per kg, by its nominal density of 151 kg/m^3 [24].

In an effort to understand (and bridge the gap) between laboratory scale and industrial scale manufacture, Fig. 10 demonstrates how altering the scaling assumptions can significantly reduce this discrepancy.

Firstly, in revision 1, the batch size for gel preparation and drying is increased to 1000 L enabling 1 m^3 of aerogel to be manufactured over one production run (as opposed to preparing 0.5 L of gel 2000 times, followed by drying 1 L of gel 1000 times). Additional changes include scaling up electricity use by 1000, assuming 100 kg of CO_2 is used during drying for LTSCD and that all methanol usage in both manufacturing methods is combusted for energy recovery. The culmination of this revision causes the magnitude of difference to reduce to 11-15x and 3.8-8.1x respectively for production energy and CO_2 burden.

Going further, revision 2, assumes that two solvent exchanges for HTSCD and three for LTSCD are carried out and the chiller

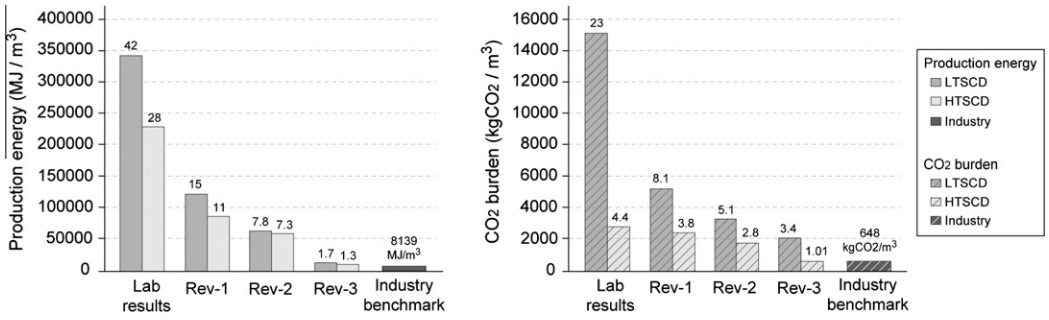

Fig. 10. Scaling revisions to bridge discrepancies between laboratory and industrial production. Left graph compares production energy. Right graph compares CO_2 burden. Bars are labelled showing the magnitude of difference compared to industry benchmarks.

efficiency in LTSCD is increased by 80%. This causes the production energy and CO_2 burden discrepancy to be reduced further to 7.3-7.8x and 2.8-5.1x respectively.

Finally, revision 3, assumes that all CO_2 used during drying for LTSCD and all methanol used in both processes is recovered/recycled (thus eliminating the impact). This causes the difference to reduce to 1.3-1.7x for the embodied energy and 1.01-3.4x for the embodied CO_2.

10. Conclusion

The aim of this study was to investigate whether the use of aerogel as an insulation technology for the building sector provides a measurable environmental benefit over its life cycle. Two methods of aerogel production have been studied to compile a data inventory for this assessment. For each, the production energy and CO_2 burden was quantified, and scaled up to produce a 1 m^3 volume of aerogel. The impact was then compared against the operational savings over 15 years, arising from retrofitting translucent aerogel to single glazing.

Preliminary results indicate that aerogel produced by LTSCD and HTSCD could recover its production cost within 0.3–1.9 years. These results are well within the predicted lifespan of building products containing aerogel. The LTSCD method of aerogel manufacture had the longest environmental payback. This was largely due to LTSCD having a higher amount of solvent use during the ageing process and because supercritical drying required more energy intensive equipment, whilst directly consumed CO_2.

The environmental impact of both manufacturing techniques could be reduced if larger batches were produced, more energy efficient equipment were used and/or if recycling or energy recovery of solvents took place. The greatest improvements are expected from LTSCD, since there is an opportunity to recycle the CO_2 used during drying. If the desire is to produce granular aerogel, there may also be opportunities to reduce the amount of solvents used, which account for a significant proportion of the total production energy. It must be emphasised that the true economies and efficiencies of scale associated with mass production are unclear due to a lack of information regarding commercial manufacturing of aerogel. Despite these factors, results have demonstrated that aerogel can provide a measurable benefit over its life cycle. Furthermore, an analysis of the scaling assumptions has shown that the discrepancies between laboratory and industrial scale manufacture can be significantly reduced.

Acknowledgements

M. Dowson thanks the EPSRC, Brunel University and Buro Happold Ltd. for funding his Research. In addition, special thanks goes to all those involved in ICAE 2011. The University of Bath aerogel project is funded by EPSRC Grant EP/F018622/1 "Aerogels in Fibre-Optics".

References

[1] British standards institution. BS EN ISO 14044:2006, Environmental management – life cycle assessment – requirements and guidelines, BSI Group, London, UK; 2006.
[2] Ashby M, Ferreira P, Schodek D. Nanomaterials nanotechnologies and design. 1st ed. Oxford, UK: Butterworth-Heinemann Publications; 2009.
[3] Fricke J, Tillotson T. Aerogels: production, characterization and applications. Thin Solid Films 1997;297:212–23.
[4] Soleimani-Dorcheh A, Abbasi M. Silica aerogel – synthesis, properties and characterization. Mater Process Technol 2008;199:10–26.
[5] Yokogawa H. Handbook of sol–gel science and technology. Thermal conductivity of silica aerogels, vol. 2. New York, USA: Kluwer Academic Publishers; 2005 [Chapter 13].
[6] Schwertfeger F, Frank D, Schmidt M. Hydrophobic waterglass based aerogels without solvent exchange or supercritical drying. Non-Cryst Solids 1998;225:24–9.
[7] Platzer WJ. Solar transmission of transparent insulation material. Solar Energy Mater 1987;16(1–3):275–87.
[8] Bahaj A, James P, Jentsch M. Potential of emerging glazing technologies for highly glazed buildings in hot arid climates. Energy Build 2008:720–31.
[9] Schultz J, Jensen K. Evacuated aerogel glazings. Vacuum 2008;82:723–9.
[10] Kistler SS. Coherent expanded aerogels and jellies. Nature 1931;27(3211):741.
[11] Steiner S, Walker W. 2010. Aerogel.org website: <http://www.aerogel.org/>.
[12] Duer K, Svendsen S. Monolithic silica aerogel in super insulating glazings. Sol Energy 1998;63(4):259–67.
[13] Deshpande R, Hua D, Smith D, Brinker J. Pore structure evolution in silica gel during aging/drying, effects of surface tension. Non-Cryst Solids 1992;144:32–44.
[14] Van Bommel M, De Haan A. Drying of silica aerogel with supercritical carbon dioxide. Non-Cryst Solids 1995;186:78–82.
[15] Tewari PH, Hunt AJ, Lofftus J. Ambient-temperature supercritical drying of transparent silica aerogels. Mater Lett 1985;3(9–10):363–7.
[16] Microstructured materials group. Silica Aerogel. Lawrence Berkeley Laboratory, California, USA; 2004. <http://eetd.lbl.gov/ecs/aerogels/sa-home.html>.
[17] Mcdonough braungart design chemistry. Cradle to Cradle Certification Program Version 2.1.1; 2008. <http://www.epea.com/documents/Outline_CertificationV2_1_1.pdf>.
[18] Green building alliance. Green Building Product Certification and Labelling; 2007. <http://www.pa-greenbuildingproducts.org/pdf/GBP_Initia tive_Product_Labeling_Grid.pdf>.
[19] Hammond G, Jones C. Inventory of carbon and energy (ICE) – version 1.6a, University of Bath, UK; 2008. <http://www.persona.uk.com/bexhill/Core_docs/CD-09/CD-09-45.pdf>.
[20] Dowson M, Harrison D, Craig S, Gill Z. Improving the thermal performance of single-glazed windows using translucent granular aerogel. Sustain Eng 2011;4(3):266–80.
[21] Neelis M, Patel M, Gielen D, Blok K. Modelling CO_2 emissions from non-energy use with the non-energy use emission accounting tables (NEAT) model. Resour Conserv Recycling 2005;45(3):226.
[22] Berge B. The ecology of building materials. second ed. Oxford, UK: Fossil oils, Architectural Press; 2009 [Chapter 9].
[23] Department of energy and climate change. SAP 2009, version 9.90, the Government's Standard Assessment Procedure for Energy Rating of Dwellings, BRE Press, Watford, UK; 2010. <http://www.bre.co.uk/filelibrary/SAP/2009/SAP-2009_9-90.pdf>.
[24] Aspen Aerogels. Spaceloft® insulation – data sheet. Revision 1.2, Aspen Aerogels, Northborough, Massachusetts, USA; 2010. <http://www.aerogel.com/products/pdf/Spaceloft_DS.pdf>.

Energy and Buildings 49 (2012) 173–187

Contents lists available at SciVerse ScienceDirect

Energy and Buildings

journal homepage: www.elsevier.com/locate/enbuild

Predicted and in situ performance of a solar air collector incorporating a translucent granular aerogel cover

Mark Dowson[a,b,*], Ian Pegg[b], David Harrison[a], Zahir Dehouche[a]

[a] School of Engineering and Design, Brunel University, London, UB8 3PH, UK
[b] Buro Happold Ltd., 17 Newman Street, London, W1T 1PD, UK

ARTICLE INFO

Article history:
Received 29 November 2011
Received in revised form 1 February 2012
Accepted 3 February 2012

Keywords:
Silica aerogel
Granular aerogel
Flat plate collector
Solar–air heater
Transparent insulation
Domestic retrofit
Mechanical ventilation
Heat recovery

ABSTRACT

There is an opportunity to improve the efficiency of flat plate solar air collectors by replacing their conventional glass covers with lightweight polycarbonate panels filled with high performance aerogel insulation. The in situ performance of a 5.4 m^2 solar air collector containing granular aerogel is simulated and tested. The collector is incorporated into the external insulation of a mechanically ventilated end terrace house, recently refurbished in London, UK. During the 7 day test period, peak outlet temperatures up to 45 °C are observed. Resultant supply and internal air temperatures peak at 25–30 and 21–22 °C respectively. Peak efficiencies of 22–36% are calculated based on the proposed design across a range of cover types. Measured outlet temperatures are validated to within 5% of their predicted values. Estimated outputs range from 118 to 166 kWh/m^2/year for collectors with different thickness granular aerogel covers, compared to 110 kWh/m^2/year for a single glazed collector, 140 k h/m^2/year for a double glazed collector and 202 kWh/m^2/year for a collector incorporating high performance monolithic aerogel. Payback periods of 9–16 years are calculated across all cover types. An efficiency up to 60% and a payback period as low as 4.5 years is possible with an optimised collector incorporating a 10 mm thick granular aerogel cover.

1. Introduction

The performance of our existing building stock must improve significantly if the UK is to meet the target of an 80% reduction in CO_2 emissions by 2050, against the 1990 baseline [1]. For instance, housing in the UK accounts for 27% of CO_2 emissions and more than 80% of the houses we will be living in by 2050 have already been built [2,3]. A range of promising new technologies are available, such as high performance translucent insulation in solar walls and solar collectors, as well as phase change materials for thermal energy storage. There is scope to retrofit these into existing buildings to make deep cuts in CO_2 emissions, but their effective implementation is no trivial task [3,4]. Solutions must account for the variety of functions, composition, size, quality, age and social value of the existing building stock, as well as the different needs, expectations and budgets of owners and occupiers.

The aim of this study is to develop and test a new retrofit technology to demonstrate its potential energy savings and payback period. In situ testing takes place in a dwelling, recently refurbished as part of the Technology Strategy Board's 'Retrofit for the Future' competition. The house is a three-storey 1960s pre-cast concrete end terrace, in South-East London, UK, with a large south facing wall, ideal to test new solar energy technologies. In its un-refurbished state, the hard-to-treat property suffered from moisture-related problems such as condensation, rising damp and mould growth made worse by insufficient supply of heating. Through refurbishment works, the property has been transformed following Passivhaus principles, from a four to a six bedroom house, super-insulated with external cladding (U-value 0.1 W/m^2 K), triple glazing (U-value 0.8 W/m^2 K, G-value 0.5) and high levels of air tightness (3.5 m^3/m^2·h @ 50 Pa). Fresh air is provided by mechanical ventilation with heat recovery (MVHR). Photovoltaic panels and vacuum tube collectors provide renewable electricity and water heating.

The focus of this paper is an innovative flat plate collector incorporated into the 2nd floor of the external insulation on the south facade. The 6 m × 0.9 m prototype is designed to provide a free source of heating to the property by elevating the temperature of the extract air used to indirectly pre-heat the supply air for the MVHR. Basic components are (i) a cover, transparent to solar irradiance whilst reducing convection and radiation losses (ii) a black perforated solar absorbing sheet inside a cavity, (iii) back insulation

* Corresponding author at: School of Engineering and Design, Brunel University/Buro Happold Ltd., London, UB8 3PH, UK. Tel.: +44 2079 279700.
E-mail addresses: mark.dowson@burohappold.com, darkmowson@hotmail.com (M. Dowson).

0378-7788/$ – see front matter © 2012 Elsevier B.V. All rights reserved.
doi:10.1016/j.enbuild.2012.02.007

Nomenclature

A_C	collector area (m^2)
A_d	exposed area of ductwork (m^2)
C_p	specific heat capacity (J/kg K)
D_h	hydraulic diameter (m)
F_R	heat removal factor
F'	collector efficiency factor
F''	collector flow factor
H	collector height (m)
H'	average cavity height (m)
h_c	convection coefficient (W/m^2 K)
h_r	radiation coefficient (W/m^2 K)
h_w	wind coefficient (W/m^2 K)
k	thermal conductivity (W/m K)
L	cube root of house volume (m)
$\dot{m}$	mass flow rate (kg/s)
Nu	Nusselt number
Pr	Prandtl number
Q_U	useful energy (W)
R	thermal resistance (m^2 K/W)
Re	Reynolds number
S	solar irradiance (W/m^2)
T_a	ambient temperature (°C)
T_{inside}	inside temperature of house (°C)
T_i	collector inlet temperature (°C)
T_{fm}	mean fluid temperature (°C)
T_L	average air temperature lost to the environment (°C)
T_o	collector outlet temperature (°C)
T_{pm}	mean plate temperature (°C)
U_{Back}	back heat loss coefficient (W/m^2 K)
U_d	loss coefficient of duct (W/m^2 K)
U_{front}	front heat loss coefficient (W/m^2 K)
U_L	overall heat loss coefficient (W/m^2 K)
v_w	wind velocity (m/s)
V	total volume of dwelling (m^3)
W	collector width (m)

Greek letters

α	plate absorptance
β	collector tilt (°)
ε	emissivity
η_1	instantaneous efficiency
μ	dynamic viscosity (kg/m s)
ρ	density (kg/m^3)
σ	Stefan–Boltzmann constant (W/m^2 K^4)
τ	cover transmittance

Subscripts: used in emissivity calculations, radiation/convection heat transfer coefficients and outlet temperature validation

1	inner surface of collector cover
2	absorber plate
3	inner surface of back insulation
i	inlet
o	outlet

to reduce conduction losses, and (iv), insulated ducts to transfer the air into the house. A novel feature of this prototype is its highly insulated translucent cover, consisting of a multi-wall polycarbonate panel filled with high performance granules of 'aerogel' insulation. This cover is predicted to reduce heat losses significantly through the collector compared to traditional glazed systems, whilst allowing sufficient solar transmission for heat collection.

2. Background

Since the late 1970s, considerable research has been undertaken to increase awareness of transparent insulation materials and demonstrate their enhanced performance over opaque and glazed elements applied to solar renovation projects [5–7]. When retrofitted to the outside of a south facing wall, as a Trombe wall, a transparent insulation material (TIM) with an air gap behind can be used to capture solar energy that can be used straight away by venting the warm air inside, or later, by allowing the heat to conduct passively through the wall. Athienitis and Ramadan [8] and Suehrcke et al. [9] demonstrate that in this application, TIMs such as glass or plastic honeycombs and flat or corrugated polycarbonate sheets can provide significant energy savings when retrofitted to residential and commercial walls. Dolley et al. [10] used a test cell to monitor the thermal performance of a polycarbonate honeycomb TIM system retrofitted to a southern wall. Extrapolating the results, for every m^2 of TIM installed, the annual space heating requirement would reduce by 150 kWh/year in a typical pre-1930s UK solid walled dwelling, or 40 kWh/year in a super insulated home [10]. In a comparative study of six houses in France, Peuportier and Michel [11] found that honeycomb TIMs can increase the efficiency of conventional solar air collectors and Trombe walls by 25% and 50%, respectively.

According to Kaushika and Sumathy [12] and Wong et al. [13] the most well documented application of TIM is in flat plate collectors for solar air or solar water heating. According to Hastings and Mørck [14], when integrated into the roof or façade of a dwelling, a solar air heater is ideal for pre-heating the ambient or return air in a mechanically ventilated dwelling. Rommel and Wagner [15] demonstrated how flat plate solar air collectors containing 50–100 mm polycarbonate honeycomb layers function well at lower temperature applications between 40 and 80 °C. Higher working temperatures of up to 260 °C can be achieved using glass capillaries, whereas plastic covers are susceptible to melting at temperatures above 120 °C [15]. Schmidt et al. [16] and Kaushika and Reddy [17] both constructed small scale solar water heaters containing TIM covers in place of conventional glazing. Solar conversion efficiencies up to 63% and storage tank temperatures of 50–60 °C were attained, indicating that these systems would be an effective pre-heater. Authors commented that the TIM was found to minimise the risk of freezing whilst also obtaining solar fractions that outperformed some conventional domestic hot water systems.

A main advantage of using TIM instead of single or multiple glazed covers is the weight reduction, which can play an important factor in retrofit applications. For example, Okalux Kapipane [18], a transparent plastic honeycomb has a density of 30 kg/m^3, compared to glass at 2500 kg/m^3. Even at 40 mm thick, this product is 12.5 times lighter than glass weighing 0.6 kg/m^2, compared to7.5 kg/m^2 for a 3 mm thick glass pane. Despite such benefits, significant implementation of outdoor solar energy systems incorporating TIM has been slow. Platzer and Goetzberger [19] estimated that over 15,000 m^2 of TIM had been installed by the mid 1990s across 85 buildings throughout Germany, Austria and Switzerland, compared to just 1000 m^2 at the start of the decade. According to the authors, this indicated that the market situation was promising, but not satisfactory. Some of the key barriers include a lack of product development guides, imperfections in honeycomb or capillary TIMs, the low working temperatures of plastics and the potential for overheating when too much solar radiation is absorbed [13,19]. Further to this, the high investment cost of TIM, shading devices and control measures has presented barriers to widespread implementation [13,19]. Conversely, Wong et al. [13] claim that with improved design guidance combined with more information on the capital cost and payback periods of TIM in use, there will be increasing evidence to outweigh the barriers currently hindering market

growth, especially as fuel prices increase in future, reducing pay back periods.

In a previous study containing a full review of transparent insulation materials applied to glazing, the corresponding author measured the in situ *U*-value and light transmittance of a 10 mm thick translucent polycarbonate panel filled with high performance granular 'aerogel' insulation, retrofitted over an existing single glazed window [20]. Aerogel is a unique class of nano-porous insulation that exhibit the lowest thermal conductivity of any solid, by suppressing heat transfer by conduction, convection and thermal infrared radiation, whilst being highly translucent to light and solar irradiance [21–23]. Applied to the inside face of a window, the prototype was found to reduce heat loss by 80%, equivalent to triple glazing, without detrimental reductions in light transmission [20]. If developed into a new retrofit product such as translucent secondary glazing or sliding shutters, payback periods between 3.5 and 9.5 years were predicted if the products were consistently used over the heating season [20]. This is considerably less than new double glazing, which can have paybacks far exceeding their 20 year product life span (for example Shorrock et al. [24] predicted a capital cost of £4000 (€4826) for double glazing in a typical 3-bedroom semi detached house, compared to just £40/year (€48) in annual energy savings). In a follow-up study, a streamlined life cycle assessment of silica aerogel was conducted to verify that the amount of energy and CO_2 required to manufacture the material does not outweigh the respective in-use savings [25]. Parity was achieved in 0–2 years, indicating that silica aerogel can provide a measurable environmental benefit [25].

Aerogel is often cited as a promising material for translucent insulation applications [26–30]. Thermal conductivities as low as 0.004 W/m K have been obtained through manufacturing solid monolithic aerogel tiles, prepared and evacuated in research laboratories [31]. Conversely, mass produced granules available to the construction industry can achieve low thermal conductivities of 0.018 W/m K [32]. According to Rubin and Lampert [33], the high cost, long processing time and difficulty manufacturing uniform samples protected from tension and moisture are key barriers hindering progress of monolithic aerogel production. By comparison, granular aerogel is cheaper, more robust and easier to produce on a commercial scale. The largest manufacturer is Cabot Corporation who produces 10,000 tonnes/year of 1–5 mm translucent, hydrophobic aerogel granules, which are completely moisture and mildew resistant [34,35]. Companies such as Kalwall, Pilkington and Okalux are now using granular aerogel across a wide range of applications [34]. Commercial products include filled polycarbonate, glass or glass-reinforced polyester glazing units, skylights and structural building panels [30].

The concept of a Trombe wall incorporating a monolithic aerogel cover encapsulated within double-glazing was originally proposed by Fricke [36]. According to modelling by Caps and Fricke [37], a 15 mm thick monolithic aerogel cover, sandwiched between double glazing, then exerted to vacuum, could achieve minimal solar heat losses compared to conventional TIM due to its high solar transmission of 50–60% and low *U*-value of 0.5 W/m^2 K. Despite this, Caps and Fricke [37] concluded that conventional TIMs are technically simpler as the evacuated system would also require a durable vacuum-tight metal rim. By comparison, Svendsen [38] constructed a 1.4 m^2 flat plate collector prototype for water heating, with measured efficiencies of 60–80% indicating that the prototype could generate up to 700 kWh/m^2/year, being twice as good as commercial flat plate collectors. Modelling by Nordgaard and Beckman [39] verified this, demonstrating that the reduction in solar transmittance compared to a single glass pane is more than compensated by the reduction in heat losses, achieving efficiencies of more than 60%.

Our literature review indentified a lack of in situ studies of solar walls and/or solar collectors incorporating granular aerogel. This paper seeks to contribute to this field, motivated by the lower cost and increased functionality of granular aerogel over monolithic aerogel, supported by its recent emergence within the construction sector. Ortjohann [40] predicted that super-insulating solar thermal collectors could be produced using granular aerogel sandwiched inside an evacuated collector design. The main benefit would be its low weight, ease of handling and ability to provide an efficient collector design without an optimised absorber technology. Conversely, the main disadvantage would be the difficulty in maintaining a long-life of the vacuum technology [40]. Countering this, the performance of granular aerogel without a vacuum has been investigated by Wittwer [41] and Reim et al. [42]. *U*-values of 1.1 to 1.3 W/m^2 K were measured for 20 mm thick glazed samples [41]. Subsequently, even lower *U*-values of 0.4 W/m^2 K were measured for 20 mm thick plastic panels filled with granular aerogel, sandwiched between two glass panes with krypton and argon gas fillings [42]. According to Reim et al. [42] without the glass panes (and gas fillings), the solar transmittance of their prototype was 65%, indicating high potential for use in insulated solar walls, with 40% less heat losses than conventional glass solar collectors.

3. Prototype description

A schematic diagram of the 'aerogel solar collector' constructed for this study, together with an outline of the monitoring equipment and control strategy, is shown within Fig. 1. A floor plan layout showing the location of the prototype, alongside the supply and extract ductwork in the mechanical ventilation system is shown in Fig. 2. The prototype is a flat plate solar air heater incorporated into an MVHR running in continuous operation. Air extracted from the kitchen and bathrooms is fed into the solar collector cavity, where it is heated by incoming solar irradiance. This heat is then used to provide additional energy to indirectly heat the incoming fresh air supply to the property's living room and bedrooms. Automatic flow and bypass controls maintain comfortable living conditions all year round, with radiators providing top-up heating when necessary.

Fig. 3 contains a section through the inlet of the aerogel solar collector. The prototype consists of a 6 m × 0.9 m timber frame, painted black, at high level, retrofitted to the outside of the dwelling's existing south facing concrete façade. Fixed to the timber is an aluminium frame to support the cover system. Two 150 mm diameter holes were diamond cut through the external wall, in the bottom left and top right corners of the collector to facilitate the inlet and outlet respectively. 50 mm of mineral insulation was inserted in the back of the collector and around the perimeter of the timber frame to reduce back and edge heat losses. The absorber consists of three black powder coated perforated aluminium sheets fixed side-by-side spanning across the width of the collector. Each sheet is 1 mm thick and contains 4.7 mm diameter perforations at 8 mm pitches, creating a 40% open area. The sheet fitted on the inlet side of the collector has a pre-cut hole enabling the inlet ductwork to penetrate through so that incoming air passes over its surface. When fitted, there is an 80 mm cavity either side of the sheet.

The cover consists of twelve 40 mm thick multi-wall polycarbonate panels connected side-by-side within the aluminium frame. This cover thickness was selected to enable the prototype to achieve an overall *U*-value below the Passivhaus target of 0.8 W/m^2 K for glazed openings [43]. This was important to the design team as the prototype was being integrated into the external cladding scheme, as opposed to being a stand-alone solar air collector mounted at roof level. This thickness was also preferred by the client over thinner covers, since it would enable a larger prototype to be constructed, more visible to the wider community, without increased

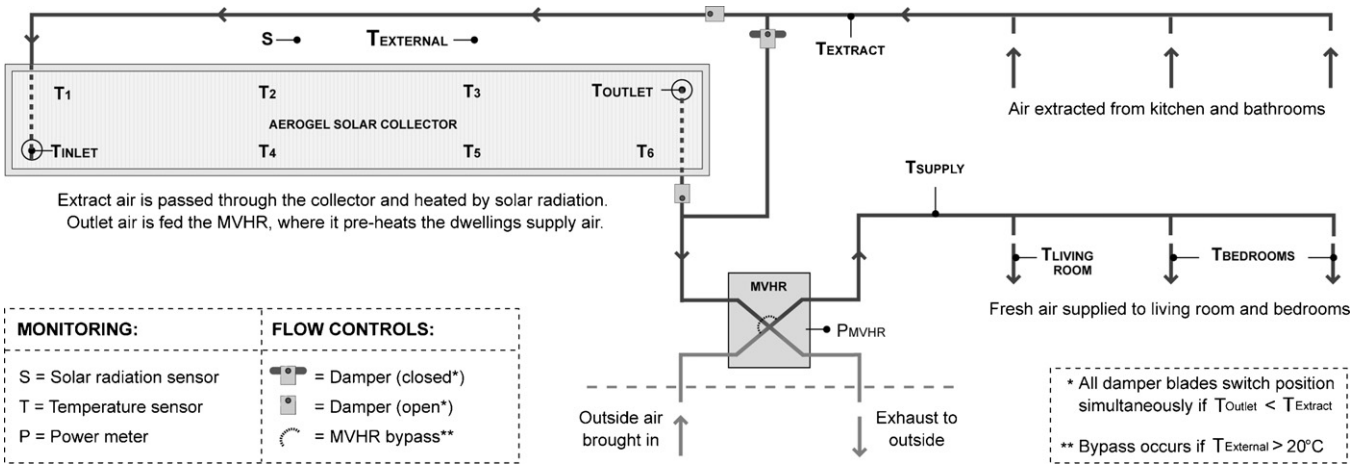

Fig. 1. Schematic of the aerogel solar collector and monitoring equipment.

risk of overheating inside the dwelling. Take note, in Section 5.1, thermal modelling demonstrates how the operational efficiency can be improved using thinner granular aerogel covers with higher solar transmittance, but worse *U*-values. Each of these polycarbonate covers can be manufactured to include additives for flame resistance and UV stabilisation, making them suitable for outdoor use and capable of withstanding temperatures up to 150 °C without warping. They have Class 1 approval and a EuroClass (B-s1, d0) fire rating, also when filled with aerogel [44].

Prior to sealing the collector, eight temperature/humidity sensors with wireless radio transmitters were fixed to the perforated absorber sheet at high and low level to monitor the profile across the collector. Each sensor head is located behind the absorber sheet and contains a plastic shield to protect against direct solar irradiance. Sensors by the inlet and outlet ducts contain small caps allowing for protection against direct solar irradiance without disrupting airflow. All transmitters were fixed to the front of the absorber sheet to obtain the clearest signal down to a data hub in the plant room. Four additional temperature/humidity sensors were installed in the supply and extract ductwork for the MVHR, as well as in the living room and a north facing bedroom (shown as Bedroom 3 in Fig. 2). A pyranometer mounted horizontally on the edge of the roof was used to measure the intensity of solar irradiance hitting the solar wall. A power meter on the MVHR measures

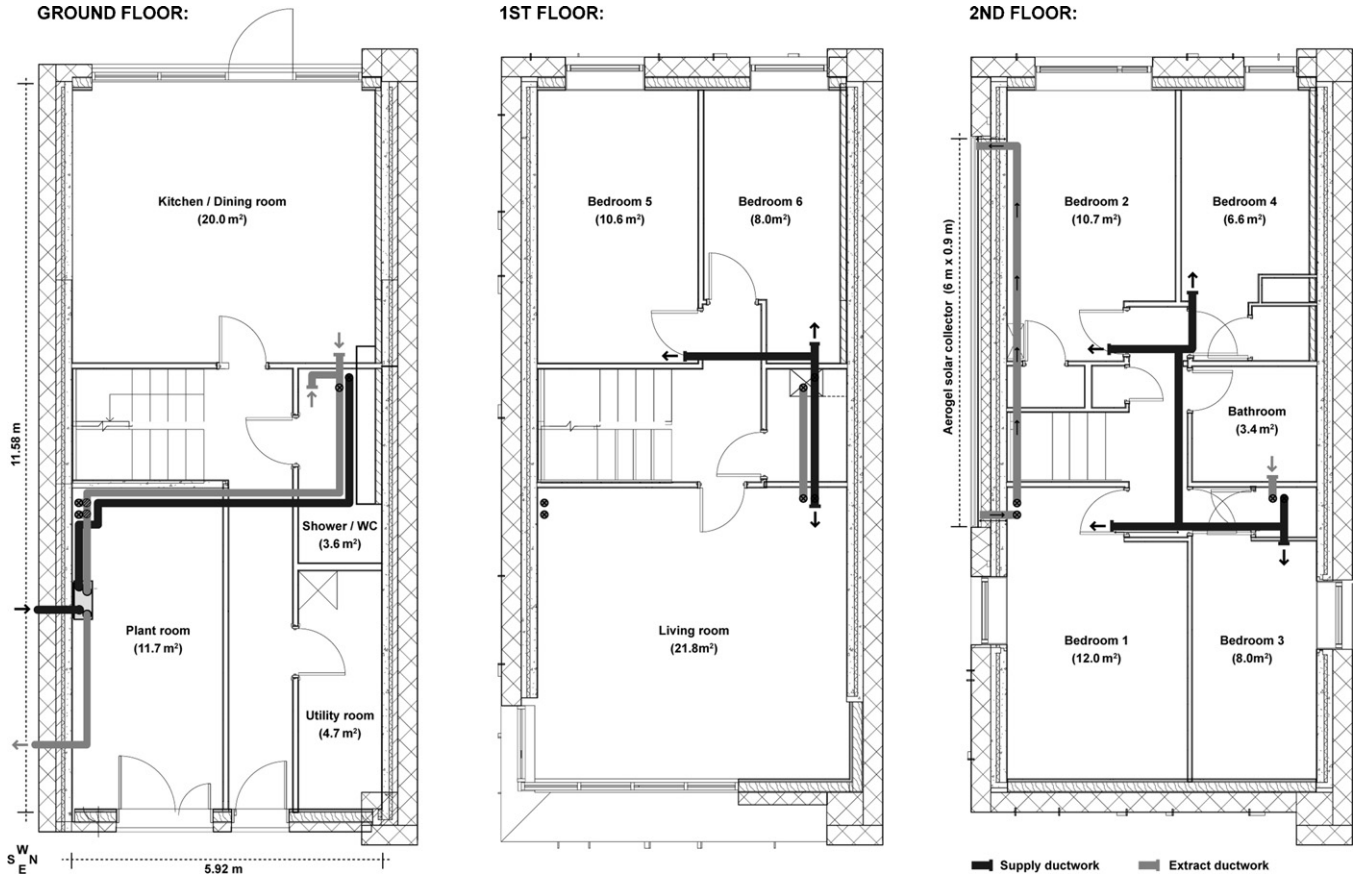

Fig. 2. Layout diagram of the house showing the aerogel solar collector and the location of supply and extract ductwork in the mechanical ventilation system.

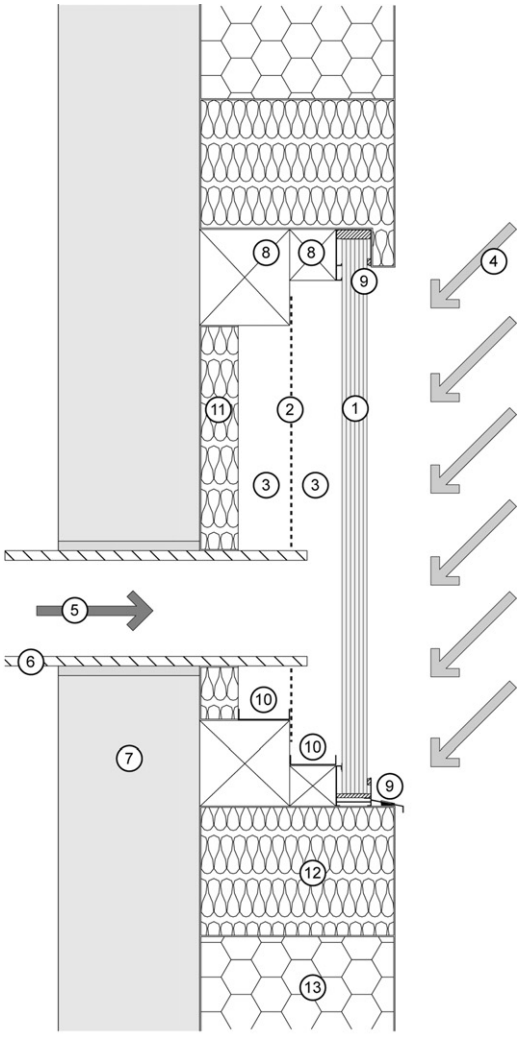

Fig. 3. Section through the inlet duct of the aerogel solar collector.

the electricity consumption of the fans. All sensors provide 5-min pulsed outputs.

Directing air to and from the solar collector are spans of 150 mm diameter pre-insulated ducts. Warm air from the collector outlet runs vertically down to a plant room on the ground floor. Inside the plant room is an arrangement of three dampers (shown in Fig. 1), to direct air flow. These dampers operate simultaneously based on a changeover relay provided by a temperature differential electronic thermostat, supplied by Titan Products Ltd. This control unit is wired to two thermistors located in the solar collector outlet and exhaust air ductwork. Its changeover relay to direct air into the collector occurs when the outlet temperature is 5 °C greater than the exhaust temperature. The MVHR is the MRXBOX95B-WH1 with optional summer bypass, supplied from Nuaire. According to its specification, the unit recovers heat at 90% efficiency when operating in a dwelling with a kitchen and three additional wet rooms. The unit's summer bypass function (independent of the three control dampers) activates when the outside air temperature exceeds 20 °C.

4. Calculation methodology

Duffie and Beckman [45] provide one of the most comprehensive and widely cited resources for predicting the performance of solar energy technologies. With the exception of the overall heat loss coefficient (U_L) and collector efficiency factor (F') equations derived by Parker [46], this reference provides the foundation for the following methodology used to predict the performance of the aerogel solar collector.

4.1. Energy balance equation

The steady state thermal performance of a flat-plate collector can be calculated from Eq. (1), taking account of thermal and optical losses to determine the distribution of incident solar irradiance into useful energy gain (Q_U).

$$Q_U = A_C F_R [S(\tau\alpha) - U_L(T_i - T_a)] \quad (1)$$

A_C is the aperture area of the collector. F_R, refers to a plate efficiency or "heat removal factor". S is the total solar irradiance on the collector surface. τ is the transmittance of the cover. α is the absorptance of the absorber plate. U_L is the overall heat loss coefficient of the collector. T_i is the inlet fluid temperature. T_a is the ambient air temperature outside.

4.2. Collector heat losses

The overall heat loss coefficient (U_L) depends upon heat losses through the front and back of the collector, convection and radiation exchanges inside the cavity and heat losses due to wind. Fig. 4 illustrates these parameters within a one-dimensional section of the aerogel solar collector. h_w is the wind heat transfer coefficient, h_r and h_c are radiation and convection coefficients, respectively, where the subscripts 1, 2 and 3 correspond to the inner surface of the collector, the absorber plate, and the inner surface of the back insulation, respectively. U_{Front} and U_{Back} are the thermal transmittance through the respective layers.

Duffie and Beckman [45] derive the loss coefficients for a variety of solar air collector layouts. However, the literature does not cover

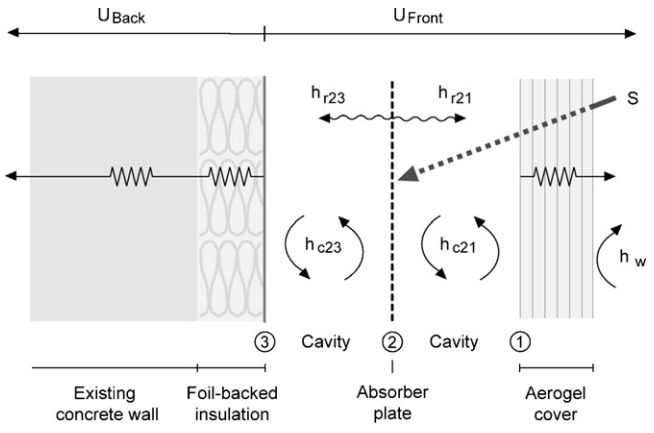

Fig. 4. Energy balance through solar collector.

solar air collectors with airflow on both sides of the absorber sheet. Addressing this issue, Parker [46] determined that the overall heat loss coefficient for this arrangement can be calculated using Eq. (2).

$$\begin{aligned} U_L = {} & \{4h_{c21}h_{c23}U_{Back}U_{Front} + 2h_{r21}[(h_{c21}+h_{c23})(h_{c23}U_{Front} \\ & + U_{Back}U_{Front} + h_{r23}U_{Back})\} + h_{c21}h_{c23}U_{Front}] \\ & + 2h_{r23}U_{Back}[h_{c21}h_{c23} + h_{c21}U_{Front} + h_{c23}U_{Front}] \\ & + h_{c21}U_{Front}[h_{c21}(2h_{r23}+h_{r21}) + h_{r23}Q \\ & + h_{c21}U_{Back}[h_{c21}(h_{r23}+2h_{c23}) + h_{r21}Q]\}/D \end{aligned} \quad (2)$$

where

$$D = \{2h_{c21}h_{c23}P + 2h_{c23}U_{Back}U_{Front} + h_{r21}[Q(h_{c21}+h_{r23}+U_{Back}) + h_{c21}h_{r23}] + h_{r23}Q(h_{c21}+U_{Front})\};$$

$$P = h_{c21} + U_{Back} + U_{Front};$$

$$Q = h_{c21} + 2h_{c23}.$$

4.3. Radiation coefficients

The radiation heat transfer coefficients between the absorber plate and the collector (h_{r21}) and the absorber plate to the back insulation (h_{r23}) can be found using Eqs. (3) and (4), respectively.

$$h_{r21} = \frac{4\sigma T_{fm}^3}{(1/\varepsilon_1)+(1/\varepsilon_2)-1} \quad (3)$$

$$h_{r23} = \frac{4\sigma T_{fm}^3}{(1/\varepsilon_2)+(1/\varepsilon_3)-1} \quad (4)$$

here ε is the surface emissivity and T_{fm} is the mean fluid temperature, expressed in Kelvin. σ is the Stefan–Boltzmann constant. Note that T_{fm}, the mean fluid temperature, must be estimated at this stage, but can be corrected later using an iterative calculation [45].

4.4. Convection coefficients

The convection heat transfer coefficients can be calculated using Eq. (5).

$$h_c = \mathrm{Nu}\left(\frac{k}{D_h}\right) \quad (5)$$

k is the thermal conductivity of air at the estimated mean fluid temperature. D_h is the hydraulic diameter of the air gap (two times the thickness). Nu refers to the Nusselt number, dependant on whether the flow regime is turbulent or laminar based on the Reynolds number, found using Eq. (6).

$$Re = \frac{2\dot{m}}{H'\mu} \quad (6)$$

μ is the dynamic viscosity. $\dot{m}$ is the mass flow rate. H' is the height of the cavity. When Re < 2300 the fluid is laminar and Eq. (7) should be used to calculate Nu, whereas if Re > 2300, then the fluid should be treated as turbulent and Eq. (8) is used.

$$\mathrm{Nu}_{laminar} = 4.9 + \left[\frac{0.0606(RePrD_h/H')^{1.2}}{1+0.909(RePrD_h/H')^{0.7}Pr^{0.17}}\right] \quad (7)$$

$$\mathrm{Nu}_{turbulent} = 0.0158Re^{0.8} \quad (8)$$

Pr is the Prandtl number, calculated from Eq. (9), where C_p is the specific heat capacity of the fluid (air) inside the collector.

$$Pr = \frac{\mu C_p}{k} \quad (9)$$

4.5. Front losses

Front heat losses through a single cover (U_{Front}) can be calculated using Eq. (10).

$$U_{Front} = \left[\frac{C}{T_{pm}}\left(\frac{T_{pm}-T_a}{1+f}\right)^e + \frac{1}{h_w}\right]^{-1} + \frac{\sigma(T_{pm}+T_a)(T_{pm}{}^2+T_a{}^2)}{(\varepsilon_2+0.00591h_w)^{-1}+((1+f+0.133\varepsilon_2)/\varepsilon_1)-1} \quad (10)$$

where

$$f = 1.07866(1+0.089h_w - 0.1166h_w\varepsilon_p);$$

$$C = 520(1-0.00005\beta^2);$$

$$e = 0.430((1-100)/T_{pm}).$$

ε_1 and ε_2 are the emissivity of the cover and absorber plate, respectively. T_a and T_{pm} correspond to ambient temperature and mean plate temperature, respectively, expressed in Kelvin. T_{pm} must be estimated at this stage, but will be corrected later using an iterative calculation. h_w is the wind heat transfer coefficient. β is the collector tilt in degrees.

4.6. Wind coefficient

The wind heat loss coefficient, h_w, accounting for free and forced convection, can be calculated using Eq. (11).

$$h_w = \max\left(5, \frac{8.6v_w^{0.6}}{L^{0.4}}\right) \quad (11)$$

here v_w is the wind velocity and L is the cube root of the dwelling volume. According to Duffie and Beckman [45], a minimum value of 5 W/m^2 K occurs in vertical solar collectors under still conditions.

4.7. Back losses

Thermal losses through the back of the collector are calculated using Eq. (12).

$$U_{Back} = \frac{1}{\sum_{i-1}^{i=n} R_i} \quad (12)$$

here $\sum_{i-1}^{i=n} R_i$ is the sum of the thermal resistances of the insulation layers. For the aerogel solar collector, these layers consist of the back insulation inside the collector, as well as the thermal resistance and internal surface resistance of the existing wall.

4.8. Heat removal factor

The heat removal factor (F_R) is a ratio between the actual useful energy gain of the collector to the maximum possible useful energy gain, obtained by setting the mean plate temperature to the inlet temperature so that heat losses are minimised. F_R is the product of two design constants: the collector efficiency factor (F') and a collector flow factor (F''), as shown in Eq. (13).

$$F_R = F'F'' \quad (13)$$

4.9. Collector efficiency factor

According to Parker [46], for solar air collectors with flow on both sides of the absorber plate, the collector efficiency factor (F')

can be calculated using Eq. (14), where the values of D, P (and Q) are given in Eq. (2).

$$F' = D/\{2h_{c21}h_{c23}P + 2h_{c23}U_{Back}U_{Front} + h_{r21}\} \times [(h_{c21} + h_{r23})(P + 2h_{c23}) + U_{Back}(2h_{c23} + U_{Front}) + h_{c21}h_{r23}] + h_{r23}[h_{c21}(P + 2h_{c23}) + 2h_{c23}U_{Front} + U_{Back}U_{Front}]\} \quad (14)$$

4.10. Collector flow factor

The collector flow factor (F'') can be calculated from Eq. (15). Here $\dot{m}C_p/(A_C U_L F')$ can be defined as the 'dimensionless collector mass flow rate'.

$$F'' = \frac{\dot{m}C_p}{A_C U_L F'}\left[1 - \exp\left(-\frac{A_C U_L F'}{\dot{m}C_p}\right)\right] \quad (15)$$

4.11. Mean fluid temperature

At this stage, it is possible to calculate Q_U, using Eq. (1). In turn, the mean fluid temperature can be calculated using Eq. (16):

$$T_{fm} = T_i + \frac{Q_U/A_C}{F_R U_L}\left(1 - F''\right) \quad (16)$$

In Eqs. (3) and (4), T_{fm} was estimated. As such, the recalculated value should be fed back into the original equations. According to Duffie and Beckman [45], typically 2–3 iterations provide sufficiently accurate values. Alternatively, computer packages can automate iteration loops updating values dependant on fluid properties such as density, specific heat capacity, thermal conductivity, dynamic viscosity and the Prandtl number.

4.12. Mean plate temperature

Similarly, the mean plate temperature can be calculated using Eq. (17). Again, the recalculated value should be fed back into the original equations, using an iterative process.

$$T_{pm} = T_i + \frac{Q_U/A_C}{F_R U_L}(1 - F_R) \quad (17)$$

4.13. Outlet temperature

The basic method of measuring collector performance is to expose it to solar irradiance and measure the inlet and outlet temperatures and the fluid flow rate. The useful gain can then be calculated using Eq. (18):

$$Q_U = \dot{m}C_p(T_o - T_i) \quad (18)$$

Rearranging this equation in terms of the outlet temperature (T_o) gives Equation (19):

$$Q_U = \dot{m}C_p(T_o - T_i) \quad (19)$$

4.14. Ductwork heat losses

Heat losses in the ductwork leaving a solar collector can be significant [45]. The temperature drop (ΔT_o) from ductwork can be calculated using Eq. (20):

$$\Delta T_o = \frac{U_d A_d (T_o T_{inside})}{\dot{m}C_p} \quad (20)$$

T_{inside} is the internal temperature, assuming ductwork runs internally through the building. A_d is the exposed area of the ductwork where thermal losses occur. U_d is the heat loss coefficient of the ducting.

4.15. Instantaneous efficiency of collector

Instantaneous efficiency can be calculated using Eq. (21):

$$\eta_1 = \frac{Q_U}{A_C S} = F_R(\tau\alpha) - \frac{F_R U_L (T_i - T_a)}{S} \quad (21)$$

4.16. MVHR supply temperature

The resultant supply air temperature leaving an MVHR, following indirect heat exchange with the exhaust air can be calculated using Eq. (22), where η_{MVHR} is the efficiency of the MVHR heat exchanger and T_o is the outlet temperature of the collector, adjusted to account for ductwork heat losses:

$$T_s = T_a + [\eta_{MVHR}(T_o - T_a)] \quad (22)$$

5. Steady state model

Table 1 displays the interface of a steady state model created to characterise the aerogel solar collector. Key inputs include the collector make-up and dimensions, the weather conditions and the inlet fluid properties. Key outputs include the overall efficiency, collector efficiency factor, overall heat loss parameter and heat removal factor, as well as the outlet temperature and useful energy before/after passing through the ductwork leading to the MVHR. The model includes an iteration loop to correct initial estimations for the mean plate temperature and mean fluid temperature. The model also calculates resultant supply air temperature leaving the MVHR based on the efficiency of the heat exchanger. Values can be compared to the baseline supply temperature without the solar collector.

When characterising the collector, the model assumes heat flow through the cover and back is one-dimensional, and construction properties are independent of temperature. Edge losses and the effects of dust, dirt and moisture are not considered. The collector is assumed to be completely airtight. Air properties are dependant on the mean fluid temperature inside the collector. Perforations in the double sided absorber plate (exposed area of 40%) are accounted for by reducing plate absorption to ($\alpha \times 0.6$). The average wind velocity is taken as 5 m/s. To account for the thickness of the granular aerogel cover, its thermal resistance is added in series to the front heat loss coefficient.

5.1. Cover efficiency investigation

To investigate the efficiency of different solar collector covers, Table 2 displays the predicted heat removal factor, overall heat loss parameter and collector efficiency factor, based upon the U-value and total solar transmittance (TST) of four multi-wall polycarbonate panels filled with granular aerogel at 10, 16, 25 and 40 mm thicknesses [47]. Values are benchmarked against properties of single glazing, double glazing and a double glazed cover encapsulating a 15 mm layer of high performance monolithic silica aerogel [48].

As shown, the single glazed cover has the highest solar transmittance at 0.85, however, its U-value is also the highest at 5.7 W/m^2 K. Conversely, the 40 mm granular aerogel cover has the lowest solar transmittance at 0.46, but also the lowest U-value at 0.54 W/m^2 K. The monolithic aerogel cover retains good properties for both, with its high solar transmittance of 0.75 and low U-value of 0.66 W/m^2 K. Regarding U_L, F_R and F', it is evident that the cover's U-value has a large influence on the overall collector losses U_L. Similarly, the collector efficiency factor and heat removal factor, representing the ability of the collector to retain heat, are strong functions of the cover's U-value. Conversely, TST has a less significant impact on U_L, F_R and F'. It should be noted, however, that higher transmittance increases the mean plate and fluid temperatures, resulting in higher

Table 1
Input and output parameters of the steady state model.

CHARACTERISE CONSTRUCTION LAYERS

				Aerogel panel	Air gap (front)	Black aluminium	Air gap (back)	Foil-backed insulation	Concrete inner- leaf	EPS insulation	Concrete outer leaf	Inner Surface
1	Thickness	x	m	0.040	0.080	0.001	0.080	0.060	0.080	0.035	0.105	-
2	Conductivity	k	W/m K	0.022	-	250	-	0.035	1.701	0.040	1.701	-
3	Resistance	R	m^2 /K/W	1.85	-	0	-	1.71	0.05	0.88	0.06	0.13
4	U-value	U	W/m^2 K	0.54	-	250000	-	0.58	21.26	1.14	16.20	7.69
5	Emissivity	ε	-	0.91	-	0.70	-	0.10	-	-	-	-

CHARACTERISE WEATHER

				Input
6	Ambient temperature	T_a	°C	7.5
7	Incident radiation	S	W/m^2	500
8	Wind velocity	v_w	m/s	5

CHARACTERISE FLAT PLATE COLLECTOR

				Input
9	Width	W	m	6.0
10	Height	H	m	0.9
11	Tilt	β	°	90
12	Cover transmittance	τ	-	0.46
13	Plate absorptance	α	-	0.54
14	Mean plate temperature	T_{pm}	°C	34.61
15	Mean fluid temperature	T_{fm}	°C	34.18

CHARACTERISE HEAT TRANSFER FLUID

				Input
16	Mass flow rate	$\dot{m}$	kg/s	0.043
17	Inlet air temperature	T_i	°C	23
18	Average cavity height	H'	m	0.687
19	Density	ρ	kg/m^3	1.1655
20	Specific heat capacity	C_p	J kg K	1006.5
21	Thermal conductivity	k	W/m K	0.02645
22	Dynamic viscosity	μ	kg/m s	1.86E-05
23	Prantl number	Pr	-	0.705

CHARACTERISE DWELLING

				Input
24	Total volume	V	m^3	400
25	Internal temperature	T_a	°C	21

CHARACTERISE OUTLET DUCTWORK

				Input
26	Duct diameter	D	m	0.15
27	Duct length	L	m	10
28	Insulation thickness	Δx	m	0.03
29	Insulation conductivity	k	W/m K	0.035

CHARACTERISE MVHR

				Input
30	Heat exchanger efficiency	η_{MVHR}	%	90

STEADY STATE CALCULATIONS

				Output
31	Stephan Boltzman constant	σ	-	5.67E-08
32	Hydraulic diameter	D_h	m	0.16
33	Reynolds number	Re	-	6748
34	Flow regime		-	*Turbulent*
35	Nusselt number	Nu	-	
36	*Laminar flow calculation*		-	n/a
37	*Turbulent flow calculation*		-	18.28
38		*Selection:*	-	18.28
39	Wind coefficient	h_w	W/m^2 K	10.16
40	Convection coefficient	h_{c21}	W/m^2 K	3.02
41	Convection coefficient	h_{c23}	W/m^2 K	3.02
42	Radiation coefficient	h_{r21}	W/m^2 K	4.30
43	Radiation coefficient	h_{r23}	W/m^2 K	0.65
44	Back losses	U_b	W/m^2 K	0.35
45	Front losses	U_f	W/m^2 K	0.47
46	Overall losses	U_L	W/m^2 K	0.78
47	Collector efficiency factor	F'	-	0.96
48	Capacitance rate	-	-	10.62
49	Collector flow factor	F''	-	0.95
50	Heat removal factor	F_R	-	0.92
51	Area of outlet ductwork	A_o	m^2	4.71
52	Loss coefficient of ductwork	U_d	W/m^2 K	1.17
53	Temperature drop from ducts	T_d	°C	1.89

PREDICTED PERFORMANCE

				Output
	Solar collector performance			
54	Useful energy	Q_u	W	555.90
55	Outlet temperature	T_o	°C	35.84
56	Mean plate temperature	T_{pm}	°C	34.61
57	Mean fluid temperature	T_{fm}	°C	34.18
58	Instantaneous efficiency	η_1	%	0.21
	Effect of ductwork leaving collector			
59	Useful energy	Q_u	W	474.29
60	Outlet temperature	T_o	°C	33.96
	Supply temperature to house			
61	Baseline (no solar collector)	T_s	°C	21.45
62	Supply temp with collector	T_s	°C	31.31

radiation and convection heat transfer coefficients, increasing the overall losses.

Hastings and Mørck [14] state that efficiency curves for closed loop solar air collectors should be produced as a function of the outlet and ambient temperature in the form $(T_o - T_a)/S$. Fig. 5 displays the overall efficiency of each collector cover, when incorporated into the 6 m × 0.9 m solar air collector designed for this study. Outlet temperatures and efficiencies are calculated for ambient temperatures ranging from −10 to +20 °C. Solar irradiance and wind speed are 500 W/m^2 and 5 m/s, respectively. The inlet air temperature is taken as 23 °C with a mass flow rate of 0.043 kg/s (based on an extract airflow rate of 37 L/s for a house with a kitchen and three additional extract points for a WC, shower room and bathroom).

Table 2
Design parameters for different collector covers calculated from the *U*-value and total solar transmittance (TST).

Collector cover type	*U*-value	TST	F_R	U_L	*F'*
Single glazing	5.70	0.85	0.63	4.36	0.78
Double glazing	2.80	0.80	0.74	2.71	0.85
10 mm granular aerogel	1.48	0.70	0.86	1.31	0.93
16 mm granular aerogel	0.97	0.62	0.89	1.06	0.94
25 mm granular aerogel	0.62	0.61	0.91	0.84	0.96
40 mm granular aerogel	0.54	0.46	0.92	0.78	0.96
15 mm monolithic aerogel	0.66	0.75	0.91	0.87	0.96

According to the efficiency calculations, the solar collector containing monolithic aerogel operates at the highest efficiency, peaking at 36% when ambient temperature is set to 20 °C. Alternatively, the 10 mm thick cover is the best performing granular aerogel system, with peak efficiencies of 31%, followed by the 25 and 16 mm thickness covers at 29%. The 40 mm cover performs less favourable with a peak efficiency of 22%. Interestingly the single glazed cover provides a higher efficiency than this system, when ambient temperature is between 10 and 20 °C. However, when ambient temperature drops below this value, the 40 mm cover provides a higher efficiency due to it improved heat retention properties, evident from the shallower gradient as seen on all of the aerogel collectors. Similarly, the double glazed collector has a higher efficiency than the 16 and 25 mm granular aerogel covers at ambient temperatures above 20 °C, but below this temperature its efficiency is lower.

Fig. 6 displays the predicted collector efficiencies at different mass flow rates. In each calculation, solar irradiance, wind speed and inlet temperatures are assumed to be 500 W/m^2, 5 m/s and 23 °C, respectively. An ambient temperature of 7.5 °C was selected to represent the average external temperature during October 1st–May 31st, the months where approximately 90% of the

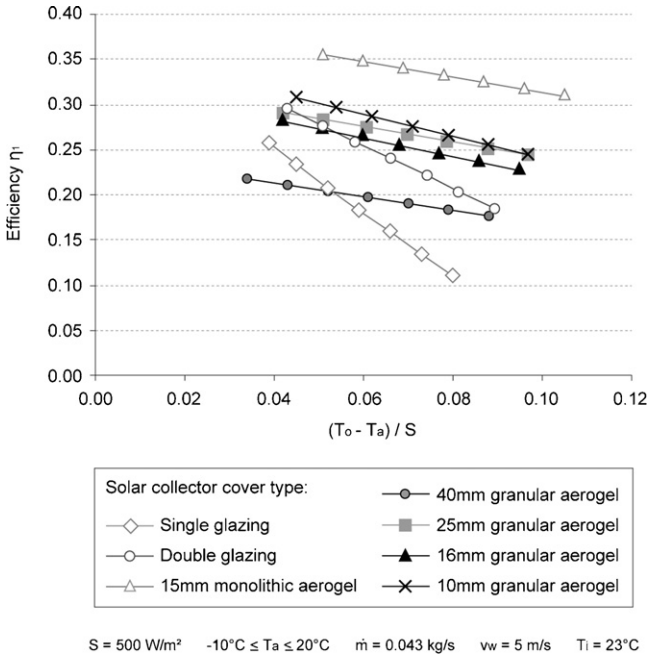

Fig. 5. Efficiency curves for different solar collector covers.

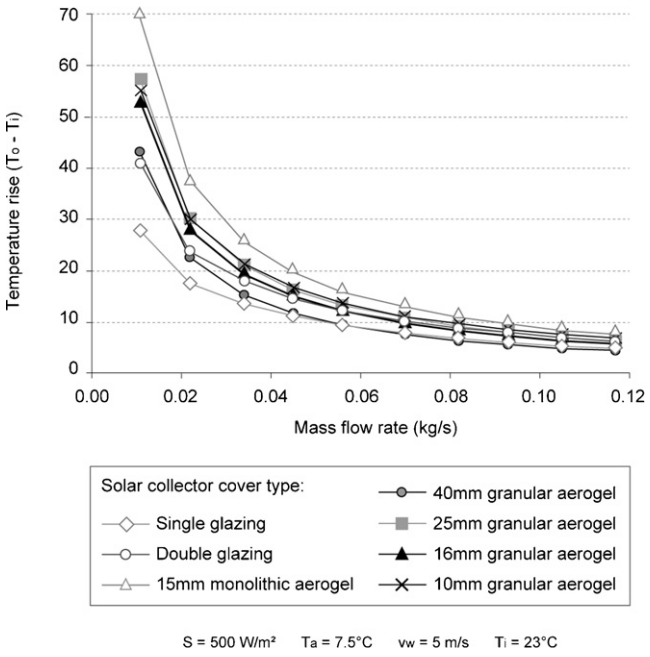

Fig. 7. Temperature rise across each collector surface.

degree-days for London Thames Valley occur [49], calculated using hourly weather data from the CIBSE TRY London weather file [50]. As shown, higher efficiencies occur at higher mass flow rates due to the mean temperature of the collector being lower, resulting in less heat losses. Again, there are conditions when the single glazed collector outperforms the 40 mm granular aerogel system. In this instance, mass flow rates above 0.050 kg/s result in the single glazed collector operating at a higher efficiency. Similarly, the double glazed collector operates at a higher efficiency than the 16 mm granular aerogel system at mass flow rates above 0.065 kg/s. By comparison, the 10 mm cover provides a higher efficiency than both glazed collectors. The 15 mm monolithic aerogel covers possess significantly higher operating efficiencies across all flow rates investigated.

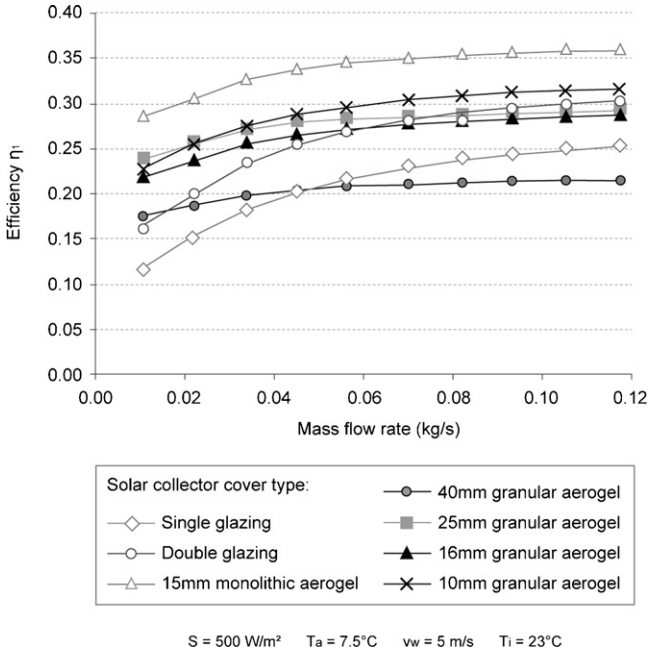

Fig. 6. Efficiency curves at different mass flow rates.

Fig. 7 displays the predicted temperature rise across the collectors at different mass flow rates. As shown, an increasing mass flow rate reduces the outlet temperature of each collector. At the lowest mass flow rate modelled, temperature rises of 28–70 °C degrees are predicted across all collectors. Conversely, at a mass flow rate of 0.043 kg/s, as modelled in Fig. 5, temperature rises of 12–20 °C degrees are predicted. In each case, the monolithic aerogel cover provides the highest temperature rise, whereas the single glazed cover achieves the lowest, until mass flow rates are increased above 0.050 kg/s. Note that some temperatures such as those predicted for the 10 and 25 mm granular aerogel collectors appear to almost trace each other, despite their differing efficiencies, particularly at higher mass flow rates. However, upon close inspection, comparing the values with Fig. 6 demonstrates a good correlation between both sets of results accounting for convergence at higher mass flow rates.

When analysing the efficiencies in Figs. 5 and 6, note that these values are strongly influenced by the tilt angle of the collector, the inlet air temperature as well as the open area of the absorber sheet, all of which are not optimised in this system. As such, if efficiencies are compared to typical solar–air collectors, such as those found in Hastings and Mørck [14], the values appear low. For example, a glazed collector with a plane black painted absorber, with flow on both sides can operate at efficiencies of 15–45% at different mass flow rates, compared to 23–32% for the 10 mm granular aerogel collector [14]. Countering this, if ambient air was fed into the cavity and the plate absorption coefficient was increased to 0.9, the steady state model gives operational efficiencies from 40 to 60% for the 10 mm granular aerogel collector across the range of mass flow rates, indicating that granular aerogel can be used in high performance collector design.

6. In situ performance

A photograph of the constructed aerogel solar collector (containing the 40 mm granular aerogel cover) is shown in Fig. 8. The collector is located at high level, spanning along the top floor of the south wall, avoiding overshadowing from surrounding buildings. In situ results are presented from 14th to 20th October 2011

Fig. 8. South-east elevation of the retrofit house.

following commissioning of air flow rates inside the dwelling. During monitoring, the building was largely unoccupied, except for periods during the 18–20th October, when internal construction works took place, resulting in the MVHR fan 'boosting' whenever PIR sensors detect movement in the kitchen or bathrooms. No auxiliary heating was used. During testing, the blinds were closed in the living room to minimise passive solar gains.

When analysing in situ results, note that commissioning of air flow rates revealed significant discrepancies between air flow and static pressure measurements upstream of the collector (measured by the inlet) and downstream of the collector (measured at plant room level). At 100% fan speed ('boost' operation) the air flow downstream of the collector was 83 L/s (static pressure −104 Pa), whereas upstream of the collector the air flow rate was 37 L/s (static pressure of −39 Pa). Similarly at 50% fan speed ('normal' operation) the air flow downstream of the collector was 54 L/s (static pressure −48 Pa), whereas upstream of the collector the air flow rate was 28 L/s (static pressure −18 Pa). In addition, at 50% fan speed an air flow rate of 34.5 L/s was measured upstream of the collector prior to the damper arrangement, indicating that 6.5 L/s was passing through the dampers rather than being directed up towards the solar collector inlet. These pressure drops and air flow reductions were later isolated and attributed to air infiltration through drainage holes running along the bottom edge of the aluminium frame, in addition to control damper blades not sealing perfectly. Nonetheless, despite these issues, promising results were observed during the monitoring phase, as follows.

6.1. Inlet and outlet temperatures

Fig. 9 displays the monitored inlet and outlet temperatures inside the solar collector compared to external temperature and solar irradiance. During the 7 day test period the average external temperature was 9.7 °C, with a maximum of 20.5 °C occurring during the 15th October and minimum of 1.2 °C that night. Irradiance levels were high for the majority of the testing phase, with mostly sunny weather conditions. Minimal cloud coverage was observed on the 19th and 20th October, resulting in fluctuations in irradiance levels throughout the day and slightly lower daytime external temperatures. Meanwhile, relatively high cloud cover was observed between early afternoon on the 16th and early morning on 18th October. Significantly higher night time external temperatures of approximately 6–7 °C were observed during this period, when compared to average night-time temperatures of 2–3 °C during clear nights. A maximum irradiance of 940 W/m^2 occurred on the 18th October at 12:40 h. Peak outlet temperatures ranged from 34.5 °C, measured at 10:00 h on 17th October (a day with relatively high cloud cover) to 46.8 °C, measured at 12:30 h on 15th October (a clear sunny day).

Other points of interest in Fig. 9 is that the inlet temperature increases by up to 5 °C during the daytime, most probably due to heat gain inside the cavity. Alternatively, the sharp decreases in the inlet and outlet temperatures during the nights demonstrate that air leakages during no flow conditions have a significant impact on collector performance. Nonetheless, an average buffer of 7 °C is found between the collector and the outside air. During the nights of the 16–17th October, it is evident that the control remained open, indicating that the temperature difference for the damper changeover relay could be reduced to improve the system efficiency.

6.2. Supply, extract and room temperatures

Fig. 10 displays the temperature profile of the extracted air from the kitchen and bathrooms (fed into the solar collector) and the supply air (fed to the living room and bedrooms following an indirect heat exchange between the outside air and solar collector outlet air). Peak supply temperatures (measured inside the duct leaving the plant room) from 25 to 30 °C were observed during the test period. At this time, peak internal temperatures of 21.5 and 21.9 °C were monitored in the living room and bedroom, respectively, indicating that the collector is capable of raising the temperature of the dwelling to comfortable levels without overheating. Comparing the living room and a north facing bedrooms temperature to the extract temperature showed a maximum temperature increases of 2.7–3 °C, respectively indicating a notable difference in the zones supplied by warm air.

When analysing Fig. 10, monitored data demonstrates that the north facing bedroom is continuously warmer than the living room. During the night time, the living room is typically 1–2 °C cooler than the bedroom. As morning approaches, the living room temperature slowly increases to reach the bedroom temperature at around noon, then dropping again towards the late evening. This behaviour is understandable since the floor area of the bedroom is 8 m^2 making it easier to heat, compared to the living room at 21 m^2. In addition, as the living room contains large areas of glazing on the South and East facades, compared to the north facing bedroom with a single window, this is expected to contribute significantly to overnight heat losses. One discrepancy that is difficult to isolate is the 1 °C difference observed during the daytimes of the 18–20th October, compared to the 14–17th October. It is thought that this discrepancy is caused by workers in the house on those days walking in and out of the living room during testing, without closing doors, resulting in cooler air from the un-heated spaces circulating in that space. By comparison, little activity was expected in the bedroom on those days.

6.3. Temperature profile through collector

Fig. 11 displays the temperature profile through the solar collector cavity, based on the eight temperature measurements taken behind the absorber sheet (visualised earlier in Fig. 1). Values are displayed for the 15th October, a clear sunny day, as well as the 18th October which was also clear, except for some scattered clouds late in the evening. As shown, there is a significant difference between the two sets of data. This is largely because the

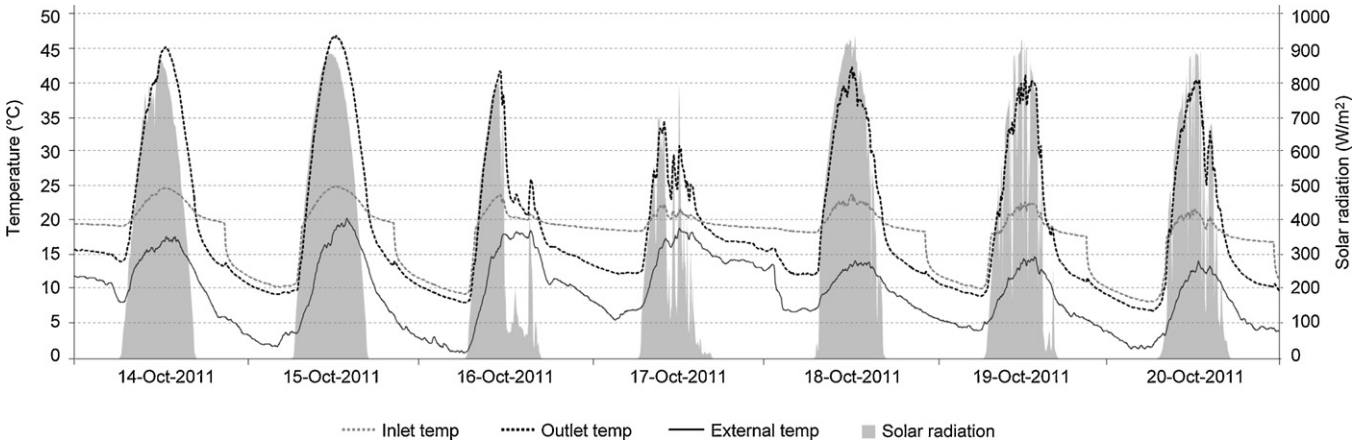

Fig. 9. Measured inlet and outlet temperature inside the collector cavity, compared to external temperature and solar irradiance during the 7 day test period.

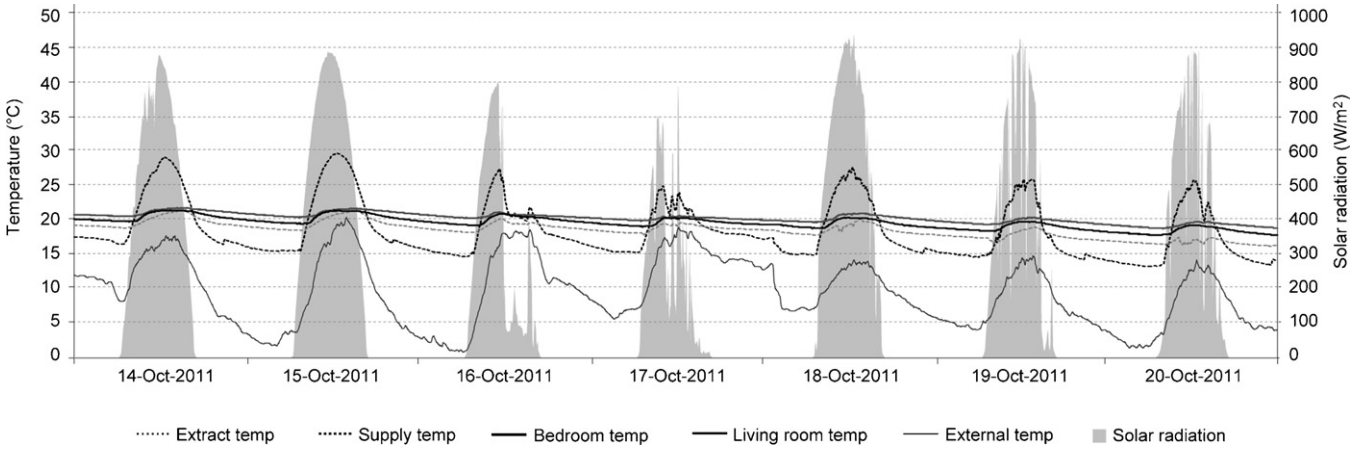

Fig. 10. Measured supply and extract temperatures, compared to the living room and north facing bedroom temperature (and external temperature and solar irradiance).

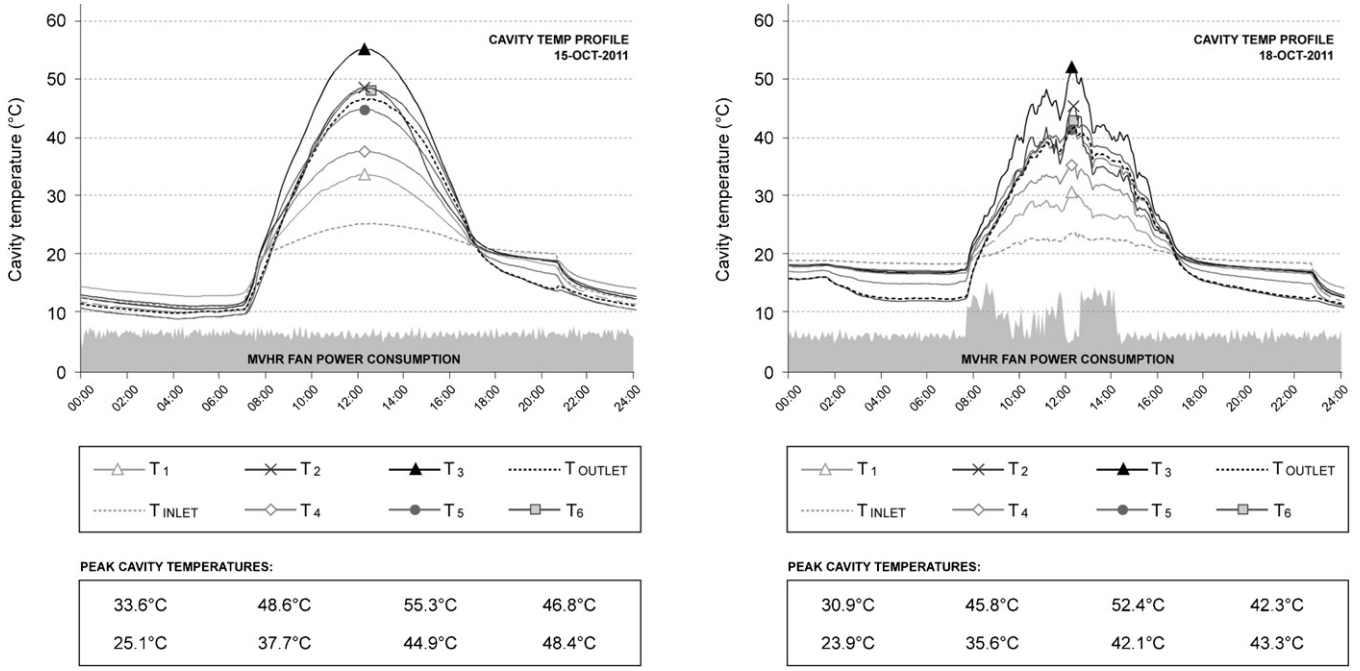

Fig. 11. Temperature profiles through the solar collector cavity. Left graph shows 15th October with the MVHR fan running in 'normal' operation. Right graph shows 18th October with the MVHR in 'boost' mode at various points in the day.

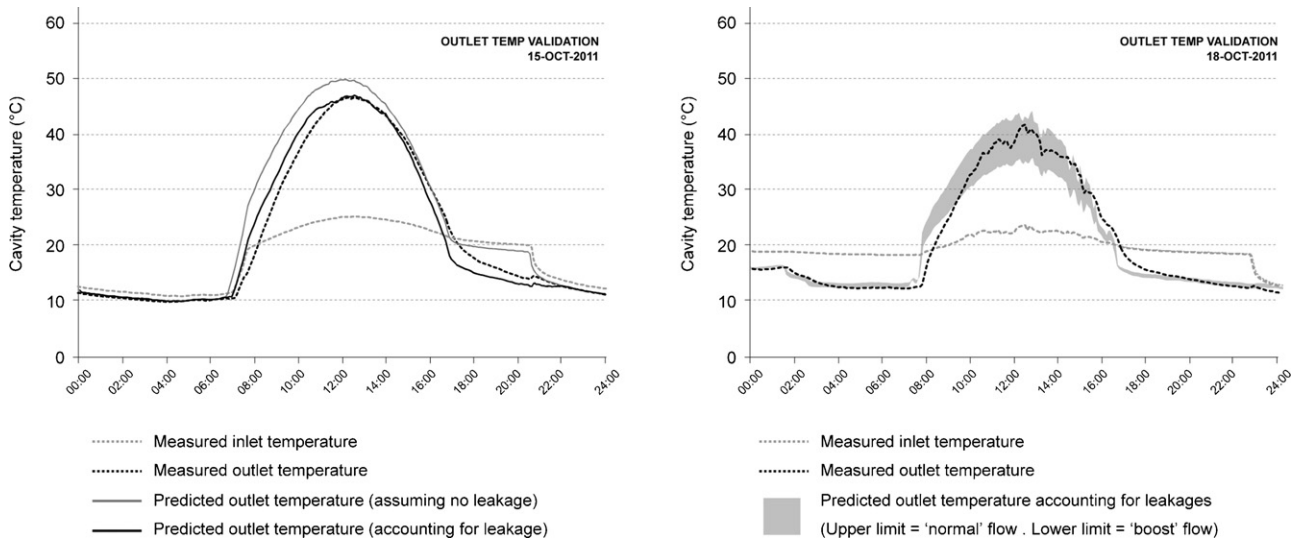

Fig. 12. Predicted vs. In situ outlet temperatures. Left graph shows 15th October, where the predictions assume the collector is perfectly sealed and also taking leakage into account. Right graph shows 18th October where the outlet temperature is predicted at 'normal' and 'boost' flow rates.

dwelling was occupied during the 18th October and occupancy sensors repeatedly activated the 'boost' on the MVHR, effectively doubling the mass flow rate through the solar collector at various points throughout the day.

An indication of when boosting occurred can be established by analysing the peaks in the MVHR power use (shown at the base of each graph). As shown, sustained periods of boosting during the 18th October occurred from 7:45 to 9:30 hrs, at 11:45 to 12:00 hrs and from 12:30 to 2:15 hrs. As a result, sharp temperature drops of up to 10 °C are observed. However, the collector quickly heats up again once 'normal' flow is resumed. By comparison, the temperature profile through the cavity on the 15th October follows a much smoother profile, with readings along the top edge being the higher than their lower counterparts. On both days, there is evidence of a 'hot spot' in the top central right zone of the cavity (T_3), up to 10 °C hotter than the outlet in peak conditions. A similar 'hot spot' was reported by the Danish Technical Institute in a study of connectable solar collectors. Here, Jensen and Bosanac [51] claimed that the most likely cause was a less even distribution of air flow over that area.

7. Validation

In order to validate the steady state model and design parameters presented in the cover efficiency investigation, Fig. 12 displays the predicted vs. measured outlet temperatures for the 15th and 18th October. In each case, outlet temperatures are calculated based on in situ data for external temperature, irradiance and the inlet fluid temperature. Average mass flow rates of 0.048 and 0.073 kg/s are applied for the MVHR under 'normal' and 'boost' operation respectively (calculated based on average air flow rates of 41 and 60 L/s in the commissioning report).

The impact of air infiltration and leakages has been accounted for by following a methodology to correct Q_U, proposed by Bernier and Plett [52]. According to Bernier and Plett [52], for collectors under negative pressure, inward infiltration can be calculated using Eq. (23).

$$Q_U = \dot{m}_{average} C_p (T_o - T_i) - (\dot{m}_o - \dot{m}_i) C_p (T_i - T_a) \quad (23)$$

Conversely, for collectors under positive pressure (or no flow conditions), outward leakages can be accounted for using Eq. (24).

$$Q_U = \dot{m}_{average} C_p (T_o - T_i) - (\dot{m}_i - \dot{m}_o) C_p (T_L - T_a) \quad (24)$$

In each equation, $\dot{m}_o$ and $\dot{m}_i$ refer to the measured mass flow rates at the inlet and outlet of the collector, respectively. T_L is the average temperature of air lost to the environment, estimated using $(T_i + T_o)/2$, where T_o is based on an initial estimate, corrected using an iteration loop.

In order to validate the collector outlet temperatures, it was first necessary to determine a reduction factor for leakages/infiltration, since the drop in mass flow rate was not just caused though leaks inside the collector. It was also caused through air passing through the damper blades, thus not going through the collector. Based on commissioning (at 50% fan speed), it was established that just 47.5 L/s (of the total 54 L/s) was extracted from the collector as 6.5L/s was passing through the dampers. Of this 47.5 L/s, only 28 L/s was measured upstream of the collector inlet, indicating that 19.5 L/s could be attributed to infiltration. Consequently, the impact of infiltration accounted for in the validation process could be reduced by 25%. Next, it was then necessary to identify the times at which air was flowing through the collector, compared to no-flow conditions. This was determined by assessing the temperature difference between the outlet temperature and the extract temperature from the house (based upon the control strategy outlined in Section 3). Following these steps, for each line of 5 min experimental data, Q_U is calculated assuming either a predicted 'leakage in' or 'leakage out'. The outlet temperature is then determined for each time period.

Predicted outlet temperatures for the 15th October are calculated assuming the collector is perfectly sealed and also accounting for infiltration. As shown, the peak outlet temperature is overestimated by approximately 4–5 °C if the collector is assumed to be perfectly sealed. Furthermore, during the evening/night, the predicted outlet temperature closely follows the inlet temperature profile, since losses are assumed to be minimal. By comparison, if leakages are accounted for, the peak outlet temperature closely matches the measured value and evening/night time losses correlate much better with the measured outlet temperature. A discrepancy inherent to both calculations due to there steady state nature is the temperature lag experienced during the morning as the collector begins to heat and during the evening as it cools. Nonetheless, if Q_U is calculated from the predicted outlet temperature taking losses into account, energy output is found to be within 5% of the measured value.

For October 18th, the predicted outlet temperature (taking losses into account) is calculated with an upper and lower limit to

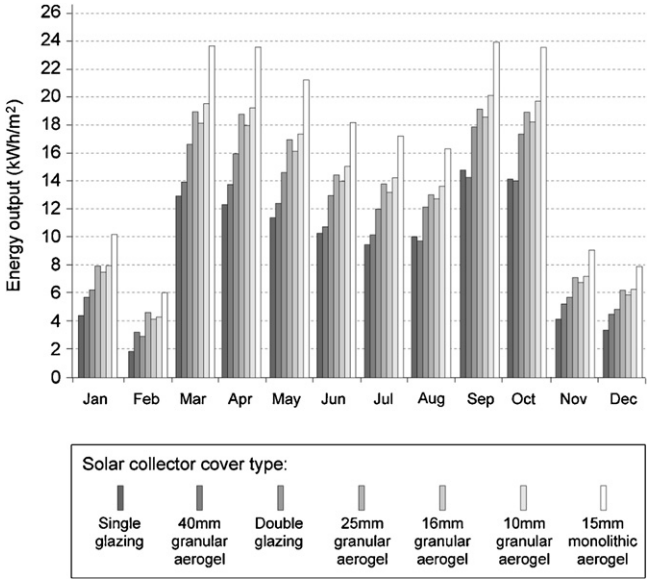

Fig. 13. Predicted annual energy output for solar collector types.

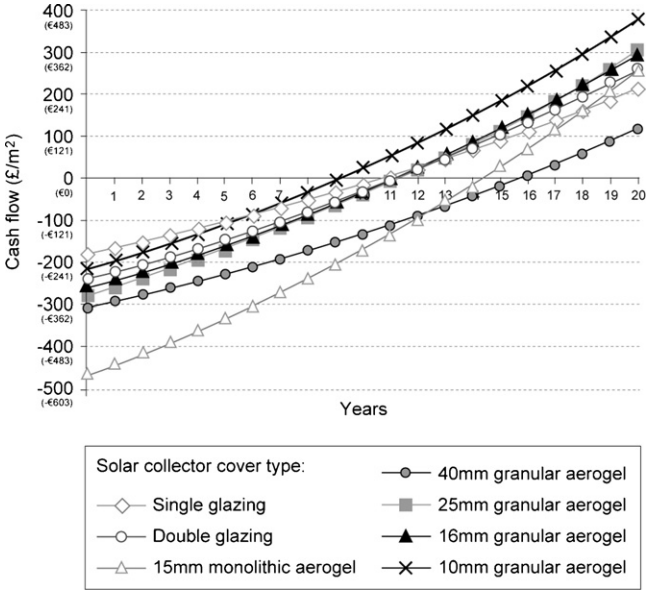

Fig. 14. Predicted payback periods for solar collector types.

account for the MVHR switching between 'normal' and 'boost' mode respectively. As shown, the measured outlet temperature is within the allowable limits of the two flow rates modelled. Again there is a discrepancy due to lag inside the collector, not accounted for in the steady state model. Nonetheless, with the air leakages properly accounted for, the predicted and measured outlet temperatures correlate reasonably well.

8. Discussion

In situ results have demonstrated that a solar air collector containing a translucent aerogel cover can function well in a domestic solar heating application. Despite air leakages/infiltration, the prototype successfully raised the temperature of the extract air in a mechanically ventilated dwelling up to 45 °C, providing additional energy to pre-heat the supply air up to 30 °C. Resultant internal temperatures of 21–22 °C indicate that the prototype will play an important role in maintaining comfortable living conditions throughout the heating season.

Although in situ results were based on a collector with a 40 mm granular aerogel cover, the reasonable correlation between predicted and measured performance has gone some way towards verifying the design parameters calculated in the cover efficiency investigation. Applying these findings, Fig. 13 displays the predicted annual energy output for comparative solar air collectors with different cover types. Climate data is generated from annual hourly irradiance (on a south facing vertical surface) and external temperature data generated using the CIBSE TRY London weather file [50]. All calculations assume a constant inlet temperature of 23 °C and mass flow rate of 0.048 kg/s. In each case, collectors are assumed to be built completely air tight. To isolate the benefits of the collector from the standard MVHR operation, calculations only count the energy output if the collector outlet temperature is higher than the inlet temperature. Alternatively, the MVHRs summer bypass function is assumed to be operational, discounting the energy output if the external temperature exceeds 20 °C. All calculated outputs are reduced by 5% to account for discrepancies observed in the steady state model.

Predicted annual energy outputs range from 110 kWh/m^2/year for the single glazed collector to 202 kWh/m^2/year for the monolithic aerogel cover. Energy outputs for the granular aerogel systems are 118 kWh/m^2/year with the 40 mm cover, 161 kWh/m^2/year with the 25 mm cover, 154 kWh/m^2/year with the 16 mm cover and 166 kWh/m^2/year with the 10 mm cover. The double glazed collector has a predicted energy output of 140 kWh/m^2/year. For each case, the largest savings are estimated during the midseason, when heating is required and incident radiation levels are high. By comparison, benefits can be obtained even during the coldest months.

Utilising these annual energy outputs, Fig. 14 displays a predicted payback curve for each collector type. To avoid uncertainties regarding fabric performance, auxilary heating systems and occupancy usage, which must be dealt with on a case-by-case basis, payback calculations assume that the collector output is offsetting an automated electric heating coil in an MVHR system. The baseline cost of electricity is assumed to be £0.12/kWh (€0.145/kWh), with a 6% annual fuel price inflation rate and 2% discount interest rate applied. The capital costs for each cover type is based on sales costs obtained through personal communication with R. Lowe (01 November 2011) from Xtralite Ltd. These costs were £190/m^2, £160/m^2, £143/m^2 and £100/m^2 (€229/m^2, €193/m^2, €173/m^2, €121/m^2) for the 40, 25, 16 and 10 mm polycarbonate panels filled with granular aerogel, respectively. The single and double glazed covers were estimated at £60/m^2 and £120/m^2 (€72/m^2 and €145/m^2) respectively. A speculative cost of £350/m^2 (€422/m^2) was given to the 15 mm monolithic aerogel cover (not available commercially). Based on this investigation an additional cost of £120/m^2 (€145/m^2) was applied to account for the timber and aluminium framing as well as the perforated absorber sheet.

According to the payback calculations, all solar collectors provide a return on investment within 9–16 years. The fastest payback is obtained from the 10 mm granular aerogel system, followed by the 25 and 16 mm systems and both conventional glazed collectors with 11 year estimated payback periods. Interestingly, the 40 mm granular aerogel system and the monolithic aerogel collector have longer payback periods at 14 and 16 years, respectively. Evidently, if future systems are designed with granular aerogel it is unnecessary to utilise cover thicknesses above 25 mm unless the solar transmittance can be improved. Furthermore, if it becomes commercially available, the cost of a monolithic aerogel must be considerably less than estimated here for it to be cost effective.

Take note, the aforementioned payback calculations (per m^2 of collector) do not include the fixed cost of controls, which were £40

(€48) for the temperature differential electronic thermostat with thermistors, and £510 (€615) for the three dampers with spring return actuators. An additional cost of £120 (€145) incurred for the 'optional summer bypass' on the MVHR was not included. If all of these costs are taken into account then payback periods (for a 5.4 m^2 collector) increase from to 9–16 years to 14–21 years across all solar collector types. Alternatively, if it is assumed that just one damper with spring return actuator is used to control air flow and the MVHR summer bypass switch was specified independently of the solar collector (thus not included in the payback calculation), then payback periods can be reduced to 10–17 years, which is more acceptable. Countering these costs, if it were assumed that solar air collectors were eligible to the £0.085/kWh (€0.103/kWh) generation tariff under the governments Renewable Heat Incentive [53], which domestic hot water solar thermal panels currently obtain, then paybacks can be reduced to 7–13 years. Evidently, even with the cost of controls included, it is possible to develop an economically viable technology.

9. Conclusion

This paper has demonstrated that incorporating granular aerogel into flat plate solar air collectors can result in improved working efficiencies over conventional glazed systems. Due to the issues regarding fragility, manufacturing difficulties, availability and the perceived higher cost of monolithic aerogel, encapsulated granular aerogel can be viewed as the preferred cover material to develop novel solar technologies such as solar air heaters, solar water heaters, and solar Trombe walls.

Long term evaluation of the aerogel solar collector prototype, incorporating the 40 mm thick cover, with leakages mended, will be conducted as part of a two year monitoring scheme funded through the Retrofit for the Future project. Once occupied, the areas of interest will include annual thermal comfort levels inside the house, the use of auxiliary heating, particularly on cold sunny days, and the effect of moisture from the kitchen and bathrooms inside the cavity. The contributions provided by the solar collector will be assessed against the property's total gas and electricity consumption, whilst being benchmarked against other renewable technologies. The overall aim of the refurbishment is to reduce the properties baseline CO_2 emissions by 80%.

At the start of this refurbishment, the design team and client were keen to use this house as a novel test-rig for new technologies. Consequently, one factor that is yet to be established is the long-term durability of this prototype compared to conventional glazed solar collectors. Under normal usage as a facade component for day lighting, the aerogel filled polycarbonate panels and aluminium support systems would possess a 15 year warranty against yellowing, light transmission and thermal degradation [44]. Alone, the aerogel granules are not expected to degrade during the foreseeable life of the solar collector. In addition, since silica is inert, the aerogel can last the life of a structure and be recycled when the building is decommissioned [44]. Instead, key areas where degradation may occur include the seals, connections and fixtures supporting the cover system and framing, due to expansion and contraction of components during summertime, general wear from wind and rain exposure, and moisture build-up inside the cavity. A further issue is the integrity of the MVHR, bypass controls and dampers in the plant room. Understandably, it is imperative that this product be systematically evaluated over its operational lifespan. If developed into a market ready solution, a minimum lifespan of 15 years would be required to justify the life cycle costs.

Take note that the prototype reported in this paper was incorporated into the 'extract' side of the mechanical ventilation system due the design team not wanting to pass the dwelling's fresh air supply through a prototype which had not been tested before. Consequently, there are opportunities to improve the overall efficiency of this system by passing ambient air into the cavity and by connecting it directly to the supply air side. Furthermore, the plate absorption coefficient could feasibly be increased to 0.9. Applying these changes to the steady state model gives operational efficiencies of up to 60% for a 10 mm granular aerogel collector, comparable to the results of Nordgaard and Beckman [39] and Svendsen [38], and hypotheses of Ortjohann [40] and Reim et al. [42]. According to our model, the predicted annual energy output for this system is 355 kWh/m^2/year with a payback as low as 4.5 years.

Further efficiency improvements could be achieved through incorporating thermal storage into the cavity or by connecting the collector outlet to an air-water heat exchanger during the summertime to avoid wasting heat. There is a need to refurbish our existing building stock to achieve energy efficiency standards, going beyond the limitations of conventional measures. Findings from this paper aim to contribute towards this challenge.

Acknowledgements

The corresponding author would like to thank the EPSRC, Brunel University, Buro Happold Ltd. and the Technology Strategy Board for funding this research project. Further thanks go to Gallions Housing Association, Fraser Brown McKenna architects, Martin Associates surveyors, Axis Europe, Xtralite, Permarock and Nuaire for their contributions during this innovative and challenging refurbishment.

All technical drawings for this prototype were drawn by the corresponding author, with support from C. Biggs (Technical Director of Nuaire), J. Richings (Technical Director of Permarock) and R. Lowe (Technical Services Manager at Xtralite) when selecting suitable components and fixings. The system was installed by Axis Europe, the lead contractors undertaking the refurbishment. Specialist items such as the granular aerogel panels and its framing were supplied and installed by Xtralite.

References

[1] Climate Change Act, Carbon Targeting and Budgeting, Part 1 – The Target for 2050, Her Majesty's Stationery Office Limited, UK, 2008 (Chapter 27).
[2] J. Ravetz, What do we know about existing buildings and their future prospects, Energy Policy 36 (2008) 4462–4470.
[3] A. Power, Does demolition or refurbishment of old and inefficient homes help to increase our environmental, social and economic viability? Energy Policy 36 (2008) 4487–4501.
[4] S.H. Hong, T. Oreszczyn, I. Ridley, Warm Front Study Group, The impact of energy efficient refurbishment on the space heating fuel consumption in english dwellings, Energy and Buildings 38 (2006) 1171–1181.
[5] International Energy Agency, Solar Renovation Concepts and Systems – a Report of Task 20 Subtask F, Solar Heating and Cooling Programme, 1999.
[6] J.O. Dalenbäck, Solar energy in building renovation, Energy and Buildings 24 (1996) 39–50.
[7] K. Voss, Solar energy in building renovation – results and experience of international demonstration buildings, Energy and Buildings 32 (2000) 291–302.
[8] A.K. Athienitis, H. Ramadan, Numerical model of a building with transparent insulation, Solar Energy 67 (1999) 101–109.
[9] H. Suehrcke, D. Däldehög, J.A. Harris, R.W. Lowe, Heat transfer across corrugated sheets and honeycomb transparent insulation, Solar Energy 76 (2004) 351–358.
[10] P. Dolley, C. Martin, M. Watson, Performance of walls clad with transparent insulation material in realistic operation, Building and Environment 29 (1994) 83–88.
[11] B. Peuportier, J. Michel, Comparative analysis of active and passive solar heating systems with transparent insulation, Solar Energy 54 (1995) 13–18.
[12] N.D. Kaushika, K. Sumathy, Solar transparent insulation materials: a review, Renewable and Sustainable Energy Reviews 7 (2003) 317–351.
[13] I.L. Wong, P.C. Eames, R.S. Perera, A review of transparent insulation systems and the evaluation of payback period for building applications, Solar Energy 81 (2007) 1058–1071.
[14] R.S. Hastings, O. Mørck, Solar Air Systems – a Design Handbook, first ed., James & James, London, UK, 2000.
[15] M. Rommel, A. Wagner, Application of transparent insulation materials in improved flat-plate collectors and integrated collector storage system, Solar Energy 49 (1992) 371–380.

[16] C.H. Schmidt, A. Goetzberger, J. Schmid, Test results and evaluation of integrated collector storage systems with transparent insulation, Solar Energy 41 (1988) 487–494.
[17] N.D. Kaushika, K.S. Reddy, Thermal design and field experiment of transparent honeycomb insulated integrated-collector-storage solar water heater, Applied Thermal Engineering 19 (1999) 145–161.
[18] Okalux Kapipane, Okalux, Retrieved January 17, 2012, from http://www.miltyr.se/Okalux_Downloads/3-Okapane/i_kapipane_twd_pmma_e.pdf.
[19] W.J. Platzer, A. Goetzberger, Recent Advances in Transparent Insulation Technology, Transparent Insulation – TI8, Fraunhofer-Institute for Solar Energy Systems, Freiburg, Germany, 2004.
[20] M. Dowson, D. Harrison, S. Craig, Z. Gill, Improving the thermal performance of single-glazed windows using translucent granular aerogel, International Journal of Sustainable Engineering 4 (2011) 266–280.
[21] W.J. Platzer, Solar transmission of transparent insulation material, Solar Energy Materials 16 (1987) 275–287.
[22] J. Fricke, T. Tillotson, Aerogels: production, characterization and applications, Journal of Thin Solid Films 297 (1997) 212–223.
[23] F. Schwertfeger, D. Frank, M. Schmidt, Hydrophobic waterglass based aerogels without solvent exchange or supercritical drying, Journal of Non-Crystalline Solids 225 (1998) 24–29.
[24] L.D. Shorrock, J. Henderson, J.I. Utley, Reducing Carbon Emissions from the UK Housing Stock, BRE Press, Watford, UK, 2005.
[25] M. Dowson, M. Grogan, T. Birks, D. Harrison, S. Craig, Streamlined life cycle assessment of transparent silica aerogel made by supercritical drying, Applied Energy (2011), doi:10.1016/j.apenergy.2011.11.047.
[26] M. Van Bommel, A. De Haan, Drying of silica aerogel with supercritical carbon dioxide, Non-Crystalline Solids 186 (1995) 78–82.
[27] R.T. Bynum, Insulation Handbook, first ed., McGraw-Hill, New York, USA, 2001.
[28] A. Soleimani-Dorcheh, M.H. Abbasi, Silica aerogel – synthesis, properties and characterization, Materials Processing Technology 199 (2008) 10–26.
[29] R. Baetens, B. Petter-Jelle, A. Gustavsend, Aerogel insulation for building applications: a state-of-the-art review, Energy and Buildings 43 (2011) 761–769.
[30] B. Petter-Jelle, Traditional, state-of-the-art and future thermal building insulation materials and solutions – properties, requirements and possibilities, Energy and Buildings 43 (2011) 2549–2563.
[31] H. Yokogawa, Thermal conductivity of silica aerogels, in: S. Sakka (Ed.), Handbook of Sol–Gel Science & Technology, vol. 243, Kluwer Academic Publishers, New York, USA, 2005, pp. 265–272.
[32] Cabot Corporation, Aerogel for Insulation, Daylighting, Additives, Retrieved February 28, 2011, from http://www.cabot-corp.com/Aerogel.
[33] M. Rubin, C.M. Lampert, Transparent silica aerogels for window insulation, Solar Energy Materials 7 (1983) 393–400.
[34] Cabot Corporation, Cabot nanogel promises unmatched energy savings – revolutionary insulating material makes the best window, wall and skylight products better, Journal of Pigment & Resin Technology 33 (2004) 345.
[35] M. Werner, L. Brand, Focus report 2010, Aerogels, General Sector Reports, Chemistry and Materials, ObservatoryNANO, 2010, p. 12.
[36] J. Fricke, Aerogels, Scientific American 258 (1988) 92–97.
[37] R. Caps, J. Fricke, Fibrous insulations with transparent cover for passive use of solar energy, Thermophysics 10 (1989) 493–504.
[38] S. Svendsen, Solar collector with monolithic silica aerogel, Non-Crystalline Solids 145 (1992) 240–243.
[39] A. Nordgaard, W.A Beckman, Modelling of flat-plate collectors based on monolithic silica aerogel, Solar Energy 49 (1992) 387–402.
[40] J. Ortjohann, Granular Aerogel for the Use in Solar Thermal Collectors, ISES 2001 Solar World Congress.
[41] V. Wittwer, Development of aerogel windows, Journal of Non-Crystalline Solids 145 (1992) 233–236.
[42] M. Reim, W. Körner, J. Manara, S. Korder, M. Arduini-Schuster, H.P. Ebert, J. Frike, Silica aerogel granulate material for thermal insulation and daylighting, Solar Energy 79 (2005) 131–139.
[43] Building Research Establishment (BRE), Passivhaus Primer, 2010, Supported Energy Saving Trust and Passiv Haus Institut, Retrieved January 12, 2012, from http://www.passivhaus.org.uk/filelibrary/Passivhaus%20Standards/BRE_Passivhaus_Primer.pdf.
[44] Cabot Corporation, Facade Systems with Nanogel, Cabot Corporation & Roda, Retrieved November 1, 2010, from http://www.cabot-corp.com/wcm/download/en-us/ae/facade%20systems%20roda.pdf.
[45] J.A. Duffie, W.A. Beckman, Solar Engineering of Thermal Processes, third ed., John Wiley & Sons Inc., New Jersey, USA, 2006.
[46] B. Parker, Derivation of efficiency and loss factors for solar air heaters, Solar Energy 26 (1981) 27–32.
[47] Lexan, Daylighting, Polycarbonate filled with Nanogel, Amerilux, 2001, Retrieved February 28, 2011, from http://www.ameriluxinternational.com/html/architectData/nanogel/documents/nanogelData.pdf.
[48] J.M. Schultz, K.I. Jensen, Evacuated aerogel glazings, Vacuum 82 (2008) 723–729.
[49] Vesma, UK Monthly and Weekly Degree Day Figures, 2009, Retrieved June 2009, from http://www.vesma.com/ddd/index.htm.
[50] Chartered Institute of Building Services Engineers, CIBSE TRY Hourly Weather Data Set – London, Test Reference Year from 1983–2004 data sets.
[51] S.Ø. Jensen, M. Bosanac, Connectable Solar Air Collectors, SEC-R-22, Solar Energy Centre Denmark, Danish Technological Institute, Denmark, 2002.
[52] M.A. Bernier, E.G. Plett, Thermal performance representation and testing of air solar collectors, Solar Energy Engineering 110 (1988) 74–81.
[53] Renewable Heat Incentive, Tariff Level Tables | RH Incentive, Retrieved November 28, 2011, from http://www.rhincentive.co.uk/eligible/levels/.

Glossary

EPS: expanded polystyrene
MVHR: mechanical ventilation with heat recovery
PIR: passive infrared sensor
TIM: translucent insulation material
TST: total solar transmittance

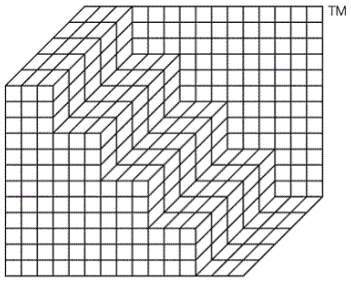

Buro Happold

Retrofit for the Future

Aerogel Solar Collector monitoring data

Retrofit for the Future
Mark Dowson, Buro Happold

Introduction:

The following report contains the preliminary monitoring data captured for the Aerogel Solar Collector installed at 55 Wolvercote Road, Thamesmead, London, as part of the Retrofit for the Future competition. This 5.4m^2 solar air collector prototype is intended to preheat the exhaust air of the property's mechanical ventilation with heat recovering (MVHR) system, providing additional energy to indirectly warm the incoming fresh air supply to the dwelling. The data is reported from 1st November 2011 - 15th August 2012. On-site retrofit works did not finish at the property until mid February. The property has been occupied by a 7 person family, since 12th June 2012. A summary table for each month is presented on the final page of this report. On-going data collection will take place as part of a two-year post occupancy evaluation programme.

Explanation of graphs:

- The first graph displays the monitored external temperature measured at roof level, and solar irradiance hitting the property's south facing wall.
- The second graph displays the temperature of the inlet and outlet air inside the solar collector cavity, against the MVHR power consumption. The inlet air has been extracted from the properties kitchen and bathrooms. The outlet air is fed down into properties plant room to indirectly pre-heat the fresh air entering the property. MVHR power consumption has been included to illustrate when the fan is operating at 'normal' and 'boost' mode.
- The final graph displays the temperature of the MVHR supply-air to the dwelling (consisting of fresh outside air that has been indirectly preheated by the solar collector outlet air), against the measured internal air temperature in the living room and a top floor north facing bedroom.

Points to note:

- The data demonstrates a significant temperature rise between the inlet and outlet temperature of the Aerogel Solar Collector during sunny conditions. This raises the temperature of the dwellings supply air from the MVHR, demonstrating that the prototype has an influence on the internal environment.
- It should be noted that the internal temperature fluctuations are also influenced by the property's high occupancy levels, air-tightness, insulation and glazing (particularly in the living room).
- To mitigate overheating the MVHR has a 'summer bypass' switch preventing fresh air being preheated if the outside air drawn into the unit is above 20°C. It should be noted that this bypass function may not be 100% effective. Opening windows when too hot has been recommended.
- Leakage inside the solar collector was addressed in early February and flow rates for the MVHR were re-commissioned before the final hand-over to the client. During this period, the MVHR was left on 'boost' mode from February 2nd-9th. The solar collector also stagnated on February 2nd (peaking at 58.8°C) when the MVHR was switched off during a sunny afternoon.

External temperature and solar irradiance:

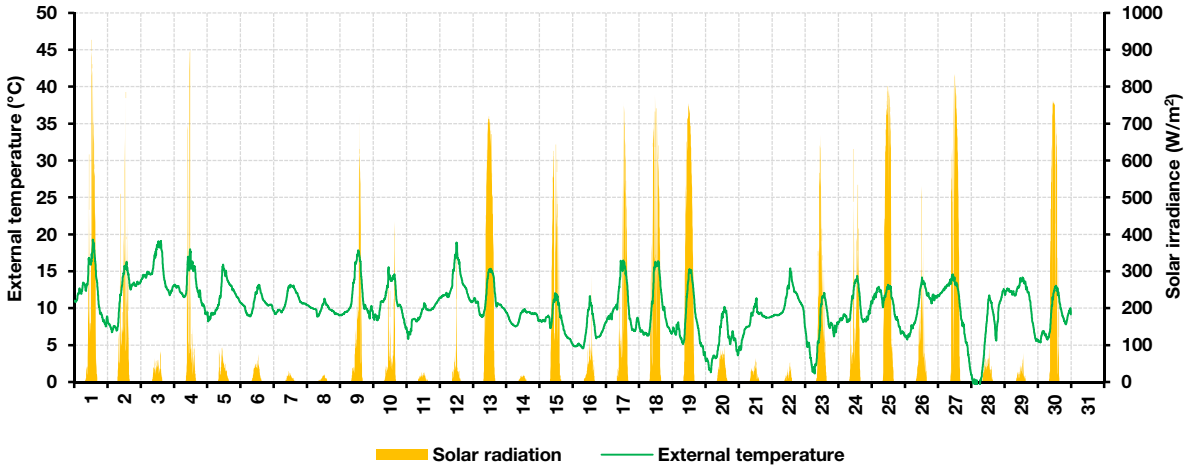

Solar collector inlet and outlet temperature against MVHR fan power:

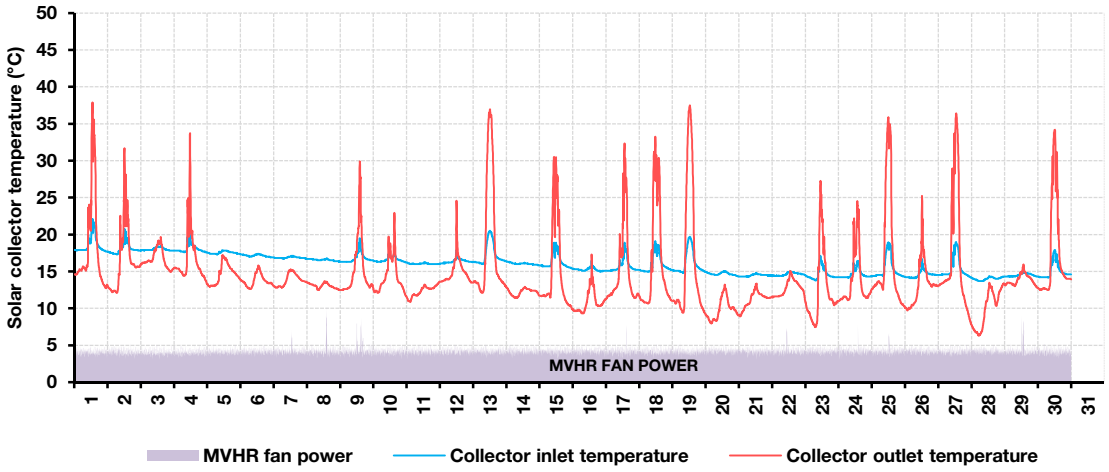

MVHR fresh-air supply, living room and bedroom temperatures:

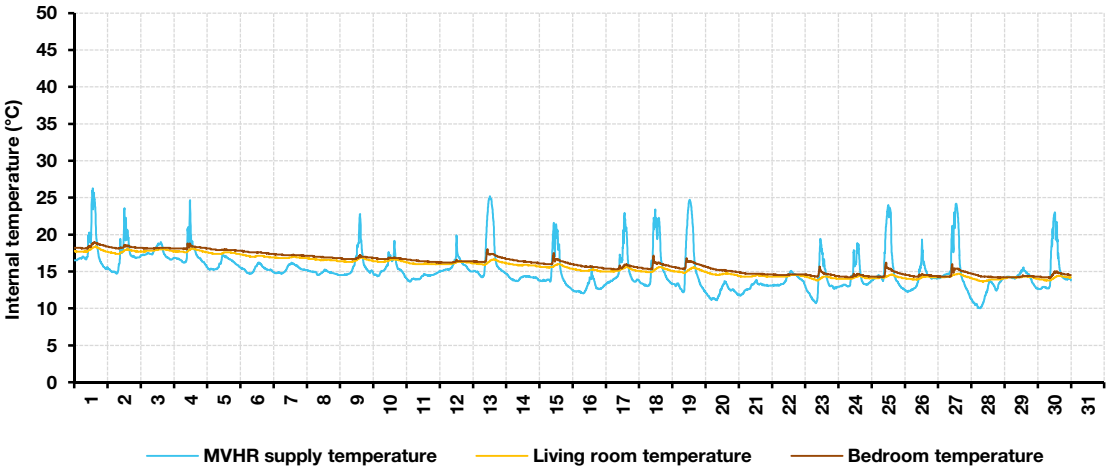

External temperature and solar irradiance:

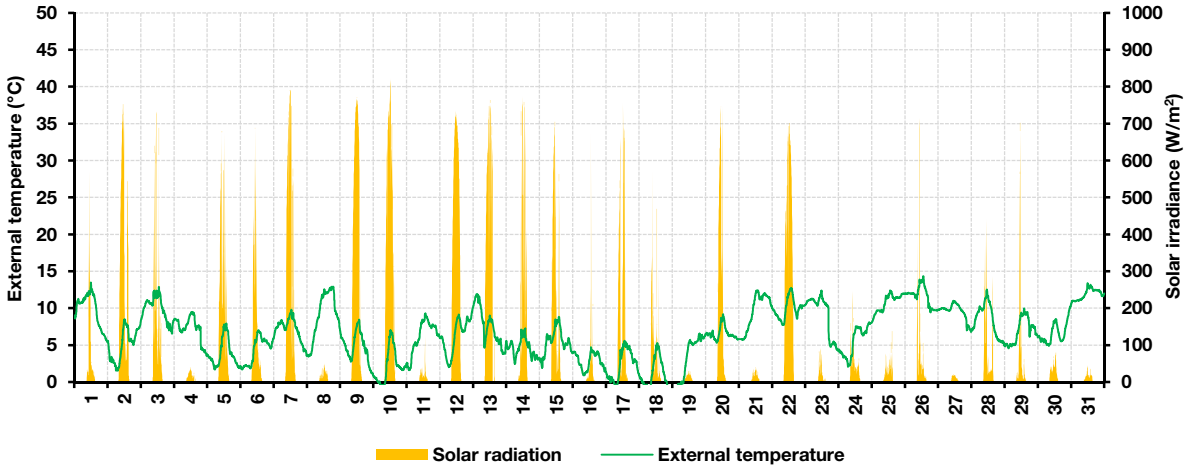

Solar collector inlet and outlet temperature against MVHR fan power:

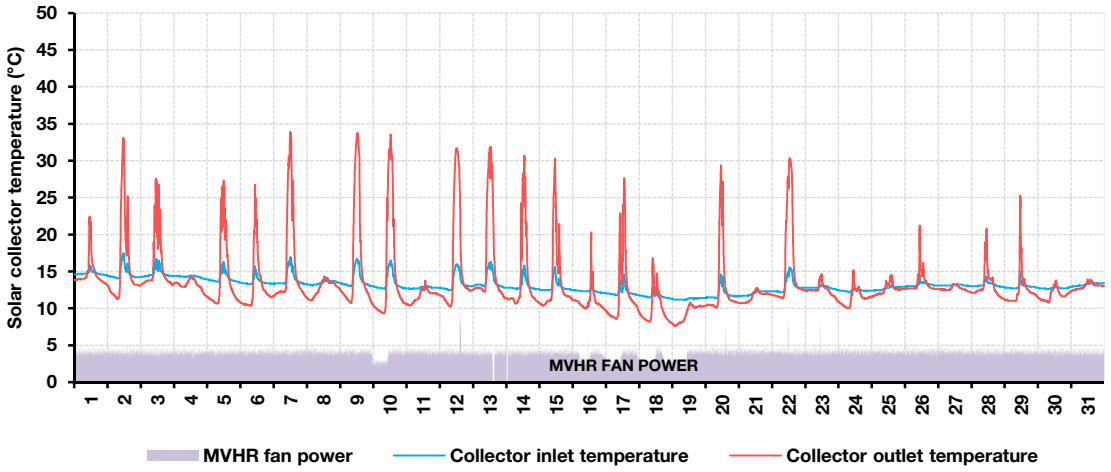

MVHR fresh-air supply, living room and bedroom temperatures:

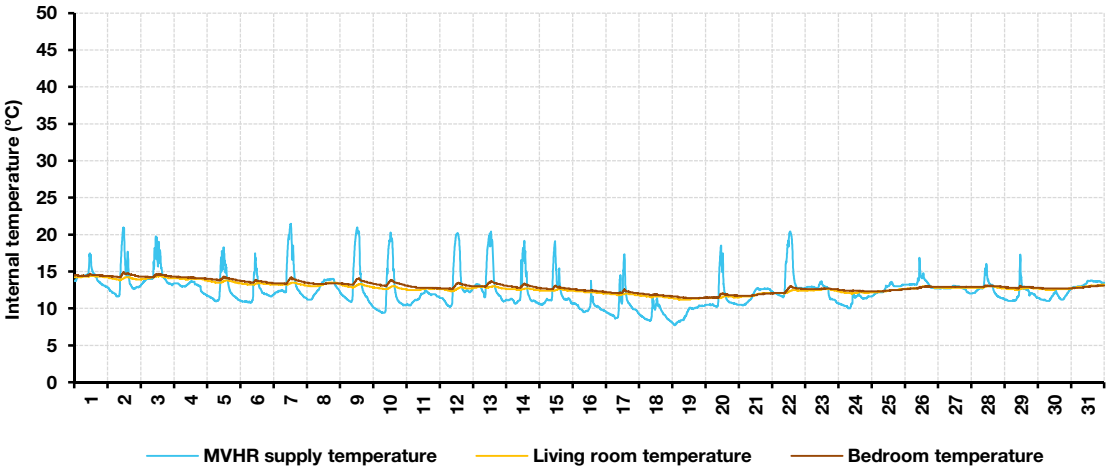

External temperature and solar irradiance:

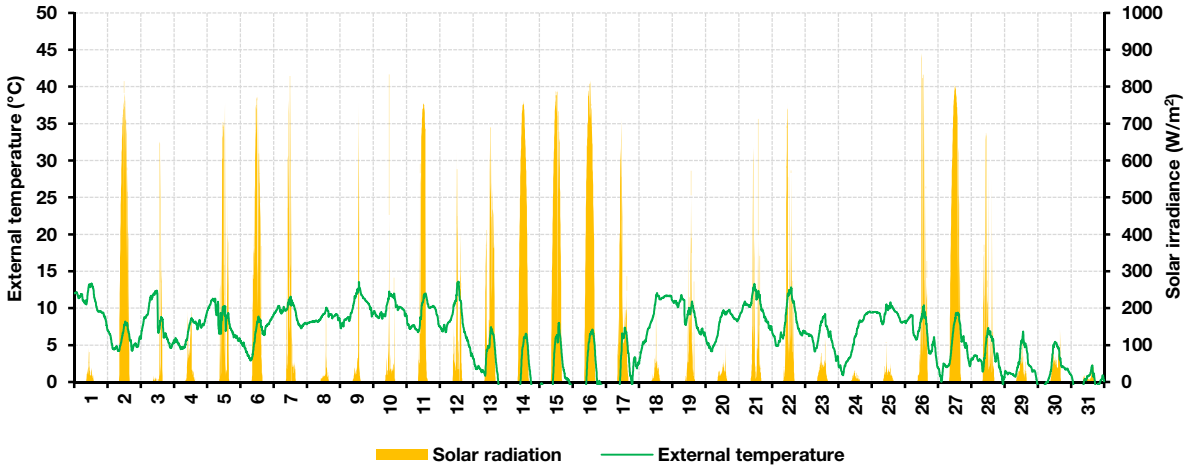

Solar collector inlet and outlet temperature against MVHR fan power:

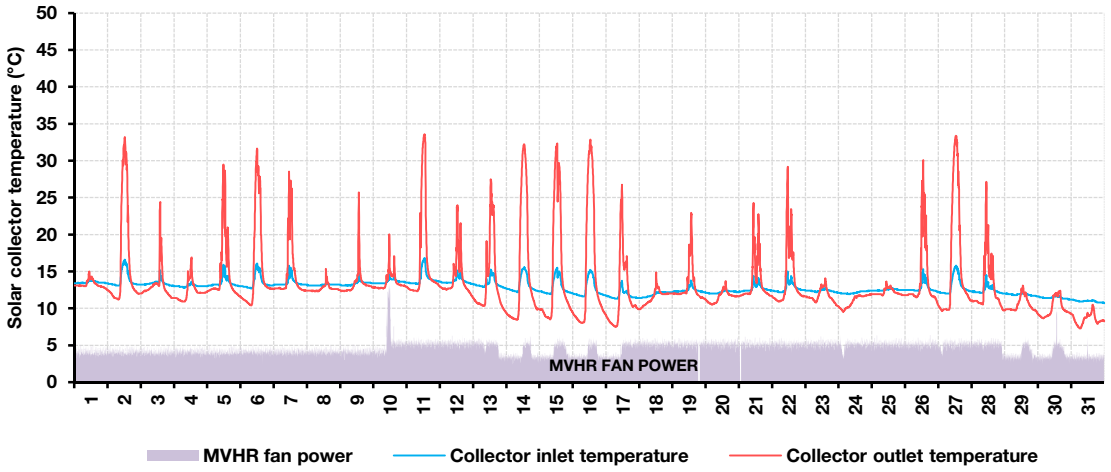

MVHR fresh-air supply, living room and bedroom temperatures:

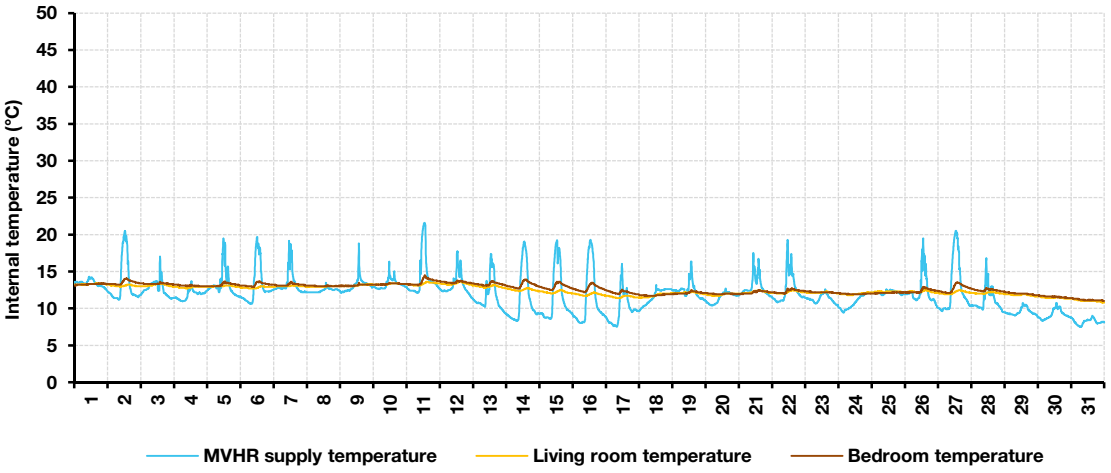

External temperature and solar irradiance:

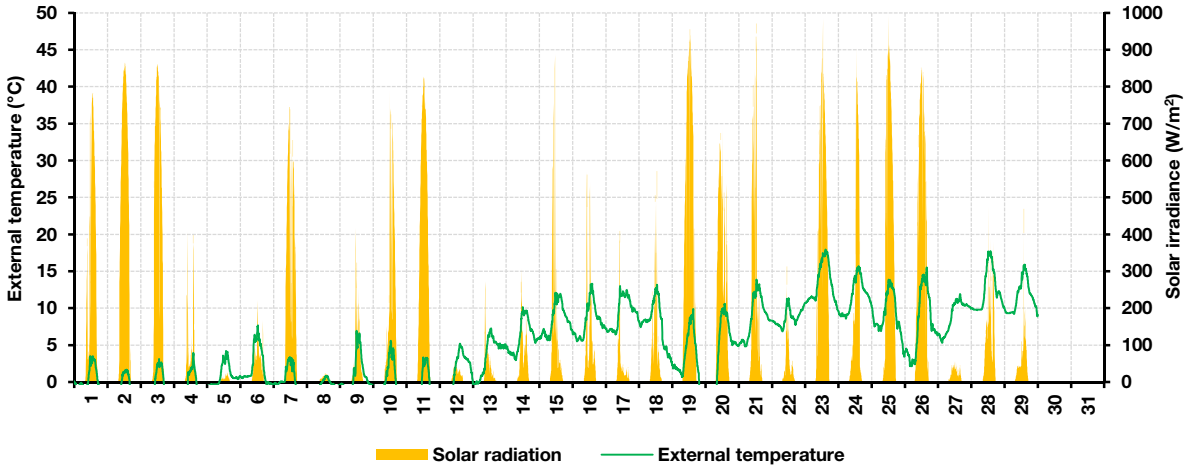

Solar collector inlet and outlet temperature against MVHR fan power:

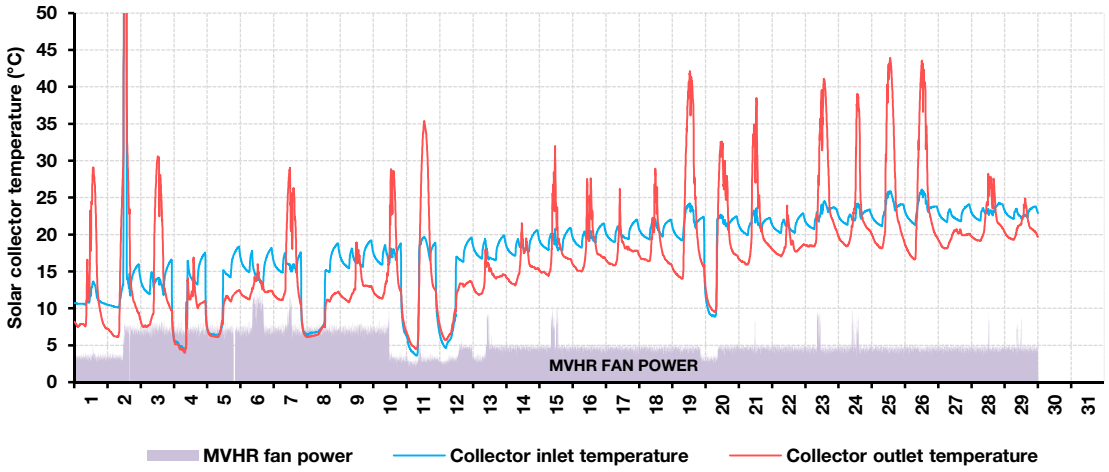

MVHR fresh-air supply, living room and bedroom temperatures:

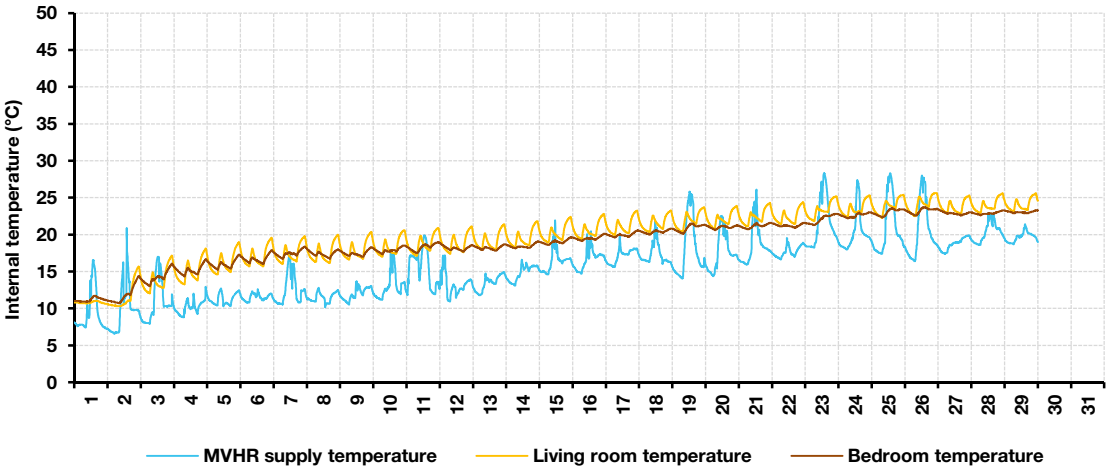

External temperature and solar irradiance:

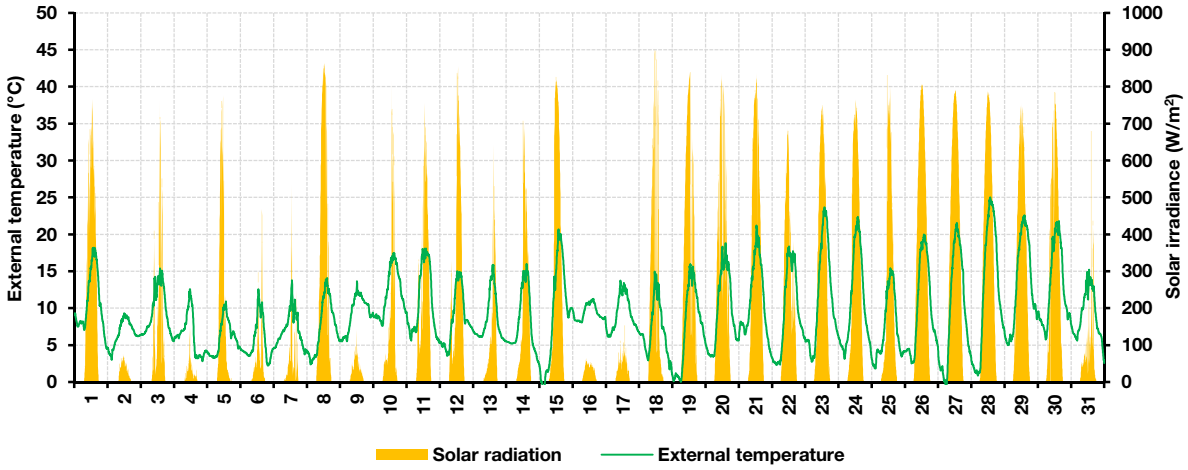

Solar collector inlet and outlet temperature against MVHR fan power:

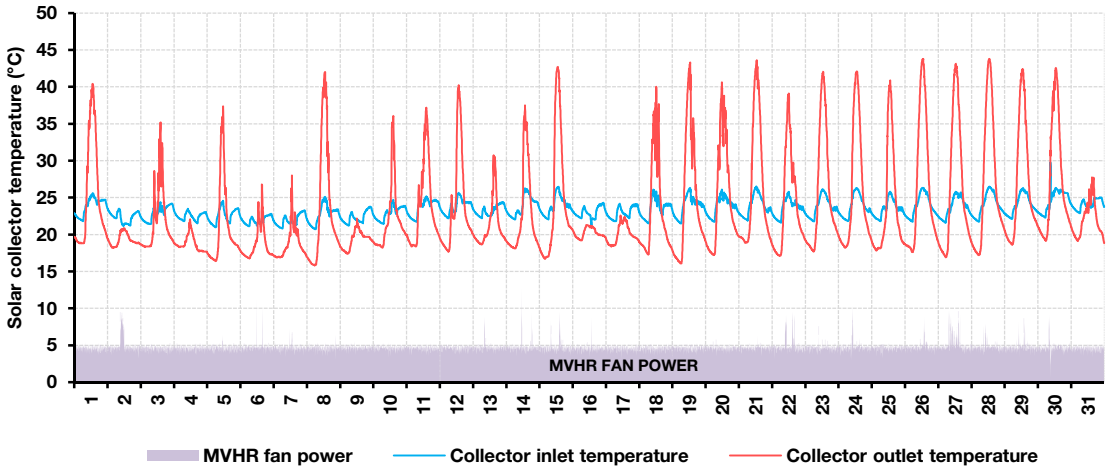

MVHR fresh-air supply, living room and bedroom temperatures:

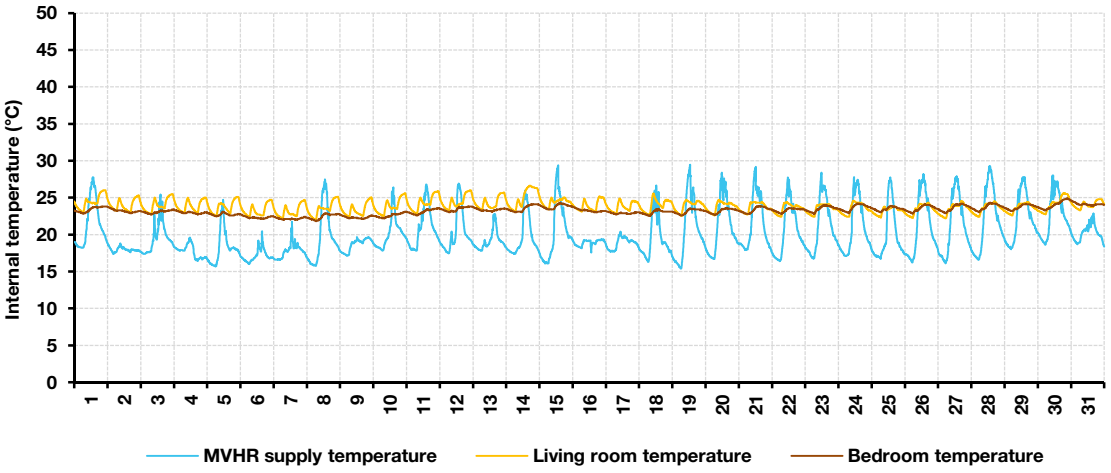

External temperature and solar irradiance:

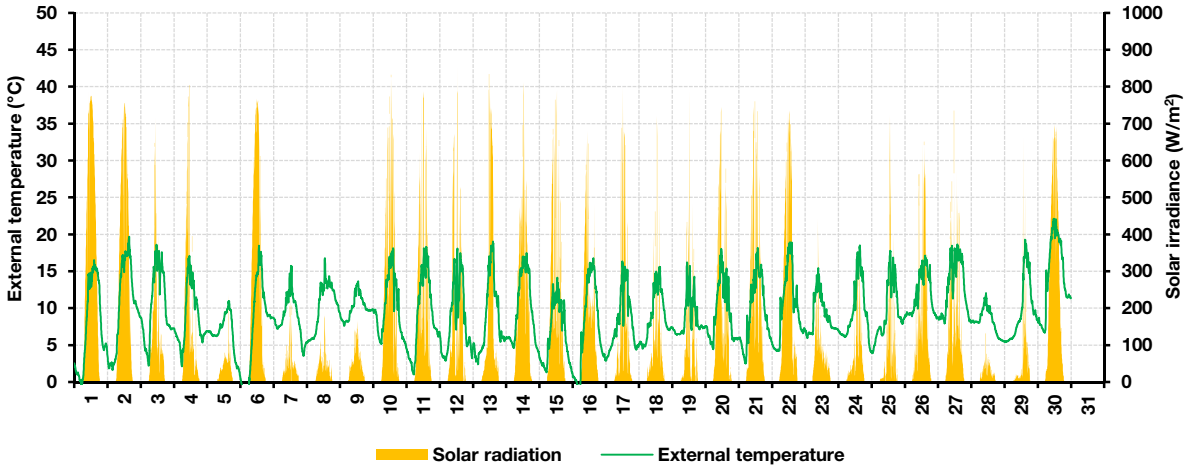

Solar collector inlet and outlet temperature against MVHR fan power:

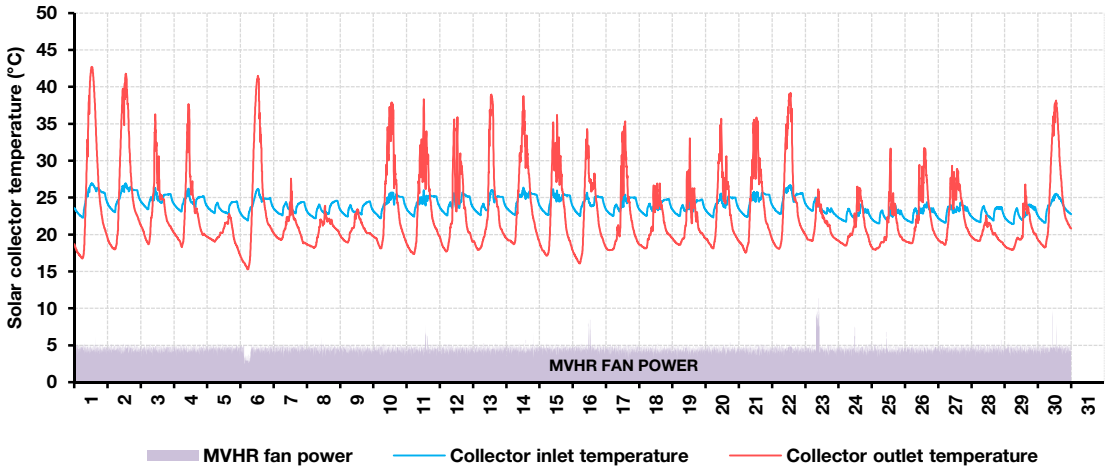

MVHR fresh-air supply, living room and bedroom temperatures:

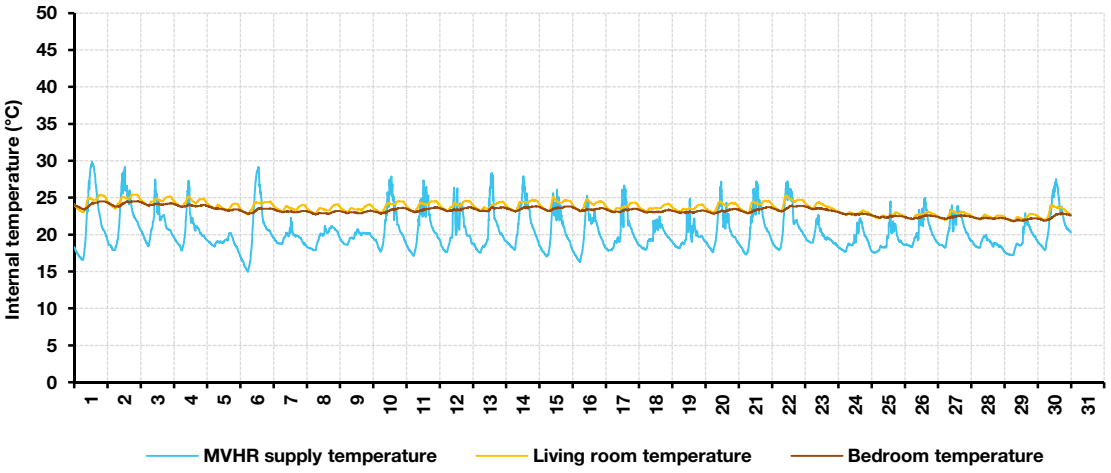

External temperature and solar irradiance:

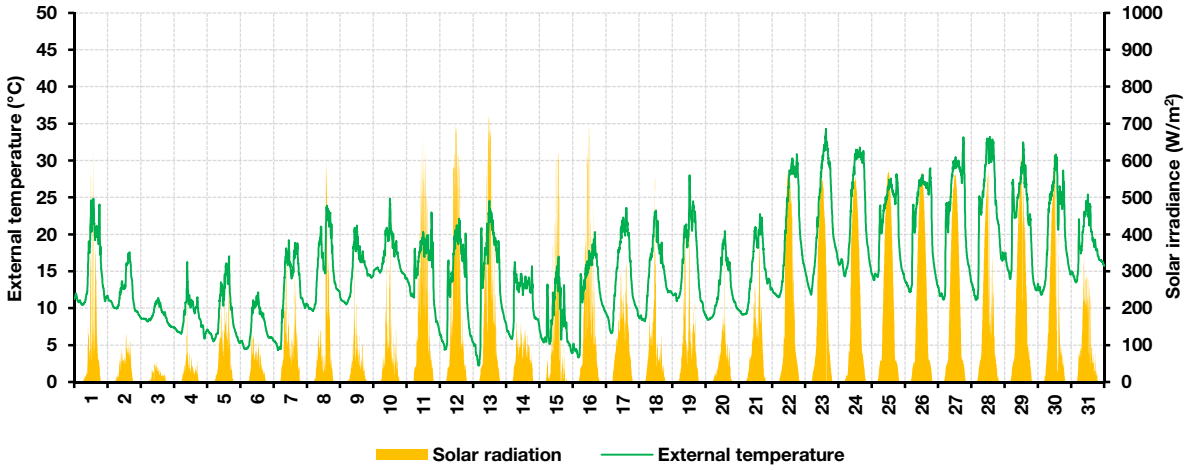

Solar collector inlet and outlet temperature against MVHR fan power:

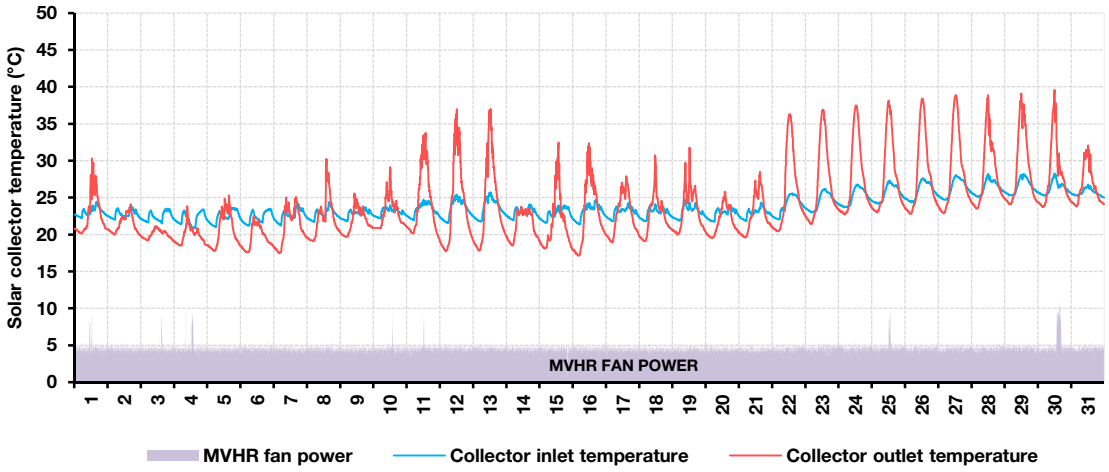

MVHR fresh-air supply, living room and bedroom temperatures:

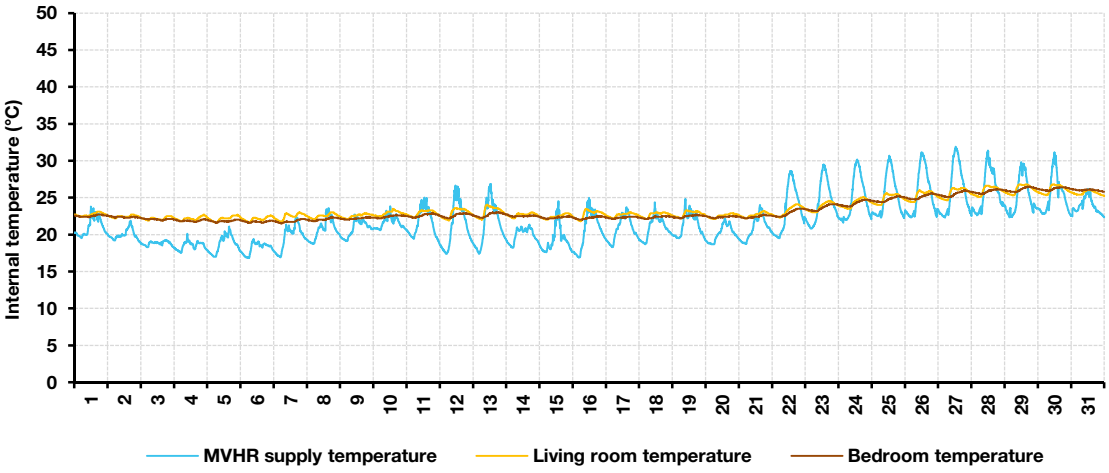

External temperature and solar irradiance:

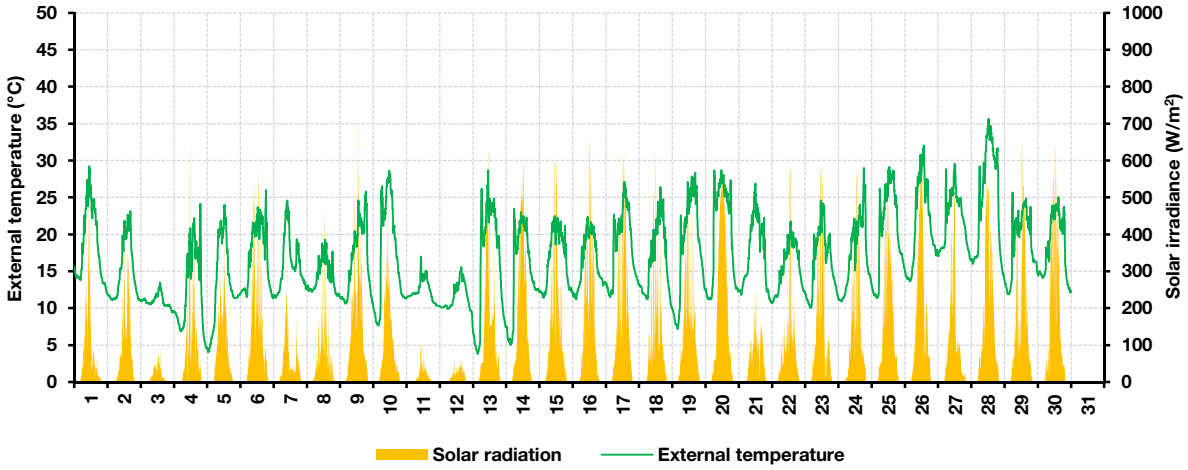

Solar collector inlet and outlet temperature against MVHR fan power:

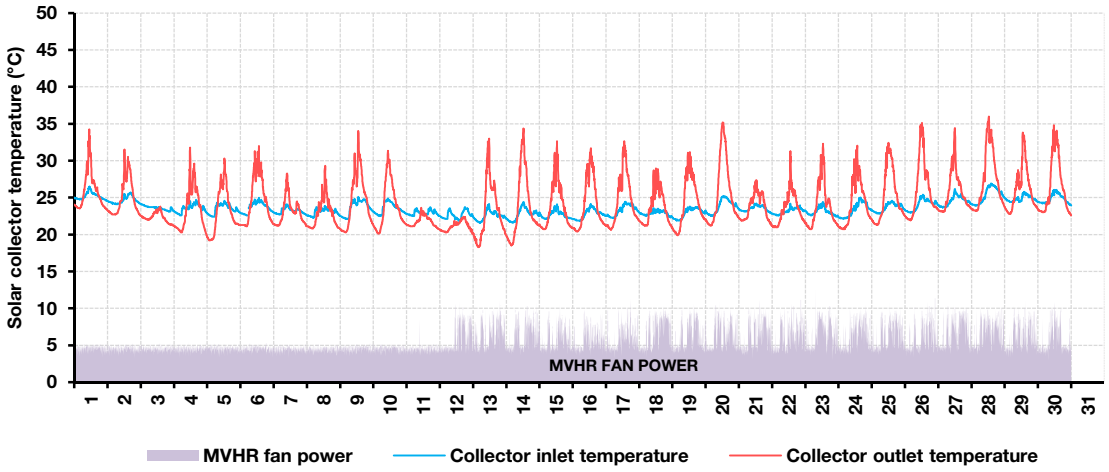

MVHR fresh-air supply, living room and bedroom temperatures:

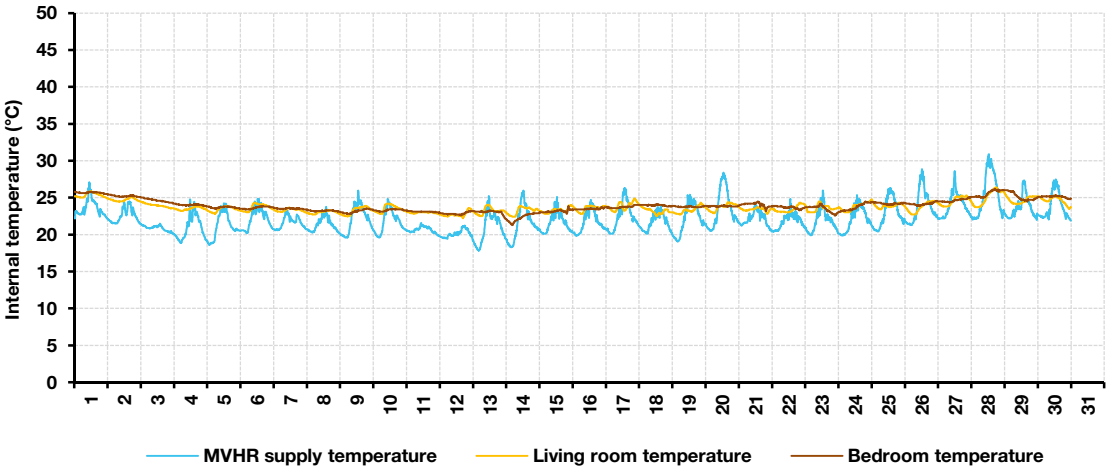

External temperature and solar irradiance:

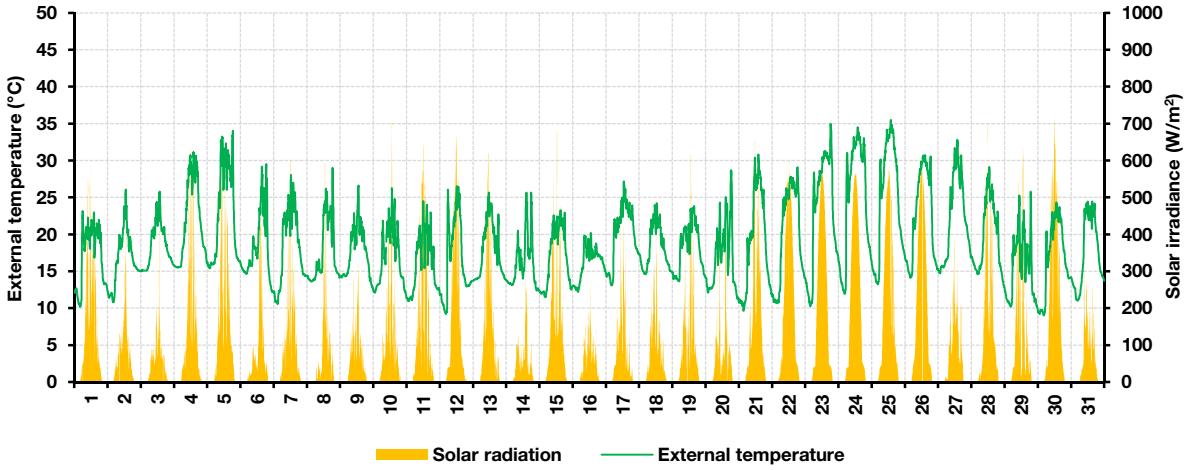

Solar collector inlet and outlet temperature against MVHR fan power:

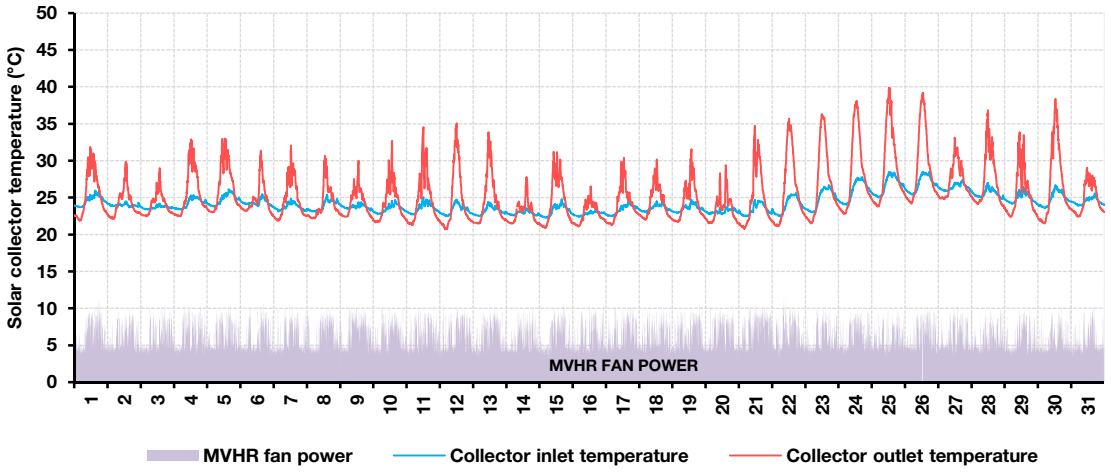

MVHR fresh-air supply, living room and bedroom temperatures:

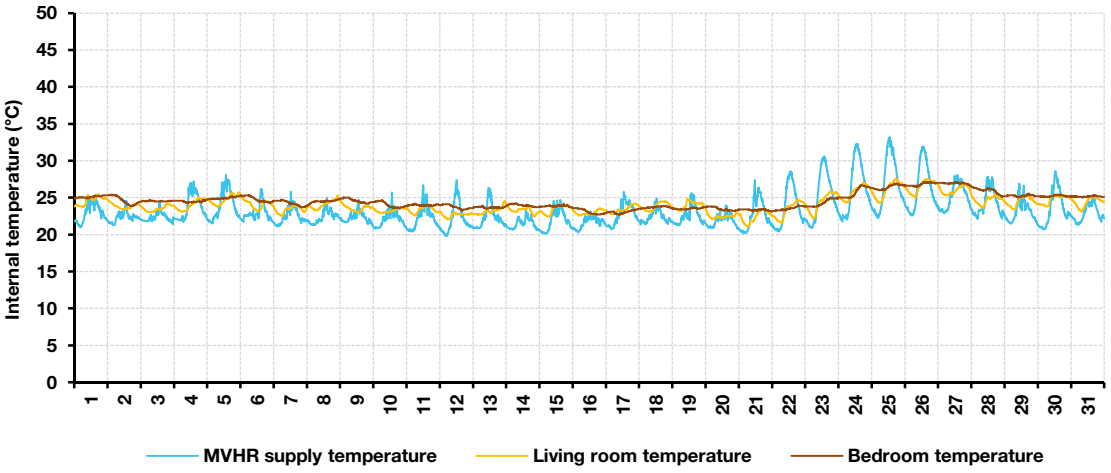

External temperature and solar irradiance:

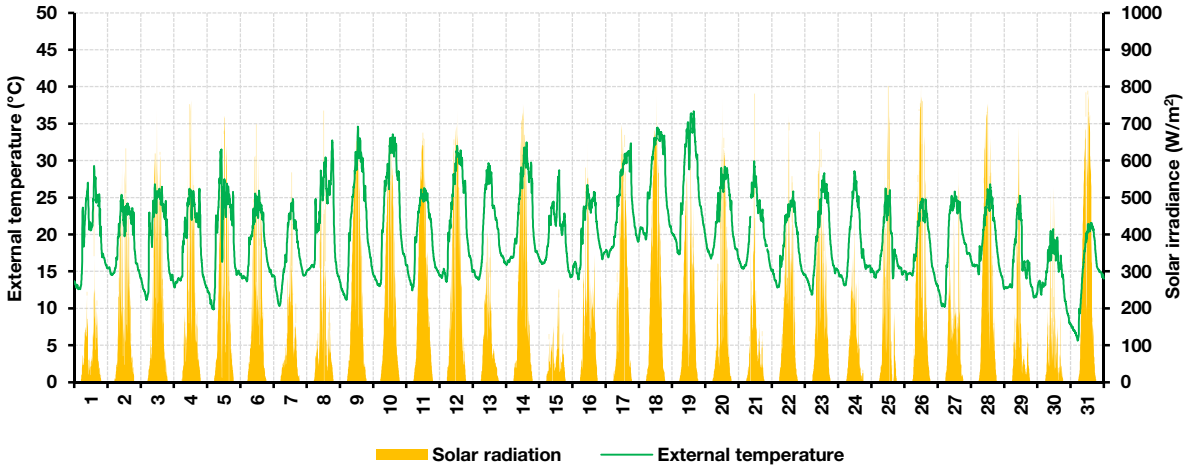

Solar collector inlet and outlet temperature against MVHR fan power:

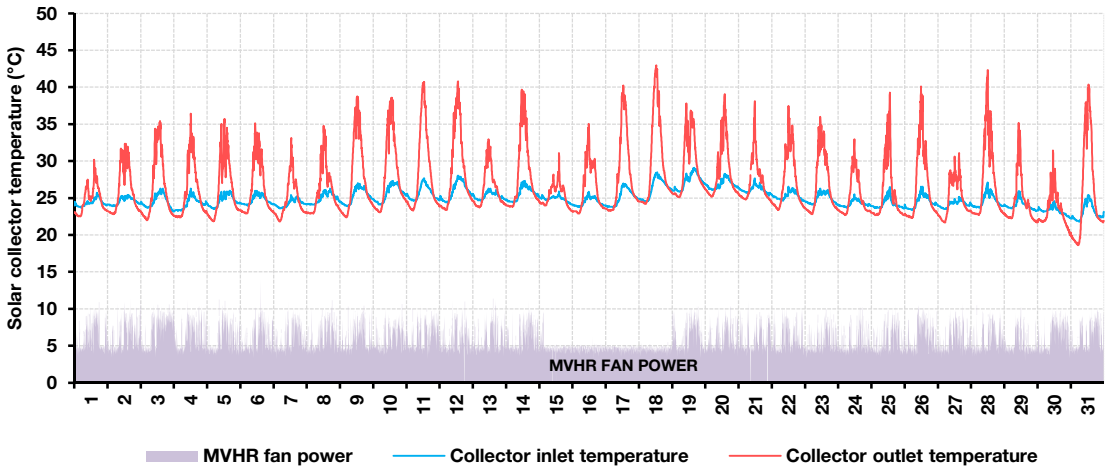

MVHR fresh-air supply, living room and bedroom temperatures:

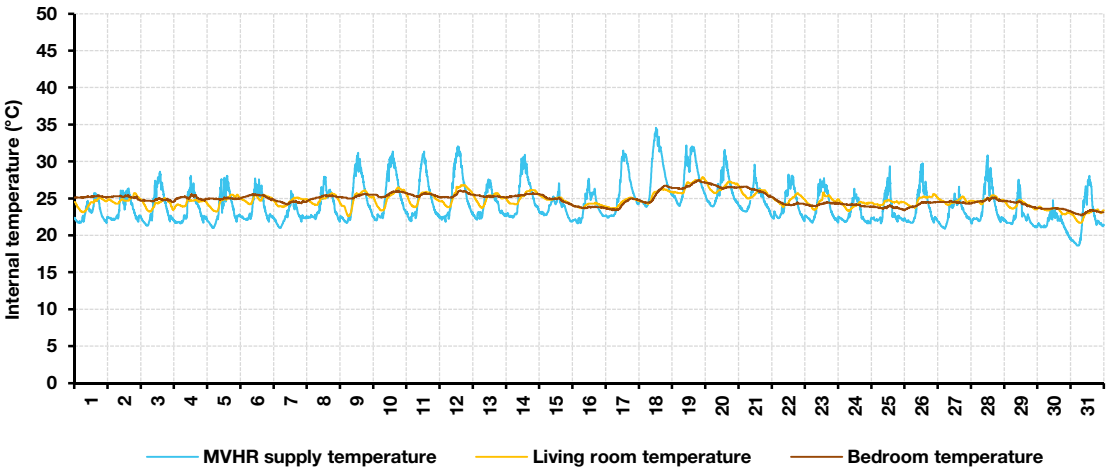

External temperature and solar irradiance:

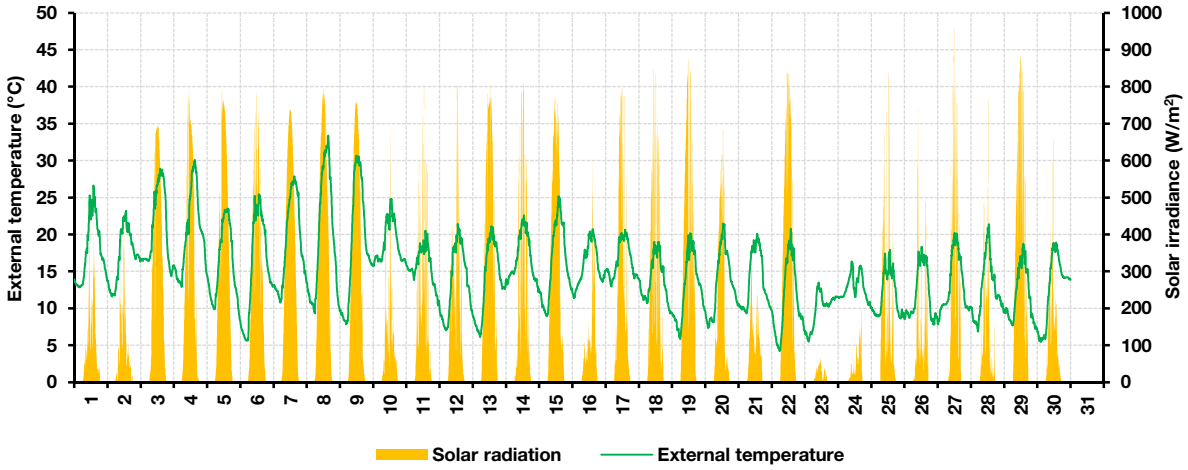

Solar collector inlet and outlet temperature against MVHR fan power:

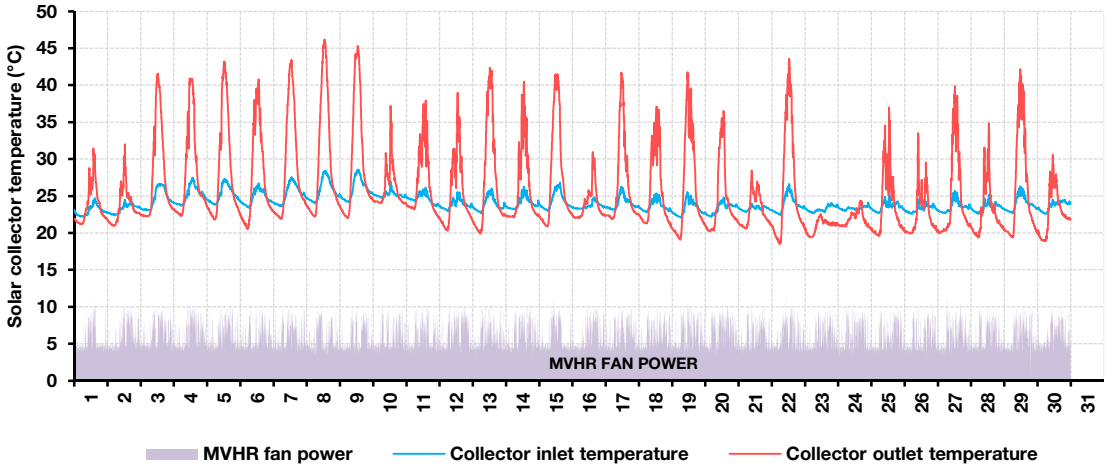

MVHR fresh-air supply, living room and bedroom temperatures:

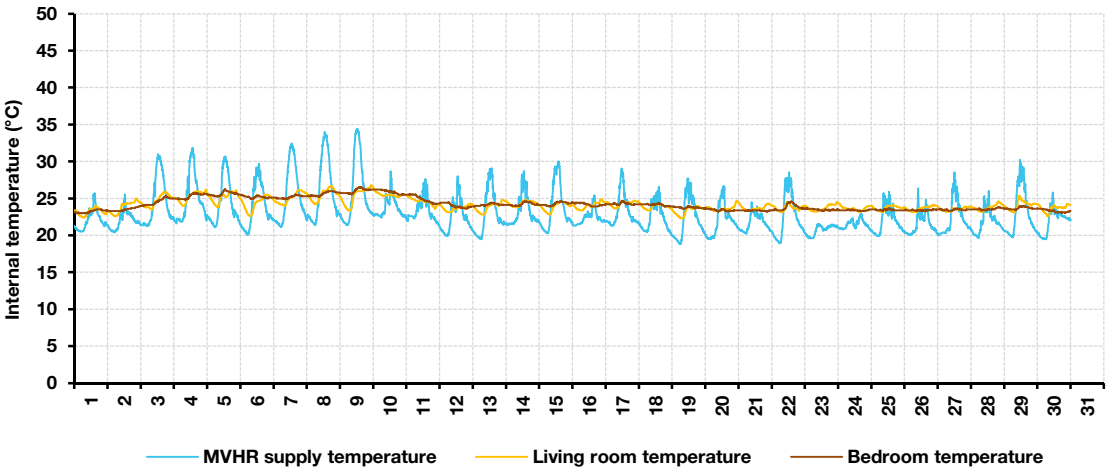

External temperature and solar irradiance:

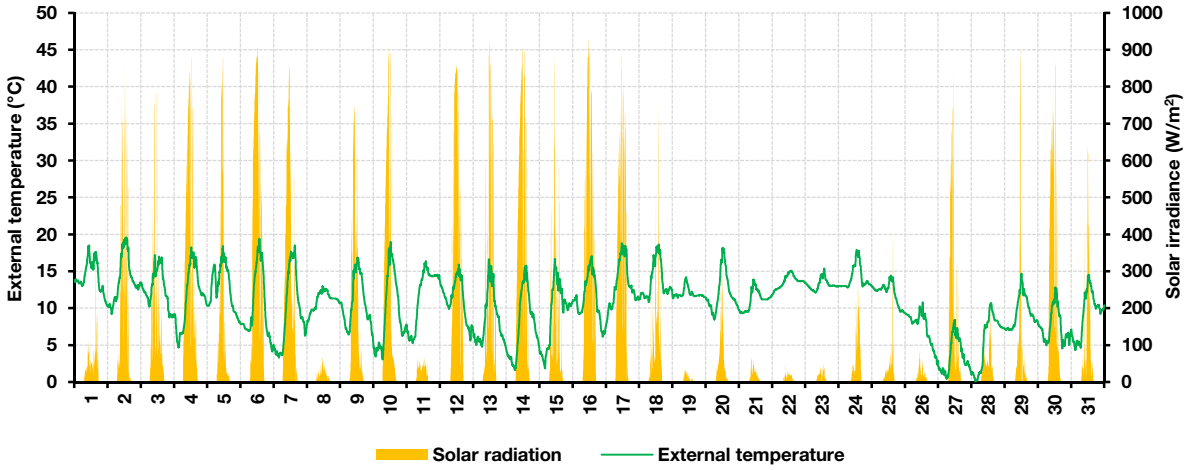

Solar collector inlet and outlet temperature against MVHR fan power:

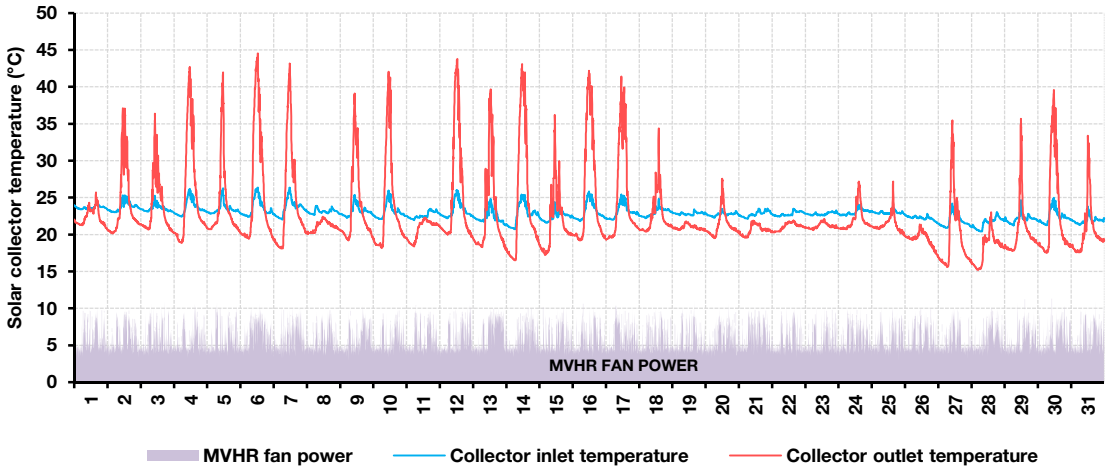

MVHR fresh-air supply, living room and bedroom temperatures:

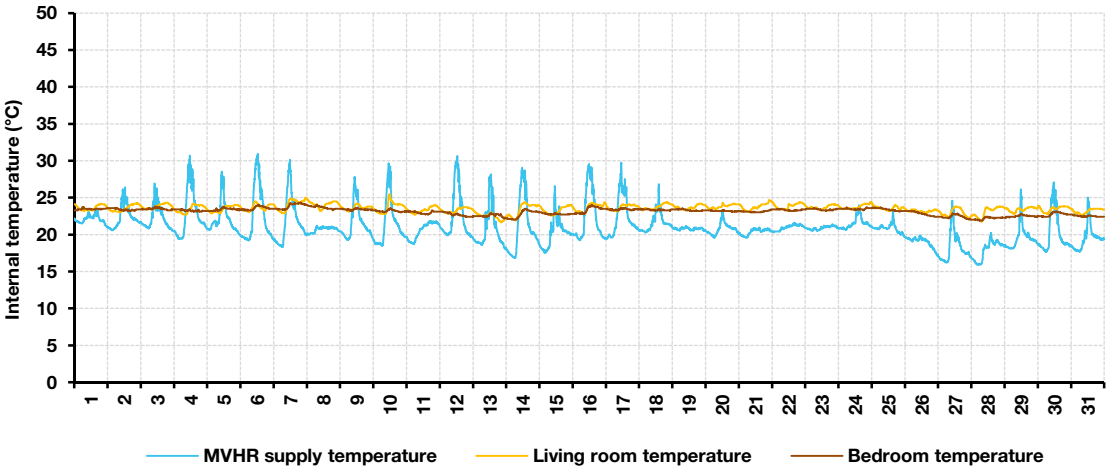

Summary of results:

External temperature and solar irradiance:

		Nov	Dec	Jan	Feb	Mar	Apr	May	Jun	Jul	Aug	Sep	Oct
External temperature (°C)	**Av.**	10.0	6.7	6.0	4.6	9.1	9.2	15.2	16.7	18.8	19.7	15.0	10.7
	Max.	19.3	14.4	13.6	17.9	25.0	22.1	34.3	35.6	35.5	36.7	33.4	19.6
	Min.	-1.1	-3.7	-5.2	-8.4	-1.1	-4.6	2.2	3.8	9.0	5.6	4.2	0.1
Solar irradiance (W/m^2)	**Av.**	55	56	62	91	128	98	92	90	97	118	134	81
	Max.	927	823	891	993	903	845	720	690	721	821	956	927
	Min.	0	0	0	0	0	0	0	0	0	0	0	0

Solar collector inlet and outlet temperature against MVHR fan power:

		Nov	Dec	Jan	Feb	Mar	Apr	May	Jun	Jul	Aug	Sep	Oct
Inlet air temperature (°C)	**Av.**	16.0	13.2	12.8	17.9	23.4	23.9	23.7	23.6	24.2	24.9	24.1	22.9
	Max.	22.1	17.5	16.8	33.8	29.8	26.9	28.3	26.9	28.5	29.1	28.6	26.4
	Min.	13.7	11.1	10.7	3.6	20.7	21.4	20.8	21.6	22.3	21.8	22.1	20.4
Outlet air temperature (°C)	**Av.**	15.1	13.3	13.1	16.8	23.1	22.5	23.8	24.2	25.2	26.6	25.5	22.4
	Max.	37.9	33.9	33.6	43.9	43.8	42.7	39.6	36.0	39.9	43.0	46.2	44.5
	Min.	6.3	7.6	7.3	4.0	15.8	15.3	17.1	18.3	20.7	18.6	18.5	15.2
MVHR in boost	**Av. %**	1.9	1.2	31.6	35.7	13.4	8.4	9.9	38.5	59.1	47.8	54.1	49.6

MVHR fresh-air supply, living room and bedroom temperatures:

		Nov	Dec	Jan	Feb	Mar	Apr	May	Jun	Jul	Aug	Sep	Oct
MVHR supply temperature (°C)	**Av.**	15.1	12.3	12.0	15.5	20.0	20.3	21.8	22.2	23.2	24.2	23.0	21.0
	Max.	26.3	21.5	21.6	28.3	29.5	29.9	31.9	30.9	33.2	34.6	34.4	31.0
	Min.	10.0	7.7	7.5	6.6	15.4	15.0	16.8	17.8	19.8	18.6	18.8	15.9
Living room temperature (°C)	**Av.**	15.6	12.7	12.4	19.8	23.9	23.7	23.4	23.7	24.0	24.7	24.2	23.5
	Max.	18.4	14.4	13.6	25.6	26.6	25.4	26.8	26.4	27.6	27.9	26.8	25.5
	Min.	13.6	11.2	10.8	10.3	22.0	21.8	21.6	22.2	21.1	21.7	22.3	21.6
North facing bedroom temperature (°C)	**Av.**	16.1	13.0	12.7	19.0	23.2	23.2	23.2	23.9	24.5	24.9	24.2	23.1
	Max.	19.0	14.9	14.5	23.7	24.9	24.6	26.5	26.2	27.1	27.5	26.5	24.4
	Min.	14.1	11.4	11.0	10.7	21.8	21.8	21.5	21.3	22.7	22.7	23.0	21.9

Excluding stagnation data on 2nd February 2012, the peak outlet temperature inside the Aerogel Solar Collector was 46.2°C measured at 1pm on September 8th 2012. At this time, the MVHR supply and living room air temperatures were 33.5°C and 26.0°C, respectively, whilst outside air temperature was 30.8°C. Through May-September, there was some evidence of overheating with peak living room and bedroom temperatures exceeding 26°C, whilst outside air temperatures are above 30°C. The minimum internal temperature was 10.3°C at night on February 11th when the dwelling was unoccupied and external temperature was below zero. The average internal temperature over the entire dataset was 20.9°C for both the living room and bedroom.

JOURNAL CIBSE

CIBSE

The official magazine of the Chartered Institution of Building Services Engineers

June 2012

HONEST ENGINEERING
CIBSE PRESIDENT CALLS FOR LESS GREENWASH

LOW CARBON REFURB
A 1960s DWELLING IS TRANSFORMED

LIGHTING FOCUS
COLOUR RENDERING FOR LED LAMPS

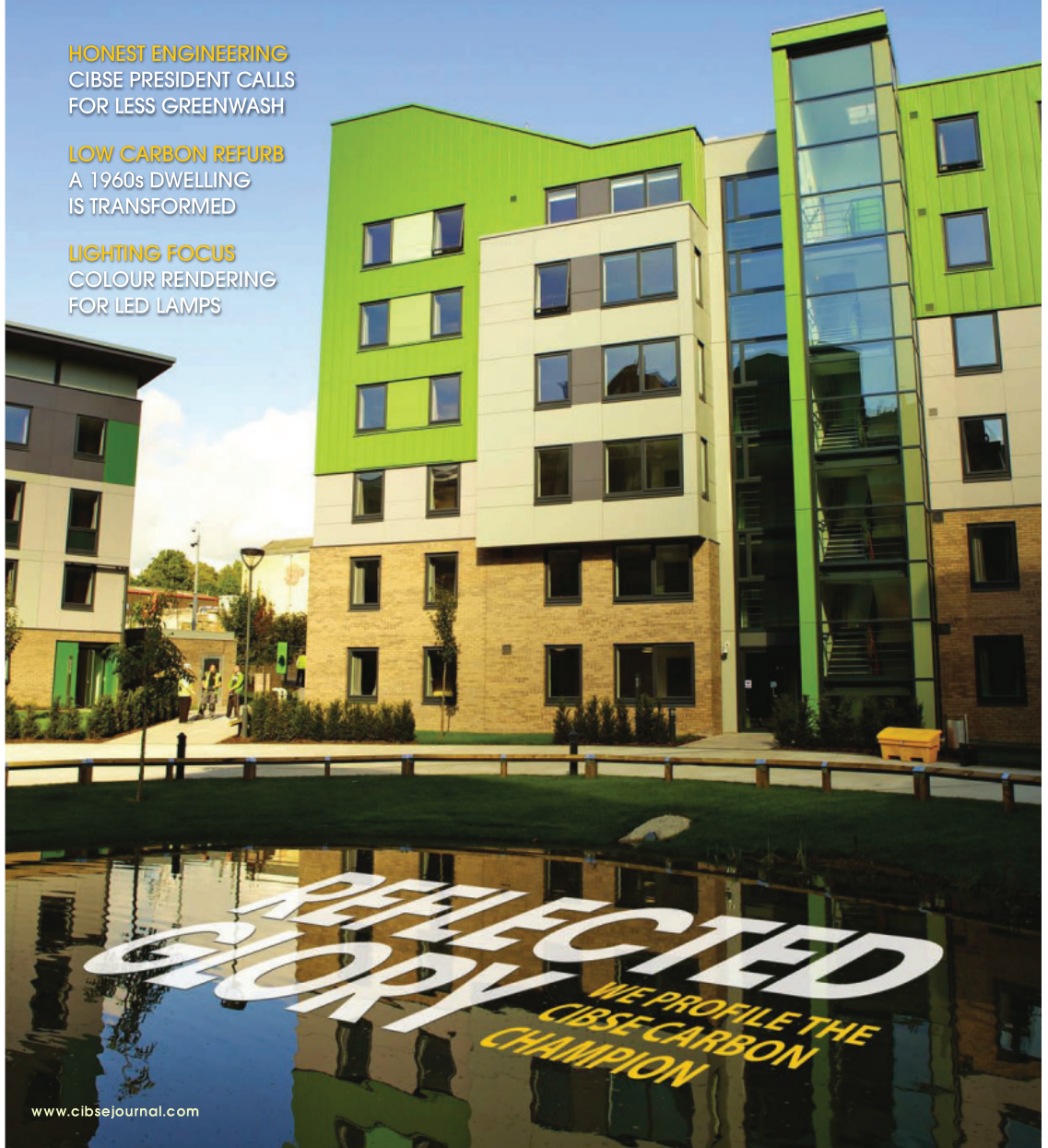

REFLECTED GLORY

WE PROFILE THE CIBSE CARBON CHAMPION

www.cibsejournal.com

BOX OF TRICKS

The transformation of a hard-to-treat 1960s property into a low carbon home involved the use of some unusual technology, writes **Mark Dowson**

A key innovation of the project is a highly-insulated solar-air collector prototype integrated into the external insulation on the south façade

The Thamesmead housing estate in south-east London is a key example of the often poorly insulated and undervalued concrete dwellings built in the 1960s. It was featured in the Stanley Kubrick film, *A Clockwork Orange*, and more recently on television in E4's *Misfits*. But its other claim to fame is that it is now part of 'Retrofit for the Future', a government-funded competition launched by the Technology Strategy Board (TSB) in 2009.

The aim of the competition was to develop innovative, scalable, whole-house refurbishment strategies with potential to reduce 80% of CO_2 emissions in low-rise social housing. Following two intense design phases, 86 teams across the UK were shortlisted and awarded £150,000 to implement their strategies with occupied dwellings. The selected properties are now being monitored over a two-year period after refurbishment, with the findings feeding into research papers and nationwide design guidance.

As a shortlisted team, Buro Happold collaborated with Fraser Brown MacKenna Architects, Gallions Housing Association, Martin Arnold Associates surveyors and Axis Europe contractors to super-insulate a pre-cast concrete end-of-terrace house on the Thamesmead estate.

Like millions of buildings across the UK, the estate consists largely of properties with solid walls, single glazing and uninsulated floors/roofs responsible for a significant amount of wasted heat. In its unrefurbished state, the hard-to-treat property suffered from moisture-related problems such as condensation, rising damp and mould growth, made worse by insufficient heating and high rates of fuel poverty. It possessed a mixture of single-glazed and old double-glazed windows, unused ground-floor garages (too narrow for modern cars) and a first-floor walkway.

Transformation

Through extensive retrofit works, the property has been transformed into a 'near Passivhaus' six-bedroom house, super-insulated with external cladding,

All images: Mark Dowson

Above: The refurbished house at the Thamesmead estate in south-east London. The brightly coloured render, bold parapet walls and pebble dashed render on the ground floor serve to show that external insulation can be achieved without losing individuality amongst the building stock. This detailing is highlighted by angular metallic fins embedded into the render casting different length shadows over the building as the sun rises and sets throughout the year.
Right: The house last year, before the refurbishment.
Top left:The aerogel solar collector prior to being sealed.
Bottom left: The plant room for the property. This contains the mechanical ventilation with heat recovery unit, photovoltaic inverter and a 500 litre domestic hot water cylinder. Three dampers on the MVHR's extract ductwork control airflow to and from the aerogel solar collector. The rear wall of the plant contains power meters to monitor each technology and a 3G hub to transmit data wirelessly to an online server.

triple glazing throughout and high levels of air tightness. Fresh air is provided by a mechanical ventilation system with heat recovery (MVHR). Ten photovoltaic (PV) panels and a vacuum tube collector on the roof provide renewable electricity and water heating. Expected U-values and other projected performance data are shown in the table on page 40.

A key innovation of the Thamesmead project is a highly-insulated solar-air collector prototype integrated into the external insulation on the south façade. The prototype consists of a cavity containing a black perforated metal sheet to absorb solar radiation and a highly insulated translucent cover, consisting of polycarbonate panels fitted with high-performance granular 'aerogel' insulation, to reduce heat losses to the outside.

Aerogel is an emerging material in the UK construction market. This unique nano-porous translucent insulation material has the lowest thermal conductivity of any solid, retaining up to four times as much heat as conventional

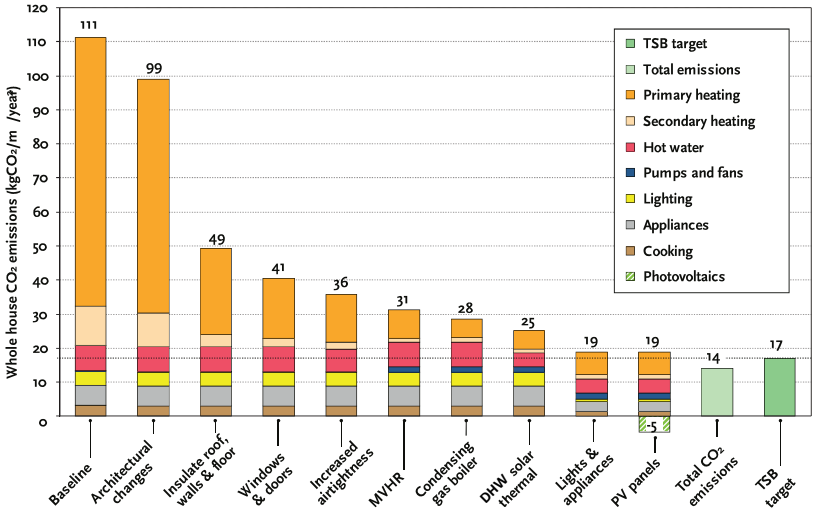

The whole-house CO2-reduction strategy

Renewable Technologies

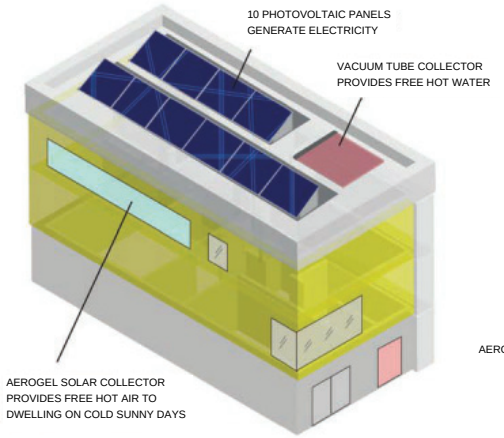

Aerogel solar collector:
(Connection to MVHR extract-air ductwork)

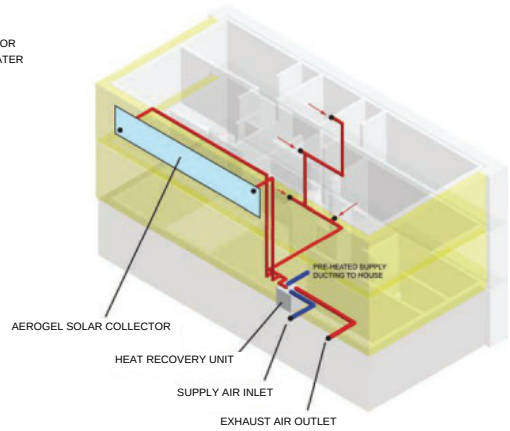

> The success of the retrofit will rely heavily on the occupants' comfort and satisfaction levels, combined with how well they engage with the new technologies and conserve energy at home

insulation, whilst being highly transparent to light and solar radiation. It is available commercially as translucent granules encapsulated within glass or multi-wall polycarbonate sheets, or as particles embedded within opaque insulation boards and blankets. The material can be applied to a building in a variety of ways.

Linked to the property's MVHR, extracted air from the kitchen and bathrooms is fed into the solar collector cavity, where it is heated by incoming solar radiation. This heat is then used to provide additional energy indirectly to heat the incoming fresh air supply to the property's living room and bedrooms. Automatic flow and bypass controls maintain comfortable living conditions all year round.

Some promising monitored results have already been observed for this system, indicating that it will play an important role in heating the property during cold-sunny conditions. During a seven-day controlled test in October 2011, the solar collector outlet reached 45C on a cold sunny day, pre-heating the supply air in the mechanical ventilation system to 30C, enabling the house to maintain comfortable living conditions at 21-22C, without additional heating.

A custom-built 'aerogel door' developed by Proctor Group was also integrated into this retrofit. The double leaf plant room door incorporates a 30 mm-thick opaque aerogel blanket, capable of achieving a central U-value as low as 0.39 W/sq m.K, or 0.65 W/sq m.K including the frames. In a separate application, 80 mm of aerogel was also applied to the ground-floor slab in a zone where the floor-to-ceiling height was limited.

Specification: Thamesmead refurbishment
Walls: 300 mm of Permarock EPS insulation to achieve U-value of 0.1 W/sq m.K. Yellow render with aluminium fins
Roof: New roof with airtight membrane, services core and PIR 300mm insulation for U-value of 0.1 W/sq m.K
Windows: Passivhaus-certified Nordan N-tech triple glazing with U-value of 0.8 W/sq m.K and solar G-value of 0.5
Doors: Passivhaus-certified front door. Plant door custom built by Proctor Group with U-value of 0.65 W/sq m.K
Ground floor: U-value of 0.15 W/sq m.K throughout. Spacetherm aerogel insulation used in zone with 80mm space available
Air tightness: Pro Clima airtight tapes, sealants and sleeves used throughout. Target: 0.6 cu m/sq m/hr @50 Pa. Best on-site : 3.5 cu m/ sq m/hr @50 Pa
Ventilation: Nuaire MRXBOX95B-WH1 unit with summer bypass. Extract air for heat recovery boosted by aerogel solar collector
Heating: Warm air supplied by MVHR. System boiler with small-zoned radiators for peak winter conditions
Hot water: 500 litre cylinder fed by electric immersion and boiler. A 3 sq m vacuum tube collector meets 42% of load
Electricity generation: Ten PV panels generate 2.30 kW peak. Array is ballasted using aluminium frame to avoid piercing insulation.
Lights and appliances: Low energy fittings and light bulbs with A-rated appliances specified throughout property
Predicted CO2 emissions **Baseline:** 111 kg CO2/sq m/year **Post retrofit:** 14 kg CO2/sq m/year **Predicted saving:** 87%

Evaluation

Onsite work at the property finished in March this year, and a large family is expected to move in over the next one to two months.

Since last August, and for another 18 months, a package of wireless monitoring equipment is being used to capture important information such as the internal temperature and CO2 levels within the house, power consumption of the MVHR, energy generation of the PV panels and solar water heater, as well as the total consumption of gas, electricity and water.

A roof-mounted solar radiation sensor, combined with temperature and humidity sensors inside the aerogel solar collector cavity and MVHR ductwork, provide a unique insight into this system's performance.

Ultimately, the success of the retrofit will rely heavily on the occupants' comfort and satisfaction levels, combined with how well they engage with new technologies and conserve energy at home. Interviews will be held to facilitate this process. Nevertheless, through this deep retrofit, the expected value of the property will have increased greatly, particularly due the extended living space, new kitchen-diner and additional two bedrooms.

There is scope to retrofit millions of buildings to make deep cuts in CO2 emissions. However, effective implementation is no small task. Solutions must account for the variety in age, size, quality, composition, function, asset value and social value across the existing building stock, as well as the different needs, expectations and budgets of homes owners and occupiers. Understanding which solutions are cost effective and deliver real savings in-use is imperative. **CJ**

● **MARK DOWSON** is a research engineer within Buro Happold's sustainability and physics team, London. **mark.dowson@burohappold.com** A full scientific paper on the aerogel solar collector's performance can be found at **http://dx.doi.org/10.1016/j.enbuild.2012.02.007**

AEROGEL SOLAR COLLECTOR

Retrofit for the Future

The Aerogel Solar Collector is a flat plate solar-air heater incorporating translucent granular aerogel insulation in the cover, designed to improve the efficiency of heat recovery systems in Passivhaus refurbishments. It was developed by Dr Mark Dowson, an Engineering Doctorate researcher sponsored by Brunel University & Buro Happold engineers. A full scale prototype was successfully installed on a 1960s end terrace house in South-East London as part of the Technology Strategy Board's Retrofit for the Future competition. In-situ testing has found that during cold sunny conditions, peak outlet temperatures up to 45°C were observed, preheating the dwelling's fresh air supply up to 30°C, facilitating internal temperatures of 21-22°C without auxiliary heating. The predicted financial and embodied CO_2 payback for a range of cover thicknesses is 7-13 years and 0-1 years, respectively. Efficiency up to 60% and a financial payback period as low as 4.5 years is possible through an optimised design.

INNOVATION

This prototype is UK's the first solar-air collector installation incorporating translucent granular aerogel insulation in the cover. Aerogel is a unique nano-porous translucent insulation material with the best insulating properties of any solid. It effectively blocks heat transfer by convection, conduction and long-wave thermal radiation. Meanwhile, it is highly transparent to light and short wave solar radiation, making it an ideal material to incorporate into the cover of high performance solar collectors. Compared to conventional single or double glazed collectors, the heat losses through an aerogel cover will be significantly reduced providing higher operational efficiencies, particularly at low ambient temperatures during the peak heating season.

PROJECT TEAM

This prototype was designed and installed as part of a collaborative effort. Detailed development of the prototype was led by Dr Mark Dowson, working with Colin Biggs (Technical Director of Nuaire Ltd), Dr Jeremy Richings (Technical Director of Permarock Products Ltd) and Richard Lowe (Technical Services Manager) at Xtralitre Ltd. The refurbishment team included Buro Happold, Fraser Brown Mackenna Architects, Martin-Arnold Associates, Gallions Housing Association and Axis Europe contractors. Monitoring equipment was installed by BSRIA and MD electrical.

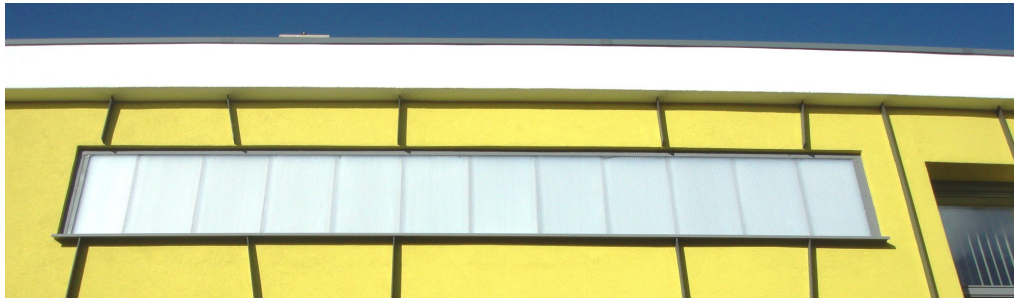

AEROGEL SOLAR COLLECTOR

Retrofit for the Future

DESIGN AND INSTALLATION

The solar collector cover thickness was selected to achieve a Passivhaus U-value below 0.8 W/m^2 K, and the system was sized to provide supply-air temperatures of 30°C. The timber and aluminium framing was incorporated into the properties external south facing wall, integrated alongside the external cladding scheme, with a fire break around the perimeter. Inside the cavity is a black perforated aluminium absorber sheet to harness solar radiation transmitted through the cover and transfer the energy to the air. The prototype is connected to the extract side of the dwelling's whole house mechanical ventilation with heat recovery system (MVHR), due the design team not wanting to pass the dwelling's fresh air supply through a prototype which had not been tested before. As such, the collector provides additional energy to indirectly heat the incoming fresh air supply to the property's living room and bedrooms. In order to mitigate overheating, the MVHR incorporates a 'summer bypass' switch to prevent fresh air being pre-heated when outside temperatures are above 20°C. Thermistors in the collector cavity and the dwelling's exhaust air ductwork from the house prevent air being fed into the collector at night when there is no energetic benefit. All joints and edges inside and around the collector were sealed with air tight tapes. Full on-site commissioning of the system and air flow rates has been carried out.

SOLAR COLLECTOR SCHEMATIC

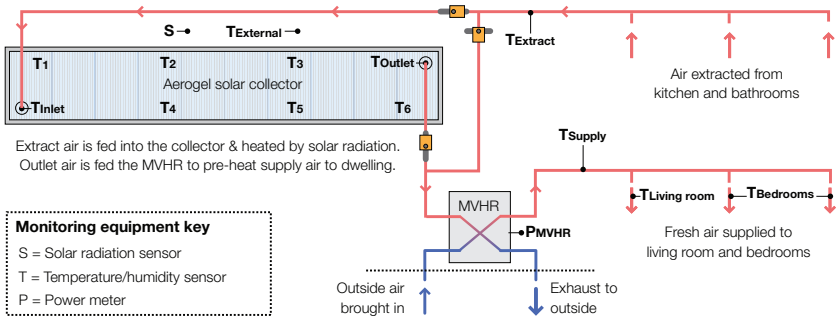

Monitoring equipment key

S = Solar radiation sensor
T = Temperature/humidity sensor
P = Power meter

SOLAR COLLECTOR SECTION

1. 40mm thick polycarbonate panel filled with aerogel granules
2. Black powder coated perforated aluminium absorber sheet
3. 80mm cavity either side of absorber sheet
4. Incoming solar radiation
5. Exhaust air from dwelling flows through inlet duct
6. 30mm thick, 150mm diameter pre-insulated ductwork
7. Existing concrete wall (south facing)
8. Timber frame (painted black)
9. Aluminium frame with housing polycarbonate panels
10. Aluminium drip trays to condense and evaporate moisture
11. 60mm thick foil backed mineral insulation
12. 300mm thick mineral insulation, 200mm around perimeter
13. 300mm thick external insulation (expanded polystyrene)

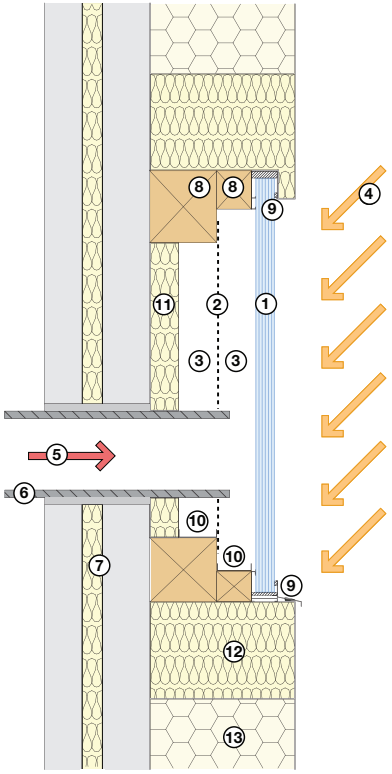

DAMPER CONTROLS IN THE PLANT ROOM

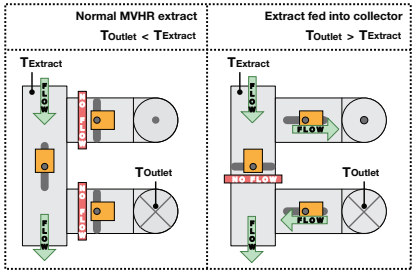

AEROGEL SOLAR COLLECTOR

Retrofit for the Future

IN-SITU PERFORMANCE

The in-situ performance of the Aerogel Solar Collector is being monitored as part of a two-year post occupancy evaluation study, led by Dr Mark Dowson, funded through the Technology Strategy Board. A package of wireless monitoring equipment is capturing information such as internal temperatures within the house, power consumption of the MVHR, solar radiation hitting the properties south facing wall and temperature/humidity inside the profile of the Aerogel Solar Collector cavity and MVHR ductwork. Over a 12 month period spanning October 2011 – October 2012, the monthly-average peak outlet temperature inside the collector was 39°C, and the monthly-average peak supply air temperature fed to the dwelling's living room & bedroom was 28.5°C. The average internal temperature in the dwelling was 20.4°C for the living room and bedroom, with no auxiliary energy for heating used during this period.

EFFICIENCY AND PAYBACK PERIOD

A scientific journal paper on the predicted and in-situ performance of the Aerogel Solar Collector has been published in '*Energy and Buildings*'. Within this paper the efficiency of the installed prototype is compared to the efficiency of an equivalent system design, but incorporating a single glazed and double glazed cover, and also different thickness of granular aerogel from 10mm-40mm. The study found that an efficiency of up to 60 % and a financial payback period as low as 4.5 years was possible for an optimised collector incorporating a 10 mm thick granular aerogel cover. In a second study, published in the '*Applied Energy journal*', the embodied CO_2 associated with aerogel manufacture was quantified. Based on these findings, the predicted environmental payback period, accounting for the embodied CO_2 associated with aerogel and all other materials inside the collector was 0-2 years, indicating that the system provides a fast environmental payback.

PUBLICATIONS

"Box of Tricks", 4-page feature article in the CIBSE Journal, June 2012, http://www.cibsejournal.com/archive/2012-06/box-of-tricks

Predicted and in-situ performance of a solar air collector incorporating a translucent granular aerogel cover, Energy and Buildings, 2012,Volume 49, pp 173-187. http://www.sciencedirect.com/science/article/pii/S0378778812000825

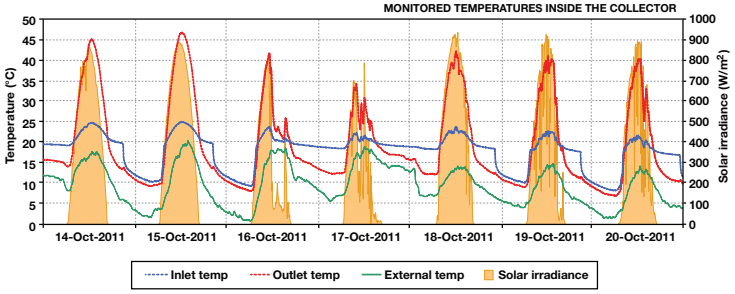

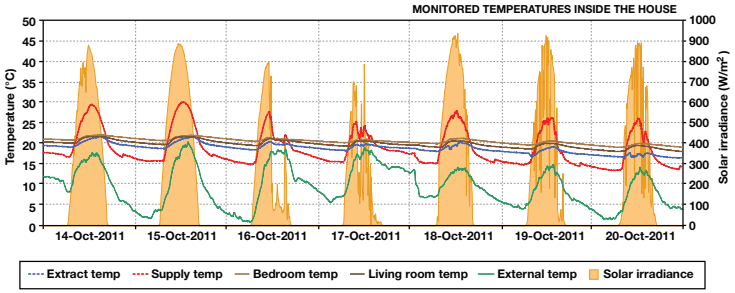

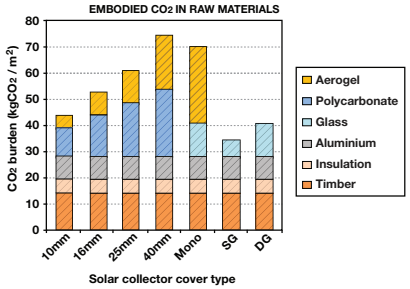

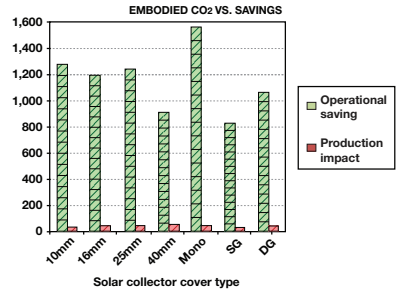

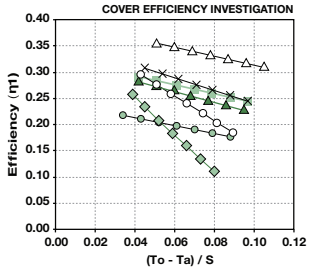

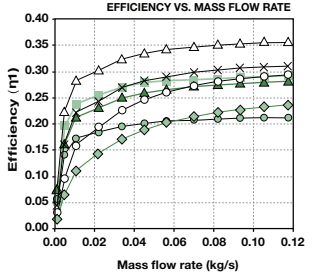

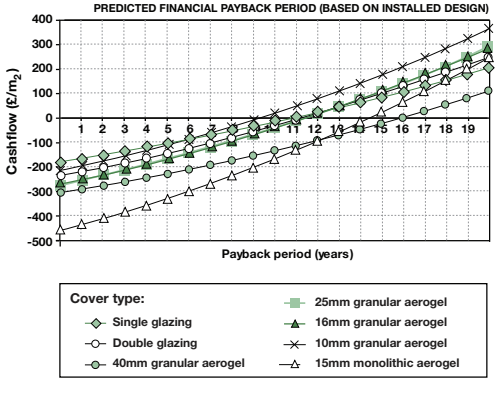

For more information please contact Dr Mark Dowson at mark.dowson@burohappold.com